



PERSATUAN GEOLOGI MALAYSIA

WARTA GEOLOGI

NEWSLETTER of the GEOLOGICAL SOCIETY OF MALAYSIA

Jilid 38
No. 2

APRIL-JUNE
2012

Volume 38
No. 2

ISSN 0126 - 5539

PP2509/07/2012(030291)



PERSATUAN GEOLOGI MALAYSIA
Geological Society of Malaysia

Council 2012/2013

<i>President :</i>	Prof. Dr. Joy Jacqueline Pereira
<i>Vice President :</i>	Dr. Mazlan Madon
<i>Secretary :</i>	Mr. Ling Nan Ley
<i>Assistant Secretary :</i>	Mr. Lim Choun Sian
<i>Treasurer :</i>	Mr. Ahmad Nizam Hasan
<i>Editor :</i>	Assoc. Prof. Dr. Ng Tham Fatt
<i>Immediate Past President :</i>	Dato' Yunus Abdul Razak
<i>Councillors :</i>	Dr. Gan Lay Chin Dr. Liaw Kim Kiat Dr. Meor Hakif Amir Hassan Mr. Nicholas Jacob Dr. Nur Iskandar Taib Mr. Robert Wong Mr. Tan Boon Kong Dr. Tanot Unjah

The Geological Society of Malaysia was founded in 1967 with the aim of promoting the advancement of geoscience, particularly in Malaysia and Southeast Asia. The Society has a membership of about 600 local and international geoscientists.

Warta Geologi (Newsletter of the Geological Society of Malaysia) is published quarterly by the Society. Warta Geologi covers short geological communications and original research, as well as reports on activities and news about the Society. It is distributed free-of-charge to members of the Society. Further information can be obtained from:

The Editor
Geological Society of Malaysia
c/o Department of Geology,
University of Malaya,
50603 Kuala Lumpur, Malaysia
Tel: 603-79577036 Fax: 603-79563900
Email: geologicalsociety@gmail.com

Warta Geologi

Newsletter of the Geological
Society of Malaysia

Editor-in-Chief

Ng Tham Fatt (University of Malaya)

Managing Editor

Ralph L. Kugler (University of Malaya)

Editorial Board

Prof. Dr. Abdul Rahim Samsudin
(Universiti Kebangsaan Malaysia)

Prof. Dr. Azman A. Ghani
(University of Malaya)

Prof. Dr. Basir Jasin
(Universiti Kebangsaan Malaysia)

Assoc. Prof. Dr. Chow Weng Sum
(Universiti Teknologi Petronas)

Prof. Dr. Felix Tongkul
(Universiti Malaysia Sabah)

Prof. Emeritus Dr. H.D. Tjia
(Universiti Kebangsaan Malaysia)

Prof. Dato' Dr. Ibrahim Komoo
(Universiti Kebangsaan Malaysia)

Prof. Dr. J.J. Pereira
(Universiti Kebangsaan Malaysia)

Prof. Dr. John K. Raj
(University of Malaya)

Prof. Dr. Lee Chai Peng
(University of Malaya)

Prof. Dr. Mohd Shafeea Leman
(Universiti Kebangsaan Malaysia)

Mr. Tan Boon Kong
(Consultant)

Prof. Dr. Teh Guan Hoe
(Consultant)

Prof. Dr. Wan Hasiah Abdullah
(University of Malaya)

Dato' Yunus Abdul Razak
(Minerals & Geoscience Department
Malaysia)

Secretariat

Anna Lim

CATATAN GEOLOGI GEOLOGICAL NOTES

Fosil moluska Trias Akhir dari kawasan Binjui, Kedah

(Late Triassic molluscan fossils from Binjui area, Kedah)

AHMAD ROSLI OTHMAN

Jabatan Mineral dan Geosains Malaysia, Wisma Persekutuan, 15200 Kota Bharu, Kelantan
Alamat emel: ahmadrosli@jmg.gov.my

Abstrak: Fosil ammonoid *Frankites apertus* (Mojsisovics), *Zestoceras birwicki* (Johnston), *Anolcites anguinus* Tozer dan *Hungarites?* sp. serta bivalvia *Halobia charlyana* Mojsisovics telah ditemui pada satu singkapan potongan jalan di kawasan Binjui berhampiran simpang Kejai-Binjui, Kedah. Fosil tersebut ditemui dalam lapisan syal dari Ahli Ridemit kepunyaan Formasi Semanggol yang berusia Perm Bawah hingga Trias Atas. Himpunan ammonoid ini mencirikan Subzon *canadensis* yang berusia Karnian Bawah (Trias Awal). Penemuan himpunan ammonoid ini dilaporkan buat pertama kalinya dalam Ahli Ridemit Formasi Semanggol dalam Zon Batuan Trias Barat, Semenanjung Malaysia.

Abstract: Fossils ammonoids *Frankites apertus* (Mojsisovics), *Zestoceras birwicki* (Johnston), *Anolcites anguinus* Tozer and *Hungarites?* sp. and the bivalve *Halobia charlyana* Mojsisovics have been discovered at a road-cut in the vicinity of Binjui near the Kejai-Binjui road junction, Kedah. These fossils were found in a shale bed belonging to the Rhythmite Member the Lower Permian to Upper Triassic Semanggol Formation. This ammonoid assemblage is characteristic of the Lower Carnian (Upper Triassic) *canadensis* Subzone. The discovery of this ammonoid assemblage is reported for the first time in the Rhythmite Member of the Semanggol Formation within the Western Triassic Rock Zone of Peninsular Malaysia.

Keywords: Ammonoid, Bivalve, Lower Carnian, Upper Triassic, Semanggol Formation

PENGENALAN

Formasi Semanggol telah diperkenalkan oleh Alexander (1959) untuk batuan sedimen yang tersingkap di kawasan Semanggol di utara Perak. Formasi ini mengunjur melepasi sempadan Thailand di mana ia boleh dikorelasikan dengan Kumpulan Lampang. Formasi ini dibahagikan kepada tiga ahli iaitu Ahli Rijang, Ahli Ridemit dan Ahli Konglomerat oleh Burton (1973). Ahli Rijang yang didominasi oleh turutan batuan rijang mempunyai fosil radiolaria yang berusia Perm hingga Trias (Basir Jasin, 1997; Basir Jasin & Zaiton Harun, 2007; Sashida *et al.*, 1995). Ahli Ridemit pula mempunyai fosil *Daonella*, *Halobia* dan *Posidonia* (= *Peribositra*) serta ammonoid yang berusia Trias Tengah hingga Trias Akhir (Kobayashi *et al.*, 1966).

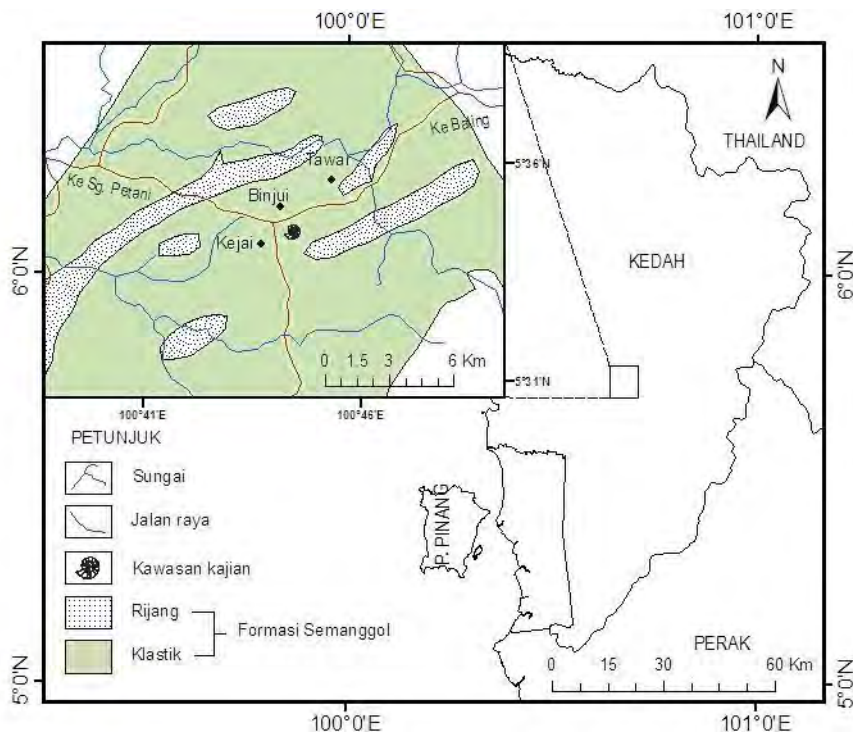
Singkapan batuan Ahli Ridemit yang mempunyai fosil moluska bivalvia dan ammonoid telah ditemui di kawasan Binjui, Kuala Ketil dalam Daerah Baling, Kedah (Rajah 1). Kajian ini mendokumentasikan penemuan tersebut merangkumi pemerihalhan fosil, kajian biostratigrafi, korelasi dan penentuan usia fosil. Fosil ammonoid dalam kajian ini adalah pertama kali dilaporkan dalam Ahli Ridemit Formasi Semanggol dan dalam Zon Batuan Trias Barat umumnya.

KERANGKA GEOLOGI

Kawasan kajian terletak dalam terain Sibumasu dalam Jaluran Barat (Melcafe, 2000) dan berada dalam Zon Batuan Trias Barat (Rajah 2) yang dicirikan oleh kebersekutuan bivalvia *Daonella*, *Halobia* dan *Peribositra* dalam lapisan syal (Kobayashi, 1963 & Kobayashi *et al.*, 1966).

Kawasan kajian berada dalam Formasi Semanggol yang berjulat usia dari Perm Awal hingga Trias (Basir Jasin & Zaiton Harun, 2007). Formasi ini mempunyai tiga unit batuan yang ditafsirkan bersentuhan secara lateral dan berjejari antara satu sama lain iaitu Ahli Ridemit, Ahli Konglomerat dan Ahli Rijang (Ahmad Jantan *et al.*, 1989; Basir Jasin *et al.*, 1989). Ahli Ridemit Formasi Semanggol ditafsirkan terenap di kawasan hujung kipas samudera dalam (Ahmad Jantan *et al.*, 1989) dan tersingkap dengan meluas di kawasan Gunung Semanggol di utara Perak serta di bahagian selatan dan utara Kedah. Di kawasan Baling, singkapan Ahli Ridemit boleh dilihat di sepanjang jalanraya yang menghubungkan Bandar Baling dan Bandar Sg. Petani.

Litologi Ahli Ridemit terdiri daripada saling lapis batu pasir dan syal atau batu lumpur dengan sedikit perlapisan atau kekanta konglomerat. Litologinya adalah menyerupai

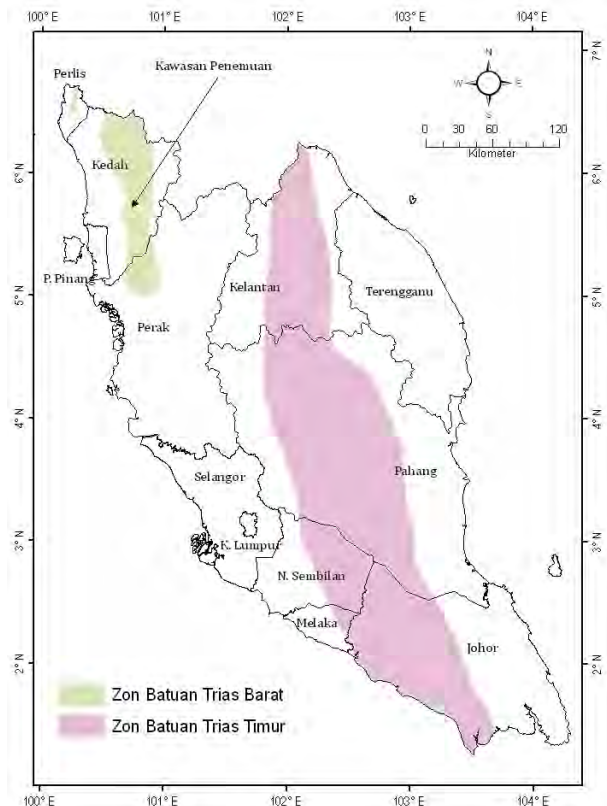


Rajah 1: Peta menunjukkan lokasi fosil dan geologi kawasan kajian.

batuan klastik dalam Ahli Rijang. Batu pasirnya adalah berkomposisi greiwak litik yang mempamerkan perlapisan silang, lapisan tergedred dan terlamniasi manakala syalnya berwarna kelabu cerah hingga kelabu gelap. Syal ini mengandungi banyak fosil bivalvia berusia Trias Tengah hingga Trias Akhir (Kobayashi *et al.*, 1966). *Halobia* dan terutamanya *Peribositra* paling biasa ditemui dalam Ahli Ridemit dan Ahli Konglomerat (Kobayashi & Tamura, 1984).

Menurut Kobayashi dan Tamura (1984), fosil bivalvia dalam Ahli Ridemit lazimnya ditemui pada satah-satah perlapisan syal di mana cengkerangnya terawet dengan baik serta tidak mengalami canggaaan. Fauna bivalvia dalam Ahli Ridemit didapati bersifat pelagik dan bercengkerang nipis yang didominasi oleh spesies-spesies dari genus *Daonella*, *Halobia* dan *Posidonia* termasuklah *Daonella burtoni*, *D. cf. kotoi*, *D. pectinoides*, *D. indica*, *D. multilineata*, *D. posidoniformis*, *D. procteri*, *D. sumatrensis*, *Halobia aotii*, *H. cf. austriaca*, *H. cf. styiaca*, *H. cf. mollukana*, *H. charlyana*, *H. comata*, *H. aotii*, *H. paralella*, *H. subquadrata*, *H. talauna*, *Peribositra cf. cycoidalis*, *B. cf. idriana*, *B. cf. japonica*, *B. kedahensis* dan *B. tawarensis*.

Menurut Kobayashi *et al.* (1966), kehadiran *Posidonia kedahensis*, *Halobia comata* dan *Halobia aotii* menunjukkan bahawa usia syal ini berjulat dari Karnian Awal hingga Norian Awal. Namun begitu penetapan julat usia berdasarkan bivalvia tersebut terlalu umum dan perlu disokong oleh kehadiran fosil-fosil lain khasnya fosil ammonoid. Fosil ammonoid memainkan peranan yang penting dalam membina biostratigrafi dan biokronologi Trias relatif terhadap usia geologi (Tozer, 1971;1994; Mietto & Manfrin, 1995; Lucas, 2010).



Rajah 2: Peta menunjukkan kedudukan kawasan kajian yang terletak dalam Zon Batuan Trias Barat. Diubahsuai dari Kobayashi *et al.* (1964).

SINGKAPAN BATUAN

Lokaliti fosil yang dikaji adalah berkedudukan pada longitud 5°34.778' U dan latitud 100°44.224' T. Fosil moluska ditemui pada jujukan batuan berketebalan lima meter yang tersingkap pada satu cerun potongan jalan raya (Rajah 3) yang menghubungkan Bandar Baling dan Sg. Petani berhampiran simpang Kejai-Binjui.

Terdapat tiga fasies batuan yang dicerap pada singkapan ini iaitu fasies batu pasir masif, batu pasir berlapis silang dan selang lapis antara syal kelabu dengan syal kelabu gelap yang miring 30° ke arah tenggara. Fosil boleh ditemui dalam lapisan syal yang berkedudukan di bahagian bawah jujukan batuan seperti yang ditunjukkan dalam Rajah 3 dan pada turus litologi dalam Rajah 4.

KOMPOSISI FOSIL

Kesemua fosil ditemui pada satu satah perlapisan syal yang kebanyakannya dalam bentuk serpihan. Fosil-fosil didapati masih terawet dengan baik dan dapat dikenalpasti walaupun lapisan syal telah mengalami luluhawa yang teruk. Sebanyak empat taksa ammonoid telah dikenalpasti iaitu *Frankites apertus* (Mojsisovics), *Zestoceras birwicki* (Johnston), *Anolcites anguinus* Tozer dan *Hungarites?* sp. Fosil bivalvia yang lazim kedapatan pada usia Karnian (Trias Akhir) turut ditemui bersama fosil ammonoid tersebut yang diwakili oleh spesies *Halobia charlyana* Mojsisovics sahaja.

BIOSTRATIGRAFI DAN USIA

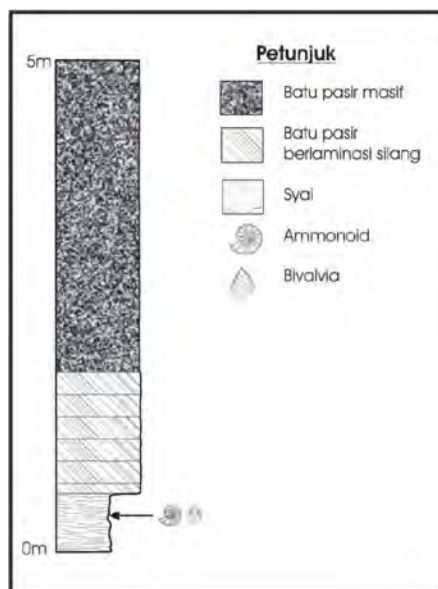
Himpunan ammonoid yang ditemui tidak menunjukkan kehadiran fosil indeks, namun begitu spesies *Frankites apertus* (Mojsisovics), *Anolcites* sp. dan *Zestoceras birwicki* (Johnston) merupakan spesies lazim bagi kedua-dua Zon *regoledanus* dari Zon *Protrachyceras* dan Subzon *canadensis* dari Zon *Trachyceras* (Mietto & Manfrin, 1995). Subzon *regoledanus* merupakan batas terakhir bagi usia Ladinian (Trias Tengah) manakala Subzon *canadensis* pula menjadi batas awal bagi usia Karnian (Trias Awal) seperti yang ditunjukkan dalam Rajah 5.

Batas antara kedua-dua subzon ini tidak dapat ditentukan di lapangan kerana fosil indeks atau fosil penanda zon tidak ditemui pada singkapan batuan tersebut. Walau bagaimanapun, himpunan fosil tersebut didapati mempunyai satu spesies *Halobia* yang lazim kedapatan pada usia Karnian, Trias Atas (Kobayashi & Tokuyama, 1959; Kobayashi *et al.*, 1966; McRobert, 2010). Oleh itu ditafsirkan bahawa usia lapisan sedimen dan fosil-fosil di kawasan kajian adalah pada subtahap Julian, Karnian (Trias Akhir).

Himpunan ammonoid ini boleh dikorelasikan dengan himpunan ammonoid di QZ467 dalam Formasi Telong, Kelantan yang terletak dalam Zon Batuan Trias Timur. Taksa *Frankites apertus* (Mojsisovics) dan *Zestoceras birwicki* (Johnston) turut ditemui di Lokaliti QZ467 bersama fosil indeks iaitu *Frankites regoledanus*



Rajah 3: Foto menunjukkan singkapan batuan Ahli Ridemit Formasi Semanggol di kawasan kajian yang mempunyai fosil moluska Trias.



Rajah 4: Turus litologi dan kedudukan lapisan fosil.

Tahap	Subtahap	Skala Piawai Ammonoid				
		Zon	Rantau Tethys	Zon	Rantau Amerika Utara	Rantau Boreal
KARNIAN	Julian	Trachyceras	Aonoides	Trachyceras	Aonoides	Seimkanites aculeatus
			Aon		Desatoyensis	"Protrachyceras" omkutchanicum
			Canadensis			Stolleyites tenuis
LADINIAN	Longorbardian	Protrachyceras	Regoledanus	F. sutherlandi	Askleopioceras laurenci	Nathorstites lindstroemi
					Frankites glaber	Nathorstites macconnelli

Rajah 5: Skala piawai ammonoid yang menunjukkan kedudukan zon ammonoid dan korelasi biostratigrafi Ladinian-Karnian bagi tiga rantau paleogeografi utama. Diubahsuai dari Tozer (1994), Mietto dan Manfrin (1995) dan Konstantinov (2008).

(Mojsisovics) dan *Daxatina canadensis* (Whiteaves), masing-masing tergolong dalam Subzon *regoledanus* dan Subzon *canadensis* (Ahmad Rosli Othman & Mohd. Shafeea Leman, 2010). Rajah 5 juga menjelaskan korelasi biostratigrafi ammonoid Ladinian (Trias Tengah) – Karnian (Trias Atas) di Rantau Tethys, Amerika Utara dan Boreal.

PEMERIHAN FOSIL

Spesimen ammonoid dari kawasan kajian ini dijumpai dalam bentuk acuan luar atau bentuk kas di mana kesemuanya tidak mempamerkan garis sutura. Kesemua spesimen dilabelkan dengan awalan KDH-BJ diikuti nombor spesimen dan disimpan di Jabatan Mineral dan Geosains Kelantan. Perbandingan spesimen adalah berdasarkan perbandingan dengan monograf-monograf dari rujukan yang telah dinyatakan sumbernya. Tatanama bagi spesies sinonim untuk tujuan perbandingan adalah seperti berikut: . → rujukan spesies yang sinonim dan diterima; ? → rujukan spesies yang diragui; non → rujukan spesies yang sebenarnya bukan seperti yang diperihalkan; p → rujukan spesies yang hanya sebahagiannya sinonim; tiada tanda → rujukan spesies tidak dapat dipastikan kesahihan tetapi tidak meragukan.

Ammonoid

Superfamili CERATITACEAE Mojsisovics

Subfamili BEYRICHITINAE (Spath)

Famili HUNGARITIDAE Waagen

Genus *Hungarites* Mojsisovics

Hungarites? sp.

Rajah 6a-b

Bahan:- Satu spesimen diperiksa iaitu KDH-BJ01 seperti yang ditunjukkan dalam Rajah 6a-b. Rajah 6a berbentuk kas manakala Rajah 6b berbentuk acuan luar tanpa umbilikus.

Perihal:- Cengkerang berlingkaran involut yang menebal di bahagian ventral dan menipis di bahagian umbilikus atau berbentuk sphaerokon. Umbilikus kecil, dalam dan sempit dengan nisbah diameter cengkerang dan umbilikus 1:5. Perhiasan cengkerang mempamerkan rib agak tebal, muncul dari pinggir umbilikus dan menghilang di bahagian lateral yang bersifat 'prosradiate'. Bahagian lateroventral dan garis sutura tidak dapat dicerap pada spesimen yang diperiksa.

Catatan:- Pengenalpastian bagi spesimen adalah sukar memandangkan hanya sebahagian cengkerang diperolehi. Spesimen ini mempunyai morfologi yang sama dengan *Hungarites* seperti yang diperihalkan oleh Arkell *et al.* (1957) dan Tozer (1994) dari segi perhiasan cengkerang dan bentuk sphaerokonya.

Superfamili CLYDONITACEAE Hyatt

Famili TRACHYCERATIDAE Haug

Subfamili ANOLCITINAE Mietto & Manfrin

Genus *Anolcites* Mojsisovics

Anolcites anguinus Tozer

Rajah 6c-e

* 1994 *Anolcites anguinus* Tozer – Tozer: Plat 80, gambarajah 7,8 dan 9.

Bahan:- Tiga spesimen diperiksa iaitu KDH-BJ02 (Rajah 6c), KDH-BJ03 (Rajah 6d) dan KDH-BJ04 (Rajah 6e). KDH-BJ02 adalah bentuk kas lengkap dengan umbilikus, KDH-BJ03 mempamerkan acuan luaran di bahagian fragmokon dan bentuk kas di bahagian umbilikus. Spesimen KDH-BJ04 pula adalah bentuk kas yang mempamerkan sebahagian fragmokon dan umbilikus.

Perihal:- Cengkerang berlingkaran agak evolut, umbilikus sederhana kecil dengan nisbah diameter cengkerang dan umbilikus 1:1.5. Rib tebal, ringkas, bersifat 'rectiradiate', semakin melebar dan mempunyai benjolan atau 'tubercles' di bahagian ventrolateral. Ketak rib yang agak sempit dengan nisbah lebar rib dan ketak rib 3:1. Spesimen tidak menunjukkan bahagian ventrolateral dan garis sutura.

Catatan:- Spesimen ini telah dibandingkan dengan spesimen dari British Columbia, Kanada yang diperihalkan oleh Tozer (1994, ms.509). Morfologi perhiasan cengkerang bagi ketiga-tiga spesimen di kawasan kajian didapati menyerupai spesimen yang diperihalkan oleh Tozer (1994) terutama di bahagian umbilikus. *Anolcites anguinus* Tozer dari British Columbia ditemui dalam Formasi Toad dan Formasi Sulphur Mountain berusia Ladinian, Trias Tengah (Tozer, 1994). Spesies ini adalah pertama kali dilaporkan dalam strata batuan Trias di Malaysia.

Genus *Zestoceras* Tozer, 1994

Zestoceras barwicki (Johnston)

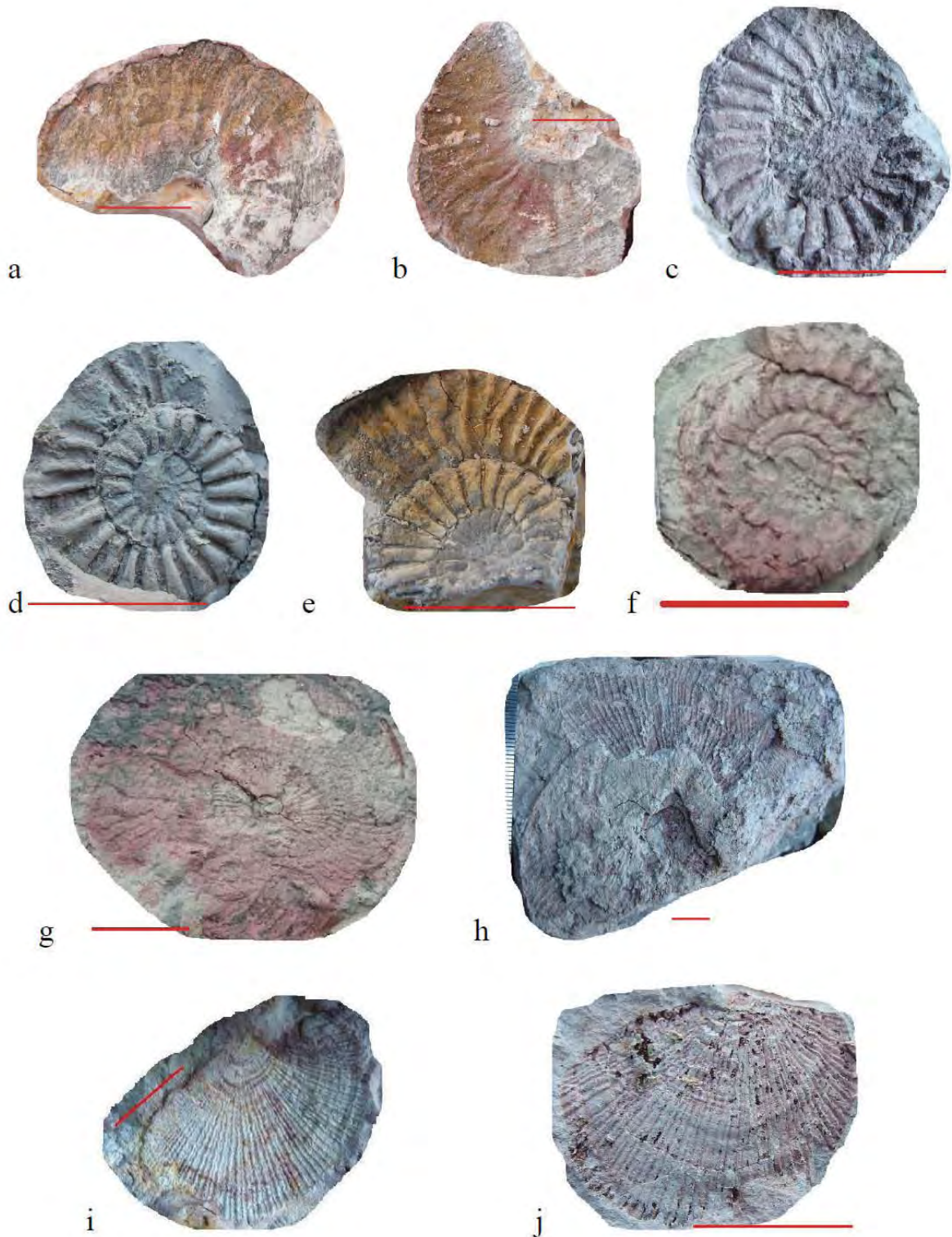
Rajah 6f

. 2008 *Zestoceras barwicki* (Johnston) - Mietto *et al.*: Plat 1, gambarajah 12, ? Plat 2, gambarajah 3-9.
non 2010 *Celtites epolensis* Mojsisovics – Ahmad Rosli Othman & Mohd Shafeea Leman: Rajah 8.

Bahan:- Satu spesimen diperiksa iaitu KDH-BJ05 (Rajah 6f) yang bentuk kas lengkap dengan umbilikus.

Perihal:- Cengkerang berlingkaran evolut, umbilikus lebar separas dengan lingkaran, bilangan rib banyak dan kasar serta kelihatan terlunjur keluar pada bahagian ventrolateral iaitu bersifat 'prosradiate'. Nisbah diameter cengkerang dan umbilikus adalah 1:1.5, manakala nisbah lebar rib dan ketak rib juga adalah 1:1.5. Ketak rib adalah lebar dan hampir sama lebar dengan rib.

Catatan:- Spesies ini sinonim dengan spesies yang ditemui oleh Ahmad Rosli Othman dan Mohd Shafeea Leman (2010) di Lokaliti QZ467, Aring (Kelantan) dalam Formasi Telong. Perhiasan cengkerang spesimen ini menyerupai *Celtites* sp. seperti yang diperihalkan oleh Manfrin *et al.* (2005) dari Latemar, Dolomites (Itali)



Rajah 6: Lima fosil moluska berusia Ladinian Akhir, Trias Tengah yang ditemui di kawasan Binjui, Kedah dalam Ahli Ridemit Formasi Semanggol. Skala bar merah mewakili 1cm. a-b: *Hungarites?* sp.; c-e: *Anolcites anguinus* Tozer; f: *Zestoceras birwicki* (Johnston); g-h: *Frankites apertus* (Mojsisovics); i-j: *Halobia charlyana* Mojsisovics. Skala bar merah mewakili 1cm.

tetapi spesies tersebut kurang evolut berbanding spesimen KDH-BJ05 dan mempunyai rib yang tidak lebar dengan ketak rib yang lebih lebar. *Zestoceras barwicki* (Johnston) dilaporkan wujud di Southern Alps (Itali), Nevada (Amerika Syarikat), British Columbia (Kanada) dan Romania (Mietto *et al.*, 2008). Spesies ini juga direkodkan dari Thailand dalam Zon *Paratrachyceras* dalam strata batuan berusia Karnian Bawah (Chonglakmani, 1983). Spesies ini mencirikan Subzon *canadensis* yang boleh dikorelasikan dengan Subzon 2 *sutherlandi* di Kanada dan Zon *desatoyense* di Nevada.

Genus *Frankites* Tozer (1971)
Frankites apertus (Mojsisovics)
 Rajah 6g-h

- v p 1964 *Trachyceras* (*Paratrachyceras*) cf. *T. (P.) regoledanus* (Mojsisovics) – Sato: Plat 4, gambarajah 2-3, 5-7, [= *Frankites apertus* (Mojsisovics)], non gambarajah 12 [= *Sirenotrachyceras thusneldea* Mojsisovics].
- p 1994 *Frankites sutherlandi* (McLearn) – Tozer: Plat 82, gambarajah 10; Plat 83, gambarajah 8-12, non gambarajah 8 dan gambarajah 9 (= *Frankites* sp. A).
- . 2008 *Frankites apertus* (Mojsisovics) – Mietto *et al.*: Plat 9d, Plat 1, gambarajah 8; Plat 4, gambarajah 5 dan 6; Plat 5, gambarajah 7-17.
- p 2010 *Frankites regoledanus* (Mojsisovics) – Ahmad Rosli Othman & Mohd Shafeea Leman: Rajah 2(1), Rajah 2(2)[= *Frankites apertus* (Mojsisovics)].

Bahan:- Dua spesimen diperiksa iaitu KDH-BJ06 (Rajah 6g) dan KDH-BJ07 (Rajah 6h). KDH-BJ06 berbentuk acuan luar yang lengkap dengan umbilikus manakala KDH-BJ07 pula berbentuk kas yang mempamerkan sebahagian fragmokon tanpa umbilikus.

Perihal:- Cengkerang berlingkaran secara involut dengan rib dari jenis ‘prorsiradiate’, padat dan berbentuk sigmoid. Rib-rib bercabang dua atau ‘bifurcation’ lebih dominan berbanding rib-rib tunggal di mana titik percabangan bermula pada satu pertiga dari bahu umbilikus. Umbilikus kecil dan sedikit tenggelam. Nisbah diameter cengkerang dan umbilikus adalah 10:1, manakala nisbah lebar rib dan ketak rib adalah kira-kira 1:1.5.

Catatan:- Spesimen ini dirujuk sebagai *Frankites apertus* (Mojsisovics) berdasarkan ciri-ciri ribnya yang padat dan berbentuk sigmoid. Perhiasan cengkerang *Frankites apertus* (Mojsisovics) dan *Frankites regoledanus* (Mojsisovics) hampir sama tetapi berbeza dari segi bentuk rib, bentuk ventral dan kedudukan titik percabangan. *Frankites regoledanus* (Mojsisovics) mempunyai rib berbentuk falkoid, mempunyai nod di hujung rib di bahagian ventral dan mempunyai titik percabangan ‘bifurcation’ hanya pada bahu umbilikus. Spesies ini sinonim dengan spesies yang ditemui oleh Ahmad Rosli Othman dan Mohd Shafeea Leman (2010) di Lokality QZ467 dalam Formasi Telong di Aring, Kelantan. Spesis

Frankites apertus (Mojsisovics) yang ditemui di Malaysia selalunya bersaiz besar seperti spesimen KDH-BJ06, KDH-BJ07 dan beberapa spesimen dari Aring, Kelantan yang dianggarkan boleh mencapai diameter sehingga 8cm. Keadaan ini menunjukkan bahawa spesies tersebut telah mencapai peringkat kematangan ontogenetik seperti yang dinyatakan oleh Mietto *et al.* (2008). Spesies ini juga mungkin tidak menunjukkan variasi intraspesifik dan mempamerkan morfologi yang tetap. Spesies induk atau spesies penanda zon iaitu *Frankites regoledanus* (Mojsisovics) tidak ditemui di kawasan kajian tetapi telah dilaporkan penemuannya di kawasan Aring, Kelantan (Ahmad Rosli Othman & Mohd. Shafeea Leman, 2010). Kesemua spesimen yang dirujuk sebagai *Trachyceras* (*Paratrachyceras*) cf. *T. (P.) regoledanus* (Mojsisovics) oleh Sato (1964) dari Yong Peng (Johor) telah dikajisemula dan dikenalpasti sebagai spesis *Frankites apertus* (Mojsisovics).

Dahulunya genus ini lebih dikenali sebagai *Paratrachyceras* yang diperihalkan oleh Mojsisovics tetapi Tozer (1971) telah menamakan semula genus ini kepada *Frankites*. Spesies *Frankites apertus* (Mojsisovics) adalah sinonim dengan *Frankites sutherlandi* (McLearn) dari rantau Amerika Utara yang hanya terdapat dalam Subzon *laurenci* (=Subzon 2) dari Zon *sutherlandi* (Mietto *et al.*, 2008; Tozer, 1994). *Frankites apertus* (Mojsisovics) didapati wujud melangkaui batas Ladinian-Karnian iaitu pada bahagian teratas Subzon *regoledanus* hingga bahagian terbawah Subzon *canadensis* (Mietto & Manfrin 1995; Mietto *et al.*, 2008). Spesies ini juga telah didokumentasikan dari Austria, Hungary, Itali, Himalaya, Greece, Turkey, Thailand dan Jepun (Mietto & Manfrin, 1995; Manfrin *et al.*, 2008).

Bivalvia

Superfamili POSIDONIOACEA Waller & Stanly
 Famili HALOBIIDAE McRobert (2010)

Genus *Halobia* Bronn
Halobia charlyana Mojsisovics
 Rajah 6i-j

- . 1963 *Halobia charlyana* Mojsisovics – Kobayashi: Plat 5, gambarajah 20.

Bahan:- Dua spesimen diperiksa iaitu KDH-BJ08 dan KDH-BJ09, kedua-duanya adalah berbentuk kas bagi cengkerang kanan.

Perihal:- Kerangka cengkerang adalah bersaiz kecil, berkerangka ‘oval’, ukuran kelebaran melebihi ketinggian dengan nisbah 1:1.5, agak *inequilateral* dan sedikit cembung. Garis engsel tidak lurus dan sedikit melengkung. Umbo terletak hampir satu perdua dari sempadan hujung anterior engsel. Cengkerang dihiasi oleh bilangan rib berjejari yang banyak dan garis pertumbuhan terpusat yang jelas terutama pada bahagian berhampiran umbo pada kedudukan satu pertiga melingkari umbo. Garis rib agak lebar berbanding ketak rib dengan nisbah 1:1.5,

sedikit berkedut dan bercabang dua.

Catatan:- Spesimen ini sinonim dengan spesimen dari kawasan Nami, Sik (Kedah) terutama dengan kehadiran rib bercabang dua. *Halobia charlyana* Mojsisovics dilaporkan wujud dalam strata batuan berusia Karnian (Trias Atas) di kawasan utara Alps, Greece dan Timor (Kobayashi, 1963). Spesies-spesies *Halobia* berkelimpahan semasa usia Karnian, Trias Atas dan juga merupakan leluhur kepada spesies *Daonella* (Kobayashi & Tokuyama, 1959; Kobayashi *et al.*, 1966; McRobert, 2010). Spesies-spesies *Halobia* juga banyak ditemui dari beberapa lokaliti di utara Kedah antaranya termasuklah *Halobia talauana* Wanner, *Halobia parallela* Kobayashi, *Halobia comata* Bittner, *Halobia styriaca* Mojsisovics, *Halobia subquadrata* Kobayashi dan *Halobia aotii* Kobayashi & Ichikawa (Kobayashi, 1964; Kobayashi *et al.*, 1966; Kobayashi & Tamura, 1984).

PERBINCANGAN DAN RUMUSAN

Ahli Ridemit Formasi Semanggol telah tersingkap pada satu cerun potongan di kawasan Binjui yang terdiri dari batu pasir dan syal. Singkapan batuan tersebut mengandungi fosil moluska ammonoid *Frankites apertus* (Mojsisovics), *Zestoceras birwicki* (Johnston), *Anolcites anguinus* Tozer dan *Hungarites?* sp. serta bivalvia *Halobia charlyana* Mojsisovics. Penemuan ammonoid ini adalah pertama kali dilaporkan dalam Ahli Ridemit Formasi Semanggol.

Himpunan ammonoid dan bivalvia ini mencirikan Subzon *canadensis* berusia Karnian, Trias Atas berdasarkan kehadiran bivalvia *Halobia*. Himpunan ammonoid ini boleh dikorelasi dengan himpunan ammonoid Subzon *canadensis* dari Lokaliti QZ467, Aring (Ahmad Rosli Othman & Mohd. Shafeea Leman, 2010) dan Yong Peng, Johor berdasarkan kehadiran beberapa spesies ammonoid yang sama. Spesies *Anolcites anguinus* Tozer dan *Zestoceras birwicki* (Johnston) yang ditemui dari British Columbia, Kanada dalam rantau Amerika Utara turut ditemui di kawasan kajian. Penemuan ini menambahkan lagi maklumat paleontologi bagi Formasi Semanggol khususnya dan dalam Zon Batuan Trias Barat umumnya.

PENGHARGAAN

Sekalung penghargaan diucapkan kepada Pengarah JMG Kelantan, Hj. Mohd. Badarudin Hasan dan ahli pasukan petugas pemetaan geologi sempadan Malaysia-Thailand khususnya kepada Hj. Ibrahim Amnan dan Dr. Asanee Meesok. Terima kasih juga diucapkan kepada En. Mat Niza Abdul Rahman atas sumbangan gambarfoto serta kepada Dr. Paolo Mietto dari Universiti Padova, Itali atas pengesahan dan pengenalpastian spesies-spesies fosil ammonoid dalam kajian ini.

RUJUKAN

- Ahmad Jantan, Basir Jasin, Ibrahim Abdullah, Uyop Said & Abdul Rahim Samsudin, 1989. The Semanggol Formation-lithology, facies association and distribution, and probable basin setting. Geological Society of Malaysia Warta Geologi 15(1), 28.
- Ahmad Rosli Othman & Mohd Shafeea Leman, 2010. Middle Triassic ammonoid fossils from Aring, Kelantan, Malaysia. Geological Society of Malaysia, Bull., 56, 53-59. (in Malay with English abstract).
- Alexander, J.B., 1959. Pre-Tertiary stratigraphic succession in Malaya. Nature, 183, 230-231.
- Arkell, W.J., Kummel, B. & Wright, C.W. 1957. Mesozoic Ammonoidea. In: Moore, R.C., (Ed.), Treatise on Invertebrate Paleontology. Part L Mollusca 4, Cephalopoda, Ammonoidea. Geological Society of America, New York and University of Kansas, Lawrence. 490 p.
- Basir Jasin, 1997. Permo-Triassic Radiolarians from Semanggol Formation, NW Peninsular Malaysia. Journal of Asian Earth Science, 15, 43-53.
- Basir Jasin, 2008. Some Permian Radiolarians from Bukit Yoi, Pokok Sena, Kedah. Geological Society of Malaysia, Bull., 54, 53-58.
- Basir Jasin, Ahmad Jantan, Ibrahim Abdullah, Uyop Said & Abdul Rahim Samsudin, 1989. The Semanggol Formation-Lithostratigraphy of the Semanggol rocks in the light of latest concept in stratigraphic practice: a suggestion. Geological Society of Malaysia Warta Geologi 15, 29.
- Basir Jasin & Zaiton Harun, 2007. Stratigraphy and sedimentology of the chert unit of the Semanggol Formation. Geological Society of Malaysia, Bull., 53, 103-109.
- Burton, C.K., 1973. Mesozoic. In: Gobbett, D.J. and Hutchison, C.S. (Eds.), Geology of the Malay Peninsular, Wiley-Interscience, New York, 97-141.
- Chonglakmani, C. 1983. The marine Mesozoic stratigraphic of Thailand. Proceeding of Workshop on Stratigraphic Correlation of Thailand and Malaysia. Vol. 1 Technical papers, Geological Society of Malaysia & Geological Society of Thailand, 105-126.
- Kobayashi, T., 1963. *Halobia* and some other fossils from Kedah, Northwest Malaya. In: Kobayashi, T., (Ed.), Geology and Palaeontology of Southeast Asia Vol. 1, 53-67.
- Kobayashi, T., 1964. On the Triassic *Daonella* Beds in Central Pahang, Malaya. In: Kobayashi, T., (Ed.), Geology and Palaeontology of Malaya Vol.1, 53-67.
- Kobayashi, T. & Tokuyama, A., 1959. The Halobiidae from Thailand. Journal of the Faculty of Science, University of Tokyo, Vol. 12, 1-30.
- Kobayashi, T., Burton, C.K., Tokuyama, A. & Yin, E.H., 1966. The *Daonella* and *Halobia* Facies of the Thai-Malay Peninsula compare with those of Japan. In: Kobayashi, T. and Toriyama, R., (Eds.), Geology and Palaeontology of Southeast Asia Vol. 3, 98-122.
- Kobayashi, T. & Tamura, M. 1984. The Triassic bivalves of Malaysia, Thailand and adjacent areas. In: Kobayashi, T. and Toriyama, R. (Eds.), Geology and Palaeontology of Southeast Asia Vol. 25, 201-225.
- Konstantinov, A. G., 2008. Debatable questions of Boreal Triassic stratigraphy: boundary between middle and upper series. Russian Geology and Geophysics 49, 64-71.
- Lucas, S.G., 2010. The Triassic timescale: an introduction. In: Lucas, S.G., (Ed.), The Triassic Timescale. Geological Society, Special Publications 334, 1-16.
- Manfrin, S., Mietto, P. & Preto, N., 2005. Ammonoid

- biostratigraphy of the Middle Triassic Latemar platform (Dolomites, Italy) and its correlation with Nevada and Canada. *Geobios* 38, 477-504.
- McRobert, C.A., 2010. Biochronology of Triassic bivalves. In: Lucas, S.G., (Ed.), *The Triassic Timescale*. Geological Society, Special Publications 334, 201-219.
- Metcalf, I., 2000. The Bentong-Raub Suture Zone. *Journal of Asian Earth Science* 18, 691-712.
- Mietto, P. & Manfrin, S., 1995. A high resolution Middle Triassic ammonoid standard scale in the Tethys Realm. A preliminary report. *Bull. Soc. Geol. France* 166 (5), 539-563.
- Mietto, P., Manfrin, S., Preto, N. & Gianolla, P. 2008. Selected ammonoid fauna from Prati Di Stuores/Stuores Wiesen and related sections across the Ladinian-Carnian Boundary (Southern Alps, Italy). *Rivista Italiana di Paleontologia e Stratigrafia* 8, 377-429.
- Sashida, K. Adachi, S., Igo, H., Koike, T. & Ibrahim Amnan, 1995. Middle and Late Permian radiolarians from the Semanggol Formation, Northwest Peninsular Malaysia. *Transection and Proceeding of the Palaeontology Society of Japan, New Series*, 177, 43-58.
- Sato, T., 1964. Ammonites du Trias de la Malaisie. In: Kobayashi, T., (Ed.), *Geology and Palaeontology of Southeast Asia Vol. 2*, 43-53.
- Tozer, E.T., 1971. Triassic time and ammonoids: problems and proposals. *Canadian Journal Earth Sciences*, 8, 989-1031.
- Tozer, E.T., 1994. Canadian Triassic ammonoid faunas. *Geology Survey of Canada, Bulletin* 467, 663p.

Manuscript received 4 July 2011
Revised manuscript received 20 February 2012

PERSATUAN GEOLOGI MALAYSIA GEOLOGICAL SOCIETY OF MALAYSIA



46th ANNUAL GENERAL MEETING & ANNUAL REPORT 2011

13th April 2012

Eastin Hotel, Petaling Jaya, Selangor



**PERSATUAN GEOLOGI MALAYSIA
GEOLOGICAL SOCIETY OF MALAYSIA (GSM)
MINUTES OF THE 45th ANNUAL GENERAL MEETING (AGM)**

Date : 15th April 2011
Time : 5.50pm
Venue : Eastin Hotel, Petaling Jaya, Selangor

Members Present

- | | |
|----------------------|----------------------------|
| 1. Ling Nan Ley | 2. Tan Boon Kong |
| 3. Askury Abd Kadir | 4. Yunus Abd Razak |
| 5. Anil Nair | 6. Joy Jacqueline Pereira |
| 7. Ng Tham Fatt | 8. Zuhar Zahir Tuan Harith |
| 9. C. S. Hutchison | 10. Ahmad Nizam Hasan |
| 11. Mazlan Madon | 12. Lee Chai Peng |
| 13. Jens Krieter | 14. Manfred Krieter |
| 15. Lim Choun Sian | 16. Tanot Unjah |
| 17. Samsudin Hj Taib | 18. Iskandar Taib |
| 19. Yip Foo Weng | 20. Ibrahim Amnan |
| 21. Leong Khee Meng | |

The President of Geological Society of Malaysia and Chairperson of the AGM, Joy Jacqueline Pereira, called the meeting to order at 5.50 pm. The President welcomed members to the AGM and thanked them for supporting GSM activities.

1. Adoption of Agenda

The Chairperson tabled the following agenda to the AGM for acceptance:

1. Welcoming Address by the President for Session 2010/2011
2. Confirmation of Minutes of the 44th AGM held on the 23rd April 2010
3. Matters arising
4. Annual Report for Session 2010/2011
 - President's Report
 - Secretary's Report
 - Editor's Report
 - Treasurer's and Honorary Auditor's Reports
5. Election of Honorary Auditor
6. Other Matters of which written notice is submitted to reach GSM Secretariat by the 8th April 2011 or by majority vote of the AGM
7. Announcement of New Council for 2011/2012
8. Presidential Address

The agenda was unanimously accepted.

2. Confirmation of Minutes of the Previous AGM

The Minutes of the 44th AGM was tabled for confirmation. As there was no amendment raised, Anil Nair proposed that the minutes be confirmed and this was seconded by Askury Abd Kadir.

3. Matters Arising

There were no matters arising from the previous AGM.

4.0 Annual Reports 2010/2011

4.1 President's Report

The President tabled the President's Report (Appendix 1). The AGM discussed the following matters:

- a. Yunus Abd Razak congratulated the President for coming up with such a forward looking report. He especially welcomed the idea of encouraging enhanced collaboration between the universities that provide geology, earth science and geophysics knowledge. The AGM agreed that GSM would initiate the collaboration and communicate with the Minerals and Geoscience Department, Institute of Geology Malaysia and the Board of Geologists on this matter. The in-coming Council would look into the details of the proposed collaboration.
- b. Askury Abd Kadir inquired who should rightfully audit the quality of the graduates. The AGM was of the view that it should be under the purview of the Board of Geologists.
- c. Mazlan Madon informed the AGM that the PETRONAS had organized a Geoscience Colloquium in Miri in 2007. The Colloquium had subsequently recommended an inter-institutional board to be set up to facilitate collaboration efforts. He further commented that the collaboration should not only be limited to between the universities but should also include the related government agencies. Zuhar Zahir Tuan Harith remarked that perhaps there is a need to organize the 2nd Colloquium.
The AGM was of the opinion that GSM, with the support from the Minerals and Geoscience Department, Institute of Geology Malaysia and the Board of Geologists, can facilitate this by providing a platform for stakeholders to come together and discuss the matter.
- d. Tan Boon Kong noted that the present 3-year geology course is not sufficiently long enough to adequately equip geology graduates and hence the course should revert back 4 years.
The AGM agreed that GSM should initiate the call to revert geology courses back to a 4-year programme.

Action: Incoming Council

Yunus Abd Razak proposed that the President's Report be accepted and this was seconded by Mazlan Madon.

4.2 Secretary's Report

The Secretary tabled the Secretary's Report (Appendix 2). The AGM discussed the following matters:

- a. Askury Abd Kadir & Zuhar Zahir Tuan Harith queried why students from UTP were not considered for the PGCE Student Excellence Awards.
Mazlan Madon clarified that the awards were decided by the PGCE Organizing Committee and not GSM. He understood that the awards were only meant for the public universities.
Iskandar Taib clarified that the original objective of the awards was to help the needy students.

The AGM suggested that the Council request the PGCE Organizing Committee to look into the matter.

Action: Incoming Council

- b. Askury Abd Kadir pointed out that in item 9.2, the Society's representative to AAPG House of Delegate is Askury Abd. Kadir of University Teknologi PETRONAS with Mazlan Madon of PETRONAS Research Sdn Bhd as the alternate and the tenure is until July 2011. He further commented that GSM should give opportunity for the representatives to attend the HOD meeting.

Yunus Abd Razak explained that GSM does not have the financial means to support the passage to the meeting. He was of the opinion that whoever being nominated by PETRONAS to the meeting should also represent GSM.

- c. C. S. Hutchison commented that the downward trend of student membership is worrying and suggested that GSM should run more programmes especially for the students.

Action: Incoming Council

- d. Yunus Abd Razak proposed that the Council should campaign for GEOSEA which is going to be held in Thailand in 2012.

Action: Incoming Council

Ng Tham Fatt proposed that the Secretary's Report be accepted and this was seconded by Askury Abd Kadir.

4.3 Editor's Report

The President informed the AGM that the Editor had sent his apology for not being able to be present at the AGM. The President tabled the Editor's Report (Appendix 3) on behalf of the Editor. The AGM commended the up-to-date publication of recent issues of *Warta Geologi*.

Yunus Abd Razak proposed that the report be accepted and this was seconded by Mazlan Madon.

4.4 Treasurer's and Honorary Auditor's Report

The Treasurer tabled the Treasurer's and Honorary Auditor's Report (Appendix 4).

Lee Chai Peng proposed that the Treasurer's and Honorary Auditor's Report be accepted and this was seconded by Samsudin Hj Taib.

5. Election of Honorary Auditor

Mr Ahmad Nizam Hassan proposed to maintain S.F Lee & Co as the Honorary Auditor for the year 2011. This suggestion was supported by Yunus Abd Razak and seconded by Ng Tham Fatt. The AGM unanimously agreed to elect S.F. Lee & Co as Honorary Auditors.

6. Other Matters

K.M. Leong submitted an item for discussion on the continuing promotion and sale of GSM's 1996 Reprinted Edition Hutchison (1989). The AGM unanimously agreed not to discuss the matter as the proposer was not in attendance at that point of the meeting.

7. Announcement of New Council for 2011/2012

The AGM was informed that nominations were called to fill the posts of President, Vice President, Secretary, Assistant Secretary, Treasurer, Editor and four 2-year Councillors posts. However, at the close of the said nomination, the election procedure was not executed for only a single nominee was received for each of the posts opened. Hence, the new Council was duly formed as in the following. One 1-year Councillor post was left vacant however, as the Councillor, Lim Choun Sian (UKM) was elected to the Assistant Secretary post.

President	:	Joy Jacqueline Pereira (UKM)
Vice-President	:	Mazlan Madon (PETRONAS Research Sdn Bhd)
Immediate Past President	:	Yunus Abdul Razak (JMG)
Secretary	:	Ling Nan Ley (JMG)
Assistant Secretary	:	Lim Choun Sian (UKM)
Treasurer	:	Ahmad Nizam Hasan (GeoSolution Resources)
Editor	:	Ng Tham Fatt (UM)
Councillors (2 years)	:	Tan Boon Kong (Freelance) Nur Iskandar Taib (UM) Gan Lay Chin (Freelance) Tanot Unjah (UKM)
Councillors (1 year)	:	Nicholas Jacob (JKR) Samsudin Hj. Taib (UM) Anil Nair (UNIGEO) (Vacant)

8. Presidential Address

The re-elected President Joy Jacqueline Pereira thanked the members for their continuing support and confidence given to the Council. She pledged that the incoming Council would devise a collaboration mechanism with various geology-related agencies and institutions for the furtherance of geosciences in the country.

9. Vote of Thanks

K.M. Leong appreciated the Council for having invited all the past GSM presidents to the PGCE 2011 opening. He also thanked the Council for listing all the GSM publications in the newly published Warta.

The AGM was adjourned at 6:50pm.

LING NAN LEY

Secretary 2010/2011

23 May 2011

**PERSATUAN GEOLOGI MALAYSIA
GEOLOGICAL SOCIETY OF MALAYSIA
PRESIDENT'S REPORT 2011/2012**

Since the 45th AGM on 15 April 2011, the Geological Society of Malaysia (GSM) has sustained its objective of actively promoting the advancement of the geological sciences in the country and surrounding region. Over the past year, GSM continued with activities that were designed to strengthen the capacity of geoscientists and embarked on initiatives to formalize collaborations and alliances with key institutions within the geoscience fraternity.

The National Geoscience Conference (NGC 2011) was successfully co-organized with the Minerals and Geoscience Department (JMG) of Malaysia and Universiti Teknologi Malaysia with the support of other partners on 11-12th June 2011 at The Puteri Pacific Johor Bahru. The outstanding Conference has set the benchmark for future events in terms of pageantry, private sector participation and collaborative legacy between geoscience institutions in Johor. We thank our co-organisers and collaborators as well as the Organising Co-Chairmen and their committee members for their support, contribution and unwavering dedication to GSM.

In 2011, the Society decided that the Petroleum Geology Conference and Exhibition (PGCE) be rebranded as the 'Petroleum Geoscience Conference and Exhibition' to truly reflect the whole spectrum of activities in the petroleum sector, as well as to capture the multi-disciplinary expansion of the knowledge domain over the decades. The Society has also initiated with co-organisers PETRONAS a new cooperative framework for PGCE, whereby the net profits from PGCE will be channeled to the Yayasan UTP and a newly created PGCE Endowment Fund. The PGCE Endowment Fund will be administered by GSM in a separate account, where the principal sum remains in perpetuity with the interest to be used to build capacity in petroleum geoscience. This new cooperative framework will be implemented in the PGCE 2012.

The 12th Regional Congress on Geology, Mineral and Energy Resources of Southeast Asia (GEOSEA 2012) was organised by the Geological Society of Thailand on 7-8 March 2012 in Bangkok, Thailand. The GEOSEA Secretariat, hosted by GSM, prepared a report for the Business Meeting held on 8 March 2012. The meeting saw the expansion of GEOSEA membership to include the Myanmar Geosciences Society, Vietnam Union of Geological Sciences and Department of Geology, Lao PDR. The Myanmar Geosciences Society graciously volunteered to host the GEOSEA XIII in 2014. Member Societies were also requested to host thematic meetings in conjunction with their annual national meetings to promote regular technical exchange between geological societies during the intervening periods between GEOSEA events. The meeting also agreed to commence on a voluntary initiative to document best geoscience practices, focusing initially on flood, earthquake, tsunami, landslide and volcanic hazards.

The Working Groups of GSM and Regional Representatives have also supported the Society's efforts in enhancing the capability of local geoscientists through the organization of technical talks and field visit. The issue of poor attendance to the technical talks, however, has not been resolved. We look forward to the operationalization of the Geologists Act, 2008 (Act 689) and a comprehensive strategy for continuous professional development. This may help to improve the situation.

The two flagship publications of GSM – *Bulletin of the Geological Society of Malaysia* and *Warta Geologi* are being continuously improved. The Editor-in-Chief, with support from the Managing Editor, is seeking ways to increase the profile of these publications to an international audience. It is hoped that these efforts will indirectly contribute to the increase in the citation index of geoscientists in Malaysia.

The linkages of GSM with national and international institutions such as the IGM, Costam, AAPG and EAGE have been maintained over the past year. Linkage has also been established with the Academy of Sciences Malaysia, specifically the Committee on Linkage with S&T Organisations and Professional Bodies. Through this linkage, GSM aims to promote the contribution of geoscience in advancing science, technology and innovation for knowledge generation, sustainable socio-economic development and improved quality of life.

The Society has also initiated an effort to formalize its relationship with IGM by establishing a joint committee to advance geoscience education and knowledge. The committee will focus mainly on ensuring the delivery of quality geoscience education programmes. Proposed members include heads of all universities that provide geology, earth science and geophysics courses as well as representatives from the Minerals and Geoscience Department, the Board of Geologists and the private sector.

The GSM Council has been instrumental in steering enhanced institutional arrangements within the geoscience fraternity and I am grateful for their ideas and support. On behalf of the Council, I thank the Organising Chairs of all our events, as well as the Working Group Chairs and Regional Representatives, for their contributions to GSM. The unwavering support of Ms. Anna Lee in the administration of GSM is also very much appreciated.

Joy Jacqueline Pereira

President

Geological Society of Malaysia

**PERSATUAN GEOLOGI MALAYSIA
GEOLOGICAL SOCIETY OF MALAYSIA
SECRETARY’S REPORT 2011/12**

1.0 Introduction

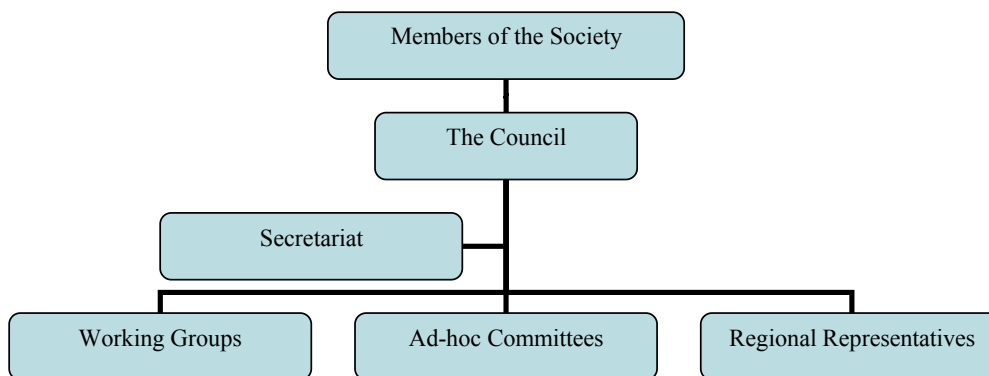
On behalf of the members of the Council of the Geological Society of Malaysia (GSM), it is my pleasure to present the Secretary’s Report for the session 2011/2012.

2.0 Society structure

The Society’s stakeholders are the members of the Society led by an elected Council. The Council’s main functions are to set directions to promote the advancement of geosciences, endorse activities and provide guidance for the execution of the activities of the Society.

The Council is supported by 5 Working Groups and 6 Regional Representatives. The Working Groups’ main function is to promote advancement and exchange of knowledge in specific geoscience areas. The Regional Representatives’ main function is to promote geosciences and implement the mission of the society within their respective geographical areas.

The Council is assisted by the Secretariat. The Secretariat assisted the Society in the administration of day-to-day activities of the Council, Working Groups and Regional Representatives.



Organisation Chart of the Society

3.0 Membership

As at 31st December 2011, the total number of members in the Society stands at 520. There is a general increase in membership across the board – overall by about 10% over the previous year’s total of 472. The surge especially in the Full and Student Membership categories could be due to the membership drive and publicity programmes carried out at various institutions. The table below presents the breakdown in membership categories and their geographical breakdown.

Breakdowns of Membership

COUNTRY	Full	Life	Inst.	Student	Associate	Honorary	Total 2011	Total 2010
Australia	-	19	-	-	-	-	19	19
Brunei	-	1	-	-	-	-	1	1
Canada	-	3	-	-	-	-	3	3
Europe	-	10	-	-	-	-	10	10
Hong Kong	-	1	-	-	-	-	1	1
Indonesia	-	8	-	-	-	-	8	8
Japan	-	4	-	-	-	-	4	4
Africa	-	1	-	-	-	-	1	1
Middle East	-	4	-	-	-	-	4	4
Philippines	-	2	-	-	-	-	2	2
Singapore	1	7	1	-	1	-	10	10
Thailand	-	3	-	-	-	-	3	3
USA	-	8	-	-	-	-	8	8
Malaysia	130	198	4	104	8	2	446	398
TOTAL 2011	131	269	5	104	9	2	520	
TOTAL 2010	108	265	3	89	4	3		472

4.0 The Council

The Council for the Geological Society of Malaysia (GSM) for 2011/2012 session resumed their office after the 45th AGM on the 15th April 2011.

4.1 Council Members

The Council Members for 2011/2012 are as follows:

President: Joy Jacqueline Pereira (UKM)
Vice President: Mazlan Madon (PETRONAS Research Sdn Bhd)
Immediate Past President: Yunus Abdul Razak (JMG)
Secretary: Ling Nan Ley (JMG)
Assistant Secretary: Lim Choun Sian (UKM)
Treasurer: Ahmad Nizam Hasan (GeoSolution Resources)
Editor: Ng Tham Fatt (UM)

Councillors:
 (2011/2012) Nicholas Jacob (JKR)
 Samsudin Hj. Taib (UM)
 Anil Nair (UNIGEO)
 (Vacant)*

(2011/2013) Tan Boon Kong (Freelance)
 Nur Iskandar Taib (UM)
 Gan Lay Chin (Freelance)
 Tanot Unjah (UKM)

*With the election of Lim Choun Sian (UKM) to the Assistant Secretary post, his previous 1-year Councilor post became vacant. The Council has co-opted Robert Wong (PETRONAS) to fill the vacant post.

4.2 Council Meetings

During the 2011/2012 session, the Council met 6 times. The attendance of the council members to the meetings is presented in the table below. All the meetings were conducted at the meeting room of the Department of Geology, University of Malaya, Kuala Lumpur.

Attendance of Council Members at Council Meetings

NAME	25/5/11	13/7/11	28/9/11	1/12/11	19/1/12	1/3/12	Total
Joy J. Pereira	/	/	/	/	/	/	6/6
Mazlan Madon	/	/	0	/	/	/	5/6
Ling Nan Ley	/	/	/	/	/	/	6/6
Ahmad Nizam H.	/	/	/	/	/	/	6/6
Ng Tham Fatt	/	/	/	/	/	/	6/6
Lim Choun Sian	/	0	/	/	0	/	4/6
Yunus Abd. Razak	0	0	0	/	0	/	2/6
Nicholas Jacob	/	0	0	/	/	/	4/6
Samsudin Taib	/	/	/	0	/	/	5/6
Anil Nair	/	/	/	0	/	0	4/6
Robert Wong	-	-	/	/	0	/	3/4
Tan Boon Kong	/	/	/	/	/	0	5/6
Nur Iskandar Taib	/	/	/	/	/	/	6/6
Gan Lay Chin	0	/	/	/	0	/	4/6
Tanot Unjah	/	0	0	/	0	0	2/6

Note: / = present, 0 = absent with apology

5.0 Working Groups

In the 2011/2012 session, the Working Groups and the Chairs are as follows:

	WORKING GROUP	CHAIRMAN
1	Working Group on Engineering Geology, Hydrogeology & Environmental Geology	Tan Boon Kong
2	Working Group on Promotion of Geoscience & Young Geologists	Tanot Unjah
3	Working Group on Economic Geology	Zakaria Endut
4	Working Group on Regional Geology	Kamal Roslan Mohamed
5	Working Group on Geophysics	Samsudin Hj Taib

6.0 Regional Representatives

The Society is keen to strengthen its delivery mechanism at the sub-national level through the appointment of Regional Representatives to work in conjunction with the local membership to advance geoscience in the respective regions. The Regional Representatives were appointed in January 2011, each for a tenure of 2 calendar years. The Regional Representatives are as follows:

	REGION	REPRESENTATIVE
1	Southern Peninsular Malaysia	Mohd For Mohd Amin
2	Perak	Askury Abd kadir
3	Northern Peninsular Malaysia	Kamar Shah Ariffin
4	Eastern Peninsular Malaysia	Mohd Pauzi Abdullah
5	Sarawak	Richard Mani Banda
6	Sabah	Baba Musta

7.0 Activities

The Society continued to undertake vigorously activities that would directly or indirectly benefit its members as detailed in the followings. The Society has successfully organised the National Geoscience Conference 2011 (NGC 2011), the GSM Photographic Competition 2011 and other activities such as talks and short courses.

7.1 The National Geoscience Conference 2011 (NGC2011)

With Minerals and Geoscience Department Malaysia and Universiti Teknologi Malaysia as co-organisers, the National Geoscience Conference 2011 (NGC2011) was successfully held from 11 to 12 June 2011 at the Puteri Pacific Hotel, Johor Bahru, Johore. The theme of NGC2011 was *Geoscientist and Ethics for a Sustainable Society*. A total of 3 keynote papers, and overwhelming 58 technical papers were presented and 73 posters were exhibited. A total of 244 geoscientists from academia as well as the public and private sectors attended the conference.

7.2 GSM Photographic Competition 2011

The organising committee received a total of 57 entries upon the expiry of the deadline, 31 December 2011 for entry submission.

The panel of judges has decided on the winners.

7.3 Others

During the session, the Council with cooperation of the Working Groups, Regional Representatives, and other organizations were able to organise a total of 18 technical talks, 1 short course and a site visit. The details are presented in the table below.

Summary of other activities

Date	Activity	Topic	Speaker	Collaborator
31.5.2011	Talk	The Pahang-Selangor Interstate Water Transfer Tunnel	Ir Dr Zullkefle Nordin (KETTHA)	
5.7.2011	Talk	Sedimentary basins and continental topography: An intergrated approach	Prof S Cloetingh, Tectonics Group, VU Amsterdam, The Netherlands	UM
8.7.2011	Malam Geologi Kejuruteraan 2011	1. Geological Investigation on "Unusual Road Heave" at Km 53, Jalan Bintulu-Bakun Dam, Bintulu Sarawak 2. Earthwork Excavation 3. Ethics in Engineering Geology	1. Tajul Anuar Jamaluddin (UKM) 2. John Kuna Raj (UM) 3. Ng Chak Ngoon (Subsurface Engineering)	
14.7.2011	Talk	Marcellus Shale – unconventional super gas play in eastern United States	Jeff Over Professor of geology, State University of New York, Geneseo	UM
18.8.2011	Talk	1. Tectonic activities in West Java. 2. Land subsidence in Jakarta, Bandung and Semarang. 3. Deformation of mud volcano in East Java	Prof. Dr. Ir. Hasanuddin Zainal Abidin, Institute of Technology Bandung, Indonesia	AAPG-UTP-SC and UTP
14.9.2011	Short Course	The Petroleum Industry in the Next Decade: An Overview to the Science, Technology and AAPG	Dr Paul Weimer, President, American Association of Petroleum Geologists	UM

PERTEMUAN PERSATUAN (MEETINGS OF THE SOCIETY)

14.9.2011	Talk	An overview to the Petroleum Geology of the Northern Deep Gulf of Mexico: Traps, Reservoirs, and Tectono-Stratigraphic Evolution	Dr Paul Weimer, President, American Association of Petroleum Geologists	UM
22.9.2011	Malam Geologi Kejuruteraan II 2011	1. Idealisation in geotechnical engineering: An essential understanding for practicing geotechnical professionals in Malaysia 2. On offshore geohazards, geophysics and geotechnics	Abdul Rasid Jaapar	
19.10.2011	Talk	On the link between orogenic shortening and “back-arc” extensional collapse in low topography orogens	L. Matenco University Amsterdam, The Netherlands	UM
21.10.2011	Malam Jurutera 2011	1. Issues in Slope Engineering 2. Slope Stabilization	1. Ir. Yee Thien Seng 2. Ir. Dr. Toh Cheng Teik	
12.11.2011	Site visit	Klang Gates Quartz Range	-	YES Network & LESTARI
16.11.2011	Talk	Offshore Geophysical Site Survey for Geotechnical Engineering – WHY, WHAT and HOW?	Abdul Hanan Ahmed Nadzeri (FGMSB)	
23.11.2011	Talk	Controls of copper and gold distribution in the Kucing Liar deposit, Ertzberg mining district, West Papua, Indonesia	Dr Brian T.E New, General Manager, Penjom Gold Mine	
19.12.2011	Talk	Modifications to the Design of Slope Remedial Works During Construction	Ir. Dr. Affendi Abdullah	
27.12.2011	Talk	1. Tectonic deformation around the eastern Himalayan Syntaxis: Paleomagnetic viewpoints 2. Differential rotation of NE and SW Japan: Opening aspect of the Japan Sea	Dr Yo-ichiro OTOFUJI, Professor of the Department of Earth and Planetary Science Kobe University, Japan	UM
13.1.2012	Chairman’s Lecture No. 17	A Tale of 2+1 Airports – the KLIA2, Sepang, the Senai and the Kuala Terengganu Airports	Tan Boon Kong	
24.2.2012	Talk	Geological and geochemical characteristics of the Tersang gold deposit in the Central Gold Belt, Peninsular Malaysia	Charles Makoundi, University of Tasmania, Australia	
28.2.2012	Talk	Some Organic Geochemical Thoughts on Concretions from New Zealand	Michael J Pearson, University of Aberdeen, Aberdeen	UM
13.3.2012	Talk	The Importance of Mineralogy in Siliciclastic Reservoirs	Dr Joseph Hamilton, ALS Ammtec, Australia	UM
19.3.2012 & 20.3.2012	Talk	1. Environmental Mineralogy for Management of Hazardous Inorganic Anions-Lessons Learnt from Natural Processes 2. Nuclear Accident at Fukushima Daiichi NPP. What happened? What can geological engineer do for our next generation? 3. A natural attenuation of arsenic in drainage from an abandoned arsenic mine dump	Professor Tsutomu Sato, Laboratory of Environmental Geology, Faculty of Engineering, Hokkaido University	SEADPRI, USM, JMG, IGM

8.0 Other Major Upcoming Events

8.1 The Petroleum Geoscience Conference and Exhibition 2012 (PGCE 2012)

This year, the prestigious event marks the 35th PGCE with a theme of *'Delivering Value: Realising Exploration & Development Potential'*. The conference will be held on 23-24 April 2012 at the Kuala Lumpur Convention Centre. The event is co-organised with PETRONAS with the inaugural participation of European Association of Geoscientists & Engineers (EAGE) as the event manager. The 2012 PGCE has opened up many exhibition booths to oil and gas companies and has provided opportunities for pre- and post-conference short courses, field trips, golf tournament, student programmes and a new initiative which will be a gala dinner.

8.2 The National Geoscience Conference 2012 (NGC2012)

The National Geoscience Conference 2012 (NGC2012) will be held from the 23rd to 24th June 2012 at the Pullman Hotel, Kuching, Sarawak. The theme of NGC2012 is *Geoscience in Everyday Life*. The Organising Committee of the Conference is chaired by Dr. Richard Mani Banda of Minerals and Geoscience Department Sarawak.

9.0 GSM Awards

GSM has set up various awards for members as follows:

9.1 Honorary Membership

No nomination received for this session.

9.2 PGCE Student Excellence Awards

PGCE Student Excellence Awards are given to outstanding students studying for a degree in Geology or Geophysics at Malaysian public universities. These awards are administered by the Organising Committee of PGCE.

9.3 Best Student Awards

These awards are administered by the Geology Departments of UM & UKM. Each award is worth RM500.00.

9.4 Young Geoscientist Award

The award shall be made to the author of the best publication in geology and related fields about Malaysia or the region and/or should be of general interest to the local community of geoscientists. The author shall not be more than thirty years of age at the time of publication of the paper or the time at the paper was accepted for publication.

The invitation for nomination of Young Geoscientist Award was published in the *Warta*. The deadline for submission is 1 May 2012.

GSM has written to all the heads of Geology Departments to invite submission for the award.

9.5 Geoscientist Award

The geoscientist award is open to any geoscientists who are members of the Society who have done excellent research and contributed significantly to the development of Malaysian geology.

The invitation for nomination of Young Geoscientist Award was published in the Warta. The deadline for submission is 1 May 2012.

GSM has written to all the heads of Geology Departments to invite submission for the award.

10.0 Linkages and Collaborations

GSM maintained linkages with national and international institutions such as the IGM, Confederation of Scientific and Technological Association of Malaysia (COSTAM), American Association of Petroleum Geology (AAPG) and EAGE over the year. Linkage has also been established with the Academy of Sciences Malaysia, specifically the Committee on Linkage with S&T Organisations and Professional Bodies. Besides that, GSM is the present host of the permanent Secretariat for GEOSEA.

For COSTAM, the Society was represented by two Council Members: Mr. Tan Boon Kong and Dr. Gan Lay Chin. Both of them were elected as Council Members.

As for the AAPG House of Delegates, the Society was represented by Dr. Mazlan Madon of Petronas Research Sdn Bhd. Mr. Askury Abd. Kadir of University Teknologi Petronas was the alternative representative.

The President represents GSM in the ASM.

For the Student's Geological Club Collaboration, at present, only AAPG Student Chapter of University of Malaya is collaborating with GSM.

11.0 Others

In keeping pace with the era of globalised communication network, GSM has set up a GSM Facebook account. Members are encouraged to visit and to post any geology-related events or news on this Facebook.

12.0 Acknowledgement

The Society would like to record its utmost appreciation to all the individuals and organizations that have helped in one way or another in the organising of the Society's activities during the session. Special mention must be made of the tremendous support by the Head and staff of the Geology Department, University of Malaya especially in the use of its premises for most of the Society's meetings and activities. The continued co-operation extended by JMG, PETRONAS, and UKM is recorded with gratitude. Thanks are also due to the members who gave much of their time and energy to serve on the Council and/or its various committees. The Council also wishes to record its appreciation of the continued dedication and hard work by the Secretariat. Last but not least, the Council also wishes to record its appreciation to all members for their advice, guidance and support throughout the session.

Ling Nan Ley

Secretary

Geological Society of Malaysia

**PERSATUAN GEOLOGI MALAYSIA
GEOLOGICAL SOCIETY OF MALAYSIA
ASSISTANT SECRETARY'S REPORT 2011**

The sales of the Society publications and the list of organizations and institutions that were exchanging publications with GSM are presented in the following tables.

Sales and stock of publications for 2011

Publications	Sales 2011	Stock remaining by end of 2010	Stock remaining by end of 2011
Bulletin 2	4	189	185
Bulletin 3	4	168	164
Bulletin 4	7	88	81
Bulletin 6	6	411	405
Bulletin 7	5	261	256
Bulletin 13	4	18	14
Bulletin 18	2	5	3
Bulletin 19	4	385	381
Bulletin 20	4	342	338
Bulletin 21	4	154	150
Bulletin 22	5	215	210
Bulletin 23	4	228	224
Bulletin 24	4	386	382
Bulletin 25	4	98	94
Bulletin 26	6	198	192
Bulletin 27	5	73	68
Bulletin 28	3	115	112
Bulletin 29	3	115	112
Bulletin 30	4	121	117
Bulletin 31	3	116	113
Bulletin 32	6	95	89
Bulletin 33	4	255	251
Bulletin 34	5	73	68
Bulletin 36	4	113	109
Bulletin 37	3	169	166
Bulletin 38	2	236	234
Bulletin 40	2	95	93
Bulletin 42	7	49	42
Bulletin 43	5	151	146
Bulletin 44	3	112	109
Bulletin 45	6	121	115
Bulletin 46	0	19	19
Bulletin 47	6	69	63
Bulletin 48	0	52	52
Bulletin 49	4	329	325
Bulletin 50	6	350	344
Bulletin 51	6	258	252
Bulletin 52	5	250	245
Bulletin 53	4	346	342
Bulletin 54	4	301	297
Bulletin 55	5	318	313
Bulletin 56	4	379	375
Bulletin 57	507*	600	93
Proceeding AGC 2000	5	32	27
Proceeding AGC 2001	4	164	160
M'sian Stratigraphic guide	2	260	258
Lexicon of stratigraphy	6	45	39
Rocks poster	3	128	125
Geology of Borneo (CD)	19	283	264
Geology of Borneo (Map)	19	902	883
Geol. Evolution of SEA	23	921	898
Geology of Peninsular Malaysia	42	1219	1177

*Distributed free to all 2011 member

List of organizations and institutions that are exchanging publications with GSM

Item	Organization	Country
1	New South Wales Dept of Mineral Resources	Australia
2	Geologica Belgica a.s.b.I	Belgium
3	Ministry of Development	Brunei
4	University of Geosciences	China
5	The Episode	China
6	Nanking Institute of Geology	China
7	National Geological Library	China
8	Peking College of Geology	China
9	SOPAC Secretariat	Fiji
10	Suomalaineu Tiedeakatemia	Finland
11	Freie Universitat Berlin	Germany
12	National Museum of Natural History	Holland
13	Geological Society of Japan	Japan
14	Dept Mineral & Planetary Science, Hiroshima	Japan
15	Museum of Nature & Human Activities	Japan
16	National Science Museum	Japan
17	Natural History Museum and Institute	Japan
18	Institute of Geosciences	Japan
19	Geological Society of Korea	Korea
20	Dewan Bahasa dan Pustaka	Malaysia
21	Jabatan Mineral dan Geosains, Ipoh	Malaysia
22	Jabatan Mineral dan Geosains, Kuching	Malaysia
23	Jabatan Mineral dan Geosains, Kota Kinabalu	Malaysia
24	Kementerian Dalam Negeri	Malaysia
25	Perpustakaan Negara Malaysia	Malaysia
26	Library Petronas Berhad	Malaysia
27	Pusat Sumber Maklumat Negeri Sarawak	Malaysia
28	Perpustakaan Tun Sri Lanang, UKM	Malaysia
29	Program Geologi, UKM	Malaysia
30	Library, UM	Malaysia
31	Library, USM	Malaysia
32	Malaysian Institute of Nuclear Technology	Malaysia
33	Library of Congress, USA Embassy	Malaysia
34	Institute of Ecological & Nuclear Science	New Zealand
35	National Library	Singapore
36	Central Geological Survey	Taiwan
37	American Museum of Natural History, New York	USA
38	CIGESE Library	USA
39	Oklahoma Geological Survey	USA
40	US Geological Survey	USA
41	University of Kansas	USA
42	AAPG Foundation Library	USA
43	Faculty of Agriculture & Natural Resources, Africa University	Zimbabwe

Lim Choun Sian

Assistant Secretary

Geological Society of Malaysia

**PERSATUAN GEOLOGI MALAYSIA
GEOLOGICAL SOCIETY OF MALAYSIA
EDITOR'S REPORT**

Three issues of *Warta Geologi* (Volume 37) and one volume of *Bulletin* (Volume 57) were published last year. Several efforts have been made to improve the citation and accessibility of the Society's publication. The *Bulletin* is now indexed by Scopus, Georef, Google Scholar and Ebsco. We are in the process of creating an online archive linked to the Society's web site, where abstract and full text of articles from past volumes of the *Bulletin*, *Warta Geologi* and conference proceedings, can be downloaded. The Society is now a member of Publishers International Linking Association (PILA) the owner of CrossRef®. Being a PILA member, we can assign doi (digital identifier) to all past and future original articles published by the Society.

The Society is planning to publish a special C.S. Hutchison Memorial Issue of the *Bulletin*, in recognition of Prof. Hutchison's outstanding contribution to geological research of Southeast Asia.

The Society is grateful to authors for their contribution, and members of the editorial board and reviewers for their time and effort to improve the quality of the Society's publications.

Ng Tham Fatt

Editor

Geological Society of Malaysia

**PERSATUAN GEOLOGI MALAYSIA
GEOLOGICAL SOCIETY OF MALAYSIA
TREASURER'S REPORT 2011**

For the Financial Year 2011, the society's posted a financial surplus of RM 679,443.00 tremendously higher compared to year 2010 RM 65,562.00. The net current asset showed increase from RM 657,916.00 for 2010 to RM 1,865,655.00 for year 2011.

Operating revenue posted higher compared to year 2010 which is total income of RM 176,407.00 to RM 778,335.00 for year 2011. Accumulations of balance payment Petroleum Geology Conference & Exhibition 2010 (PGCE 2010) and collection of the PGCE 2011 posted net total collection of RM 748,253.00. The revenue posted for Subscription shows slightly lower to RM15,070.00, Sales of Geology Peninsular Malaysia by RM 2,189.00 from RM 22,140.00 of year 2010 and Sales of publications from RM 4,994.00 of year 2010 to RM 3,253.00 for year 2011.

Total operating expenditure for Financial Year 2011 posted lower from RM 110,845.00 for year 2010 to RM 98,892.00. Nevertheless, there are an increasing expenditure recorded from printing of Bulletin, speakers' account and income tax. National Geological Conference that was held in Johor Bharu posted a healthy deficit of RM 5,945.00 compare to previous year 2010 of RM 25,466.00.

The Hon. Treasure would like to express a great appreciation to all organizing committee of PGCE 2011 lead by En Abdul Manaf Mohamad that contribute a tremendous income, NGC 2011 joint chaired by Tuan Hj Shahar Effendi Abdullah Azizi Director of JMG Johor and Associates Prof. Mohd For Mohd Amin of UTM Skudai; that managing a self funded conference by procuring sponsors given a minimal impact on deficit. Last but not least the donors and sponsor for their contributions and supports throughout the year.

Ahmad Nizam Hasan

Treasurer

Geological Society of Malaysia

NOTES

1. The RM 26,745.00 is still held in trust for the Evaluation Formation Working Group and RM 567.00 was loan to AAPG-UM student chapter fund to finance their activities.
2. The income from the sales of Geology Peninsular Malaysia of RM 2,189.00 would be divided between GSM and Department of Geology University Malaya as joint publishers.
3. Young geoscientist award fund of RM 3,143.00 still held as no candidates nominated.
4. Petroleum Geology Fund means PGCE 2012 was created as specific item as to detail out the account activity in that particular years without accumulate either income or expenditure from previous year.

**PERSATUAN GEOLOGI MALAYSIA
(GEOLOGICAL SOCIETY OF MALAYSIA)
(Registered in Malaysia)**

**REPORT AND ACCOUNTS
31 DECEMBER 2011**

**S.F. LEE & CO.
CHARTERED ACCOUNTANTS**

**PERSATUAN GEOLOGI MALAYSIA
(GEOLOGICAL SOCIETY OF MALAYSIA)
(Registered in Malaysia)**

**REPORT AND ACCOUNTS
31 DECEMBER 2011**

CONTENTS

	Page
Statement by Council	1
Statutory Declaration	2
Auditors' Report	3
Balance Sheet	4
Income and Expenditure Statement	5
Cash Flow Statement	6
Notes to Accounts	7 - 9

**PERSATUAN GEOLOGI MALAYSIA
(GEOLOGICAL SOCIETY OF MALAYSIA)
(Registered in Malaysia)**

MEMBERS INFORMATION

President	:	Joy Jacqueline Pereira
Vice-President	:	Mazlan Madon
Secretary	:	Ling Nan Ley
Assistant Secretary	:	Lim Choun Sian
Treasurer	:	Ahmad Nizam Hasan
Editor	:	Ng Tham Fatt
Councillors	:	Tan Boon Kong Nur Iskandar Taib Gan Lay Chin Tanot Unjah Nicholas Jacob Samsudin Hj. Taib Anil Nair Robert Wong
Immediate Past President	:	Yunus Abdul Razak

PERSATUAN GEOLOGI MALAYSIA (GEOLOGICAL SOCIETY OF MALAYSIA)
STATEMENT BY THE COUNCIL

We, Joy Jacqueline Pereira and Ahmad Nizam Hasan, being the President and Treasurer respectively, of the Persatuan Geologi Malaysia (Geological Society Of Malaysia) do hereby state that, in the opinion of the Council, the financial statements set out pages 4 to 9 are properly drawn up in accordance with applicable approved accounting standards so as to give a true and fair view of the state of affairs of the Persatuan Geologi Malaysia (Geological Society of Malaysia) as at 31 December 2011, and of the result and cash flows for the year then ended.



Joy Jacqueline Pereira
President



Ahmad Nizam Hasan
Treasurer

Kuala Lumpur

Dated : **22 MAR 2012**

PERSATUAN GEOLOGI MALAYSIA (GEOLOGICAL SOCIETY OF MALAYSIA)
DECLARATION BY THE OFFICER PRIMARILY RESPONSIBLE FOR THE
FINANCIAL MANAGEMENT OF THE SOCIETY

I, Ahmad Nizam Hasan, the officer primarily responsible for the financial management of the Persatuan Geologi Malaysia (Geological Society Of Malaysia), do solemnly and sincerely declare that the accompanying financial statements set out on pages 4 to 9 are, to the best of my knowledge and belief correct, and I make this solemn declaration conscientiously believing the same to be true and by virtue of the provisions of the Statutory Declarations Act, 1960.

Subscribed and solemnly declared by)
the abovenamed Ahmad Nizam Hasan)
at Kuala Lumpur in Wilayah Persekutuan)
on **22 MAR 2012**)



Ahmad Nizam Hasan

Before me,



NO. 102 & 104 1st FLOOR BANGUNAN
PERSATUAN YAP SELANGOR
JALAN TUN HS LEE
50000 KUALA LUMPUR

Commissioner for Oaths



S.F. LEE & CO (AF: 0670)


**REPORT OF THE AUDITORS TO MEMBERS OF THE
PERSATUAN GEOLOGI MALAYSIA (GEOLOGICAL SOCIETY OF MALAYSIA)**

We have audited the financial statements set out on pages 4 to 9. These financial statements are the responsibility of the Council Members of the Society. It is our responsibility to form an independent opinion, based on our audit, on those financial statements and to report our opinion to you, as a body, and for no other purpose. We do not assume responsibility to any other person for the content of this report.

We conducted our audit in accordance with approved auditing standards in Malaysia. Those standards require that we plan and perform the audit to obtain reasonable assurance about whether the financial statements are free of material misstatement. An audit includes examining, on a test basis, evidence supporting the amounts and disclosures in the financial statements. An audit also includes assessing the accounting principles used and significant estimates made by the Council Members, as well as evaluating the overall financial statements presentation. We believe that our audit provides a reasonable basis for our opinion.

In our opinion, the financial statements give a true and fair view of the statement of assets and liabilities of the Society as at 31 December 2011 and of its statement of income and expenditure and cash flows for the financial year ended 31 December 2011 in accordance with the MASB approved accounting standards in Malaysia.


S.F. LEE & CO. (AF 0670)
Chartered Accountants


LEE SIEW FATT
(1179/9/12J)
Chartered Accountant

Kuala Lumpur

Date : **22 MAR 2012**

**PERSATUAN GEOLOGI MALAYSIA
(GEOLOGICAL SOCIETY OF MALAYSIA)
(Registered in Malaysia)**

STATEMENT OF ASSETS AND LIABILITIES AS AT 31 DECEMBER 2011

	Note	2011 RM	2010 RM
FUND ACCOUNTS			
GENERAL FUND	3	1,315,658	636,215
STUDENT LOAN FUND		656	656
EVALUATION FORMATION WORKING GROUP FUND		26,745	16,207
YOUNG GEOSCIENTIST AWARD FUND		3,143	3,143
AAPG-UM STUDENT CHAPTER FUND		(567)	1,695
PETROLEUM GEOLOGY FUND		520,020	-
		<u>1,865,655</u>	<u>657,916</u>
Represented by:			
NON-CURRENT ASSETS			
PLANT AND EQUIPMENT	4	24,236	27,235
CURRENT ASSETS			
Inventories	5	35,118	44,159
Other receivable		2,765	-
Deposits		600	600
Fixed deposits with licensed bank	6	293,580	193,580
Cash and bank balances		1,509,356	392,342
		<u>1,841,419</u>	<u>630,681</u>
NET CURRENT ASSETS		1,841,419	630,681
		<u>1,865,655</u>	<u>657,916</u>

The accompanying notes are an integral part of these statements

PERSATUAN GEOLOGI MALAYSIA
(Registered in Malaysia)

**STATEMENT OF INCOME AND EXPENDITURE FOR THE YEAR ENDED
31 DECEMBER 2011**

INCOME	2011	2010
	RM	RM
Entrance fee	1,300	1,360
Fixed deposits interest income	6,936	4,506
Subscription	15,070	16,787
Sales of publications	3,253	4,994
Petroleum Geology Conference	748,253	121,820
Photostat	734	-
Geosea	-	4,800
Advertisement (Warta Geologi)	600	-
Geology of Peninsular Malaysia	2,189	22,140
	<u>778,335</u>	<u>176,407</u>
EXPENDITURE		
Annual dinner	2,480	2,474
Annual General Meeting	348	345
Audit fee	900	800
Bank charges	78	166
Department of Geology	1,620	200
Depreciation on plant and equipment	2,999	3,408
Honorarium	21,000	20,410
Income tax	1,200	-
National Geological Conference	5,303	25,466
Photo competition	-	2,300
Photostat	-	541
Postages	5,945	6,981
Printing and Stationery		
- Miscellaneous	524	740
- Warta Geologi	31,290	33,175
- Bulletin	12,025	7,140
Refreshment	750	370
Speakers' account	7,393	2,570
Subscription to COSTAM	200	-
Sundry expenses	2,443	2,244
Telefax	780	469
Telephone	1,614	1,046
	<u>98,892</u>	<u>110,845</u>
Surplus for the year	<u>679,443</u>	<u>65,562</u>

PERSATUAN GEOLOGI MALAYSIA
(Registered in Malaysia)

CASH FLOW STATEMENT FOR THE YEAR ENDED 31 DECEMBER 2011

	2011 RM	2010 RM
Cash flows from operating activities		
Surplus of income over expenditure for the year	679,443	65,562
Adjustments for:-		
Depreciation on plant & machinery	2,999	3,408
Interest income	(6,936)	(4,506)
Surplus before working capital changes	<u>675,506</u>	<u>64,464</u>
Increase in Petroleum Geology Fund	520,020	-
Increase in other receivable	(2,765)	-
Decrease / (Increase) in inventories	9,041	(12,224)
Increase in Student Fund	-	500
Decrease in AAPG-UM Student Chapter Fund	(2,262)	(4,050)
Increase / (Decrease) in Evaluation Formation Working Group Fund	<u>10,538</u>	<u>(31,998)</u>
Cash generated from operations	<u>1,210,078</u>	<u>16,692</u>
Purchase of plant and equipment	-	(2,482)
Interest income	<u>6,936</u>	<u>4,506</u>
Net cash generated from operating activities	<u>1,217,014</u>	<u>18,716</u>
Net increase in cash and cash equivalents	1,217,014	18,716
Cash and cash equivalents at beginning of the year	585,922	567,206
Cash and cash equivalents at end of the year	<u>1,802,936</u>	<u>585,922</u>
Cash and cash equivalents comprised of:		
Deposits held with licensed banks	293,580	193,580
Cash and bank balances	<u>1,509,356</u>	<u>392,342</u>
	<u>1,802,936</u>	<u>585,922</u>

**PERSATUAN GEOLOGI MALAYSIA
(Registered in Malaysia)**

NOTES TO THE FINANCIAL STATEMENTS - 31 DECEMBER 2011

1. PRINCIPAL OBJECTIVES

The objective of the Society is to promote the advancement of the geological sciences in Malaysia.

2. ACCOUNTING POLICIES

(a) Basic of Accounting

The financial statements have been prepared under the historical cost convention and comply with applicable Approved Accounting Standards issued by the Malaysian Association Standards Board.

(b) Plant and Equipment

Plant and equipment is stated at historical cost less accumulated depreciation. Depreciation on plant and equipment is computed on the reducing balance basis calculated to write-off the cost of the assets over their estimated useful lives. The principal annual rates used are:-

Office equipment	10%
Computer	20%

The carrying values of the assets are reviewed for impairment when there is an indication that the assets might be impaired. Impairment is measured by comparing the carrying values of the assets with their recoverable amounts.

An impairment loss is charged to the income and expenditure account immediately, unless the asset is carried at revalued amount. Any impairment loss of a revalued asset is treated as a revaluation decrease to the extent of previously recognised revaluation surplus for the same asset.

Subsequent increase in the recoverable amount of an asset is treated as reversal of the previous impairment loss and is recognised to the extent of the carrying amount of the asset that would have been determined (net of amortisation and depreciation) had no impairment loss been recognised. The reversal is recognised in the income statement immediately, unless the asset is carried at revalued amount.

c) INVENTORIES

Inventories consists of compass and maps valued at the lower of cost and net realizable value.

PERSATUAN GEOLOGI MALAYSIA
(Registered in Malaysia)

d) **INCOME RECOGNITION**

Membership subscription is payable annually at the beginning of the financial year. All subscriptions received during the financial year are recognised as income.

Income from sale of publications is recognised upon delivery of goods.

Income from organising conference is recognised on received and receivable basis.

Fixed deposit interest income is recognised on an accrual basis.

3. GENERAL FUND	2011	2010
	RM	RM
At 1 January	636,215	570,653
Surplus for the year	679,443	65,562
At 31 December	<u>1,315,658</u>	<u>636,215</u>

4. PLANT AND EQUIPMENT

<u>2011</u>	<u>Cost</u>			<u>Balance at 31/12/2011</u>
	<u>Balance at 1/1/2011</u>	<u>Additions</u>	<u>Disposal</u>	
	RM	RM	RM	RM
Office equipment	130,155	-	-	130,155
Computer	5,078	-	-	5,078
	<u>135,233</u>	<u>-</u>	<u>-</u>	<u>135,233</u>

	<u>Accumulated depreciation</u>			<u>Balance at 31/12/2011</u>
	<u>Balance at 1/1/2011</u>	<u>Charge for the year</u>	<u>Disposal</u>	
	RM	RM	RM	RM
Office equipment	105,671	2,449	-	108,120
Computer	2,327	550	-	2,877
	<u>107,998</u>	<u>2,999</u>	<u>-</u>	<u>110,997</u>

<u>Net Carrying Amount</u>	2011	2010
	RM	RM
Office equipment	22,035	24,484
Computer	2,201	2,751
	<u>24,236</u>	<u>27,235</u>

PERSATUAN GEOLOGI MALAYSIA
(Registered in Malaysia)

5. INVENTORIES	2011	2010
	RM	RM
Maps	3,091	3,482
Compass	14,918	19,668
Magazines	17,109	21,009
	<u>35,118</u>	<u>44,159</u>

6. FIXED DEPOSITS WITH LICENSED BANK

The fixed deposits with licensed bank have a maturity of between 3 to 15 months (2010 : 3 to 15 months). Interest rates for the deposits ranged from 3.75% to 5% (2010 : 3.75% to 5%) per annum.

**PERSATUAN GEOLOGI MALAYSIA
GEOLOGICAL SOCIETY OF MALAYSIA
ANNOUNCEMENT OF NEW COUNCIL FOR 2012/2013**

President	:	Joy Jacqueline Pereira (UKM)
Vice-President	:	Mazlan Madon (Petronas Research Sdn Bhd)
Immediate Past President	:	Yunus Abdul Razak (JMG)
Secretary	:	Ling Nan Ley (JMG)
Assistant Secretary	:	Lim Choun Sian (UKM)
Treasurer	:	Ahmad Nizam Hasan (GeoSolution Resources)
Editor	:	Ng Tham Fatt (UM)
Councillors (2 years)	:	Meor Hakif Amir Hassan (UM) Liaw Kim Kiat (BHP Billiton) Robert Wong (PETRONAS) Nicholas Jacob (JKR)
Councillors (1 year)	:	Tan Boon Kong (Freelance) Nur Iskandar Taib (UM) Gan Lay Chin (Freelance) Tanot Unjah (UKM)



Petroleum Geoscience Conference and Exhibition 2012

The 35th edition of Petroleum Geoscience Conference and Exhibition (PGCE) was held at the Kuala Lumpur Convention Center until the 24th of April 2012. Aspiring to be Asia's Premier Geosciences Event, PGCE is co-organised by the Geological Society of Malaysia and PETRONAS. PGCE has hosted various international and domestic oil and gas companies, oilfield service providers and educational institutions. The event has been graciously officiated by the Chief Operating Officer & Executive Vice President of Downstream Sector PETRONAS, YBhg Datuk Wan Zulkiflee Wan Ariffin. Also in attendance, Datuk Yunus Abdul Razak, Director General of Mineral & Geoscience Department of Malaysia.

A total of 50 oral presentations and 42 technical posters, including a keynote address on the future global energy outlook will be presented during the 2 day event covering a wide range of topics, focusing on new ideas and technological advancement in Petroleum Geoscience. The theme for this year's PGCE is "Delivering value: Realising Exploration & Development Potential". It is hoped this could bring new dimension and perspective to petroleum geoscientist's role to keep up with the dynamic of oil and gas business landscape.

The 2 day event has set much precedence, including registering for the first time more than 2000 delegates and 44 exhibitors. PGCE is currently playing host to international speakers from 4 continents, further cementing its position as Asia's Premier Geoscience event. Additionally, PGCE will be hosting its first Gala Dinner, to promote networking among industry professional in a more relaxed environment, treating our delegates to a night of fine cuisine and entertainment.

This year marks the first time, PGCE made a contribution of RM 200,000 each to Yayasan UTP and the newly established PGCE Endowment Fund. Top students from 8 universities were also recognised through the PGCE Student Excellence Award. The objective of the contribution is to assist the continuous advancement and sustained growth in the knowledge areas of earth science, particularly in Malaysia and the region.

Ku Rafidah Ku Shafiee
Communication & Promotion Committee, PGCE2012

Organized by:



Managed by:

EAGE

PGCE 2012 Organizing Committee

Patron	Effendy Cheng B Abdullah
Advisor	Idris B Ibrahim
Chairman	Peter Majid
Vice Chairman	Gerard Wieggerink
Technical Program	
Communication & Promotion	
Exhibition	
Short Courses	
Student Program	
Secretary	Haizum Nadirah Mohd Zaideen
Treasurer	Ahmad Nizam Hassan
Venue & Budget	M Rashidi Abd Hamid
Venue & Budget	Basiron B Jalil
Corporate Sponsorship	Liau Min Hoe
Publication & Editor	Dr. Nur Iskandar Taib
Communication & Promotion	Ku Rafidah Ku Shafiee
Protocol & Stage	Kamarul Hadi B Roselee
	M Amar B Amir
IT & Registration	Tg M Syazwan B Tg Hassan
	Anna Lee
Golf	M Zin B Che Lah
Short Courses	Dr Deva Prasad Ghosh
Field Trip	Dr Bernard J M Pierson
	Boniface B Bait
Souvenirs & Gifts	Ahmad B Abas
	Ali Andrea B Hashim
Gala Dinner	Rizal Bakar





Back row, left to right: M Rashidi Abd Hamid, Liau Min Hoe, Rizal Bakar, Basiron Jalil, Tg Syazwan Tg Hassan, Boniface Bait, Haizum Nadirah Hassan, Kamarul Hadi Roselee, M Zin Che Lah, Ali Andrea Hashim, Ahmad Abas, Dr Deva Ghosh, Anna Lee, M Amar Amir, Gerard Wieggerink, Ahmad Nizam Hassan

Front row, left to right: Peter Majid, Idris Ibrahim, Effendy Cheng Abdullah, Dr Bernard Pierson



Not in photo: Ku Rafidah Bt Ku Shafie, Dr. Nur Iskandar Taib

PGCE 2012 Sponsors

Platinum Sponsors

	ExxonMobil	Opening Ceremony	Poster Display	Program Book
	PETRONAS	OC Apparel		

Gold Sponsors

	PGS	Lanyard	Student Sponsorship	
	Shell	Luncheon Day 1	PGCE Website	



Silver Sponsors

	CGGVeritas	Conference Premium		
	JX Nippon	Luncheon Day 2		
	Murphy	Conference Premium		
	TOTAL	Directional Signage	Golf Souvenir Item	
	BHP Billiton	Registration	Conference Badge	
	Hess	Oral Sessions		
	Halliburton	Golf Souvenir Items	3 Piece Orchestra (Happy Hour)	

Bronze Sponsors

	FugroJason	Rest & Relax Booth		
	Lundin	VIP Lounge		
	Mitsubishi	Morning Coffee Break Day 1	Wireless Cybercafe	
	Mubadala (Pearl Energy)	Afternoon Tea Break Day 1	PGCE Growth Fund	
	Newfield	Happy Hour Reception		
	Talisman	Afternoon Tea Break Day 2		
	Baker Hughes	Golf Souvenir Item		
	ConocoPhillips	Morning Coffee Break Day 2		
	Schlumberger			

Other Sponsors

	Kencana	Golf Souvenir Item	PGCE Growth Fund	
	Weatherford	Golf Souvenir Item		

Oral Presentations - Monday, 23rd April

	Banquet Hall	Plenary Theater	Room 302
	ADVANCES IN SEISMIC	NEW PLAY CONCEPTS I	FORMATION EVALUATION
	Ahmad Riza Ghazali (PETRONAS EPTC) & M. Tham (Schlumberger)	P. A. Restrepo-Pace (Mubadala) & V. Cathey (KPOC)	L. Riepe (PETRONAS Carigali) & J. Phillips (Schlumberger)
13:30	<p>Keynote: Better, Faster and (Possibly?) Cheaper: Recent Advances and the Road Ahead in Seismic Marine Acquisition and Processing Craig Beasley* (WesternGeco/Schlumberger)</p>	<p>B01 The Role of Play-Based Exploration in Heartland Portfolio Rejuvenation, Offshore and Onshore Sarawak, Malaysia S. J. Gough* (Sarawak SHELL Berhad), E. W. Adams (Sarawak SHELL Berhad) & T. Evers (Sarawak SHELL Berhad)</p>	<p>C01 Petrophysical Evaluation of "Quasi Wet Pay Zones" (QWPZ) via Integration of Advanced and Conventional Wireline Data S. Ismail* (PETRONAS Carigali Sdn Bhd), M. M. Altunbay (PETRONAS Carigali Sdn Bhd) & N. Aula (PETRONAS Carigali Sdn Bhd)</p>
13:55	<p>A01 Marine Broadband Seismic Data Acquisition: PETRONAS Perspective C. F. Low (PETRONAS Carigali Sdn Bhd), S. Chandola (PETRONAS Carigali Sdn Bhd), Z. M. Zawawi* (PETRONAS Carigali Sdn Bhd), A. Aziz Muhamad (PETRONAS Carigali Sdn Bhd), S. Kumar (PETRONAS Carigali Sdn Bhd), & M. Shah Sulaiman (PETRONAS Carigali Sdn Bhd)</p>	<p>B02 Deepwater Exploration in Malaysia, Offshore Sarawak P. Baltensperger* (Newfield Exploration), K. Robinson (Newfield Exploration), A. Finlay (Newfield Exploration) & A. Thomas (Newfield Exploration)</p>	<p>C02 Applications of 3D Micro-CT Images and 2D BSEM-EDS for Petrophysical Reservoir Characterization L. Riepe* (PETRONAS Carigali Sdn Bhd)</p>
14:20	<p>A02 Simultaneous Sources: The Inaugural Full-Field, Marine Seismic Case History from Australia I. Moore* (WesternGeco), D. Monk (Apache Energy Ltd), L. Hansen (Apache Energy Ltd) & C. Beasley (WesternGeco)</p>	<p>B03 Hydrothermally Enhanced Fractured Reservoirs – A New Play? A. A. Bal* (Baker Hughes Inc), R. Bray (Consultant) & R. Sigit (Geo-Connection)</p>	<p>C03 Integrated Interpretation of an Iron-Rich Sediment, Jansz-lo Field, Northwest Shelf, Australia G. R. Heavysage* (ExxonMobil Exploration and Production Malaysia) & A. Mills (ExxonMobil Australia)</p>
14:45	<p>A03 Geophysical Innovation and Technology Meeting Challenges of a Transition Zone OBC Survey in Malaysia S. K. Chandola* (PETRONAS Carigali Sdn Bhd), M. Z. Zawawi (PETRONAS Carigali Sdn Bhd), C. T. Law (PETRONAS Carigali Sdn Bhd), R. Faizal (PETRONAS Carigali Sdn Bhd), M. Adura (PETRONAS Carigali Sdn Bhd), R. Roslan (PETRONAS Carigali Sdn Bhd), J. Ismail (PETRONAS Carigali Sdn Bhd) & M. A. Ariff (PETRONAS Carigali Sdn Bhd)</p>	<p>B04 "Pre-MMU" Carbonates and the Influence of Age and Tectonic Regimes on Their Growth Styles, Sarawak, Malaysia E. W. Adams* (Sarawak SHELL Berhad), R. E. Besems (Sarawak SHELL Berhad) & S. J. Gough (Sarawak SHELL Berhad)</p>	<p>C04 An Integrated Petrophysical Analysis of Low Resistivity Low Contrast (LRLC) Pays in Clastic Reservoirs in SE Asia L. Riepe (PETRONAS Carigali Sdn Bhd), M. N. Zain (PETRONAS Group Research Sdn Bhd) & N. S. Zainudin* (PETRONAS Group Research Sdn Bhd)</p>
15:10	TEA BREAK		

	Banquet Hall	Plenary Theater	Room 302
	DEVELOPMENTS IN EM	NEW PLAY CONCEPTS II	HYDROCARBON PREDICTION FROM SEISMIC & ROCK PROPERTIES
	M. Farouki (PGS) & S. K. Chandola (PETRONAS Carigali)	H-J. Meyer (SHELL) & Jamlus Md Yasin (PETRONAS Exploration)	C. H. Sim (ExxonMobil) & G. Hodgkiss (CGGVeritas)
15:30	A04 Marine CSEM with A Novel Towed Acquisition System F. L. Engelman* (PGS Asia Pacific Pte Ltd), J. Mattsson (PGS) & J. Linfoot (PGS)	B05 Sepat Barat Deep-2: The Deepest and Hottest HPHT Well in North Malay Basin S. Osman* (PETRONAS), M. F. Nianamuthu (PETRONAS), F. A. Ismail (PETRONAS), J. J. M. Idris (PETRONAS) & J. Ping (PETRONAS)	C05 Lithology Discrimination Through Elastic Inversion D. Ghosh* (Universiti Teknologi PETRONAS)
15:55	A05 Pitfalls in CSEM Inversion; A Case Study of A False Positive V. Ganesan* (EMGS Asia Pacific Shd Bhd), H. T. Pedersen (EMGS Asia Pacific Sdn Bhd), S. K. Chandola (PETRONAS Carigali Sdn Bhd) & N. N. Halim (PETRONAS Carigali Sdn Bhd)	B06 Brittle versus Mobile Shale Tectonics in Deltas: Structural Constraints Derived From Regional Seismic Interpretations P. A. Restrepo-Pace* (Mubadala Oil & Gas)	C06 Estimating Porosity from Deterministic Inversion M. Sams* (Ikon Science/ Fugro-Jason (M) Sdn Bhd), T. J. Focht (Newfield Peninsula Malaysia Inc) & J. Ting (Fugro-Jason (M) Sdn Bhd)
16:20	P45 Key features of TEM and EM-IP investigations in South-East Asia Y. A. Agafonov (Irkutsk Electroprospecting Company), M. V. Sharlov (Irkutsk Electroprospecting Company), O. V. Tokareva (Irkutsk Electroprospecting Company), I. V. Buddo* (Irkutsk Electroprospecting Company), I. V. Egorov (Irkutsk Electroprospecting Company), M. M. Salleh (Onyx Engineering), S. K. Chandola (PETRONAS Carigali Sdn Bhd), T. Velayatham (PETRONAS Carigali Sdn Bhd), S. Shukri (PETRONAS Carigali Sdn Bhd), I. Ismail (PETRONAS Carigali Sdn Bhd) & S. Fatimah (PETRONAS Carigali Sdn Bhd)	B07 Maturation of a New Play Concept in Northern Provinces of Offshore Sarawak Basin, Malaysia S. R. Iyer* (PETRONAS Exploration), H. Rosidah (PETRONAS Exploration) & A. S. Amar (PETRONAS Exploration)	C07 The Evolving Role of Geophysics in Exploration. From Amplitudes to Geomechanics E. C. Andersen* (Talisman Energy Malaysia) & D. Gray (Nexen Inc., Calgary, Alberta, Canada)
16:45 - 17:10	POSTERS		

Oral Presentations - Tuesday, 24th April

	Banquet Hall	Plenary Theater	Lecture Room 302
	CARBONATES	RISK MITIGATION IN BASINS & COMPLEX PETROLEUM SYSTEMS	ROCK PHYSICS
	M. Jones (Murphy Oil) & Azhar Yusof (PETRONAS PMU)	D. Basu (Schlumberger) & Mohd Hasni Hashim (PETRONAS EPTC)	T. Focht (Newfield) & J. Ting (Fugro Jason)
08:30	A07 Seismic Imaging and Interpretation of Paleo-Cave Systems in Karstified Carbonate Reservoirs of Tarim Basin C. Luo (CNPC Tarim Oil Company), F. Xue* (Schlumberger), Q. Miao (CNPC Tarim Oil Company) & P. Yang (Schlumberger)	B08 Tectono-Stratigraphy and Development of the Miocene Delta Systems on an Active Margin of Northwest Borneo, Malaysia A. Balaguru* (Talisman Energy) & T. D. Lukie (Talisman Energy)	C08 Xu and White Revisited M. Sams* (IkonSciences/ Fugro-Jason (M) Sdn Bhd), T. J. Focht (Newfield Peninsula Malaysia Inc) & N. Azuairi Che Sidik (Newfield Peninsula Malaysia Inc)
08:55	A08 A Novel Technique for Carbonates to Enhance Static and Dynamic Models A. F. Zakeria* (PETRONAS Carigali Sdn Bhd), M. Altunbay (PETRONAS Carigali Sdn Bhd), R. Poit (PETRONAS Carigali Sdn Bhd) & J. Kijam (PETRONAS Carigali Sdn Bhd)	B09 Integrated Bio- and Seismostratigraphy of the Southern Sabah Offshore, Malaysia J. J. Lim* (Sarawak SHELL Berhad)	C09 New Joint Categorical/Continuous Simultaneous Inversion Technology M. Kemper (Ikon Science Ltd) & D. Flett* (Ikon Science)
09:20	A09 Mapping the Kinta Valley Karst System, Peninsular Malaysia: Implications for Better Insight of Subsurface Karst Features S. Kassa* (Universiti Teknologi PETRONAS), B. J. Pierson (Universiti Teknologi PETRONAS), W. S. Chow (Universiti Teknologi PETRONAS) & B. A. T. Jasmi (Universiti Teknologi PETRONAS)	B10 New Seismic Insight At Keabangan Field: KPOC Gears Up for A Development Drilling Campaign At a New Major Gas-Oil Hub in Offshore Sabah V. L. Cathey* (Kebabangan Petroleum Operating Company Sdn Bhd) & C. M. Curtis (Kebabangan Petroleum Operating Company Sdn Bhd)	C10 Evaluation of Thin-Bedded Heterogeneous Sands Using Geophysical Applications & Well Data For A Robust Development Plan M. S. Mohd Adnan* (ExxonMobil Development Company) & F. Fahmi (ExxonMobil Exploration & Production Malaysia Inc)
09:45	TEA BREAK		

	Banquet Hall	Plenary Theater	Room 302
	RESERVOIR MODELING	PORE PRESSURE	SEISMIC RESOLUTION
	A. Everts (Leap Energy) & R. Kugler (UM)	S. Bordoloi (Baker Hughes) & Wan Ismail Wan Yusoff (UTP)	M. Sams (Ikon Science) & C. F. Low (PETRONAS Exploration)
10:15	<p>A10</p> <p>A New Perspective of Structural and Property Modelling: A Case Study of Baram Oil Field, Offshore Sarawak, Malaysia.</p> <p>A. I. Latief* (ROXAR), A. MacDonald (ROXAR), G. Rahman (ROXAR), M. E. Rahman (PETRONAS), W. A. Nasir (PETRONAS), A. I. Ridzuan (PETRONAS) & P. A. Faehrmann (SHELL)</p>	<p>B11</p> <p>Overpressured Carbonate Reservoirs, Offshore Sarawak; Methods of Pore Pressure Prediction</p> <p>P. Baltensperger* (Newfield Exploration), W. Zanussi (CGGVeritas), S. Bordoloi (Baker Hughes) & S. Nath (Baker Hughes)</p>	<p>C11</p> <p>Improved Resolution of Thin Turbiditic Sands in Offshore Sabah With Bandwidth Extension – A Pilot Study</p> <p>G. Yu* (Geotrace), N. Shah (Geotrace), M. Robinson (Geotrace), N. H. Nghi (PETRONAS Resource Development/Petroleum Management Unit), A. A. Nurhono (PETRONAS Resource Development/Petroleum Management Unit) & G. S. Thu (PETRONAS Resource Development/Petroleum Management Unit)</p>
10:40	<p>A11</p> <p>Seismic Reservoir Characterisation of a Channel Sand Oil and Gas Field, Malaysia</p> <p>T. J. Focht* (Newfield Peninsula Malaysia Inc), M. Sams (Ikon Science/ Fugro-Jason (M) Sdn Bhd), D. Brookes (Newfield Peninsula Malaysia Inc) & J. Ting (Fugro-Jason (M) Sdn Bhd)</p>	<p>B12</p> <p>Pore Pressure Modeling How to Overcome HPHT Challenges</p> <p>S. Bordoloi (Baker Hughes Inc. (GMI)) & A. Ghosh* (Baker Hughes Inc. (GMI))</p>	<p>C12</p> <p>Seismic Resolution and Analysis of Thin Pay Beds</p> <p>M. Sajid* (University Technology PETRONAS), D. P. Ghosh (University Technology PETRONAS) & Z. T. H. Zuhar (University Technology PETRONAS)</p>
11:05	<p>A12</p> <p>Value & Insights from Synthetic Seismic Validation of Reservoir Models in Carbonate Gas Fields, Offshore Sarawak</p> <p>K. N. Baharaldin* (Sarawak SHELL Berhad) & A. Kayes (Sarawak SHELL Berhad)</p>	<p>B13</p> <p>Drilling Risks Associated With Hydraulic Fractures and Reactivating Faults Due to High Mud Weight/Pore Pressure And Miti</p> <p>A. A. Bal (Baker Hughes Inc), D. Maya* (Baker Hughes Inc), K. K. Kyi (PETRONAS Carigali Sdn Bhd), R. Guha (PETRONAS Carigali Sdn Bhd), M. I. Gabreldar (PETRONAS Carigali Sdn Bhd) & D. Abang Indi (Baker Hughes Inc)</p>	<p>C13</p> <p>Cascading Inversion Application for Lithology And Porosity Estimation Of Deepwater Thinly-Bedded Reservoirs</p> <p>A. Nurhono* (PETRONAS Petroleum Management Unit), B. Kantaatmadja (PETRONAS Petroleum Management Unit), S. T. Goh (PETRONAS Petroleum Management Unit), V.W.T. Kong (Schlumberger), M. R. Abdul Rahman (Schlumberger) & N. M. Hernandez (Schlumberger)</p>
11:30	POSTERS		
12:00	LUNCH		

	Banquet Hall	Plenary Theater	Room 302
	IMAGING THROUGH COMPLEX OVERBURDEN	INTEGRATED SUBSURFACE SOLUTIONS FOR FIELD DEVELOPMENT	GEOCHEMISTRY & UNCONVENTIONAL RESOURCES
	C. Notfors (CGGVeritas) & D. Ghosh (UTP)	M. Challis (ConocoPhillips) & R. Jones (Lundin)	P. Abolins (PETRONAS Exploration) & C. L. Wong (SHELL)
13:00	A13 Imaging Solutions for Geophysical Challenges in South East Asia N. El Kady* (PETRONAS Carigali Sdn Bhd), Z. Mohd Dom (PETRONAS Carigali Sdn Bhd), Y. Prasetyo (PETRONAS Carigali Sdn Bhd), M. Bayly (WesternGeco), G. Nyein (WesternGeco), P. Vasilyev (WesternGeco) & N. M. Don Ya (WesternGeco)	B14 Integrated Reservoir Characterisation of Turbidite Deposits within a Submarine Canyon, Offshore Sabah, Malaysia. K. Maguire* (SHELL Malaysia Exploration & Production), C. W. Hong (SHELL Malaysia Exploration & Production), T. M. Ting (SHELL Malaysia Exploration & Production) & G. Stone (SHELL Malaysia Exploration & Production)	C14 Hydrocarbon Source Rock Characteristics of The Gondwana Coals from Barapukuria Basin, Bangladesh M. Farhaduzzaman* (University of Malaya)
13:25	A14 Enhanced Seismic Imaging of a Mature Oilfield A. Nalonnil (Schlumberger), T. Handayani (Pertamina), W. Triyoso (Institut Teknologi Bandung (ITB)) & S. Dogra* (Schlumberger)	B15 Application of Innovative & Unconventional Techniques Enhanced Subsurface Interpretation of the J Sands, B Field J. Ranggon (Petrofac Energy Developments Sdn Bhd), M. H. Abdul Halim* (PETRONAS), W. N. Wan Mohammad (Petrofac Energy Developments Sdn Bhd), S. Dang Do (Petrofac Energy Developments Sdn Bhd) & M. H. Hashim (Petrofac Energy Developments Sdn Bhd)	C15 Source Potential and Hydrocarbon Maturity Modeling of the Onshore Masila Basin, Eastern Yemen M. Hakimi* (University of Malaya), W. H. Abdullah (University of Malaya) & M. R. Shalaby (University Brunei Darussalam)
13:50	A06 A Decade of 4D Seismic Monitoring of Carbonate Gas Reservoirs in Offshore Sarawak, Malaysia P. F. Hague* (SHELL) & B. H. Chiem (SHELL)	B16 An Integrated Approach for Infill Drilling Opportunity Maturation in a Mature Malay Basin Oil Field A. A. Abdul Rahim* (ExxonMobil Exploration & Production Malaysia Inc), H. K. Lim (ExxonMobil Exploration & Production Malaysia Inc) & F. Fahmi (ExxonMobil Exploration & Production Malaysia Inc)	C16 Geological Controls on Well Productivity and Reservoir Performance in Select North American Shale Gas Plays P. A. L. Winder* (Talisman Malaysia Limited), R. Herbert (Talisman Energy), G. Schmidt (Talisman Energy), M. Lawford (Talisman Energy) & B. Faraj (Talisman Energy)
14:15 - 14:40	A16 Geomechanical Approach to Resolve Severe Velocity Variations and Remove Image Distortions Below Rugose Seafloor S. Birdus* (CGGVeritas Australia), A. Artyomov (CGGVeritas), L. Li (CGGVeritas) & S. Xin (CGGVeritas)	B17 Well Architecture and Design Criteria for Complex Reservoirs in Mature Fields K. S. Chan (PETRONAS), R. Masoudi (PETRONAS), B. P. Kantaatmadja* (PETRONAS) & M. Othman (PETRONAS)	C17 Application of Dual Well Micro-Seismic Monitoring in Hydraulic Fracturing Stimulation in a Tight Oil Reservoir T. K. Lim (Schlumberger China SA), Y. Li* (Schlumberger) & X. G. Yang (PetroChina)

<h2 style="text-align: center;">Posters</h2> <h3 style="text-align: center;">Monday 23rd April</h3>	
<h3>Pore Pressure</h3>	
P01	Foresee the Unforeseen: Modeling West Baram Delta Overpressure C. A. Ibrahim* (PETRONAS Exploration), L. Light (Sarawak SHELL Berhad), J. Mennie (Sarawak SHELL Berhad) & C. K. Ngu (Sarawak SHELL Berhad)
P02	Pore-Pressure and Subsurface-Plumbing Patterns in Central Luconia; Offshore Sarawak, Malaysia E. Kosa* (Sarawak SHELL Berhad)
<h3>Carbonates</h3>	
P03	Application of Stable Isotope Analysis from Central Luconia, Sarawak: Insights into Reservoir Development and Diagenesis K. K. Ting* (Sarawak SHELL Berhad), B. J. Pierson (South-East Asia Research Laboratory, SEACARL, UTP) & O. S. Al-Jaaidi (Sarawak SHELL Berhad,*Qatar Petroleum (*current))
P46	CSEM Application in Carbonate Environment: A Case Study A. S. Saleh* (PETRONAS Carigali Sdn Bhd), S. K. Chandola (PETRONAS Carigali Sdn Bhd), P. K. Lee (PETRONAS Carigali Sdn Bhd), T. Velayatham (PETRONAS Carigali Sdn Bhd), P. Kumar (PETRONAS Carigali Sdn Bhd), M. S. Wahid (PETRONAS Carigali Sdn Bhd) & J. Beenfeldt (EMGS Sdn Bhd)
<h3>Imaging Through Complex Overburden</h3>	
P04	Converted Waves Seismic Imaging : Importance of Gamma Estimation A. G. Mohd Adnan* (PETRONAS Research Sdn Bhd), M. H. M. Zahir (PETRONAS Research Sdn Bhd) & A. R. Ghazali (PETRONAS E&P Technology Centre)
P05	Application of TTI Reverse Time Migration, Deepwater Offshore Malaysia J. Sun* (CGGVeritas), B. Mishra (CGGVeritas), C. Jiao (CGGVeritas), J. Sun (CGGVeritas), G. Hodgkiss (CGGVeritas) & A. Bisset (Murphy Corporation)
<h3>Rock Physics</h3>	
P06	Application of Upscaling Permeability Workflow: Pore to Core Plug Scale on Malay Basin Thin Sections L. A. Lubis* (Universiti Teknologi PETRONAS), Z. Z. Tuan Harith (Universiti Teknologi PETRONAS), K. A. Moh Noh (Universiti Teknologi PETRONAS), H. Khairy (Universiti Teknologi PETRONAS) and A. Moh Salih (PETRONAS E&P Technology Centre)
<h3>Unconventionals Resources</h3>	
P08	Status of Exploration on Shale Gas Resources in India A. Boruah* (University of Baroda, Gujarat, India)
P09	Time-Pressure Correlation to Estimate Dewatering Time for Coalbed Methane Reservoir at Saturated and Undersaturated Condition D. C. I. Hutami* (Institute Technology of Bandung), I. K. Alhamzany (Institute Technology of Bandung), I. G. Permana (Institute Technology of Bandung), S. K. H. Wicaksono (Institute Technology of Bandung), H. W. Alam (Institute Technology of Bandung) & U. W. R. Siagian (Institute Technology of Bandung)
<h3>Risk Mitigation in Basins & Complex Petroleum Systems</h3>	
P10	Systematic Evaluation of Play and Prospect Risk Using a New Play-Based Exploration Methodology A. Neber* (Schlumberger), I. Bryant (Schlumberger), G. Koller (Schlumberger), T. Levy (Schlumberger), M. Neumaier (Schlumberger) & N. Tessen (Schlumberger)
P11	Systematic Application & Play-based Exploration Methodology Using ArcGIS in Sabah Exploration Block SB309 & SB310 S. Jamil* (PETRONAS), A. Ngau (Talisman Malaysia Limited) & C. H. Tan (Talisman Malaysia Limited)
P12	Deepwater Reservoir Geometry and Characterisation: Analogue from the Semantan and West Crocker Formations H. H. Ismail* (PETRONAS Research Sdn Bhd), M. Madon (PETRONAS Research Sdn Bhd), Z. A. Abu Bakar (PETRONAS Research Sdn Bhd) & M. S. Leman (National University of Malaysia)
<h3>Geochemistry</h3>	
P13	Well Log Application in Source Rock Evaluation: Using Committee Machine with Intelligent Systems M. Verdiyari (Petroleum University of Technology), F. Kamyabi* (Petroleum University of Technology), A. Nazarpour (Petroleum University of Technology) & M. K. Ghassem Alaskari (Petroleum University of Technology)
P14	Geochemical Evaluation of Oil Reservoirs in the World's Largest Gas Field from Persian Gulf, Iran P. Hassanzadeh* (NIOC-EXP), M. Khaleghi (NIOC-EXP), A. Ahanjan (NIOC-EXP), M. Kobraei (NIOC-EXP) & R. Bagheri Tirtashi (NIOC-EXP)
P15	Common Liptinitic Constituents of Mukalla Coals in The Offshore Qamar Basin, Eastern Yemen: Implication for Hydrocarbon M. Hakimi* (University Of Malaya) & W. H. Abdullah (University Of Malaya)
<h3>Reservoir Modeling</h3>	
P17	Generating a New Approach for Continuous Reservoir Model Updating: Non-Gaussian Priors & Nonlinear Data Functions in ENKF S. Forghany* (Research Institute of Petroleum Industry (RIPI)), A.A. Asgari (Research Institute of Petroleum Industry (RIPI)) & T. Behrouz (Research Institute of Petroleum Industry (RIPI))
P18	Diverse Origins of Carbonate Cements Revealed By Carbon and Oxygen Isotopic Analysis. D. M. Ince* (PETRONAS Carigali Sdn Bhd)
P19	Conceptual Geology of Dulang Using Sedimentology, Stratigraphy and Netsand Distribution. S. C. Kurniawan* (PETRONAS), K. Saraton (PETRONAS) & U. Deliza Aleesha (PETRONAS)
P20	Reservoir Characterization Enhancement Through Integrated Wellbore-Reservoir Flow Model and Pressure Transient Analysis K. Khadivi* (Sharif University), R. Masoudi (PETRONAS), M. Soltanieh (Sharif University) & F. A. Farhadpou (Sharif University)
P21	EB Field: Doubling a Marginal Field's Reserves by Understanding the Application of "Enabling" Technology K. Afzan* (Newfield Peninsula Malaysia Inc), O. T. Suan (Newfield Exploration Company), M. Lambert (Newfield Sarawak Malaysia) & B. Goodin (Senergy Australia Pty Ltd)

Posters Tuesday 24th April

New Play Concepts

P23	Unravel New Exploration Opportunity in Central Luconia A. H. W. Abdullah* (PETRONAS), J. Singh (PETRONAS), S. Osman (PETRONAS) & C. Abdullah (PETRONAS)
P24	Structuration & Stratigraphic Influence in Post Carbonate Trap Geometry of "K" Prospect, SK315 Block, Offshore Sarawak K. A. K. Amry* (PETRONAS Carigali Sdn Bhd), M. S. M. Sharir (PETRONAS Carigali Sdn Bhd), S. S. Wafa (PETRONAS Carigali Sdn Bhd) & A. M. S. Azlan (PETRONAS Carigali Sdn Bhd)
P25	Sedimentological Characterization of Deeper Group M Reservoirs in Malay Basin S. A. M. Yusak* (PETRONAS Carigali Sdn Bhd)
P26	The Exploration Strategic Potential of Rajang Delta System Z. Ibrahim* (PETRONAS Exploration), B. H. WEI (PETRONAS Exploration) & A. Rauf (PETRONAS Exploration)
P27	Shallow Reservoirs, The Neglected Play in The Malay Basin - A Case Study From The A Field S. H. So* (PETRONAS Carigali Sdn Bhd), S. Shahar (PETRONAS Carigali Sdn Bhd) & N. Ahmad (PETRONAS Carigali Sdn Bhd)
P28	Pre-Tertiary Fractured Basement of Mega Host Block A, Malays Basin in Light of Current 3D Seismic Data Interpretation N. H. Ngoc* (PETRONAS Carigali Sdn Bhd)
P29	3D Near-Wellbore Structural Modeling, Natural Fracture Characterization and in-Situ Stress Analysis in A Complex Thrust R. Dashti* (Schlumberger)

Advances In Seismic

P30	CRS-Stack and NIP-Wave Tomography Implemented to the SH-Wave Reflection Seismic Data for Shallow Hydrocarbon Prospecting M. R. Sule (Institut Teknologi Bandung), A. A. Valencia* (Institut Teknologi Bandung), A. Hendriyana (Institut Teknologi Bandung), U. Polom (Leibniz Institute for Applied Geophysics) & C. M. Krawczyk (Leibniz Institute for Applied Geophysics)
P31	Workflows to Improve the Resolution of Post-Stack Seismic Data and Attributes from the Malay Basin A. E. Barnes* (PETRONAS Research Sdn Bhd), M. F. A. Rahim (PETRONAS Research Sdn Bhd) & A. R. Ghazali (PETRONAS EXPLORATION/ PETRONAS Carigali Sdn Bhd)

Hydrocarbon Prediction from Seismic & Rock Properties

P32	Integrated Fluid Analysis Technique to Improve Evaluation on Fluid Potential in Downthrown Structure Prospect T. Aldha* (PETRONAS Carigali Sdn Bhd) & G. Taslim (PETRONAS Carigali Sdn Bhd)
P33	Integration of Sequence Stratigraphy and Elastic Inversion Improved Understanding on Reservoir Characterization N. Mohamud* (PETRONAS Carigali Sdn Bhd), O. A. Mahmud (PETRONAS Carigali Sdn Bhd), N. A. Razali (PETRONAS Carigali Sdn Bhd) & M. H. M Nor (PETRONAS Carigali Sdn Bhd)

P44	Application of Seismic Inversion To Mitigate Reservoir Heterogeneity Uncertainty For Optimized Well Planning M. F. Mohd Fuad* (ExxonMobil Exploration & Production Malaysia Inc.), F. Fahmi (ExxonMobil Exploration & Production Malaysia Inc.) & A.G. Williams (ExxonMobil Exploration & Production Malaysia Inc.)
-----	---

Integrated Subsurface Solutions for Field Development

P34	An Efficient Development 2011 Case History from the Gulf of Thailand R. C. Roever* (Coastal Energy), J. Moon (Coastal Energy), R. Ripple (Coastal Energy), D. Cox (Coastal Energy), N. Htein (Coastal Energy), J. Mitchell (Coastal Energy), S. Rubio (Coastal Energy), J. Pringle (CEC International, Ltd (Thailand)), R. The (CEC International, Ltd (Thailand)), G. Peace (CEC International, Ltd (Thailand)) & A. Laird (CEC International, Ltd (Thailand))
P35	Reservoir Characterisation of Mishrif Formation of Garraf field, Iraq, using 3D seismic and AI Inversion M. Embong (PETRONAS Carigali Sdn Bhd), M. Higashi* (PETRONAS Carigali Iraq Holding BV), H. H. Abu Bakar (PETRONAS Carigali Iraq Holding BV), K. A. Zamri (PETRONAS Carigali Iraq Holding BV), F. H. M Ali (PETRONAS Carigali Iraq Holding BV), S. Moriya (PETRONAS Carigali Iraq Holding BV), S. B. M Said (PETRONAS Carigali Iraq Holding BV) & A. T. Patrick Panting (PETRONAS Carigali Sdn Bhd)
P36	Geo-Information & GIS: Adding Value to Exploration and Development Activities G. G. Tan* (Sarawak Shell Berhad)
P37	A Structured Approach Towards Quantification of Subsurface Parameter Ranges A. J. W. Everts* (Leap Energy Partners Sdn Bhd), L. Alessio (Leap Energy Partners Sdn Bhd), P. Friedinger (Leap Energy Partners Sdn Bhd) & F. Rahmat (Leap Energy Partners Sdn Bhd)
P38	Biostratigraphic Real-time Well-site Support for a NW Palawan, Offshore Philippines Appraisal Well. C. T. Naih* (Sarawak SHELL Berhad), J. J. Lim (Sarawak SHELL Berhad) & R. Sandom (Sarawak SHELL Berhad)
P39	A Sedimentologic and Petrographic Perspective of the Miocene Stage IVA from the Klias Peninsula to Labuan Island T. D. Lukie* (Talisman Malaysia Ltd) & A. Balaguru (Talisman Malaysia Ltd)
P40	An Integrated Approach Towards Delineating Hydrocarbon Prospectivity in Untested Fault Blocks Within a Brown Field. A Case Study in B Field, Offshore Sarawak, Malaysia. A. Azami* (PETRONAS Carigali Sdn Bhd), A. Hashim (PETRONAS Carigali Sdn Bhd), N. Alias (PETRONAS Petroleum Management Unit), N. Ujal (PETRONAS Carigali Sdn Bhd), M. Bhattacharya (PETRONAS Carigali Sdn Bhd), A. Roy (PETRONAS Carigali Sdn Bhd), S. Pamungkas (PETRONAS Carigali Sdn Bhd) & T. Aldha (PETRONAS Carigali Sdn Bhd)
P41	Integrated Geoscience Interpretation of Selected Group B Sands In Beta Field, Malay Basin C. H. Sim* (ExxonMobil Exploration and Production Malaysia Inc) & F. Fahmi (ExxonMobil Exploration and Production Malaysia Inc)
P42	Geohazards Assessment, Data Integration and Visualization via ArcGIS M. Zulkifli* (Sarawak SHELL Berhad), D. A. Bean (Sarawak SHELL Berhad) & T.K. Tiong (Sarawak SHELL Berhad)
P43	The Evolution of Tiltmeter-Based Reservoir Monitoring: From Risk Mitigation to Production Optimization S. Marsic* (Pinnacle, a Halliburton Service), M. Machovoe (Pinnacle, a Halliburton Service) & W. Roadarmel (Pinnacle, a Halliburton Service)

THANKS TO.....

In addition to all the speakers, the organizers wish to thank the following persons for their valuable contributions to the PGCE 2012 technical program:

Technical Program Subcommittee:

Deva Gosh (Universiti Teknologi PETRONAS) co-chairman	Michael Challis (ConocoPhillips)
Ralph Kugler (Universiti Malaya) co-chairman	Michelle Tham (Schlumberger/ WesternGeco)
Azlina Anuar (PETRONAS Carigali)	Mohamad Rizam Sarif (ExxonMobil E & P Malaysia Inc.)
Bernard Pierson (Universiti Teknologi PETRONAS)	Mohammad Yamin Ali (PETRONAS RESEARCH)
Chung Lee Wong (Shell E & P)	Pedro A. Restrepo-Pace (Mubadala)
Craig Myers (Leap Energy)	Simon Molyneux (Talisman)
Firdaus Halim (PETRONAS RESEARCH)	Thomas Focht (Newfield Exploration Company)
Graham Hodgkiss (CGGVeritas)	Yashkor Yunus (Murphy Sarawak Oil Co., Ltd)
Jesmee Zainal Rashid (PGS)	Zuhar Zahir Tuan Harith (Universiti Teknologi PETRONAS)
Klaus Soffried (Halliburton)	

Reviewers:

Abdelaziz Abdeldayem (Universiti Teknologi PETRONAS)	John Phillips (Schlumberger)
Adam Betteridge (PSG Asia Pacific)	Juhari Ismail (PETRONAS Carigali)
Adriaan Bal (Baker Hughes)	Klaus Soffried (Halliburton)
Alain Morash (Total Malaysia E&P)	Lutz Riepe (PETRONAS Carigali)
Arjen Rolf (ConocoPhillips)	Maarten Wiemer (Shell E & P)
Arnout Everts (Leap Energy)	Marie Lefranc (Schlumberger)
Azlina Anuar (PETRONAS Carigali)	Michael Challis (ConocoPhillips)
Bernard Pierson (Universiti Teknologi PETRONAS)	Michelle Tham (Schlumberger/ WesternGeco)
Carl Curtis (ConocoPhillips)	Mohamad Rizam Sarif (ExxonMobil E & P Malaysia Inc.)
Chee Hui Sim (ExxonMobil E & P Malaysia Inc.)	Mohammad Yamin Ali (PETRONAS RESEARCH)
Chung Lee Wong (Shell E & P)	Mohd Rohani Elias (ExxonMobil E & P Malaysia Inc.)
Craig Myers (Leap Energy)	Patrick Gou (Newfield Sarawak Malaysia Inc)
Debnath Basu (Schlumberger)	Pedro A. Restrepo-Pace (Mubadala)
Deva Ghosh (Universiti Teknologi PETRONAS)	Peter Lee (PSG)
Eduard Kosa (Shell E & P)	Ralph Kugler (Universiti Malaya)
Erwin Adams (Shell E & P)	Scott Jaynes (ExxonMobil E & P Malaysia Inc.)
Fariz Fahmi (ExxonMobil E & P Malaysia Inc.)	Simon Molyneux (Talisman)
Firdaus Halim (PETRONAS RESEARCH)	Tanwi Basu (Schlumberger)
Graham Hodgkiss (CGGVeritas)	Thomas Focht (Newfield Exploration Company)
Hock Kuang Lim (ExxonMobil E & P Malaysia Inc.)	Vivian Cathey (Kebangsaan Petroleum Op. Co.)
Jan de Jager (University of Utrecht)	Yashkor Yunus (Murphy Sarawak Oil Co., Ltd)
Javier Guerrero (Universiti Teknologi PETRONAS)	Zuhar Zahir Tuan Harith (Universiti Teknologi PETRONAS)
Jesmee Zainal Rashid (PGS)	

Session Chairmen:

Deva Ghosh (UTP)	Mohd Hasni Hashim (PETRONAS EPTC)
Michelle Tham (Schlumberger)	Thomas Focht (Newfield)
Pedro Restrepo-Pace (Mubadala)	Jimmy Ting (Fugro Jason)
Vivian Cathey (KPOC)	Arnoud Everts (Leap Energy)
Lutz Riepe (PETRONAS Carigali)	Ralph Kugler (UM)
John Phillips (Schlumberger)	Sanjeev Bordoloi (Baker Hughes)
Maz Farouki (PGS)	Wan Ismail Wan Yusoff (UTP)
Sandeep K. Chandola (PETRONAS Carigali)	Mark Sams (Ikon Science)
Hans-Jurg Meyer (SHELL)	Cheng Foo Low (PETRONAS Exploration)
Jamlus Md Yasin (PETRONAS Exploration)	Carl Nottfors (CGGVeritas)
Chee Hui Sim (ExxonMobil)	Ahmad Riza Ghazali (PETRONAS EPTC)
Graham Hodgkiss (CGGVeritas)	Michael Challis (ConocoPhillips)
Mark Jones (Murphy Oil)	Richard Jones (Lundin)
Azhar Yusof (PETRONAS PMU)	Peter Abolins (PETRONAS Exploration)
Debnath Basu (Schlumberger)	Chung Lee Wong (Shell)

And of course the chairmen who stepped in at the last minute.

Fieldtrip Leaders:

Bernard J. Pierson (Universiti Teknologi PETRONAS)
Chow Weng Sum (Universiti Teknologi PETRONAS)
Abdul Hadi Abd. Rahman (Universiti Teknologi PETRONAS)
Mazlan Hj Madon (PETRONAS)
Narender Pendkar (PETRONAS Carigali)
Mohd. B. Kadir (PETRONAS Carigali)

Short Course Instructors:

Ahmad Riza Ghazali (PETRONAS)	Mark Sams (Ikon Science)
Deva Ghosh (Universiti Teknologi PETRONAS)	Jamaal Hoesni (PETRONAS)
Mehmet F. Akalin (PETRONAS Carigali)	Wan Ismail Wan Yusoff (Universiti Teknologi PETRONAS)
Lorie Bear (ExxonMobil)	Othman Ali Mahmud (PETRONAS)
M Nabil El Kady (PETRONAS Carigali)	Peter Abolins (PETRONAS)
Arthur Earl Barnes (PETRONAS)	Azlina Anuar (PETRONAS)
Nguyen Huy Ngoc (PETRONAS)	Zailani Abdul Kadir (Schlumberger)
Martin Stephen Brewer (PETRONAS)	Alexander Neber (Schlumberger)

PETRONAS Technical Review Committee

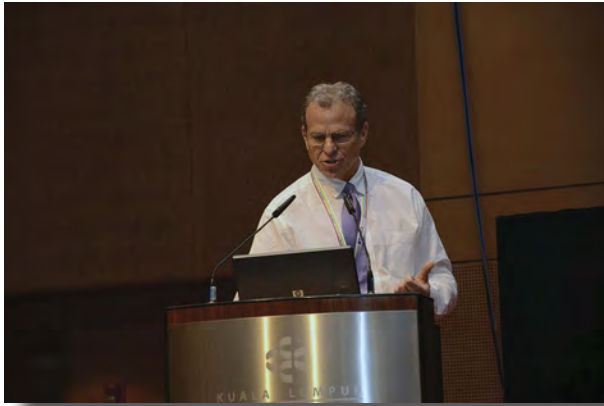
Joseph Justin Soosai (PETRONAS PMU)	Jamin Jamil B M Idris (PETRONAS PMU)
Badrul Hisam B Ismail (PETRONAS PMU)	Rizal B Abdullah (PETRONAS Group Corporate Affairs)

Others:

Meor Hakif (UM)
Malaysian Philharmonic Orchestra (MPO)







Marine Broadband Seismic Data Acquisition: PETRONAS Perspective

C. F. Low (PETRONAS Carigali Sdn Bhd), S. Chandola (PETRONAS Carigali Sdn Bhd),
Z. M. Zawawi* (PETRONAS Carigali Sdn Bhd), A. Aziz Muhamad (PETRONAS Carigali Sdn Bhd),
S. Kumar (PETRONAS Carigali Sdn Bhd), & M. Shah Sulaiman (PETRONAS Carigali Sdn Bhd).

Introduction

Broadband seismic data is the primary requirement for improving resolution, enhanced imaging of thin beds and stratigraphic features, seismic inversion etc. In recent past, advancements in marine seismic acquisition have evolved around improving the bandwidth of recorded seismic signal. These include the improvement in the low frequency response of the streamer, higher fidelity of recording units and more recently, broadband acquisition techniques aimed at attenuating the source and receiver ghost notches.

The hydrophone in a towed streamer always records two wavefields that constructively interfere with each other. The up-going pressure wavefield propagating directly to the hydrophone from the earth below and the down-going pressure wavefield reflected from the “free air” sea surface immediately above the streamer. The consequence is that a series of “ghost” notches are introduced into the frequency spectra and the reflection wavelet is undesirably elongated, reducing the temporal resolution. For zero angle reflections, the frequency of notches is always at 0 Hz and integer multiples of $V_w/2d$ where V_w is the speed of sound in water and d is the receiver depth. In conventional acquisition, the streamer is towed close to the sea surface so that the first ghost notch occurs beyond the desired high frequency band. However, this results in attenuation of the lower frequencies (Fig. 1). Thus, streamer depth in a conventional marine acquisition has historically been a trade-off between low and high frequency requirement.

Marine Broadband Acquisition Technologies

Different acquisition technologies have been proposed to overcome the receiver ghost notch problem and deliver an improved low and high frequency spectral response. These include deep-towed dual sensor streamers, the variable depth streamer and pairs of over-under streamers towed at different depths. Currently, the following three proprietary marine acquisition techniques are commercially available in the market, which use different ways to deliver broadband seismic data:

- **Dual sensor streamer:** Dual-sensor streamer acquisition technique combines collocated pressure and velocity sensors in a single streamer. The spectral notches in the frequency spectrum of the velocity sensor are complimentary to those for hydrophone. Thus the combination of pressure and velocity data removes the ghost event (down-going wavefield) and therefore delivers broader signal frequency bandwidth.

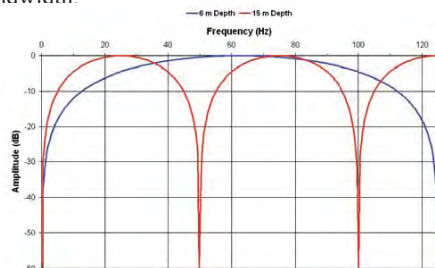


Fig. 1: Receiver ghost amplitude spectra for a hydrophone towed at 6 m (blue) and 15 m (red) depth. The wavefield is assumed to have vertical propagation (zero angle of incidence).

- **Variable depth streamer:** In this technique, a combination of solid streamers and a variable depth towing configuration is used to deliver an improved bandwidth in the final image. In variable depth configuration, the receiver ghost notches vary along the cable and this ‘notch diversity’ is exploited by the proprietary deghosting and imaging techniques (e.g. joint deconvolution and mirror migration) to enhance the signal bandwidth.
- **Over-under streamer:** This acquisition technique uses a sparse deep towed marine acquisition spread in combination with a conventional shallow towed spread. The shallow spread gives the high frequencies while the deep spread provides the enhancement in low frequencies and therefore can be more sparsely sampled.

Broadband Technology Application

PETRONAS Carigali has applied each of the above marine broadband acquisition technologies over the past couple of years to address some specific seismic imaging issues in Malaysia. These technologies have been applied to different geological settings and part of the data is still under processing. We present here our current assessment of the potential of these technologies based on the results of these surveys and the challenges which need to be overcome before their full potential is exploited.

Dual sensor streamer surveys

Two dual sensor 2D streamer surveys were carried out offshore Malaysia in 2009-10. In the first survey area, hydrocarbons have been discovered in pre-carbonate stratigraphic clastic sequences. However, structural interpretation, seismic attribute analyses and resources evaluation are hampered due to poor quality of the conventional 3D streamer data, especially below the thick carbonate formation (Fig. 2a). The dual sensor streamer survey was intended to improve the seismic image of the pre-carbonate sequence. Several 2D lines were shot with a 6 km long dual sensor streamer towed at 25m depth. The multi-level source was also tested along one 2D line to address the source notch issue. A few 2D lines were acquired on top of the legacy seismic lines and processed through pre stack time migration concurrently, to allow a fair comparison of the conventional and dual sensor streamer data. Key data processing steps included low frequency compensation (LFC) for the velocity sensor data and dual sensor summation. The second survey was a regional 2D survey, acquired with a streamer length of 8 km to assess the hydrocarbon potential of deeper sediments.

The comparison of processed datasets shows that a combination of dual sensor streamer and multi-level source achieves improved seismic image at both shallow and deeper levels (Fig. 2a & 2b). However, a significant portion of the improvement in the data quality in the deeper portion is contributed by the multilevel source. Also, the improvement in the target zone remains marginal, primarily because of the thick carbonate section which absorbs and scatters major part of seismic energy in a 3D sense. The future dual sensor streamer acquisition in such geological setting should probably be of 3D nature with a multi-level/detuned source array and probably a

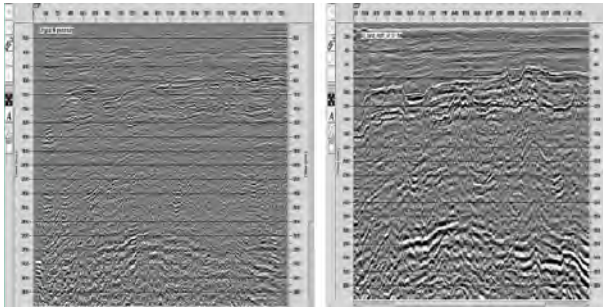


Fig. 2a: (left) PreSTM section of Legacy 2D seismic data reprocessed using identical processing flow as the dual sensor streamer data. Fig. 2b: (right) PreSTM section of pilot test data recorded with dual sensor streamer and multi-level source. The target pre-carbonate sequence is marked in red ellipse & the deeper prospects in blue ellipse. Improvement at both shallow and deeper levels is observed in the dual sensor streamer data.

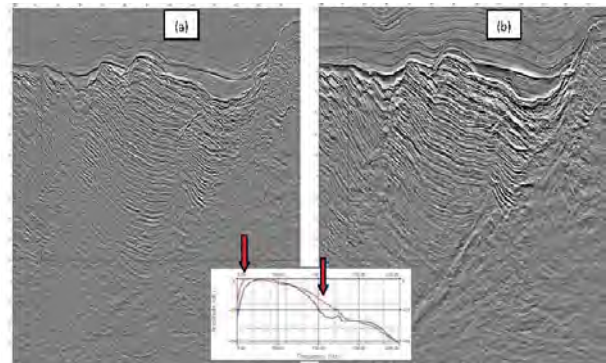


Fig.3: Fast track PreSTM sections from the variable depth streamer survey. (a) Conventional 2D seismic data and (b) Variable depth streamer data. Significant improvement is observed in overall quality of the image in the section to the right as well as in the signal bandwidth at both low and high frequency ends (inset-red arrows). The two lines were located on top of each other to allow a fair comparison.

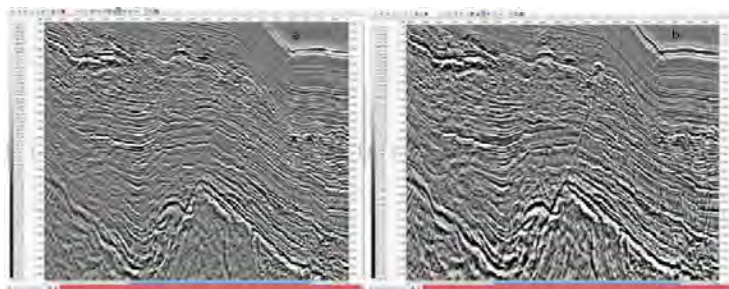


Fig.4: Fast track 2D PreSTM sections from the over-under streamer survey. (a) shallow streamer (b) combination of shallow and deep streamer and (c) amplitude spectrum of shallow and combination of shallow and deep streamer for full window. Incremental improvement is observed in overall quality of the image in the section to the right (above) as well as in the signal bandwidth at low frequency ends (inserted red arrow-left)

multi-azimuth (MAZ) or a wide azimuth (WAZ) survey, for better results.

Variable depth streamer surveys

Three variable depth 2D streamer surveys were carried out by PETRONAS Carigali in the year 2011, offshore Malaysia with the objective to improve the imaging of both shallow and deep clastic targets. The depths of the exploration targets in these areas vary between 1 to 7 km which necessitated broadband acquisition to preserve both the low as well as the high frequencies. The data were acquired with 6 km long streamer in the shallow water area and with 8 km long streamer in the deep water area. The streamer depth varied from 5m at the shallow end to 50m at the deep end. The data were processed through PreSTM and the key steps included the proprietary joint deconvolution and mirror migration to remove the receiver ghost notches.

A comparison of the fast track PreSTM outputs of the conventional and the variable depth streamer datasets (Fig. 3a and 3b) reveals that the variable depth streamer delivers a much improved seismic image and amplitude spectrum at both low and high frequency ends.

Over-under streamer surveys

A 3D over-under streamer survey was conducted by PETRONAS Carigali in 2010 in deepwater offshore Malaysia. The depth of the clastic targets in the survey area varied between 2-6 km and the acquisition was carried out using two sets of 8 km long streamers. The shallow spread consisting of 8 streamers was towed at a depth of 7m (@ 100m separation) and the deep spread consisting of 2 streamers (@400m separation) towed at a depth of 20m.

The key steps in data processing included-wavefield interpolation for the deeper streamers and proprietary optimized deghosting scheme to deliver a broadband spectrum. Based on the fast track processing, the over-under combination shows improvement in the overall signal bandwidth (Fig 4). However, at the time of writing this paper, the data processing is still ongoing and the final evaluation of the results shall be based on the processed outputs.

PETRONAS Perspective

As evident from the above examples, each of the broadband acquisition technologies described here enhances the signal bandwidth and therefore improves the seismic imaging through effective removal of receiver ghost. In addition, these technologies offer the following operational and geophysical advantages over the conventional towed streamer acquisition:

- Better estimation of quality factor (Q) during data processing
 - Better S/N ratio and extended operational window due to deep tow depth
 - Better potential for seismic inversion due to richer low frequency content
- Some of the challenges which need to be addressed to effectively implement and leverage these technologies include:
- Application domain for dual sensor, variable depth and over-under streamer technologies is currently confined to approximate water depths > 35m, >70m and > 40m respectively due to the streamer towing configuration.
 - Each of these technologies need to be combined with multi-level or detuned sources in order to remove the source ghost. The dual sensor streamer has already been combined with the newly introduced multi-level/detuned source to address

the source notch issue.

- The processing of the above datasets is proprietary up to a certain stage and therefore restricted to the respective acquisition contractor.
- In dual sensor streamer, the low frequency portion (<15-20 Hz) of the velocity sensor currently needs to be reconstructed using the pressure sensor data. This limits the usage of velocity sensor data for low frequency enhancement.
- In variable depth streamer, the key process of deghosting using proprietary joint deconvolution and mirror migration is still under evaluation by the users, especially in terms of amplitude preservation.
- For over-under streamers, the trade-off between the wavefield sampling requirement and the separation between the deep streamers is critical in terms of the quality of end results. Also, the vertical and lateral alignment of the two sets of streamers needs to be maintained within tight tolerances for effectiveness of the wavefield interpolation.

Conclusion

The current focus of exploration has shifted to stratigraphic and deeper plays. The broadband surveys conducted by PETRONAS Carigali have demonstrated their ability to enhance the seismic bandwidth and address some of the imaging issues commonly encountered in Malaysian basins. However, the ultimate choice of the optimum technology should be based on the geological setting, operational environment and the cost and the quality of end results may also vary accordingly. In order

to realize the full potential of these technologies, some of the operational and data processing challenges mentioned above need to be addressed. The future marine seismic acquisition trends are expected to involve multi-azimuth (MAZ), wide azimuth (WAZ) or full azimuth (FAZ) implementations of the broadband acquisition technologies.

Acknowledgement

Authors would like to thank the PETRONAS management for the permission to publish this work. Direct and indirect contribution by several colleagues in PETRONAS and the service providers (M/s PGS, CGGVeritas and WesternGeco) is also gratefully acknowledged.

References

- Moldoveanu, Nick et.al., 2007, Over/under towed-streamer acquisition: A method to extend seismic bandwidth to both higher and lower frequencies. *The Leading Edge*, January issue, 41-58.
- Soubaras, Robert and Dowle, Robert, 2010, Variable-depth streamer – a broadband marine solution. *first break*, December issue, 89-96.
- Tenghamn, R., Vaage, S., and Borresen, C., 2007, A dual-sensor, towed marine streamer; its viable implementation and initial results. *Annual Meeting Expanded Abstracts, SEG*, 989-993.

(*Corresponding Author Email: zabudz@petronas.com.my, subodh_kumar@petronas.com.my)

Simultaneous Sources: The Inaugural Full-Field, Marine Seismic Case History from Australia

I. Moore* (WesternGeco), D. Monk (Apache Energy Ltd.),
L. Hansen (Apache Energy Ltd.) & C. Beasley (WesternGeco)

Introduction

Simultaneous-source acquisition is an established technology for land data, and has a proven record of providing enormous increases in acquisition efficiency. A plethora of associated acronyms bear witness to the rapid development of the technology over recent years. Notable methods are slip-sweep (Rozemond, 1996), HFVS (Allen et al., 1998), DSSS (Bouska, 2010), ISS (Howe et al., 2008) and DSS (Bagaini and Ji, 2010). A useful summary was provided by Bagaini (2010). All of these methods provide efficiency gains through firing two or more sources sufficiently close together in time that the recorded energy interferes. The interference is then handled in processing.

The corresponding techniques for marine acquisition have seen somewhat slower development, despite being introduced over a decade ago (Beasley et al., 1998). The main reasons for this are consequences of the extra constraints marine acquisition places on its sources. Specifically, marine sources typically lack the ability to shape the source wavelet as can be done for land vibrators. Moreover, each source must move continuously at constant speed, and introducing extra source boats to achieve significant distance separation between sources is expensive.

Initially, most marine, simultaneous-source studies involved wide-azimuth (WAZ) data (Stefani et al., 2007; Fromyr et al., 2008; Dragoset et al., 2009). WAZ acquisition typically involves multiple source vessels, and may require several passes for each line. Simultaneous sources can be used to reduce the shot interval for each pass, thereby reducing aliasing effects or improving efficiency by reducing the number of passes that are required.

In this study, we consider the application of simultaneous source (SimSource™) technology to a conventional, narrow-azimuth (NAZ) survey. Data from the region have previously been acquired using a standard “flip-flop” technique, in which the sources fire alternately every 18.75 m, leading to a 37.5-m shot interval for each source line. The use of simultaneous sources, such that both sources are fired every 18.75 m, halves the shot interval for each source line, thereby providing better-sampled data for coherent noise attenuation and imaging. No extra vessels are required, and the overall acquisition time is unaffected.

In principle, the SimSource methodology is very simple. The sources are dithered relative to one-another to enable separation using a sparse inversion technique (Moore et al., 2008; Akerberg et al., 2008). Once separated, the data can be processed conventionally, and will benefit naturally from the improved sampling. The key to success is, therefore, the quality of the source separation. To mitigate the risk associated with the separation process, concept studies were performed on similar data sets. These studies indicated that source separation was possible at the proposed shot interval.

The SimSource separation process depends on the dithers, and does not require that the sources be physically separated by a significant distance. In fact, the close proximity of the two sources for this survey ensured that the relative signal strengths were comparable, avoiding problems that can occur if the signal from one source dominates the record.

Only minor software modifications to the Q-Marine™

acquisition system were required to acquire data in SimSource mode. However, some of the standard quality control processes were no longer applicable because of the interference between sources, and additional processes were required to check that the firing times and navigational data were correct. In practice, these processes worked well, and no specific problems were encountered.

Processing is ongoing, but source separation results so far, both for prestack data and for stacks of imaged data, indicate that the separation step performs well, as expected from the concept studies.

Concept Studies

Concept studies were performed to assess the viability of the method for the proposed survey. In the primary study, a line was acquired in both conventional and SimSource modes. The conventional data had a 12.5-m shot interval, and were used to simulate SimSource data with 12.5-m, 18.75-m and 25-m shot intervals (using shot interpolation where necessary) by adding shot gathers to dithered versions of themselves. The separated data can then be compared to the original data to assess the quality of the separation process. It should be noted, however, that we cannot expect to separate ambient noise because it is not source-generated. The results indicated that separability was reasonably good, but decreased, as expected, with increasing shot interval.

Real SimSource data were shot with 12.5-m and 18.75-m shot intervals, allowing separation tests to be run at the same shot intervals as for the simulated data. The results validated the conclusions from the simulated data tests, and it was decided that SimSource acquisition with an 18.75-m shot interval was viable for the upcoming survey.

As a final test, separation tests were run on a simulated SimSource line from the proposed survey area to have water depths and noise levels that were representative of the proposed survey. The separation results (Figure 1) were also considered satisfactory.

Data Acquisition

The acquisition geometry, apart from the use of SimSource, was a conventional NAZ geometry using 10 x 6000-m Q-Marine cables with 75-m separation. The two sources were fired simultaneously (apart from the dithers) every 18.75 m. One source was considered to be the “master” and shot on position. The “dithered” source fired with prescribed time differences (dithers) relative to the master source. The dithers were essentially randomly distributed over a small time window.

Conventional QC products were used whenever they were appropriate. In addition, QC products were designed specifically to check that the firing times were in agreement with the planned dithers. Two main methods were used to do this:

1. Passively separated data were inspected in the common channel domain for both sources (Figure 2). Passive separation simply involves aligning the data in time such that time zero corresponds to the firing time for the chosen source. The energy associated with that source becomes coherent, and any observed

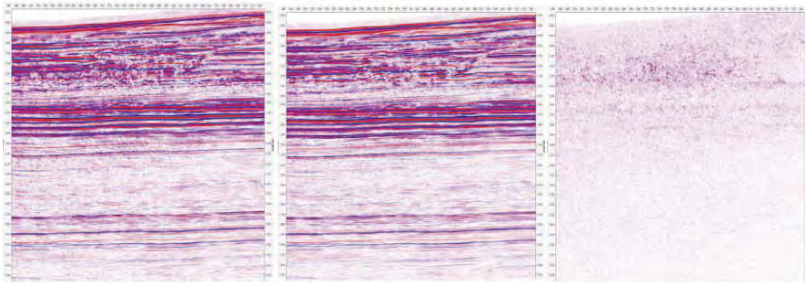


Figure 1: Conventional (left) and simulated SimSource (centre) images from the concept study. The difference (right) indicates that signal loss is minor, and some of this signal loss is due to imperfections in the interpolation used to create the conventional data set.

lack of coherency is an indication of a potential problem with the associated dither.

2. Autocorrelations were computed and the secondary peaks, which are related to the timing dithers, were auto-picked and compared with the planned dithers to provide an automated QC. Any discrepancies were then investigated manually.

In practice, the SimSource aspects of the acquisition proceeded without any problems. Some lines were reshot due to weather, and there was a small amount of infill.

Method and Results

Recorded SimSource data differ from conventional data in that each trace has two shot locations associated with it, as well as a dither time. At this stage, the data volume is the same as for the equivalent conventional survey. Any processes applied before separation must preserve the signal from both sources. The separation process cannot, of course, separate noise that is not source generated, and it is, therefore, desirable to remove this noise component prior to separation. Noise attenuation of this kind must generally be run in the common shot domain where the signal from both sources is coherent. In other domains, the signal from one source will not be coherent and the noise attenuation process is likely to attenuate that signal.

Active separation was performed using a sparse inversion method (Moore et al., 2008) applied to common channels. Sparseness is promoted using a time-domain, linear Radon transform that effectively separates each trace into estimated components for each source, together with a (small) residual of unseparated energy. Figure 3 shows an example that demonstrates the effectiveness of the separation process. The residual contains both ambient noise and signal that has not been modelled, typically because it is weak or complex. To avoid attenuating this signal, the residual was added back to the separated data for both sources. After separation, the data volume is doubled and each trace is associated with only a single source. Conventional processing can be used from this point onwards.

Conclusions

Although data processing is not yet complete, a preliminary conclusion is that the SimSource acquisition technique was successful. No issues were encountered during the data acquisition phase, indicating that the method is sufficiently robust to be used on full-scale 3D surveys. The critical source-separation step in the processing sequence performed well. There was very little signal leakage between sources, and results so far have been in accordance with expectations based on the concept studies.

Whilst it is often difficult to make a quantitative evaluation of the benefits associated with the application of such new technology, in this case, a conventional survey was acquired within three months of the SimSource survey with significant overlap in the imaged areas. The line orientations were not

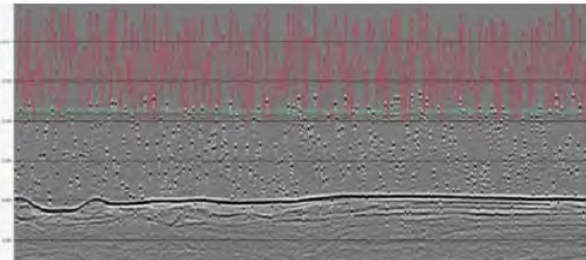


Figure 2: Part of a common channel section after passive separation for the dithered source, as used for onboard QC. The coherency of the water bottom reflection and the direct arrival (green graph) indicate that the data were acquired using the planned dithers. The red graph shows the predicted direct arrival times for the master source, taking the dithers into account. The close agreement between this graph and the observed direct arrivals also indicates that the data were acquired correctly.

the same and the processing was performed separately, but expectations based on previous experience are that the SimSource acquisition will yield better attenuation of the coherent noise, and that doubling the fold will lead to an improved signal-to-noise ratio in the image.

This project involved the use of advanced technology in a new area, and minimizing the associated risks was extremely important. The preliminary concept tests were very valuable in providing confidence that the method would work, and in assisting with the survey design.

Although the motivation for this project was to acquire well-sampled data to improve our ability to attenuate coherent noise, SimSource technology also has potential advantages with respect to ambient noise. The acquired data have higher signal-to-noise ratio than the equivalent conventional data because the signal content of each trace is increased. There exists, therefore, the potential to shoot SimSource data in more adverse weather conditions than would be used for conventional data, although it is, of course, important that the presence of the ambient noise does not affect signal separability too much. This will be the subject of further study.

Acknowledgements

The authors would like to acknowledge the contributions made to the acquisition and processing of the SimSource data, as well as to the preparation of this manuscript, by Jim Ross, Paul Anderson and Rob Kneale (Apache), and by Bart Szydluk, Jason Gardner, Richard Bisley, Chris Semeniuk, Dea Mustafa Hudaya, Ted Phillips and Morten Svendsen (WesternGeco), as well as the crew of the Western Spirit.

We also thank the JV partners for blocks WA-290-P and WA-450-P, namely Apache Energy, Finder Exploration, Santos, OMV Australia, Nippon Oil Exploration and Tap Oil, for permission to publish.

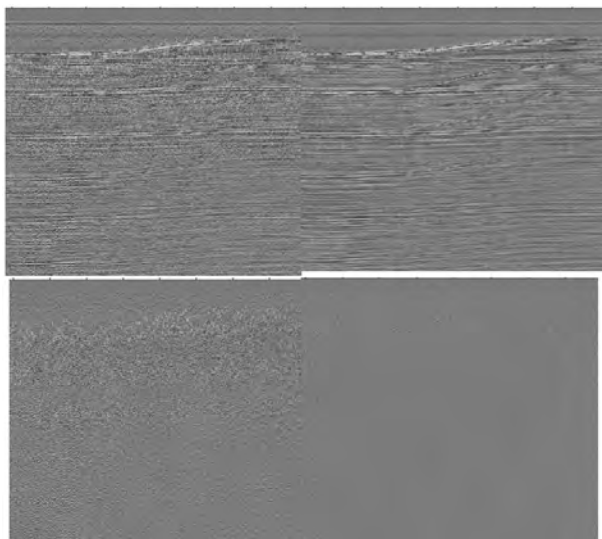


Figure 3: Separation of part of a common offset plane. The input data (top left) are separated into S1 (top right) and S2 (bottom left) components, plus a residual (bottom right) of unseparated energy. The residual is small and contains mainly noise. The S2 data are shown in S1-time and the lack of coherent energy in this section indicates a low level of leakage. In S2-time, the separated S2 data look much like the separated S1 data due to the close proximity of the sources. About 3 s of data are shown, and the lateral extent is about 7.5 km.

References

- Akerberg, P., Hampson, G., Rickett, J., Martin, H., and Cole, J., 2008, Simultaneous source separation by sparse Radon transform: 78th Meeting, SEG, Las Vegas, Expanded Abstracts, 2801-2805.
- Allen, K.P., Johnson, M.L., and May, J.S., 1998, High Fidelity Vibratory Seismic (HFVS) method for acquiring seismic

data: 68th Meeting, SEG, New Orleans, Expanded Abstracts, 140-143.

- Bagaini, C., 2010, Acquisition and processing of simultaneous vibroseis data: Geophysical Prospecting, 58, 81-99.
- Bagaini, C., and Ji, Y., 2010, Dithered slip-sweep acquisition: 80th Meeting, SEG, Denver, Expanded Abstracts, 91-95.
- Beasley, C.J., Chambers, R.E., and Jiang, Z., 1998, A new look at simultaneous sources: 68th Meeting, SEG, New Orleans, Expanded Abstracts, 133-135.
- Bouska, J., 2010, Distance separated simultaneous sweeping for fast, clean, vibroseis acquisition: Geophysical Prospecting, 58, 123-153.
- Dragoset, W.H., Li, H., Cooper, L., Eke, D., Kapoor, J., Moore, I., and Bealsey, C., 2009, A 3D wide-azimuth field test with simultaneous marine sources: 71st Meeting, EAGE, Amsterdam, Extended Abstracts, Z037.
- Fromyr, E., Cambois, G., Loyd, R., and Kinkead, J., 2008, Flam – A simultaneous source wide azimuth test: 78th Meeting, SEG, Las Vegas, Expanded Abstracts, 2821-2825.
- Howe, D., Allen, A.J., Foster, M.S., Jack, I.J., and Taylor, B., 2008, Independent simultaneous sweeping - a method to increase the productivity of land seismic crews: 78th Meeting, SEG, Las Vegas, Expanded Abstracts, 2826-2830.
- Moore, I., Dragoset, W., Ommundsen, T., Wilson, D., Ward, C., and Eke, D., 2008, Simultaneous source separation using dithered sources: 78th Meeting, SEG, Las Vegas, Expanded Abstracts, 2806-2810.
- Rozemond, H.J., 1996, Slip-sweep acquisition: 66th Meeting, SEG, Denver, Expanded Abstracts, 64-67.
- Stefani, J., Hampson, G., and Herkenhoff, E.F., 2007, Acquisition using simultaneous sources: 69th Meeting, EAGE, London, Extended Abstracts, B006.

Geophysical Innovation and Technology - Meeting Challenges of a Transition Zone OBC Survey in Malaysia

S. K. Chandola* (Petronas Carigali Sdn Bhd), M. Zabuddin Zawawi (Petronas Carigali Sdn Bhd), C. T. Law (Petronas Carigali Sdn Bhd), R. Faizal (Petronas Carigali Sdn Bhd), M. Adura (Petronas Carigali Sdn Bhd), R. Roslan (Petronas Carigali Sdn Bhd), J. Ismail (Petronas Carigali Sdn Bhd) & M. Asraff Ariff (Petronas Carigali Sdn Bhd)

Introduction

A Transition Zone Ocean Bottom Cable (TZ-OBC) survey was recently conducted by PETRONAS Carigali in offshore Sarawak. The OBC survey covered the onshore and offshore region with water depth up to approximately 30m. TZ-OBC technique was adopted due to flexibility of acquisition geometry, greater surface consistency and more flexibility in working around obstructions. The geological setting in the survey area is characterized by deltaic setting dominated by growth faults and strike slip faults. The faults play significant role in hydrocarbon migration and accumulation. The OBC survey was aimed at enhancing fault definitions and improving reservoir characterization, prospect identification and maturation.

Operational challenges

TZ-OBC survey posed several technical and operational challenges. These include:

Diverse operational environment

The area of operation could broadly be divided into three parts;

- The shallow water portion comprising of water depth in the range 7-30m. Dual sensor OBC system was deployed in this part together with the large air gun array (~1780 cu.in).
- The transition zone extending from water depth of 7m to the coast. This region is operationally most challenging due to the surf zone, tidal variations etc. Single hydrophones flushed to depth of 6m (Fig. 1a) were deployed in this portion together with the smaller air gun array (~680cu.in). Marsh phones in clamshell housing (Fig. 1b) were deployed up to the coast where flushing of hydrophones was not feasible due to the Marine Park.
- The onshore component of the survey was introduced relatively later in the project, based on exploration priority. Accordingly, vibroseis units were mobilized together with the Geospace standalone recording nodes (Fig. 1c) for acquiring data in this portion.

Noise Characteristics

The following types of noise were observed on the field data:

- Seismic interference caused by the 3D streamer survey being acquired ~30km from the OBC survey. The data was also affected by the noise from vessel movement and drilling activities.
- Mud-roll affecting both the geophone and the hydrophone components.
- Random noise occasionally observed on the data due to the wave action and swell in the shallow water portion.

During the in-field data processing, the mud-roll and the random noise were handled using an FK filter more effectively in common-receiver domain than the common-shot domain, due to finer sampling in receiver domain (Fig. 2a and 2b).

Sub-surface coverage gaps

- The eastern boundary of the OBC survey required an onshore component of sources and extended receiver lines in order to improve fold coverage near the coast (Fig. 3a and 3b).

- Part of the survey area was located inside the marine park and there were pipelines and platforms in the vicinity of survey area. Prior to the commencement of the seismic data acquisition, bathymetry survey was conducted in order to study any potential subsurface hazards. Meticulous acquisition management and coverage analysis were adopted to maintain desired fold coverage and offset-fold distribution throughout the survey area.

Data Acquisition workflow

Survey design

Industry standard 3D survey design and analysis software was used to design the acquisition geometry. Various 3D attributes like fold coverage, offset and azimuth distribution, average stack response; source and receiver effort etc. were generated for candidate designs for comparison.

The following design was adopted for data acquisition based on the technical, operational and economic considerations:

Bin Size : 25m x 12.5m	Type of Geometry : Orthogonal (Full Swath Roll Extended Salvo)
Nominal Fold : 80	No. of Channels per Receiver Lines : 200
No. of Shots / Salvo : 96	No. of Receiver Lines in a Patch : 4
Receiver Interval : 50m	Receiver Line Interval (RLI) : 300m
Source Interval : 25m	Source Line Interval (SLI) : 250m

Operational planning

Information from the detailed bathymetry survey and the DGPS survey in the onshore portion was used to determine the optimum source and receiver configuration for the survey area. Intelligent orientation of the source lines and shooting during high tide resulted in significant gains in sub-surface coverage (Fig. 4).

The following measures were taken to improve the operational efficiency and sub-surface coverage;

- No dynamite shots due to environmental restriction and habitation.
- Reduction in receiver group interval from 50m to 25m for the onshore portion.
- Adding infill source lines parallel to the shore line in the costal part.
- Air gun array deployment in the river to compensate the middle and far offsets near the coast.
- Deployment of vibroseis units on the beach to improve sub-surface coverage.

Dynamic acquisition

Near-real time monitoring of the 3D coverage was adopted to monitor the sub-surface coverage and modify the survey design as and when required. Some of the steps taken included;

- Additional infill sources to compensate for the fold drop in the anchorage area.
- Considering the cost of line clearing and bridging in swamp area, receiver undershoot was adopted to recover the mid and far offsets.

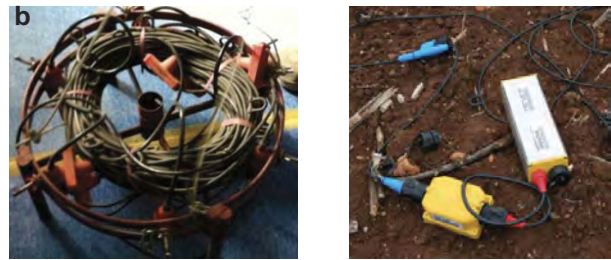
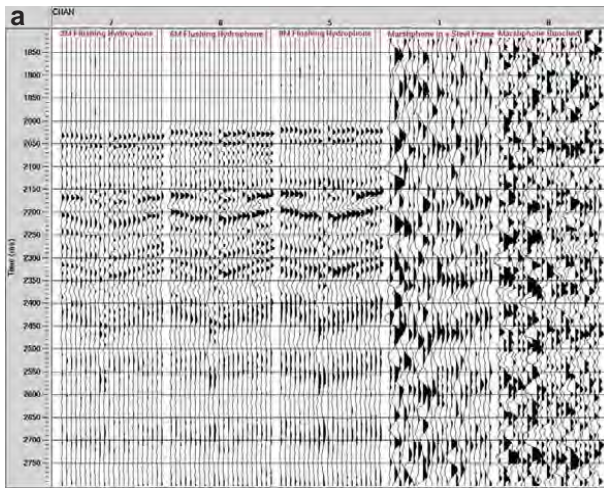


Fig.1a: Raw data comparison between 3, 6 and 9 meters flushing depths shows that deeper flushing gives better quality data. Marsh phones in clamshell housing have a better quality data compared to the bunched ones. Fig.1b: Clamshell marsh phones. Fig.1c: GeoSpace Seismic Recorder (GSR).

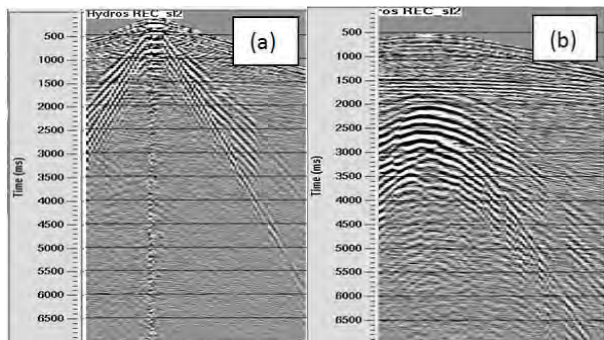


Fig.2: Typical hydrophones data from the survey (a) shot gather and (b) receivers gather. Common receiver domain is the appropriate for applying FK filtering.

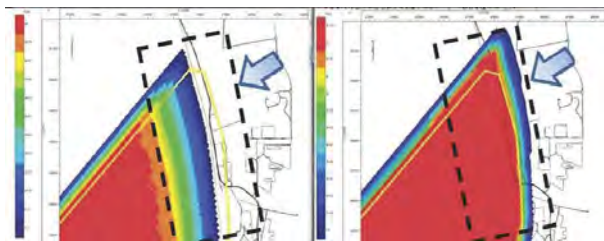


Fig.3a (left): Original design : Sources until 3 meter water depth and receiver lines upto the shore. Fig.3b (right): Infill Source in shallow water and onshore receiver line extension from shore.

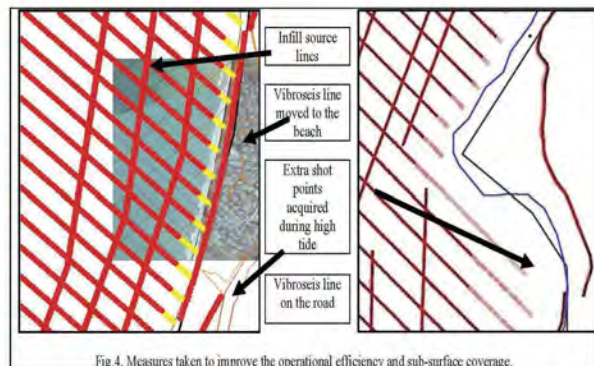


Fig.4. Measures taken to improve the operational efficiency and sub-surface coverage.

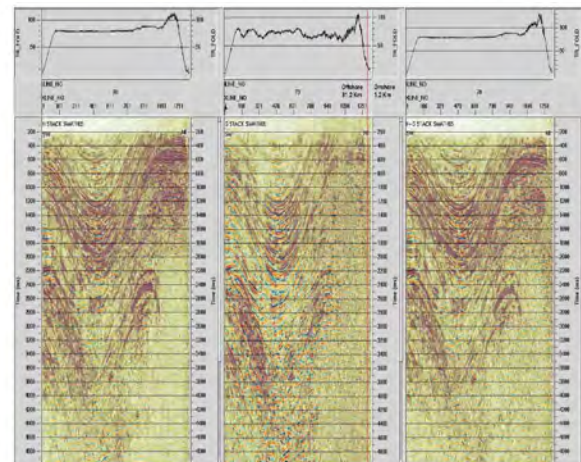


Fig. 5. A typical brute stack image from the survey showing overall good data quality. Hydrophone (left), Geophone (centre) and Summed stack (right).

Data Quality

A three tier Quality Assurance and Quality Control system was implemented throughout the survey consisting of stringent QC by contractor, onsite QC representatives and the specialized geophysical and geomatics team of PETRONAS. Excellent interaction amongst the crew, data processing group and the seismic interpretation team helped in ensuring good quality of seismic and positioning data (Fig.5).

Geophysical innovation

The Geospaces Seismic Recorder (GSR) is an autonomous, light weight and cable-less onshore nodes recording system. For the first time, this system was used in Malaysia. It allowed flexibility of deployment and reduced the manpower needed to deploy and maintain the spread. It also helped immensely in minimizing the environmental impact and improving the efficiency and HSE aspects of the survey.

Conclusion

The data acquisition was completed in a safe and environment friendly manner, within the allocated time frame and with significant cost savings. Excellent sub-surface coverage and data quality was achieved using a robust acquisition workflow combined with innovative acquisition techniques. The results of the survey are expected to deliver a high quality 3D volume to accelerate the exploration and appraisal activity in this area.

Reference

- S.K. Chandola, K. Ramakrishna, A.K. Sharma, ONGC, India; Nabeel Yassi, PGS Onshore, Houston; A. Saha, M.V.R. Murthy, A. Sanyal, ONGC, India, 2003, Dynamic Fold Solutions for Improved Sub-surface Imaging: A Transition Zone 3D-OBC Survey in East Coast of India, SEG Expanded Abstracts.

Marine CSEM with A Novel Towed Acquisition System

F. L. Engelmark* (PGS Asia Pacific Pte Ltd), J. Mattsson (PGS) & J. Linfoot (PGS)

Introduction

Marine controlled source EM has ever since its inception been based on a sparse grid of stationary receivers placed on the sea-floor and a dipole source towed close to the sea-floor. An early survey is described by Ellingsrud et al. (2002). Further evaluations followed by Amundsen et al. (2004) and by Jurgen et al. (2009). The receivers contain all the signal recording equipment together with very accurate clocks. When the survey is finished, the receivers are recalled to the surface where they are collected. The data is then downloaded, quality controlled and processed.

Towed EM, as described by Anderson and Mattsson (2010), has numerous advantages:

- Improved efficiency: source and receiver towed from the same vessel.
- Operationally similar to marine seismic.
- Real time monitoring and QC of source and receiver cable.
- On-board pre-processing.
- Dense sub-surface sampling.
- Receivers towed above the seafloor. The influence of strong local anomalies at the seabed is minimized.
- Facilitates simultaneous acquisition of EM and 2D seismic.

The reason towed EM has not been available until now is that the relative movement between the receiver sensors and the seawater generate a voltage that is typically much larger than the signal voltage. This was a crucial issue that had to be resolved before bringing the system to the market.

The two surveys described here were acquired in the North Sea. The Peon gas field is located very shallow at 540 m below sea-level with 380 m water depth. The second survey was over the Troll Oil and Gas field where the water depth is 320 – 350 m and the target depth is around 1,100 – 1,200 m below mud-line. Both surveys were successful and the data was processed and inverted to delineate all targets.

The commercial towed EM system

The acquisition system shown in Figure 1 below is operationally similar to 2D seismic.

The EM dipole source was 400 m long for the Peon survey and 800 m long for the Troll survey. The source strength was in both cases 800A and the dipole was towed 10 m below the sea surface. The EM receiver cable was towed at a depth of 100

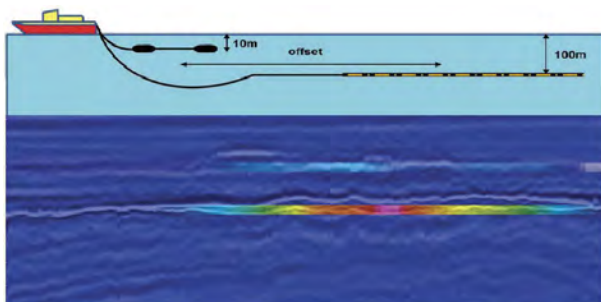


Figure 1: Schematic layout of the towed acquisition system showing the EM dipole-source, receiver-cable and the seismic streamer. A preliminary unconstrained inversion of the Peon reservoir is shown by warm colours in the subsurface.

m and had offsets from 2,500 m to 5,500 m. The conventional seismic streamer was towed at 6 m.

The commercial system introduced in 2012 differs in the following aspects: The strength of the source current is increased to 1,500 A, and the receivers range in offsets from 1,000 – 7,300 m. When combined with a seismic streamer for simultaneous acquisition, the dual-sensor de-ghosting streamer will be implemented.

Any kind of source signal can be used. So far we have tried the pseudo random binary sequence (PRBS), a standard square-wave, and an optimized repeated sequence (ORS), which can be described in terms of spectral content as a square-wave with the addition of the even harmonics.

The towing speed was 4 knots and the acquisition parameters are shown in Table 1 below. Notice that the source length was reduced to half the nominal length for the Peon survey, since the field is so shallow.

Following deconvolution and noise reduction the amplitude and phase spectra of the measured signal were compared with the modelled signal for a range of offsets. The agreement between modelled and measured data was found to be very good.

The Peon gas field

The Peon gas field is located very shallow at only 540 m below sea-level whereof 384 m is the water depth. The reservoir thickness in the discovery well is 33 m with recoverable gas at the top 18.5 m followed by 9 m residual gas and a 5.5 m brine layer at the bottom. The target is easy to detect, but we wanted high quality data to confirm the inverted values of intersecting survey-lines show similar absolute values at the point of crossing, and this was confirmed. We also found that there are some differences between the areal extent of the field as mapped and published based on seismic data and the edge detection defined by the EM-data. This is to be expected and the EM boundary is more likely to show the economic limits of the field, whereas the seismic can show volumes with very low gas saturation that is unlikely to contribute to the recoverable volumes of gas. Seismic can also resolve very thin gas-charged reservoir sections that have too low transverse resistance to be detected by the EM system.

In Figure 2 below the QC result is shown for the inverted volume. A group of 10 closely spaced parallel lines were acquired to create a 3D image of the northern part of the gas charged reservoir. This also gives us an idea of how much spatial variation in transverse resistance can be seen within the reservoir. Then there are a set of longer acquisition lines placed along the main axis of the gas field and one line investigates

Table 1: Acquisition parameters for the Troll and Peon Fields. Nominal towing speed was 4 knots.

Parameter	Peon	Troll
Source depth/length	10/400 m	10/800 m
Source current	800 A	800 A
Source waveform	ORS	ORS
Shot-point interval	250 m	250 m
Shot length	120 s	120 s
Receiver depth	100 m	100 m
Offset range	650-3,650 m	2,500-5,500m

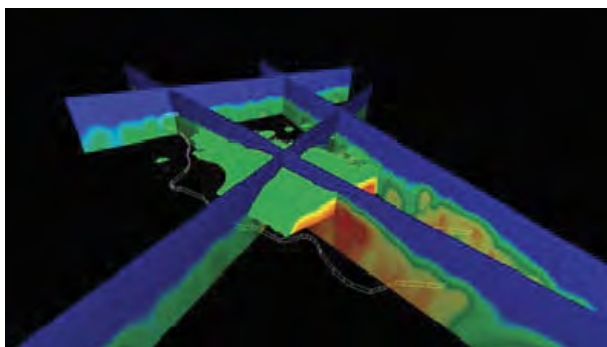


Figure 2: The Peon Field where the body in light green is the inverted 3D rendition of the transverse resistance. The four long regional lines tie the 3D volume together with the two existing well locations and also evaluate some potential satellite deposits.

some of the potential satellite deposits in close proximity to the main volume. Two of these lines also cross the two existing well locations to facilitate calibration.

The Troll oil & gas field

The Troll Field is located in the northern part of the North Sea. The water depths range from 320 – 350 m with the top of the reservoirs around 1,100 – 1,200 m below mud-line. The Troll West oil province (TWOP) has an oil column 22-26 m thick under a thin gas column. The Troll West gas province (TWGP) has a gas column up to 200 m thick over a 12-14 m oil column making it a much stronger target. A suite of 9 densely spaced lines were acquired to create an image in 3D.

In addition there were three regional lines acquired. One line was acquired simultaneous with 2D seismic as a proof of concept. The potential for the source dipole to induce electrical noise in the seismic streamer was found to be an issue only if the dipole cable and the seismic streamer came in direct contact with each other. The issue was completely resolved by maintaining a vertical and lateral separation between the dipole and streamer and the processed seismic is of expected quality.

The Troll West Oil Province (TWOP) is the more difficult field to image due to the lower transverse resistance (2,000 ohm-m²) compared to the Troll West Gas Province (TWGP) where the transverse resistance reaches 6,500 ohm-m². The difference is due to the fact that the resistivity is lower in the oil saturated reservoir and the charged reservoir thickness in TWOP is also reduced compared to the TWGP.

Figure 3 shows the measured transverse resistance for the TWOP where the red colour represent maximum transverse resistance and the dark blue the lowest transverse resistance.

Conclusions

The two field trials were completely successful. Over a period of 138 hrs of acquisition time 615 line km of high quality EM data was acquired. This was achieved with no Lost Time Incident (LTI) in spite of 3.5 m high waves (sea state 5) during parts of the acquisition.

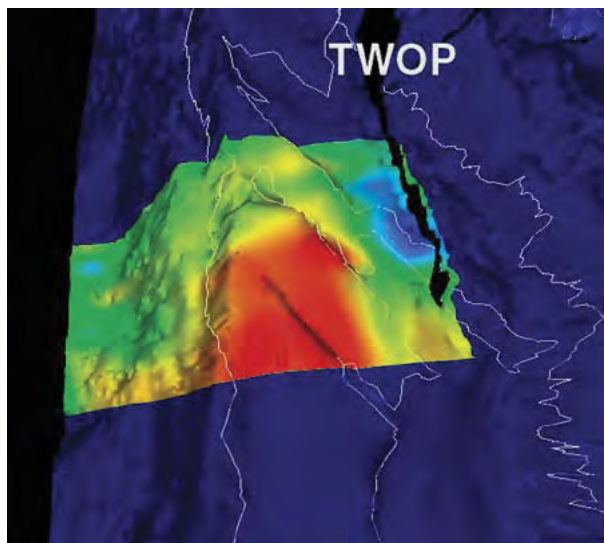


Figure 3: The measured transverse resistance for the TWOP where the red colour represent maximum transverse resistance and the dark blue the lowest transverse resistance.

A total of 13 lines were acquired over the Peon field with 10 of them in parallel in sufficient proximity to facilitate 3D imaging of the target. Inversion of intersecting lines displayed similar values at the point of crossing, confirming that the inversions are robust. The edge of the field as defined by the EM differs somewhat from the published seismic interpretation.

Acknowledgements

We thank Statoil for supporting our work on the Peon field and the collaboration they have provided. We also thank Statoil for permission to carry out the survey over the Troll field. We would also like to thank our colleagues that have contributed to the successful development and field testing of the towed EM system. Finally, we also thank Petroleum Geo-Services for permission to present this work.

References

- Amundsen R.E.F., Johansen S., and Rosten T., 2004, A Sea Bed Logging (SBL) calibration survey over the Troll Gas Field: EAGE 66th Conference and Exhibition, Expanded Abstracts.
- Anderson C., and Mattsson I, An integrated approach to marine electromagnetic surveying using a towed streamer and source: First Break, vol 28.
- Ellingsrud S., Eidesmo T., Johansen S., Sinha M.e., MacGregor L.M., and Constable S., 2002: Remote sensing of hydrocarbon layers by seabed logging (SBL): Results from a cruise offshore Angola: The Leading Edge, October, 872-982.
- Jurgen J.Z., Frenkel A.M., Ostvedt-Ghazi A-M., de Lugao, P., Ridyard D., 2009: Marine CSEM methods for 3D hydrocarbon field mapping and monitoring: 11th International Congress of the Brazilian Geophysical Society

Pitfalls in CSEM Inversion; a Case Study of a False Positive

V. Ganesan* (EMGS Asia Pacific Shd Bhd), H. T. Pederson (EMGS Asia Pacific Sdn Bhd),
S. K. Chandola (Petronas Carigali Sdn Bhd) & N. N. Halim (Petronas Carigali Sdn Bhd)

Introduction

All sediments exhibit electrical anisotropy to some extent. Certain sediments are more prone to have a higher electrical anisotropy ratio than others, e.g. shale has usually larger anisotropy ratio than sands (Ellis et al., 2010). Within a basin, one should then expect both micro level electrical anisotropy (within a geological sequence) and macro level electrical anisotropy (measured over several sequences). Trying to reproduce an anisotropic resistivity volume with an isotropic approach can generate artifacts due to oversimplification. In this paper, we show an example of such an artifact and demonstrate the importance of taking the electrical anisotropy into account when interpreting CSEM data.

With the Controlled Source Electro Magnetic (CSEM) method, a horizontal electric dipole emits EM-fields which induce telluric currents (Eidesmo et al., 2002). The inline component of the electric field is mostly sensitive to the vertical resistivity while the electric broadside component is more sensitive to the horizontal resistivity (Lu and Xia, 2007; Morten et al., 2010). In an anisotropic geological setting where both inline and broadside components of the measured data are inverted using an isotropic scheme, one should expect to be able to fit one component, but not both (Mohamad et al., 2010). In 3D inversion of CSEM data, the goal is to recover a realistic resistivity volume based on the information in the recorded data.

CSEM inversion case study

Two criteria should be fulfilled when investigating CSEM inversion results; 1) acceptable fit between measured and synthetic data and 2) the inverted resistivity volume should be geologically feasible. In the following case study, we shall discuss these two criteria using inversion results from a CSEM survey in deep water Malaysia. The prospect was covered with 93 receivers and towed in both EW- and NS- direction (Figure 1). All the receivers were active for all towlines assuring full azimuth data coverage. At the time of the survey, only an isotropic 3D inversion scheme was commercially available with the service provider (Støren et al., 2008; Zach et al., 2008).

The start model for the unconstrained isotropic inversion was based on 1D CSEM inversion results and did not include any structures from seismic. Upon inspection of the data fit, the inline data is fitted within the acceptance level. However, the broadside component shows poor data fit. The isotropic 3D inversion scheme introduces oscillating resistivity (Figure 2), which is a red flag and should be investigated as a possible inversion artifact. In addition, the isotropic inversion generated a high resistive feature within the structural closure. So, for the isotropic inversion neither criterion for successful CSEM inversion was properly fulfilled.

3D inversion was rerun in 2011 with identical data input and inversion parameters, but now with an anisotropic scheme and a start model anisotropy ratio of 1.5. The result of the anisotropic inversion is shown in Figure 3, and we see that for this inversion no high resistive feature is reconstructed within

the closure. Figures 4 and 5 show a comparison of the data fit for the isotropic and anisotropic inversions and one can clearly see that the latter has a much better data fit, especially for the broadside component. In Figure 6, the inverted anisotropy ratio is superimposed onto a seismic cross section and one clearly observes that changes in the seismic character coincide with anisotropy alterations. The inverted volume is distinguished into four major sequences and within the second sequence; the largest relative increase in resistivity is seen to coincide with a strong seismic amplitude event.

Calibration of CSEM 3D inversion results:

Post-drilling analysis shows that the horizontal resistivity behavior of the unconstrained anisotropic 3D inversion match the resistivity log reasonably well (Figure 7). The well encountered a thin limestone layer and 1D CSEM modeling was performed to investigate if this limestone layer could be a possible cause of the resistor observed in the isotropic 3D inversion results. Based on the modeling results, this thin resistive layer had minimum effect to the measured fields (<2%). Therefore the inverted high resistive feature observed in the isotropic inversion is interpreted as an inversion artifact related to not taking anisotropy into account rather than a real event.

References

- Eidesmo, T., S. Ellingsrud, L. M. MacGregor, S. Constable, M. C. Sinha, S. Johansen, F. N. Kong, and H. Westerdahl, 2002, Sea bed logging (SBL), a new method for remote and direct identification of hydrocarbon filled layers in deepwater areas: *First Break*, 20, 144–152.
- Ellis, M. H., M. Sinha, and R. Parr, 2010, Role of fine-scale layering and grain alignment in the electrical anisotropy of marine sediments: *First Break*, 28, (9), 49–57.
- Lu, X., and C. Xia, 2007, Understanding Anisotropy in Marine CSEM Data: 77th Annual International Meeting, SEG, Expanded Abstracts, 633–637.
- Mohamad, S.A., L. Lorenz, L. T. Hoong, T. K. Wei, S. K. Chandola, N. Saadah, and F. Nazihah, 2010, A practical example why anisotropy matters - A CSEM case study from South East Asia: 80th Annual International Meeting, SEG, Expanded Abstracts, 696–700.
- Morten, J. P., A. K. Bjørke, and A. K. Nguyen, 2010, Hydrocarbon reservoir thickness resolution in 3D CSEM anisotropic inversion: 80th Annual International Meeting, SEG, Expanded Abstracts, 599–603.
- Støren, T., J. J. Zach, and F. Mao, 2008, Gradient Calculations for 3D Inversion of CSEM data using a fast finite-difference time-domain modelling code: 70th Conference & Exhibition, EAGE, Expanded Abstracts.
- Zach, J. J., A. K. Bjørke, T. Støren, and F. A. Maaø, 2008, 3D inversion of marine CSEM data using a fast finite-difference time domain forward code and approximate Hessian-based optimization: 78th Annual International Meeting, SEG, Expanded Abstracts, 614–618.

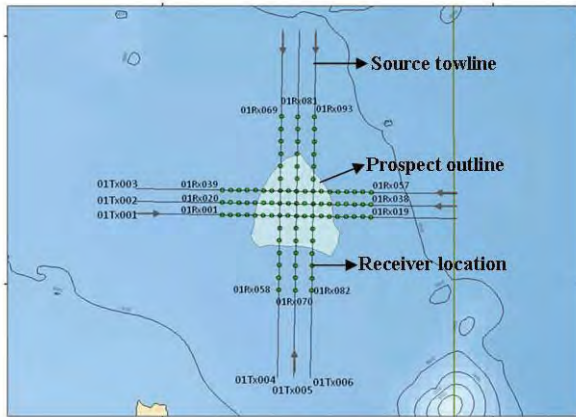


Figure 1: Acquisition survey layout for the 2008 dataset from Malaysia

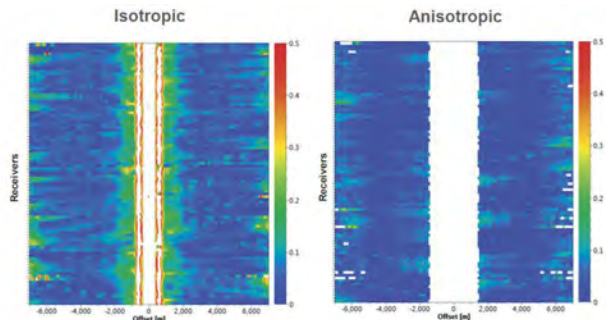


Figure 4: Inline data misfit illustrated by plotting the Ex component of inline towlines for isotropic 3D inversion (left) and anisotropic 3D inversion (right). The misfit is slightly better in the anisotropic inversion.

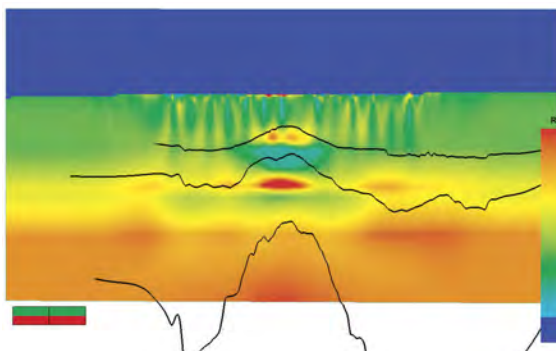


Figure 2: Inverted vertical resistivity model from isotropic 3D inversion scheme displayed along line 01Tx005 shows oscillation effects due to inversion artifacts (marked in circle).

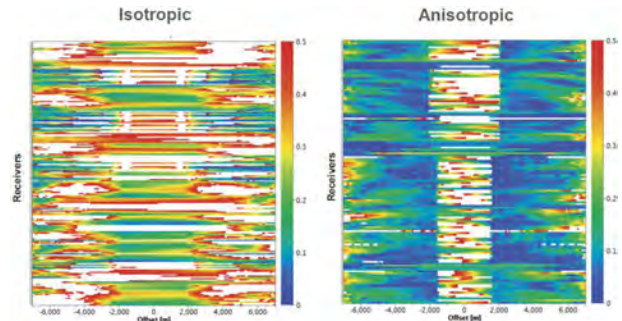


Figure 5: Broadside data misfit illustrated by plotting the Ey component of azimuth towlines for isotropic 3D inversion (left) and anisotropic 3D inversion (right). There is a significant improvement for the Ey component in the anisotropic inversion.

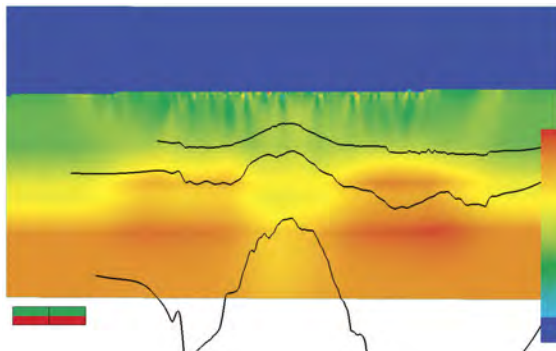


Figure 3: Inverted vertical resistivity model from anisotropic 3D inversion scheme displayed along line 01Tx005 shows no increased resistivity at the target structure.

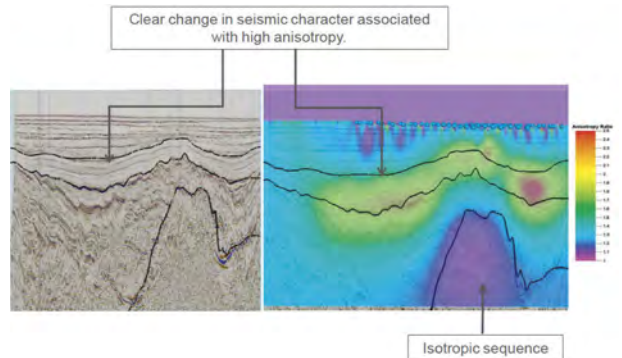


Figure 6: Seismic section displayed along line 01Tx002 (left) and anisotropy ratio (Rv/Rh) from anisotropic 3D inversion superimposed on seismic for line 01Tx002 (right).

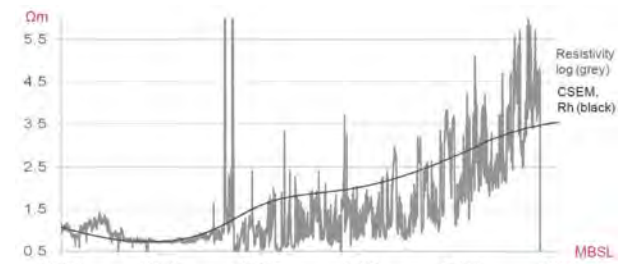


Figure 7: Well log correlation with anisotropic 3D inversion result (horizontal resistivity).

A decade of 4D seismic monitoring of carbonate gas reservoirs in offshore Sarawak, Malaysia

Paul Hague & Chiem Boon Hong (Sarawak Shell Berhad)

Introduction

In recent years 4D seismic monitoring has been widely used to monitor production effects in clastic reservoirs, to the extent that the seismic response of such reservoirs to saturation and pressure changes has become reasonably well understood and is well documented in the published literature. However, given that carbonate reservoirs account for approximately half of the world's oil and gas reserves, it is perhaps surprising that the use of 4D seismic data to monitor production effects in carbonate reservoirs has received considerably less attention. This is largely due to the fact that the acoustic response of carbonates has been shown to be highly variable and there has been some debate regarding the applicability of Gassmann's equation for predicting the impact of changes in saturation on the acoustic properties of carbonates (eg. Baechle et al. 2005; Rasolofosaon et al. 2008). Of particular relevance to the carbonate gas fields of offshore Sarawak is the fact that Gassmann's equation predicts that water influx into a gas reservoir would produce a relatively minor acoustic response, which might be expected to be swamped by non-repeatable noise on 4D seismic data.

For these reasons, Shell has adopted a cautious approach to implementing 4D seismic monitoring of the Miocene carbonate gas reservoirs of offshore Sarawak, Malaysia. This approach has involved a gradual shift from 2D repeat seismic acquisition to targeted 3D seismic swaths and more recent plans for platform undershoots to provide repeatable pre-production data for future surveys. At each stage of this journey important lessons have been learned regarding the applicability of 4D seismic data for monitoring production behaviour in carbonate gas reservoirs and these lessons have laid the foundation for further 4D seismic monitoring to maximise ultimate gas recovery in future.

Repeat 2D seismic acquisition at the M3 field

The first attempt at time-lapse seismic monitoring of a carbonate gas reservoir in offshore Sarawak was undertaken in 2001, when 6 repeat 2D seismic lines were acquired over the M3 field, which had experienced unexpected water breakthrough just three years after first gas. Despite the limitations of repeating 2D seismic data, two of the six lines appeared to show a relatively strong coherent seismic amplitude response at both the original gas-water contact and the point which coincided with the logged producing gas-water contact in the wells. Furthermore, robust time-shifts between the base and monitor surveys were also observed. These can be attributed to seafloor subsidence and stress relaxation in the overburden, due to pressure depletion and compaction in the reservoir and provided evidence that it was possible to use time-lapse seismic data to monitor the aerial extent of pressure communication in these reservoirs.

Repeat full field 3D seismic acquisition at the M4 & Serai fields

These encouraging results prompted the first full-field repeat seismic survey, covering two smaller subsea fields in 2005 (Barker et al. 2008). Both of these fields were developed with two horizontal subsea wells at the crest of the structures. The only real difference was the geometry of the structures

with the M4 field having a 180ft gas leg and the Serai field having a 560ft gas leg. By the time of acquisition, M4 had been producing for three years, whilst Serai had been producing for less than a year. However, it was apparent that the two fields were in pressure communication, because Serai already showed signs of pressure depletion when it came onstream, which was attributed to two years of production from M4.

Water breakthrough in one of the M4 wells was observed in 2004, two years after first gas, whilst water breakthrough at the second M4 well was observed within months of completing the repeat 3D seismic acquisition. At this point in time, the field had produced less than 50% of its GIIP and it was believed that the early water breakthrough may have been a localised effect and that the ultimate recovery could potentially be increased by drilling an additional subsea well into an unswept part of the field. However, when the 4D seismic data became available in early 2006, a clear amplitude response was observed at the original gas-water contact and another clear amplitude response was observed very close to the crest of the structure (Figure 1). This implied that the contact rise was broadly uniform, leaving no real pockets of by-passed gas. Based on this observation, the decision was taken not to drill a costly additional subsea well or sidetrack on this field.

The 4D seismic data over the Serai field showed a slightly unexpected amplitude response which seemed to imply an expansion of the gas cap into the aquifer, due to pre-production depletion. Interestingly, this signal is much stronger than the signal related to water influx at M4, which is precisely what Gassmann's equation predicts. In addition to the 4D seismic amplitude response, both fields showed clear time-shifts between the base and monitor surveys, due to seafloor subsidence and stress relaxation in the overburden, once again demonstrating the use of 4D seismic data for understanding pressure communication.

Repeat 3D seismic swath acquisition at the F6 field

In 2006 another repeat seismic survey was acquired at the F6 field. This field came onstream in 1987 and had already been producing for 15 years when the first 3D seismic survey was acquired over the field in 2002. Pulsed neutron capture logs showed clear evidence for water influx in the central part of the field. However, owing to the size of the field (130 sqkm) and the fact that it had been developed from a single platform, there was considerable uncertainty surrounding the remaining gas volume on the flanks. Dynamic simulation studies indicated that the degree of water influx was likely to be greater in the central part of the field than on the flanks and that any further gas-water contact rise on the flanks between 2002 and 2006 was likely to be small (<50ft). This represented a challenge for 4D seismic monitoring. Never-the-less, synthetic seismic modelling using Gassmann's equation for the replacement of gas with water showed that it should be possible to observe a 50ft contact rise above the expected levels of non-repeatable noise.

Because of the cost of full-field 3D seismic acquisition over such a large field and the relatively low probability of success, it was decided to acquire a targeted 3D seismic swath over the

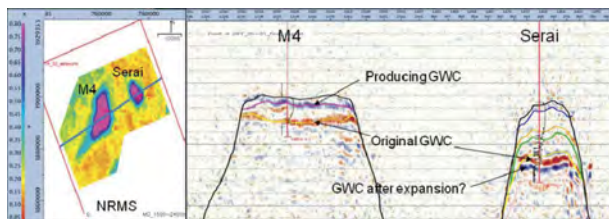


Figure 1: 4D seismic difference data at M4 and Serai.

western flank of the field. When processed, this swath showed a weak 4D amplitude response, which is interpreted as evidence for partial sweep of the western flank (Figure 2). However, it also implies that there is a sizeable volume of gas remaining in this area. As a result, plans are in place to drill an 18,000ft extended reach development well into the western flank of the field in late 2012. Part of this plan involves drilling a pilot hole in this area to confirm the depth of the current contact and validate the predictions of the 4D seismic data.

Repeat 3D seismic swath acquisition at the Jintan field

In 2008 a similar approach of targeted 3D seismic swath acquisition was adopted at the Jintan field. This field came onstream in 2004 and was covered by a full-field pre-production 3D seismic survey in 1992. However, in this case, the acquisition of two 3D seismic swaths, rather than a full-field repeat seismic survey was partly dictated by the desire to keep costs down and partly by the fact that the Jintan platform precluded the acquisition of seismic data over the central part of the field. By the time of repeat seismic acquisition in 2008, pulsed neutron capture logs at 3 deviated wells showed evidence for no more than 55ft of water influx in the northern part of the field, which was considered to be just above the lower limit of resolution. However, when the two processed seismic swaths were delivered, they showed strong, but patchy 4D seismic difference responses (Figure 3). These patchy seismic responses are attributed to an irregular water influx, which may be related to the presence of high permeability regions of the reservoir, such as karstified zones. So far, the locations of two subsequent infill wells on this field have been optimised based on the 4D seismic observations.

Conclusions and future plans

Although the effects of pressure and saturation changes in carbonates are believed to be highly variable and the applicability of Gassmann's equations is still the subject of some debate, these empirical examples from offshore Sarawak conclusively demonstrate that 4D seismic monitoring of carbonate gas fields can yield meaningful signals, which can be used to optimise further field development.

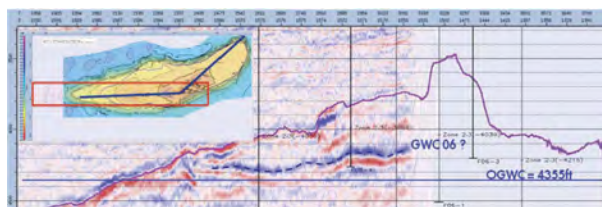


Figure 2: 4D seismic difference data at F6.

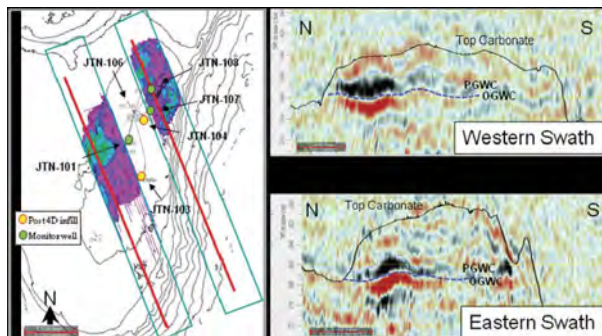


Figure 3: 4D seismic difference data at Jintan.

As a result of the successes to date, a campaign of activities is planned for 2012 and beyond. This involves extended repeat swath surveys over Jintan and pre-production seismic undershoots of the platform locations at two currently undeveloped fields, which are designed to lay the foundation for future repeat seismic surveys to maximise ultimate gas recovery from offshore Sarawak.

Acknowledgements

The authors would like to thank Tim Barker, Chen Bao Ning, Wong Kah Luk, Cameron Dinning, Lee Bor Seng, Elvis Chung, Shuh Wen Yee, Khaw Lay Hong & Kok Yip Cheong for their contributions to this work.

References

- Baechle, G.T., Weger, R.J., Eberli, G.P., Massafiero, J.L. and Sun Y-F. 2005. Changes of shear moduli in carbonates rocks: implications for Gassmann applicability. *The Leading Edge*, 24, 507–510.
- Rasolofosaon, P., Lucet, N. and Zinszner, B. 2008. Petroacoustics of carbonate rocks. *The Leading Edge*, 27, 1034-1039.
- Barker, T.B., Chen, B.N., Hague, P.F., Majain, J. and Wong, K.L. 2008. Understanding the Time-Lapse Seismic Response of a Compacting Carbonate Field, Offshore Sarawak, Malaysia. IPTC abstract No.12514.

Seismic Imaging and Interpretation of Paleo-Cave Systems in Karstified Carbonate Reservoirs of Tarim Basin

C. Luo (CNPC Tarim Oil Company), F. Xue* (Schlumberger), Q. Miao (CNPC Tarim Oil Company) & P. Yang (Schlumberger)

Introduction

Paleocave systems are extensively developed within the deep karstified Ordovician carbonate reservoir in the Tarim Basin, West China. The reservoirs associated with these paleo-cave systems contribute the majority of hydrocarbon storage space and production in the tight Ordovician carbonates. The newly reprocessed seismic data has significantly improved the seismic images of the paleo-caves and effectively revealed the complex cave systems through the area (Figure 1).

Method

Based on seismic characteristics, and combined with well log interpretation, drilling results and production data more than one thousand caves are interpreted over an area of 230 square kilometers. This cave interpretation provide basis for seismic attribute analysis in order to extract cave reservoir parameters (Figure 2).

Cave entrances and exits have been identified in seismic sections. Combined with cave distribution tendency and associated seismic anomaly continuity, the

coalescing karst patterns have been delineated to illustrate the connectivity of the caves and the Paleo-cave systems.

Result

At least 5 levels of conduit cave development have been interpreted in the upper 200m of the Ordovician section in the study area (Figure 3 and 4). They were likely formed in response to changes in the underground-water tables in the phreatic zone during Late Paleozoic exposure events. The caves of different levels are connected in many place and form complex cave systems. Combined with structural mapping and production analysis, the paleo-cave system analysis provides an effective approach to predict cave fillings and fluid types. Hundreds of oil-bearing caves are predicted in the study area. Dozens of drilling locations are selected based on potential and risk ranking of the predicted oil-bearing caves. This study was completed in early 2011. The result has been applied in drilling deployment since then. Drilling on these locations in late 2011 has successfully led to high productive wells after unsuccessful drilling in 2009 and 2010.

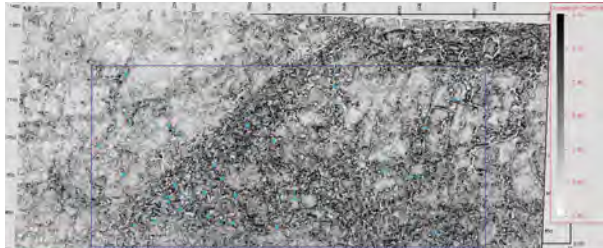


Figure 1. A correlation type of seismic attribute map 50~150ms below the Ordovician top reveals the subtle paleo-cave systems. The linear features are the seismic response of large cave passages (underground rivers). The blue box is the focused area. The light blue dot is the key wells in study.

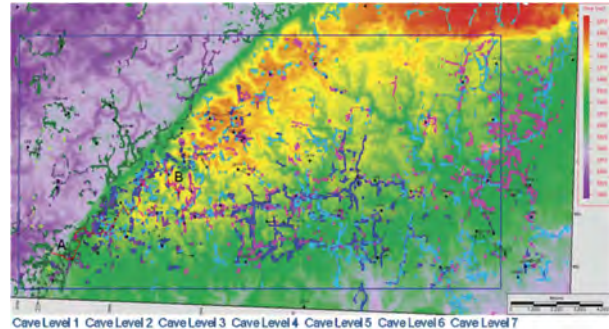


Figure 3. The overlap of Time Map of Ordovician top with interpretation of all Cave levels. Seismic section AB is shown in Figure 6.

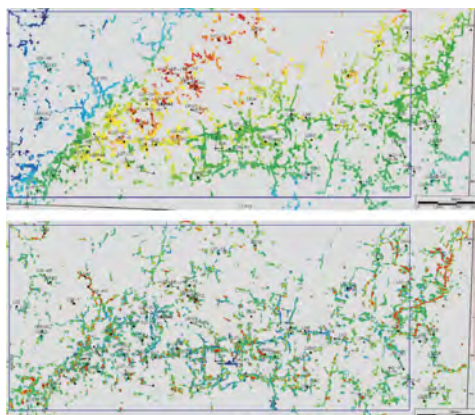


Figure 2. The interpretation of paleo-caves illustrated in Figure 1. The upper figure is the time map of cave interpretation. The lower one is the amplitude map of the cave interpretation.

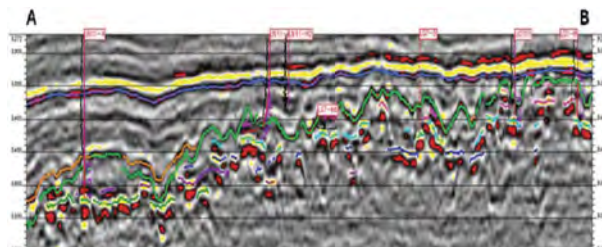


Figure 4. Seismic section showing multi-levels of caves. The seismic line position is shown in Figure 5.

Carbonate Petrophysics Leading to Productivity Analysis in Support of Static Modeling

F. Zakeria* (PETRONAS Carigali Sdn Bhd), M. Altunbay (PETRONAS Carigali Sdn Bhd),
R. Poit (PETRONAS Carigali Sdn Bhd) & J. Kijam (PETRONAS Carigali Sdn Bhd)

Carbonates pose extreme challenges in petrophysical studies that lead to higher uncertainty levels for static modeling of reservoirs. Consequently, economic viability studies for the field suffer from low levels of confidence. The difficulties in mapping "controls of fluid flow" exponentially increase when/if basic data availability is hindered by limited or failed wireline logs. We had taken two wells in a carbonate structure in which the control well had wealth of wireline data while the second well lacked vital wireline data due to operational difficulties. The objective of this study was to generate all petrophysical data from the control well and to devise models to propagate them to the second well. The subject carbonate was minimally fractured and had minimal number of vugs (a well behaving carbonate). Although, lesser challenge was experienced in modeling, possible remedies for extreme heterogeneities were also formulated and presented. A new formulation was derived for determining the irreducible wetting phase saturation for the cases with no NMR log data in which resistivity-based water saturation (Swi) can be in check with for more realistic determination of zones with water-free hydrocarbons. The study produced all relevant petrophysical and productivity information for the well with less than minimum wireline data by using the models created from the control well. The outcome of the model-driven petrophysical data set and reservoir engineering treatment of it for productivity estimations were in agreement with the actual productivity verifying the efficacy and reasonable accuracy of the models. The study yielded and verified models for usage in static modeling for the reservoir circumventing the issues originating from the lack and/or quality of actual data.

Introduction and Methodology

No simple/apparent linear-relationship existed between permeability and porosity; hence, multiple non-linear regressions were used for evaluating co-dependence of wireline logs to Flow Zone Indicator (FZI)1.

$$FZI = \frac{0.0314 \cdot (1 - \phi_e) \cdot \sqrt{k \cdot \phi_e}}{\phi_e^2}$$

where:

FZI : Flow zone indicator, microns

ϕ : porosity, fraction

k : permeability, mD

FZI amalgamates permeability, porosity, tortuosity and shape factor in a single term; hence, lessening the non-correlatable nature of porosity and permeability. By using FZI, explicit dependency of wireline responses to permeability was revealed and strong co-dependent correlations of FZI versus Sonic transit time (DTC) and density log (RHOB) were obtained.

However, DTC log had to be modeled and corrected in the subject well due to a missing section before the FZI-model equation can be used.

The permeability profile was then computed from the equation that is algebraically manipulated from the intrinsic correlations of permeability and porosity in the definition of FZI, reservoir quality index (RQI) and normalized porosity of the hydraulic units by using predicted FZI for the subject well:

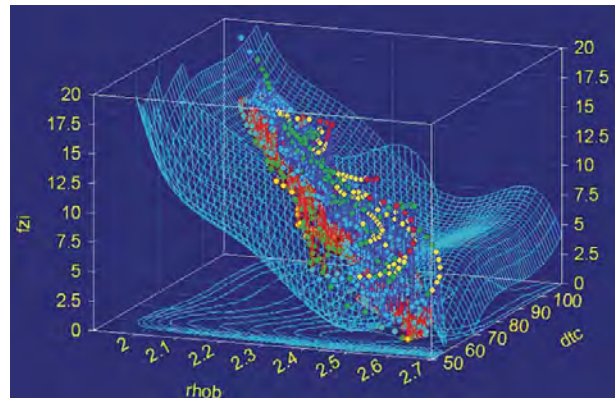
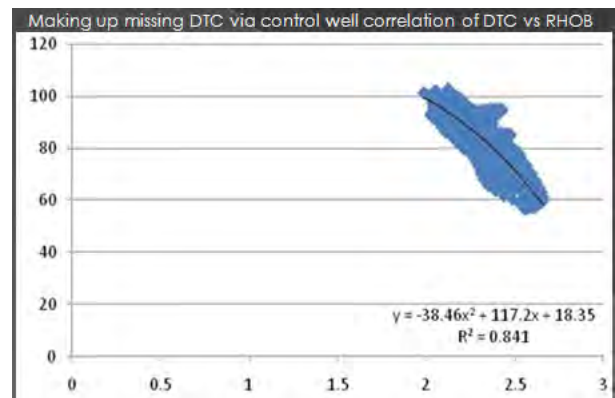


Figure 1: FZI correlating to density and sonic transit time.



$$k_p \cdot mD = \frac{\left(FZI_p \cdot \frac{\phi_e}{1 - \phi_e} \right)^2 \cdot \phi_e}{0.000986}$$

where:

kp : predicted permeability, mD

FZI_p : predicted/modeled Flow Zone Indicator, microns

ϕ_e : effective porosity, fraction

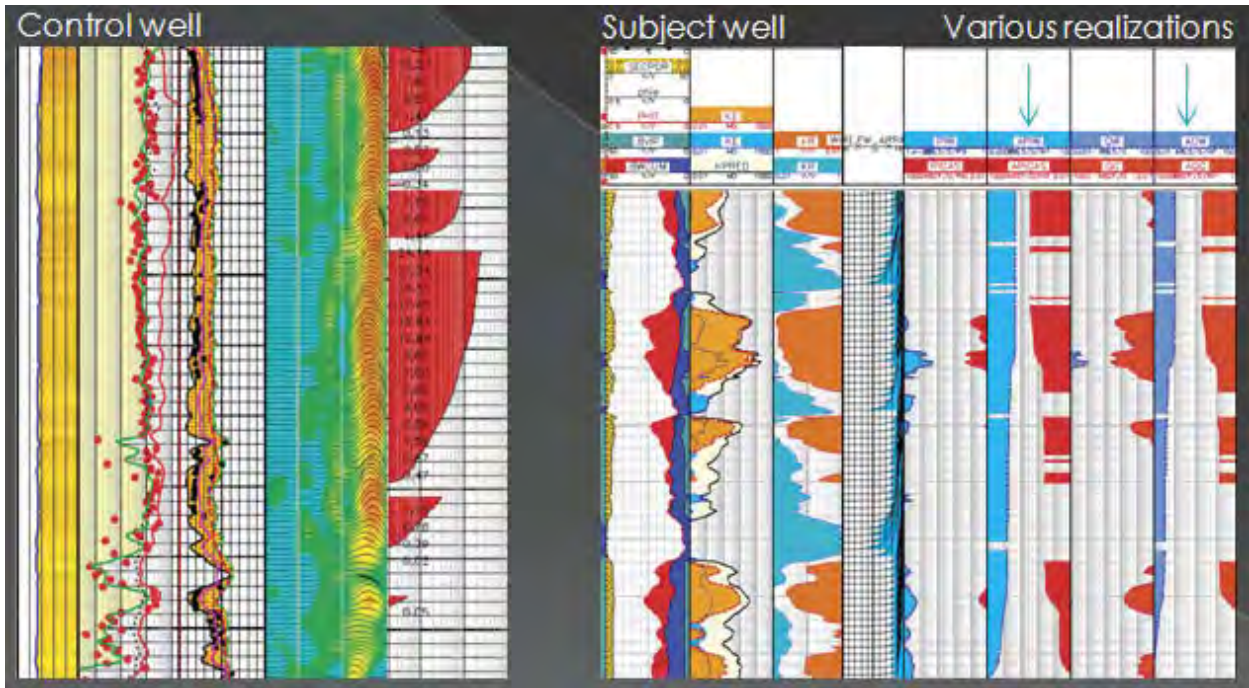
0.000986 : conversion factor from mD to microns

The predicted matrix permeability profile for the subject well is statistically tied to the control well based on the core/Formation Tester calibrations of permeability profile of the control well and; there from, calibrated nature of the FZI_p.

The bulk-volume-irreducible (BVI), there from, Swirr (Swirr=BVI/ ϕ_e) for the subject well is required deriving Corey-Burdine type relative permeability equations which will be used in reservoir engineering treatment of the petrophysical data for Productivity Index (PP)/rate estimations. We either could base BVI formulations to a general capillary pressure model or to calibrated Timur-Coates permeability equation. We have taken the latter avenue.

$$k = \left(\frac{\phi_e}{C} \right)^m \cdot \left(\frac{BVM}{BVI} \right)^n$$

Core calibrated Timur-Coates equation (above) is algebraically manipulated to the following form for the BVI



estimation of the subject well:

$$BVM = \phi_e - BVI$$

$$BVI, pu = \frac{\phi_e}{\left[\frac{k}{\left(\frac{\phi_e}{C} \right)^m} \right]^n + 1}$$

where:

BVI : bulk volume irreducible, pu

BVM : bulk volume movable, pu

k : permeability, mD

ϕ_e : effective porosity, pu

C, m and n : coefficient and exponents from the FT calibration of permeability profile of the subject well

Connectivity-based permeability is also required if the carbonate exhibits vuggy nature. The delineation of permeability into matrix permeability and the connected-vug permeability becomes an important issue when the productivity estimation requires averaging of permeability. For the vuggy cases, we would like to calibrate the average permeability as a function of well test permeability for PI estimations. Our case study did not exhibit a fractured/vuggy nature.

We have computed well productivity indices² for gas and brine for various scenarios of skin factor, drawdown, drainage

radius and well placements by using the driven Sw, Swirr (BVI/effective porosity), permeability, porosity, Corey-Burdine relative permeability and capillary pressure data for gas-brine carbonate systems. The resultant estimation of water-free gas production for the control well was in agreement with the actual test results. However, the subject well estimations indicated minor water influx.

Conclusions

The study produced models for deriving reasonable estimates of Swirr, permeability, effective permeability, productivity indices (and/or rates) for any well in the same depositional environment with similar levels of diagenetic changes with minimum requirements of basic wireline logs (RHOB, DTC, Resistivity).

A methodology, a set of generic equations and a workflow have been produced for treating carbonate cases with minimal wireline data to produce petrophysically sound information with economic implications.

References

Amaefule, J.O., Altunbay, M., Djebbar, T., Kersey, D.G., Keelan, D.K., "Enhanced Reservoir Description: Using Core and Log Data to Identify Hydraulic (Flow) Units and Predict Permeability in Uncored Intervals/Wells", SPE 226436, 1993

Mapping the Kinta Valley Karst System, Peninsular Malaysia: Implications for Better Insight of Subsurface Karst Features

S. Kassa* (Universiti Teknologi PETRONAS), B. J. Pierson (Universiti Teknologi PETRONAS),
W. S. Chow (Universiti Teknologi PETRONAS) & B. A. T. Jasmi (Universiti Teknologi PETRONAS)

Introduction

The Kinta Valley is characterized by remnant limestone hills, which are part of the expansive bedrock that once covered the whole valley. These hills are honeycombed with karst caves and shattered by tectonic structures. The development of karst in carbonate rocks by meteoric water, during subaerial exposure, is believed to be an important geologic phenomenon that can lead to the formation of petroleum reservoirs (Wang and Al-Aasm, 2002 and references therein). To define reservoir geometry, scale, pore networks, and spatial complexities for purposes of exploration and development, near-surface histories of karst features and their later burial modifications must be understood (Loucks, 1999). The existence of paleokarst channels, collapsed caves and sinkholes, commonly indicated by analyzing the seismic reflection characteristics of these features and from well logs (Vahrenkamp, 2004; Shen et al., 2007; Zheng et al., 2011).

According to Golf-Racht (1982), a carbonate reservoir is defined as being "fractured" only if a continuous network of various degrees of fracturing is distributed throughout the reservoir. In general, the most intense karst occurs along linear fault and fracture-controlled karst channels, and such faults and fractures have an important impact on reservoir connectivity (Shen et al., 2007). In spite of that, it can be difficult to interpret continuity of fracturing in matured subsurface karst system, but comprehending subaerial karst features can be a way forward to unearthing the most likely trend of the subsurface structures. And may help to fill gaps in the knowledge base that still exist, concerning particularly connectivity (how individual fractures link to form coherent networks) and scaling (how small features are related to large ones) (Odling, 1999).

This study is initiated by the curiosity of (1) identifying the peculiar nature of the Kinta Valley karst landform and to illustrate how it can be a good analogue for subsurface karst, (2) identifying the role of faults and joints, and whether it is possible to infer their continuity considering the location of the isolated hills scattered in the valley. And it is hypothesized that, having a good knowledge of subaerial karst system, including distribution, dimensions, and factors responsible for their formation, among others, is key to comprehend and interpret subsurface karst features, which are commonly inferred from indirect evidences.

Methods

In order to identify the prominent factors controlling the development of karst, cave surveying and lineament analysis were conducted. To map the various karstic caves, standard method of cave mapping using clinometers, compass and laser distance measuring instruments were employed. And the survey data were analysed using COMPASS software.

Spot image, with a resolution of 2.5 m, was used for the extraction of lineaments. Two methods of lineament extraction techniques exist: manual (visual interpretation) and automatic; for this study we used the former, as it is easier to manually identify geological elements from non geological ones. In order to enhance the interpretability of the image, the commonly used image enhancement techniques, i.e. directional filtering and

color composite, were employed. And to enhance linear features in specific directions, directional filtering was conducted, and color composite was used to achieve maximum contrast by combining different bands (RGB), for the ease of identifying linear patterns of geological elements.

Image enhancement has been undertaken using PCI Geomatics software, and Arc GIS 9.3 software used to digitize the lineaments and make the final map, and GOrient software was employed to indicate the lineaments' orientations using rose diagrams.

Result and Discussion

After a number of caves were surveyed and their passage orientations analyzed, the main cave passages trend appeared to be in the NNW-SSE. Lineaments extracted from the vestige hills also indicated similar prominent orientation. The overall trend of the cave passages (fig.1a) and the lineaments (fig.1b) appeared to be almost the same, and it leads to deduce that the karst development, most likely, attributes to the pre-existence of tectonic structures oriented in the NNW-SSE. Furthermore, this similarity has also enabled to infer the continuity of fracture traces, albeit continuous fault system that traverses the whole valley was not evident. The multi-fracturing phenomenon clearly observed on the hills appears to have been imprinted on the caves passage morphology, as rectilinear, circular and convoluted conduits typifies the pattern of karstic caves passage of the area. For instance, figure 2b-d exemplifies this phenomenon.

Although direct comparison is not always possible, the Kinta Valley karst system is a good analogue to envisage the possible continuity of fracture traces in carbonate reservoirs, which might have undergone intensive subaerial karstification process. As a matter of fact, because of the intensive subaerial karstification process, positive paleokarst features may not appear in seismic section, and it can be difficult to infer the continuity of associated negative karst features and fracture traces. Nonetheless, such a problem can be alleviated by comprehending the relation between structures and associated karst features in a matured karst system, such as the one in the Kinta Valley.

Despite the fact that a carbonate terrain is immensely shattered by fracturing, multiple channel development via the fractures may not occur, if one considers the Kinta Valley karst system as analogue. This is because, whenever fracture traces are interconnected, channels in the form of sinuous (fig.2b and c) or loop (fig.2d) will take place, following the ease of solute attacks along the fractures. It has to be noted that, the convoluted and curvilinear passage morphologies may not necessarily suggest the prime influence of fracturing. At times, similar conduit pattern can be controlled by bedding-plane partings or predominance of intergranular pores (Palmer, 1991) than being merely a consequence of the pre-existence of structures; hence, it may be difficult to infer as to what controlled the development of similar pattern of subsurface karst features. However, according to Palmer (1991), solutionally enlarged joints and high-angle faults tend to produce fissure-like passages with lenticular cross sections and angular intersections. But bedding-plane partings lead to the formation of branchwork or anastomotic pattern. Thus,

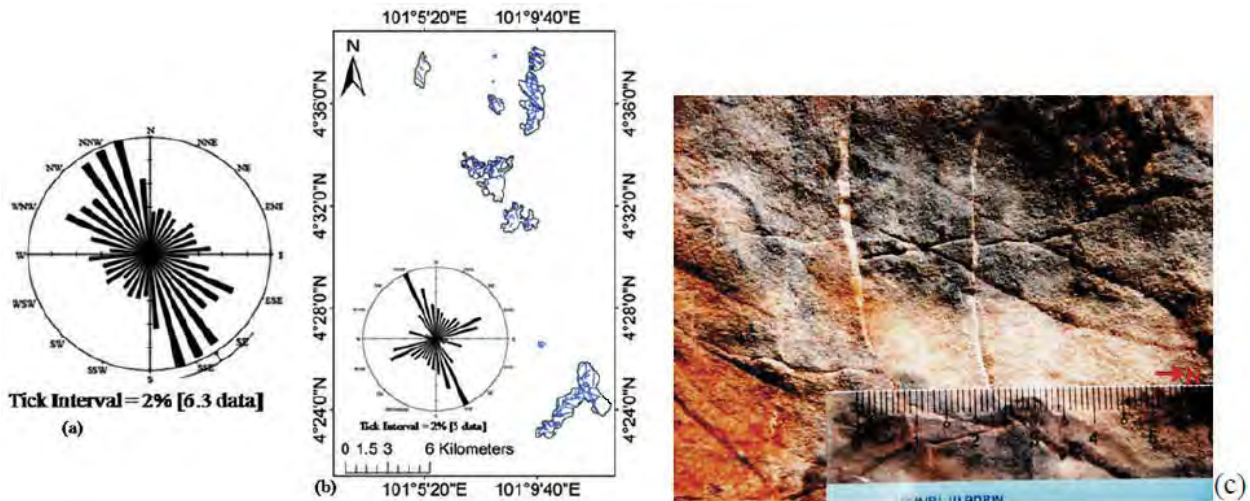


Figure 1: (a) indicates the prominent NNW-SSE trend of conduits analyzed for twelve caves, and (b) inset rose diagram depicting the general orientation of lineaments extracted from the vestige hills, and (c) illustrates fracture sets observed on the wall of a precipitous hill.

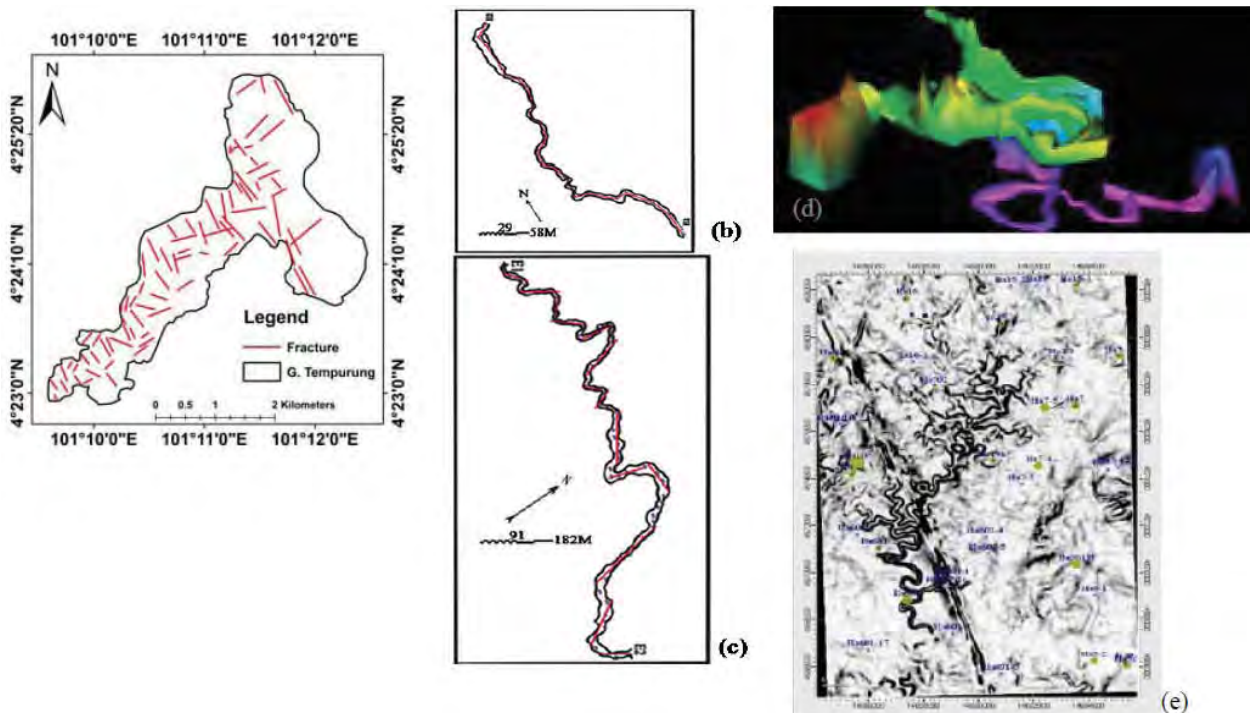


Figure 2 Indicates Tempurung hill which is shattered by fractures (a), and the two sinuous passage caves, Anak Tempurung (b) and Tempurung (c) located close to each other in this hill. The red lines, in the caves passage, indicate the possible trend of fractures along which conduit development might have taken place, (d) 3-D map of the multi-layered and circular passage Kandu cave, and (e) paleokarst channels observed with seismic discontinuity and dip attributes (Zheng et al., 2011).

we can deduce that, good know-how of the origin and patterns of modern karst system may help to improve the interpretation and structural understanding of 3D seismic data.

The karstic caves conduits dimension in the study area do not exceed 10 m and in many caves it is about 1.5-2.5 meters. Though most of the channels appear collapsed, forming various scales of chambers, there are also conduits that survived the collapse. The multi layered Kandu cave (fig.2d) is a prime example that illustrates collapsed and extant conduits. Coalesced collapsed paleocave reservoirs that may extend for hundreds of kilometres are believed to have formed from later burial and compaction process (Loucks, 1999); nonetheless, considering the fact that commonly the average conduits diameter is within

the range of 2-3 meters and the distance between the channels is in the order of 10 m, the possibility of coalescing of channels, after burial, might be doubtful. At times, the possibility of occurrence of spongework patterns of solutional caves, in poorly lithified carbonates, and its resemblance with coalesced collapsed paleocave systems, needs to be taken in to consideration, so as to be able to alleviate the erroneous interpretation of these karst features.

Identifying the relation between karst channels and fractures is indispensable to understand complexity of subsurface karst. In the Kinta Valley, the complex structures that characterize the carbonate rock are also visible at the micro fracture scale (fig.1c). Fractures are also quite visible on the ceiling of cave chambers.

This fracturing phenomenon will be more aggravated when the subaerial karst features are subjected to burial, further enhancing the interconnection between fracture traces, which may lead to the formation of good fracture reservoir. It is obvious that fractures are below seismic resolution, but the resulting fracture porosity can potentially be extracted from seismic data (Eberli et al., 2004); therefore, understanding the complex fracturing phenomenon and the associated occurrence of karst features is an intrinsic part of acquiring information that can be crucial in the modeling of karst reservoirs.

Conclusion

The integrated approach of lineament analysis and cave surveying clearly indicated that the Kinta Valley karst morphology is controlled by tectonic structures. The possible continuity of fracture traces has also been inferred. As subsurface karst features are the result of subaerial karstification process and later burial, understanding the geometry of modern karst enables to visualize the possible geometry and scale of paleokarst features, which in turn strengthen the interpretations to be made from indirect evidences. Although subsurface karst features consistent with the scale and dimensions of modern karst can be inferred, a direct correlation or comparison is not always possible. In spite of that, the Kinta Valley karst system is considered as good analogue to envisage the continuity of fracture traces in carbonate reservoirs, which might have undergone intensive subaerial karstification process.

References

- Eberli, G.P., Masafarro, J.L. and Sarg, J.F. 2004. Seismic Imaging of Carbonate Reservoirs and Systems. AAPG Memoir, 81, 1-9.
- Golf-Racht, T. D. van, 1982. Fundamentals of fractured reservoir engineering: Elsevier Scientific Publ. Co., Inc. pp.710.
- Loucks, R.G., 1999. Paleocave Carbonate Reservoirs: Origins, Burial-Depth Modifications, Spatial Complexity, and Reservoir Implications. AAPG Bulletin, 83, 1795-1834.
- Odling, N. E., Gillespie, P., Bourguin, B., Castaing, C., Chile, J-P., Christensen, N. P., Fillion, E., Genter, A., Olsen, C., Thrane, L., Trice, R., Aarseth, E., Walsh, J. J. and Watterson, J., 1999. Variations in fracture system geometry and their implications for fluid flow in fractured hydrocarbon reservoirs. Petroleum Geoscience, 5, 373-384.
- Palmer, A.N., 1991. Origin and morphology of limestone caves. Geological Society of American Bulletin, 103, 1-21.
- Shen, F., 2007. Characterization and preservation of karst networks in the carbonate reservoir modeling. Society of Petroleum Engineers, 1-8.
- Vahrenkamp, V.C., David, F., Duijndam, P., Newal, M., Crevello, P., 2004. Growth Architecture, Faulting, and Karstification of a middle Miocene carbonate platform, Luconia Province, offshore Sarawak, Malaysia. In Eberli, P., Masafarro, J.I. and Sarg, J.F. (Eds.) Seismic imaging of carbonate reservoirs and systems. AAPG Memoir, 81, 329-350.
- Wang, B. and Al-Aasm, I.S., 2002. Karst-controlled diagenesis and reservoir development: Example from the Ordovician main reservoir carbonate rocks on the eastern margin of the Ordos basin, China. AAPG Bulletin, 86(9), 1639-1658.
- Zheng, D., Zhang, L. and Shen, F., 2011. Characterization and Modeling Study of Karst Networks in the Ordovician Carbonate Reservoirs, Tarim Basin. AAPG Annual Convention and Exhibition, Texas, USA, Poster presentation #40795.

A New Perspective of Structural and Property Modelling: A Case Study of Baram Oil Field, Offshore Sarawak, Malaysia.

A. I. Latief* (ROXAR), A. MacDonald (ROXAR), G. Rahman (ROXAR), M. E. Rahman (PETRONAS), W. A. Nasir (PETRONAS), A. I. Ridzuan (PETRONAS) & P. A. Faehrmann (SHELL)

Introduction

Baram is a giant mature oil and gas field located in the Baram Delta area of offshore Sarawak Malaysia. Reservoirs are Late Miocene to Early Pliocene deltaic to shoreface sands with an approximate thickness of 7000 feet and comprise of over 200 sand-shale zones. The field is outlined in a very complex structural setting of Sarawak Basin where early growth faulting, followed by compressional phase has created numerous unconventional fault geometries.

The field complexity, poses a real challenge to effectively manage and optimize the reservoir. An integrated reservoir model will be a prudent solution for interdisciplines communication platform and database, and also effective tool to support optimum reservoir management process. This is especially true, considering huge amount of data available in the field, in combination with over 40 years of production history.

An attempt has been made in 2006 to construct static model of Baram Field. However, due to technology limitation to address complexity of fault geometries, the model has to be segmented into 10 pieces. It restricts establishment of vertical reservoir communication (through wellbore or faults) and also lateral inter fault blocks interaction. Unfortunately, both event clearly observed and reflected in well production performance.

An innovative approach has been put in place in 2011, taking advantage of "state of the art" structural modelling technology and parallel property modelling technique. This has made construction of Baram Field integrated static model possible within a very effective timeframe. A static model which incorporate over 150 zones, 150 wells and 6000 compartments, been established in six months time. The model has set a new level of technology utilization in mature and complex field reservoir management.

Methodology

There are two important aspects, as described below, which contribute to the project success.

Automated fault geometry modelling

A modern algorithm for modelling the complex fault geometries in the Baram field (Figure 1 to 4) was used. This algorithm is fully automated and data driven and can model complex growth faulting and antithetic/synthetic conjugate structures. This would not have been possible using more conventional pillar gridding based fault modelling approaches.

Parallel property modelling

The geological grid were split into separate key stratigraphic intervals to allow parallel property modelling work. When completed the results were simply re-combined by upscaling into a single simulation grid to enable integrated reservoir simulation. This parallel approach to property modelling was one of the key measures which allowed the static model to be built within an effective timeframe.

In addition to the above, all the work processes from structural modelling up to volumetric uncertainty analysis were included in an automated (batch) workflow. This optimized the time used in modelling iterations and also provides the foundation for model updates as new well are drilled on the field.

Examples

To illustrate geometrical complexity of faults in Baram field, several examples are provided below. These examples has been chosen to represent most geometries exist in Baram field and posturing a real challenge to be modelled. It could be used as reference to tackle similar problem which may occur in other fields.

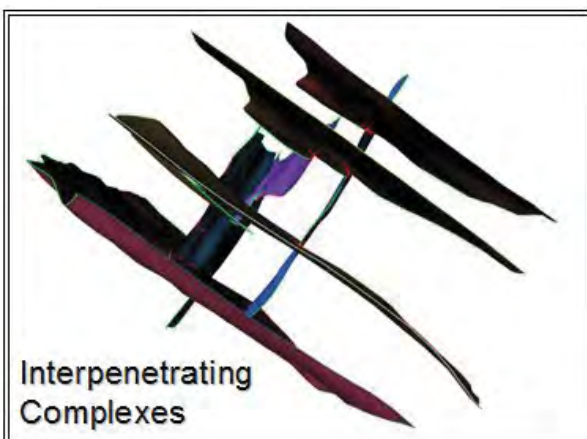


Figure 1: Example of interpenetrating complexes of faults in Baram field. This is the most complex geometry to be modelled as fault shapes are irregular, and only partly penetrating one into another, both laterally and vertically.

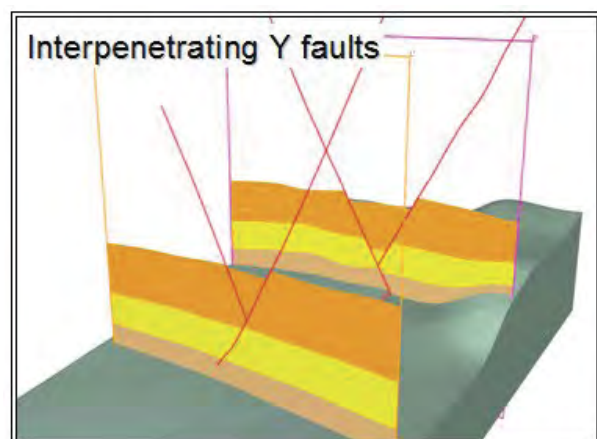


Figure 2: Interpenetrating Y faults, in which faults are change from synthetic to the antithetic side laterally.

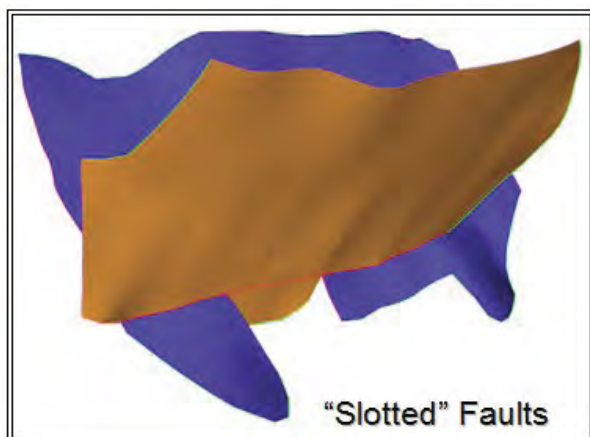


Figure 3: Example of slotted faults where faults are partly penetrate and intersect each other.

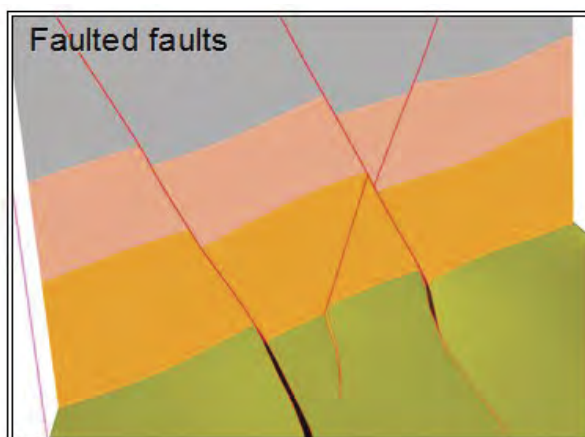


Figure 4: Example of faulted faults where faults are displaced by younger ones.

Conclusions

The construction of full field static model of a giant oilfield with a complex structural setting is non-trivial, but not an impossible task. A full focus on the importance of the timeline and early investment, plus the adoption a variety of strategic project management measures and use “state of the art” modelling technology can allow fit-for-purpose static models to be delivered within effective timeframe.

Acknowledgements

We would like to express our gratitude to the Management of Petronas Carigali Sdn Bhd (PCSB), and Petronas Petroleum Management Unit (PMU) for permission to publish the paper. Our special thank also to Budi Rahim Permana, Doan Hoang Thang, Vu Quach, and Khong Kheng Ting who was very cooperative and dedicative to accomplish the study.

References

- Darling, T.J., 1992. Baram field : Petrophysical analysis of BA-16ST3 core.
- Hoffman, K.S., Neave, J.W., 2007. The fused fault block approach to fault network modelling. Special Publications January 1, 2007. Geological Society, London, v. 292, p. 75-87.
- Lancelot Serling., 1991. Geological evaluation of cores from well BA-16ST3, Baram field, offshore Sarawak.
- Rizzi, G., Wood, J., Mathison, F., Phillips, I., 2003. Sedimentological, petrographic, SEM, and XRD investigation of core from well BA-50ST1, Baram field, offshore Sarawak.
- SIEP., 2006. Baram full field review phase 1 report.
- SIEP., 2007. Baram re-development field development plan report.

Seismic Reservoir Characterisation of a Channel Sand Oil and Gas Field, Malaysia

T. J. Focht* (Newfield Peninsula Malaysia Inc), M. Sams (IkonScience/ Fugro-Jason (M) Sdn Bhd), D. Brookes (Newfield Peninsula Malaysia Inc) & J. Ting (Fugro-Jason (M) Sdn Bhd)

Introduction

A regional, straight sandstone channel of mid-Miocene age within the Malay Basin forms a reservoir at several areas where the flow direction abruptly turned forming large meanders. One such meander constitutes the study field where oil and gas have been stratigraphically trapped. The seismic response to this channel is complicated by the laterally varying fluid type. The channel when wet gives a Class II AVO response and Class III when sufficient thickness of gas is present. The response changes depending on the height of the channel above the gas and oil contacts. The oil leg is only 12 meters thick. The response is also complicated by smaller channels just above and below this large channel. An underlying coal that varies in thickness and in some places appears to have been cut by the large channel also can distort imaging. With three exploration wells available, a seismic inversion study was conducted to try to extract more reliable and quantitative information from the seismic. As a result of the inversion the interpretation of the channel has been modified (Figure 1) and the inversion predictions have so far been confirmed by an additional two appraisal and four development wells.

Geology

The sole reservoir of the field is a fluvial channel sand and the hydrocarbons are stratigraphically trapped. The channel sand was deposited in an incised valley cutting into upper-coastal plain deposits consisting of siltstone and coals. All of the vertical wells to date have encountered a sandstone with a consistent thickness of 30 meters. A conventional core was acquired in one well which shows a fining-upwards grain size and a gravel lag at the base. The sandstone in the core is of good quality. Porosity ranges from 25 to 27 pu and net-to-gross exceeds 90 percent. Petrophysical analysis of all the wells in the field indicates that the reservoir shares common gas-oil and oil-water contacts.

Rock physics

At the time of the seismic characterisation study there were three wells drilled within the channel (Figure 1). One was wet, drilled on an amplitude anomaly down dip to the south. Two encountered gas, oil, and water. All three penetrated approximately 30 meters of good quality, channel sandstone.

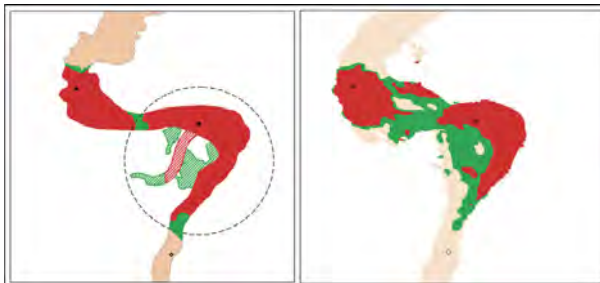


Figure 1: The channel distribution with the predicted fluids prior to the inversion study (left) and after the inversion study (right). Gas is shown in red and oil in green. The study field is circled. The line on the right represents the line of cross-section shown in Figure 3.

The logging suites in all of the wells were good quality with shear sonic measured in the wet well and one of the hydrocarbon bearing wells. At this time core data was not available. After further drilling with one appraisal well cored, it was found that the clay content of the channel sand was around the 25% level and the porosities were in the 25 to 27 pu range. The oil encountered has an API of 39. Cross-plotting of the P-impedance and Vp/Vs logs showed that there was separation such that at log resolution gas, oil and brine sands and shales could be differentiated. A rock physics model was developed that could predict to a reasonably high degree of accuracy the elastic logs based on a petrophysical interpretation in terms of volume of clay, porosity and saturation. During this modelling it was apparent that the elastic logs were affected by invasion and corrections were applied. Shear sonic data were predicted for the one well with no measured shear, and various fluid scenarios were modelled to try to understand the seismic response to various scenarios. Forward modelling of the AVO response indicated that the seismic response would be Class II to Class III and the ability to use high angle data would greatly enhance the ability to identify the channel and fluid fill. The rock physics modelled logs were used for tying the wells to the seismic and extracting wavelets for inversion.

Seismic conditioning

The seismic data available at the time had been stacked into 3 angle sub-stacks between 5 and 40 degrees, which initially seemed to be sufficient for the purpose of extracting useful Vp/Vs information from seismic inversion. However, a look at the NMO corrected seismic gathers showed that the events were not flat across the entire offset range and deviated upwards significantly at far offsets. The far traces appeared to contain useful amplitude information. It was decided to re-pick the seismic velocities and include the effects of anisotropy to flatten the gathers (Figure 2) and then re-stack to 5 angle stacks between 5 and 55 degrees. Validation for this process came with the drilling of a highly deviated well, which showed that the shales within the section above the channel are indeed highly anisotropic. After removing the residual moveout the seismic gathers were further processed to reduce random noise and multiples. The removal of multiples has had a significant impact in terms of cleaning up the image of the channel. A cross cutting channel depicted in Figure 1 in the pre-inversion channel distribution was found to be a multiple.

Despite this conditioning there remained a significant acquisition footprint. This footprint was assessed through RMS attributes at various intervals. These attributes were used to scale each of the seismic sub-stacks individually. Quality control checks were made to ensure that this process did not introduce artificial variations in the inversion results.

Inversion

Seismic inversion is run to convert seismic reflectivity to elastic properties. Due to a lack of low frequency information in the seismic data a low frequency model is required. This model is integrated during the inversion to provide a broadband result.

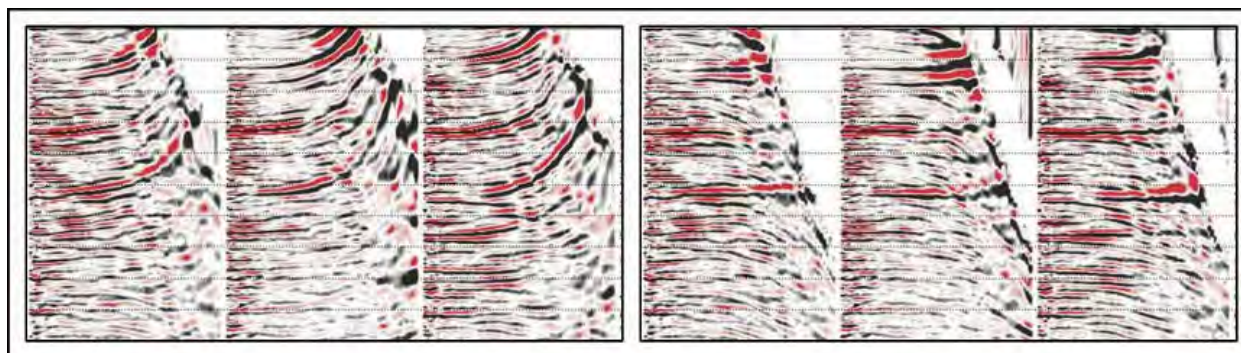


Figure 2: Seismic gathers before (left) and after (right) correction for anisotropic moveout. The channel is the event at the centre of the time interval and is clearly a Class II AVO. After anisotropic moveout correction further conditioning was applied.

When a number of angle stacks are inverted simultaneously the results are in terms of P- and S-impedance (or combinations of these) and density, though the later is most often not well constrained. This means that low frequency models for P- and S-impedance are required. These low frequency models must be geologically reasonable and can often only be determined through the interpretation of intermediate inversion results. For example, in this case all the well data penetrate the channel sand with various thicknesses of hydrocarbons.

Clearly the elastic properties of the sandstone cannot be extrapolated beyond the channel limits across the entire area to form a low frequency model. To overcome this, a detailed model of the sandstone reservoir and encasing strata was made and updated with intermediate inversion results. The detailed model is filtered back to 8 Hz to provide the low frequency component for the inversions and filtered back to 60 Hz to provide a comparison with the inversion output. Differences between the model and inversion are used to update the model.

The model is primarily based on an interpolation of the wells after the channel properties have been removed and replaced by a linear interpolation. Outside of the channel there is a high degree of correlation between the wells that justifies this procedure. The distribution of the channel is initially determined from an inversion of the ultra-far angle stack using a simple trend as a low frequency model. This proves to give a good prediction of the top and base of the channel at the well locations. Within the interpreted channel the porosity from the wells is interpolated. The porosity is then transformed to elastic properties based on the rock physics model and the fluid contacts. The fluid contacts are placed in time based on a time to depth conversion as described next.

Time to depth conversion

Time to depth conversion is important in this project. The structural dips are low and therefore small variations in time to depth prediction can have impact to the structural maps. The development plan that includes drilling long horizontal wells within the 12 meter oil column also requires accurate time to depth conversion.

Despite the apparent lateral consistency of the elastic properties above the channel, the time to depth relationships at the wells indicated that a simple model was not sufficient. The seismic velocities from the re-picking were conditioned and calibrated to the wells to provide a velocity model with which to convert the top of the channel to depth. This top channel in time and depth can then be used as a datum and velocities from the detailed low frequency modeling scheme used to time-depth convert data at other levels.

Interpretation

Interpretation is an iterative procedure in a seismic inversion workflow. There are a couple of critical items that are required from the interpretation. First is the ability to identify and pick the top and base of the channel. It is important to know where the channel exists and whether it has the same reservoir quality as penetrated by the wells. The top and base were interpreted on a number of inversion results, based on forward modelling studies that highlight the impact of fluid fill on how to pick the top (and base) of the sand. The inversion of the very far stack and the Vp/Vs from the simultaneous inversion of all the angle stacks, proved most useful. The P-impedance on its own is not helpful in determining the presence of channel sand (Figure 3).

Secondly, reservoir quality and fluid prediction are required. Due to uncertainties in the time to depth relationships across the field, it is important to get confirmation of the distribution of the fluids. Bayesian analysis was applied to generate fluid and lithology probabilities from the P- and S-impedance from the inversion. Due to the resolution and seismic noise these can not give detailed interpretations but it was possible to extract the most likely fluid at the top of the reservoir for comparison with that derived from the time to depth conversion of the top channel.

The P- and S-impedance from the inversion are affected by the presence of fluids and in combination with the limited resolution make identifying variations in porosity (or clay content) rather difficult. However, since a detailed model of the reservoir has been built to support the low frequency model, it is possible to look at the differences between this model filtered back to the seismic bandwidth and the seismic inversion results. These differences were interpreted in terms of variations of porosity from that initial assumption of interpolating the well porosities.

Early development drilling

Since the inversion study was completed, another six wells have been drilled. The first was an appraisal well drilled within the main channel at a location with a significant gas expression in the seismic. The well came in as prognosed in terms of depth, channel thickness and fluid content. The second well was also an appraisal well, but this time drilled outside of the main channel. Prior to the inversion study there was no clear idea of what sub facies of the channel system to expect at this location. The inversion study indicated an oil bearing channel sand of similar thickness to the other wells. The well penetrated a 30 meter channel sand with porosities similar to the other wells. No gas was encountered and the same oil-water contact as seen in the other wells was observed extending the

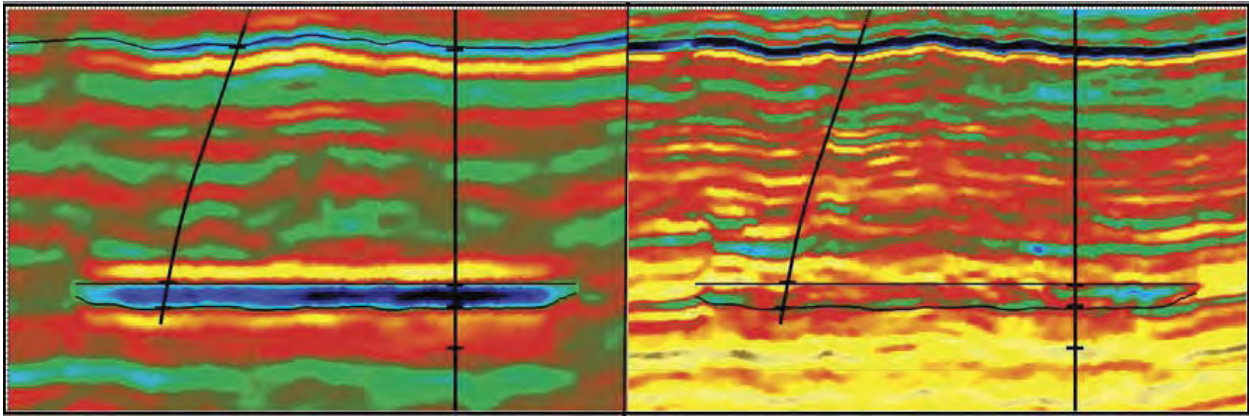


Figure 3: A cross-section through two recently drilled wells. The direction is south to north along the line indicated in Figure 1. The left hand panel shows the bandpass inversion results of the ultra-far angle stack that has been used for the initial interpretation of the top and base of the channel. On the right is the P-impedance from a simultaneous inversion. In both cases the data have been flattened to the top of the channel and blues represent low impedances. These wells were drilled after the inversion study and both came in as predicted in terms of channel thickness and fluid content.

size of the field. However, the well came in structurally low limiting some of the development potential.

The next four wells were horizontals with 1.5 kilometer lengths within the oil leg. The wells encountered the top of structure giving four more depth points. Two of the horizontal wells exited the top of structure at the heel providing two additional depth points. All of these data points were close to prognosis. Therefore if we trust the pick of the top of the reservoir in time we have more velocity control points for interpolation. Of course, there will be uncertainties in the top channel pick as it relies to a large extent on the far angle stacks, whose moveout correction is determined by a reasonably sparse velocity picking which included anisotropy corrections.

Conclusion

Seismic inversion can be used to improve our understanding and interpretation of seismic data. In fact, seismic inversion should be considered an integral part of seismic interpretation,

where both mutually benefit the other. Naturally, interpretation is also based on both geological understanding and rock physics models. Rock physics scenario modelling provides the framework for interpreting the elastic properties from the seismic inversion. In this case, interpretation has improved as different inversions have been applied and the inversion results have become more quantitative as the interpretation has improved. The results for this channel sand are semi-quantitative allowing for the prediction of the channel thickness and the fluid at the top of the channel. Estimates of porosity variation have been made but resolution issues and the small variations in the sand porosity make validation difficult.

Acknowledgements

We would like to thank the management of Newfield and PETRONAS for permission to present these data.

Value & Insights from Synthetic Seismic Validation of Reservoir Models in Carbonate Gas Fields, Offshore Sarawak

K. N. Baharaldin* (Sarawak Shell Berhad) & A. Kayes (Sarawak Shell Berhad)

Introduction

Robust static and dynamic models of the offshore Sarawak gas fields are of paramount importance for reliable volumetric estimation, production forecasting and optimum gas planning in order to maintain the security of gas supply. A tool for performing quick and timely health checks of reservoir models is therefore invaluable for providing confidence in model-based predictions. In Shell, a synthetic seismic workflow is used for validating carbonate reservoir models against seismic data and effectively “closing the loop”, which began with the interpretation of the seismic data in the first place. To facilitate this, an effective software solution has been developed to shorten the cycle time of the validation process, so that different subsurface scenarios can be assessed and key insights can quickly be incorporated into the modelling workflow. The workflow and examples presented here focus on the use of synthetic seismic validation to gain key insights into the reservoir architecture, properties and production behaviour of the carbonate gas fields of offshore Sarawak.

Method

Figure 1 illustrates the principal steps in the synthetic seismic validation of reservoir models. The first step is to convert the reservoir properties in the model (primarily porosity in the case of carbonates) to acoustic properties (V_p , V_s , and Density), based on water-wet rock property regressions derived from well data. Gassmann fluid substitution is then used to convert the acoustic properties to their gas saturated state.

As an initial QC of the model, the predictions of acoustic properties are compared to the measured acoustic logs at the well locations. The quality of this comparison establishes the confidence for the predictive value of seismic between the wells.

After that, synthetics based on the model can be generated by convolving the AI property model with a seismic wavelet extracted from the seismic dataset. Once the synthetics are generated, they are compared to the actual seismic.

Application to the Sarawak carbonate fields

1. Validating reservoir architecture & vertical porosity variations

Synthetic validation of static models can provide valuable insight into the “quality” of the final structural framework, including the internal reservoir zonation. The carbonate gas fields of offshore Sarawak generally exhibit significant porosity contrasts. Low porosity zones are generally attributed to episodic drowning events and can have a significant impact on vertical fluid flow and water breakthrough, particularly in fields with thin gas columns and strong aquifers. Ensuring that such zones are correctly modeled is therefore important, not only for predicting the distribution of GIIP, but also for predicting the location and timing of water breakthrough.

Converting intra-carbonate depth horizons back into the time domain using velocities derived from the model enables them to be compared with the time horizons from the original seismic interpretation. Zone thickness difference maps can then be quickly generated for each zone, in order to identify significant anomalies. These anomalies can either be attributed to errors in

the porosity model or errors in the original depth conversion; in any case they can be “fixed” accordingly.

Often synthetic seismic validation of reservoir models can reveal additional zonation which has been overlooked. In one instance an observation of this nature led to a timely review of the trajectory of a planned development well and the associated drilling risks ahead of drilling. In another instance, synthetic seismic validation revealed that vertical porosity variation, which had been present in the fine-scaled static reservoir model, was “averaged out” during initial upscaling for dynamic simulation purposes, resulting in an over-estimation of the vertical connectivity of the reservoir.

2. Validating lateral porosity variations

For the carbonate gas fields of offshore Sarawak, the preferred method for generating porosity models is to populate a pre-defined structural framework, using co-kriging of well log derived porosity with seismic acoustic impedance (AI) data as a secondary variable. Although the relationship between AI and porosity in carbonates is known to be highly variable at the core plug scale, it is considered to be reasonably well constrained at the seismic scale (>50ft). Nevertheless if the lateral variogram range used during porosity modeling is too large or the correlation coefficient is too low, lateral variations in amplitude can be “smeared out”.

Extracting attributes from the synthetic seismic data and comparing them with attributes generated from the actual seismic data can reveal errors or anomalies. A “good” match between synthetic and actual seismic amplitude maps can provide confidence in the both the structural framework and the property modeling approach, which in turn provides confidence in the GIIP estimate. Furthermore, since permeability is generally modeled as a function of porosity it will also have an impact on aquifer influx during dynamic simulation.

3. Validating karst properties

The presence of karst networks throughout the carbonate reservoirs is known to have a significant impact on both the GIIP and aquifer behavior. It is therefore important to incorporate secondary karst related porosity into Static Model

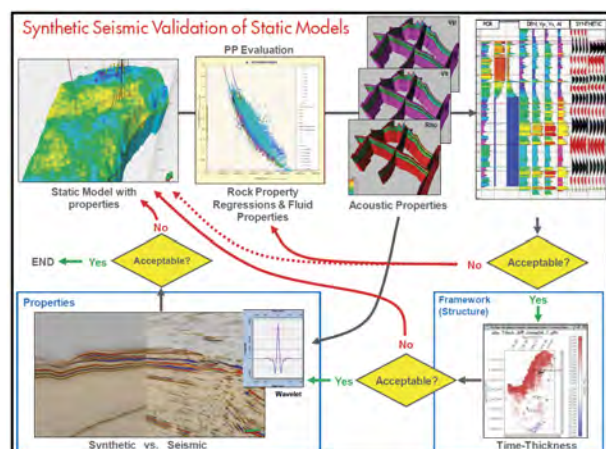


Figure 1: Summary of the principal steps in the synthetic seismic validation of reservoir models.

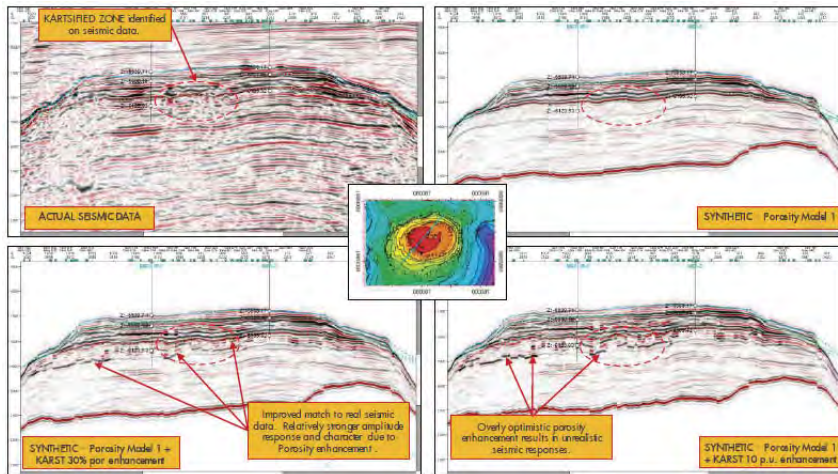


Figure 2: Example of using synthetic seismic validation on a number of alternative scenarios for constraining karst porosity in static models.

realizations. This enables more accurate volumetric estimates and better predictions for the nature and timing of expected water breakthrough at producing well locations. As well as the distribution of “karst” throughout a reservoir (derived from other seismic attributes such as semblance data), another important parameter to consider is the properties assigned to these regions. The synthetic validation process has been applied to great effect to test a number of sensitivities around karst modeling and porosity enhancement (in this case varying karst fill porosity uplift between a 10 pu absolute or 30% relative increase over background) by generating synthetics and comparing back to the real seismic response. As illustrated in figure 2, through this iterative approach, it has been proven that karstified type seismic responses and character can be replicated in synthetics and constraints applied to the modeling approach.

4. Validating dynamic simulation results

The next step from performing a 3D static model validation is to use available 4D seismic difference to attempt dynamic model validation. 4D seismic difference data is compared with synthetic seismic data that can be generated from dynamic simulation models using base case property volumes and the time-step water saturation cubes. By generating difference volumes between resulting time-step AI volumes, a direct comparison with the observed 4D signal can be carried out to assess the quality of the match of predicted aquifer response (HC fluid contact rise) with production against observed.

This approach has been applied in several instances to compare 4D seismic results with dynamic simulation results. To shorten the cycle time, the % AI difference between monitor and baseline time can be compared to the RMS amplitude of the measured 4D difference quadrature data. This is a more qualitative comparison made in the depth domain, but can still highlight spatially where water movement is correctly or incorrectly modeled. Subsequent modifications can then be made to the static or dynamic models to improve the match and provide more reliable predictions of water breakthrough at wells, which is a key risk for production forecasting in the field.

Conclusions

Developing and implementing a workflow for validating our carbonate reservoir models against seismic data has come with many benefits. As a tool for integration it enables different disciplines to integrate and be consistent; it helps production geologists to “think seismic”, and helps reservoir geophysicists to “think geology”.

As an early detection tool, it can alert subsurface teams to issues inherent in their modeling approach/strategy, interpretation and depth conversion, which can be addressed in a timely manner to avoid surprises with respect to volumetric estimates, forecasting and well planning.

The process has been applied to a number of fields in the Sarawak gas portfolio and to-date some of the key learnings are:

- The technique promotes a better understanding of the relevance of seismic amplitude variations on a model, such as the effects of tuning, and the effects of rock and fluid property variations. This can lead to better interpretation of key horizons that are used to constrain the model.
- Variations in internal reservoir architecture & layer thickness are often modeled incorrectly, or obliterated during upscaling. Synthetic seismic validation can be used to identify these issues and put them right.
- The technique of using AI data as a secondary variable to constrain porosity distribution in models produces good match to seismic amplitudes.
- Porosity enhancement in features, which are interpreted as karst, produces features in synthetic seismic, which are similar to those we see in actual seismic data, but too much porosity enhancement can be shown to be unrealistic.
- 4D synthetic seismic validations of dynamic simulations against available 4D seismic data can be used as an additional history matching parameter.

Acknowledgements

From Sarawak Shell Berhad; Tim Barker, Paul Hague, Mas Nur Afikah Rabani and Yee Shuh Wen.

Imaging Solutions for Geophysical Challenges in South East Asia

N. El Kady* (PETRONAS Carigali Sdn Bhd), Z. Mohd Dom (PETRONAS Carigali Sdn Bhd), Y. Prasetyo (PETRONAS Carigali Sdn Bhd), M. Bayly (WesternGeco), G. Nyein (WesternGeco), P. Vasilyev (WesternGeco) & N. Mat Don Ya (WesternGeco)

Introduction

Significant improvements in seismic acquisition, signal processing, imaging algorithms and computing power during the last 3 to 5 year period have made possible robust, reliable and effective solutions for most geological and geophysical challenges facing oil exploration companies in the South East Asia region. Improved illumination and resolution at target level, enhanced signal to noise ratio are possible through better noise and multiple attenuation and improved imaging techniques – these combine to provide higher confidence in the final image delivered to the interpreter and prospect generation group. This in turn, can lead to significant reduction in uncertainty and risk in prospect delineation and subsequent drilling.

In this paper we discuss seismic challenges in imaging and solutions for offshore Malaysia and other SE Asian basins. With depth imaging now a standard component of the seismic data processing workflow, the necessity for obtaining geologically plausible and geophysically reliable velocity models is critical. To match the expectations from the depth imaging outcome, velocity model building techniques have become increasingly complex, shifting towards the derivation of “earth models”. The “earth model” not only includes interval velocity (V_p) referenced in space and depth, also other subsurface properties such as Thomsen’s anisotropy parameters, dip magnitude and azimuth, faults, surfaces and geo-bodies. This requires more information from different geophysical methods, such as acoustic well logs and interpretation.

There are many geophysical challenges when it comes to earth model building for depth imaging, including region dependency, so we wish to cover several main issues for SE Asia and demonstrate possible technical solutions. The challenges we describe in this paper include: the near seabed and shallow velocity anomalies, major faulting and “fault shadow” effect, and seismic velocity anisotropy estimation and implementation. We will address each part and provide existing solutions based on several projects performed in SE Asia.

Data setting

The examples based on the prospect which is geologically placed within the highly prospective North Malay Basin, located Offshore West Malaysia. The main reservoir rocks are Oligocene to Middle Miocene in age, and are fluvial clastics. The anticlines draped on fault blocks and were formed during mid to late Miocene transpressional tectonic inversion phase are important hydrocarbon traps. This prospect contains challenging

geological and geophysical issues such as shallow biogenic gas, gas leakage from deep reservoirs, shallow channels and gas pockets, a major bounding fault system and many minor faults systems and generally layered geology with VTI anisotropy.

Methods

Near seabed and shallow velocity anomalies.

In case of shallow or leaking gas zones, the data can exhibit near vertical bands of weak reflection strength and very often deeper target reflectors show anomalous attenuated amplitudes with frequency (Ghosh et al., 2010). This is obviously not the true subsurface reflectivity response, but rather an “imprint” of overburden effects. The wave phenomena that can cause these bands may include, but are not limited to:

- Absorption and Transmission,
- Simple mis-stacking of the data due to an inadequate earth model and or imaging methods.

To solve this issue, the seismic data processing geophysicist must address the amplitude attenuation and associated frequency loss due to shallow gas, and derive an accurate velocity model for the near surface which ideally will include a high level of spatial detail. In this paper we propose a solution that is comprised of amplitude and frequency recovery prior to the imaging step, combined with the use of Diving (or Turning) Wave Tomography (DWT) with high resolution reflection tomography (Woodward, 2008) to produce an accurate and high-resolution near-surface (and deeper) earth model. This can be used for both time and depth imaging (Fig 1).

Fault shadow effect

From observation the PSDM gathers around the major bounding fault, on first view, an apparent velocity speed-up is required (Fig 2 left), however contrary this observation, when viewing an initial Depth stack, in a structural context, a slowdown in velocity is indicated. This is due to short spatial lateral velocity changes of an order shorter than a spread length. This is also expressed as a fault shadow or zone of weak data (Fig 4 upper panel). If the velocity model is not sufficiently detailed across major fault boundaries, then distortions in the depth of the structure can be introduced (Fig 3 & Fig 4). The potential for rapid lateral velocity change across a fault, if not resolved, can result in poor seismic images and non-hyperbolic moveout.

For this project a Fault Constrained Tomography (FCT) approach has been presented as a special depth processing technique that solves this problem through construction of detailed, high resolution interval velocity models for such zones

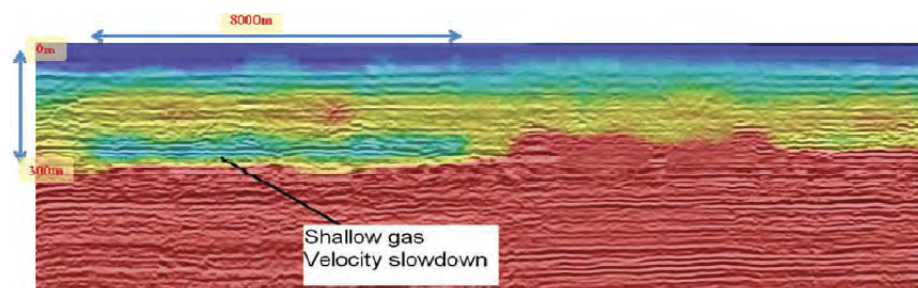


Figure 1: The Depth interval velocity model with DWT information included and after incorporating high-resolution tomography.

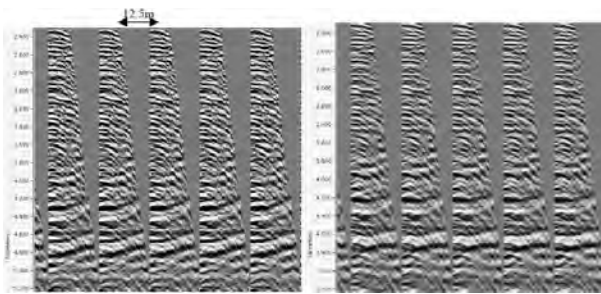


Figure 2: The Depth migrated gathers before applying FCT (Left) approach showing the apparent need for a velocity increase, however what is actually required is a slow velocity anomaly (pull up) in the vicinity of the near traces at a shallower depth around the fault. The Depth migrated gathers after applying FCT (Right) showing improved flatness. (note change in depth of the near traces.)

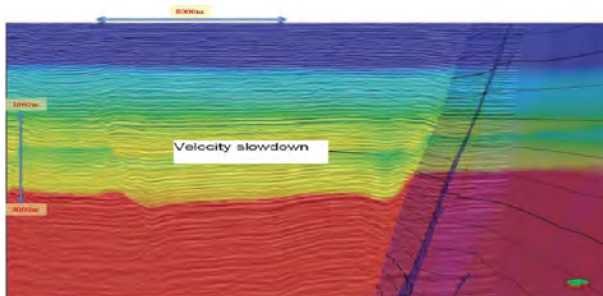


Figure 3: The Depth interval velocity model with fault information incorporated, showing the velocity anomaly (green zone) "stepped" across the fault causing the "fault shadow" effect.

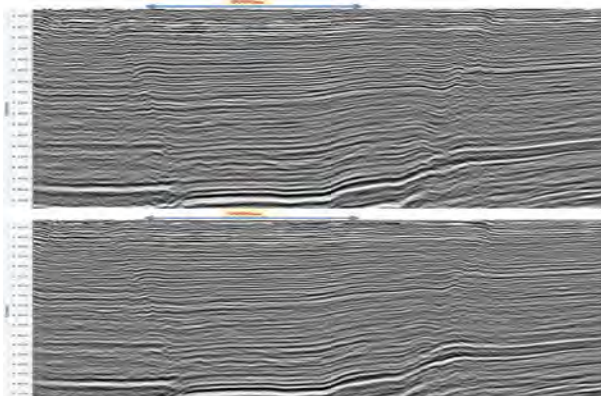


Figure 4: The Depth migrated stacks showing the structural positioning and difference in imaging around the fault before (Top) and after (Bottom) applying FCT approach.

(Birdus et al., 2007). The main steps in this approach are:

- Build as accurate velocity model as possible using conventional "global" reflection tomography approach.
- Interpret major fault planes and included them into the depth-velocity earth model.
- Perform Non-hyperbolic multi valued Residual Moveout Analysis performed on the dense grid around the selected fault .
- Run High-resolution 3D seismic tomography using the fault planes as a "soft" constraint to update the interval velocity. This is achieved via weighting of the RMO "picks" that relate to the fault or close by.

Anisotropic velocity model building.

At present we believe that all Earth Models constructed for depth imaging must include anisotropic parameters, as

their inclusion, has been shown to produce more geologically plausible and accurate seismic images. The estimation of accurate anisotropy parameters requires acoustic well data which helps constrain the possibilities for anisotropy variations. However this only provides information locally to the well and difficulty arises in extrapolation of the anisotropic parameters spatially and vertically across the prospect where typically, well coverage is sparse. One particular solution can be a workflow that incorporates: general knowledge and structural information of the area, analysis of data anellipticity (Interval eta) during time processing (using ray tracing) , derive Thomsen's δ from wells in the survey area or from a neighboring area, and to use spatially variable ϵ and δ fields, whilst honoring the variation of the anellipticity and guiding the extrapolation / interpolation of the field by interpreted structural surfaces (Zdraveva, Cogan, 2011).

In our example we had 3 wells which were analyzed and used to produce the required velocity scalar to match the well markers and initial epsilon and delta values. These values were found to be spatially constant within the interpreted geological boundaries, but vertically variant for each zone. After several iterations of reflection tomography with current anisotropic model updating only the vertical velocity, we observed that we cannot achieve the desired gather flatness as this initial simple anisotropic model was not quite suitable for the majority of areas away from the wells. The decision of introducing spatially and vertically variable gridded epsilon and delta values was made. In our paper we will demonstrate the method we used to produce a structurally consistent and plausible anisotropic earth model for the final depth imaging.

Conclusions

The main challenges for this project, as for many projects in South East Asia, have been: the near seabed and shallow velocity anomalies, major faulting and "fault shadow" effect, and seismic velocity anisotropy. We showed possible solutions for imaging in case of these issues using technologies to compensate for amplitude attenuation with frequency, producing high fidelity velocity models, honoring geological interpretation and faults and producing structurally consistent anisotropic models.

Acknowledgements

We'd like to thank Petronas Carigali for allowing the use and presentation of this data.

Reference

- Nabil El Kady, Shah Sulaiman, Zabidi M Dom, Tang Wai Hoong, Lee Mei Lu, Pavel Vasilyev, Martin Bayly. 2011. Seismic imaging near and within the basement offshore Malaysia, including comparisons of imaging algorithms. Petroleum Geology Conference and Exhibition, Malaysia 2011
- Zdraveva, O., Cogan, M.,Hydal, S.,Derbala, R., 2011. Large-scale TTI Imaging in Areas of Limited to No Well Control., Twelfth International Congress of the Brazilian Geophysical Society
- Woodward, M., Nichols, D., Zdraveva, O., Whitfield, P., and Johns, T., 2008. A decade of tomography. *Geophysics*, 73, VE-5-VE11.
- Dr. S. Birdus, 2006, Resolving fault shadow problem by fault constrained tomography, Petroleum Geology Conference and Exhibition, Malaysia 2006
- D.Ghosh, M.Firdaus, M.Brewer, B. Viratno, N.Darman, 2010, Geophysical issues and challenges in Malay and adjacent basins from an E&P perspective, TLE April 2010

Enhanced Seismic Imaging of a Mature Oilfield

A. Nalonnil (Schlumberger), T. Handayani (Pertamina),
W. Triyoso (Institut Teknologi Bandung (ITB)) & S. Dogra* (Schlumberger)

Introduction

Crosswell seismic is an emerging technology which provides enhanced resolution seismic imaging between wells. The technology has the potential to delineate complex structure and deliver enhanced imaging to reduce the inherent uncertainty in surface seismic where shallow attenuation and scattered coals impede the surface seismic method. The problem is compounded in complex plays, where traditional interpretation involving 3D surface seismic combined with log information retains a large degree of uncertainty since the imaging between the two scales of information requires in-depth geological knowledge combined with geostatistical best-fit approaches. Crosswell seismic reduces this uncertainty as it represents a physical measurement of sound waves between wells.

In this paper, some of the key results will be discussed with the focus on enhanced resolution. Initially, a brief description of the measurement theory and its capabilities is provided, followed by a description of the processing workflow and finally a discussion of the acquired results. Two main products were obtained from each profile: tomographic velocities and reflection images for both compressional (P) and Shear (S) arrivals. A further discussion on an integrated workflow to enhance existing surface seismic with the help of crosswell data is presented with key results.

Method

The technology employs tomographic surveying, whereby the transmitter and receiver are deployed in separate wells and traverse alongside the reservoir. The source-receiver geometry records the direct as well the reflected raypaths; thus providing the velocity tomogram and the reflection seismic between the wells (Figure 1). With its own inbuilt velocity model and higher frequency bandwidth, the migrated crosswell seismic reflection section provides an enhanced image between wells to diagnose the structural and stratigraphic potential of key areas in the field.

Example

In this paper, a case study from a mature oilfield in Indonesia (Handayani et al., 2011) is described highlighting the benefits of the crosswell technique in an area where surface seismic is difficult to interpret for infill well planning. A brief description of the measurement, assessment of enhanced resolution and additional value provided by the crosswell data is discussed (Figure 2).

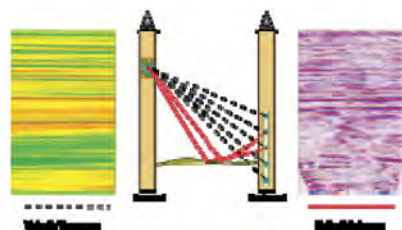


Figure 1: Data are acquired by having a receiver string recording seismic signals from a source deployed in another well. This allows for velocity (dashed black) and reflection (solid red) imaging to be processed.

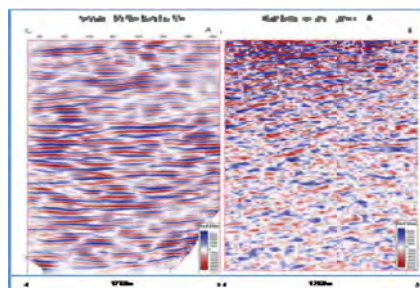


Figure 2: Crosswell seismic reflection section (left) at world record spacing of 1780m compared with equivalent surface seismic extraction in the same plane from the 3D cube (right).

These results at the Bunyu oilfield have led to a new understanding of the field and aim to improve the in-fill well selection process by combining with existing seismic, production and geological knowledge of the field. The data consisting of multi-well pairs will form the basis for advanced processing and interpretation including seismic attribute analysis (Figure 3), tomographic velocity control to help surfaces seismic processing and a new approach in seismic inversion leading to a clearer picture and validation of the surface seismic.

Conclusion

The crosswell profiles exhibit significant improvement in the seismic imaging in Bunyu field. The images reveal new stratigraphic plays that were not visible before in the existing seismic and achieve the overall project objective. The crosswell migrated sections and the related attributes such as acoustic impedance and others will provide useful data for in-fill drilling location identification and field optimization.

Acknowledgments

We thank Pertamina for the use of the seismic images.

References

- Handayani T., Irwanzah Z., Taslim M., Dogra S., Nalonnil A., Marion B., Carrillo Reyes, P., 2011. Enhancing Seismic Interpretation using Crosswell Seismic: Case Study from Indonesia, Proceedings from IPA, Thirty-Fifth Annual Convention & Exhibition, May 2011, IPA11 G-179
- Handayani T., Irwanzah Z., Taslim M., Dogra S., Nalonnil A., Marion B., Carrillo Reyes, P., 2011. Crosswell Seismic: Step Change in Seismic Imaging – A Case Study from Indonesia, SPE APOGCE, Sep 2011, SPE 147827

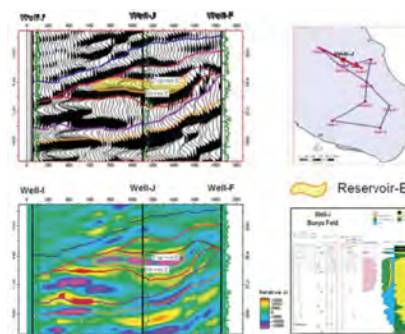


Figure 3: Preliminary structural and advanced interpretation of crosswell reflection profile between wells I and F. Sequence boundaries and GR log correlation with the reflection seismic (top) show potential sand pinchouts in the region of Well J (highlighted lens section). The bottom image shows the same interpretation overlain with relative acoustic impedance attribute - useful for identifying intra reservoir detail. Bottom right shows the petrophysical evaluation with hydrocarbon potential. Vertical axis is depth in meters.

Depth Imaging Coil Data: Multi Azimuthal Tomographic Earth Model Building and Imaging of Tulip

S. Chen* (WesternGeco Indonesia), M. Buia (ENI E&P), L. Livraghi (ENI Indonesia), M. Bakhrudin (ENI Indonesia), M. Tham (WesternGeco), M. Bayly (WesternGeco), S. Ng (WesternGeco) & O. Zdraveva (WesternGeco)

Introduction

The Tulip survey is located over the continental slope east of Kalimantan, offshore Indonesia in a water depth of 300-1500m. The overburden geology is extremely complex due to rugose water bottom, very bright Bottom Simulating Reflectors (BSR), very heavy faulting, sub-surface channels, and shallow overburden patchy gas pockets throughout the survey area. The target reflectors have very low acoustic impedance contrast and are heavily contaminated by surface and diffracted multiple energies. The consequence of these complexities results in overall poor seismic response, very low amplitude or near invisible target reflections, very low signal-to-noise ratio (S/N). With conventional narrow azimuth marine acquisition, this results in poor imaging and poor illumination of the reservoirs. A different approach was required not only in terms of acquisition method, but also a tailored processing workflow to improve the imaging and illumination of the reservoirs.

After an extensive survey design and feasibility study effort, eni chose a Coil shooting geometry (French, Cole, 1984; Tozzi et al., 2009) to more densely and diversely illuminate the reservoir for an appraisal campaign.

The benefits of an extended azimuth (multi, wide, rich, full, etc) datasets include not only illumination improvement, increase in signal-to-noise and event continuity, reducing multiples and enhancing amplitude fidelity, but also improving the tomographic velocity model updating and imaging stages.

However, velocity model building with full multi-azimuth data not only requires the use of a tomographic solver method that can comprehend the ray-path direction between the source and receiver, but also correctly account for the source to receiver azimuth contribution of traces in common image point gathers (CIPs) when performing residual moveout (RMO) analysis (Woodward et al. 2008). This paper will discuss the multi azimuthal tomography velocity model building workflow and depth imaging of the Tulip survey. In addition, a comparison will be made of individual azimuth sectored migration volumes combined using a straight sum compared to an optimum weighted summation.

Multi Azimuthal Anisotropic Tomographic Velocity Model Building and Depth Imaging Workflow

The Coil configuration and geometry used in this survey recorded a very high density (offset, fold, and azimuth), rich azimuth dataset. This additional azimuth information allows for a improved constraint for the full multi azimuth tomography enabling a detailed velocity model with higher degree of accuracy. With this geometry we were able to sector the full azimuth dataset into 29 offset groups and three azimuth sectors with 60 degree wide for azimuthal tomography velocity model building. Figure 1 shows the multi azimuth workflow.

All three azimuth sectors were iteratively prestack depth migrated for common image point (CIP) gather production for the model building loops. These gathers were produced on a dense 50mx50m grid to drive a high spatial resolution tomography solution. The gathers were individually analyzed

to measure multi-valued residual moveout (RMO) for each azimuth sector. All three sets of RMO picks were provided to a single "all azimuths" Grid Tomography to update the model. The assumption being that velocity change seen on individual CIP locations at this early stage with initial earth models is most probable to be unresolved overburden heterogeneity rather than true azimuth anisotropy.

Extensive auto-picking of gathers was used, and both smooth and complex moveout were used in the tomographic back-projection, depending on the scale length of the solution. This process was iterated until a satisfactory velocity model was achieved. Figure 2 shows the illustration of the Grid Tomography workflow.

The initial velocity model for grid tomography was derived from edited time domain interval velocities with strong smoothing. The first two iterations were isotropic with tomography resolving features to a scale length of 5000m horizontally and 1000m vertically. Further iterations used generalized Tilted Transverse Isotropy (TTI) modeling approach (Zdraveva, Cogan 2011). The following three tomography iterations converged to resolving features of a scale length of 1700m in the horizontal direction and 200m in the vertical direction. Each model loop was checked with quality control (QC) plots of the RMO gamma attributes as histograms and maps. Figure 3a and 3b show the RMO gamma QC maps over a window containing the main target depth for 1st iteration and 3rd iteration. Notice how the histograms have converged from being bi-modal (some zones too slow and some too fast) at the first iteration to a normal distribution around zero by the third iteration, for all azimuth sectors. This indicates the single earth model being produced is reducing the residual moveout for all azimuths.

This further indicates that the bulk of the residual moveout seen at earlier iterations is due to previously undefined overburden heterogeneity (lateral velocity change) and not change of velocity with direction due to potential HTI anisotropy. As noted by Whitfield et al. (2009), overburden lateral velocity heterogeneity needs to be reduced first before indications of Azimuthal Anisotropy can be investigated. In this case, observation of azimuth and offset organized butterfly gather QC displays indicated that azimuth velocity change appears to be minimal once the earth model was refined in this manner. Figure 4 shows the initial model and fifth iteration model overlaying the seismic data, this displays velocity details corresponding to the geology and reflection boundaries. Figure 5 shows a comparison stack of the prestack time imaging (stretched to depth) compared to the improvement of depth imaging using the multi azimuthal velocity model building technique. The depth imaged data shows improved data continuity, visibility and sharpness of the key dipping events.

Following an initial depth migration of the entire survey, a subset volume of data was extracted for a more detailed work program. Two additional iterations of TTI tomography were performed on this subset volume, resolving to a scale length of 1000m horizontally and 200m vertically. This further improved the earth model and the details can be seen in Figure 6.

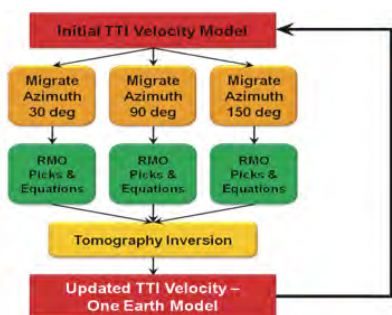


Figure 1. Multi azimuth tomographic workflow

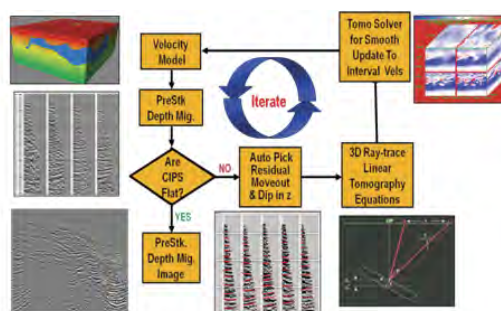


Figure 2. Illustration of the Grid Tomography workflow.

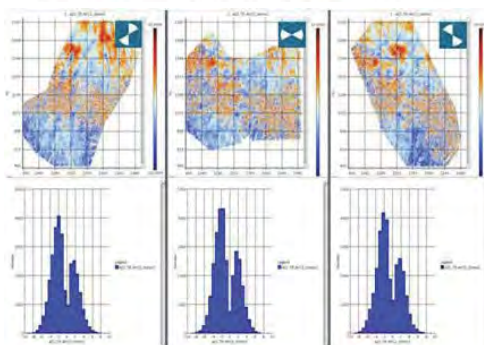


Figure 3a. RMO Gamma maps and histograms QC of 1st iteration

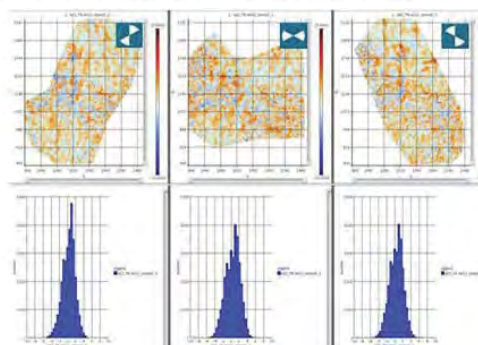


Figure 3b. RMO Gamma maps and histograms QC of 3rd iteration

During the entire earth model building process, the developing model was constantly monitored against geological knowledge and expectations; in order to give a physical meaning to the velocity anomalies observed. A good match was observed between the velocity model and the single available VSP derived interval velocity measurement (Figure 7). This confirmed the interval velocity gradient changes with depth computed by the tomography. Also of note were the slow velocities indicated below the seabed, these are likely to be due to free, patchy gas. This not only produces very slow P wave velocities but contributes to the strong absorption effects present in the dataset. Furthermore, although the tomography did not use interpreted horizons as constraints, the resulting model matches the geologic boundaries; for example a slow velocity zone from the model correlating to an overpressure zone encountered during the first exploration well.

Azimuth Sector Migrations and Optimum Weighted Stack

Although the original project timeline only allowed for the initial migration of the data as an “all azimuth” migration, there was an opportunity later to perform azimuth sector migrations with the coil dataset. By deferring the summation of the different azimuths from the migration step to a separate sum later enables analysis of event illumination in differing directions.

The individual azimuth sector migrations show depth and space variant quality differences of stacking response, signal to noise level and data continuity depending on the azimuth sector. Different azimuth sectors illuminate different areas of the zone of interest with varying signal to noise ratios. Ideally, the optimal dataset will be a combination of the best stacking response and highest signal to noise data regions from each azimuth sector thereby producing an optimized final stack volume. To analyze the benefit of this approach, a comparison stack was

produced by straight summing the three azimuth migrations; another stack was then produced using an optimum weighted stack technique. This method derives azimuth, depth and space variant weights based on comparative data quality so that the best data zones from each azimuth sector are given more weight in the stacking process. As a consequence, maximum coherent/illuminated events are favoured on the resultant weighted stack output. Figure 8 and 9 show the comparison of the two methods and the advantage of the optimum weighted stack method is clearly visible.

Conclusion

The success and value of the multi azimuthal TTI anisotropic earth model building using grid tomography and following depth imaging workflow has been demonstrated. The final velocity model matches the VSP data very well. The resulting images in this challenging prospect are demonstrably better in terms of data continuity, visibility and sharpness of the dipping events compared to traditional methods. The azimuth sector migrations and optimum weighted stack also showed another advantages of rich azimuthal diversity datasets.

Acknowledgement

The authors would like to thank eni E&P Management, eni Indonesia, BPMIGAS, and WesternGeco for permission to publish this paper

References

- French, W., 1984, Circular seismic acquisition system: US Patent No. 4,486,863.
- Cole, R.A., and French, W.S., 1984, Three-dimensional marine seismic data acquisition using controlled streamer feathering: 54th SEG Annual Meeting, Expanded Abstracts, 293-295.
- Durrani, J.W., French, W., and Comeaux, L.B., 1987, New

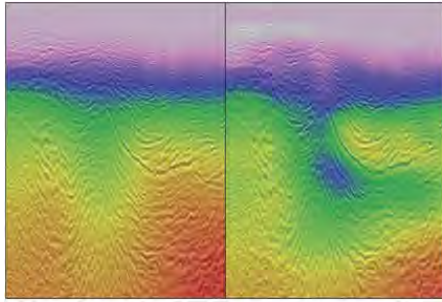


Figure 4. Initial (left) and 3 iterations TTI modeling (right)

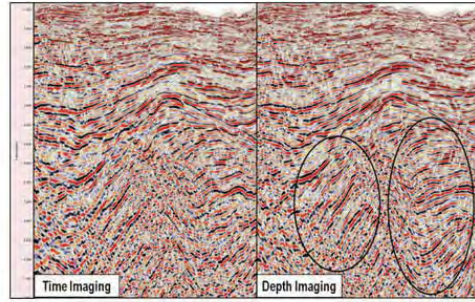


Figure 5. Comparison stacks of time imaging and depth imaging - the depth imaged data shows improved data continuity, visibility and sharpness of the key dipping events

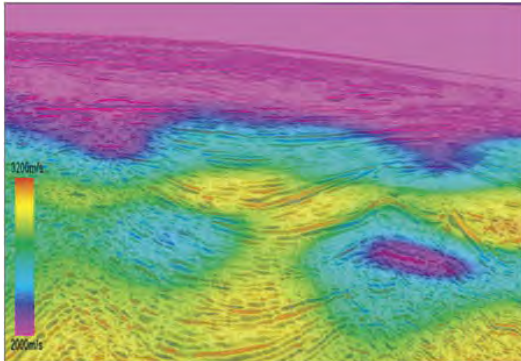


Figure 6. Velocity after two further iterations of TTI tomography updates

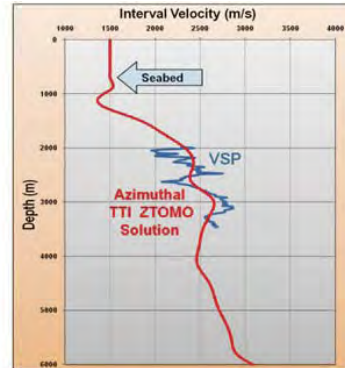


Figure 7. TTI azimuthal tomography velocity and well VSP

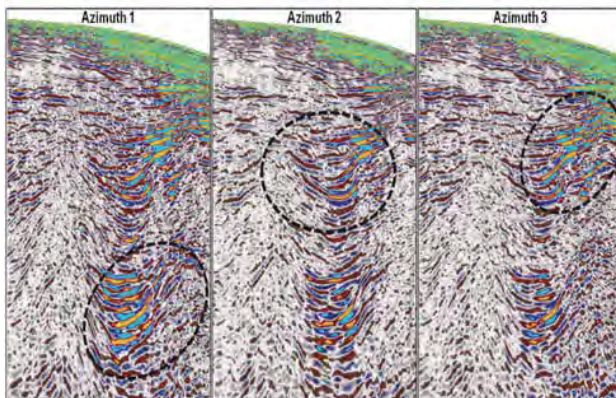


Figure 8. Azimuth sectored migrations

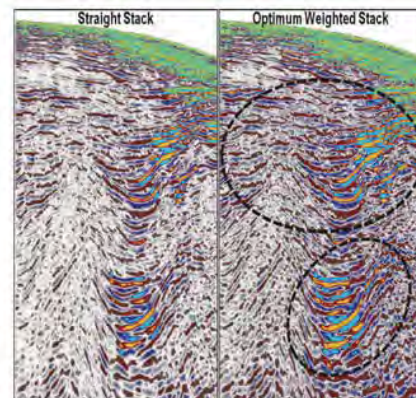


Figure 9. Straight stack vs. optimum weighted stack.

directions for marine 3D surveys: 57th SEG Annual Meeting, Expanded Abstracts, 177-181.

Whitfield, P.J., Woods, R.T., Manning, T., and Baptiste, D., 2009, Multi-azimuth QC for velocity model building - A Nile Delta Case Study: 71st Conference and Exhibition, EAGE,

Extended Abstracts, paper V015.

Buia, M., Vercesi, R., Tham, M., Ng, S.L., Waluyo, A.T., Chen, S., 2010, 3D Coil Shooting on Tulip field: Data processing review and final imaging results: 80th SEG Annual Meeting, Expanded Abstracts, 31-35.

Geomechanical Approach to Resolve Severe Velocity Variations and Remove Image Distortions Below Rugose Seafloor

S. Birdus* (CGGVeritas Australia), A. Artyomov (CGGVeritas),
L. Li (CGGVeritas) & S. Xin (CGGVeritas)

Introduction

Seismic imaging and depth-velocity modelling below a seafloor with complex topography are always challenging. The problems are caused by two types of lateral velocity variations: (1) contrast between the water and sediments and (2) velocity variations within shallow sediments created by the variable water depth.

A few years ago geomechanical modelling (Birdus, 2009) was included into the depth-velocity modelling toolkit to solve velocity variations within shallow sediments caused by variable stress and differentiated compaction below a rugose seafloor.

In this paper, we propose a new version of tomographic inversion that is focused (constrained) to recover spatially variable velocity anomalies caused by geomechanical effects below rugose seafloor. Applied together with geomechanical modelling and standard seismic tomography it helps to solve the strongest and most complicated water bottom related velocity anomalies. Synthetic and real data examples illustrate how it works.

Geomechanical velocity anomalies below seafloor with complex topography

We know that a stress applied to given sediments changes seismic velocities. Variable water depth always creates some variations in overburden pressure and corresponding anomalies in interval velocities. These compaction driven velocity anomalies can extend far away from the seafloor and seriously affect seismic rays travel times and geometry. In case of severe variations in the water depth (seafloor channels, cliffs, prominent reefs, etc) these anomalies can be much stronger than typical velocity variations associated with lithological changes.

Standard seismic tomography often fails to correctly recover these velocity anomalies because (a) acquisition parameters may be selected for illumination of much deeper target intervals, so we do not have enough offsets to estimate moveout immediately below the seafloor and (b) the anomalies can have significant magnitudes (up to more than 20%) with complex 3D shapes and rapid variations.

Luckily, the geomechanical anomalies obey laws of solid mechanics and petro-physical relationships between stress and

interval velocities. We can calculate such anomalies using this knowledge.

Geomechanical velocity modelling consists of 3 major steps:

1. Determine the sources of anomalous geo-stress. If we know the seafloor topography and difference in density between the shallow sediments and the water, we can calculate variations in overburden pressure caused by the variable water depth.
2. Calculate how the stress propagates away from the sources in 3D geological media using principles of solid mechanics. These stress anomalies (color overlay on Figure 1.b) extend far away from the seafloor.
3. Transform anomalous geo-stress into interval velocity variations.

Seismic reflection tomography constrained to geomechanical velocity anomalies

The following equation describes how geomechanical modelling calculates interval velocity variations below rugose seafloor:

$$\text{Vanomaly}(X, Y, Z) = \text{WB}(X, Y) * \text{Propagate}(X, Y, Z) \times \text{SV}(X, Y, Z). \quad (1)$$

The first term is the source of variable overburden pressure - the seafloor topography; in practice it is well known. The second term is a convolution operator that describes how variations in overburden stress propagate in 3D medium away from their source - rugose seafloor; this term is well determined by solid mechanics theory. The convolution of the first two terms is a variable overburden stress in sediments caused by the seafloor topography; it can be relatively easily calculated with sufficient accuracy. This convolution describes anomalies shown in colour on Figure 1.b in units of pressure. The third term is the most challenging part of the equation; it sets relationships between variations in overburden stress and interval velocities. The third term is responsible for the absolute values of the anomalies shown on Figure 1.b in units of velocity. In general, an increase in overburden stress leads to higher interval velocities but in practice we found it difficult to derive the necessary numerical functions with sufficient accuracy. In order to solve this uncertainty we use seismic tomography approach. We build an initial interval velocity volume using geomechanical modelling with parameters based on our best a-priori estimation. Then we run PSDM, measure depth-residual moveout and set tomographic inversion to find velocity anomalies that would (a) minimize the measured residual moveout and (b) have 3D shape of stress anomalies corresponding to the given water bottom topography. In this way, the tomography is constrained to estimate only the magnitude of anomalies with known shapes. It makes such hybrid tomography-geomechanical inversion robust and accurate even in the most difficult situations where the standard unconstrained tomography fails. As soon as geomechanical modelling and geomechanical constrained tomography build an accurate velocity model for the shallow sediments affected by variable stress fields we switch to standard tomographic sequence to recover other geologically determined velocity variations at all levels.

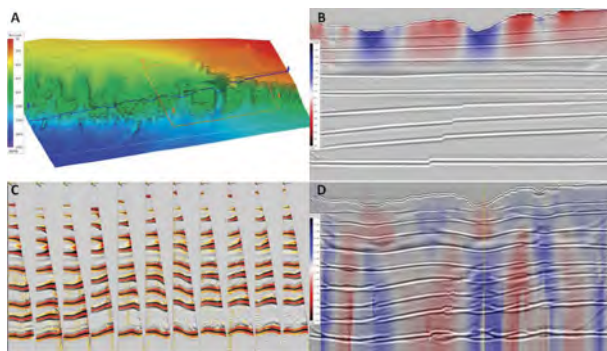


Figure 1: Some results of synthetic modelling. See text for the details.

Synthetic and real data examples

In reality, there is always have a combination of lithology dependent and compaction driven velocity variations, along with other types of velocity anomalies. In order to test different processing sequences and to provide some illustrations we created a synthetic dataset with geomechanical velocity anomalies corresponding to a fragment of a real seafloor with complex topography (Figure 1). The orange polygon on Figure 1.a shows the extent of the 3D synthetic dataset, the blue traverse is the location of the real seismic section shown on Figure 2. The velocity volume for synthetic modelling consisted of three components: (a) water layer with sipican based vertical velocity profile (range from 1480m/s to 1530m/s), (b) smoothed compaction driven trend for the sediments and (c) geomechanical velocity anomalies caused by the given seafloor topography. All these contribute to the real velocity field, we just excluded lithology dependent variations from the model. The smoothed trend "b" can be seen in colour on Figure 2.a. The geomechanical velocity anomalies are displayed in colour on Figure 1.b, they have magnitude up to plus/minus 300m/s and extend down to approximately 1.5 km below the seafloor. Red colour corresponds to positive velocity anomalies (increased overburden pressure), blue colour - negative anomalies (decreased pressure). PSDM section migrated with correct velocity can be seen on Figure 1.b. Figures 1.c and 1.d show PSDM gathers and stack migrated with the smoothed velocity model that excluded geomechanical anomalies. Colour overlay on Figure 1.d is the residual moveout section. The section on Figure 1.d is a synthetic equivalent of the real data section from Figure 2.a. The rugose seafloor topography with up to 600m deep channels leads to strong image distortions. The real seismic section has been also affected by lithology dependent velocity variations but their impact seems to be much weaker than that of geomechanical anomalies. These results confirm that geomechanical velocity anomalies are responsible for the majority of imaging problems below rugose seafloor.

All types of seismic tomography use PSDM gathers (Figure 1.c) to determine velocity variations (colour overlay on Figure 1.b). Geomechanical constrained tomography benefits from the a-priori knowledge of 3D shapes of geomechanical velocity anomalies. We used the synthetic data to compare (1) standard tomography, (2) geomechanical modelling followed by standard tomography and (3) geomechanical modelling followed by geomechanical constrained tomography. We saw noticeable increases in the quality of the results as we evaluated the workflows in this sequence. We started with a "perfect" synthetic dataset (Figure 1.c); then, to make the study more realistic, we excluded shallow events from the analysis and reduced number of valid residual moveout picks for deeper events, in these latter cases we observed increased importance of geomechanical constraint as the standard tomography started to fail whereas the geomechanical constrained version was still producing reliable results.

Figure 2.b shows real 3D PSDM section after geomechanical modelling and several iterations of tomography including geomechanical constrained inversion. This workflow removed all image distortions caused by the rugose seafloor.

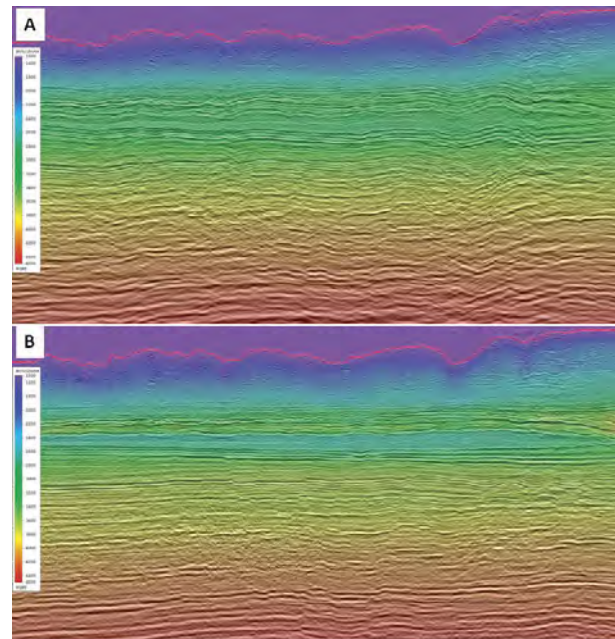


Figure2: 3D PSDM sections migrated (A) with the initial velocity model that includes only contrast between the water layer and the sediments with smoothed velocity field, (B) after depth-velocity modeling including geomechanical constrained tomography. Depth scale. Interval velocities are overlaid in colour. NW Australian shelf. Data courtesy CGGVeritas Multi-client Data Library.

Conclusions

Compaction driven velocity variations are important components of real velocity models.

Geomechanical approach to building velocity models in areas with complex seafloor topography:

- enhances our understanding and representation of real velocity fields and seismic data;
- allows us to achieve distortion free seismic images below rugose seafloor.

Geomechanical constrained tomography:

- uses seismic data to estimate vital parameters of geomechanical velocity models;
- provides a robust and accurate solution even in cases of inadequate illumination, poor seismic data quality or structural complexity.

Acknowledgement

The authors thank CGGVeritas management and Multi-client Data Library for permission to present these results.

References

- Birdus S., 2009. Geomechanical modeling to resolve velocity anomalies and image distortions below seafloor with complex topography. 71st EAGE Conference & Exhibition, Extended Abstracts, U014.

The Role of Play-Based Exploration in Heartland Portfolio Rejuvenation, Offshore and Onshore Sarawak, Malaysia

S. J. Gough* (Sarawak SHELL Berhad), E. W. Adams (Sarawak SHELL Berhad) & T. Evers (Sarawak SHELL Berhad)

Shell has a long history of exploration in Sarawak, with the first discovery being made over one hundred years ago. Historically, exploration has largely focused on three main plays: Central Luconia carbonates situated above a maximum flooding surface known as the mid-Miocene unconformity (MMU), post-MMU clastics in the Baram Delta, and pre-MMU clastics in the southern Balingian region. Continued recent discoveries in the mature Balingian acreage to the south and, more importantly, recent high profile discoveries proving a working petroleum system in North Luconia, pointed to yet un-creamed pre-MMU plays and the potential for large discoveries in an area previously unexplored by Shell.

For these reasons, Shell has recently renewed its focus on heartland portfolio rejuvenation, using play-based exploration (PBE) techniques to assess the remaining exploration potential of the pre-MMU stratigraphy of onshore and offshore Sarawak. This paper shows how fully integrated regional studies based on a PBE approach can effectively quantify existing and identify new plays in a varied and complex basin environment. This play-based approach to portfolio rejuvenation culminated in Shell being awarded coveted exploration blocks during the recent Malaysia exploration bid-round.

Regional evaluation work focused on offshore and, subsequently, onshore Sarawak. Access to a large regional well and 2D seismic dataset, combined with recent advances in our biostratigraphic understanding of the region allowing reliable correlation between wells throughout the basin, presented an opportunity to undertake a fully integrated re-interpretation and a full revision of the biostratigraphy, tectonostratigraphy and sequence stratigraphy of Sarawak, and a simultaneous enhancement of the (mega-) regional structural framework. This built a strong foundation on which to redefine a number of megasequences, within which were developed a series of gross depositional environment maps, recording our understanding of the palaeogeographic evolution of the basin and, ultimately, helping to describe and constrain a number of key plays. The fresh interpretation of >65 key pre-MMU wells drilled in the basin since 1960 formed the basis of a comprehensive well look-back evaluation, incorporating results from parallel studies such as re-interpretation of overpressure trends, estimation of depth to basement (including potential fields modeling), and basin modeling. Expansion of the regional evaluation to include older Eocene to Early Miocene stratigraphic units onshore Sarawak also provided an opportunity to enhance our understanding of central and northern Sarawak, thus rapidly expanding and

refining our evaluation. Together, this enabled the creation of a detailed set of play maps showing the location and extent of sweet-spots throughout the basin, providing focus for prospect maturation, and culminating in the fast delivery of defined prospect portfolios in coveted acreage.

The study confirmed the legacy view that the objective pre-MMU sequence in Central Luconia has poorly developed, deep and highly overpressured reservoir potential. Three main pre-MMU sweetspots were identified in Sarawak. One, the shelfal clastics play in the southern Balingian region, was confirmed as being largely creamed. A potential Oligocene-Early Miocene carbonate play in southeast Sarawak was not pursued, steered partly by regional play-based views of this carbonate from elsewhere in the basin. In contrast, high-graded Cycle I and II shelfal clastics play segments in North Luconia have few well penetrations, and several large undrilled structures have been identified as having big cat potential.

Figure 1 shows the palaeogeographic evolution of Sarawak, from Late Eocene to Mid Miocene. In the Late Eocene (Pre-Cycle I), speculative isolated thrust-top platform carbonates developed within widespread marine shales in front of the Rajang accretionary wedge. By the Late Oligocene (Upper Cycle I), a relatively stable, regionally extensive coastal plain and shelf system was established, with parallel coastline and shelf edges trending northwest-southeast. In the Early Miocene (Lower Cycle II), extensional and transtensional faulting and in some areas major uplift took place, the clastic shelf system retreated to the southwest, and widespread passive shelf-margin carbonate deposition occurred in distal northeast Sarawak, before being largely smothered by prograding shelf clastics. In the early Mid Miocene (Cycle III), Sarawak was dominated by shale-rich topset beds during a flooding stage.

In conclusion, by integrating all available data using a PBE workflow, a solid regional understanding of the Sarawak basin has been established, including a modified tectono-stratigraphic framework distinguishing two megasequences, and a revised understanding of palaeocoastline and shelf evolution. Based on these strong foundations, a series of easily updateable play and CRS maps has been compiled. These have enabled identification of sweetspots in previously overlooked plays, the definition of an internally consistent new lead portfolio, and the addition of a ranked list of coveted acreage for these plays, primarily focusing on potential big cat opportunities in pre-MMU Cycle I and II shelfal clastic plays in North Luconia.

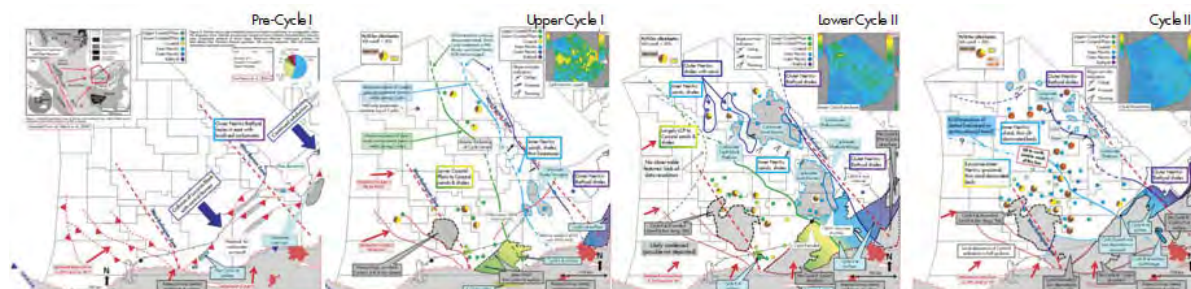


Figure 1: Gross Depositional Environment (GDE) maps illustrating the palaeogeographic evolution of the pre-Mid Miocene unconformity ("pre-MMU") stratigraphy of Sarawak.

Deepwater Exploration in Malaysia, Offshore Sarawak

P. Baltensperger* (Newfield Exploration), K. Robinson (Newfield Exploration),
A. Finlay (Newfield Exploration) & A. Thomas (Newfield Exploration)

Introduction

Recent exploration drilling by Newfield and their partners, PETRONAS Carigali and Mitsubishi Corporation, has proven a new hydrocarbon province in Deepwater Sarawak, Malaysia. The Newfield operated JV have drilled 2 wells since signing the Deepwater PSC in 2004 resulting in 2 hydrocarbon discoveries.

The offshore Sarawak region has been divided into a number of structural-stratigraphic geologic provinces. The study area lies in the North Luconia province, beyond the continental shelf and north of the prolific hydrocarbon producing Luconia province (estimated reserves of > 33TCF and 2.4 Bbl) which produces mainly from Miocene carbonates. Alternatively, the prospectivity in the deepwater province is in the Late Oligocene-Miocene clastics. Water depths in the block extend to greater than 2000m.

Exploration methods and results

Previous drilling in this deepwater region had been unsuccessful before the 1st exploration well in 2006/2007 and 2nd exploration well in 2009 (figure 1). Historical deepwater oil discoveries have been limited to offshore Sabah. The 2nd exploration well (figure 1) was the 1st well to encounter an oil column in an Oligo-Miocene reservoir in deepwater Sarawak.

Various geophysical, geochemical and remote sensing methods have been used in the exploration efforts on the block including CSEM, drop cores, seep studies and detailed mapping from recent 3D PSDM.

The tectonic feature tested by exploration well #2 is a large paleostructure present during Late Eocene-Early Oligocene which has undergone a complex tectonic history with recent extension and sediment slumping as indicated by near surface faulting in the Plio-Pleistocene. A NE-SW trending extensional fault system dominates the structural architecture and act as the trapping mechanism for numerous prospective tilted fault blocks and a conduit for vertical gas leakage. Large gas chimneys are present 300-400m below mudline at the crest of the structure due to leakage along older major faults which have been reactivated in the Pliocene. The crestal portion of the fault blocks is very poorly imaged on seismic due to P-wave transmission loss below shallow gas accumulated in the Pliocene which has made definitive mapping of the structural geometry of prospective fault blocks difficult. The application of modern seismic depth imaging has improved data quality and resulted in significant changes in structural mapping (figure 2).

Primary reservoir targets are Late Oligocene to Early Miocene shoreface and shallow marine sandstones. Fault juxtaposition of Miocene shoreface sands and marine claystones act as a lateral seal. Reservoir sand and interbedded shales form intra-formational seals while >1000m of overlying Pliocene bathyal claystone acts as a regional topseal. The Post MMU sediments are poorly consolidated and present a seal capacity risk for large gas columns in the Cycle I reservoir.

Source rock in the late Oligocene section in the form of 1-3m thick coal units were encountered in discovery well #2. These rich sapropelic coals act as the primary source rock in offshore Sarawak. Coals of similar geochemical properties are present as in-situ and re-deposited coals in offshore Sabah and Eastern Kalimantan. Pre-drill analysis of drop cores, gas chimneys and

flats spots indicative of fluid contacts in various fault blocks suggest that the structure has received hydrocarbon charge. Fluid escape features evident on the seafloor were sampled with drop cores and indicate the presence of thermogenic and biogenic gas (figure 3). The results from the 2 exploration wells prove that an active source kitchen is present and that both gas and liquids have been generated.

Well #2 was drilled as a deviated well to test the potential of stacked clastic reservoirs at a crestal location in the prospective fault block. The surface location was positioned to avoid drilling through the shallow gas hazard resulting in a 49deg deviated well trajectory through the objective reservoir interval. The well plan consisted of a shallow vertical hole section then building angle and a deeper hole section with constant angle paralleling the major west bounding fault. All objectives were normally pressured and evaluated without any significant drilling problems. An appraisal to the 2nd discovery well is planned in 2012.

Acknowledgments

The authors would like to thank PETRONAS for their support and cooperation during the exploration phase of this PSC and also Mitsubishi Corporation for their support as our joint venture partner.

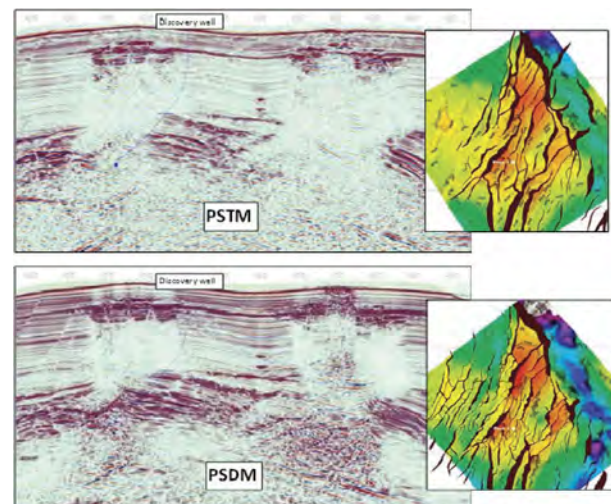


Figure 2: Comparison of PSTM vs PSDM illustrating the improved imaging and related changes to structural mapping in the prospect area.

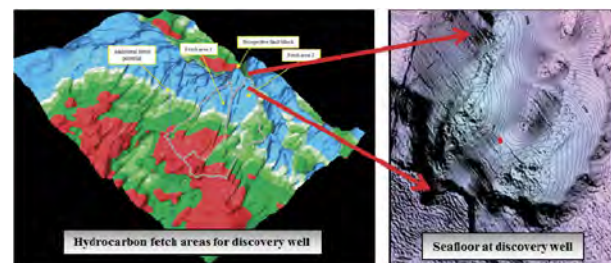


Figure 3: Source kitchen and hydrocarbon fetch area. Expanded seafloor view on the right illustrates recent tectonic inversion and sediment slumping with abundant fluid release features on the crest.

Hydrothermally Enhanced Fractured Reservoirs – A New Play?

A. A. Bal* (Baker Hughes Inc), R. Bray (Consultant) & R. Sigit (Geo-Connection)

Introduction

Have we ignored the possibility of hydrothermally enhanced fractured reservoirs as a play type in its own right? With the exception of Nang Nuan (Heward et al., 2000) and some references to the fractured granites in Vietnam (e.g. Hung and Le 2003), hydrothermally altered hydrocarbon reservoirs are largely unreported in the rocks of Southeast Asia. This contrasts with the extensive literature concerning hydrothermally altered reservoirs in Europe and North America (e.g. Davies et al 2006).

Under-reporting in Southeast Asia is perhaps due to the failure to appreciate and distinguish hydrothermal fabrics and behavior. Recognition and acknowledgement of the role of hydrothermal fluids, however, is important because adherence to incorrect or insufficient analogues will result in erroneous prospect risking and ranking, and results in incorrect estimates of hydrocarbons in place. Hydrothermal solutions may include seawater and meteoric water circulating through fractured rock, formational brines and metamorphic fluids created by dehydration of hydrous minerals during metamorphism. These solutions are considered hydrothermal if they are approximately 20-30°C above the surrounding rock. Three case studies are presented from hydrothermally altered fractured reservoirs; two from Southeast Asia, a carbonate and a granitoid study, with the key elements that suggest hydrothermal activity highlighted.

Nang Nuan “karst buried hill” play

The Nang Nuan Permian carbonate reservoirs display karst features initially believed to be due to subaerial exposure and meteoric diagenesis. After drilling six wells based on this play it was shown to be fractured reservoirs enhanced by hydrothermal processes within rifted horst blocks (Figures 1 and 2). The most significant lesson from this case study is the absence of a multidisciplinary approach to interpreting and integrating the conflicting datasets (Heward et al., 2000). For example an adjacent well experienced large losses in sandstones and produced fluids with temperatures 20°C higher than formation temperature did not result reconsidering the play concept (Figure 2). Working on the assumption of the karst buried hill play; the least prospective location was reluctantly drilled last but turned out to be the most productive well producing up to 10,000 b/d for several years after losing 350,000 bbls of drilling fluids and

seawater (Heward et al, 2000). The evidence of hydrothermally enhanced fractured reservoir changes the play concept, prospect ranking, and well trajectory planning.

Fractured granites in Vietnam

The question of where hydrocarbons are stored in the fractured granites of Vietnam remains controversial and equivocal. A review of the literature shows that each field has its own unique conditions and explanation for hydrocarbon habitat. In some cases the upper granite regolith and underlying fractured granite comprises the reservoir (e.g. Hung and Le 2003). In others, production is deep seated, up to 500m below the top granite (e.g. Hien et al., 2006). Measured fracture apertures (thin sections) range from 0.025-0.1 mm (Tien et al., 2008); many 1-3mm fractures are filled with secondary minerals (Tien et al., 2008). However, vuggy fracture porosity is commonly referred to and core samples from fractured zones frequently show large (>0.5cm) crystals developed along fracture surfaces. These are indicators of dissolution and precipitation from hydrothermal fluids. Of six listed porosity-creating mechanisms, Tien et al (2008) consider tectonic fracturing and hydrothermal fluid enhancement to be the primary controls on porosity distribution. Where hydrothermal fluids are active, vuggy porosity may locally be 2-15%. Analyses of some production tests indicate a dual porosity and dual permeability systems are not uncommon (e.g. Quy et al., 2008), suggesting the fractured granites reservoirs are not Type-1 reservoirs sensu Nelson (2000).

Hydrothermal dolomite (htd) reservoir plays

Hydrothermal dolomite (HTD) reservoirs are important hydrocarbon producers in North America and are now subject to increased interest globally (Davies and Smith 2006). HTD hydrocarbon reservoirs, and their close relatives, the Mississippi Valley-type (MVT) mineral deposits, are commonly hosted in platform carbonates, most often dolomite although also limestone. The most important structural controls for HTD reservoirs and MVT deposits are extensional faults, including wrench, transtensional and normal faults, and the associated fracture and dilatancy zones (Leach et al 2010). Most commonly, transtensional sags above negative flower structures are the drilling sites for HTD reservoir (Davies and Smith 2006).

Table 1: Indicators and best-practice logging programs to help identify the effects of hydrothermal activity on the reservoir. These indicators are not exclusive. For example the occurrence of saddle dolomite, commonly assumed to be the result of hydrothermal activity, is not necessarily indicative of hydrothermal activity or fluid flow.

INDICATORS OF HYDROTHERMAL ACTIVITY	BEST PRACTICE WORKFLOW (BOREHOLE)
<ul style="list-style-type: none"> • Fluids hotter than formation temperature. • Association of unusual mineral species (e.g. saddle dolomite, sphalerite, fluorite). • Euhedral crystals developed on fracture walls • Well-developed veining. • Presence of CO₂. • Mass-balance calculations and DSTs are difficult to reconcile with mapped volumetric and expected connected pore volumes. • Unusual development of porosity, e.g. pervasive “pin-pick” to pervasive excessive high values 25-30% (“Swiss cheese”). • Absence of typical meteoric karst fabrics (spelothems and cave sediments). • Collapse breccias 	<ul style="list-style-type: none"> • Core (whole rock Ø & K) • Core description • Thin sections, XRD, • Focused diagenetic studies to understand mineral associations and precipitation temperatures (including fluid inclusion and isotope analyses) • Logging <ul style="list-style-type: none"> –Conventional logs and –X-dipole acoustic –Images resistivity & ultrasonic –Sampling program (water & HC) –PLTs (temperature logs) –DST and extended production testing for material balance analyses

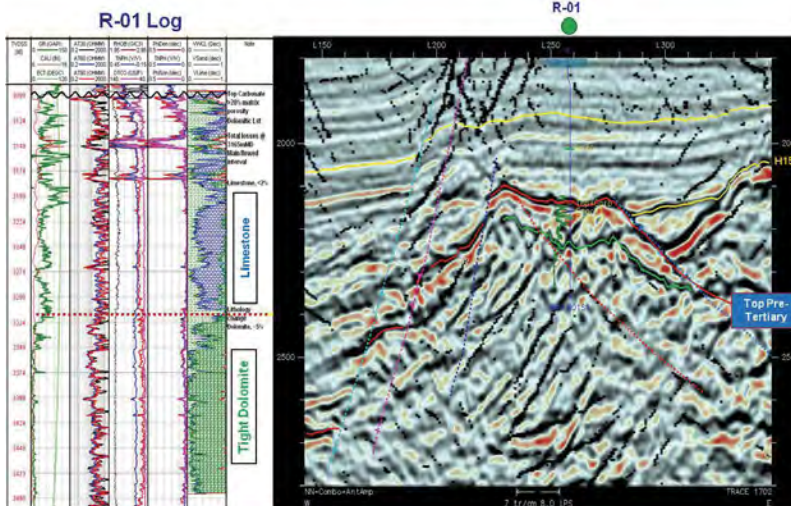


Figure 1: Seismic section and well results.

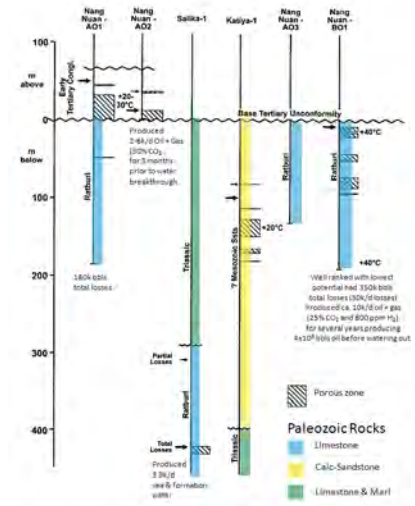


Figure 2: Wells drilled in B6/27 Thailand based in an erroneous conventional buried hill karst play. (After Heward et al., 2000 with minor modification).

Dolomite, especially the saddle dolomite cement ubiquitous in many HTD reservoirs and MVT deposits, is associated with hydrothermal fluids. Nevertheless, seawater-derived brines most commonly are responsible for the replacement dolomite of the host rock (Leach et al., 2010).

Indicators of hydrothermal activity and best practice

Table 1 presents a list of primary features and fabrics to watch out for and that may indicate the influence of hydrothermal fluids on the reservoir. This table also presents a best-practice, borehole perspective, evaluation workflow to help identify and quantify the effects of hydrothermal activity. It is important to recognize that any one feature is not indicative and interpretation of mineral associations is a task for specialists. Recognizing and distinguishing hydrothermal effects is difficult because meteoric karst is often associated with hydrothermal karst.

Implications and conclusions

Plays and analogs are fundamental to our business. They are used to help optimize exploration and development decisions minimizing costs. In the case of a hydrothermal play, or overprint on meteoric karst, we might expect higher porosities associated with deep-seated fluid conduits (fault systems). The conduits may tap into very deep seated systems, as with many of the Mississippi Valley-type examples, or into surrounding dewatering basin shales and source rocks, as in the Thailand and Vietnam examples. Porosities may be higher than expected and not necessarily associated with unconformities. Furthermore, fluid contacts may not be related to structural spill points.

References

Davies, Graham R. and Smith, Langhorne B. Jr., 2006. Structurally controlled hydrothermal dolomite reservoir facies: an overview. AAPG Bulletin November 2006 v. 90 no. 11 p. 1641-1690

Heward, Alan p.; Chuenbunchom, Supamittra; Makel, Gerard; Marsland, David; and Spring, Laurent 2000. Nang Nuan oil field, B6/27, gulf of Thailand: karst reservoirs of meteoric or deep-burial origin? *Petroleum Geoscience*, vol. 6 2000, pp.15-27.

Hien, Ngo Quang; Krisadasima, Supakorn; Bal, Adriaan 2006. Fracture identification, characterization, and quantification using borehole images, full wave form acoustic, high definition laterolog and other drilling data from 9-2-CNV-1X (Ca Ngu Vangu Field). *Fractured Basement Reservoir - The 1st International Conference for Basement Reservoir conference proceedings 2006*. pp.98-105.

Hung, Nguyen Du and Hung Van Le, 2003. *Hydrocarbon Geology of Cuu Long Basin – Offshore Vietnam* AAPG International Conference, Barcelona, Spain, September 21-24, 2003

Leach, D.L., Taylor, R.D., Fey, D.L., Diehl, S.F., and Saltus, R.W., 2010. A deposit model for Mississippi Valley-Type lead-zinc ores, Chap. A of *Mineral deposit models for resource assessment: U.S. Geological Survey Scientific Investigations Report 2010–5070–A*, 52 p.

Nelson, R.A., 2001. *Geologic analysis of naturally fractured reservoirs*. Gulf Professional Publishing 332p.

Quy, Hoang van; Son, Pham Xuan; Nhuan, Xuan Tran; Lan, Tran Duc 2008. Reservoir parameter evaluation for reservoir study and modelling of fractured basement White Tiger oil Field. *Fractured Basement Reservoir - The 2nd International Conference for Basement Reservoir conference proceedings 2008*, pp. 97-107.

Tien, Hoang Ding; Dung, Nguyen Ngoc; Chau, Ho Trung; Iuan, Bui Thi 2008. The factor forming and developing porosity and permeability of granitoid basement rocks in Cuu long basin. *Fractured Basement Reservoir - The 2nd International Conference for Basement Reservoir conference proceedings 2008*. pp.169-180.

“Pre-MMU” Carbonates and the Influence of Age and Tectonic Regimes on Their Growth Styles, Sarawak, Malaysia

E. W. Adams* (Sarawak SHELL Berhad), R. E. Besems (Sarawak SHELL Berhad) & S. J. Gough (Sarawak SHELL Berhad)

Introduction

In Shell, recent exploration activities have focused on portfolio rejuvenation and play-based exploration (PBE) studies to assess the remaining exploration potential of onshore and offshore Sarawak. Historically, in Sarawak, carbonate exploration has mostly focused on the renowned Middle to Late Miocene Luconia Province carbonates. The base of the Luconia Province carbonates demarcates a time of major flooding and is commonly referred to as the “Mid-Miocene unconformity (MMU)”. In contrast, the older stratigraphy, i.e. the “pre-MMU”, was given less attention but discoveries continued in the mature Balingian acreage in the south and, more importantly, recent high profile discoveries proved a working “pre-MMU” petroleum system in North Luconia.

A back-to-basics PBE study was conducted on the “pre-MMU” section, covering the South China Sea plate tectonic to regional Sarawak scale, and including integrated reinterpretation and full revision of the biostratigraphy, tectonostratigraphy, and sequence stratigraphy. The PBE study refocused efforts on the Late-Eocene-Oligocene-Early Miocene carbonate intervals that are located deeper than the renowned Luconia Province carbonates. A key result was the establishment of a regional framework connecting the tectonic regime with carbonate occurrences and growth styles since the Late Eocene.

Basin Evolution, Basin Fill, and Carbonate Growth

Upper Eocene-Lower Oligocene carbonates, found in the subsurface and outcropping onshore in Sarawak, developed speculatively as isolated thrust-top platforms. Carbonate growth is envisaged to have taken place atop basinward propagating thrusts and tectonic highs which developed in front of the Rajang accretionary wedge as a result of the rigid Luconia Block docking against Borneo.

In the Late Oligocene, a relatively stable, regionally extensive shelf system was established that continued developing

until present day. The Sarawak shelf succession has been traditionally subdivided into eight transgressive-to-regressive cycles. In this paper, it is proposed to group the eight cycles into four lower-order sequences bounded by flooding surfaces. During deposition of the Sarawak shelf succession three major extensional and one compressional event took place.

Figure 1 illustrates the basin evolution and basin fill of the “pre-MMU” stratigraphy. The first identified extensional event occurs during the early Late Oligocene (~28 Ma) through the early phase of Sequence 1 (or Lower Cycle I). In Central Luconia, extensional grabens developed, however, most extension occurred in North Luconia where deposition took place in a horst and half-graben type setting. Based on seismic interpretation, it is speculated that carbonate platforms fringed horst blocks during this time, while clastics were deposited in the grabens. Towards the end of the Oligocene stable conditions returned and Sequence 1 (Upper Cycle I) deposition ultimately blanketed and levelled the rift topography. In the Lower Miocene, at the end of Sequence 1, a sand-prone, regionally widespread and maximally eastward extending shelf system was established. During the subsequent transgression low-relief outer shelf carbonate banks developed.

At the onset of Sequence 2 (Cycle II), in the Early Miocene (~20 Ma), extensional and transtensional faulting and in some areas major uplift took place. Because the clastic shelf system retreated to the southwest, widespread passive shelf-margin carbonate deposition occurred in the distal shelf area in the east and northeast of Luconia. A pronounced high-relief carbonate platform margin developed along the shelf edge, whereas proximally, a mixed carbonate-siliciclastic shelf developed. Eventually, prograding shelf clastics smothered most carbonates. However, in the northeast of Central Luconia, the high-relief platforms that developed during Sequence 2 provided the basis for later carbonate growth and hence provide extensions to the base of Middle-to-Late Miocene Luconia Province carbonates. The final flooding stage of Sequence 2 (Cycle III) recorded shale-

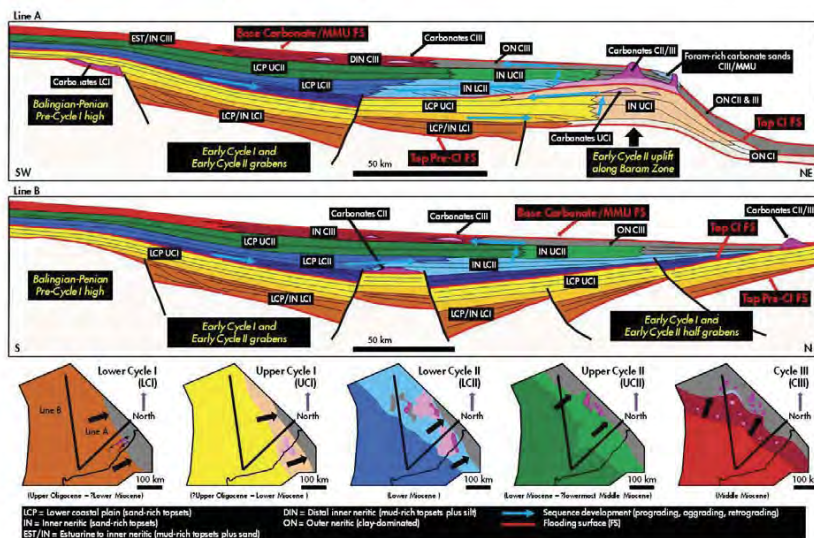


Figure 1: Cross-sections(above) and environment of deposition (EoD) maps (below) illustrating the basin evolution and basin fill of the pre-Mid Miocene unconformity (“pre-MMU”) stratigraphy of the Sarawak Shelf. Note Line A and B are only schematically located on the EoD maps.

rich topset beds and low-relief carbonate banks and platforms.

The base of Sequence 3 (Cycle IV) demarcated a time of major flooding in the Middle Miocene during which many of the Luconia Province carbonates initiated (aka the “MMU”). A major extensional event ending in the early Upper Miocene (~10 Ma) amplified and differentiated several structural domains in Sarawak. Numerous NW-SE extensional normal faults developed. During the Middle-to-Late Miocene (Cycles IV and V), in Central Luconia, large-scale, flat-topped, fault-block carbonate platforms developed on regional highs whereas keep-and give up pinnacles occurred in tectonic lows.

In Sequence 4 (Cycles VI-VIII), Pliocene and younger carbonates locally developed. Unattached, long-lived platforms that initiated in the early Miocene and are still growing today are present and most distally located.

Summary

Clearly, since the Eocene, the tectonic evolution and basin fill history in Sarawak encountered different styles of carbonate growth including thrust-top platforms, subsiding passive margin platforms, fault-block platforms, keep-and give-up pinnacles, and long-lived offshore banks. Besides the change in growth styles, several global evolutionary trends have been imposed influencing the type of carbonate being deposited and hence the potential of having variable reservoir quality. Examples include the extinction of larger benthic forams at the end of the Eocene and the shift from foram-and-algal to coral-dominated carbonate deposition at the Oligocene-Miocene boundary.

The present study, focusing on “pre-MMU” carbonates, demonstrates how play-based exploration (PBE) and the placing of carbonate occurrences in a tectonic and age context helps to understand and derisk carbonate plays in complex settings.

Sepat Barat Deep-2: The Deepest and Hottest HPHT Well in North Malay Basin

S. Osman* (PETRONAS), M. F. Nianamuthu (PETRONAS), F. A. Ismail (PETRONAS),
J. J. M. Idris (PETRONAS) & J. Ping (PETRONAS)

Since the late 60s, exploration activities had started in the North Malay Basin region which resulted in the discoveries of Jerneh, Lawit, Bintang, Damar, Noring, Guling and Tujoh by several operators (Figure 1). Most of the exploration target is the conventional play type; Upper Miocene clastics of Groups D, E and Top F (Figure 2). The play is generally located within the hydrostatic to slightly over pressured zone (upper zone of pressure ramp up). The play is characterized by siliclastics prone of Group E where most of the hydrocarbon accumulations are trapped within the east to west faulted anticlines. The hydrocarbon types are generally gas with condensates and some of the structure also had discovered oil rims (Sepat, Dulang, Semangkok and Bujang). This play is also characterized by having variable CO₂ concentrations. Given the pressure range at the groups F, H, I and J depths as well as temperature gradient in the North Malay Basin, only complex architecture HPHT type of wells could successfully allow the exploration of the deeper prospects.

Malay Basin had undergone three major structure movements; extension, thermal subsidence and basin inversion. The important result of the inversion is the compressional anticline, which includes the low relief structure. The possible low relief traps lies between high relief structures or beneath the major gas fields which may be overlooked because they are not obvious in the time domain and affected by gas sagging (Ji Ping, 2010). Hence a comprehensive seismic analysis is required, especially to generate the correct velocity model. The seismic data in the Sepat Barat area is poorer in the deeper levels and also effected by the gas cloud from shallower reservoir. The reservoirs are consists of fluvial and coastal reservoirs most often fluvial meandering channel. Traps associated with this play are 4 way-dips anticline (Figure 3).

The Middle to Lower Miocene HPHT play of Group F, H, I and J is characterized by the simultaneous occurrence of high pressure and high temperature. Most of the previous exploration wells had penetrated until top of Group F, due to inability to drill through high temperature and pressure region.

In addition, as experienced in Sepat Barat Deep-2 well, expected less than 1 ppg drilling margin (margin between formation pressure and fracture gradient) and possible to encounter another pore pressure ramp in F and H groups. High mud weight was used, up to 18.2 ppg with bottom hole temperature reaching 360 degree Fahrenheit and challenges of the presence of shallow gas that required surface casing to

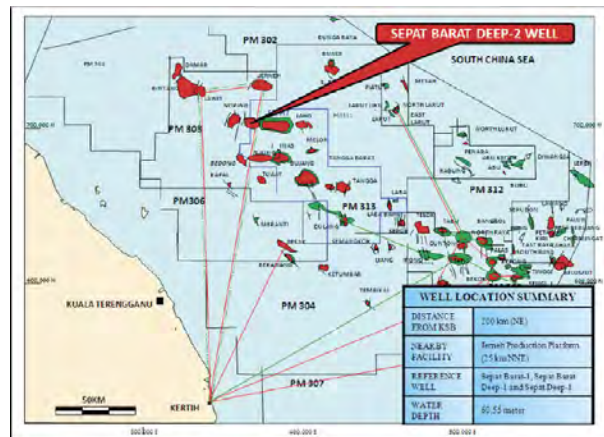


Figure 1: Sepat Barat Deep-2 well location in the North Malay Basin Region.

be set shallower (resulted in a very long 17-1/2" section up to 1850 meters).

Sepat Barat Deep-2 well was the only well which successfully evaluates the deeper reservoir of Group F and H in the North Malay Basin area with a total drilled depth of 2768mss. The reservoir pressure system is over-pressured starting at depth 1748mss, penetrated steep pressure ramp which is 3 ppg pressure increments for 200 meters until lower of Group F sand. The maximum recorded formation pressure was 7826psi at 2623mss and maximum bottom hole static temperature recorded was 340 degree F (Figure 4).

Based on the new well data, depositional environment for Group F is interpreted as delta front to shallow marine while Group H is interpreted as delta plain. A total of 8 new hydrocarbon bearing sands were encountered with gross thickness of 69 meters. The well had proved that Group F and H have significantly good porosity and permeability. F sands which are over-pressured reservoirs had preservation of its porosity up to 24% and this resulted had challenged the previous hypothesis of reservoir porosity quality decreases with depth. Minimum CO₂ content (11%) was recorded in H80 and H90 sands concluded that there is no CO₂ trend with depth in the area (Figure 5).

The Sepat Barat Deep-2 well had recorded a milestone as the first successful HPHT well in North Malay Basin region. Advanced tools and technologies were applied such as Manage

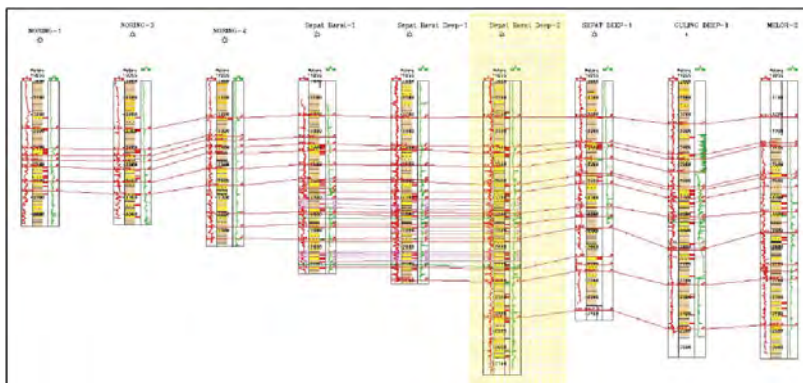


Figure 2: NW-SE Well to Well Correlation from Noring-1 to Melor-2.

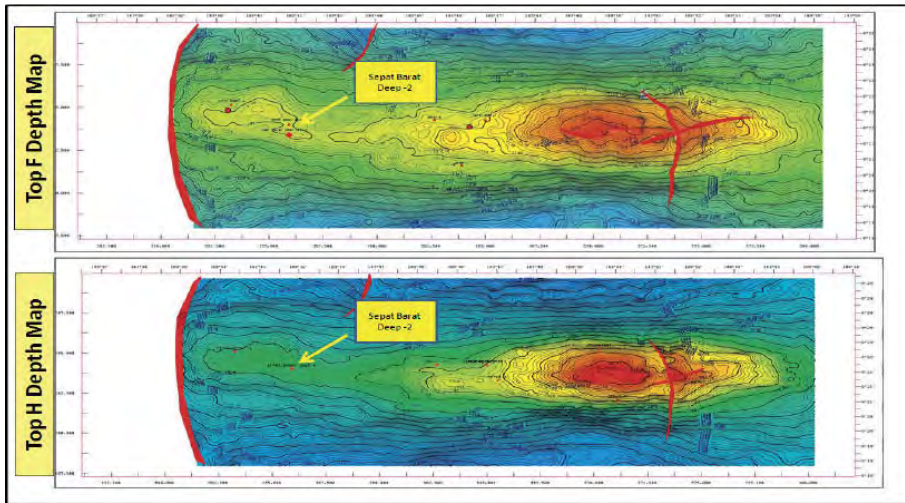


Figure 3: Low relief structure at the deeper reservoir of Sepat Barat.

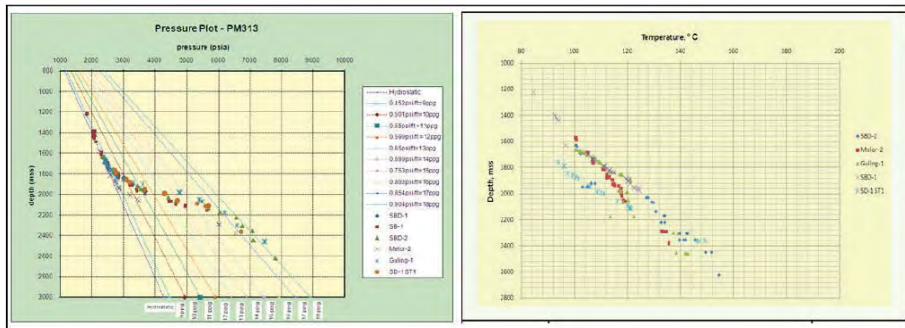


Figure 4: Sepat Barat Deep-2 Pressure and Temperature Data.

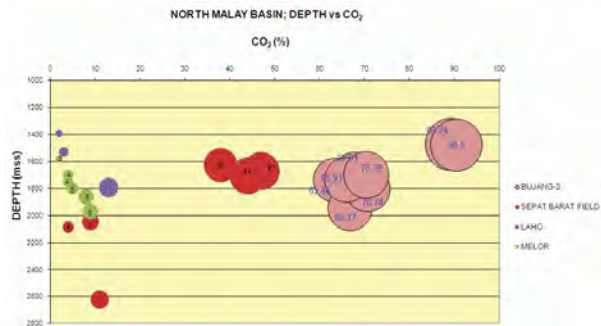


Figure 5: CO₂ trend in Sepat Barat Field is non depth dependent.

Pressure Drilling (MPD), high temperature wireline tools, StethoScope and Insitu Fluid Analyser (IFA). With the same technologies and well design, all the others deeper prospect could be explored.

Discovery of Sepat Barat Deep-2 well will open up the deeper reservoir of Sepat Complex and similar plays within surrounding area i.e Bujang, Inas and Guling. North Malay Basin region had proved to be highly prospective with the current available facilities. With thorough well-planning and application of relevant technologies had not only ensured the well objectives was meet but importantly drilling operations was optimized and safely conducted.

Brittle versus Mobile Shale Tectonics in Deltas: Structural Constraints Derived From Regional Seismic Interpretations

P. A. Restrepo-Pace* (Mubadala Oil & Gas)

Many deltas e.g. NW Borneo exhibits extensional growth systems landward and compressional structures at the present day slope and deep-water positions. The link between the extensional and compressional systems is hard to pin down as deep seismic data is of poor quality in these areas. Extension is generally believed to be accommodated by volume changes of a mobile substratum (mobile shale interpretation) Figure 1.

This view has been prevalent primarily due to:

- Poor seismic imaging at depth
- Evidence of overpressure
- Pock marks on the sea floor
- Sandbox and numerical structural models
- Seismic interpretation bias introduced by workstation interpretation i.e. large vertical exaggeration
- Structural geometry similarities between of shallow structures in many regions (Nigeria, Angola, Trinidad, Gulf of Mexico or Brazil salt basins)

- Operational driven interpretation i.e. prospect generation and very few seismically intensive regional studies
- Small amount of shortening at the toe thrust area that cannot account the amount of extension up dip

Careful examination of long cable data offshore Nigeria provides sufficient evidence to indicate that though mobile shale is present, may not be as extensive as currently believed. In the latter view extension and compression are linked via a basal detachment system (brittle interpretation) Figure 2.

The evidence for such interpretation is presented here; seismic examples, concepts and analogue models from sandbox experiments are also utilized. Future improvements on deep penetration long cable seismic imaging should provide better constraints and thus new plays may emerge (many with drilling challenges). In addition, the alternative structural interpretations may lead to improved charge modelling in complexly deformed delta systems.

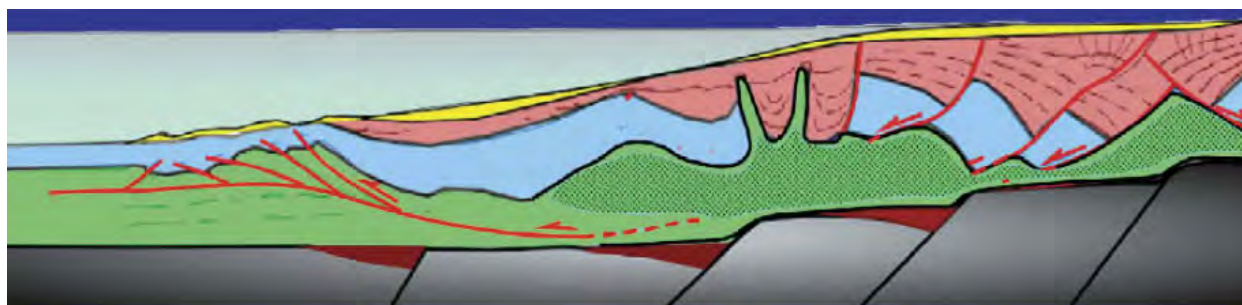


Figure 1: Schematic cross-section depicting the internal structure of a typical delta wedge. Extension/accommodation space of the updip section is accommodated by displacing mobile shale from the overpressured deeper portions of the delta.

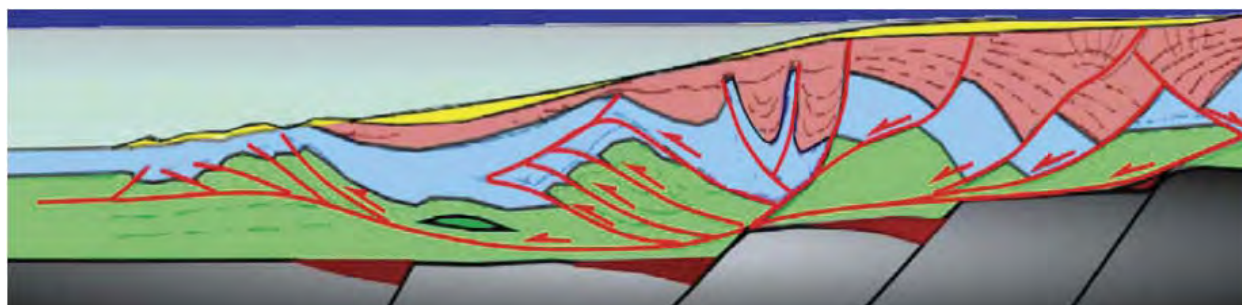


Figure 2: Alternative interpretation for a typical delta wedge. This model links the extensional systems landward with the compressional systems basinward.

Maturation of a New Play Concept in Northern Provinces of Offshore Sarawak Basin, Malaysia

S.R. Iyer* (PETRONAS Exploration), H. Rosidah (PETRONAS Exploration) & A. Shahrul Amar (PETRONAS Exploration)

Northern provinces of Offshore Sarawak Basin represent a frontier area with low well density and relatively fair understanding of the petroleum system. Hydrocarbon prospectivity evaluation integrating seismic, gravity, and well data of northern provinces of offshore Sarawak facilitated modeling of tectono-stratigraphic framework and geological evolution of the area, culminating in the development of a new play concept, hitherto untested in this part of Sarawak Basin. Stratigraphy of the study area is characterized by a lower synrift sequence, consisting of transitional to shallow marine sediments, unconformably overlain by passive margin sag phase deep water sediments. Exploration to date has focused on hydrocarbon plays in upper part of synrift section. Present paper deals with maturation of Sequence-A play as a new concept, primarily based on seismic evidence. This sequence, consisting of postulated lacustrine sediments, filled the early formed half grabens during the first phase of extension. Uplifted sections of this sequence on footwall closures are potential hydrocarbon plays with charge from adjoining grabens. Regional review of equivalent sections suggests clastic sequence similar to Sampaguita-1 as the most likely analogue. Proving this play will open up substantial exploration potential in the northern provinces of Offshore Sarawak Basin, with significant economic value.

Introduction

Offshore Sarawak Basin, located towards south western part of South China Sea, is an area of active hydrocarbon exploration and development for more than a century. The present paper covers North and West Luconia Provinces of Offshore Sarawak Basin, where active exploration commenced from 1990. The study area (Fig.1) is a frontier basin with low well density, and poor to fair understanding of the petroleum system. Regional hydrocarbon prospectivity study integrating all geoscientific data facilitated modeling of tectono-stratigraphic framework and geological evolution of the area, culminating in the development of a new play concept, hitherto untested in this part of Sarawak Basin.

Geological Background

General stratigraphy of the study area is shown in Fig.2. Northern provinces of Offshore Sarawak Basin initiated as intracratonic rifts on attenuated continental crust, on the foreland bulge part, during Late Cretaceous (?) to Late Eocene. The general structural style during this stage is characterized by N-S and NE-SW trending half grabens, dipping to the east and southeast (Fig.3). Sequence-A (Pre Cycle-I sequence of earlier authors), consisting of possible lacustrine facies (?), filled the early formed half grabens. The extensional phase continued, with opening of South China Sea during Early Oligocene, and also during subsequent drift phase up to Early Mid Miocene. Unequal subsidence in the half grabens over the study area during this stage, accommodated variable thickness of infill sequences B and C, represented by Cycles I to III (Fig.4), showing diverse facies distribution as evidenced by the wells. It can be inferred that the study area consisted of a complex of minibasins/grabens with uneven subsidence history, bounded by intervening horsts,

often forming localized provenances. Subsequent regional uplift in the area associated with plate convergence during Late Early Miocene to Middle Miocene, resulted in a major unconformity, designated Middle Miocene Unconformity (MMU). Post unconformity easterly and northeasterly sag of the basin through Late Miocene to Recent lead to a deep water setting, ensuing in deposition of hemipelagics, overlain by mass transport dominated sequence.

Sequence-A Play Concept

Exploration to date has focused on hydrocarbon plays in sequences B and C, wherein, a few subcommercial HC accumulations have been discovered. Sequence-A, which constitute the pre rift/early synrift section, is quite evident in the 3D seismic data of the area (Fig.5), and shows unequivocal sedimentary characters like layering, angular unconformity etc. Multiple units can be mapped within this sequence, showing distinct seismic characters representing discrete facies. The postulated lacustrine clastic sediment fill includes the source, reservoir, and intraformational seal elements of Sequence-A petroleum system. Regional top seal for this play is transgressive shale (?) overlying the Sequence-A unconformity. Uplifted sections of this sequence on footwall closures are ideal exploration targets for this play. Prospect-A is an example of Sequence-A play with three way footwall closure against a fault forming a structural trap (Fig.5). The predicted depth to the target is less than 2000m below mudline and reasonably good porosity is expected based on offset well porosity-depth plots. Reservoir temperature predicted is less than 125°C and any oil accumulated is likely to be preserved without cracking.

Regional screening of equivalent sections for analogues has brought out Sampaguita-1 well in Reed Bank Basin towards NE as the most likely, suggesting a clastic play in Sequence-A (Fig.6). Transitional to non marine sand/shale sequence of Early to Mid Cretaceous age, up to 600m thick, was reportedly penetrated in equivalent section in Sampaguita-1. Two shallow offshore wells in the SW part of Sarawak drilled in 1970's encountered tight, feldspathic sandstone of Eocene (?) age, unconformably overlain by Cycle V section, and possibly represents Sequence-A equivalent in the southern part of Sarawak, around 600 km from the study area. Several seismic profiles indicate likely carbonate reflection character in Sequence-A highs, similar to a Pre Tertiary hydrocarbon discovery in Vietnam (Fig.7). Consequently, carbonate reservoir in Sequence-A is a likely scenario. Metasediments varying in age from Late Cretaceous to Eocene constitute the economic basement in several deep wells in East Natuna basin, fringing the western boundary of the study area, making up a possible case. True basement represented by granodiorite has been observed in only one well in East Natuna, which is an unlikely scenario for Sequence-A, based on seismic character.

Proving this play will open up substantial exploration potential in the northern provinces of Offshore Sarawak Basin, where, a significant number of potential leads have been identified, similar to the prospects shown in Fig.4, with significant commercial value.

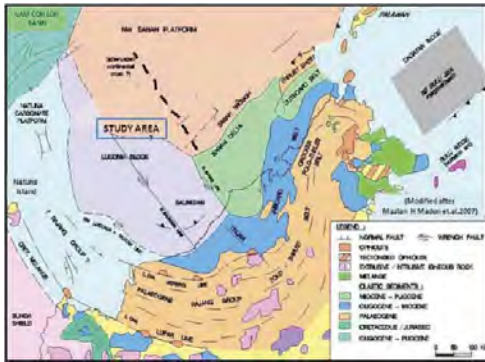


Figure 1: Regional geological map of the study area.

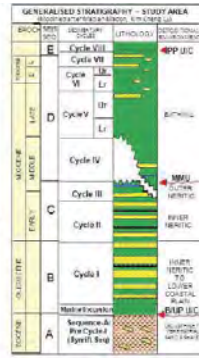


Figure 2: General stratigraphy

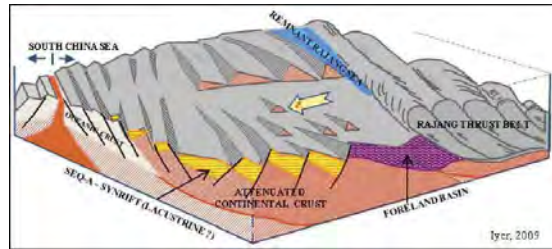


Figure 3: Schematic model showing NE-SW trending half grabens on attenuated continental crust developed during Phase-I extension (Late Cretaceous? to Eocene). Sequence-A consisting of possible lacustrine sediments filled these grabens. Phase-II extension is associated with opening of SCS around 30 Ma and the spreading phase which continued up to 19 Ma, and deposition of Synrift sequences B, C, & C2.

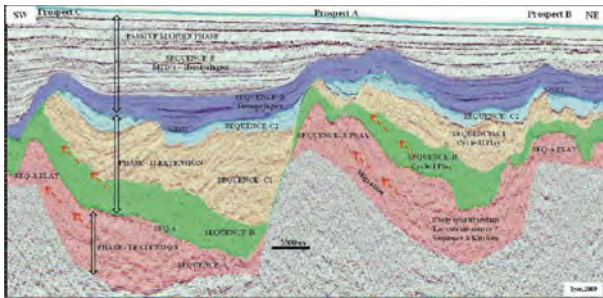


Figure 4: Representative SW-NE profile depicts the mapped sequences and main play types in the study area. Prospect A, a footwall closure at Sequence A level is ideally located to test the new play concept.

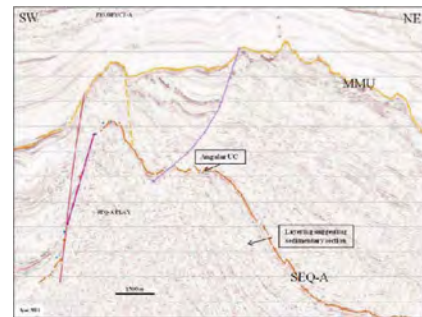


Figure 5: SW-NE seismic profile through Prospect-A shows the internal character of Sequence-A. Reflection character suggests sedimentary section with layering and obvious angular unconformity on the highs. Multiple subsequences can be identified within Sequence-A.

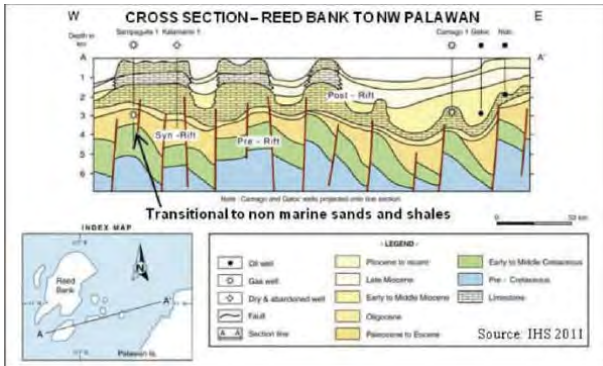


Figure 6: Cross section from Reed Bank to Palawan is located towards the NE part of the study area. Transitional to non marine sands and shales were reported in Early to Mid Cretaceous and early Tertiary sections in Sarnpaguita-1 well. This section has been considered as the closest analogue for Sequence A in the study area.

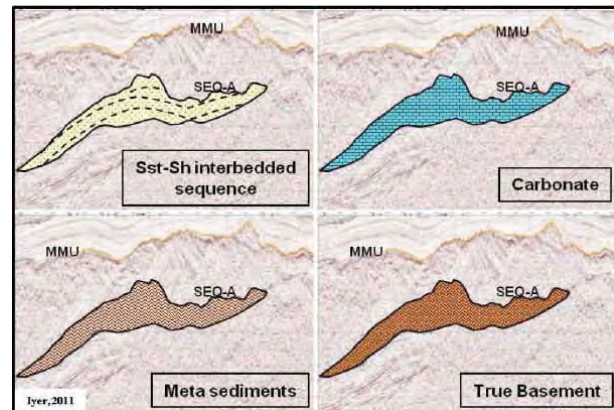


Figure 7: Reservoir scenarios considered for Sequence-A play based on regional studies. Clastic sequence similar to Sarnpaguita-1 well is the most likely case. Carbonate case similar to Pre Tertiary carbonate discovery in Vietnam is a likely scenano. Metasediments are possible considering East Natuna basin wells as analogue. True igneous basement is an unlikely case.

Conclusions

Sequence-A play is a new concept targeting Pre/Early Tertiary sequence, hitherto untested in thenorthern provinces of Offshore Sarawak Basin.

Proving this play will open up substantial exploration potential in the study area, with significant commercial value.

References

Andrew Cullen, Paul Reemst, Gijs Henstra, Simon Gozzard and Anandaroop Ray, 2010. Rifting of South China Sea: new perspectives. *Petroleum Geoscience*, 16, 273-282.

Kenneth Thies, Mansor Ahmed, Hamdan Mohamad, Richard Bischke, Jeffrey Byer and Daniel Tearpock, 2006. *Structural and Stratigraphic Development of Extensional Basins: A Case Study Offshore Deepwater Sarawak and Northwest*

Sabah, Malaysia. Search and Discovery Article #10103 (2006).

Mazlan H Madon, Kim C Ly, Robert Wong, 2007. *The Structure and Stratigraphy of deep water Sarawak, Malaysia. Implications for the Tectonic Evolution of NW Borneo continental margin. AAPG Annual Convention and Exhibition, 2007, Long Beach, CA.*

Tectono-Stratigraphy and Development of the Miocene Delta Systems on an Active Margin of Northwest Borneo, Malaysia

A. Balaguru* (Talisman Energy) & T. Lukie (Talisman Energy)

Introduction

The Paleogene regional tectonic setting of Sabah is very complex with southeasterly subduction of the proto-South China Sea in NW Borneo (Hall, 1996), followed by a period of continued deposition of deep marine Rajang Group turbidites. The Late Eocene tectonic deformation is characterized by folding, thrusting and regional uplift related to the collision of the Luconia Continental Block against NW Borneo (Sarawak Orogeny; Hutchison, 1996).

Barkhausen & Roeser, (2004) reinterpreted paleomagnetic data and concluded that the sea floor spreading in the South China Sea, which began at 32 Ma, had already ceased by 20.5 Ma. This indicates that subduction ceased in the Early Miocene as opposed to the previously interpreted Middle Miocene (Brias et al. 1993) when the Dangerous Grounds micro-continental fragments collided with NW Borneo (Clennell, 1996; Hutchison et al., 2000. This predates the timing of the Sabah Orogeny including the earlier 20 Ma timing proposed by Balaguru & Hall (2008), and it coincides with the Base Miocene Unconformity (BMU) in Sabah (Figure 1). The Early Miocene (22-20 Ma) deformation is a major tectonic event involving the formation of the Sabah mélanges, significant uplift and erosion; patches of Burdigalian limestone formed during this uplift. This period was followed by a change in depositional environment from deep-water clastics to a shallow-water deltaic setting.

The Miocene to recent regressive fluvio-deltaic systems have been progressively deformed and overlie the Oligocene Crocker accretionary complexes generally regarded as the economic basement (Stage II or TB1.5sb). The Oligocene comprises slightly metamorphosed, highly deformed deep-water turbidite sediments known as the Crocker and Temburong Formations of onshore equivalents.

The overlying Neogene section has an unconformable relationship with the underlying section and can be divided into three deltaic complexes that generally young from east to west. The Meligan Delta (Stage III or TB 2.1-2.3) is the oldest and it accumulated in the mid-Early Miocene, forming the sand-dominant Meligan and shale-dominant Setap formations. The Meligan Formation is dominated by thick sandy deltaics with subordinate sandy shallow marine facies; the Setap Formation contains thin interbeds of sandstone within an overall shaley succession representing the distal equivalent facies of the Meligan Delta. All of offshore Sabah was under slope- to deep-marine conditions during Early Miocene to early Middle Miocene time.

A significant Middle Miocene unconformity (also known as Deep Regional unconformity) (MMU/DRU) separates the Meligan Delta from the overlying middle to late Miocene Champion Delta (Stage IV-ABC). This stage generally is characterized by coastal aggradation and progradation sequences comprising the onshore outcrop equivalents of the Belait, Miri and Sibuti Formations of NW Sabah (Figures 1 & 2). The Stage IVA (TB2.4-2.5) is a widespread regressive lower coastal plain to marginal marine (deltaic to shoreface) succession, whereas the Stage IVB (TB 2.6) is a major transgressive sequence of offshore marine deposits. The Stage IVC (TB3.1) is a major regressive sequence with widespread coastal to shallow marine

and deep-water deposits followed by a period of prolonged sea-level lowstand. The Belait and Miri Formations are dominated by a fluvio-deltaic sandstones with laterally equivalent coastal plain to marine sandstone successions that comprise the topsets of the Champion Delta depositional system. The Lambir and Seria formations are lithologically similar, but contain more fine-grained sandstone interbedded with mudstone representing the foresets of the delta. The shale-dominated marine deposit of the Sibuti Formation represents the distal equivalent or bottomsets of this relatively large delta system. Outcrop studies indicate that the Champion Delta is a complex NW prograding delta system with stacked sequences (from bottom to top) of fluvial sands, marginal marine (estuarine & deltaic) and shoreface deposits (Figures 1 & 2).

The Baram Delta succession is the youngest of the three deltaic systems. The late Miocene Shallow Regional Unconformity (SRU) separates the Champion Delta sequence from the younger Baram Delta (Stage IV-DEFG) succession; this most prominent unconformity in Sabah coincides with significant regional uplift and erosion. Stage IV (DEFG) of the Late Miocene to Pliocene is composed of stacked fluvio-deltaic sequence of the Baram Delta System with equivalent offshore shales and deep-water turbidite deposits. The late Miocene to Pliocene was a period of active regression with moderate aggradation punctuated by short periods of minor transgression. The deposits include the onshore equivalent of the Liang Formation of NW Sabah and Brunei (Figure 1) that unconformably overlie the Belait Formation. The Liang formation also consists of fluvial sandstones and conglomerates, marginal marine sediments and shoreface sandstones and shales.

The stratigraphy of northern Labuan, island and Klias Peninsula were re-examined using sequence stratigraphic and biostratigraphic studies resulting in a revised geological map (Figure 3). This study concurs with the original and correctly subdivided stratigraphy of Wilson (1964) where Labuan was divided into the Setap and Belait Formations. This study does not support the stratigraphy proposed by Madon (1994 & 1997) where the stratigraphy was subdivided into the much older Temburong and younger Belait Formations. The steeply dipping argillaceous strata that underlie the sequence boundary of Belait conglomerate ridge near Layang Layangan are more typical of the Setap/Meligan Formations; this interpretation is also supported by biostratigraphic analysis. This lower section is interpreted as shelf edge prodelta to upper slope with the progradation of thicker sand beds interpreted as distal delta front. The conglomeratic sandstone cap reflects the incision of the Stage IVA lowstand fluvial deposits cutting into the underlying Stage III Setap/Meligan formations, suggesting that the Temburong Formation is absent here but well exposed in Sipitang and Lawas areas. This unconformity between the stages is the Deep Regional or Middle Miocene Unconformity (DRU/MMU). Similar observations were made at the Ganggarak Quarry in Labuan and at Batu Luang Quarry in the Klias Peninsula. Sequence of deep water turbidites, slope channels, turbidite fans and mass-transport deposits of the distal equivalent of the Meligan Delta System are exposed at the northern tip of the Klias

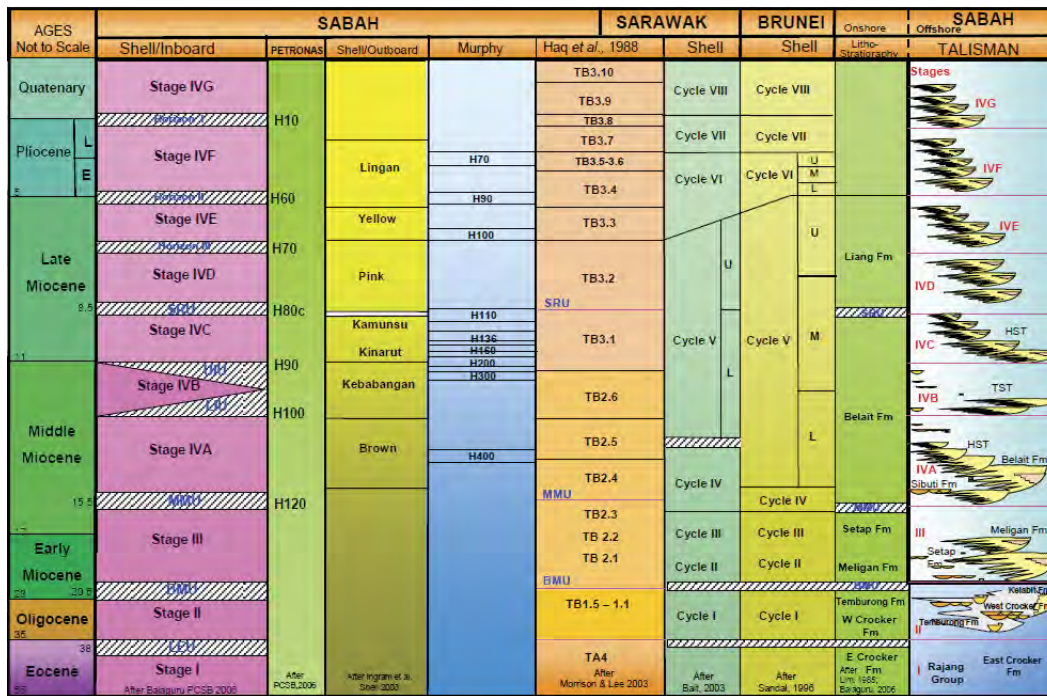


Figure 1 : Integrated Chronostratigraphic Nomenclature of NW Borneo.

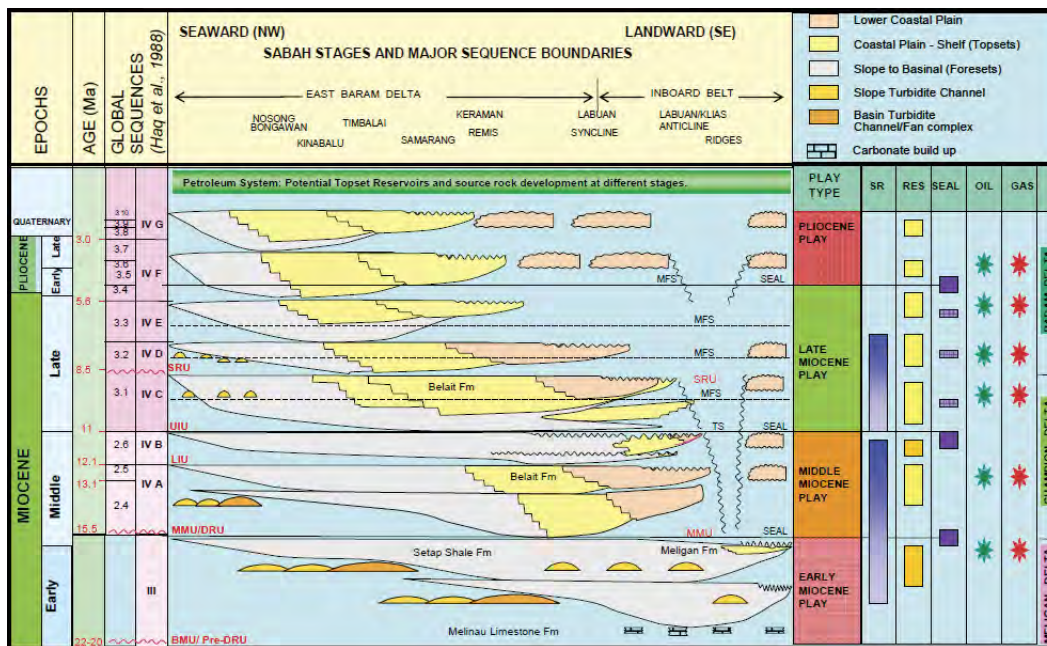


Figure 2 : Chronostratigraphy and Petroleum System of Offshore NW Sabah.

Peninsula and southwestern part of Labuan Island. This sandy deep-water sequence has been mapped as the Meligan Formation (Stage III). The Base Miocene Unconformity (BMU) between the Stage III and Stage II is observed during this field study at the Kalamunian Damit Island, north of the Pulau Tiga, Sabah.

Conclusions

Integrated evaluation indicates that the NW Borneo Delta province evolved during the Early Miocene to present day from a foreland basin to a shelf margin. Multiple phases of compressional folding and faulting events have affected the region, causing uplift of the hinterland, large deltaic progradational events, and

inversion of gravity-related faults. New geological mapping, detailed field studies and reinterpretation of existing data suggest that the region consists of west-vergent fold-thrust belts formed in the Early Miocene with syn- and post-deposition of the large Meligan, Champion and Baram Delta Systems on an active margin in NW Borneo. Most folds are detached, buried and thrust cored anticlines and they are younging towards west. The Labuan and Jerudong/Morris anticlines and Belait syncline formed during the Late Miocene as fault-bend and fault propagation folds. The prodelta shale was progressively buried by the prograding delta front and likely became overpressured and mobilized above reactivated basement structures during

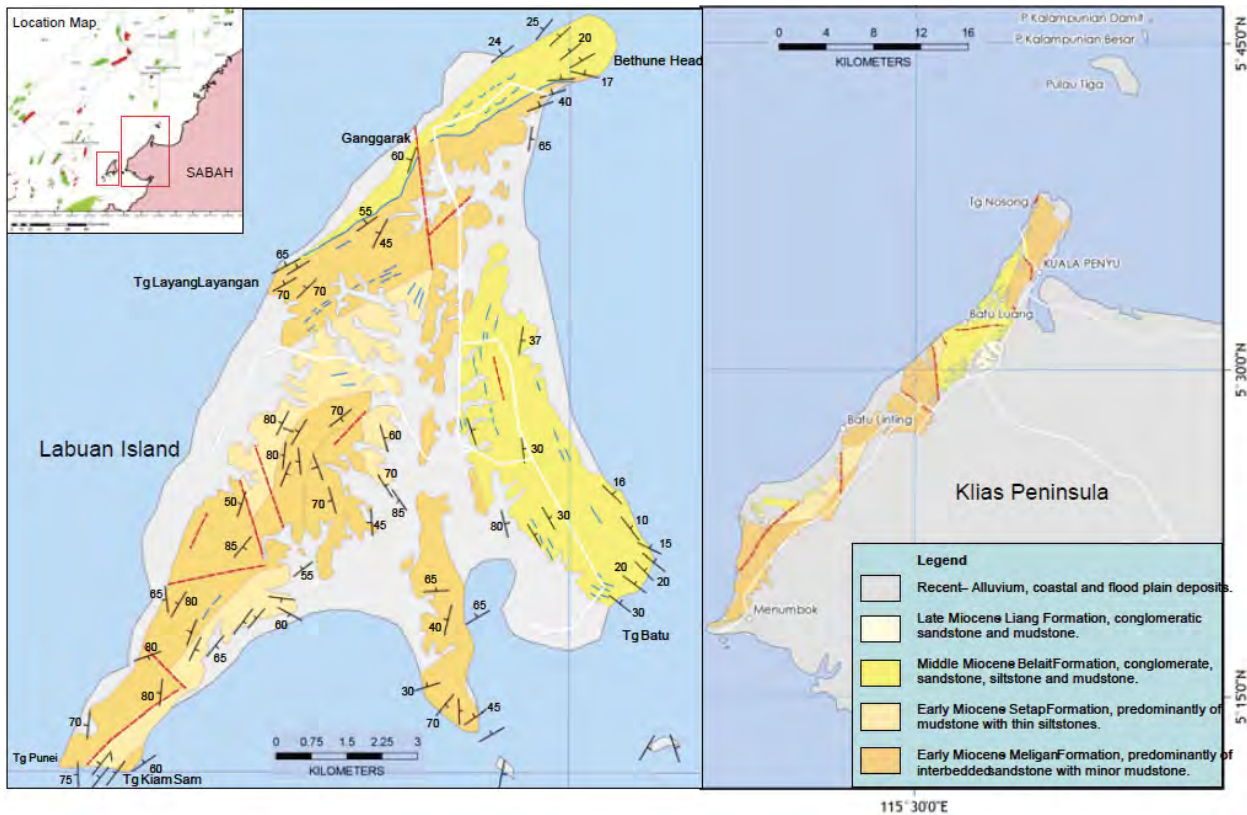


Figure 3 : Geological Map of Labuan Island and Klias Peninsula, modified and revised after Wilson (1964)

Pliocene, further complicating the deformation style. Pliocene-Pleistocene inversion on NNE- and N-trending structures with continued growth on NE-trending structures is most likely controlled by the regional NW-trending sinistral shear zones. Flower structures and thrust cored anticlines were developed above the reactivated structures.

This study provides new insight into the tectonic evolution of rapidly prograding Tertiary delta systems and reveals how the compressional tectonics have migrated basinward as the delta system prograded.

Acknowledgements

The author wishes to thank the management of Talisman Energy for their support of several field studies conducted in NW Sabah and permission to present this paper. We also thank all the Sabah exploration team members for their support and assistance during the integrated field studies. Thanks to the drafting unit for their assistance in drawing the ArcGIS maps.

References

Balaguru, A. & Hall, R. 2008. Tectonic evolution and sedimentation of Sabah, North Borneo, Malaysia. Extended abstract, presented at the American Association of Petroleum Geologists 2008 International Conference, Cape Town, South Africa.

Barckhausen, U. & Roeser, H.A. 2004. Sea floor spreading anomalies in the South China Sea revisited. In : Clift, P., Wang, P., Kuhnt, W. & Hayes, D. (eds) Continent-Ocean Interaction with Asian Marginal Seas. American Geophysical Union, 140, 121-125.

Brias, A., Patriat, P. & Tapponnier, P. 1993. Updated interpretation of magnetic anomalies and sea floor spreading stages in the South China Sea: Implications for the Tertiary tectonics of Southeast Asia. *Journal of Geophysical Research*, 98 (B4), 6299-6328.

Clennell, B. 1996. Far-field and Gravity Tectonics in Miocene Basins of Sabah, Malaysia. In: Hall, R. & Blundell, D.J. (eds.), *Tectonic Evolution of SE Asia*, Geological Society of London Special Publication, 307-320.

Integrated Bio- and Seismostratigraphy of the Southern Sabah Offshore, Malaysia

J. J. Lim (Sarawak SHELL Berhad)

Recently, the Sarawak Shell Berhad Biostratigraphy team has reviewed a selection of key wells from the Southern Sabah Offshore, and has built a consistent biostratigraphic zonation and framework, largely based on nannoplankton and planktonic foraminifera. The biostratigraphic zonation has been tied to regional seismic lines in order to create a robust bio- and seismic stratigraphic framework. A work flow has been set-up and the value of such an approach has been demonstrated in the regional evaluation projects.

Biostratigraphic resolution limitations are caused by both geological and sampling factors. Sampling is best done on cuttings, provided they are representative for the interval drilled. Areas of rapid deposition, especially in the slope and / or slump scar fill depositional environments tend to have a poor microfossil yield.

In parallel, seismic stratigraphic analysis has been carried out to establish the regional stratigraphic framework in an ongoing attempt to unravel sand fairway systems transporting sand from the Sabah inboard to the deep water. The delineation of these 'sand fairways' is a key element in the assessment of reservoir risk in the Sabah deep water Hydrocarbon plays.

Mapping of clinoform packages (foreset corridors) is the key to understanding sediment supply and progradational patterns. Flattening on a continuous seismic reflector above the mapped

foreset corridor clearly shows the depositional architecture (Figures 1 and 2). Shelf margin (clinoform geometry) mapping in the Sabah inboard area has increased the understanding of the location and direction of the sediment supply to the deep water. Progradation and aggradation stacking patterns demonstrate the influence of actively forming anticlines and synclines during the deposition.

The nature of reflection termination patterns define a range of significant stratigraphic surfaces such as unconformity, onlap, downlap and toplap surfaces. Divergent and convergent reflection packages demonstrate the active growth phases of the anticlinal and synclinal structures, which in turn have a major impact on the sand fairway distribution and morphology.

Wheeler diagrams have been generated to compile all available stratigraphic information, i.e. both bio- and seismic stratigraphic data. They are an excellent way to demonstrate the depositional links between inboard and outboard depositional areas, as well as across zones of poor data, i.e. often the slope (Figure 3).

The Sumandak – Ranau system has been investigated in some detail and a potential fairway can be demonstrated, although linkage to the Sabah deep water reservoir units still remains to be proven.

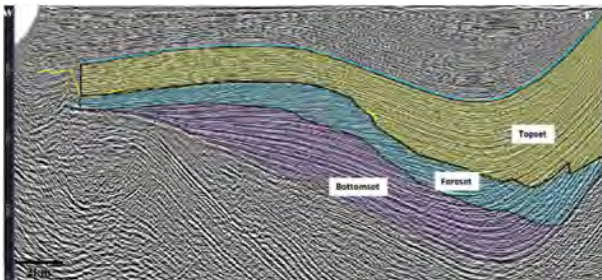


Figure 1: Clinoform aggradation and progradation patterns.

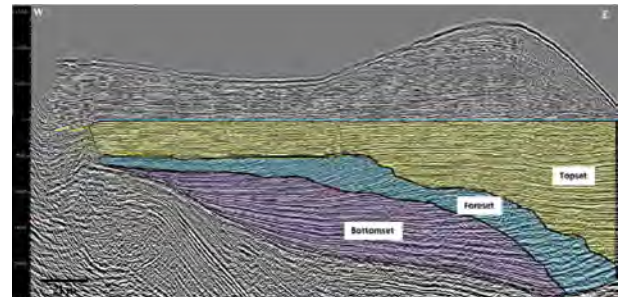


Figure 2: Clinoform aggradation and progradation patterns (flattened on blue line).

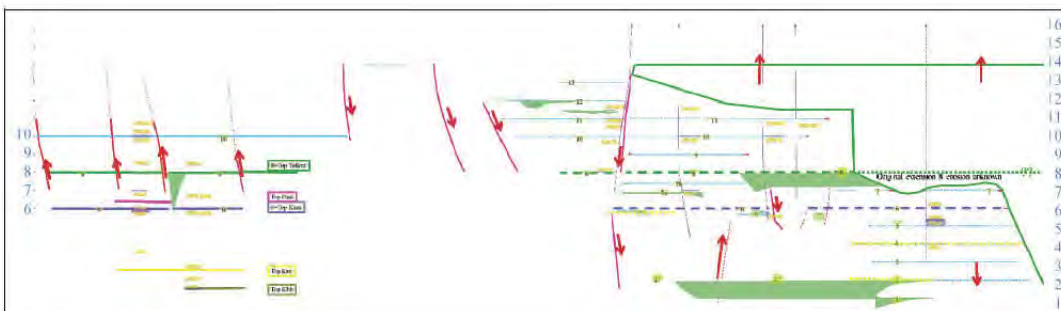
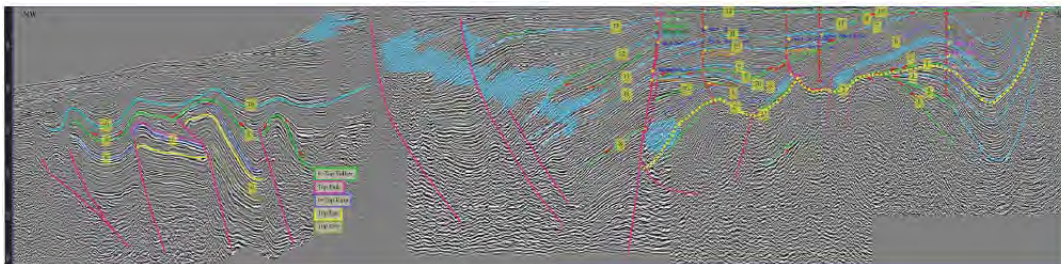


Figure 3: Wheeler (Time-Rock Synopsis) diagram.

New Seismic Insight At Keabangan Field: KPOC Gears Up for a Development Drilling Campaign At a New Major Gas-Oil Hub in Offshore Sabah

V. L. Cathey* & C. M. Curtis (Keabangan Petroleum Operating Company Sdn Bhd)

Introduction

Keabangan Petroleum Operating Company (KPOC), a joint-operating company owned by PETRONAS Carigali Sdn Bhd, ConocoPhillips Sabah Gas Ltd and Shell Energy Asia Ltd, has the green-light to begin construction on a new major gas-oil hub at Keabangan Field (KBB) in offshore Sabah (Figure 1). The platform's strategic location will enable the tie-back and development of otherwise remote deepwater Sabah opportunities. In conjunction with the KBB platform installation, KPOC will kick off a major drilling campaign. A newly reprocessed seismic volume has boosted confidence in the development well program.

Method

KBB Field, situated at the edge of the continental shelf, is a Miocene age turbidite reservoir. The field's characterization has long been hindered by the presence of a shallow gas chimney directly over the crest of the reservoir, which results in a sizable seismic image washout through the crestal region of the KBB structure (Figure 2a). The secrets hidden in the washout area have caused the field's history to take many interesting turns.

The Keabangan concession was originally awarded to Shell, which drilled the Discovery Well in 1994 based on 2D seismic lines. The exciting, thousand-foot (gross) gas discovery was followed the next year by the acquisition of a 3D seismic survey and a number of reprocessing attempts in the early 2000's to resolve the poor seismic image using various migration technologies. The PreSDM reprocessing exercises resulted in only minor improvements in imaging quality (Figure 2b). Two appraisal wells were drilled using the 3-D seismic data.

In a twist of fate, the second appraisal well, drilled in the poor seismic image area, proved a predominant oil accumulation rather than gas accumulation. This surprising result prompted the invalidation of the field development plan for a gas development.

The Keabangan oil concession was then awarded to Carigali-ConocoPhillips Oil JOC. The 3D seismic data was reprocessed again, with modest imaging improvement (Figure 2c). A third appraisal well was drilled to assess the oil. The field's crest in the problematic imaging area beneath the gas chimney, was targeted. Ironically, the well proved gas.

To facilitate progression of the field's development, a new three-company joint-operating company, KPOC, was ultimately formed in 2007. This synergism enabled the three companies to pool KBB learnings to pursue the development of the oil and gas field efficiently.

In 2009/10, PreSDM seismic reprocessing was again carried out, this time applying both a Shell-proprietary migration technology for resolving highly dipping structural geometries



Figure 1: Location of the KBB development. The platform's strategic location will enable the tie-back and development of deepwater opportunities in northern Sabah. (source of map: PETRONAS public website)

and a collaborative interpretative approach to model the gas chimney. The investment paid off in a step-change improvement in imaging quality (Figure 2d). The emergent picture has sparked some new ideas about the internal geometry of the KBB structure.

Conclusions

As KPOC gears up to execute its development drilling campaign, the improved seismic has confirmed the gross KBB structure and has facilitated the refinement of the well targets, conferring greater confidence to realize the culmination of a patiently awaited dream.

Acknowledgements

The authors would like to recognize their colleagues who were instrumental in enhancing the geologic understanding of KBB Field: Ms. Amalia Bolhassan, Ms. Aslinda Azman., Ms. Bernice Ho Soong Sheah, Mr. Fernando Dasquez, Mr. Gary Wu, Mr. Leong Hon Yoong, , Mr. Mohamed Rafizal Mohammad Nor, Ms. Nor Hazlijah Sukri, Ms. Pauline Chung; and Mr. Luk Chee-Khieng (Shell Geosolutions) and Mr. Rodrigo Heidorn (now at Norske Shell). ... and recognize KPOC's management for facilitating their effort: Mr. Michael Challis (Senior Manager, KBB Subsurface) and Mr. Rob Willis (General Manager Petroleum Engineering). Our thanks to PMU and to the KPOC shareholders, PETRONAS Carigali Sdn Bhd, ConocoPhillips Sabah Gas Ltd and Shell Energy Asia Ltd, for supporting the sharing of this work.

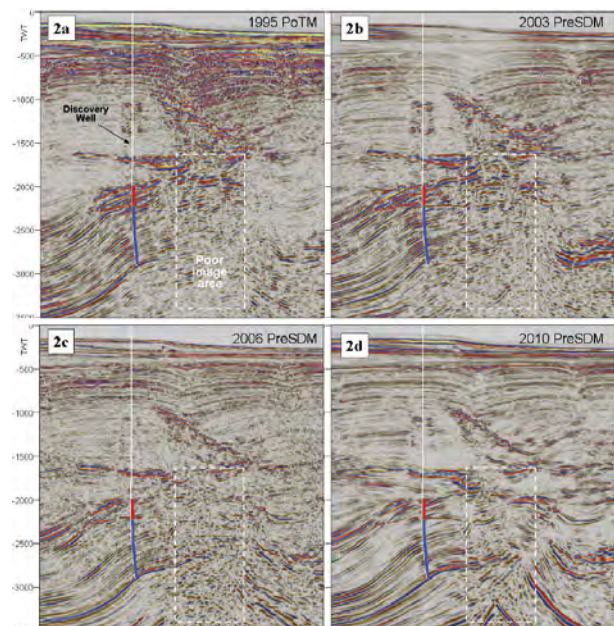


Figure 2: The progression in 3D seismic imaging improvement from: 2a) the original post stack time migration in 1995, 2b) and 2c) two earlier pre-stack depth migrations in 2003 and 2006, and 2d) the latest pre-stack depth migration in 2010. The 2010 reprocessing applied a Shell-proprietary migration technology for resolving highly dipping structural geometries and incorporated a collaborative, interpretative approach to model the gas chimney. Displayed on the Discovery Well is the thick column of gas (red) that was encountered.

Overpressured Carbonate Reservoirs, Offshore Sarawak; Methods of Pore Pressure Prediction

P. Baltensperger* (Newfield Exploration), W. Zanussi (CGGVeritas), S. Bordoloi (Baker Hughes) & S. Nath (Baker Hughes)

Introduction

Recent exploration drilling by Newfield and their partners, PETRONAS Carigali and Mitsubishi Corporation, in offshore Sarawak has encountered hydrocarbons in a highly overpressured carbonate pinnacle. Pressure prediction and safe, effective drilling is challenging and requires an integrated technical approach. The Newfield operated JV recently successfully drilled, tested and evaluated a highly overpressured exploration well in offshore Sarawak.

The offshore Sarawak region is divided into a number of structural-stratigraphic geologic provinces. The study area is located on the eastern edge of the Central Luconia province, east of the prolific hydrocarbon producing carbonate gas fields in offshore Sarawak.

Although pore pressure varies in carbonate reservoirs in offshore Sarawak, the variance rarely exceeds 1,500psi over hydrostatic. The highly overpressured trend is restricted to the eastern edge of the Luconia platform along the Baram line where pore pressure is over 10,000psi (>5,000psi over hydrostatic). There are currently no commercially developed fields in this overpressured trend.

Methods and Results

The primary cause of overpressure is related to partially de-watered, undercompacted claystone rapidly deposited from clastic sources of the Baram Delta to the southeast, together with seal development in thick shale-dominated sequences. These claystones overlie and in some areas are in pressure communication with the carbonates. Another possible source of overpressure in the carbonate reservoirs is related to vertical fluid migration along faults from a deeper aquifer in the Cycle I and II clastics below the carbonates. Possibilities of thermal mechanisms causing overpressure generation due to unloading also exist, but need further verification with more drilled well data. In order to mitigate seal risk and accurately estimate hydrocarbon resource for carbonate prospects in such an overpressured environment a thorough analysis of lithofacies distribution and pore pressure must be done.

Pore pressure prediction relies on offset well analysis, high-end seismic velocities and an understanding of the regional stress field caused by sediment loading and tectonics. Porosity-based pore pressure estimation techniques utilizing both petrophysical and velocity data can be used to accurately predict pressure in shales when calibrated with offset well data. However, unlike

typical pore pressure prediction methodology in clastic lithology, where it can be assumed that porosity is intrinsically linked to compaction, which is controlled by effective stress, in case of carbonates, inherent porosity is mostly controlled by cementation history rather than by effective stress.

Moreover, carbonates do not usually generate overpressure internally due to early development of carbonate cements restricting pore collapse and overpressure in carbonates is principally controlled by associated overpressured shales. In the prospect area porosity maps on the top carbonate were derived from elastic inversion and used to determine where pressure communication exists between the carbonate reservoir and the overlying undercompacted shale (figure 1).

The overpressure trend in Eastern Luconia is not depth related. The depth of the onset of overpressure is controlled by a 600-800m thick NW directed overlapping prograding clastic unit. Elastic seismic inversion products (P-imp, S-imp, VP/VS and PR) were used to characterize the vertical lithofacies in the prograding clastic wedges overlying the carbonate to distinguish sand prone, normally pressured stratigraphic packages from shale prone, overpressured stratigraphic packages. These progrades are sand prone in the updip, proximal region and are predominantly shale prone in the distal region resulting in a highly variable depth profile for the onset of overpressure (figure 2). The result is a distribution of overpressure in the prospect area that is complex and highly variable.

Since the pore pressure model relies highly on seismic velocities, geologic input to detailed velocity analysis using a stratigraphic interpretation of the prograding clastic wedges is critical. This process provides a velocity model which can be calibrated to nearby well information in a predictive and deterministic approach. Seismic velocities were picked at 50m intervals on PSTM gathers and specific picking criteria are established based on well ties and the seismic facies relationship to RMS velocity trends (figure 3).

The retention capacity and hence hydrocarbon column height in carbonate pinnacles can be greatly restricted in overpressured reservoirs due to the relative proximity of the pore pressure, fracture and lithostatic gradients. Column height estimates are only as accurate as the predicted pore pressure profile. An analysis of reservoir pressure in hydrocarbon bearing wells in the study area indicate column heights less than maximum closure are often due to overpressured reservoir and not the presence of thief sands.

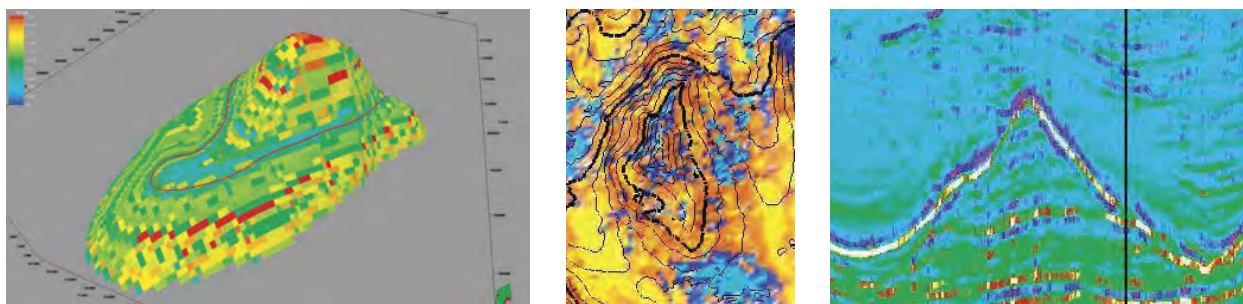


Figure 1: Porosity distribution on the surface of the carbonate pinnacle (porosity derived from AI)

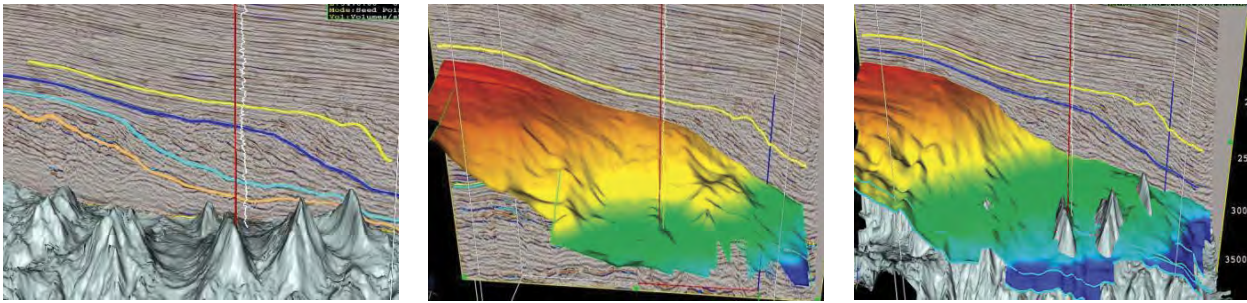


Figure 2: Images depicting the stratigraphic position of the carbonate pinnacle's relative to the overlying prograding clastic units.

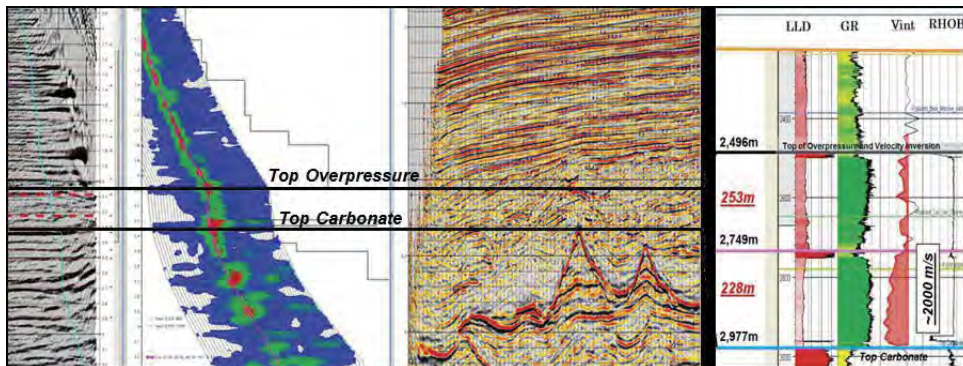


Figure 3: PSTM gathers, semblance and log used to calibrate and characterize seismic velocities to pore pressure trends.

Accurately predicting reservoir pressure is critical for hydrocarbon resource estimates and well design. A miscalculation of 1ppg in pore pressure prediction can relate to 150m of gas column or 200-400bcf of GIIP. Pore pressure also greatly affects depth conversion and estimates of GRV. Accurate prediction of the overpressure magnitude in overlaying shale sequence along with the thickness and distribution of this shale interval therefore has significant economic impact.

An integrated approach to estimate the hydrocarbon resource in carbonate pinnacles uses high end fit to-purpose seismic velocities constrained by stratigraphic facies mapping as an essential input to pore pressure estimation. The calculated

pore pressure can then be used for depth conversion and column height estimation to assist in risking, sizing and ranking an exploration prospect portfolio in an overpressured environment. Newfield and their partners plan to drill and evaluate another high pressure carbonate pinnacle in 2012.

Acknowledgments

The authors would like to thank PETRONAS for their support and cooperation during the exploration phase of this PSC and also Mitsubishi Corporation and their Malaysian subsidiary Diamond Energy Sarawak Sdn. Bhd for their support as our joint venture partner.

Pore Pressure Modeling - How to Overcome HPHT Challenges

S. Bordoloi (Baker Hughes Inc. (GMI)) & A. GHOSH* (Baker Hughes Inc. (GMI))

Introduction

Well planning and designing in HPHT environment have numerous challenges starting from play identification and prospect de-risking to drillability and finally development and production. Overpressure prediction is one of the principal challenges facing the oil industry today, as exploration focus worldwide is moving more and more into the HPHT environment. Pressure related problems in HPHT wells include well control incidents, lost circulation, differential sticking, reduced rates of penetration, and reservoir damage. These often lead to expensive sidetracks, well abandonments and even underground blowouts. A better understanding of the prevalent pore pressure regimes in terms of generating mechanisms, pressure maintenance and dissipation through geologic time offers invaluable insight and perception about these challenges and also on our ability to mitigate or minimize them. It is important to analyse these challenges and develop an understanding of the same, prior to drilling so that, various plans and systems can be put in place.

Understanding of Pressure Regimes

Mitigation of various associated risks in HPHT well planning requires detail pre-job pore pressure and fracture gradient modeling. Integration of predrill pore pressure estimation with geological understanding is the key to avoid possible drilling surprises or plan for alternate scenarios so that the wells can meet their intended objectives.

Modelling approaches are required to help understand the causes of overpressure. In addition to stress related fluid retention causes, thermal mechanisms leading to diagenetic changes and fluid volume increase also play a defining role in generating high pore pressure in HPHT environment. Moreover, once overpressure is generated in the subsurface, it also wants to equilibrate to hydrostatic and therefore fluid redistribution in permeable zones, usually leading to pressure inflation, can not only alter the pressure regimes locally, but also results in a reduction of the already narrow mud window available to drill and complete a well successfully. That makes pressure prediction so much more difficult and challenging, requiring an integrated approach involving basin modeling, velocity and petrophysical-based analysis, offset well studies and combined with a detail understanding of the geological model and seismo-stratigraphical interpretation (Bordoloi, 2009).

Understanding the in-situ stress state in the area and the geological model plays an important role in providing solutions on how to manage HTHP well drilling to ensure stable wellbore. This may involve detail workflows to improve the quality of input data, including special seismic velocity processing, geobody mapping and understanding of seal integrity as well as modeling of possible hydrocarbon column heights.

The commonly used methodologies, either 1D or 3D, based on log or and seismic velocities as well as basin modeling approaches are primarily based on the assumption that pore pressure is a function of rate of loading and the accompanied changes in porosity and its effect on permeability, depending on the sediment type. This leads to the modeling of shale pressure evolution, but sand pressures can be in pressure disequilibrium compared to the bounding shales. The sands usually show a positive imbalance compared to the shale background pressure,

particularly in case of wells drilled in virgin exploratory areas. Precise modeling of sand pressure is challenging. This requires detail integration of offset well studies, pressure cell modeling and information from improved seismic imaging. Use of high-end seismic data provides significant advantage by analysing different seismic attributes for identifying the possible reservoir bodies (or permeable zones) and their spatial distribution as well as connectivity.

Fracture Pressure Modeling

In addition to pore pressure, fracture gradient modeling also plays a critical role as it limits the maximum allowable mud weights for a particular hole section. When the section is overpressured, and particularly when high pressures close to fracture pressure are expected – either in shales or due to sand-shale pressure differential, casing setting depths are dictated by the proximity of the pore pressure to the fracture gradient rather than the length of open hole which can be drilled without difficulty. The fracture pressure is the effective upper limit to the pore pressure, above which fluids can escape and pressures will bleed-off (Ward, et. al 1994). The retention capacity of a pressure cell is therefore bounded by the fracture propagation pressure, the knowledge of which is important for planning and drilling HPHT wells as it forms the effective upper limit for mud weight and therefore Leak-Off Tests (LOT) or Extended Leak-off Tests (XLOT) becomes crucial.

Reliable pressure prediction techniques are not only important during the exploration phase when virgin pressures are likely to be encountered, but also important in case of depleted reservoirs, particularly when in-fills are planned. During production in high pressure areas, it is not just the pore pressure that changes rapidly, but also the entire stress regime in the rocks around the wellbore along with the depleting reservoir. The changes in the reservoir pressure also leads to a reduction of the fracture gradient due to the coupling effect and this requires the mud weights to be adapted accordingly.

Uncertainties and Real-time Monitoring

Even with good seismic and well data, uncertainties still exist. Even the most sophisticated pore pressure prediction techniques cannot rule out that kicks cannot be experienced. Real-time pressure monitoring while drilling therefore becomes necessary to avoid pressure related drilling complications. The key for successful real-time pore pressure monitoring is to develop a collaborative effort by thorough understanding of the predrill model assumptions and the possible geological uncertainties. This helps to quickly update the predrill pressure models with real-time predictions leading to better constrained ahead-of-bit predictions and thereby influencing the drilling procedures.

Conclusions

In many areas around the world deep HPHT targets are being increasingly targeted. Accurate pore and fracture pressure determinations are some of the key considerations in these wells. Optimum mud weights and casing point selections are crucial for safe, efficient and cost effective planning and drilling. In HPHT areas, pore pressure modeling requires a very

detail understanding of the possible causes combined with an integrated modeling from a geological perspective – so that the workflows cover the analysis of various possible mechanisms to minimize drilling surprises. This may require improving the quality of input data, including special seismic velocity processing, detail seismic interpretation leading to geobody mapping and understanding of possible hydrocarbon column heights. In addition to pore pressure, fracture gradient modeling is also crucial in HPHT wells as it forms the effective upper limit for mud weights. Extended Leak-off Tests (XLOT) or at-least Leak-Off Tests (LOT) are therefore critical data to have for a better understanding of the fracture propagation pressure. Real-time pressure monitoring plays an important role to reduce the inherent uncertainties in such areas, but requires a very good integration with the predrill models and concepts for ensuring better predictions.

References

- Bordoloi, S., 2009, Geopressure Estimation– An Integrated Approach: Petroleum Geology Conference and Exhibition (PGCE), Kuala Lumpur, Malaysia, March 02-03, 2009.
- Ward, C.D., Coghill, K., Broussard, M. D., 1994. The Application Of Petrophysical Data To Improve Pore And Fracture Pressure Determination In North Sea Central Graben HPHT Wells, SPE 69th Annual Technical Conference and Exhibition, New Orleans, LA, U.S.A, September 25-28, 1994, SPE paper # 28297, p. 53-68.

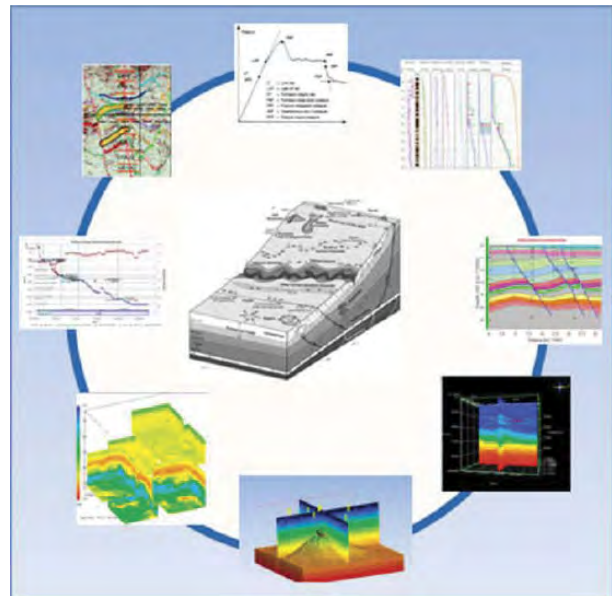


Figure 1: A best practice approach for pore pressure modeling in HPHT areas requires a combination of various input data, application of different methods & techniques and a workflow which is highly focussed on understanding and replicating the possible geological processes responsible for overpressure generation.

Drilling Risks Associated With Hydraulic Fractures and Reactivating Faults Due To High Mud Weight/Pore Pressure and Miti

A. A. Bal* (Baker Hughes Inc), D. Maya (Baker Hughes Inc), K. K. Kyi (Petronas Carigali), R. Guha (Petronas Carigali Sdn Bhd), M. I. Gabreldar (Petronas Carigali Sdn Bhd) & D. Abang Indi (Baker Hughes Inc)

Introduction

In the wake of the Deepwater Horizon accident, a proper safety process and qualification is being given highest attention in the industry. Process safety refers to the procedures for minimizing risk generally (Deep Water Final Report 2011, Chpt 8). One of these risks is deciding on the appropriate mud weight to balance the pore pressure without fracturing or damaging the formation. The decision is generally based on a pore pressure prediction study resulting from modeling seismic or well-log data (e.g. Zoback 2007). Two case studies are presented here that illustrate where the optimal balance between mud weight and pore pressure as well as fracture gradient was unexpectedly crossed, and its effects on the formation and drilling process. One example comes from a recently drilled offshore Sabah exploration well, and another from Venezuela.

High mud weight increases pore pressure and reactivates a pre-existing fault

Significant losses were experienced in the 15 ¼" section of a well recently drilled offshore Sabah, Malaysia. The mud system was oil based. It was assumed that the fracture gradient was surpassed and the mud weight was consequently lowered to 10.6 ppg to control losses. Post drill estimated pore pressure was 9.2 ppg. Despite having a logging-while-drilling (LWD) bottomhole assembly comprising resistivity, density, neutron, gamma tools, the defensive decision was made to log the planned wire-line suite before reaching the planned section total depth to secure data in case the well was lost.

During post wireline logging processing and analysis it was observed that there was a significant difference between the LWD and wireline resistivity logs over a large interval: with all the resistivity curves showing a wide separation (Figure 1). Normally we would expect similar results. The wide separation suggests the formation was hydraulically fractured after the LWD log acquisition and before the wireline acquisition. The high resistivity values are due to the invasion of oil-based mud into the inferred hydraulic fractures. Subsequent attempts to obtain formation pressure tests were unsuccessful over the interval where losses were experienced. It was suspected that the fractured formation precluded the possibility of a good seal.

Analysis of the Stoneley permeability index derived from the full wave acoustic tool (Tang and Cheng 1996), which is sensitive to the presence of fractures, confirms the zone around the recorded losses is highly permeable. This analysis supports the hydraulic fracture hypothesis. The features observed on the borehole image log, however, are equivocal due to the poor condition of the damaged borehole (Figure 2). There is however a suggestion of steeply dipping dips in the borehole image log ranging from 55-80° dip - these poorly developed features are not typical tensile fractures characteristic of vertical wells.

Although it was suspected that high mud weight resulted in hydraulic fracturing, analysis of bedding dips from the borehole images derived from above and below the damaged zone shows an upward steeping pattern (arrows in Figure 3). This pattern is interpreted to be bedding deformation as a result of fault drag. A great circle fitted to the deformed bedding suggesting the deforming feature (fault) has a near NW-SE orientation. Although hydraulic fracturing cannot be ruled out, it is likely that a poorly imaged pre-existing fault was reactivated into which fluid were lost.

To further test the existence of the inferred fault, a processing methodology following Tang et al (2007) was applied to the full waveform acoustic data (XMACTM). Implementation of this method to acoustic-logging data processing provides analysis of the reflected wavefield, making it possible to image near-borehole geologic structures up to 20 metres away from the borehole using conventional array acoustic-logging. Processing confirms the presence of a fault plane that dips 68° striking approximately N-S and intercepting the borehole at a depth consistent with the deformed bedding trend and feature observed in Figure 2A. Moreover, the acoustic processing confirms the fault plane is imaged up to 20m beyond the borehole.

From the point of view of safety, the above situation was controlled, data was defensively acquired, and the operation was able to continue drilling to planned section total depth. However this situation was potentially critical as a minor increase in mud weight leads to increased mud loss and a decrease in mud weight potentially leads to kicks. Such a situation is described in Rupdip et al (2006). In that case, modeling shows the hydraulic fracturing length extends up to 6m beyond the well bore.

A mitigating well planning strategy for this situation is to undertake a predrill geomechanical model (Zoback 2007). These models help to define upper-mud-weight limits that avoid the costly formation fracturing (or fault activation) and

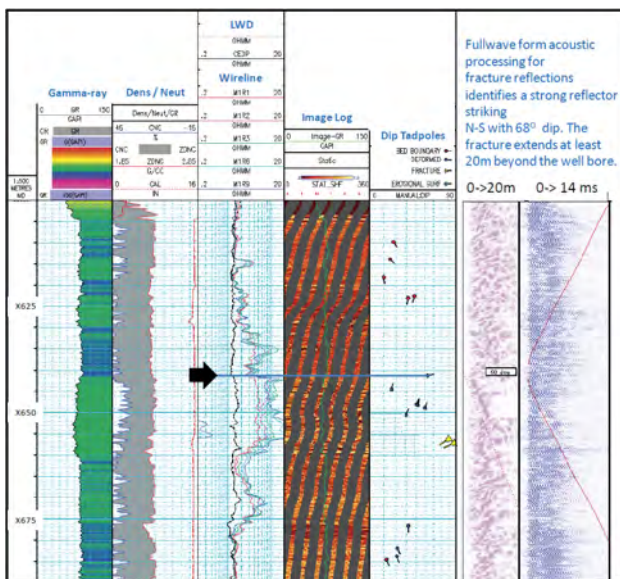


Figure 1: The resistivity track (black arrow) shows the LWD resistivity (black curve) reading about 1.5 ohm.m. The wireline resistivities, in contrast, are an order of magnitude larger. This interval of anomalously high wireline resistivities coincides with deformed bedding (see dip track and Figure 2) and a fracture (fault) imaged using the full waveform acoustic data. The imaged fracture intercepts the borehole at approximately the depth of the bold black arrow.

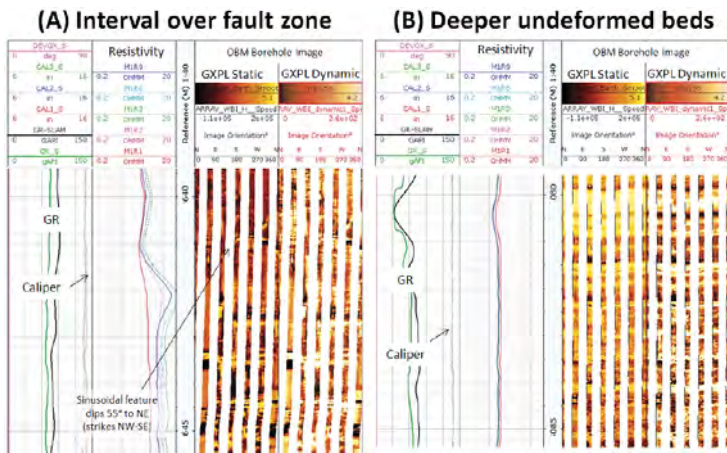


Figure 2: (A) Borehole image log over fault zone. Sinusoidal feature marks probable fault at borehole wall. Image quality is poor over the damaged zone. (B) Borehole image from below the damage shows a markedly improved quality in image. Borehole is vertical and 15 ¼ inches; approximately 5m of image is displayed.

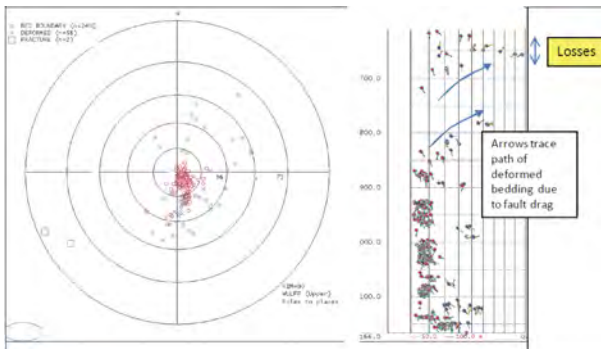


Figure 3: Stereonet with poles to bedding planes (red) and deformed bedding (blue). To the right is a compressed scale tadpole plot showing dips along the borehole (m), approximately 500m is shown. Blue arrows trace deformed bedding steeping upwards is best explained by fault-drag folding. Stereographic analysis of deformed beds indicates the deforming structure (fault) has a NW-SE orientation.

consequent losses, loss mitigation procedures, time spent for intermediate logging, and borehole damage that precludes formation pressure seals.

Underbalanced drilling assessment and implementation — Economic impact

In this case study from Venezuela, hydrocarbon bearing structures conform by a sequence of aligned domes that are structurally complex and affected by high compressive and tensile stresses. The reservoir contains light oil and gas. Drilling is challenging since the sequence comprises interbedded depleted sands (2000 psi below expected pressure) with normally pressured shales.

More specifically, the challenge is to provide enough borehole support for the normal or over-pressured zones, and avoiding fluid losses through drilling-induced fractures (DIFs) in low-pressure zones. Moreover wells with high or total losses generally results in damage that affects acquisition of data needed to identify the problem zones.

Underbalanced drilling operations are often expected to prevent unwanted fractures or fault reactivations. However, it could lead to borehole collapse due to the lack of positive support by borehole mud. An accurate evaluation of in-situ stresses and realistic estimations of formation rock mechanical properties is recommended at the well planning stage.

Using available logs, pressure data, and drilling history, a geomechanical model was developed (pore pressure and stress profiles). Caliper and image logs were crucial in the in-situ stress model determination. Acoustic logs provided the information

for rock mechanical properties. With the model in place, a new mud window (that avoids shear failures, tensile fractures) was estimated and implemented. After implementation in the field, the result was a cost benefit of \$1 MM over five wells, lost circulation was avoided, and improvements in rig time and penetration rates were achieved.

Discussions and conclusions

Drilling induced fractures (DIF) or reactivated faults pose serious threats to drilling operations. A critical situation may result as a minor increase in mud weight leads to increased mud loss and a decrease in mud hydrostatic column potentially leads to kicks (e.g. Guha et al. 2006). DIFs can also affect cementing jobs. In this case, cement is channelled into the DIFs, resulting in channelling opposite the DIFs. The value of a geomechanical model with regards to mitigating drilling problems, reducing drilling risk, and cost savings should not be underestimated. Equally important, contingency plans should be in place to acquire the correct data so that effective mitigating strategies can be developed or to understand the problem at hand.

Acknowledgments

The authors thank Baker Hughes and PETRONAS Carigali for permission to publish this paper. We also thank Doug Patterson for assistance in processing the the compressional body waves generated by the dipole which allows us to see the fault beyond the borehole.

References

National Commission on the BP Deepwater Horizon Oil Spill and Offshore Drilling, 2011. Deep Water – the gulf oil disaster and the future of offshore drilling <http://www.oilspillcommission.gov/final-report>

Rupdip G., Tyagi, A. K., Corley, B., Rabinovich, M., Tang, X., 2006. Integration multi-senor acoustic and resistivity data for improved formation evaluation in the presence of drilling induced fractures. SPWLA 47th Annual Logging Symposium, June 4-7.

Tang, X., Zheng, Y., and Patterson, D., 2007. Processing array acoustic-logging data to image near-borehole geologic structures *Geophysics*,72, NO.2, March-April.

Xiaoming Tang and C. H. Cheng, 1996. Fast inversion of formation permeability from Stoneley wave logs using a simplified Biot-Rosenbaum model *GEOPHYSICS*, VOL. 61, NO. 3 (MAY-JUNE 1996); P. 639-645.

Zoback, M.D., 2007. Wellbore stability p.301-331. In *Reservoir Geomechanics*. Cambridge University Press, pp.449.

Integrated Reservoir Characterisation of Turbidite Deposits within a Submarine Canyon, Offshore Sabah, Malaysia.

K. Maguire* (SHELL Malaysia Exploration & Production), C.W. Hong (SHELL Malaysia Exploration & Production), T.M. Ting (SHELL Malaysia Exploration & Production) & G. Stone (SHELL Malaysia Exploration & Production)

Introduction

One of the main subsurface uncertainties that impacts waterflood and enhanced oil recovery (EOR) projects is reservoir connectivity. Reservoir connectivity is controlled by structure (faults) and stratigraphy (reservoir architecture). An understanding of structural connectivity in a field can often be determined by detailed structural mapping from seismic. However, due to seismic resolution limitations, an understanding of stratigraphic connectivity often relies on detailed reservoir characterisation in order to understand the depositional processes, depositional setting, and resultant reservoir architecture of a field. Due to the inherent uncertainty in characterising an entire reservoir from a limited sample set of wells, alternative stratigraphic scenarios must be considered and field development plans screened against the different scenarios to ensure the most optimal development plan is selected to cover the range in subsurface connectivity outcomes.

An integrated approach to reservoir characterisation of turbidite deposits within a submarine canyon located in offshore Sabah, North West Borneo will be presented in this paper. This involved detailed sedimentological analysis of core, borehole image, dipmeter and wireline data combined with detailed seismic mapping. This, together with outcrop and subsurface analogues, provided the basis for the construction of two alternative depositional models. It is proposed that these models will be used to screen the field development plan for the field particularly with respect to the range of reservoir connectivity and the associated impact on water injection and EOR schemes.

Field Information and Data Available

The studied field has a total of eleven wells and is located in offshore Sabah, North West Borneo in a water depth of 70ft. Two phases of development drilling have been completed since the field was discovered in the late 1990s. The field has a northwest-southeast orientated structure and is cross cut by northeast-southwest trending faults (Figure 1). There are three main sandstone reservoir intervals which are separated by mudstone sequences (Figure 2). Generally, the reservoirs are

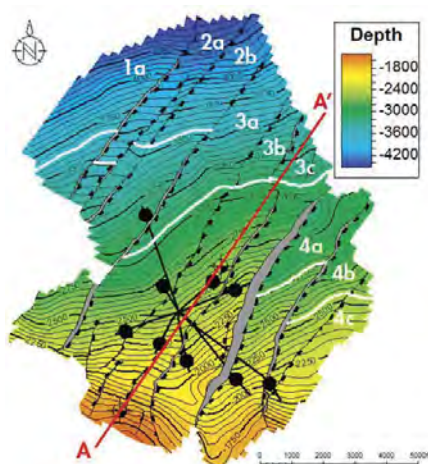


Figure 1.

subdivided into upper and lower reservoirs with the lower units holding the majority of the hydrocarbon reserves. Full suites of conventional logs (gamma ray, resistivity, neutron porosity and bulk density and sonic) were acquired in all wells. Core was taken across the main reservoir intervals, as well as the intervening mudstones in three of eleven wells (Figure 2). Good quality image logs were available for six of the wells.

Seismic Interpretation

Good quality 3D seismic data with pre-stack depth migration processing is available and this together with regional seismic data led to the early recognition of the canyon geometry of the field (Figure 3). Seven consistent seismic horizons were interpreted and used to constrain the reservoir intervals. Seismic attribute analysis including waveform classification, volume sculpting and horizon probe techniques were employed as part of the seismic stratigraphic work in an attempt to identify stratigraphic boundaries and depositional features such as meander belts, channels and/or lobes. In addition, amplitude-versus-offset (AVO) inversion and lithology cubes were used for loop level interpretation.

Depositional Models and Impact

Detailed sedimentological analysis of cores and image log data further indicates that the reservoirs comprise stacked sandstone sequences deposited by turbidity currents. Integration of this data with the regional and field scale seismic interpretation indicates that the studied field lies in an incised canyon or slump-scar close to the shelf-slope break.

Integrated reservoir characterisation using new core and image log data and detailed seismic stratigraphic work has resulted in the construction of two alternative depositional

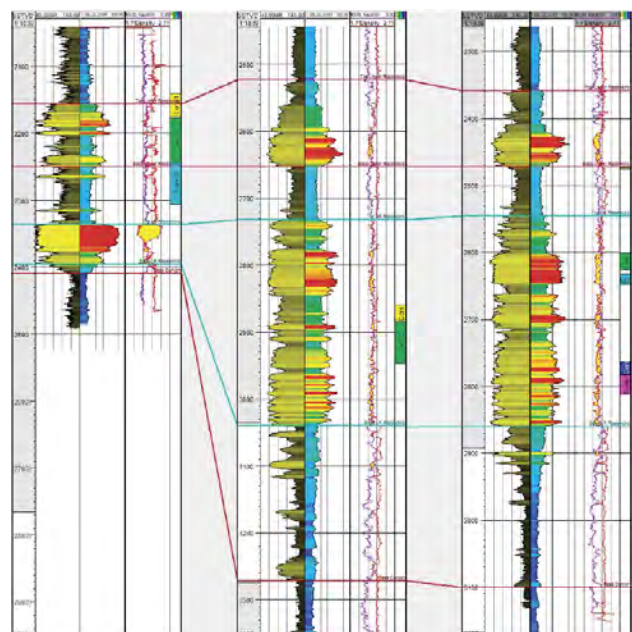


Figure 2: Well Correlation Panel.

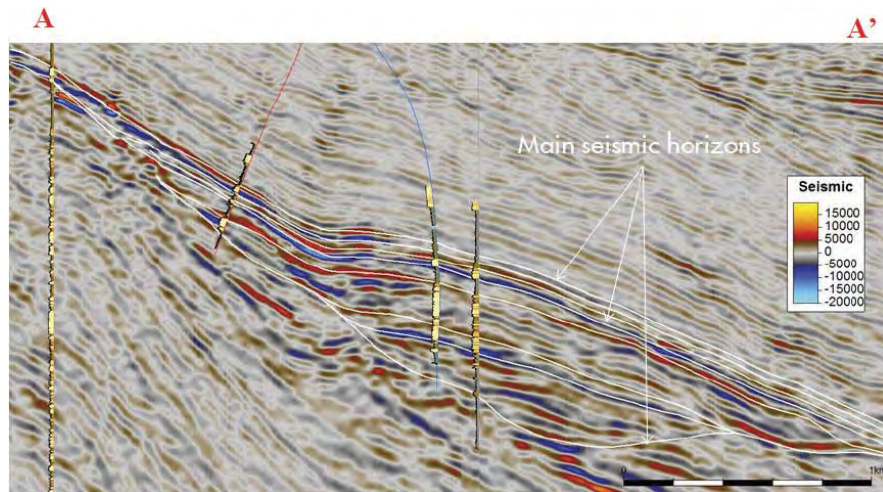


Figure 3: Seismic cross section showing canyon geometry and internal fill.

models. In the first model, the environment of deposition is interpreted as an incised canyon, within which the lower reservoirs were deposited in a channel-levee system, with reservoir quality deterioration away from the channel levee axis, while the upper reservoirs are interpreted to have been deposited within a lobate system

The second model provides an alternative interpretation with deposition associated with backfilling of a slump scar. In this model the lower reservoirs are interpreted as more lobate in nature (rather than channelized), and the upper reservoir remaining lobate in nature. This model results in the internal architecture of the lower reservoirs being interpreted as more sheet-like compared to the first model. It is envisaged that the lobate model will result in improved reservoir connectivity within the same fault block compared with the channel levee model.

Both models are based on the same data set and the same data observations. It is the interpretation of those observations which differ for the two models, and result in quite different representations of reservoir connectivity. This illustrates the importance of observation based (rather than direct interpretation based) reservoir characterisation and this topic will be discussed further in this paper. The two models represent end members which will be used to test the effectiveness of different water injection schemes and optimise well placement for further field development.

Acknowledgements

The authors would like to acknowledge the publication permission granted and constructive feedback given by the management of Shell Malaysia Exploration & Production and Petronas Carigali Sdn. Bhd.

Application of Innovative & Unconventional Techniques Enhanced Subsurface Interpretation of the J Sands, Berantai Field

J. Ranggon (Petrofac Energy Developments Sdn Bhd), M. H. Abdul Halim* (PETRONAS), W. N. Wan Mohammad (Petrofac Energy Developments Sdn Bhd), S. Dang Do (Petrofac Energy Developments Sdn Bhd) & M. H. Hashim (Petrofac Energy Developments Sdn Bhd)

The Berantai field is fast track development project under a Risked Service Contract (RSC) agreement. The oil and gas are planned to be produced from multiple reservoirs, ranging from the F to the J sandstones. The development potential for the shallower reservoirs (F to I sands) is well defined due to good subsurface data coverage and tested productivity.

Although these J sands are known prolific hydrocarbon producers in nearby fields, but due to limited or inconclusive data by conventional analysis, the subsurface definition and development potential of these reservoirs are less certain. This paper will focus on how detailed analysis and the use of an alternative interpretation methodology of the all available data have enhanced the subsurface definition.

In the original Berantai FDP, the reservoir characterizations of the J sands were based on log data from three pre-2007 appraisal and exploration wells (C, D and E, Figure 1). The acquisition of cores and additional subsurface data from another J sand well drilled in mid 2011 (well F), provided valuable information on reservoir properties to enhance geological and petrophysical interpretations, and reservoir engineering analysis. Improved sedimentological understanding was made possible by integrating the data from this well with earlier wells.

The J reservoirs comprise of sand and shale intercalation. The sandstones are very fine to silty grained, heavily bioturbated, abundance marine micro faunas, well compacted and display coarsening upward trends. Based on a combination of lithology, sedimentary features, stacking pattern, ichnofacies assemblages and facies association analysis, the J sand in Berantai area have been interpreted as being deposited within a low energy setting, as reworked shoals/bars in lower shoreface/distal shelf areas. The shoals and bars are frequently being reworked, resulting in a sheet like sandbodies which can be correlated field wide and across to nearby fields.

Based on regional trends, a WNW-ESE trending shoreline is located towards the northern part of the Berantai field, whereby the sediments in well F area is deposited in the most distal part of the shelf and display poorer reservoir properties (Figure 2). The J sandstones penetrated by wells C and D, located in areas north of well F represent a more proximal shelf environment.

These wells display better reservoir properties with calculated mobility value up to 22 mD/Cp. In addition, the ability to recover gas samples from LFA and bottom hole sampling runs in well D confirmed the presence of moveable gas.

Petrophysical interpretation of the J sands is not straightforward. Although mud logs and LWD logs indicated the presence of gas, the inability to flow during DST renders fluid identification inconclusive. Several innovative non-conventional petrophysical interpretation techniques using Rock Physics analysis principles were applied to help firm-up the fluid types (Figure 3). A detailed assessment of the acoustic properties was used to assist in discriminating gas-filled sand from wet sand and shale. Assessment using other well data, such Near versus Far neutron counts, and Compressional versus Shear curves was used to compliment and validate the interpretation results. The results from the alternative interpretation approaches supported the presence of gas.

The data from well F indicates a lower formation pressure of about 3200 psia compared to an expected 4500 psia, recorded in previous wells drilled in 2007. As the higher pressure was recorded from the adjacent fault block, it is possible that the lower pressure in the Fault Block A could have been drawdown by nearby large and matured producing fields. Based on an improved subsurface understanding of the Berantai J reservoirs, several optimizations were made to the development plan in the area of well placement, well design, and drilling and completion techniques.

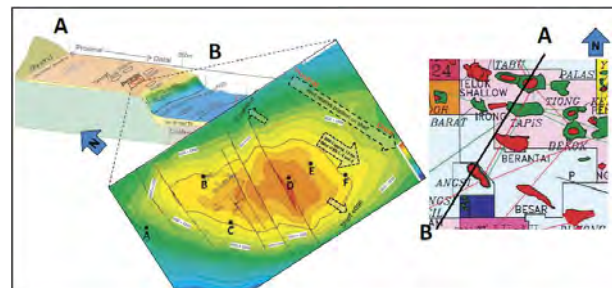


Figure 2: Berantai J Group, conceptual depositional model.

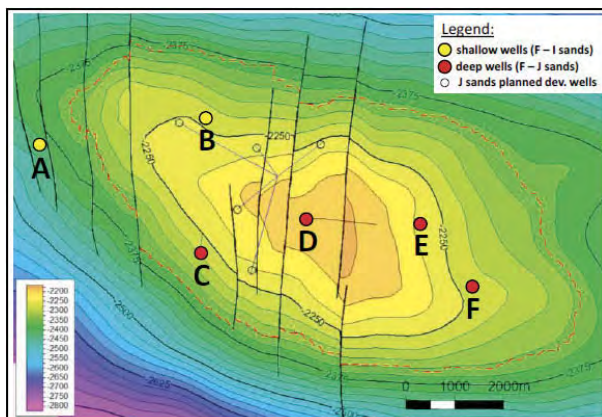


Figure 1: Berantai structure map, Top J Group reservoirs.

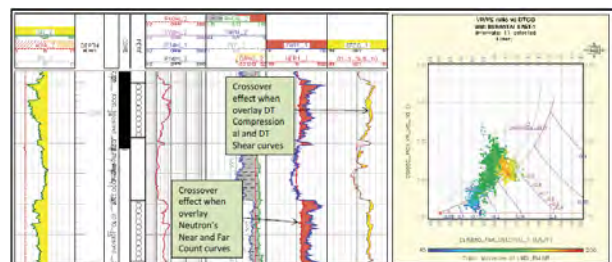


Figure 3: Petrophysical interpretation using Near vs Far neutron counts and rock physics analysis.

The Success and Pitfalls of Seismic Application for Infill Drilling In Alpha Field, Malay Basin

A. A. Abdul Rahim* (ExxonMobil Exploration & Production Malaysia Inc), L.H.K. Lim (ExxonMobil Exploration & Production Malaysia Inc) & F. F. Fahmi (ExxonMobil Exploration & Production Malaysia Inc)

Introduction

Alpha field, located approximately 240 km east of Kerteh, comprised of generally east-west trending anticlinal complex with four main culminations. Development began in 1989 with a total of 228 development wells drilled from 8 platforms. Cumulative field production to-date has reached 93% of the total estimated EUR; infill programs were planned targeting bypassed oil and undeveloped areas to maximize field production. Integrated seismic interpretation techniques were applied on various 3D seismic cubes to help identify and mature these infill opportunities.

Two vintages of 3D seismic data, acquired in 1987 and 1998 were available; the latter was reprocessed by applying Q-migration technique to improve imaging. In addition, derivative seismic data such as AVO, impedance and coherency volumes were generated to supplement the geophysical evaluation and infill prospects generation. This paper discusses how the integrated seismic interpretation results were used in identifying and de-risking two of the Alpha infill prospects in A1 and A2 reservoirs.

Method and/or Theory

The south-eastern part of Alpha field is one of the primary infill areas known to have high degree of geologic uncertainty. The primary infill objectives identified in A1 and A2 reservoirs carry significant geologic risks due to uncertainty in reservoir quality and oil column thickness.

Integrated analysis including detailed evaluation of offset wells (core data, rock properties and logs characteristics) and the associated production performance data together with seismic attributes were analysed for better prediction of the distribution of the A1 productive facies.

Early field development primarily focused on the northern and western part of Alpha field where a 23m rim oil column was

proven by exploration wells and seismic DHI. No development wells were planned for the southern area due to uncertainty in oil column thickness, whilst the south-eastern closure has thinner oil column of 4m. A recent field study revealed that there is potentially a thicker oil column in A2 based on seismic DHI analysis.

Examples

The A1 reservoir, interpreted to consist of estuarine deposits is well developed in the northern Alpha field. However, reservoir quality deteriorates to the south, where the A1 opportunity is located. The prospect was assessed to have a producibility risk due to learnings from a nearby well which intersected poorer quality tidal flat sands. Seismic attributes were calibrated to productive facies thickness observed in existing wells, which was defined by resistivity cut-off (figure 1). The analysis suggested that there was potential for an economically-viable infill opportunity in the prospective area, which was eventually proven by the drill well result.

The deeper A2 reservoir, interpreted as deltaic sand deposits, is observed to be laterally extensive. The prospect identified in A2 is located within a small closure bounded by a fault in the southern area, and the opportunity could be stacked with the shallower A1 opportunity discussed earlier (figure 2). The key risk is oil column thickness, governed by structural spill depth and seal integrity of the bounding fault. Mitigating this risk was further challenged due to different structural mapping scenarios using the original 1998 and 2010 reprocessed seismic data (figure 3). Considering the associated risk and impact on prospect resource, a decision was made to deepen the well from the primary A1 objective into the A2, and 8m oil column was successfully encountered.

Due to the successful well result, an additional opportunity was identified to test a potential thicker oil column in the A2.

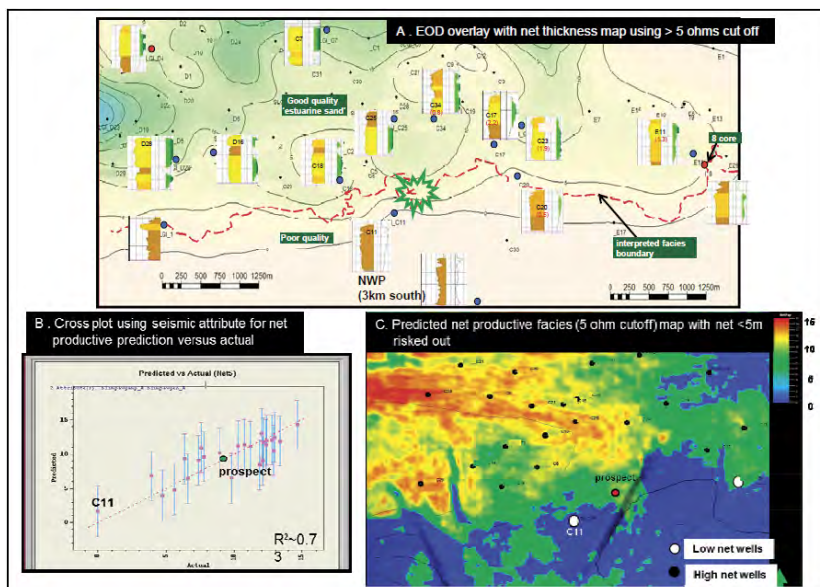


Figure 1: Integrated analysis conducted for prediction of A1 productive facies boundary; Diagram A - Showing EOD distribution of good quality productive facies to the north and poorer reservoir quality to the south. Diagram B & C - Seismic attributes analysis giving correlation factor ~70% together with performance behavior of analogs in the vicinity of the opportunity support presence of productive facies from the A1 sand.

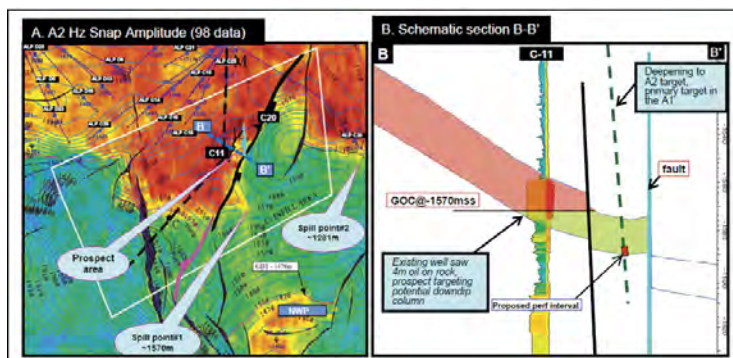


Figure 2: Shows the A2 opportunity that was identified in the southern Alpha area; Diagram A –Shows A2 amplitude map highlighting the location of the prospect and the bounding NE-SW fault that separate it from the spill point#1 (mapped at -1570m, which is shallower than proven oil as low as at -1573m). Diagram B illustrating the A2 prospect targeting possible oil trapped within small closure.

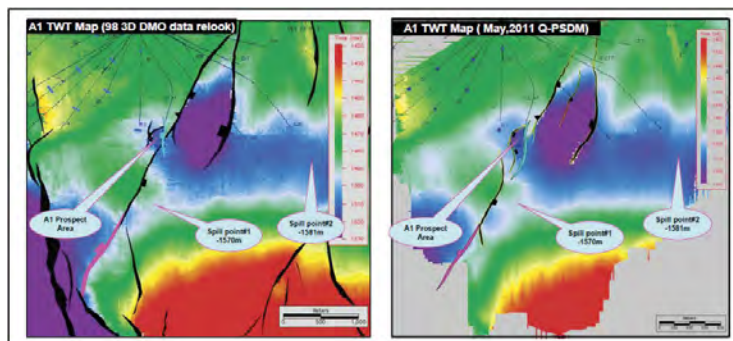


Figure 3: Comparison between 2 seismic datasets giving different fault interpretation, the interpretation based on 2010 dataset shows prospect not isolated from the spill point #1; possess significant risk to oil presence below the spill mapped at -1570m.

The well location has a potential seismic DHI in a sub-block northeast of the earlier A2 well penetration. Similar to the earlier prospect, this sub-block is bounded by two normal faults in the east and west. The key risk for this prospect was fault seal, as the reservoir could be juxtaposed against another fault block to the east that has a thinner oil column of 4m. The pre-drill assessment predicted an approximately 23m oil column at the prospect area, based on deeper termination of the DHI, which was structurally consistent with the developed northern area of the field. Reservoir connectivity analysis integrating seismic and well data also supported this interpretation. However, the well results encountered a shallower current Gas Water Contact (CGWC) at a depth equivalent to the Oil Water Contact (OWC) observed in the A3 reservoir in the eastern fault block.

Preliminary post-drill evaluation suggests potential hydrocarbon movement post production between the A2 and the A3. The DHI is potentially due to residual hydrocarbon or the pre-development OWC. The observed CGWC in the drilled well may represent the break-over point or the shallowest leak point along the east bounding fault between A2 and A3.

Conclusions

Integrated analysis, incorporating seismic and geological interpretations together with production performance was essential in de-risking an infill opportunity proven to be successful in the A1 reservoir. However, the results of the follow-up well in the A2 highlights potential pitfalls in using seismic data alone in a mature field setting.

Well Architecture and Design Criteria for Complex Reservoirs in Mature Fields

K. S. Chan* (PETRONAS), R. Masoudi (PETRONAS), B. P. Kantaatmadja (PETRONAS) & M. Othman (PETRONAS)

In the quest of reducing the field development and production cost in Malaysia in the complex multi stacked compartmentalized mature fields, a new initiative is to couple the reservoir dynamic simulation with reservoir geo-mechanical modeling. Reservoir rock properties, stress regime, wellbore stability, fault sealing behavior, reservoir connectivity and communication can be significantly changed during the long time production and injection history in mature fields. Any successful field rejuvenation plan should carefully take into account of these changes. The objective is to plan, drill and complete cost effective wells having high productivity, high recovery per well, and high borehole stability during production life in mature fields.

This “Well Architecture” initiative involves studies for optimal well placement, maximizing reservoir reserve contact, evaluating potential drilling risks, determining optimum sequential hole-sizes before reaching reservoir targets,

simplifying well trajectory, and minimizing well count. A starting point is to construct a mobile oil productivity (MOP) 3D map and super-imposed with a well-bore stability critical drawdown pressure (CDP) 3D map constructed by the geo-mechanical modeling. In addition, this approach which entails studies of rock mechanical stress change in the reservoir during production and injection can also yield the optimal well orientation, well inclination, and perforation orientation, selecting the most effective well type, simplifying the well completion for achieving optimal well productivity and ensuring expected oil and gas recovery.

In this paper, suggested workflow and key tasks with the desired results are to be presented and demonstrated with a few selected field case studies for examples. The applications of new and smart technologies to optimize furthermore the well completion in thin oil-rim, multiple-stacked, and compartmentalized reservoirs are illustrated.

Petrophysical Evaluation of “Quasi Wet Pay Zones” (QWPZ) via Integration of Advanced and Conventional Wireline Data

S. Ismail* (PETRONAS Carigali Sdn Bhd), M. M. Altunbay (PETRONAS Carigali Sdn Bhd) & N. Aula (PETRONAS Carigali Sdn Bhd)

A “low resistivity-low contrast” (LRLC) and low porosity-permeability sand earns a new name “quasi-wet-pay zone” (QWPZ) encompassing the hindrances of recognition due to lesser conductivity-contrast and diminished hydraulic properties. As we know from each components of this new definition, the evaluation of QWPZ sands by traditional methods has historically proven to be inadequate in deciding if the testing/completion/stimulation of a zone(s) is economically feasible. We have studied new avenues for advanced data gathering and interpretation methods to address the Petrophysical and decision-making challenges of QWPZ interests. We added the NMR, directional resistivity and the image log tools to the conventional wireline string. We have also devised a new workflow for the challenge by evaluating the electrical anisotropy from directional resistivity device together with movable porosity from NMR data as an indicator for hydrocarbons. The apparent electrical anisotropy due to bioturbation is discounted from the decision-tree by screening the source of anisotropy through image log of the subject intervals. However, for the case study QWPZ challenges doubled up with the masking of formation oil with the invading OBM filtrate. Hence, the hydrocarbon typing feature of NMR log evaluation is added to the workflow to differentiate the formation oil from the OBM filtrate. The merits, limitations and the outcome of this study are presented.

Introduction and methodology

The data acquired from the conventional resistivity tool is first treated with Waxman-Smiths application in our sand-silt-clay (SSC) model. The results were compared against the results from directional resistivity-based Thomas-Steiber (TS) technique together with the NMR-driven Diffusion-T₂intrinsic (DT₂) maps and saturation computations. Our intent was to look for co-existence of a resistivity-anisotropy (R_v/R_h) and moveable porosity (BVM-Bulk volume movable- from NMR) in subject intervals that can be surmised as a “direct pay indicator”. We have seen the “direct pay indicator” and sufficient permeability for one of the studied intervals. We also have seen the same pay indicator with very low possibility of production (due to low permeability and PI) in another section. However, the interpretation was challenged due to masking of formation oil by the oil-based mud (OBM) filtrate. Therefore, we have used the “Diffusion versus T₂ intrinsic” algorithm in NMR data evaluation to differentiate the OBM-filtrate from the formation oil. Due to an appreciable contrast between the viscosities of OBM-filtrate and the formation oil, we were able to observe different placements of their respective signals on the “Diffusion versus T₂ intrinsic” maps.

Differentiation and quantification of the formation oil signal from the OBM filtrate enabled the computation of formation oil saturation profile by using NMR data. Both conventional and directional resistivity tools calculated high water saturation values doubting the economic feasibility of the newly found interval. However, the inversion of NMR data with a default T₂cutoff of 33 ms yielded very high irreducible water saturations for the formation signaling the sand pack being a QWPZ (Quasi-wet pay zone).

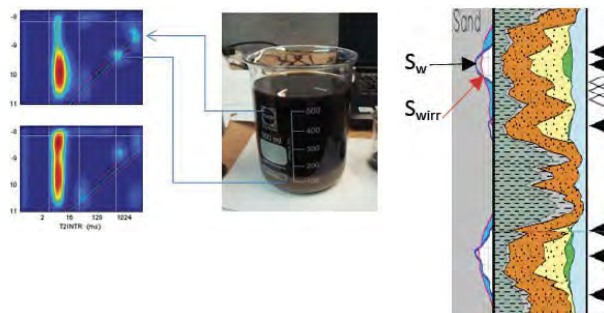
Confirmation of water in the subject interval being at irreducible state (due to capillary retentive forces –NMR BVI data-), it was decided to calculate the Productivity Index (PI) of the interval before sampling and testing the zone. With the direct input of irreducible wetting phase saturation and viscosity from NMR log data, synthetic capillary pressure, Corey-Burdine relative permeability transformations and; there from; the effective permeability profiles were computed from NMR. Productivity Index (PI) profiles were generated via radial flow of Darcy equations for various scenarios of skin factor, Bo and drainage radii. The PI curves for various permutations provided the economics information required in running a well test and sampling.

Then, the samples were taken and fingerprinted and compared against the OBM filtrate proving the presence formation oil. Well test sustained a production of 2600 bbls/d for 13 hours at 96/64” choke with zero water production agreeing what was seeing on the NMR log as %65-70 of Swirr for the subject interval.

The volume of laminar shale driven from directional resistivity measurement (V_{lam}) should compare well with that V_{lam} driven from Thomas-Stieber V_{shale} distribution model. However, we have evidenced the need for “a degree of caution” that is required when the V_{lam} estimates differ, as in the upper sand of this study. The difference between the estimates contains information concerning the nature and scale of the sedimentary fabrics. In our study, image log showed the bioturbation as the causative agent for the disparity between the V_{lam} estimates. Electrical anisotropy as a function of bioturbation rendered itself insufficient as a “pay indicator” for the upper sand.

Conclusions

The addition of advanced wireline log data to the conventional analysis proved to be fruitful by yielding a highly productive oil-sand which was previously thought to be “being wet” and ruling out the main target for the original study as “being-wet” which was previously thought to contain oil. The sampling/testing of the subject sands revealed the efficacy of the tools/methods used in the interpretation and proved the “value added” nature of advanced wireline data.



Applications of 3D Micro-CT Images and 2D BSEM-EDS for Petrophysical Reservoir Characterization

L. Riepe* (PETRONAS Carigali Sdn Bhd)

The paper provides an overview on the application of 3D imaging and Pore Network Modeling (PNM) technology to establish a direct relationship between rock micro-structure parameters from 3D via micro-tomographic images, and the simulation of petrophysical properties of reservoir rocks. Accurately mapping the pore and grain structure and mineralogy in 3D and the interconnectivity of primary and secondary porosity illustrates the role 3D imaging plays in a comprehensive reservoir characterization program.

The computed petrophysical properties (e.g. porosity, permeability, formation resistivity factor, hydraulic radii and drainage capillary pressure) are compared with routine and special core analysis results measured on conventional core samples. The use of 3D micro-tomograms at different scales and PNM provides a quick complimentary method to characterize the distribution and nature of different pore types and matrix components to characterize the static, elastic and dynamic rock properties even on rock fragments (2mm to 1cm diameter) that are not suitable for conventional core analysis techniques.

Introduction

In the recent years significant progress has been made in the development of high resolution 3D tomographic imaging and registration techniques to directly image rock microstructures across a continuous range of length scales (from 10nm to cm scales). This emerging new technology provides a direct characterization of multi-modal pore size distributions and allows one to predict petrophysical flow properties and the producibility of complex reservoir types. Rock properties derived from small fragments of core material have been compared with conventional laboratory measurements and shown to be in good agreement for a wide variety of clastic and carbonate rocks (Knackstedt et al., 2004).

The very encouraging results of this emerging 3D imaging technology for “conventional” reservoirs rocks, has triggered the application of these digital core technologies to very complex “unconventional” reservoirs, like “shale gas” and “fractured basement”, where the rocks are characterized by nano- to micro-porosity and resulting extremely low matrix permeabilities (Riepe et al., 2011).

In this paper case studies will be shown applying high resolution X-ray microtomography (μ -CT), and Pore Network Modeling (PNM) for the 3D visualization and understanding of the nature and variability of the rock fabrics and the related storage and flow capacity of the major rock types. In addition an integration of μ -CT, SEM-EDS and other high resolution imaging techniques has been applied to characterize the dependency of the petrophysical properties from petrographic/mineralogical parameters in 3D (pore/grain shapes & orientations, mineralogy, grain contacts, pore/grain connectivity).

We will present the results of a blind screening test and the first pass evaluations of the μ -CT for three samples from a “Tight Gas” clastic reservoir in the Sultanate of Oman (Riepe et al., 2011). Results for petrophysical flow properties are in good agreement with routine core analysis (RCA) data previously derived for the same samples. Examples are given of combining

the 3D data with conventional SEM based petrographic methods allowing one to map in detail the pore and grain structure of the rocks and to characterize the interconnectivity of the primary and secondary porosity. Constituent mineral distribution, composition and habitat can be mapped in 3D; pore network analysis and pore connectivity can also be correlated to potential hydrocarbon recoveries.

The workflow undertaken on each sample is outlined in Fig. 1. It is based on experimental imaging, image quality control, phase characterization, static and dynamic property analysis.

Experimental Methods

X-ray -CT Imaging

3D images of the miniplugs (small samples extracted from plug scale samples of 38 mm in diameter) at ~2-3 mm in diameter are imaged. The tomogram images were obtained using a μ -CT facility at voxel sizes down to ~1.5 μ m resolution. Images are all composed of 20483 voxels.

SEM

All 2D Backscattered Scanning Electron Microscopy (BSEM) images were taken on a Hitachi 4300 SE/N (Schottky Field Emission SEM, 2006). Automated image analysis for the identification of mineralogy was performed using an FEI QEMSCAN®, a fully automated mineral and petrological analysis system that comprises a SEM integrated with multiple light element X-ray detectors and pulse processor technology. Back-scattered electrons (BSE) and energy dispersive (EDS) X-ray spectra are used to create digital mineral and textural maps. Minerals are accurately identified by their chemical compositions.

Image Registration (2D-to-3D)

The microporosity in the 3D image can be directly correlated with high-resolution microscopy data using 2D-to-3D image registration. The 3D imaged core is then cut and a face within the 3D field of view was polished for the acquisition of an SEM image. The polished section image in 2D was registered to the corresponding slice of the tomogram. The SEM provides a higher-resolution image (down to nm scales can be probed) and allows the evaluation of the pore-filling material and identification of microporous regions. The polished face of the core was also scanned using SEM-EDS which quantifies the in-situ mineralogy. The mineralogy map of the registered

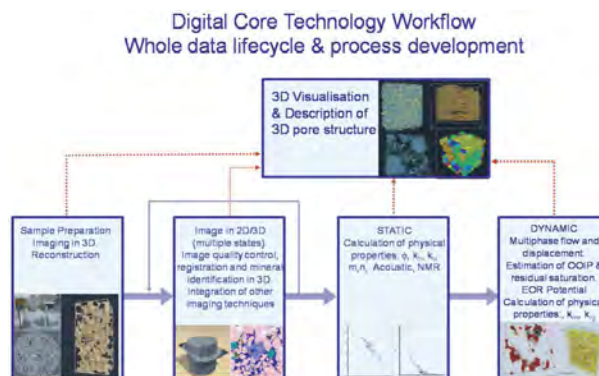


Figure 1: Workflow undertaken for Digitalcore analysis.

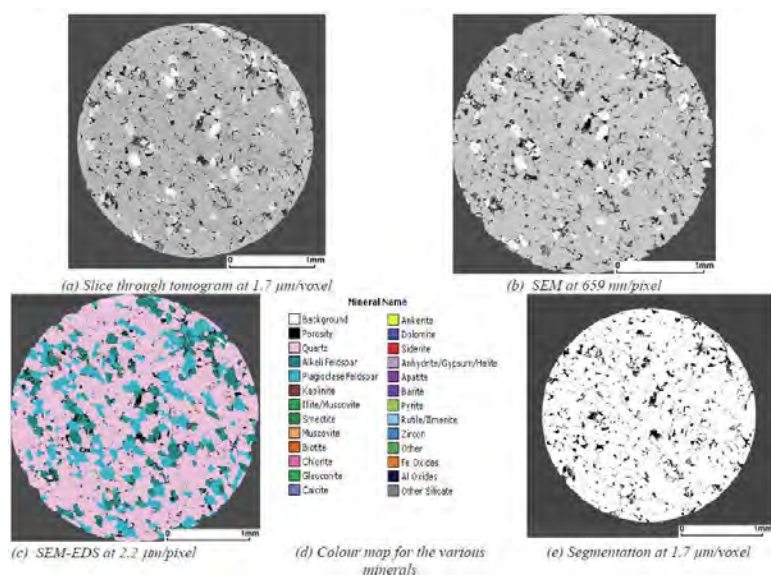


Figure 2: (a) single slice from the μ -CT image (b) SEM (c) SEM-EDS (d) Mineral colour map for the SEM-EDS slice (e) Phase Partitioning into pore (black), clay (grey) and solid (white) for a “tight gas” sample from Oman.

polished section allows one to directly calibrate the mineralogy to the estimation of microporosity .

Phase Identification

The tomographic image consists of a cubic array of reconstructed linear x-ray attenuation coefficient values each corresponding to a voxel of the sample. Different phases (pore, mineral grains and clays) have different attenuation values and may be distinguishable within the 3D data. In these clastic samples we use an advanced image processing and analysis approach based on filters and masks to sharpen phase edges and improve phase characterization]. Use of these filters coupled with image registration and quality control methods allows one to identify the quartz, feldspathic, clay or microporous phases (often mixtures of clays). Higher attenuation minerals/cements (e.g., iron-bearing minerals, zircon, calcite) can also be identified and spatially characterized in 3D.

Pore and grain partitioning of the sample

Pores and grains can be partitioned in the 3D image allowing one to obtain statistics on the image data. Quantities associated with the rock texture and fabric can be derived from image data including grain size, shape, orientations, distributions, roundedness, and connectivity for different mineral phases. Factors such as pore/throat size, shape, and connectivity can also be derived from image data. 3D pore structure information can be central to understanding recoveries and multiphase flow properties.

A slice from the 3D image is shown in Fig. 2(a). Ideally we need to have a well separated multi-modal distribution of the x-ray attenuation coefficients (grey scale), that gives an unambiguous phase assignment of the pore and various mineral phase peaks. For this “tight gas” sample it was obvious that we needed at least a three phase segmentation to further distinguish additional micropores below the resolution of the μ -CT, which are associated to clay fractions or other detrital cements. One can achieve more direct quality control on the different pore types in 3D image data of reservoir sandstone by comparison with standard 2D microscopic analysis. Figure 2(b) illustrates the 3 mm x 3 mm inset of a 2D SEM slice which has been registered to the slice of the 3D tomogram. Fig. 2(c) shows the same slice after SEM-EDS analysis. The presence of porosity, clay, feldspathic and quartz grains is evident from all three images. This registration assists in high quality image segmentation of the data. The SEM-EDS data quantifies the mass

composition of the major mineral phases; ~66% quartz, ~9% alkali feldspars, ~16% plagioclase feldspar, ~2% illite/muscovite. These minerals, quantified in 2D, can also be identified in the 3D image; in particular the spatial distribution of the quartz, illite/muscovite and alkali feldspar phases are easily differentiated. Figure 2(d) shows the 3D tomogram now phase separated into the three primary regions (mineral, clay and pore) identified via registration of the 3D image to the SEM-EDS data; the confidence in the phase identification of clay rich, open porosity, feldspathic rich and quartz grain phases is enhanced greatly by the integration of the data. The measured porosity is ~9.2% from the image. Simulation of fluid permeability on the image gives an estimate of ~0.4mD.

Conclusions

High resolution μ -CT Imaging and PNM is a very fast developing new technology for the visualization and characterization of the microstructures of reservoir rocks. It allows a quick evaluation of static and dynamic petrophysical properties to complement conventional routine and special core analysis measurements and petrographic analysis. The application of this technology for “unconventional” reservoir rocks, like low porosity, low permeability “tight gas” reservoirs, is a promising alternative approach for an improved understanding and the evaluation of the storage and flow capacity for the optimization of development concepts for these challenging reservoirs.

References

Knackstedt, M. A., Arns, C. H., Limaye, A., Sakellariou, A., Senden, T. J., Sheppard, A. P., Sok, R. M., Pinczewski, W. V. & Bunn, G. F., 2004. Digital Core Laboratory: Properties of Reservoir Core Derived from 3D images. Society of Petroleum Engineers Paper No. 87009-MS, 1–14. Presented at the Asia-pacific Conference on integrated Modeling for Asset Management.

L.Riepe,, M. H. B. Suhaimi, Malaysia, M. Kumar, SPE, M. A. Knackstedt, 2011. Application of High Resolution Micro-CT Imaging and Pore Network Modeling (PNM) for the Petrophysical Characterization of Tight Gas Reservoirs - A Case History from a Deep Clastic Tight Gas Reservoir in the Sultanate of Oman. SPE-142472-PP, presentation at the SPE Middle East Unconventional Gas Conference and Exhibition held in Muscat, Oman, 31 January–2 February 2011

Integrated Interpretation of an Iron-Rich Sediment, Jansz-lo Field, Northwest Shelf, Australia

G. R. Heavysage* (ExxonMobil Exploration and Production Malaysia) & A. Mills (ExxonMobil Australia)

Low Resistivity (LR) and Low Contrast (LC) pays have been identified in many clastic and carbonate reservoirs all over the world. Typical LRLC zones in PETRONAS operated fields show resistivities of 2-4 Ohmm, which are similar to the resistivities of the adjacent shale beds and very close to the resistivities of the (fresh) formation water bearing zones (1-2 Ohmm). This study is focussed on the investigation of clastic reservoirs in the Malay, Sarawak and Sabah Basins, which are mainly shaly and silty sandstone zones, that were not obvious and not classified as "net pay" from previous conventional formation evaluation techniques. Based on an integrated petrophysical analysis of modern log data (including Nuclear Magnetic Resonance (NMR), Borehole Imaging), and Special Core Analyses (SCAL) data (including electrical, hydraulic and NMR properties), improved concepts and workflows were developed for the identification and evaluation of productive hydrocarbon bearing LRLC zones.

Introduction

There are two main types of problems associated with the identification of producible hydrocarbons and with the correct evaluation of LRLC zones:

1. The water saturation S_w as derived from conventional resistivity logs is incorrect (too high)! This can be attributed to the following reasons:

- 1a. Resistivity Logging Tool related effects, i.e. the measured resistivity "Rt" is incorrect or not properly corrected for:
 - Borehole, shoulder bed and invasion effects
 - High dips or high well deviations
 - Thin bed effects (laminations, anisotropy)

In most of the above cases, R_t has been underestimated.

- 1b. The resistivity of the formation water R_w is incorrect or unknown, e.g. due to variable salinity and/or variable ion composition.

- 1c. The saturation equation and parameters are incorrect, e.g. due to "Non Archie" more complex relationships between S_w and resistivity, reflected by variable or unknown:
 - Cementation exponent "m", saturation exponent "n"
 - Excess surface/interlayer conductivity effects (Cx), Cation Exchange Capacity (CEC)
 - Conductive minerals (e.g. Pyrite, Siderite)

2. The water saturation S_w as derived from conventional resistivity logs is correct, but very high, and a conventional S_w -cutoff might eliminate these zones! These rock type related high ("irreducible") water saturations can be due to:

- Grain size/pore size effects (high specific internal surface S_v)
- Bioturbation effects (high amount of bioturbated fine silts and shales)
- High amount of clays with high Cation Exchange Capacity (CEC, Q_v)

For these zones with a high amount of "capillary bound" water, it is crucial to determine up to which S_{wirr} the reservoir will be productive to establish permeability predictions based on the analysis of capillary pressure and relative permeability data, and to correlate these S_{wirr} with NMR derived T2 spectra,

for later calibration of NMR log derived continuous S_{wirr} and permeability profiles.

In many case histories, we have experienced a combination of several of the above causes for LRLC reservoirs, which underlined the need to first apply advanced resistivity modelling techniques to get reliable R_t values from logs, and to investigate alternative methods like NMR measurements for an independent evaluation of correct water saturations, and to predict the amount and type of mobile fluid phases.

Work program

Special Core Analysis

The SCAL investigations were concentrated on the analysis and reconciliation of three independent measurements to evaluate the irreducible water saturations S_{wirr} in case of LRLC effects due to the pore structure (see Fig.1):

1. NMR T2-Spectra at different S_w .
2. Capillary Pressure Curves $p_c = f(S_w)$.
3. Electrical measurements, i.e.
 - a. Conductivities C_o at different salinities/conductivities C_w of the formation water: $C_o = f(C_w)$, "Multi Salinity method".
 - b. Resistivity Index R_t/R_o at different saturations: $RI = f(S_w)$.
 - c. Cation Exchange Capacity (CEC) from the "wet chemistry method".

The results of the T2 spectra at $S_w = 100\%$, were compared with the capillary pressures curves from the same plug.

From the comparison of the cumulative T2 distributions at $S_w = 100\%$ with the cumulative T2 spectra at S_{wirr} , T2-cutoff criteria were defined to derive S_{wirr} from T2 distributions. The resulting "Bound Fluid Volumes (BFV or BVI)" from the NMR core spectra were compared with the S_{wirr} from the cap curve and later applied to derive continuous S_{wirr} profiles from NMR logs in the uncored sections of the key wells based on analytical empirical functions or a statistical analyses based on Neural Net applications.

From the electrical resistivity measurements at different salinities and saturations, the formation resistivity factor (FRF), the excess conductivity C_x (or BQ_v), the "cementation exponent" (m or m^*), and the "saturation exponent" (n or n^*) were derived. The "traditional" relationships of $\log FRF$ vs $\log \Phi$ or $\log RI$ vs $\log S_w$ were applied to test the validity and the potential application of different saturation equations, e.g. "Archie's Clean Sand Model" vs "Shaly Sand Models" (e.g. "Dual Water", Waxman/Smits) or "Interlayer Conductivity Models" (Pape et al., 1987) for the later evaluation of the resistivity logs.

Well Log Analysis

In the first stage of this study, the log evaluations were focussed on the processing

and evaluation of resistivity logs and NMR logs in order to derive and compare saturation profiles from these two independent log measurements (see Fig. 2).

For the resistivity logs some special processing and R_t -modelling was required to correct for borehole and environmental effects (including invasion and shoulder bed

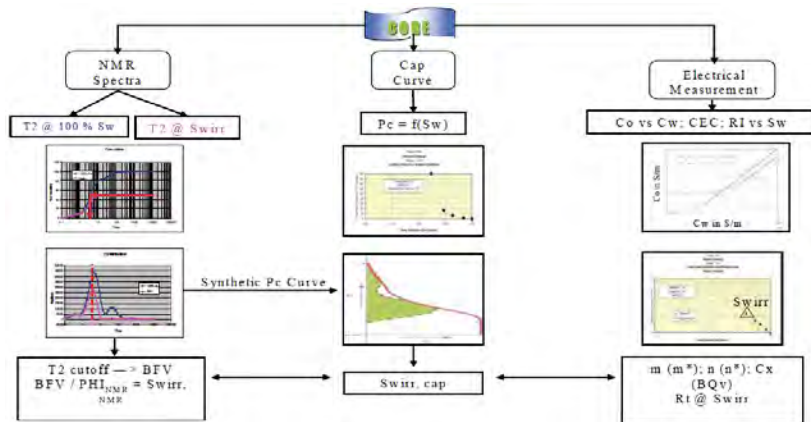


Figure 1: Workflow for the evaluation and reconciliation of irreducible water saturation Sw_{irr} from Special Core Analysis.

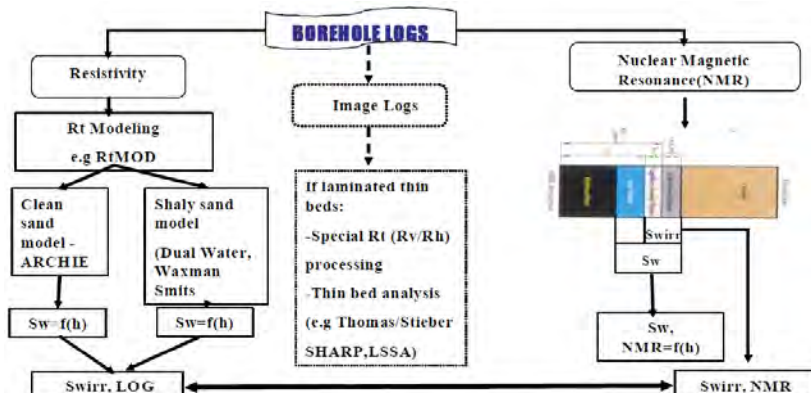


Figure 2: Workflow for the evaluation and reconciliation of irreducible water saturation Sw_{irr} from Resistivity Logs and NMR Logs.

effects) and to generate reliable R_t profiles for the evaluation of Sw from different saturation models and equations. In hydrocarbon bearing reservoir zones above the identified FWL and above the assumed “transition zones”, the Sw_{irr} from the resistivity logs were reconciled with the Sw_{irr} from the NMR log, by applying the T2 cutoffs that have been established from the NMR core spectra. In case of major discrepancies between the electrical and the NMR derived Sw profiles, the T2 cutoff and the electrical parameters (m , n , C_x) and the saturation equations have been varied until a best fit is achieved. The saturation profiles from the saturation height (SHF) modelling based on the capillary pressure curves have been used as a final reference and guidance until a reconciliation within ± 5 saturation units is achieved.

Examples & discussion

Figure 3 shows a typical example of a LRLC zone with resistivities of 1.5-3 Ohmm, that has tested dry gas at very high log derived water saturations of $Sw = 60-80\%$, even at rather high porosities of $\Phi = 25-28\%$ (with moderate average permeabilities of 5-50mD). The core was described as a silty/shaly argillaceous sand, which was confirmed by the high V_{sh} and V_{silt} fractions based on a GR and D/N crossplot analysis. The cap curve and the T2 measurements confirmed the high amount of “irreducible bound water”, and a type of a “bimodal” pore size distribution, where the majority of pores were classified as “micro”-pores ($< 0.5 \mu m$), and a smaller fraction as “meso”-pores, (in the range of $> 0.5 \mu m$ to $< 5 \mu m$), that provide the flow path and storage for the gas. The Bound Water Volume (BVW) from the NMR log (Baker Atlas MREX) confirmed the high Sw_{irr} evaluations

at the top of the tested “sand”, and also indicated that the further reduced resistivities below 1025m (s. Fig.3) are most likely due to lithology effects (nearly pure silt/shale) and not associated with a possible transition zone with moveable water. The saturation height function as derived from a cap curve (centrifuge air/brine) analysis confirmed a free water level (FWL) about 10m deeper than originally assumed from the analysis of the log derived saturation profiles, which resulted in a significant increase in reserves and a revised development strategy that justifies perforation to deeper zones than originally anticipated.

Conclusion

Based on an integrated petrophysical analysis of modern log data (including NMR and Borehole Imaging) and advanced SCAL data, new workflows and correlations were established to reconcile electrical and NMR parameters, and to evaluate LRLC reservoirs in order to unlock additional reserves. For wells and fields with limited core and log data, a multivariate statistical analysis, including Neural Net solutions, were used for the calculation of true water saturations and to predict the amount and type of mobile fluid phases.

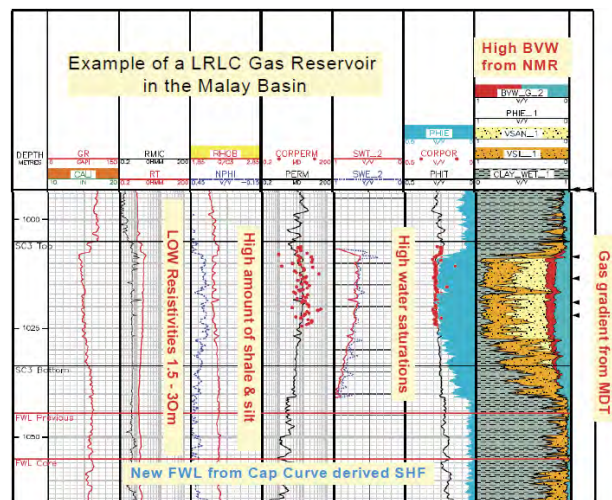


Figure 3: Log and Core results for a typical LRLC gas reservoir in the Malay Basin.

References

Pape, H., Riepe, L., Schopper, J.R., 1987. Interlayer Conductivity of Rocks-A Fractal Model of Interface Irregularities for Calculating Interlayer Conductivity of Natural Porous Mineral Systems”, *Colloids and Surfaces*, 27, 97-122.

An Integrated Petrophysical Analysis of Low Resistivity Low Contrast (LRLC) Pays in Clastic Reservoirs in Se Asia

L. Riepe* (PETRONAS Carigali Sdn Bhd), M. N. Zain (PETRONAS Group Research Sdn Bhd) & N. S. Zainudin (PETRONAS Group Research Sdn Bhd)

Jansz-10 Field is part of the Greater Gorgon Liquefied Natural Gas (LNG) Project on the Northwest Shelf of Australia. The reservoir consists of sub-tidal marine sandstones that will be developed in a present day deep water setting. The majority of the reservoir is highly bioturbated shaly sandstones with significant amounts of potassium feldspar and glauconite. The reservoir is capped with a medium to coarse grained sandstone with abundant iron-rich ooid grains and iron-rich cements including siderite, hematite, limonite, and an amorphous green clay mineral identified as berthierene, a form of chamosite.

The iron content strongly affects the Resistivity, Neutron and Density logs. As a result, previous conventional analyses mistakenly identified the interval as being clay bearing, in spite of the relatively clean Gamma Ray (GR). Applying the Elemental Capture Spectroscopy (ECS) interpretation using the standard WALK2 processing also incorrectly identified the interval as shale. Consequently, the grain density was significantly underestimated. This in turn resulted in a significant underestimation of porosity and permeability for the interval. In contrast, the full waveform sonic data clearly demonstrated the presence of a gas-bearing reservoir, and NMR data confirmed producible porosity and invasion of oil-based mud (OBM).

Apparently, the WALK2 ECS processing model was initially settled on due to the difficulty in distinguishing the iron and

aluminum signals. A constant ratio of Al/Fe was assumed. At the recently drilled Jansz-4 well the NMR log was run at a relatively slow speed of 170 fph to facilitate full polarization of the gas. As a result, the combined ECS log was able to separate the measured Iron and Aluminum signals. Another lesser known ECS processing model, ALKNA, was then used to effectively identify the proper mineralogy. Based on the patent submission, this was the originally preferred processing model; however the Al/Fe issue rendered it impractical for most conventional reservoirs.

The ALKNA processing predicted the very high grain densities measured in core. The resulting higher porosity compounded with the large grain size of the upper sand facies resulted in much higher estimates of permeability. This new log-derived permeability-thickness has an improved match with the permeability derived from pressure transient analysis of production tests in two recent appraisal wells.

Iron-rich reservoirs remain as one of the most challenging FE interpretation environments. Detailed knowledge of mineralogy, mineral effects on all logging tools and an open mind in selecting processing methods is essential for a successful interpretation.

Lithology Discrimination Through Elastic Inversion

D. Ghosh* (Universiti Teknologi PETRONAS)

Introduction

Since the advent of Bright spot DHI bright spot technology in the early 80's, prospect evaluation and reservoir development using amplitudes, or some form of this attribute, is an accepted norm in the oil and gas industry and PETRONAS is no exception. Most of the experience and rules to circumvent pitfalls were practiced elsewhere (GOM) and are not always applicable to our situation. In order to better understand these pitfalls, this work documents some of our successes and failures and analyses the pitfalls. In particular we will define processes to identify the response relating and discriminating different lithologies starting from zero offset reflection amplitudes and extending to full Elastic Inversion reflection.

Defining Amplitude

The term amplitudes in geophysical evaluation sometimes, is used loosely to mean any or all of the following: Reflection strength (Sweetness); Reflectivity; AVO; Acoustic impedance (AI); Elastic impedance (EI); Vp/Vs; Poisson's ratio; and Fluid factor.

None of the above associations or interpretations is right or wrong, but they have to be clarified as to which context they are being used. If the amplitude is being related to signify hydrocarbon presence it is the total anomaly (A) divided by the background (B) that is of importance. This (A/B) quantity is what interpreters need to map. A/B is high in the presence of gas (about 4.5) and low (1.2) when the reservoir is wet. In a hydrocarbon related province. This normalized amplitude is generally a good hydrocarbon indicator.

Factors Affecting Seismic Amplitudes

In order to relate seismic amplitudes to geology, i.e. to lithology and/ or pore fill, it is required to understand all physical factors that influence seismic amplitudes in one way or the other. Anstey (1971) defined some of them, and these are listed below.

1. Wave Field Divergence or Spreading
2. Angle dependent Reflection and Transmission losses
3. Angle dependent Ghosting in Marine situation
4. Inelastic Absorption
5. Internal Peg-leg Multiple energy loss
6. Geometric effect of structures causing Focusing / Defocusing
7. Scattering and non Specular reflection
8. Mode Conversion (P->S)

Significance of Amplitudes

In this paper we will concentrate on the relationship of amplitudes to reservoir quality, thickness, net-to-gross, porosity and pore fill. In order to be able to achieve this objective we should be able to understand factors that seismic amplitudes can be caused by a variety of geological factors including but not limited to:

- 1) Quality of sand: Net-to-Gross.
- 2) Porosity.
- 3) Pore fill: gas, oil or brine.
- 4) Lithology, hard on soft shale, coal.

In most cases the hydrocarbon sands are softer than the bounding shale producing a strong negative or a trough response

(often called a bright spot or DHI). Unfortunately, a large number of geologic and lithologic situations can also cause this negative response: Hard shale/soft shale; Coal layers; and High quality brine sand.

3D Seismic Rock Properties

The three most important rock and elastic parameters that play a critical role in interpretation of the seismic response are as follows: P wave velocity, Vp; S wave velocity, Vs; and Density of rocks, ρ .

In a 3D representation of the variables Vp, Vs and Rho (figure 1), the three faces of the cube are: Acoustic Impedance, AI, ($\rho \cdot V_p$); Poisson's Ratio, σ or Vp/Vs; and Shear Impedance, SI ($\rho \cdot V_s$).

Bright Spot (DHI) & AVO

Explorers in Gulf of Mexico, particularly Shell under leadership of Mike Forest observed that hydrocarbon anomalies often gave a bright spot, the start of Bright spot Technology. However, several pitfalls were recognized. A hard shale underlain by an acoustically soft shale also gave a bright spot at zero offset, however using AVO response (Rising/ falling) this lithology problem could be solved. However, as discussed earlier a wet sand with good reservoir properties could be mistaken as HC sand. This still remains a problem. AVO rotation techniques and Rutherford & Williams fluid factor also contribute to the solution of this problem.

AI Vs EI

Although effectively in the AVO domain the lithology can be effectively discriminated, the Elastic domain is preferable as we will perform a full inversion particularly suitable for thin beds as the so called " Tuning " interference will be removed. This is the focus of this paper.

The output of an AI is basically a lithological section indicating the softness in terms of AI. As the softness can be caused by a jump from a hard shale to a sand or from a hard shale to soft shale, AI is unable to distinguish. Hence, it cannot separate lithological effects from fluid effects.

The counterpart of AVO in reflectivity is elastic inversion (EI) in impedance. The formula was derived by Connolly (1999) state that :

$EI(\alpha) = V_p^l \cdot V_s^m \cdot \rho^n$, where l, m, n are functions of angle of incidence and gamma ie Vp/Vs .

Several example of lithology discrimination will be given in this paper:

- Discriminating Sand From Coal & Shale
- Discriminating Soft Shale From Soft Hc Sands
- Seismic Interpretation – Lithology Vp/Vs Cube
- Coal-HC Discrimination in Elastic Domain

Discriminating Soft Shale From Soft Hc Sand

With AI alone, soft shale and HC sand cannot be separated since both have soft impedance. Shale has higher Vp/Vs. This difference is utilized for lithology discrimination by performing elastic inversion on near and far angle stacks which determines Vp, Vs and less reliably density. To avoid this pitfall inherent in AI inversion by using elastic inversion. The example is from

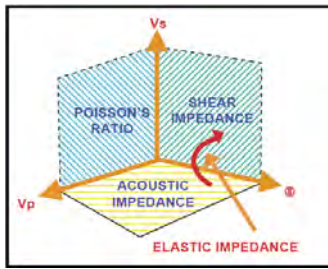


Figure 1: 3D representation of elastic parameters.

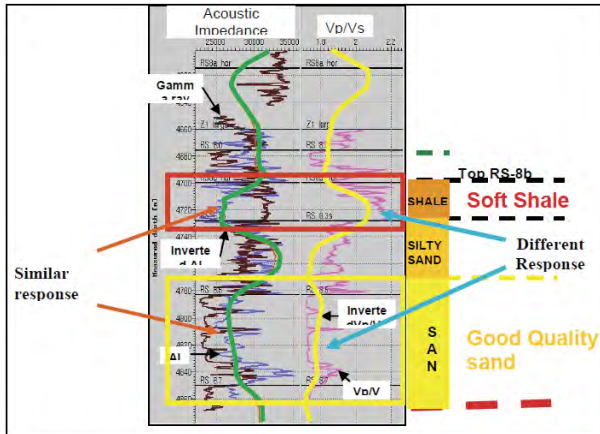


Figure 2: Example from Turkmenistan of using Vp/Vs to identify lithology. From porefill.

Turkmenistan where soft hydrocarbon sands have the same AI as soft shales. On the other hand we have a different value for Vp/Vs between shale and good quality sand. Vp/Vs is higher for the shales (figure 2).

Elastic Inversion

Input to elastic inversion is the near and far section (mid offset optional, only for stability). The solution is done simultaneously and any of these products can be output: EI cube; Vp/Vs cube; and Density cube.

On the AI (Acoustic Impedance) vs σ (Poisson Ratio) plot (figure 3 (c)) we can discriminate the gas sands (low σ & Vp/

Vs) from shale/coal with high σ . In the AI domain gas sands and coal are both soft negative amplitude responses and are inseparable. However, in the Poisson's ratio or Vp/Vs domain, they are separable because sands have lower σ and Vp/Vs. The AI and Vp/Vs volumes are obtained by simultaneous inversion of the near, mid and far angle stacks.

Coal effect is one of the pitfall in Malay Basin. The coal beds are generally from one to five meters thick. And the coal sometimes stratigraphically conformable with the hydrocarbon structures. The coal bed, geophysical response, is close to a hydrocarbon sand response. It has low density, low velocity, small thickness, one to five meters, weak gamma ray. Therefore, they could be mistaken for hydrocarbon sand. However the Poissons ratio or Vp/Vs are different.

This example is from central malay basin (figure 3). When we look in the acoustic impedance domain, the coal is soft. It has a high AI, and also the hydrocarbon are soft. Therefore, the coal dominant the response (figure 3a). However, if we look in the EI domain (figure 3b), the EI or the Vp/Vs separates the coal from the hydrocarbon sand can be separated well as the channels. This is a technique, interpretation in the elastic domain through elastic inversion.

Conclusion

We have shown that Vp/Vs is an effective parameter in discriminating lithologies. Lithology and fluid discrimination needs further work and possibly calibration.

Acknowledgement

I like to thank Petronas and its PSC partner to allow us work on this problem. Individual who have contributed to this paper are Martin Brewer, Liau Min Hoe, Ahmad Bukhari and El Saadany. This paper is compiled by Mr Najmi Sani a MSC research student.

References

- Conolly, 1999. Elastic Impedance, TLE.
- Ghosh, D.P. et al., 2010. Geophysical Issues and Challenges In Malay basin, TLE April
- Ghosh D.P. et al., 2010. Seismic attributes in Prospect Evaluation, SEG Annual Meeting, Denver

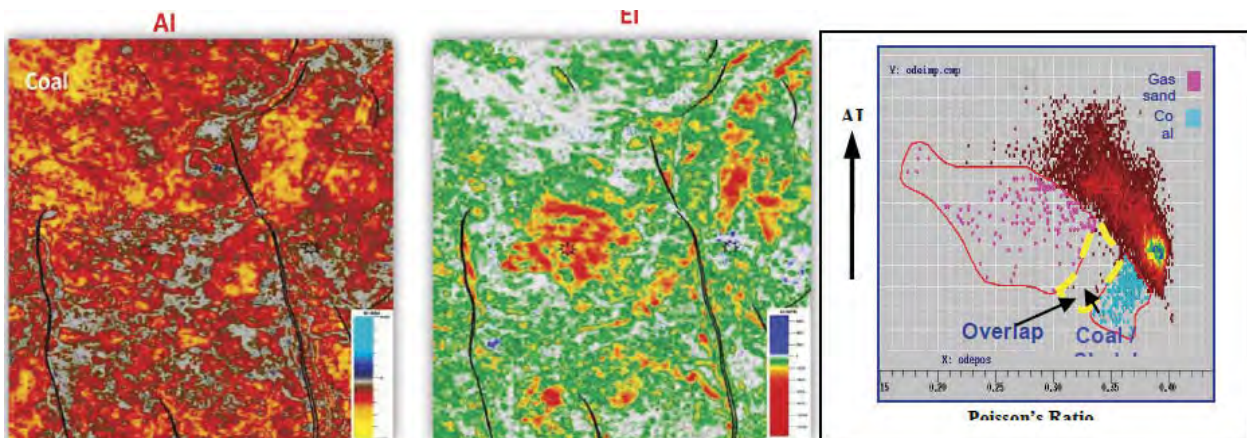


Figure 3: At the left (a) showing the AI domain there is a effect of coal musk and figure at the center (b) showing the coal effect being removed in EI domain and (c) AI vs. Poisson's ratio cross plot showing lithology zones.

Estimating Porosity from Deterministic Inversion

M. Sams* (IkonScience/ Fugro-Jason (M) Sdn Bhd), T. J. Focht (Newfield Peninsula Malaysia Inc) & J. Ting (Fugro-Jason (M) Sdn Bhd)

Introduction

In quantitative reservoir characterisation we try to extract absolute information about reservoir rocks from the seismic data. One method is to invert the seismic data to elastic rock properties and then interpret these rock properties in terms of reservoir properties. There are a number of problems that hamper this process. First we have to make estimates of the absolute elastic properties of the rocks which means that we have to provide accurate low frequency information. Second, these estimates of elasticity will always be band-limited at the high-frequency end and thus lack resolution. As such relationships between elastic and reservoir properties derived at log scale are not directly applicable. In addition, these relationships may be affected by the type of fluid present and therefore the distribution of fluids needs to be understood in advance. One solution would be to apply geostatistical inversion that would allow for the application of reasonable constraints whilst assessing the uncertainties. However, such a method is time consuming to apply. Here we present a solution based on deterministic inversion that results in a low resolution image of the porosity within a channel sand reservoir, yet permits an understanding of the general variations in the distribution useful for well planning and field development.

Field

The reservoir in question is a mid-Miocene channel sandstone located in the Malay Basin. The sand sediment was deposited into an incised valley that cut through an inter-bedded sequence of claystone, siltstone and coals. The channel sand, penetrated in five conventional wells, shows a consistent thickness of approximately 30 meters, with 25% clay content (from core) and average porosities of 25 to 26 porosity units.

The trap type of the channel sandstone is purely stratigraphic and is developed where the regionally straight channel system turns abruptly and forms a large meander at the field. Structural dip is uni-directional and low magnitude. The majority of the field comprises an area of water overlain by oil overlain by gas. The oil column is 12 meters thick.

The channel within the field area has been encountered by nine wells of which five were vertical exploration wells. There are currently four horizontal development wells with each obtaining over one kilometre of oil bearing sandstone. All of these wells provide a significant number of porosity estimates that show the modal porosity is approximately 25 pu. and ranging from 12 to 29 pu. The wells show a trend of lower porosities nearing the top of this fining-upward channel and locally, spatially coherent variations in porosity.

Rock physics

Before discussing the methodology for porosity estimation it is important to understand the relationship between the elastic properties and the porosity of the channel sand for the different fluids present. The rock physics model that provides this relationship is reasonably well constrained. The five vertical wells all have a suite of logs for formation evaluation in addition to P-sonic logs. S-sonic logs are available in four of the wells including one well that was drilled down dip and is wet. One well has core measurements that show average clay content of

25%. The clay content in all of the wells can be derived from the gamma-ray calibrated to the core measurements. The porosities are derived from the density and neutron porosity logs and the saturations are estimated using the Dual-Water equation. These petrophysical results are then used in a rock physics modelling scheme that aims to replicate the measured sonic data.

The rock physics model used is the self-consistent inclusion based model which utilizes a variable aspect ratio dependent on the porosity and clay content. The results show a very-high degree of predictability of the elastic properties. The major uncertainty, and key for the purposes of this work described herein, is the effect of fluids. It is clear from analysis that the sonic measurements are affected by invasion. However, it is not clear how much of the effect is due to invasion and how much is caused by the patchiness of the fluid distribution in the rock. Nor is it clear whether the response at sonic frequencies is what would be observed at seismic frequencies. Assumptions are made and the uncertainties assessed in interpreting the results of the complete workflow.

Methodology

The idea behind the proposed methodology is to build a model of the reservoir and surrounding rocks in terms of elastic properties. The model within the reservoir will be based on an underlying porosity model converted to P-impedance through the rock physics relationships and estimates of the location of the fluid contacts in time. This model proposal will be used to contribute the low frequency information in a seismic inversion. The results of the inversion will then be compared with the model within a common bandwidth and differences used to update the porosity model within the reservoir. This process can be iterated until the differences are reduced sufficiently. Prior to applying this to the real data, it is applied to synthetic seismic models of the real data to understand the likely success and limitations.

Using a wavelet derived from a near angle stack of the real seismic data, we generate through convolution a synthetic seismic based on the rock physics logs with the measured petrophysical properties. Then the porosity is changed to a constant value of 25 pu within the reservoir section, the elastic properties generated from the rock physics relationship and another synthetic generated. The originally created synthetic is then inverted using the second model to supply the low frequency content. The ratio between the high-cut filtered constant porosity model and the inverted impedances are then used to adjust the porosity within the channel sandstone. This process can be repeated, with the updated porosity used to generate a new elastic model that can be used for the next inversion. It can be seen from Figure 1 that this process results in reasonable convergence towards the channel porosity in the three wells chosen for this test. However, it should be noted that the changes made are only within the frequency band of the seismic data.

This test proves that all else being equal we should see a convergence towards a low resolution porosity model. However, there have been a number of assumptions. First, it has been assumed that the top and base of the sand is known. Clearly the P-impedance profiles suggest that this might not be possible

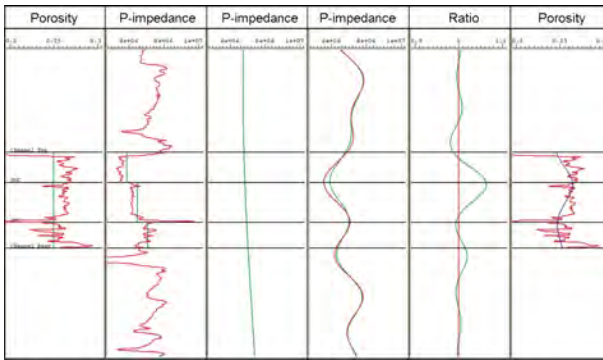


Figure 1: The panels show from left to right (a) the measured porosity (red) and the starting porosity (green) (b) the measured impedance and the model impedance (c) the low frequency component used from the model impedance (d) inversions from the measured (red) and modelled (green) synthetics (e) the ratio of the inversions (green) (f) the measured (red) and updated (green) porosity.

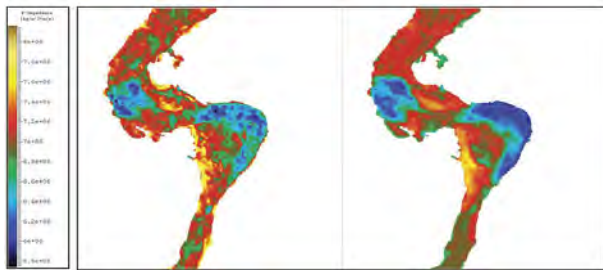


Figure 2: The P-impedance extracted at the top of the reservoir from the inversion of the real data (left) and from the model data based on an interpolated porosity (right). The differences are potentially caused by actual variations in the porosity.

from the P-impedance as the contrasts are low with respect to the surrounding rocks. Second, it has been assumed that the impedances of the surrounding rocks are known and thirdly that the fluid contacts in time are known. These assumptions will be addressed as the methodology is applied to the real data.

Application

Analysis of the log data from the wells which sample the area suggest that the main characteristics of the surrounding rocks are reasonably consistent in general. That is a simple interpolation of the well logs with the channel sand removed, provides a good estimated of the background. There are some complications though. A thin coal bed sits towards the base of the channel. Indeed, as well as varying in thickness, the coal sits at various distances from the base of the channel and has in some places been eroded by the channel. This is important because differences between an inversion and a model are going to be used to update the porosity and although thin, the coal has very low impedances. If the coal is modelled incorrectly, this will affect the porosity update. The coal has also been removed from the well logs before interpolation for the background model. The coal has then been modelled based on interpretation of first pass inversions, though in some places significant uncertainty remains.

The next step is to introduce the channel by placing it within this interpolated background. The top and base of the channel cannot be determined from the p-impedance at all locations as the wet and oil sands have small P-impedance contrasts with the surrounding rocks. However, the Vp/Vs contrast is quite high for all fluids. An elastic inversion of a far angle stack (45-55 degrees) using a simple trend as a low frequency model, produces a bandlimited result that is consistent with the time thickness for all the vertical wells. A velocity model derived from the seismic velocities and calibrated to the wells was used to place the top of the channel in depth. The contacts are well known in depth. The velocities between the top channel and the contacts can be estimated from the rock physics relationships for the fluids and the current porosity model. This then allows for the contacts to be placed in time. To get this to work perfectly obviously requires iterations as the porosity needs to be placed in depth first.

The P-impedance within the channel can now be generated based on the assumption that the porosity of the channel is a simple interpolation of the well data. This model is used to provide the low frequency information for an inversion of the near angle stack seismic data. The model is also high-cut filtered to the upper-seismic limit and compared with the inversion results. The differences are used to update the porosity model and the process iterated. An example of the differences is shown in Figure 2 which displays extractions from the top of the reservoir from inverted and modelled data at the end of the first iteration. The differences observed here are potentially due to variations in the porosity not yet included in the model. The variations may also be due to uncertainties in the rock physics model, the picking of the top and base of the channel, wavelet estimation and a number of other factors. Therefore the predicted variations in the porosity must be treated with some caution.

Results

The final results of this process are variations in the porosity at the scale of the seismic data. From these results it can be observed that there are some areas of potentially poorer and better quality reservoir. The variations in the porosities are reasonable in scale, but there are still a number of uncertainties due to seismic noise, time to depth conversion, rock physics modelling and the background model. These results can be used to improve a well only based static model.

Conclusions

A methodology has been proposed to estimate the general variations in porosity for a channel sandstone where the presence of gas and oil mask the effects of porosity. The method relies on the existence of a strong rock physics relationship between porosity and P-impedance for each fluid case. The background model needs to be understood and predictable. The location of the channel and the position of the contacts in time also need to be predictable. For the example given, these requirements are all met to a reasonable degree. The results indicate that there are systematic changes in the lateral and vertical distribution of porosity that are consistent with the well information.

Acknowledgements

The authors thank the management of Newfield and PETRONAS for permission to present this paper.

The Evolving Role of Geophysics in Exploration. From Amplitudes to Geomechanics

E. C. Andersen* (Talisman Energy Malaysia) & D. Gray (Nexen Inc., Calgary, Alberta, Canada)

Over the last 25 years, geophysical analysis of seismic data has greatly evolved. However, in the routine utilization and daily workflows of many exploration and development teams, geophysical technology is at a standstill.

The purpose of this paper is to review a few of the major milestones of geophysical innovations, as we see them. The aim is to provide insight into how geophysics has evolved and provide a glimpse into the direction of the technology and its application to improving exploration and production solutions.

In school we – geologists, engineers, and geophysicists - learned how reflectivity equations provide us with the basics for what is needed to interpret seismic data. It gives us an understanding of the time required for a seismic impulse to travel to and through a reservoir. It also gives us some understanding of the amplitude we should expect to record by way of acoustic impedance properties encountered by the traveling seismic wave.

This has been the status quo for more than 40 years. Seismic amplitudes were revolutionary in the 1960's (see e.g. Schneider, 1971). Many exploration teams still rely solely on time structure and horizon amplitude maps to present their exploration prospects to management or drilling engineers.

The first innovation came through the simplification of the work of Zoeppritz (1919) by Aki and Richards (1980) and particularly by Shuey (1985). At the same time, Ostrander (1982) observed that seismic amplitudes changed with offset in the presence of gas. The Zoeppritz equations provide an explanation for this effect, especially through the use of the simplifications introduced by Aki and Richards, and Shuey. Castagna et al (1985) started to quantify this effect with their development of the "Mudrock Line" (Figure 1). This effect was further quantified with the "Fluid Factor" of Smith and Gidlow (1987). The importance of this innovation was the ability to evaluate fluid properties from seismic data.

With the evaluation now focusing on angles, the shear wave component to the seismic ray path came under scrutiny. This brought rock physics into play – the next great innovation. Backus et al. (1993) describe the incorporation of petrophysics and borehole properties into seismic interpretation. A further extension of this was the work by Goodway et al (1997) who incorporated these principles with his paper on rock properties - Lambda-Mu-Rho (LMR). This innovation provided for more direct estimation of lithologies and fluids from seismic data. (Figure 2).

Thomsen (1985) simplified the concept of seismic anisotropy, the variation of physical properties in different directions, by introducing the concept of weak anisotropy. Lynn et al (1996) showed that these effects could be seen in seismic data and Gray et al (1999) showed that fractures could be detected using 3D wide-azimuth seismic data– the next innovation. This was done by examining the shear wave component, which is affected differently depending whether it is traveling parallel or perpendicularly to the fracture system due to its anisotropy.

The impact of this was that engineering decisions could now be influenced directly by seismic recordings. Geophysics was not strictly regulated to geologic interpretations.

So where are we now? By incorporating the concepts of stress and strain into the anisotropic calculations, we are now

deducing Geomechanical properties from seismic data (Figure 3). Young's Modulus and Poisson's ratio, although present in geophysical algorithms for years for fluid calculations, they are also parameters the engineering teams use for well planning and frac'ing.

Modern geophysicists should consider themselves a partner in the drilling and development of the field. We are no longer just producing structural maps. We now have the capability of providing key links between geology and engineering through the use of seismic data. Expensive drilling decisions can be influenced in a positive way with the use of these seismic techniques.

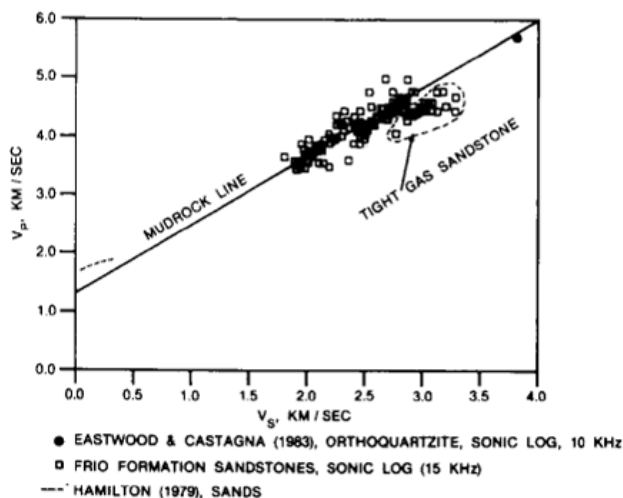


Figure 1: Sonic Log Velocities in Sandstone (Castagna et al, 1985).

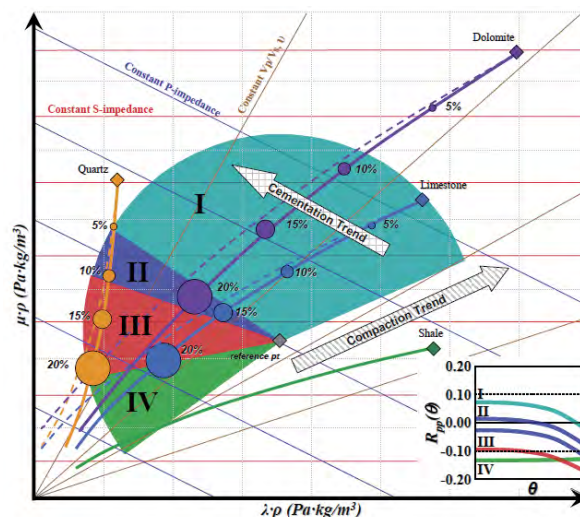


Figure 2: LMR crossplot showing effects of lithology, porosity and fluids. Hoffe et al (2008).

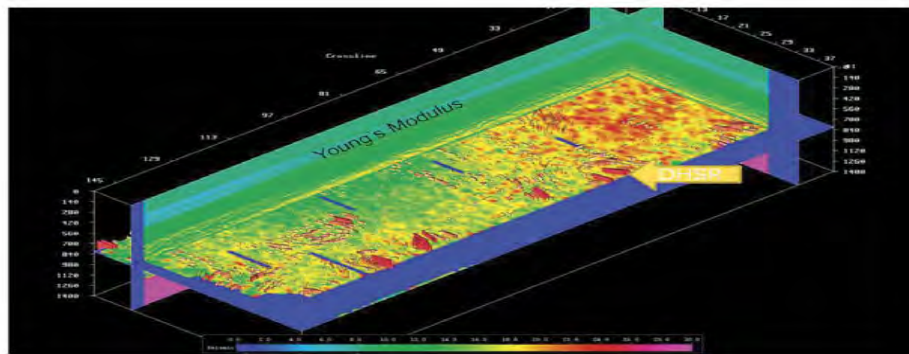


Figure 3: Young's Modulus Cube (Gray, 2010)

References

- Aki, K. and Richards, P.G., 1980. Quantitative Seismology, W.H. Freeman and Co.
- Backus, M.M., Kan, T.K., Castagna, J. P. and M. L. Batzle, 1993. Rock physics - The link between rock properties and AVO response, SEG Books, 135-171.
- Castagna, J.P., Batzle, M.L. and Eastwood, R.L., 1985. Relationships between compressional-wave and shear-wave velocities in clastic silicate rocks, *Geophysics*, 50, pp. 571-581.
- Goodway, W., Chen, T., and Downton, J. 1997. Improved AVO fluid detection and lithology discrimination using Lamé petrophysical parameters; "Lambda-Rho", "Mu-Rho", & "Lambda/Mu fluid stack", from P and S inversions: 1997 CSEG Meeting Technical Abstracts Book, 148-151.
- Gray, F.D., Head, K.J., Chamberlain, C.K., Olson, G., Sinclair, J. and Besler, C., 1999. Using 3-D Seismic to Identify Spatially Variant Fracture Orientation in the Manderson Field, 1999 Canadian SEG Convention Technical Abstracts, 59-63.
- Gray, D., 2008. Fracture Detection Using 3D Seismic Azimuthal AVO, CSEG Recorder, Vol. 33, No. 3, pp. 38-49.
- Hoffe, B.H., Perez, M.A. and Goodway, W., 2008. AVO Interpretation in LMR Space: A Primer, CSEG, Expanded Abstracts.
- Lynn, H.B., Simon, K.M. and Bates, C.R., 1996. Correlation between P-wave AVOA and S-wave travelttime anisotropy in a naturally fractured gas reservoir, *The Leading Edge*, Vol. 15, No. 8, pp. 931-935.
- Ostrander, W.J. 1982. Plane wave reflection coefficients for gas sands at nonnormal angles of incidence, SEG, Expanded Abstracts, 1, no. 1, 216-218.
- Schneider, W.A., 1971. Developments in seismic data processing and analysis (1968-1970), *Geophysics*, 36, 1043-1073.
- Thomsen, L., 1995. Elastic anisotropy due to aligned cracks in porous rock, *Geophysical Prospecting*, Vol. 43, pp. 805-829.
- Larry, S. M., Curly, H., and Moe, W. W., 1955, Prestidigitation, strabismic filtering and ocular violations in the San Andreas strike slip fault zone: *Geophysics*, 24, 338-342.

Xu and White Revisited

M. Sams* (IkonSciences/ Fugro-Jason (M) Sdn Bhd), T. J. Focht (Newfield Peninsula Malaysia Inc) & N. Azuairi Che Sidik (Newfield Peninsula Malaysia Inc)

Introduction

Xu and White (1995) proposed a workflow for estimating the elastic properties of sand and clay mixtures based on the petrophysical analysis of well log data. The workflow was aimed at generating synthetic shear data in wells, where none was measured, for the purposes of seismic reservoir characterisation. Despite some criticism, primarily aimed at the idealised representation of the pore space as ellipsoids, the method has proved effective and thus popular. The workflow mixes the elastic properties of quartz and clay using the time average equation. The total pore space is assigned to either quartz or clay on a volume weighted basis and assigned a different aspect ratio dependent on whether it is a quartz or clay pore. The empty pores are then included into the quartz-clay mix using the Differential Effective Medium method and finally the fluids are introduced through Gassmann. The effective elastic properties of the clay component and the aspect ratios assigned to the quartz and clay pores are adjusted until a match with measured data is achieved.

The recognition that the effective aspect ratio of the pore space associated with each mineral differs was a significant contribution to the ability to effectively model real rocks using pore shapes as the control for the rock micro-structure. However, it does seem rather a gross assumption and intuitively one might expect that there is more variation in the aspect ratios than can be modelled through the choice of two fixed values. On the other hand, if a higher degree of variability in the aspect ratio produces an improved fit to the data, the problem becomes one of being able to predict those variations so that the modelling method can be applied to other wells with poorer quality data or where elastic logs were not measured.

In this paper we show that a single aspect ratio applied to the total porosity of a sand-clay mixture can accurately model both P- and S-sonic data. We also show that the variation of this optimal aspect ratio can be predicted from the petrophysical properties of the rocks, whilst keeping the effective elastic properties of the minerals constant over large geological intervals. The use of one variable aspect ratio applied to the total porosity provides a much better fit to the data than using a single aspect ratio for each mineral.

Dataset

The dataset shown here comes from a field in the Malay Basin. The rocks penetrated are a sequence of Mid-Miocene claystones, siltstones, sandstones and coals. A sand-filled incised valley forms a 30 meter thick, channel-reservoir with both oil and gas. Five vertical wells penetrate this sandstone channel, four in the hydrocarbon interval and one entirely in the aquifer. These wells were logged with a comprehensive suite of logs that allow for formation evaluation. All the wells have measured P- and S-sonic except for one well that has only p-sonic measurements. Core samples have been taken within the reservoir sand that indicate the clay content is substantial ranging from 15 to 25%. Total porosity within the reservoir generally varies by only a few porosity units (pu), approximately 26 pu.

A petrophysical analysis has been applied that keeps the link to the input data straight forward. Clay content has been

derived from the gamma ray log calibrated to the volume of clay measurements from core. The total porosity has been estimated from the density and neutron logs and the saturation using the Dual-Water equation. The coals are not included in the rock physics modelling and have been identified where possible and removed from the analysis. The analysis described will be carried out between two regional coal markers. This interval represents over 450 metres of rock.

Effective aspect ratio

The first step is to assess whether an effective aspect ratio applied to the total porosity can model both P- and S-sonic measurements. This assessment is made using a slight modification to the Xu and White approach, whereby the time average equation is replaced by the Hill average of the component minerals. The aspect ratio at each depth is adjusted until the modelled velocity matches the measured velocity. This was carried out for both the compressional and shear velocities independently. The values found will not necessarily be the same, but the elastic properties of the clay can be adjusted to fit the data. Although this is an arbitrary adjustment there are some valid reasons and limitations. Unlike quartz, the elastic properties of clay are not well established and are also typically anisotropic. The effective elastic properties of the clay observed in the vertical direction (parallel to the borehole) are therefore probably a function of the clay type and the orientation of the clay particles (inter alia), neither of which are readily determined from standard petrophysical analysis. The effective properties are therefore unknown, but here are assumed to be constant over the interval of interest.

There is sufficient room for a range of aspect ratio and elastic property combinations that are reasonably effective. For example, if the shear velocity of clay is set high then the effective aspect ratio required to match the s-sonic is reduced. This increases the V_p/V_s of the model results that can in turn be compensated by a decrease in the V_p/V_s ratio of the clay. By applying this approach to the wet well in the dataset, this well is chosen to initially avoid the complications of hydrocarbons, it is possible to find a combination of elastic properties for clay that minimises the difference between the optimal aspect ratios for P- and S-sonic data. Figure 1a shows the correlation of the optimal aspect ratios to match the P-sonic versus those required to match the s-sonic. Note that some of the scatter is due to the effect of washouts on the calculation of porosity as will be discussed later.

It is noticeable that the optimal aspect ratios tend to cluster based on the clay content. The cleaner sands require higher aspect ratios than the shales. This is consistent with the findings of Xu and White (1995). However, the distribution suggests that a fixed aspect ratio for quartz and clay pores might not provide an accurate prediction of all the velocities. A direct comparison with the standard Xu and White approach is made later in this abstract after dealing with a number of issues.

Aspect ratio prediction

The methodology of using a variable aspect ratio is most useful if the values can be predicted from other data. Visual

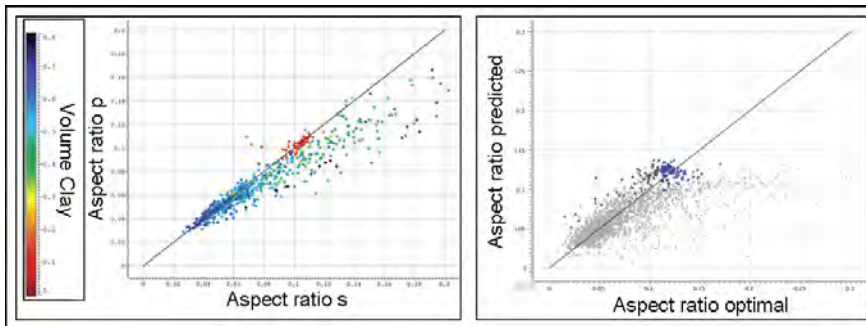


Figure 1: (a) Crossplot of the aspect ratio required to model the P-velocity versus that required to model the S-velocity coloured by volume of clay. The line of perfect match is shown. (b) Crossplot of optimal aspect ratio for modelling S-velocity versus aspect ratio predicted from porosity and clay content. Shales are shown in grey and wet sands in blue.

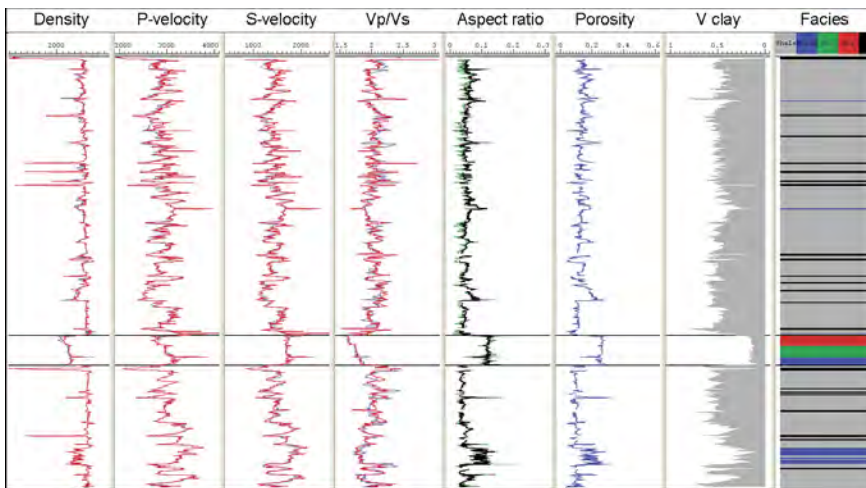


Figure 2: Panel 1-4 modelled (red) and measured (blue) density, p-velocity, s-velocity and vp/vs respectively. Panel 5 optimal aspect ratio for P- and S-velocity (magenta and green) and predicted aspect ratio (black). Panel 6-8 total porosity, volume of clay and facies/fluids respectively.

observation indicates that the aspect ratio varies with both clay content and porosity. In this case a simple, linear combination of porosity and clay content was rapidly found through trial and error that gave a reasonable prediction of the estimated optimal aspect ratio for all of the wells for shales and wet sands (Figure 1b). Some of the shale points drift away from the line of parity and observation of the log data indicates that many of these points are associated with poor borehole conditions where the density and neutron logs are affected by the borehole rugosity. The prediction for the wet sands is reasonable but not highly accurate. By taking a different relationship within the channel sand an improved prediction can be found. Interestingly this improved fit in the channel sand requires the aspect ratio to increase with increasing clay content, whereas the opposite is true in the rest of the interval.

Further improvements

There are a couple of areas in which the results obtained so far can be improved. The borehole conditions in a number of wells in the section above the channel are such that the density and neutron logs are affected. This can easily be seen by observing unusual scatter in the relationship between P-velocity and density. A correction was applied to the density log to improve the consistency with the P-velocity log. This correction changed the porosity and thus the predicted aspect ratios. The changes in porosity resulted in much greater consistency between all predictions of elastic properties and the measured data. Although this is self-fulfilling for the P-velocity, the improvements to the S-velocity prediction, as well as the improved match between optimal P- and S-velocity aspect ratios, justifies the changes.

In the section below the channel there are a number of areas where the predictions are also poor. However, it was observed

that the clay content derived from the gamma ray log and the neutron-density combinations is very different at these points. If the neutron-density combination is used for clay content in this lower section, all the modelling improves considerably.

Fluids

The presence of hydrocarbons causes a number of problems. Hydrocarbons are often displaced by drilling fluids away from the borehole wall and thus many logging tools with a shallow depth of investigation do not measure the properties of the in-situ hydrocarbon saturated rocks. There is uncertainty about what effective saturation many tools measure, but density, neutron and sonic tools are usually affected. In addition, the fluids in the rocks are potentially not evenly distributed across the pore space. There can be heterogeneities that mean the standard Wood's mixing law for fluids is not applicable. Brie et al. (1995) provided an equation to mimic the heterogeneity of the fluid distribution in rocks using a power law for the saturation. The effect of invasion is also often mimicked through a power law for the saturation. Therefore the combination of invasion and heterogeneity are here modelled through a power law, where the power term is empirically found based on the assumption that the model of a single aspect ratio for P- and S-velocities is valid. It is found that the power law required for gas and oil are different, but there is no direct evidence from the data how much of the effect is due to invasion and how much is due to fluid distribution heterogeneity.

Comparison with Xu and White

The final model based for one of the wells is shown in Figure 2. The match to the measured data is very-high as a result of the accurate prediction of the optimal effective aspect ratios. Using the same approach to fluid modelling and correction for

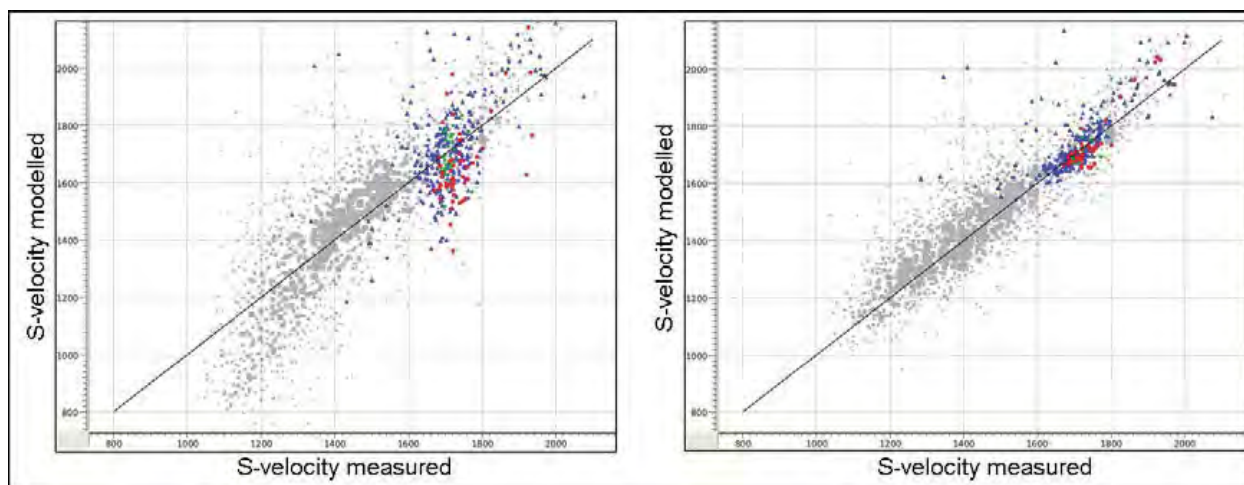


Figure 3: Cross-plots of measured S-velocity versus modelled S-velocity using (a) fixed aspect ratio for quartz and clay and (b) variable aspect ratio for total porosity.

washouts it was found that this methodology gives a significant improvement over the use of fixed aspect ratios for quartz and clay pores as per the original Xu and White methodology. A comparison with the fixed aspect ratio method is shown in Figure 3. For the fixed aspect ratios the optimisation has caused systematic over- and under-estimation for shales with different degrees of shaliness and porosity. Clearly a constant aspect ratio for all clay and quartz pores is not appropriate. Although the use of fixed aspect ratios predicts the mean properties of the channel sands, the variable aspect ratio methodology shows a much better prediction.

Conclusions

The standard Xu and White approach to modelling clay-sand mixtures can be improved by assuming a variable aspect ratio that is applied to the total porosity. These aspect ratios can be predicted from measurements other than the velocity logs after calibration in one well. This means that elastic properties can be predicted in wells with no measured sonic data provided the other

log data are of a reasonable quality. In addition, this approach allows for the identification and correction of errors in the log data and petrophysical analysis, providing a means to understand the influence of hydrocarbons on the rock elastic properties. The methodology results in a complete, consistent and corrected dataset suitable for use in seismic reservoir characterisation. Once the rock physics model has been established, there is the possibility to constrain the petrophysical analysis with the elastic logs in a joint inversion where the aspect ratio becomes the link between the rock physics and the petrophysics.

Acknowledgements

The authors thank the managements of Newfield and PETRONAS for permission to present these data.

References

- Xu, S. and White, R.E., 1995, A new velocity model for clay-sand mixtures, *Geophysical Prospecting*, 43, 91-118.
- Brie, A., Pampuri, F., Marsala, A.F., and Meazza, O., 1995, Shear-sonic interpretation in gas bearing sands, SPE 30595.

New Joint Categorical/Continuous Simultaneous Inversion Technology

M. Kemper* (Ikon Science Ltd)

Introduction

In this paper we will first review the industry-standard continuous simultaneous inversion methods and point out some shortcomings. We will then introduce our new joint categorical/continuous simultaneous inversion technology, which reformulates the problem to address these issues. We present some examples and wash up with conclusions.

Note that in this paper, it is assumed that the seismic to be inverted is a suite of true amplitude partial angle stacks with calibrated wavelets available from well ties.

1. Simultaneous inversion to date

A) Deterministic method

We start in this case with the Fatti (1994) equation (other approximations to the Zoeppritz (1919) equation are possible also):

$$R_{pp}(\theta) = aR_{AI} + bR_{SI} + cR_p \quad [1]$$

Where:

$$R_{AI} = \Delta Vp/(2Vp) + \Delta\rho/(2\rho)$$

$$R_{SI} = \Delta Vs/(2Vs) + \Delta\rho/(2\rho)$$

$$R_p = \Delta\rho/(2\rho)$$

$$a = 1 + \tan 2\theta; b = -8 K \sin 2\theta; c = 4 K \sin 2\theta - \tan 2\theta; [K = (Vs_{avg}/Vp_{avg})^2]$$

Note that a, b and c are constant per incidence angle θ .

We can turn reflectivity $R_{pp}(\theta)$ in [1] into synthetic seismic $S_{pp}(\theta)$ by convolving with wavelet $W(\theta)$:

$$S_{pp}(\theta) = a W(\theta)R_{AI} + b W(\theta)R_{SI} + c W(\theta)R_p \quad [2]$$

Subsequently we can use the small contrast approximation $RAI = (RAI2 - RAI1) / (RAI2 +$

$$RAI1) \approx \frac{1}{2} \Delta AI / AI = \frac{1}{2} \Delta \ln(AI) \text{ to rewrite [2] as}$$

$$S_{pp}(\theta) = a/2 W(\theta) \Delta \ln(AI) + b/2 W(\theta) \Delta \ln(SI) + c/2 W(\theta) \Delta \ln(\rho) \quad [3]$$

Formula [3] is the essence of all continuous simultaneous inversion methodologies (i.e. no inversion to categorical/discrete properties takes place): plug in a starting model of AI, SI and ρ , take the natural logarithm, difference, for each partial angle stack convolve with the corresponding wavelet $W(\theta)$, scale (using $a/2$, $b/2$ and $c/2$) and for each partial angle stack incidence angle θ compare the synthetic seismic $S_{pp}(\theta)$ so obtained with the real seismic $S_{real}(\theta)$. Use some optimization apparatus (e.g. the conjugate gradient method, or least squares optimization) to iteratively change AI, SI and ρ until the difference between $S_{pp}(\theta)$ and $S_{real}(\theta)$ is minimized for all partial angle stack incidence angles θ , typically in some least squares sense (solving for AI, SI and ρ directly is possible also; not discussed here).

Because of the convolution by $W(\theta)$, this formulation cannot be used sample-by-sample. Instead it is typically used trace-by-trace (this can be extended to multitrace; not discussed here). Therefore $\ln(AI)$, $\ln(SI)$ and $\ln(\rho)$ can be seen as column vectors which we stack on top of one another to obtain $\ln(Z)$. The difference operation Δ , applied to each of $\ln(AI)$, $\ln(SI)$ and $\ln(\rho)$, can be expressed as an (almost diagonal) matrix D . And lastly the convolution can be expressed by a (banded) matrix W (typically a different W matrix per partial angle stack). The product of W and D we can call system matrix X , into which the scaling parameters a, b and c (and the $1/2$ factor) can be subsumed. So [3] in block matrix form reduces to

$$S = X \cdot \ln(Z) \quad [4]$$

It is useful to sketch (Fig. 1) the sizes of the various block-vectors/block-matrices in the case where we invert for 3 impedances (i.e. AI, SI and ρ) given 4 partial angle stacks at, say, 5o, 15o, 25o and 35o incidence angle, over a gate of 100 samples.

So the optimization typically consists of minimizing an objective function $\|S_{real} - X \cdot \ln(Z)\|^2$, by changing $\ln(Z)$. This in itself is usually wildly unstable, so normally one adds a regularization term to ensure the impedances do not drift away too much from the initial impedances Z_0 . The total objective function to be minimized is something like $\|S_{real} - X \cdot \ln(Z)\|^2 + \mu \|\ln(Z) - \ln(Z_0)\|^2$, where μ , the so-called model weight, should be as small as possible to ensure the inversion is driven mostly by the data (i.e. the seismic S_{real}), and as little as possible by the initial model (Z_0). Note that the objective function is quadratic, which makes optimization relatively easy.

It is well known that the methodology described in some detail above gives results that are not credible when compared to the impedances from wells. A major reason for this is that the band-limited convolution destroys high and low frequency information, making the inverse problem very underdetermined, and the regularization term introduced above is too simplistic a cure for this. In other words, in the deterministic inversion scheme introduced so far we need to incorporate more sophisticated regularization information for it to provide useful results. We'll come back to this in section 2.

B) Statistical method

Clearly simultaneous inversion can be seen as a statistical problem, given the noise component of the seismic signal. The most common way to proceed is to cast it as a Bayesian problem, in which the prior information, if well chosen, will provide sufficient regularization. Bayes' Theorem in this case can be written as:

$$\pi(Z|S_{real}) \approx L(S_{real}|Z) p(Z) \quad [5]$$

Where π is the posterior distribution, L the likelihood function and p the prior distribution. Again Z represents the impedances (say AI, SI & ρ in case of Fatti)

It is customary (Buland and Omre, 2003) to represent the distributions as being (multi)normal; this is often very reasonable, and makes the mathematics a lot more tractable.

The prior distribution can be obtained from a depth trend of, say, AI and cross-plots between AI vs. SI and AI vs. ρ (all derived from well data, and all with an assessment of uncertainty). These trend fits can be expressed as a multi-normal prior distribution of form

$$p(Z) \approx \exp\{-\frac{1}{2}(Z - Z_0)^T C_p^{-1} (Z - Z_0)\} / |C_p|^{1/2} \quad [6]$$

Where C_p is the covariance matrix describing the variance of and the correlation between the impedances

The likelihood function can be expressed as

$$L(S_{real}|Z) \approx \exp\{-\frac{1}{2}(S_{real} - F(Z))^T C_d^{-1} (S_{real} - F(Z))\} / |C_d|^{1/2} \quad [7]$$

Where $F(Z)$ is the function to derive synthetic seismic from the impedances Z , as described under 'A) Deterministic method', and C_d is the covariance matrix representing the 'effective' seismic noise.

The (un-scaled) posterior distribution can be derived using [5], from which we can derive the maximum a-posteriori (MAP) model of Z (kind of like a P50 estimate), or we can use MCMC

sampling to obtain marginal distributions of interest (see also Gunning and Glinsky, 2004).

2. Why not optimal?

The inversion schemes described above have a number of shortcomings. Firstly, the additional regularization information needed to ensure reasonable comparisons between the deterministic inversion results and well impedance profiles at best contains only global or 'pooled' rock physics trends (i.e. one rock physics trend for all facies) and at worst no rock physics at all. As an example, one 'trick' often applied is to approximate $\text{Ln}(\text{SI})$ as linear in $\text{Ln}(\text{AI})$: $\text{Ln}(\text{SI}) = \alpha_{\text{SI}} \text{Ln}(\text{AI}) + \beta_{\text{SI}} + \delta \text{Ln}(\text{SI})$ (same for $\text{Ln}(\rho)$). This changes [3] to

$$S_{\text{pp}}(\theta) = a'/2 W(\theta) \Delta \text{Ln}(\text{AI}) + b/2 W(\theta) \Delta \delta \text{Ln}(\text{SI}) + c/2 W(\theta) \Delta \delta \text{Ln}(\rho) \quad [8]$$

Where $a' = a + \alpha \text{SI}$ $b = \alpha \rho$ c

So now we invert to $\text{Ln}(\text{AI})$, $\delta \text{Ln}(\text{SI})$ and $\delta \text{Ln}(\rho)$, i.e. for SI and ρ we invert for the deviation from the global linearizations. So how accurate are these linearizations? In Fig. 2 you see that the relationship between $\text{Ln}(\text{AI})$ and $\text{Ln}(\text{SI})$ can be reasonably linear, but that the same cannot always be said for $\text{Ln}(\text{AI})$ and $\text{Ln}(\rho)$!

Secondly, most energy in the seismic S_{real} comes from interfaces between different facies, but the inversion methodologies described so far are entirely continuous (whereas of course facies are categorical). This means that away from facies interfaces, where the energy wanes, the impedance tends to the pooled rock physics trend value (or background value), as shown in figure 3.

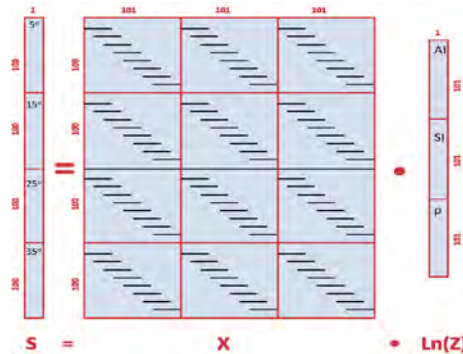


Figure 1: Matrix sizes (in red) for 4 partial angle stacks, 3 impedances, and a time gate of 100 samples. The black lines show that the blocks within matrix X are banded; in the top right and bottom left are many zeroes (especially if the wavelet is small and/or the gate is long), which speeds up calculation. Note 1: Each block of the system block matrix X contains an almost diagonal difference matrix D multiplied by a banded wavelet matrix W, making each block banded and thus quite sparse. These blocks are not identical, as vertically the convolution matrix changes (different wavelets for different incidence angles θ), and horizontally the scaling factors change from a/2 to b/2 to c/2 respectively. Note 2: The impedance traces are 1 longer than the synthetic seismic traces, as we need 2 impedances to calculate 1 reflectivity!

These two shortcomings lead to the following realizations:

1. We need to ensure the regularization is based on un-pooled, one-per-facies rock physics trends, as a pooled rock physics trend (one rock physics trend to describe all facies) is demonstrably unrealistic/inaccurate
2. Therefore we need to jointly invert for facies and for impedances per facies!

3. Joint categorical/continuous simultaneous inversion

For the avoidance of doubt, 'joint' here means that we invert both for facies (a categorical variable) and impedances (continuous variables), and 'simultaneous' means that we invert more than one seismic dataset (e.g. near, mid and far partial angle stacks) to more than one impedance (e.g. AI, SI and ρ) in one go. So for example we can jointly invert for a categorical facies label (e.g. 1=shale, 2=waterbearing sandstone, 3=oil-bearing sandstone etc) and for continuous AI, SI and ρ estimates (if the Fatti equation is used).

This joint inversion we desire is mathematically demanding, as it cannot be written down in closed form (such as [4] above), nor can it be solved using standard optimization apparatus. We use an iterative method where we first invert for impedances (given a starting facies model), then given these impedances we invert for facies labels, then given these facies labels we re-invert for impedances and so forth, until a suitable solution has been obtained. This method is called the Expectation-Maximization algorithm, or E-M for short. In the M step we estimate the impedances given the expected facies labels, and in the E step we estimate the expected facies labels given the impedances.

Again using Bayes' theorem, the joint-model posterior distribution equivalent of [5] is now more complex

$$\pi(Z, F | S_{\text{real}}) \approx L(S_{\text{real}} | Z) p(Z | F) p(F) \quad [9]$$

The likelihood function $L(S_{\text{real}} | Z)$ is the same as [7], and the prior distribution $p(Z | F)$ is very similar to [6], the only difference being that the prior mean Z_0 depends on the facies label F:

$$p(Z | F) = \exp\{-1/2(Z - Z_0(F))^T C_p(F)^{-1}(Z - Z_0(F))\} / C_p(F)^{1/2} \quad [10]$$

This facies-dependent prior distribution can be obtained from depth trends of, say, AI and cross-plots between AI vs. SI and AI vs. ρ . The difference with section 1 is that now we develop these depth trends and cross-plots per facies, each one complete with an assessment of uncertainty.

That leaves $p(F)$, the facies prior distribution. For this we use a discrete Markov Random Field. Expressed simply, any 3D seismic lattice consists of many pixels. We define a set of edges connecting the direct neighbours of each of the pixels in the inversion window. Each pair of connecting neighbours forms a so-called clique, and so each pixel belongs to six cliques (except at edges, corners). The probability of a configuration F of the whole lattice is then defined by the sum of potential energies over all the cliques in what is usually called a Gibbs distribution:

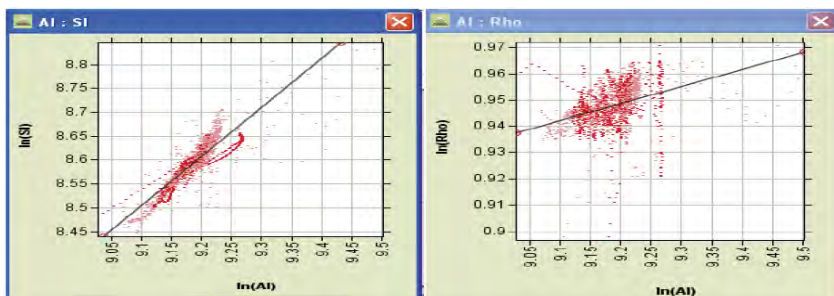


Figure 2: Typical $\text{Ln}(\text{AI})$ vs. $\text{Ln}(\text{SI})$ (left) and $\text{Ln}(\text{AI})$ vs. $\text{Ln}(\rho)$ (right) cross-plots over all facies excluding hydrocarbon bearing intervals. Whereas the $\text{Ln}(\text{AI})$ vs. $\text{Ln}(\text{SI})$ cross-plot is reasonably linear, the $\text{Ln}(\text{AI})$ vs. $\text{Ln}(\rho)$ relation is more complex.

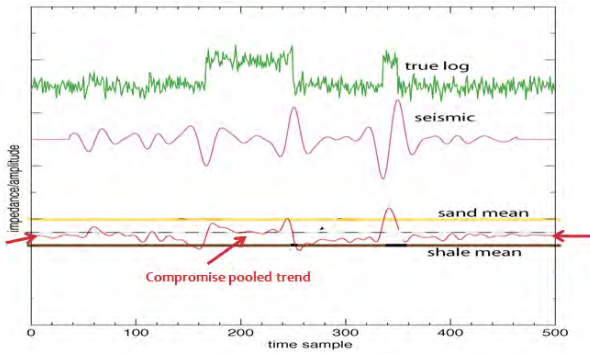


Figure 3: An impedance model (top), the corresponding synthetic (middle) and the inverted impedance trace (bottom). Note how away from seismic energy (at the ends, and also in the centre of the thick sand interval; all indicated by red arrows) the impedance tends to a value not representative of any rock.

$$p(F) \approx \exp(-\sum V_c(F_c)) \quad [11]$$

where V_c represents the “potential energy” of the set of labels F_c seen by each clique c .

Comparing the central pixel with each of the 6 individual neighbour we can write the potential energy as $V_c = \frac{1}{2} \beta I(F_{\text{centre}}, F_{\text{neighbour}})$ where the discrete indicator function I is 1 if labels F_{centre} and $F_{\text{neighbour}}$ are different and is 0 if they are the same, and β is a positive smoothness/continuity parameter. So we can rewrite [11] as ...

$$p(F) \approx \exp(-\sum \sum \frac{1}{2} \beta I(F_1, F_2)) \quad [12]$$

where the first summation is over all pixels and the second summation is over the 6 cliques per centre-pixel ... and thus we penalize (reduce) the probability $p(F)$ if 2 labels are different.

We have implemented different β 's for horizontal and vertical smoothness, as geologically horizontal continuity is typically larger than vertical continuity. However, as geology is seldom perfectly horizontal, we use the concept of stratigraphic age to determine neighbours of the same age, which may not be simply the neighbouring pixel at the same time index. This is explained in Fig 4.

In the E-step, the facies distribution needs to be updated based on the current estimate of the impedances (and the per facies rock physics model trends). I.e. we also need to optimize $p(F|Z) \approx p(Z|F) p(F)$. For this graph-cutting and so-called loopy Bayesian Belief Propagation techniques are used, which are beyond the scope of this paper.

Presently the tool inverts only for the maximum a-posteriori probability (MAP) estimate (i.e. no sampling, such as MCMC). As all 3 probabilities in [9] are of exponential form, determining where the maximum is achieved is equivalent to determining where the minimum of the sum of the exponents is achieved, which simplifies the algebra.

4) Examples

The first example shows a trace from a wedge model with a slow ca. 2450 m/s sand encased in fast ca. 2800 m/s shale (black model in Fig. 5). It is clear the final iteration (number 7, grey dashed) of the new Joint Categorical/Continuous inversion is superior to the continuous inversion result (number 0, red) as described in section 1, which is the industry standard at present.

In the second example we have applied the new Joint Categorical/Continuous inversion to the 3D seismic of the Stybarrow field, offshore Western Australia, as shown in Fig. 6.

The inversion to AI was performed twice, once with horizontal β values equal to 0 (no horizontal continuity), and once

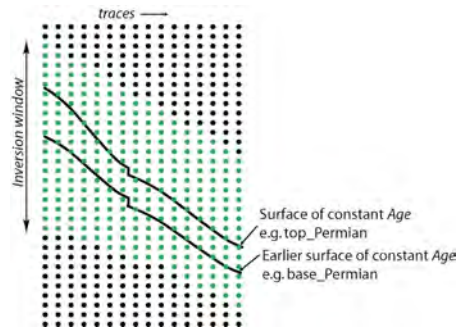


Figure 4: A stratigraphic age 'field' assists in determining neighbours of the same age.

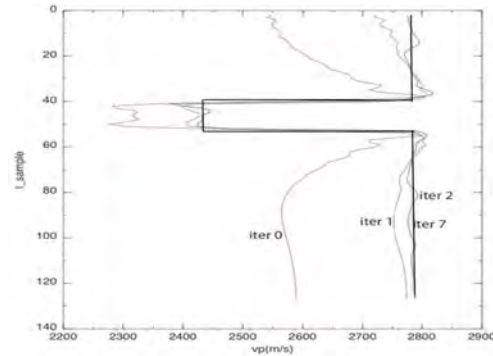


Figure 5: A sand embedded in a shale. Iterations 0, 1, 2 and 7 (the last one) are labelled. Note that iteration 0 is the normal continuous inversion result, and shows familiar problems: the sand value 'overshoots' (2300 m/s instead of the real ca. 2450 m/s sand value), a dip to higher velocities in the middle of the sand, and away from the shale/sand and sand/shale interfaces the impedance value tends to a neither-sand-nor-shale value.

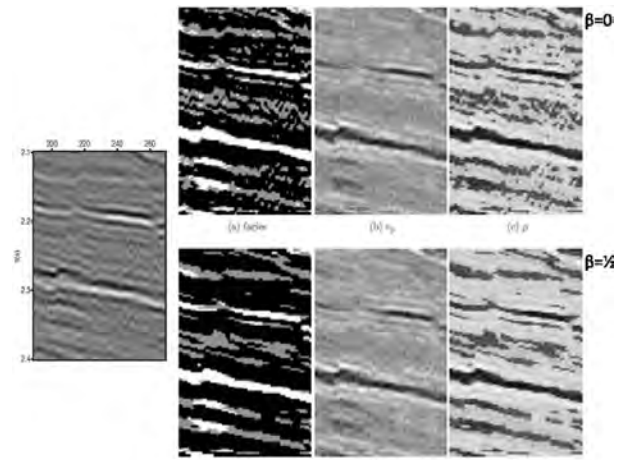


Figure 6: The normal incidence section (left), inverted with horizontal β values equal to 0 (top), and horizontal β values equal to 0.5 (bottom)

equal to 0.5. We see that imposing some horizontal continuity in this case (bottom of Fig. 6) improves both the facies inversion (less salt and pepper effect, and therefore more geological) and the density inversion (a less dappled ρ image). The velocity image is less sensitive to the β values, which is understandable, as V_p has most effect on the impedance.

5) Conclusions:

In-depth analysis of the present industry standard continuous simultaneous method highlighted some shortcomings, which require the following remedies:

1. Prior constraints based on un-pooled (i.e. per facies) rock physics trends need to be incorporated in the ideal inversion algorithm, as rock type is crucial.
2. This means the ideal inversion needs to invert not only to continuous impedances, but also jointly to categorical facies!

In this paper we have introduced a new joint categorical/continuous simultaneous inversion method which implements these two remedies, and which does not show the unsightly artefacts of standard methods such as impedances tending to a non-geological value away from seismic energy.

En passant the new technique has some other attractive features, such as the ability to hardwire the facies labels at wells. This is quite a unique way to use well data directly in seismic inversion (normally it is only used indirectly, and in inversion QC).

References

- Buland, A. and Omre, H., 2003. Bayesian linearized AVO inversion, *Geophysics*, 68, 185–198.
- Fatti, J.L., Smith, G.C., Vail, P.J., Straus, P.J. and Levitt, P.R., 1994. Detection of gas in sandstone reservoir using AVO analysis: a 3D seismic case history using the Geostack technique, *Geophysics*, 59, 1362-1376.
- Gunning, J. & Glinsky, M.E., 2004. Delivery: an open-source model-based Bayesian seismic inversion program. *Computers & Geosciences*, 30, 619–636.
- Gunning, J. and Kemper, M., 2011. Some newer algorithms for joint categorical and continuous inversion problems. Inversion Workshop, 73rd annual conference, EAGE, Vienna
- Zoeppritz, K., 1919. Erdbebenwellen VIII B. On the reflection and penetration of seismic waves through unstable layers. *Goettinger Nachrichten*, 1, 66-84.

Evaluation of Thin-Bedded Heterogeneous Sands Using Geophysical Applications & Well Data for A Robust Development Plan

M. S. Mohd Adnan* (ExxonMobil Development Company) &
F. Fahmi (ExxonMobil Exploration & Production Malaysia Inc)

Introduction

A comprehensive technical evaluation was conducted in a gas field in the Malay Basin, offshore Peninsula Malaysia, to describe the degree of reservoir heterogeneity in the thinly stacked non-associated gas (NAG) reservoirs in the Middle Miocene Group D and E sandstones. This paper focuses on two major reservoirs, D-1 and E-1, using AVO modeling and seismic Vp/Vs inversion with well log and MDT pressure integration to better understand sand distribution for subsequent drillwell development planning in 2014.

The field is a low relief compressional anticline with a discovery well drilled in 1979. Two additional appraisal wells were drilled to delineate the field. There are 34 stacked reservoirs with up to 46 gas-water contacts penetrated by the wells. The individual reservoirs rarely exceed 15 meters in thickness, separated by sealing shales or coals. Based on the well log, MDT static pressure, and the presence of numerous GWC's, there is significant stratigraphic heterogeneity interpreted.

Method and/or Theory

Due to the thinly bedded nature of the reservoirs, the seismic could not be fully utilized to evaluate internal stacking geometries. This was further complicated by attenuation from the overlying coals. However, attribute analysis was effective to determine overall sand presence where bed thickness ranges from 7 – 15m in thickness (seismic detection is ~ 7m).

Rock property analysis was performed to calibrate both acoustic impedance and Vp/Vs to gamma ray for indication of sand presence. The Vp/Vs derivative was used instead of acoustic inversion because of the extra information obtained in both the elastic and AVO domain. In addition, AVO modeling was performed to differentiate gas from wet sand and coals.

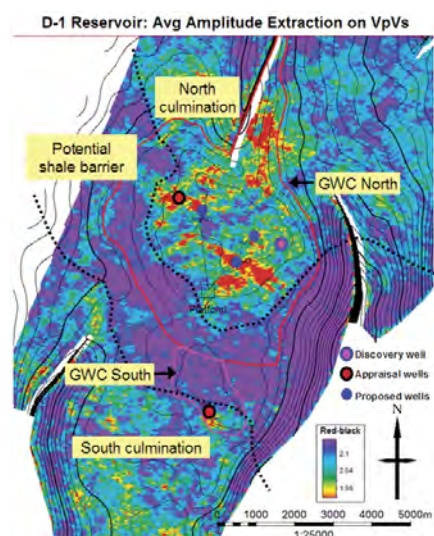


Figure 1: Average amplitude extraction on a seismic inversion volume (Vp/Vs) to help identify potential stratigraphic barrier based on MDT pressure data. Development wells are planned to target better sand quality and mitigate reservoir connectivity uncertainty and aquifer strength in the water leg.

The seismic data was used to qualitatively condition a 3D geologic model to better distribute sand presence for well planning optimization. However, given the remaining degree of heterogeneity in these thinly-bedded sands with multiple GWC's, a robust well planning and commingling strategy was considered to mitigate this uncertainty.

Examples

The D-1 reservoir is deposited in tidal channel bar complexes surrounded by inter-channel overbank muds. Reservoir pressure data supported that the northern and southern culminations are not in pressure communication in the water leg. Integration of seismic Vp/Vs and fluid sample data added support that the central shale was a stratigraphic barrier (Figure 1).

The E-1 reservoir sandstone was deposited in fluvial channels and is overlain by shales formed in interdistributary bays. Seismic AVO analysis is challenging because of interference from the overlying shales and coal. Reservoir fluid determination utilizing AVO modeling, combined with Vp/Vs sand distribution, enables the separation of the gas and water responses and outlining the reservoir distribution (Figure 2).

Conclusions

Full integration of the seismic Vp/Vs inversion and 2D AVO modeling with MDT pressures has resulted in an improved understanding of reservoir distribution, and reduced the degree of uncertainty in reservoir connectivity, thus allowing a more robust development strategy. Work is currently on-going to incorporate the remaining uncertainties in sand distribution and facies quality.

References

Basin History and Evolution [1995] Esso PETRONAS Integrated Collaborative (EPIC) Study

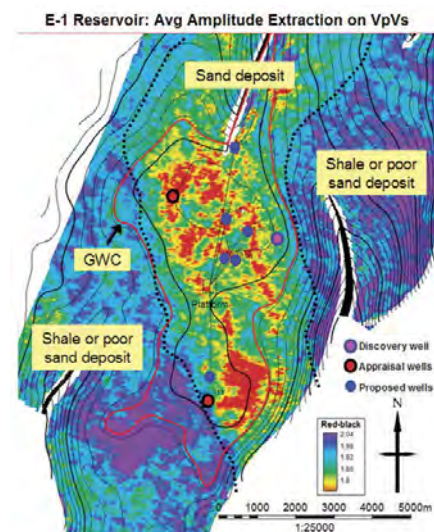


Figure 2: Average amplitude extraction on a seismic inversion volume (Vp/Vs) to differentiate lithology responses. Development wells are planned to target good quality sands to maximize recovery efficiency.

Improved Resolution of Thin Turbiditic Sands in Offshore Sabah with Bandwidth Extension – A Pilot Study

G. Yu* (Geotrace), N. Shah (Geotrace), M. Robinson (Geotrace), N. H. Nghi (PETRONAS Resource Development/Petroleum Management Unit), A. A. Nurhono (PETRONAS Resource Development/Petroleum Management Unit) & G. S. Thu (PETRONAS Resource Development/Petroleum Management Unit)

Introduction

Many of the deepwater reservoirs offshore Sabah are characterized by thinly bedded turbidite sands. The main interpretation challenge in the area of interest is to define the thickness, extension, and geometry of these sands. The net pay of the sands encountered by the wells varies, from centimeters to tens (10s) of metres. The conventional 3D seismic data doesn't have the appropriate frequency content and resolution to properly image the reservoir where thin turbiditic channels and lobes exist and to discriminate the different units possibly present. The data is further limited by the presence of shallow gas.

The latest seismic data available over the reservoirs in question (Figure 1) has a usable frequency range at target level of 5 to 27Hz rendering it unsuitable for imaging the thin turbidite sands. The pilot study was designed to test the potential of Geotrace Technologies proprietary methodology known as Bandwidth Extension (Smith et al., 2008) to recover higher frequencies that may be carried in the existing data and to verify that these higher frequencies corresponded to geology. An inline was selected from the 3D dataset that passes through a well that has good correlation with the seismic. It was observed that the correlation coefficient of 0.85 is dominated by a few high amplitude low frequency events. A cross-line was also included in the study that passes through a blind test well used by Petronas to verify the results.

Methodology

Bandwidth Extension algorithm utilizes the Continuous Wavelet Transform (CWT) to model harmonics and sub-harmonics to recover both high and low frequencies. The algorithm attempts to recover the lost wavelet characteristics by using the available bandwidth in the recorded seismic data. The available bandwidth acts as the fundamental frequencies, for which harmonics and sub-harmonics will be computed from, and added back into the wavelet by a convolutional-like process in the CWT domain as illustrated in Figure 2. This effectively reshapes the wavelet and broadens the spectrum. Any harmonic and sub-harmonic frequencies that do not match reflectivity

above the ambient noise level will not remain in the final result.

This resolution enhancement technique can be applied before and after migration. In this pilot study it was applied to the migration stack provided by the client. First, the given known well data was used to make the seismic zero phase, create the synthetics, and calibrate with the geology. Then, the pilot study tested extending the bandwidth by one and two octaves, extension beyond this was limited by the temporal sampling of the recorded seismic and possibly by the filters applied during the processing. Finally the results were evaluated with the blind well data by the client for resolution enhancement, reservoir identification, and interpretation improvements.

Results and Conclusions

Based on this technique it was possible to extend the usable maximum frequency from 27Hz to 83Hz as shown in Figure 3. The correlation with the known well reduced to an acceptable 0.65 given the significant increase in the events being correlated and the high frequency attenuation and distortion effects of the gas. In other words the greatly increased bandwidth up to 83Hz offered rich geological information that can be tied with the well for detailed interpretation and reservoir characterization badly needed for this field characterized by thin turbidite sands with widely variant thickness and spatial distribution.

The result was further verified by the client using a blind well that was not available to Geotrace during the testing and processing phases. Figure 4 illustrates the blind well and seismic correlation using the synthetics computed from the sonic and density logs of the said blind well with a broader bandwidth wavelet comparable to the extended seismic bandwidth. All log curves and computed reflectivities are displayed to the left-side of Figure 4. The synthetics (in blue) and seismic trace at the blind well locations are repeated 5 times (in red) to its right for comparison and visual correlation. Also a small seismic section around the blind well is displayed at the far right of Figure 4.

Most importantly, by comparing the input (Figure 1) and the output (Figure 3), the enhanced result significantly improves the resolution of thin sands identification enabling a more accurate

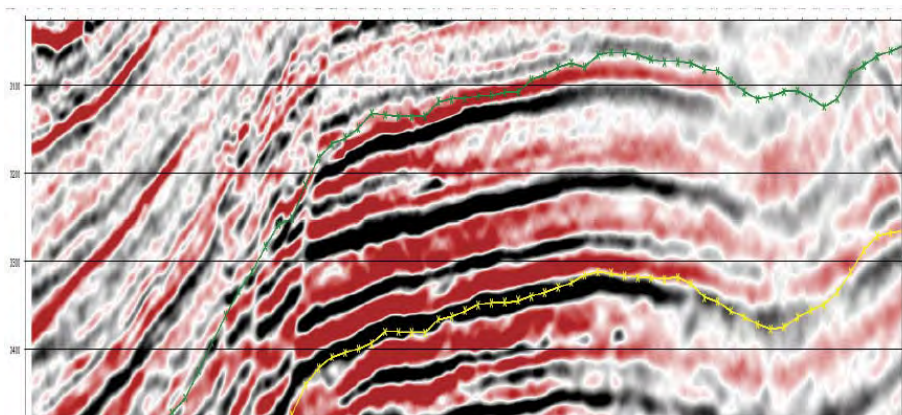


Figure 1: Input seismic (inline) with the top and bottom of the target zone identified by the green and yellow horizons respectively. The seismic to the right of the section degrades as it approaches the gas affected areas. Maximum frequency in the zone of interest is approximately 27Hz resulting in poor resolution of the thin bed sands in the target zone.

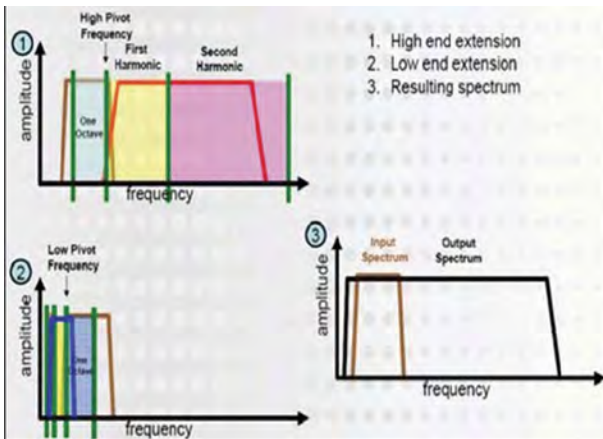


Figure 2: A schematic rendition of Bandwidth Extension theory, implementation and key steps of the bandwidth evolution in the processing.

interpretation, has good correlation with the blind-well (Figure 4) and geology, improves fault definition on the flanks of the gas chimney, and meet client's objectives and needs for reservoir management, production enhancement, and appraisal decision making and activities.

Acknowledgements

The authors would like particularly to thank Petronas for permission to show the data. The authors would also like to thank Petronas and Geotrace for permission to publish this paper and gratefully acknowledge the work done by Petronas technical team and Geotrace Reservoir Services team.

Reference

Smith, M., Perry, G., Bertrand, A., Stein, J., and Yu, G., 2008. Extending seismic bandwidth using the continuous wavelet transform. *First Break*, 26, 97-102.

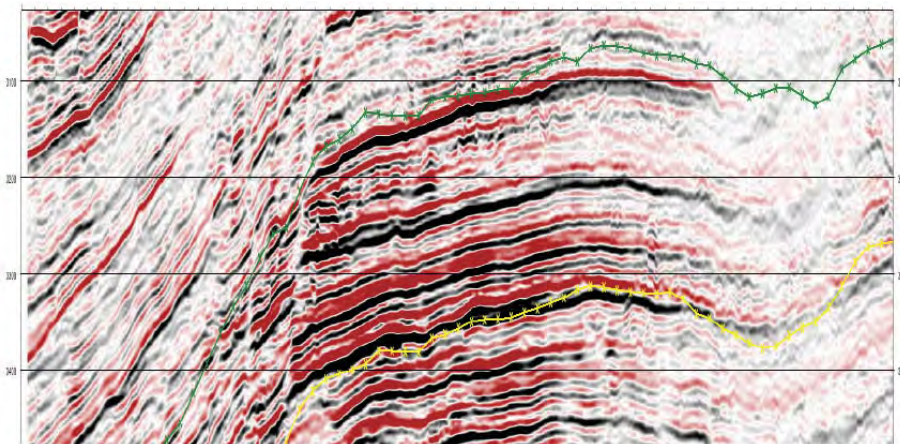


Figure 3: Output seismic (inline) the usable high frequency has been extended to 83Hz at target resulting in the addition of many additional reflectors and clearer definition of both large and small scale faults.

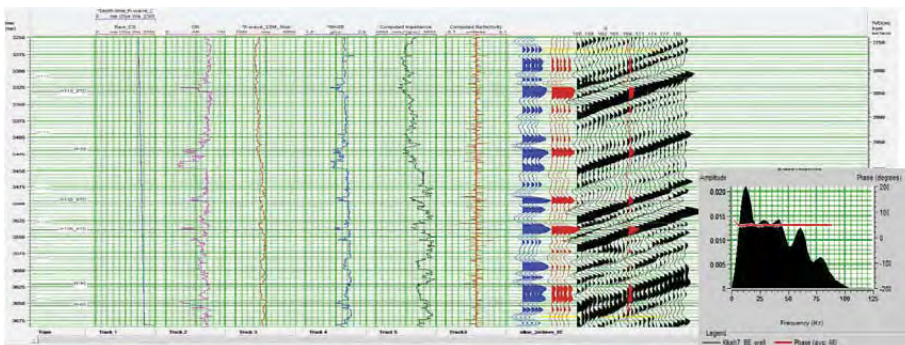


Figure 4: Blind well comparison of the 2 octave Bandwidth Extension result performed by Petronas. The extended seismic has significantly more events that correlate well with events seen on the synthetic trace. The correlation coefficient in the reservoir zone is 0.69.

Seismic Resolution and Analysis of Thin Pay Beds

M. Sajid* (University Technology PETRONAS), D. P. Ghosh (University Technology PETRONAS) & Z. T. H. Zuhar (University Technology PETRONAS)

New purposed algorithm is based on derivation of seismic trace amplitude with respect to time. Each order of differentiation represents the finer level of change in signal i.e. higher the order of derivation represents finer the change in signal. Each output of derivation operation has higher frequency that follow by adding extra half cycle and 90° phase shift. So the differential operator can be considering being a low cut filter.

Derivation of signal has many uses in digital signal processing. First derivative of signal y with respect to independent variable 't' represents the slope of signal at that point. If the sample interval of independent variable 't' is constant than first derivative is defined by eq.(1). The Second derivative measures the curvature of the signal which can be obtained by taking twice successive derivative of the signal i.e. $y'' = \frac{d(y')}{dt}$

Similarly for higher order derivatives.

$$y'_j = \frac{y_{j+1} - y_j}{t_{j+1} - t_j} \text{ where } j \in R(1 \leq j < n - 1)$$

$$t_{j+1} - t_j = \text{Constant}$$

$$y'_j = \frac{y_{j+1} - y_j}{\Delta t} \quad (1)$$

Maximum resolvable thickness by Widess (1973) is $\lambda/4$ of the wavelength. Wavelet has two lobes, one on each side of inflection point. So with respect to side-lobes, resolvable thickness is half the size of the wavelet side lobe. Derivatives provide the ability to study in detail the variation in these side lobes. 1st derivative splits these lobes into two half at the point of maximum inclination as shown in Figure 1a.

Now the features with the size of $\lambda/4$ are more easily identifiable. Similarly 2nd derivative splits the side-lobe of 1st derivative into two half and the polarity depends on the direction of slope, Figure 1b.

Similarly for 3rd and 4th derivatives. It can be observe that 4th derivative focuses on the detail $1/4h$ of the size of side lobe or $1/8$ h of the wavelet, Figure 1d. So in comparison in details of information between derivatives, each successive derivative focuses two times finer detail than its inputs, Figure 1.

Effect of derivatives on wavelet relative amplitudes

Successive derivative of the signal increase the amplitude ratio of high frequency event to low frequency event, as shown in Figure 2 and focus on high frequency event in wavelet. These two properties of derivatives i.e. focus on finer event in wavelet and Increase in amplitude ratio lead us for creation of new seismic attribute based on signal derivatives.

Methodology

In digital Seismic data processing, derivation process can be best approximated by using the difference function (as sample interval is small and constant i.e. 2msec, Nyquist frequency 250Hz). Difference function means the difference between two consecutive sample values in each seismic trace. If the sample interval is 2mSec and samples are represented by $y(1), y(2), y(3), \dots, y(n)$. Then difference function calculates $ydiff(2) = y(2) - y(1)$, $ydiff(3) = y(3) - y(2)$, $ydiff(4) = y(4) - y(3)$, $ydiff(n) = y(n) - y(n-1)$. Second derivative is the application of differential function again on first derivative and similarly for third and fourth derivative. Each derivatives operation

gives one sample less than the original input of operation. To balance, 0 is padded at beginning and at the end alternatively in successive derivatives.

Creation of differential resolution algorithm

As the sample rate is 0.002 Sec with Nyquist frequency of 250 Hz so difference function can be a good approximation of derivative. Derivative can be written as eq.(2). Similarly, III & IV represents the 3rd and 4th derivative of the signal. Amplitude (Ay) of each successive derivative is less than its predecessor (i.e. $Ay > Ay' > Ay'' > Ay''' > Ay^{IV}$). So the amplitude is normalized eq.(3) Before the calculation of differential resolution algorithm eq.(4).

$$\frac{dy}{dx} = \frac{y_2 - y_1}{t_2 - t_1}$$

$$y' = \frac{y_2 - y_1}{\Delta t} \quad (2)$$

Δt is constant (i.e. 0.002 Sec in this case).

$$Ay_i = \frac{[Ay_i]}{\text{maximum}([Ay_i])} \quad (3)$$

$$Ay_{DR} = \frac{Ay_n - (0.5) \cdot [Ay_n'''] + (0.5) \cdot [Ay_n^{IV}]}{3} \quad (4)$$

Response of the differential resolution algorithm on Butterworth wavelet of frequencies (fmin = 10 and fmax = 60 and slop 24db/octave) is shown in Figure 1a. Red curve represents the input wavelet whereas the magenta and blue curves represents the

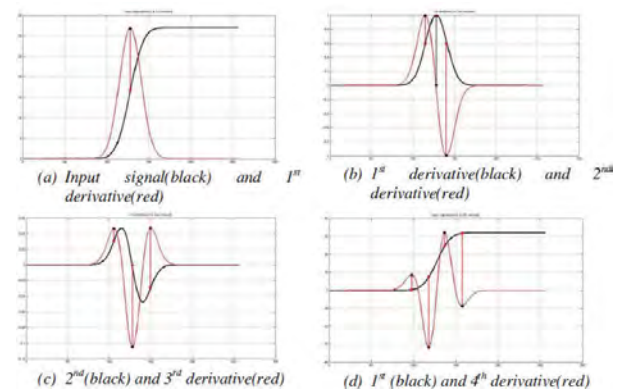


Figure 1: Comparison in details of information between derivatives.

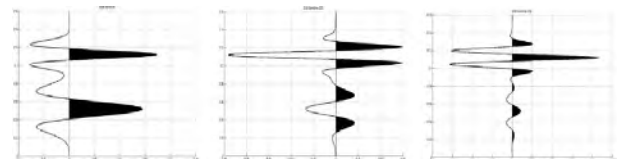
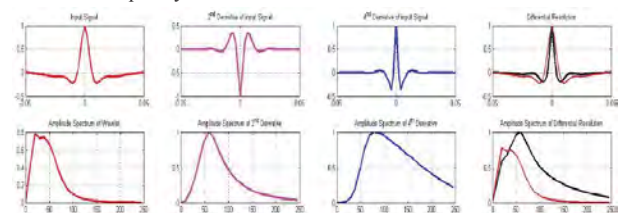


Figure 2: Relative change in amplitude of interface with different dominant frequency.



Application of differential resolution algorithm on butter-worth wavelet.

Figure 3: Differential resolution algorithm analysis.

2nd and 4th derivative respectively. Black curve represents the differential resolution output and their corresponding amplitude spectrum. Figure 3b show the tuning analysis of butter-worth wavelet before and after the application of differential resolution algorithm. It can be observe that the resolution limit of the wavelet is decrease from 0.01Sec to 0.007 Sec.

Application of differential resolution algorithm on 1D synthetic model

1D synthetic model is created using Butterworth wavelet with frequency (10,60,240 slope both sides). Two events are separated by 8mSec or 4 Sample which produce flat spot(below tuning thickness) according to Ricker criteria (Kallweit and Wood, 1982). Figure 4a, 4b blue and red curve represents the 1st and 2nd event respectively whereas the black curve represents the combined effect respectively. Similarly black curve in the second row of Figure 4a, 4b represents the differential resolution output. Analysis shows the differential resolution algorithm developed in eq.(4) successfully separated the two seismic events.

Application of differential resolution on 2D synthetic Seismic

2D synthetic is created from geological model of stratigraphic layer of known thickness and Elastic properties. In this analysis 0o offset synthetic seismic section is created by using zero-phase butterworth wavelet with the frequency range (8,10,50,60), sample rate of 2mSec and length 0.1Sec. Normally distributed noise with S/N ratio of 3 is added in the original synthetic seismic shown in Figure 5b. Figure 5d show output of the algorithm developed on eq.(4) Whereas the Figure 5c shows the result of Differential resolution algorithm from synthetic seismic without noise.

Conclusion

Differential resolution algorithm which is based on variation of amplitude with respect to time provides the ability to study in

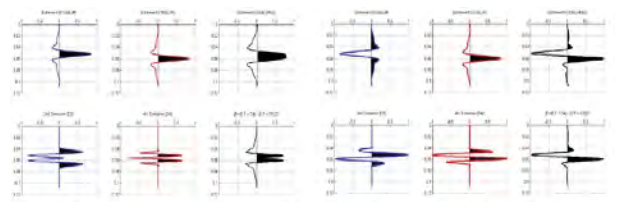


Figure 4: Differential resolution application on 1D Model.

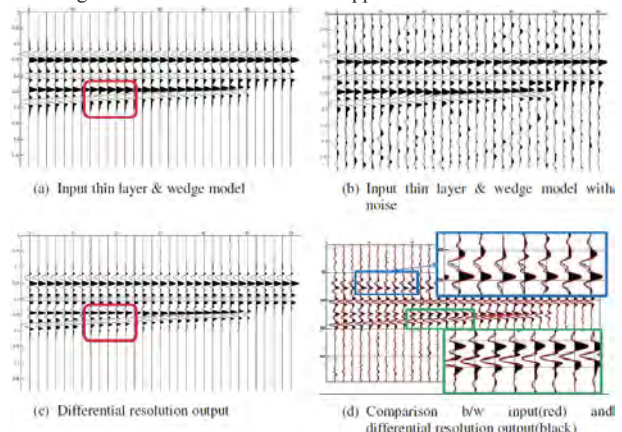


Figure 5: Application of differential resolution algorithm.

detail the thin layers response in seismic. Differential resolution algorithm increases the amplitude spectrum of high frequencies and decrease tuning thickness of the seismic wavelet. This make is possible to separate the events at the place of tuning without application of low-cut filter.

References

M. B. Widess, 1973. How thin is a thin bed?," Geophysics, vol. 38, pp. 1176-1180
 R. S. Kallweit and L. C. Wood, 1982. The limits of resolution of zero-phase wavelets, Geophysics, vol. 47, pp. 1035-1046,.

Cascading Inversion Application for Lithology and Porosity Estimation of Deepwater Thinly-Bedded Reservoirs

A. Nurhono* (PETRONAS Management Unit), B. KANTAATMADJA (PETRONAS Management Unit), S. T. GOH (PETRONAS Management Unit), V.W.T. KONG (Schlumberger), M. R. ABDUL RAHMAN (SLB) & N. M. HERNANDEZ (Schlumberger)

The deep water basins are major targets for hydrocarbon exploration to contribute a significant undiscovered resources. The geological processes in DW environments commonly include deposition of thinly-bedded pay zones that are difficult to characterize using standard seismic and logging techniques, and are often left unexploited and even overlooked during drilling.

This pilot project was the first collaboration study conducted in Malaysia for DW Thinly-Bedded Reservoir Characterization. The essential of reservoir model is including the Cascading Inversion of an integrated multiple disciplines workflow: (1) Seismic Data Conditioning, (2) Sedimentology, SHARP and Rock Model Building, (3) Simultaneous AVO Inversion, (4)

Lithology and pay prediction, (5) Stochastic inversion and Geo-Modeling, and (6) Validation.

This paper emphasized on a calibrated deterministic Simultaneous AVO Inversion of 4ms samples and utilized as one of the essential inputs to the stochastic seismic inversion to produce a higher resolution 1ms dataset. In essence, the stochastic inversion workflow incorporated 7 exploration wells with SHARP logs are used as the definitive model, and a number of realizations generated within the given geo-cellular grid over the zone of interest. These simulated realizations afforded the improved lithology and porosity computations which would lead to more robust volumetric computations of thinly bedded reservoirs.

Hydrocarbon Source Rock Characteristics of the Gondwana Coals from Barapukuria Basin, Bangladesh

M. Farhaduzzaman* (University of Malaya)

Introduction

Barapukuria coal deposit, one of the five important coal basins of Bangladesh (Figure 1), was discovered at Dinajpur district in 1985 by Geological Survey of Bangladesh (GSB). On the basis of borehole information and seismic survey, the study reveals that the stratigraphy of Barapukuria basin includes four different formations namely Basement Complex, Gondwana Group, Dupi Tila Formation and Barind Clay (Madhupur Clay) Formation and corresponding ages of the formations are Archaean, Permian, Tertiary and Quaternary respectively (Wardell Armstrong, 1991; Islam & Islam, 2005, Islam & Hossain, 2006; Islam & Kamruzzaman, 2006; Farhaduzzaman et al., 2011). Gondwana Group contains the important coal resource of Barapukuria basin. This sedimentary basin lies above the basement complex within which Permian age formations have been preserved by down faulting and subsequently in filled with unconsolidated Tertiary and Quaternary sediments.

The aim of this study is to characterize the petroleum source rock properties of these Permian Gondwana coals based on organic geochemical and organic petrological methods.

Methodology

The coal samples have been collected directly from the underground mine. The samples have been crushed to fine powder and subsequently analyzed using Source Rock Analyzer (SRA-Weatherford)-TOC/TPH of Rock-Eval equipment. Approximately 15g of the powdered samples have also been

Soxhlet extracted using an azeotropic mixture of dichloromethane (DCM) and methanol (93:7) for 72 hours. The EOM have been separated by means of column liquid chromatography into aliphatic, aromatic and polar fractions using petroleum ether, DCM and CH₃OH respectively. For the purpose of petrographic study (e.g., vitrinite reflectance analysis), the samples have been prepared by mounting whole rock fragments in slow setting polyester (serifix) resin together with resin hardener that allow to set and subsequently polished using water lubricated silicon carbide paper of different grades (P800, P2400 & P4000). Finally, the samples were polished to a highly reflecting surface using progressively finer alumina suspension (1µm, 0.3 µm & 0.05 µm). Petrographic examinations were performed using a Leica CTR 6000-M microscope with white and ultraviolet (UV) light sources. The percent of random vitrinite reflectance (R_o) were measured using a 50x oil immersion objective and a sapphire standard having 0.589% R_o.

Results and discussion

The SRA data (Table 1) indicate that the organic matter is a mixture of Type-III and Type-II kerogen. The TOC (Total Organic Carbon) ranges from 61 to 74 wt.% and the results based on high EOM (Extractable Organic Matter = 27561- 41389 ppm) suggest that the coals are excellent source rock following the classification established by Peters and Cassa (1994). In support, the hydrocarbon yield (14.77-30.66 mg HC / g TOC) is also high (Table 2).

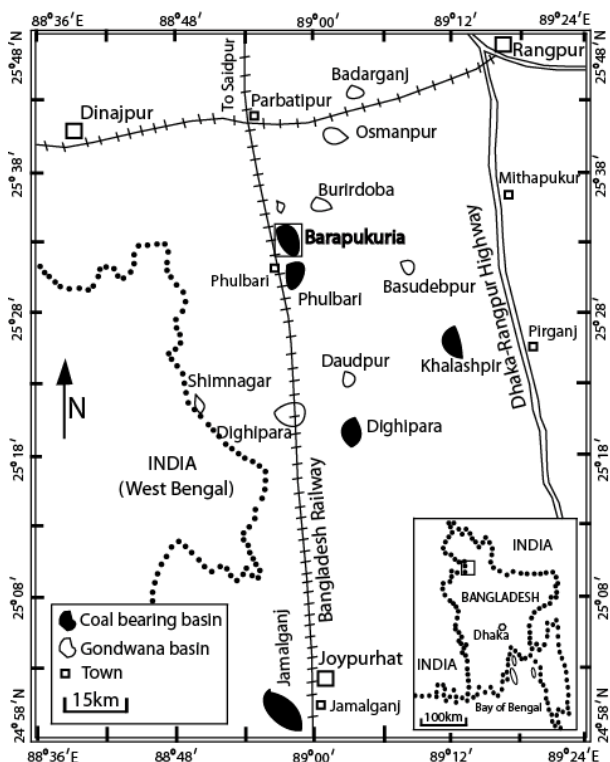


Figure 1: Location map of the study area showing other Gondwana basins, NW Bangladesh.

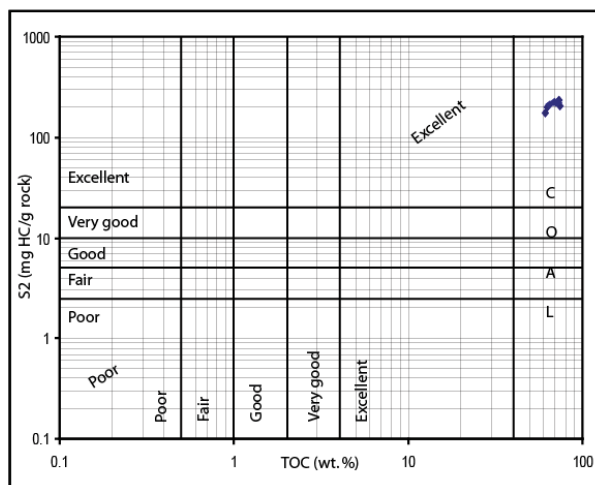


Figure 2: Plot of total organic carbon (TOC in wt.%) versus remaining hydrocarbon potential (S2 in mg HC/g rock) of coal samples which show an excellent source rock generative potential.

Source Potential and Hydrocarbon Maturity Modeling of the Onshore Masila Basin, Eastern Yemen

M. Hakimi* (University of Malaya), W. H. Abdullah (University of Malaya) & M. R. Shalaby (University Brunei Darussalam)

The Masila Basin is one of the most hydrocarbon-prolific sedimentary basins in the Republic of Yemen and is located in the Hadramaut region in East Central Yemen (Fig. 1). The hydrocarbons produced from Masila Basin are predominantly oil with minor amounts of natural gas. This basin formed as a rift during the Late Jurassic-Early Cretaceous due to the Gondwana breakup. This paper will present subsidence histories, maturation window, hydrocarbon generation and expulsion analysis. The main points are the vertical extent of strata which can be the source rock for mature hydrocarbon generation and the thermal history of the source rock. According to hydrocarbon exploration records and source rock studies in the onshore Masila Basin, substantial oil reserves occur in the Lower Cretaceous clastic and carbonate rocks as well as fractured basement reservoir rocks. In this study, we have chosen a location within the western central Masila Basin (East Shabowah Block 10), which is close to the major fields of hydrocarbon accumulation in the Masila Basin, as a representative site to model the timing of hydrocarbon generation (Fig. 1). The Upper Jurassic Madbi shales source rock were evaluated and incorporated into the basin modeling in order to improve our understanding of timing of oil generation, expulsion and migration. The Madbi Shales are characterised by a high total organic matter (TOC >2.0 wt %) and have a very good to excellent hydrocarbon generating potential. Kerogen is predominantly algal Type II with minor Type I. The Madbi Shales are mature and, at present, are within the oil window with measured vitrinite reflectance (%Ro) values in the range of 0.65–0.91%. This work on the stratigraphic sequence for of

each well optimized the model of the source rock due to the available geochemical and geological data. This technique is important to develop the burial history, hydrocarbon maturation, and generation history and was achieved by 1-D basin modeling (PetroMod) specialized software to cover the full history of petroleum formation for the selected fields. Modeling results suggest that the oil generation from Upper Jurassic Madbi Formation began in the Late Cretaceous and maximum rates of oil expulsion occurred during the Early Tertiary (Fig. 2). On the basis of the hydrocarbon generation modeling, one can deduce the time of hydrocarbon migration after expulsion. It is believed that hydrocarbon migration in the Masila Basin has continued approximately since Tertiary time, probably during Oligocene and Miocene time, which associated with the Gulf of Aden and Red Sea rifting. The result of the study provides an avenue for exploration strategies of the known location of Upper Jurassic Madbi source rock and exploiting effectively the existing petroleum system.

Acknowledgements

The authors would like to thank the Petroleum Exploration and Production Authority (PEPA), Yemen for providing the samples and data for this study. The authors are more grateful to the Department of Geology, University of Malaya for providing facilities to complete this research. Special thanks are offered to Mr. Peter Abolins, PETRONAS Carigali, Kuala Lumpur for his helpful comments on the basin modeling.

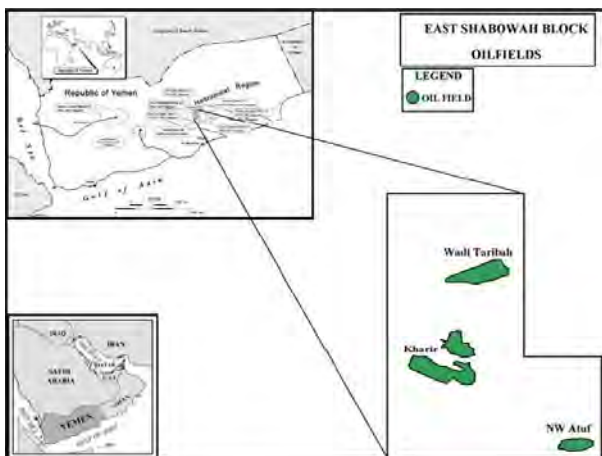


Figure 1: Location map showing the oil fields in the East Shabowah Block 10, western central Masila Basin, Republic of Yemen.

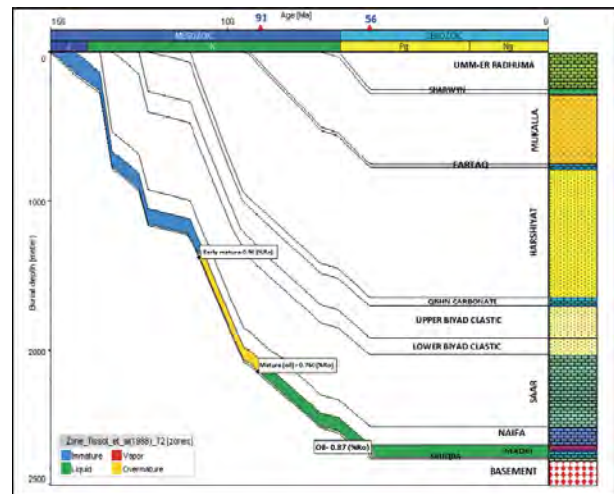


Figure 2: Burial history curves with hydrocarbon zones for the Madbi shale in wells KHA 1-23 in the western central Masila Basin.

Geological Controls on Well Productivity and Reservoir Performance in Select North American Shale Gas Plays

P. A. L. Winder* (Talisman Malaysia Limited), R. Herbert (Talisman Energy), G. Schmidt (Talisman Energy), M. Lawford (Talisman Energy) & B. Faraj (Talisman Energy)

North American shales typically exhibit geological variability on a macro and micro scale that results in marked variability in well performance. In the era of unconventional development, technology is driving well performance, but geology still underpins the potential for commercial development. Three North American shale gas plays, the Marcellus Shale in Pennsylvania, USA, the Montney Shale in Western Canada and the Eagle Ford shale in Texas, USA are the current focus of active piloting activity and in the case of the first two of these shales, development (figure 1).

To date, approximately 500 wells have been drilled by Talisman in the Marcellus, Montney (figure 2), and Eagle Ford Shales. The pace of evolution of shale plays is growing exponentially.

Therefore, it is critical to acquire data early and develop geological models to establish a clear understanding of the

technical controls on commercial development.

The results described will include the data obtained from 23 cored wells, which recovered over 1,000m of full-diameter core. Extensive analysis of samples, including XRD, SEM, geochemical analysis, as well as porosity, permeability and saturation measurements that are designed specifically for shales were conducted early in the life of the play. These data are integrated into basin-wide depositional and maturity models to establish a prospective fairway.

The complex interplay between shale mineralogy, tectonics, and reservoir fluid composition determines the response of the shale to hydraulic fracturing (figure 3), and subsequent reservoir performance (figure 4).

The combination of these characteristics and their effect on well productivity and reservoir performance will be discussed and contrasted for each of the shales.

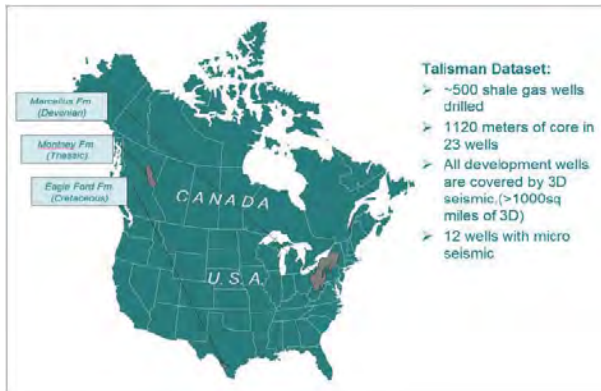


Figure 1: Location map of 3 North American shale gas plays.

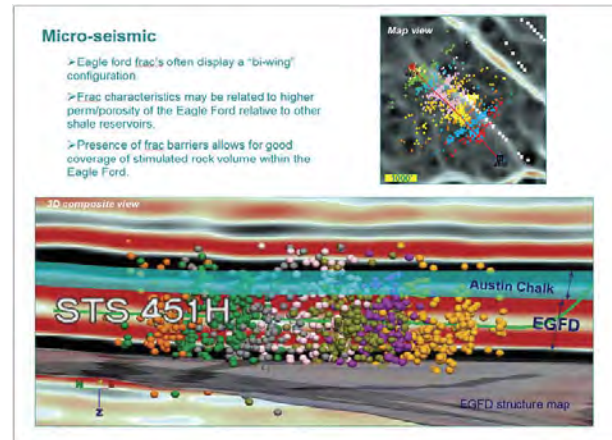


Figure 3: Micro-seismic example from the Eagle Ford Formation, USA.

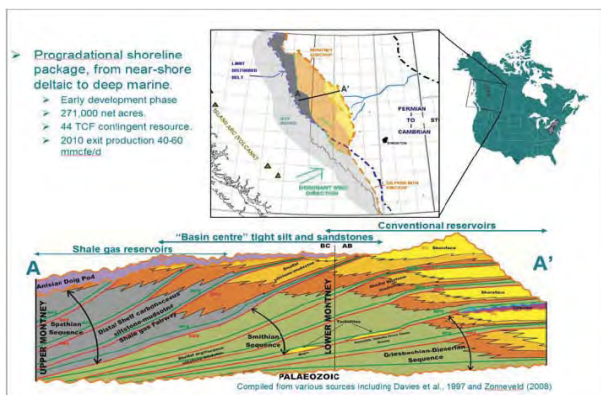


Figure 2: Montney Formation, Western Canada.

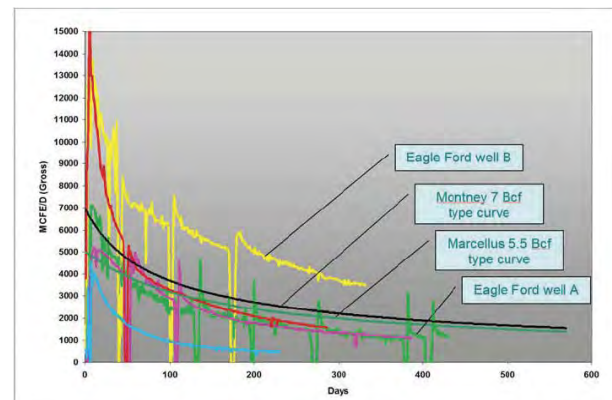


Figure 4: Comparison of Eagle Ford, Marcellus and Montney gas production.

Application of Dual Well Micro-Seismic Monitoring in Hydraulic Fracturing Stimulation in a Tight Oil Reservoir

T. K. Lim* (Schlumberger China SA), Y. Li (Schlumberger) & X. G. Yang (PetroChina)

The tight sand oil reservoir found in the Urdos basin is known for its very low porosity and permeability. Almost every well has been stimulated using hydraulic fracturing techniques. The average production for a vertical well is approximately 4-5 ton per day. Among such a large number of fracture jobs, enhanced production after stimulation does not always meet expectations. Since 2005, hydraulic fracturing monitoring service has been carried out widely in PetroChina field to understand the fracture geometry generated by hydraulic stimulation that would help optimize well placement. With the implementation onsite real time hydraulic fracture monitoring, the pumping procedure can be adjusted accordingly based on the mapped micro-seismic events.

Based on the past hydraulic fracturing monitoring experience in this field, an average microseismic event detectable distance range around 300m is expected for the case of geophones inside a monitor well. Two parallel horizontal wells were thus drilled at 600m apart. Horizontal section length is around 1500m for both wells. The original hydraulic fracture plans for each well consisted of 18 stage stimulations but were subsequently adjusted to 13 stages based on real time hydraulic fracture monitoring results. Three monitoring wells were drilled from toe to heel as shown in Figure 1. These monitor wells will also be used as water injection wells in later stimulation process. So hydraulic fractures generated by the pumping from both horizontal wells are not expected to extend far enough to reach the monitor wells.

With this favorable well layout, simultaneous dual well hydraulic fracture monitoring was proposed and conducted for this simultaneous horizontal well stimulation project. In order to obtain the optimized fracturing parameters first, the initial 3 stages of each treatment well was conducted at one stage per well i.e. stimulate well-1 and then move to frac well-2. Simultaneous hydraulic fracturing began after the initial six stages were completed.

Result

Based on the real time dual well monitoring results, a few main features are observed:

- Fractures generated under initial stage design overlay with each other. The fracturing design was modified to lengthen the perforation distance between stages.
- Single well monitoring depends on travel T_s - T_p travel time difference and hodogram angle to locate events. Multi-well monitoring allows for travel time triangulation plus

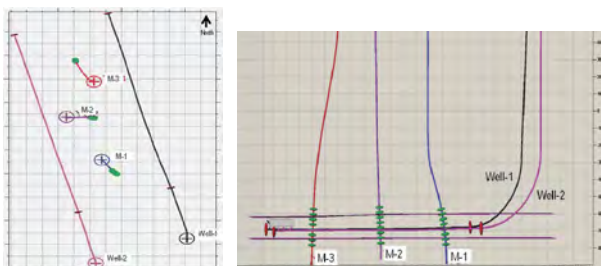


Figure 1: Left: treatment wells (Well-1 and Well-2) and monitoring wells layout, Right: side view of the seismic receivers in each monitoring wells.

hodogram angles. This reduced micro-seismic event location uncertainty, thus improving mapped fractures locations. In Figure-2, we can clearly differentiate and identified two fractures were developed instead of one, which might be mapped as single fracture if single monitoring well was used (processed individually). This observation is in agreement with geomechanics theory.

- The recorded fractures length suggested that horizontal spacing between these two treatment wells can be further increase to 700m~800m to improve the fracture coverage.
- A fault near one treatment well is detected apparently based on abnormally high event magnitude. Microseismic events resulting from fault activation typically have higher seismic magnitude than events from the hydraulic fracture.

Conclusion

Single well micro-seismic monitoring has been widely used to understand hydraulic fracture geometry in unconventional reservoir stimulation. The use of 2 wells to simultaneous monitor should be done when more wells are available within the required distance, as we have demonstrated in this case. Dual well technique can delineate feature in much detail and accurate as uncertainty is reduced. This example is the first dual well monitoring in China.

Both two treatment wells show astonishing production after stimulation, which is 25 times higher that the neighbor wells in this area.

References

- Cipolla, C. L. and C. A. Wright, 2000, State-of-the-art in hydraulic fracture diagnostics: SPE paper 64434, Asia Pacific Oil and Gas Conference and Exhibition, Society of Petroleum Engineers, 1618.
- Maxwell, S.C., 2008, Microseismic location uncertainty, CSEG Recorder.
- Warpinski, N. R., S. L. Wolhart, and C. A. Wright, 2004, Analysis and Prediction of Microseismicity Induced by Hydraulic Fracturing: SPE: Journal of Petroleum Technology, 24-33.

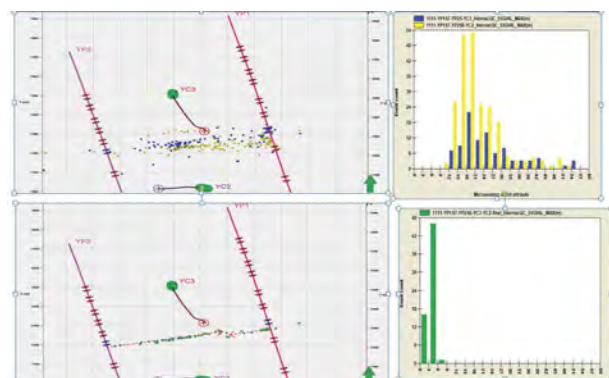


Figure 2: Top map show the mapped events using single well processing approach with the estimated uncertainty histogram and the bottom map show the combined dual-well processing result. The dual-well approach shows much lower uncertainty and clearly delineate the fracture as two separate patterns.

Foresee the Unforeseen: Modeling West Baram Delta Overpressure

C. A. Ibrahim* (PETRONAS Exploration), L. Light (SHELL Sarawak Berhad), J. Mennie (SHELL Sarawak Berhad) & C.K. Ngu (SHELL Sarawak Berhad)

PETRONAS Carigali and Shell Sarawak Berhad commenced a drilling campaign in SK307 in 2011 that constituted the first HPHT wells to be drilled with a 15K capacity rig in the West Baram Delta. Understanding regional overpressure behaviour will allow more accurate modelling of the pore pressure behaviour for future HPHT exploration opportunities and robust well planning.

Data from 62 West Baram Delta wells (MDT/RFT, Mudweight, Kick, FIT and LOT) indicates that the onset of overpressure occurs at different depths within these wells, which is both controlled structurally and stratigraphically.

Seismic velocity overpressure modelling was undertaken in 25 wells using both VP_VES Tau transform and Eaton exponent methods. Using a Tau function, it was observed that seismic velocities under predict the overpressure build-up. There is a large variation in Eaton exponents required to calibrate wells in the broader West Baram Delta and location specific exponents must be applied. A large number of 3D seismic datasets covered the area of interest and it was observed that short cable data (3km) have limited use with poor match to well data. Datasets

with 4.5km cable length demonstrated more robust tie to the modelled wells.

Under-compaction overpressure was identified as the predominant overpressure mechanism in the region. Under-compaction was driven by the rapid sedimentation underneath the prograding delta. In the southern West Baram Delta, late inversion resulted in unloading due to the structural overprint. Observation showed a significant pressure increase beyond the under-compaction trend in some wells which was inferred as inflationary overpressure. Prediction of this overpressure mechanism was difficult due to limited expression of seismic velocities and log responses.

The development of an integrated geological model incorporating all available well and seismic data underpins the prediction of overpressures in exploration prospects. Subsequently, this will significantly influence the well and subsurface target locations, well casing design (casing type and setting depth), mud weight program, evaluation and well monitoring program for well planning.

Pore-Pressure and Subsurface-Plumbing Patterns in Central Luconia; Offshore Sarawak, Malaysia

E. Kosa* (Sarawak Shell Bhd)

Introduction

Central Luconia is a geological province extending over an area of some 40,000km² offshore Sarawak, NW Borneo (Fig. 1). More than 200 Miocene-Recent carbonate build-ups are found in this province, many of which contain commercial hydrocarbons. Pore-pressure regimes within the carbonate reservoirs range from hydrostatic to lithostatic, and as such have a strong bearing on hydrocarbon prospectivity as well as on safety and performance of drilling operations.

The ability of low-permeability shale to contain hydrocarbons within porous reservoirs relates to the ratio between the ambient stress in the caprock and the pressure exerted by the reservoir fluids. Elsewhere in the sediment column, the pore-pressure regime depends on the ability of sediments to release water and compact in response to burial. In exploration, understanding of these processes allows for successful prediction of hydrocarbon presence as well as of pressure-limitations on hydrocarbon-column lengths attainable in a trap. Understanding of pore-pressure profile in the subsurface is also crucial for safe and efficient wellbore delivery.

Despite more than 40 years of intense exploration and development activities in this Province, however, hydraulically blown traps and pressure-related operational issues are still encountered by the petroleum industry. The present study tackles this persistent issue by summarising pore-pressure data from drilled carbonate reservoirs and subsequent analysis of these within the context of the tectono-stratigraphic evolution of the Province. Five principal pressure domains are identified, characterised by different drainage mechanisms. The result is a predictive model of overpressure, which has a clear link to geology and has been successfully tested in recent exploration wells.

Geological Setting

The Central Luconia Province is surrounded by deep basins on the NE, N and W sides. In the South it borders the heavily compressed Balingian Province flanking the shores of NW Borneo. Although relatively stable and flat compared with the surrounding areas, the substrate of the carbonate province is structurally divided into a number of regional highs and troughs, which are themselves dissected into localised highs and lows (Fig. 1).

Three structural events have significantly affected the block's evolution in times relevant for the carbonate play discussed here: (i) dilation and associated growth-faulting giving birth to the 'Mid-Miocene Unconformity' or 'MMU' at c. 15MA, (ii) rapid subsidence of the Eastern fringes of the Province across the so-called West Baram Line and in the area known as the East Trough some 12-9MA, and (iii) compression in the Late Pliocene leading to inversion and denudation in the South, concurrent with tilting and a rapid deposition in the North (Fig. 2).

Carbonate build-ups were mostly initiated at the MMU and evolved in interaction with contemporaneous clastics and their depositional environs. In general, build-ups are observed to have died earlier, and have lower relief (<2000ft) in the South,

while they become gradually longer-lived, higher (>3500ft) and reaching into younger levels of the overburden stratigraphy, northwards. Mild differences in subsidence seem to have had profound effect on carbonate growth. Regional highs are typically occupied by large platforms, while pinnacles mostly populate regional troughs.

The overburden clastics are organised into shallowing- and sanding-up sequences and parasequences on various scales (Fig. 2). Regional sequence-stratigraphic framework established for the Province allows subdivision of the overburden into domains according to inferred ability of the strata to conduct fluid flow. This relates to predominant lithology (i.e., shale vs. sand) and connectivity of flow units.

Pore Pressure and Subsurface Plumbing

Overpressures in the carbonate build-ups in Central Luconia may be generated through inflation by tapping into pre-MMU clastics, where pressures are generally 2000-6000psi above hydrostatic, and/or by insufficient draining of fluids from the post-MMU sediments. The latter mechanism seems to be chiefly responsible for the observed overpressures, as in all deep wells distinct ramp-ups in formation pressure are observed below the carbonates. Five plumbing systems are recognized in the post-MMU stratigraphy, which seem to act to relieve pressures in different ways (Fig. 3).

'Jintan Aquifer Plumbing' comprises carbonate build-ups located along the edges of the Jintan Trough in the NW of Central Luconia (Fig. 1), which show consistent overpressure of 1200-1300 psi. The inflation in pressure is likely caused by the deep burial of the central part of the trough, and the communication within the apparent 'pressure cell' is thought to be via connected carbonates in the underlying 'Megaplatform' and/or via the Upper Cycle V clastics.

'Lower Cycle V Plumbing' is interpreted to drain excess fluids from early buried carbonate build-ups whose overburden lithologies consist of shale, ratty sands, and marls. Great variations in overpressure in the order of 5000psi are observed between build-ups located near to each other, and are interpreted to result from variable connectivity of permeable streaks

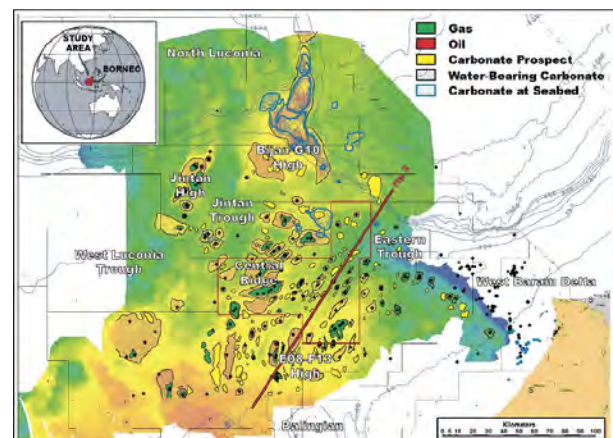


Figure 1: Study area.

contained within the generally low-permeability lithologies. This interpretation is corroborated by the apparently random exploration success in build-ups in this group: dry wells are found in the neighborhood of build-ups filled-to-spill, with no obvious variations in the surrounding geology. Overpressures do seem to respond to subsidence. High overpressures are found in the centre of the East Trough and near West Baram Line, while build-ups on the E08-F13 High consistently show about 100psi of overpressure (Figs. 1, 3A).

'Upper Cycle V Plumbing' appears to be responsible for draining of build-ups culminating between the upper TB3.2 and the lower part of TB3.6 (Figs. 2, 3B). The upper part of TB3.2 and the whole of the TB3.3 sequences are sandy elsewhere in Central Luconia, while the TB3.4 and TB3.5-Lower TB3.6 are predominantly made up of shale (Fig. 2). This pattern corresponds to Cycle-scale sea-level fluctuation: the upper part of Cycle V is a product of a prolonged highstand during which sand-prone sediments were dispersed across the shallow shelves, while the overlying Cycle VI was initiated with a major transgression and a switch from sand-rich to virtually sand-free sediment content (Figs. 2, 3B). Carbonate build-ups benefiting from this mode of fluid release show a distinct regional trend in overpressure, from pressure-blown traps in the North to hydrostatically pressured build-ups in the South. This pressure gradient is observed to correspond to thickness of young sediments of the TB3.7-TB3.8 sequences deposited in response to a regional tilt of the province beginning c. 3MA ago (Fig. 2). This interpretation is corroborated by the fact that hydrocarbon columns within this group of build-ups are systematically truncated at the tops of the TB3.2 and TB3.3 sequences, indicating good connectivity of sands observed in the upper parts of these sequences elsewhere

in the region.

'Young Clastics Plumbing' links high-relief build-ups in the northern part of Central Luconia with flanks overlapped by sands building much of the shallow part of the stratigraphy (Figs. 2, 3C). Extremely short HC columns, and a low exploration success rate encountered in this group of build-ups, seem to corroborate this interpretation.

'Blown Shale' forms a peculiar way of pressure release through otherwise impermeable overburden. Central Luconia is renowned for spectacular examples of blown traps. Carbonate build-ups located near the outer fringes of the Province appear to be particularly prone to forcible ejection of fluids into the overburden. This is evidenced by fluid-escape structures such as craters, disturbed bedding and mounds on the seabed, and interpreted to result from excess pressure generated by the weight of the TB3.7-TB3.8 wedge of undercompacted, muddy foresets deposited in response to the regional tilting of Central Luconia since some 3MA ago (Figs. 2, 3D).

Conclusions

Five plumbing systems have been identified in Central Luconia. The concept presented here accords with sequence stratigraphy and with variations in lithology derived from well logs and inferred from seismic data, and is corroborated by hydrocarbon occurrences. The model has been successfully tested in recent exploration wells, and shall serve as a basis for future pore-pressure prediction for well planning in Central Luconia. Implications for future exploration can be drawn from identification of carbonate build-ups prone to hydrocarbon columns limited by high pressures and weak overburden.

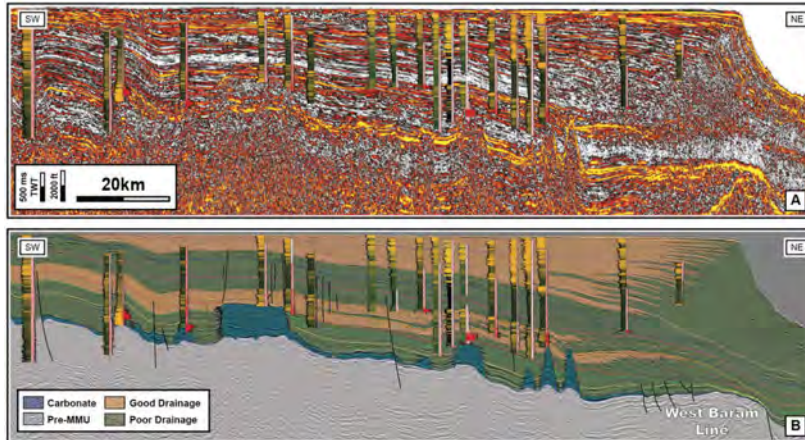


Figure 2: Regional seismic line, c. 115km long, through Central Luconia. A. Well-log data (GR/RES) and seismic amplitude as indicators of lithology. Bright colours in seismic correspond to sand in wells and vice versa. B. Interpretation of the ability of clastic sediments around and above carbonate build-ups to drain excess fluids during burial.

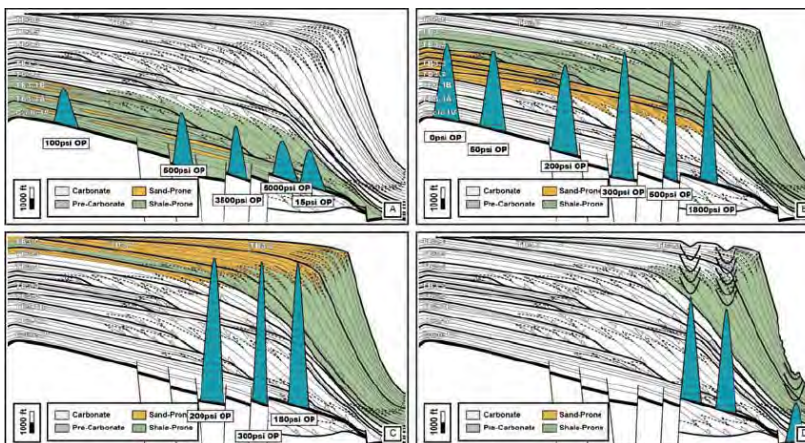


Figure 3: Four plumbing systems identified by this study. A. Lower Cycle V Plumbing. B. Upper Cycle V Plumbing. C. Young Clastics Plumbing. D. Blown Shales.

Application of Stable Isotope Analysis from Central Luconia, Sarawak: Insights into Reservoir Development and Diagenesis

K. K. Ting* (Sarawak Shell Berhad), B. J. Pierson (South-East Asia Research Laboratory, SEACARL, UTP) & O. S. Al-Jaaidi (Sarawak Shell Berhad, *Qatar Petroleum (*current))

Introduction

During the late Oligocene and Miocene period, the Central Luconia area was characterized by the development of shallow-water carbonate platforms. The study area, part of the so-called Mega-Platform and referred to as MPB-2 is a 30-x 50-km-large and 1.2-km-thick carbonate platform located in the Northern part of the Luconia province (Fig.1). The platform experienced several phases of evolution in response to syn-depositional tectonics movement of different magnitude (Ting et al, 2011). This paper is focused on the last sequence before the platforms drowns, referred to as sequence of zone 5, interpreted as a highstand sequence capped with a subaerial exposure unconformity. This sequence has core coverage in three wells, namely MPB-2a, MPB-2b, and MPB-2g. MPB-2a was drilled in the southern flank of the field, while MPB-2b and MPB-2g are located towards the northern part of the platform (Fig.1). The current model invokes a single exposure at the top of the sequence but gives no detail regarding the control of rock properties and the spatial distribution of the exposure horizon. It is therefore crucial to identify the sequence of events that led to the final range of rock properties and pore characteristics that are found today in the studied sequence.

Methodology

The study started with a detailed core inspection to recognize the facies changes, cyclicity pattern and to understand how the original depositional fabrics were modified by diagenetic processes. Dissolution patterns, cements and the geochemical signature are clues that can help identify these processes. Petrographic analysis is used to provide insights into grain-cement relationships. The isotopic geochemical signature is of particular significance in carbonates. The two most naturally abundant isotopes in carbonates, for oxygen, ^{18}O and ^{16}O and for carbon, ^{13}C and ^{12}C are commonly used in geochemical investigations. Limestones from immediately beneath a subaerial exposure surface generally have ^{13}C values that are more negative than values from otherwise similar limestone from several metres further below the exposure surface. This is attributed to the incorporation of light carbon from soil gas CO_2 into the carbonate lattice during recrystallization and cementation within the shallow vadose environment (Allan and Matthews, 1982). The carbonates precipitated in different

environments of diagenesis will generally reflect the oxygen and isotopic composition and temperature of precipitating fluid, as controlled by temperature and isotopic fractionation between liquid and mineral phase. Meteoric calcite cement therefore will exhibit relatively low oxygen isotopic ratios due to the addition of lighter meteoric-derived ^{16}O . Strontium (Sr) also provides information regarding the diagenetic environment. Carbonate minerals which precipitate directly from seawater or as a direct result of the dissolution and re-precipitation of marine biogenic carbonate, should exhibit the $^{87}\text{Sr}/^{86}\text{Sr}$ ratio of the sea water at the time of their precipitation.

In contrast, later diagenetic carbonates incorporate ^{87}Sr released during the dissolution and recrystallization. Such carbonate cements inherit the $^{87}\text{Sr}/^{86}\text{Sr}$ ratios of the evolved formation waters from which they crystallised, which typically have Sr ratios greater than contemporaneous seawater.

Results and Discussion

Detailed inspection of the core and logs reveals a stacking pattern of shallowing upwards cycles separated by a tight interval, referred as SE1 (Fig.2). This tight interval consists of coral floatstone in the mottled fine-grained bioclastic packstone at MPB-2a. Towards the north of the field, MPB-2b and MPB-2g SE1 is a heavily cemented and recrystallised horizon. This interval is also marked by strongly depleted carbon values. The downward increase of both ^{13}C and Sr compositions indicates that meteoric alteration progressively decreases downwards, suggesting less alteration, possibly due to shorter subaerial exposure events in the lower part of the section. SE1 could possibly be a single or multiple exposure horizons with an intricate pattern of dissolution channels in MPB-2a and a crystalline and cemented fabric in MPB-2b and MPB-2g (Fig. 3a). A similar trend of geochemical shift in Sr is observed in a thick coral rubble rudstone (24 ft thick at MPB-2a and 15ft at MPB-2a) that was deposited at the base of the sequence and is referred to as SE2. The fabric consists of poorly sorted angular dark grains in a fine packstone and is fining upwards to mottled fine to medium grained burrowed bioclastic packstone, interpreted as another exposure horizon.

The upper sequence, above SE1, records another facies transition from the mottled fine grained burrowed bioclastic packstone to coral floatstone at the top. This pattern is correlatable across the platform with the texture changing to coarser grain dominated towards the northern part of the buildup.

The top of the cored section at MPB-2a and MPB-2b consists of a crystalline fabric like what has been observed in SE1; it exhibits fabric-selective calcite mosaic with ghost fabrics (Fig3b). This type of delicate replacement mechanism could have been achieved via very thin films of fluids in the vadose zone (Tucker and Wright, 1990). The final exposure at the top of zone 5 does not display a geochemical signature similar to SE1, possibly because the exposure horizon was not preserved or, more likely, because the exposure period was shorter and had less impact on the limestone.

The repeated occurrence of vadose and meteoric phreatic cement textures and intracycle variation of ^{13}C and porosity

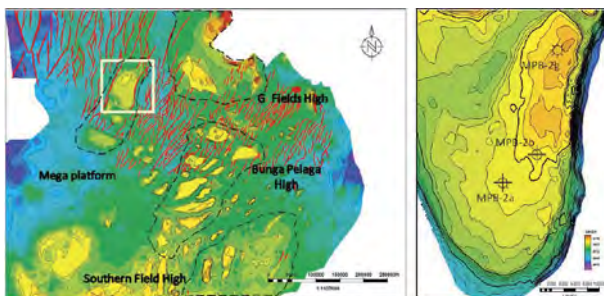


Figure 1: (Left) Top carbonate structure map showing the location of the study area (highlighted with a white box). (Right) Top carbonate structure map showing MPB-2 and the well locations.

pattern suggests that these meteoric vadose and meteoric-phreatic regimes were established at multiple stages in the evolution of the platform. This suggests high frequency exposure events where a thin freshwater lens was established, affecting only the underlying cycle or a part of it.

This observation suggests a simple carbonate island karst model (Mylorie and Mylorie, 2007). During major karst events a thick freshwater lens was established and meteoric alteration extended deeper and overprints the cyclic 13C curve. Due to the dissolution, the top of the tight interval of SE1 is characterized by the presence of isolated vugs; this type of pore structure will give a low porosity but a high permeability. The lower sequence is dominated by mouldic pores in a grainstone to packstone while the upper section is more poorly sorted and most of the porosity occurs as mini-moulds in a mud matrix (Fig 3c and 3d).

Conclusions

These isotope patterns could prove to be useful for identifying diagenetically induced porosity trends in carbonate rocks. The relevance of recognizing exposure events cannot be overstated. Their recognition has added to the understanding of

regional processes controlling carbonate platform development in the basin. Moreover, this knowledge has helped put diagenetic processes into their proper context and has aided in the understanding and prediction of reservoir-scale. This will be crucial information for further detailed study of porosity and permeability relationship and its spatial distribution.

References

- Allan, J.R. and Matthews, R.K., 1983. Isotope signatures associated with early meteoric diagenesis, *Sedimentology*, 29, 797-817.
- Mylorie, J.R. and Mylorie, J.E., 2007. Development of the carbonate island karst model: *Journal of Cave and Karst Studies*, 69(1) 59-75.
- Ting, K.K., Pierson, B.J., Al-Jaaidi, O.S. and Hague, P.F., 2011. Effects of syn-depositional tectonics on platform geometry and reservoir characters in Miocene carbonate platforms of Central Luconia, Sarawak. International Petroleum Technology Conference IPTC, IPTC 14247
- Tucker, M.E and Wright, P.V., 1990. *Carbonate Sedimentology*. Blackwell Science.

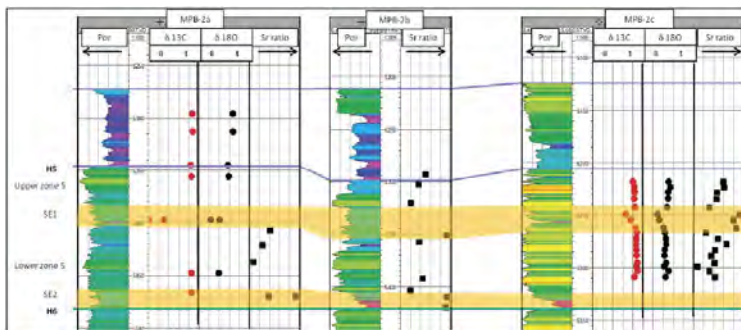


Figure 2: Vertical and lateral trends in geochemical data with porosity. SE1 and SE2 interval are marked by the strongly depleted carbon and oxygen value with increasing Sr ratio value.

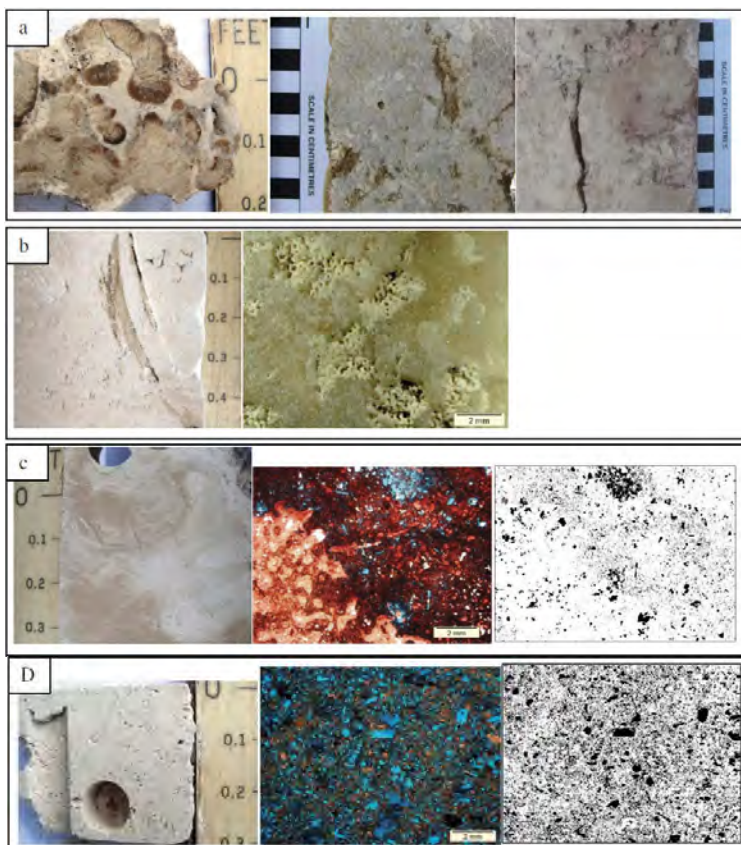


Figure 3: a) Core photo of SE1 interval, coral floatstone in the fine-grained bioclastic packstone at MPB-2a (first left), heavily cemented and recrystallised fabric with occurrence of large vug at MPB-2b and MPB-2g (right). b) Core photo of crystalline fabric on top of sequence of zone 5 (left, close up inspection of hand specimen (right)). c) Core photo of poorly sorted coral floatstone in mud matrix (first left). Thin section and binary picture of shows cemented coral grain with most of the porosity occurs as mini-moulds in a mud matrix (pore in black color) (right). d) Core photo on lower sections of grain dominated fabric (first left). Thin section and binary picture shows dominated mouldic type porosity (pore in black color) (right).

Converted Waves Seismic Imaging : Importance of Gamma Estimation

A. G. Mohd Adnan* (PETRONAS Research SDN BHD) & A. R. Ghazali (PETRONAS E&P Technology Centre)

Introduction

There are several seismic methods to image gas cloud areas such as multi-component Ocean Bottom Seismic (4C OBS) (Li et al., 2001 and Akalin et al., 2010) and full waveform redatuming operators (Ghazali, 2011). Converted wave (S-wave) travels through the subsurface rock matrix and not affected by the compressibility or the bulk modulus of the rock properties. It is used to improve imaging within and below gas accumulation, and increased the vertical resolution for the P-wave image. One of the most crucial steps to achieve an optimum subsurface response of the converted shear wave (PS) from compressional wave (PP) is to apply an accurate V_p/V_s ratio (gamma) operator in the stack and migration process. In this paper, we studied gamma estimation for 4C seismic imaging and a case example from an offshore field Malaysia is shown. Other special processes that we applied in the processing of the P and S-wave are anisotropic rotations, S-wave receiver statics, asymmetric and anisotropic binning and pre-stack migration with scanned gamma (VP/VS) to improve the final result.

Data preparation

Primary step in converted wave processing is to ensure the vector fidelity of a dataset which involved in positioning and orientation correction of the receivers into radial and transverse vector directions. Figure 1 shows the radial and transverse stack results after XY transformation where Figure 1b display the radial stack that provide a better image as compared to the transverse stack (Figure 1a). This is due to the direction of the radial is coaxial to the source while the transverse only recording the reflection of shear data. Low energy distribution on transverse stack section suggests that minimum polarization of shear wave occurs in the area. This is important for deghosting, multiple attenuation and separation of P and S-waves (Hokstad et al., 2002).

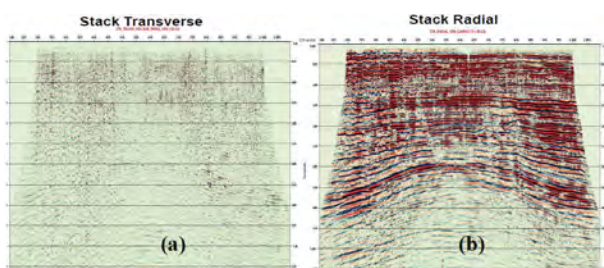


Figure 1: (a) Radial stack section, and (b) transverse stack section.

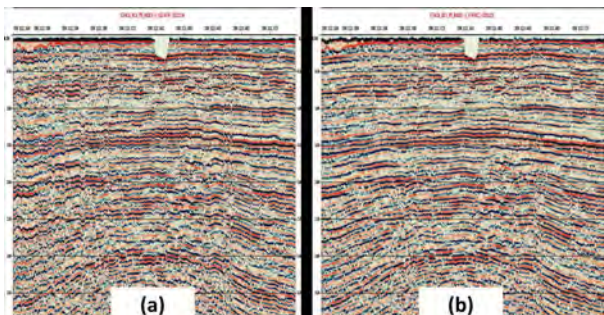


Figure 2: (a) No static correction, (b) Reflectors are more continuous after static correction.

In this field data example, the receiver static values are calculated from the P-wave data that is then used as a reference in the shear wave static calculation. In Figure 2a shows PS reflectors static time shift jittering due to the slowness of the shear wave velocities in the near surface and Figure 2b shows result after the static correction that gives better reflectors continuity.

Estimation of gamma operators

We derive the gamma analysis by two methods: vertical gamma analysis and variable gamma analysis. Vertical gamma operator is determined by correlating trace to trace PP and the stretched PS (time stretched to the same level to the PP time). In the variable gamma analysis, we use several constant gamma values to stack and scan the optimum stack image in the asymptotic common conversion point (ACCP) binning. By selecting the best stack bin associated with specific gamma values, we then build the time and space variant gamma operators that are then applied throughout the whole seismic data. In order to QC the quality of the gamma operator, we then pre-stack migrate the data using Kirchhoff pre-stack time migration and check the degree of flatness of the common image gathers (CIG) after pre-stack time migration. The rows, as illustrated in a matrix form of Figure 3, shows variation of gamma values by a certain percentage; and the columns, shows percentage variation of PS velocities. In the final section, Gamma value with 2.25 with 98 percent of velocity which provide the best ratio of V_p/V_s to flatten the common image gather for to this data set. The other gamma value is not suitable due to the high and low V_p/V_s ratios. After migration, vertical gamma is then used to stretch the PS migration time to the same level with the PP section. This is to ensure the geological structural integrity of PP and PS section is similar.

Conclusions

A case study on the effectiveness of gamma estimation in converted wave imaging is shown. Although the analysis of the gamma estimation is expensive as it involved pre stack migration process, it is required to get an accurate gamma operator for optimum PS image. An accurate gamma operator in converted wave has improved the imaging within and below the gas clouds as shown in the Malay Basin data example.

Acknowledgement

We would like to thank PETRONAS Research, for giving permission to publish this work. We would also like to express our appreciation to the PETRONAS E&P Technology Centre (EPTC) and PETRONAS for the support.

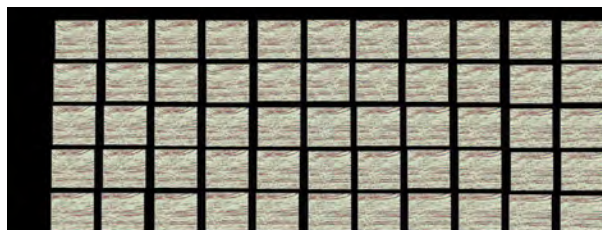


Figure 3: Velocity and Gamma analysis on common image gathers (CIG)

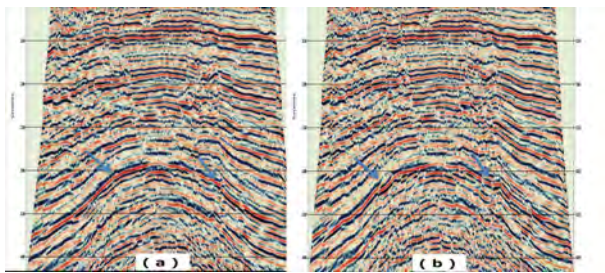


Figure 4: (a) Gamma estimation for asymptotic common conversion point binning (ACCP), $\gamma=2.5$, (b) $\gamma=3.0$.

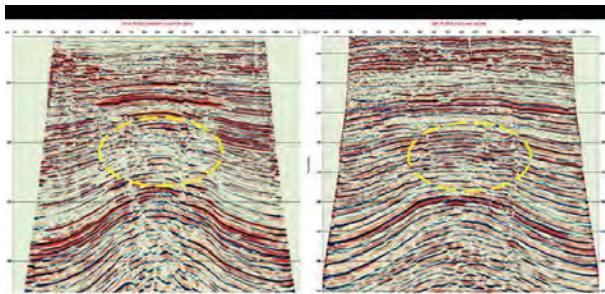


Figure 5: Result of the 2D processing of PP & PS multicomponent data set. a) 2D PP Pre-Stack Time Migration and b) 2D PS Pre Stack Time Migration.

References

- Akalin M. F., et al., 2010, 3D-streamer and 4C-OBC seismic imaging in gas cloud affected area offshore Malaysia: Mediterranean Offshore and Exhibition, MOC 2010.
- Ghazali A. R., 2011. True Amplitude Seismic Imaging Beneath Gas Clouds, PhD Thesis. DELFT University of Technology
- Hokstad, K, Mjaaland, S., Maaø, F. and Don, H., 2002, Vector Fidelity of Ocean-Bottom Seismic Data, Offshore Technology Conference.
- Li, X.-Y., Dai, H., Mueller, M., and Barkverd, O. I., 2001. Compensating for the effect of gas clouds on C-wave imaging: A case study from Valhall: The leading Edge, 20, no.12, 1351-1360

Application of TTI Reverse Time Migration, Deepwater Offshore Malaysia

J. Sun* (CGGVeritas), B. Mishra (CGGVeritas), C. Jiao (CGGVeritas), J. Sun (CGGVeritas), G. Hodgkiss (CGGVeritas) & A. Bisset (Murphy Corporation)

Introduction

In this paper we present a case history of applying TTI RTM (Reverse Time Migration) for imaging in a deep-water area offshore Malaysia. Use of RTM is not new but examples tend to come from areas such as the Gulf of Mexico and North Sea and as such, the example presented here may be the first of its kind in South East Asia. The project was started in 2009 and completed in 2010.

The value of RTM lies in its ability to handle energy propagation through complex velocity models and to image steeply dipping reflectors. It is the preferred imaging tool in areas where sharp velocity contrasts due to salt, or other high velocity bodies, cause other imaging algorithms to be less successful primarily due to multi-pathing of the recorded seismic energy. A unique feature of the current example is that the multi-arrivals are due to low velocity zones rather than high velocity bodies as in other recorded cases. We show, using impulse response analysis and actual data, that RTM is superior to Kirchhoff migration even in the absence of high velocity bodies.

Processing Flow

There are four main stages in the processing.

1. Noise removal. The seismic data are very noisy, mainly due to surface-related multiples and diffractive multiples. 3D SRME, Radon and amplitude/frequency-based diffractive multiple removal methods were used in the noise removal. Dip filters were also applied in the deep part to control remaining noise patterns. Despite the process, the signal/noise ratio is still relatively low.
2. Data regularization. For Kirchhoff migration, the data was regularized within common offset using a dense subsurface grid of 12.5m x 12.5m. For RTM, the traces were further adjusted to a shot point interval of 50m and a surface receiver grid of 25m x 25m. Shot line spacing is 400m.
3. Velocity model building. ATTI (Tilted Transverse Isotropy) anisotropic velocity model was built using six iterations of 3D tomography incorporating well logs and geological constraints.
4. Imaging. Migration half-aperture is 5km for both Kirchhoff and RTM. For RTM, common shot migration was used, with maximum frequency of 40 Hz.

Seismic Data Comparison

One inline and one crossline were selected for comparison of Kirchhoff and RTM imaging. Figure 1 shows part of the inline stack section. The Kirchhoff stack on the left has more noise than the RTM stack. The difference in signal/noise ratio increases with depth. Some structures shown in the RTM stack are hardly visible on the Kirchhoff stack. Since the input and the velocity model are the same for the two results, the difference in quality can only be attributed to migration algorithm.

Figure 2 shows a comparison on the crossline, which cuts across the dominant folding structures. In zone 1, the vertical flank of the fold is imaged in both stacks but the RTM result is clearer with less migration swing artefacts. The vertical flank terminates at the lower end by a fault (zone 2) that is interpretable in the RTM stack but not in the Kirchhoff one. Finally in zone 3, the Kirchhoff stack has strong migration swings while the RTM stack is clean. Note that a 40Hz high cut filter was applied to the Kirchhoff stack (in time domain) to ensure that the observed difference is not due to difference in frequency content.

Impulse Response

We performed impulse response analysis in order to better understand the observed differences. In Figure 3, A and C show a Kirchhoff impulse response on an inline section and a depth slice, while B and D show a corresponding RTM impulse response on the same inline section and depth slice. The red line on the vertical sections is the water bottom, and the area coloured purple is a low velocity zone due to gas accumulation. The low velocity zone caused severe distortion and multi-pathing as the seismic wave passes through it. The RTM impulse indicates that all the arrivals are accounted for whereas the Kirchhoff result has only a limited subset. That means the Kirchhoff migration is less likely to migrate all recorded energy to its correct location than the RTM, which accounts for the presence of significantly more noise in the Kirchhoff images. Note that the effect of multi-pathing gets more prominent as the wave front moves away from the low velocity zone. Therefore we should expect to see more difference in image quality in the deeper section, which is what we observed in Figures 1 and 2.

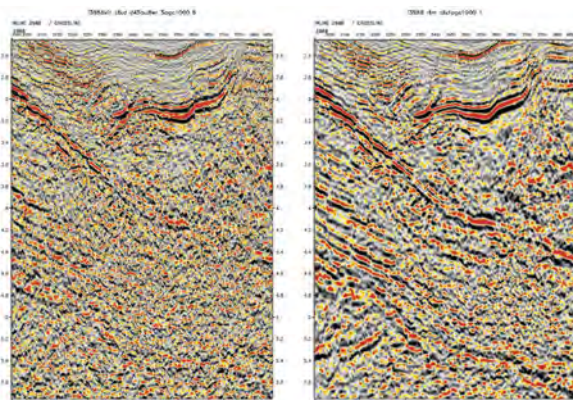


Figure 1: Left is Kirchhoff migration; right is RTM.

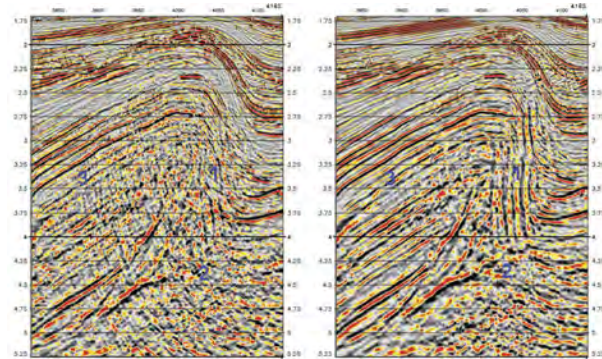


Figure 2: Left is Kirchhoff migration; right is RTM.

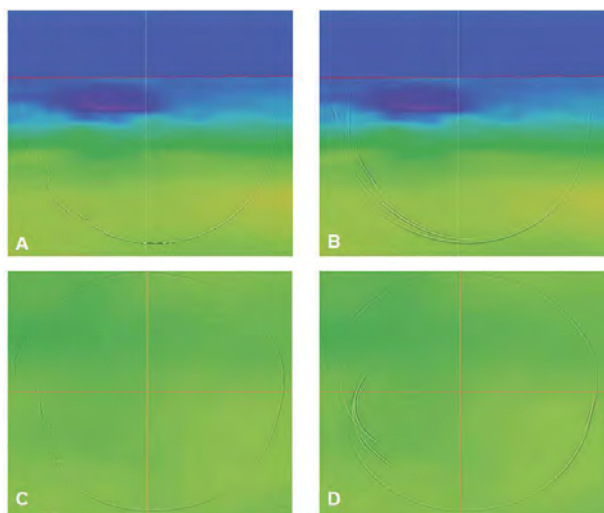


Figure 3: Impulse response analysis.

Conclusion

We have presented a case history of applying RTM for imaging subsurface structures, and presented comparisons to show that RTM is a better imaging tool than Kirchhoff migration in this context. We noted that the advantage of RTM gets more obvious in the deeper section, away from the low velocity zone that is responsible for the multi-pathing.

Acknowledgement

We thank Murphy Corporation, Petronas Carigali and CGGVeritas for permission to publish this paper. We thank Joe Zhou, Christian Milne, Xie Yi, Melanie Vu, Khek Lay Kin, Rahim Arshad, Wan Zurushdi and all other people who contributed to this study in various ways.

Application of Upscaling Permeability Workflow: Pore to Core Plug Scale on Malay Basin Thin Sections

L. A. Lubis* (Universiti Teknologi PETRONAS), Z. Z. Tuan Harith (Universiti Teknologi PETRONAS), K. A. Moh Noh (Universiti Teknologi PETRONAS), H. Khairy (Universiti Teknologi PETRONAS) & A. Moh Salih (PETRONAS E&P Technology Centre)

Introduction

Permeability is the most difficult parameter to describe. Unlike porosity, detailed distribution of permeability cannot be remotely mapped since it poorly correlates with elastic properties, parameter that usually obtained from remote acquisition such as seismic and well log. Collecting physical core plugs along selected depths of petroleum wells and measuring permeability of core plugs in the laboratory, until now, is the most reliable and essential way to obtain special distribution of permeability.

For unconsolidated samples such as cuttings, chips and sidewall core plugs, although can be obtain from almost all depth of the wells however these type of samples cannot be measured using usual equipment for measurement, as their do not have enough range size to conduct experiment in laboratory. Most of these types of samples were used to created thin section for geological evaluation and mineralogy sorting purposes, stored in oil companies samples database and it's rarely used to estimate physical properties.

The main purpose of this paper is to present the application of our newly develop permeability prediction workflow which can be implemented in real time on standard personal computer. The workflow was applied on three thin sections from Malay Basin. We used the concept of upscaling permeability to estimate laboratory scale permeability from pore scale information. Pore scale permeability is calculating on 3D generated porous media using fluid flow simulation. In our work, we modified Keehm's methodology (Keehm et al., 2004) and adding new parameter to improve computational time of 2D to 3D porous media reconstruction and compared with known sample from 3D CT-Scan image.

To cover core plug scale information from thin section, full thin section image was acquired. Once full thin section image is obtained, the grain size vertical profile trends were calculated from images.

The building blocks were determined based on the trends showed from grain size vertical profile. The building blocks were used as a benchmark to upscale permeability from pore to core plug scale. The results from this workflow will be compared with lab data to show the accuracy of our workflow.

Methodology

Full thin section image is required as an input for the new workflow to predict laboratory scale permeability. We assume the length of full thin section image has the same length with core plug. To obtain this objective, 12.5 times magnification was used to acquire the images. Figure 1 shows steps to obtain full thin section image.

The next step is to calculate grain size vertical profile. Grain size vertical profile is used to define the heterogeneity on full thin section image. We define the heterogeneity as the coarse and fine part of the section. The first concept of this method was first employed on sand sediment by Rubin (2004). In our study we modified the MATLAB algorithm to fit the thin section scale. The actual grain size cannot estimated with this method but enough for tracking changes in sediment grain

size, which in some settings related flow changes. Figure 2 shows how effective this method to determine coarsening and fining trends of digital image of sandstone. Area b with yellow arrow determines the fining part of thin section. This area can be clearly observed on the image. Area a with yellow arrow determines the coarsening part of thin section.

The reconstructed 3D porous media is generated using geostatistics algorithm from SGEMS. Figure 3 shows inputs for simulation. Once the 3D porous media generated, permeability is estimated by conducting numerical flow simulations on the 3D porous media. The Lattice Boltzmann Method (LBM) for fluid simulation is used to estimate pore scale permeability. This method is a robust technique that simulates flow according to simple rules governing local interactions between individual particles and recovers the Navier-Stokes equations at the macroscopic scale.

Final step is to upscale permeability from pore to core plug scale. The same concept as conventional reservoir upscaling is used in this step. The bulk permeability horizontal (K_h) and vertical (K_v) to bedding are calculated as weighted arithmetic and harmonic averages (Weber & Van Geuns, 1990), respectively, using the corresponding values. The fractions of Building blocks are determined from grain size vertical profile.

Once the coarse and fine parts are identified, images are selected which represent each part. The following formulas are the examples of effective permeability formulas for three fractions of building blocks.

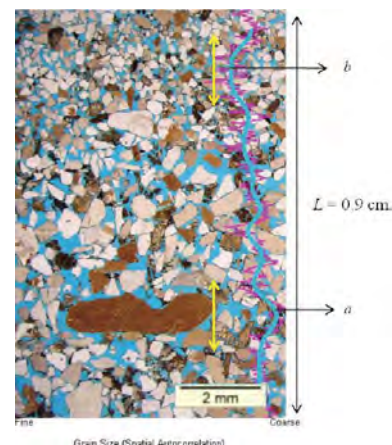


Figure 2: Grain size vertical profile of thin section. a arrow with yellow line is the coarse area (porous) and b arrow with yellow line is the fine area (tight).

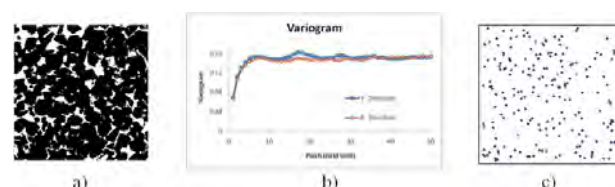


Figure 3: Input parameters for simulation: porosity, variogram and sample points extracted from training image.

$$K_h = \frac{k_a l_a + k_b l_b + k_c l_c}{L} \quad (1)$$

$$K_v = \frac{k_a k_b k_c L}{k_a k_b l_c + k_c k_b l_a + k_c k_a l_b} \quad (2)$$

Results

This part presents the application of our newly developed permeability prediction workflow. Since we calculate laboratory scale permeability from pore scale permeability, we need to examine and show the accuracy of fluid flow 3D reconstructed porous media for calculating pore scale permeability. The methodology was tested on 2D (training image) which was cut and selected by considering the REV (Representative Elementary Volume) concept from 3D CT-Scan image of sandstone. We adopted Keehm's methodology (Keehm et al., 2004) and modified this method by adding sample points as a new parameter to improve computational time for reconstruction of 3D porous media. Table 1 shows the accuracy of pore scale permeability on reconstructed porous media compare to 3D CT-Scan image of sandstone.

Figure 4 shows the steps and results of permeability prediction workflow application on Well B Malay Basin thin section.

Table 1: Comparison of physical properties between reconstruction method and CT-Scan image.

Sample	Original 3D CT-Scan		Reconstructed 3D Porous Media	
	ϕ (%)	K (mD)	ϕ (%)	K (mD)
B	19.6	1360	19.8	1512
S(8)	34	13169	35.1	13105
F	14.7	2262	15.1	1550
S(2)	24.6	3898	25.8	4244

Table 2: Comparison between upscaling permeability workflow application on Malay Basin thin sections with core plug measurement.

Thin Section	Upscaling K Workflow			Lab Data	
	ϕ (%)	K_v (mD)	K_h (mD)	ϕ (%)	K (mD)
Well A	20.2	544.4	1186.6	28.7	1085
Well B	22.5	715.3	3215.9	30.6	3700
Well C	20	274.1	590.3	24.3	287.6

section. From left to right, result of full thin section image on Well B thin section, blue line is grain size vertical profile trends calculated on the thin section which is also the average trends of pink line. The representative 2D images were selected on each building block and fluid flow simulation was applied on each generated 3D porous media.

Table 2 describes the accuracy of application of the workflow on three Malay Basin thin sections. The results on three thin sections showed good agreement with laboratory data. The accuracy of this workflow is ~85 - 90 % on each thin section compare to physical lab measurement. This workflow can be applied on standard personal computer with reasonable running time (~180 seconds).

Conclusions

We have demonstrated that our new workflow is efficient to predict laboratory scale permeability of sandstone using thin section image information. The results showed good accuracy with laboratory measurement. This approach is practical, easily repeatable (in real time) and can be used as an alternative method when core plugs for permeability measurement is not available.

References

- Keehm, Y., Mukerji, T., and Nur, A., 2004. Permeability prediction from thin sections: 3D reconstruction and Lattice-Boltzmann flow simulation. *Geophysical Research Letters*, 31, L04606.
- Rubin, D. M., 2004. A simple autocorrelation algorithm for determining grain size from digital images of sediment. *Journal of Sedimentary Research*, 74, pp. 160-165.
- Weber, K. J. and Van Geuns, L.C., 1990. Framework for constructing clastic reservoir simulation models. *Journal Petroleum Technology*, 10, pp. 1248-1297.

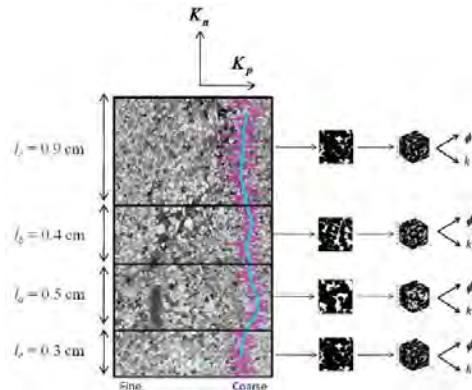


Figure 4: Building blocks for upscaling permeability workflow on full thin section image of well B Sandstone.

Studying Carbonate AvO Response

Y.F. Tiong* (Sarawak Shell Berhad)

AvO inversion has not been done for carbonate fields because carbonate rock does not normally display AvO effects. However, there is no hard evidence for that, so this project was setup to investigate if there are any meaningful AvO effects in Sarawak carbonates.

The project was started by studying some similar works done in the past. Some studies hinted at the existence of two types of overburden shale in Sarawak carbonate fields, i.e. hard and soft shales. There was another study that encouraged the usage of physics-based equations, instead of well data based regressions. These findings were input into this project.

Eight wells are used in this study: E6-3, E8-101, E11-106, E11 Deep-1, F14-2, F28-2, Jintan-3 and Serai-1. They are selected based on well log quality and the availability of Gassmann brine substituted logs. These wells also have measured vs logs, so that data driven rock property trends can be derived.

To model any kind of AvO response, there must be rock property trends. A set of trends were derived each for shale and carbonate. There are two kinds of overburden shale, hard and soft, so the depth (TVDss)-vp and vp-vs trends differ. The vp- ρ trend is the same for both types of shale. As for carbonate, the equations are porosity (ϕ)-vp, vp-vs and ϕ - ρ . A set of the equations were derived each for gas- and brine-filled carbonate.

With a complete set of rock property trends, the next step of the project is modeling AvO response. There are three types of interfaces modeled: top carbonate, intra carbonate and gas-water contact. Two types of modeling were employed in

this project. Blocky modeling synthesizes rock property values from the derived trends, so the AvO responses are obtained from there. Monte Carlo modeling assigns an uncertainty range for each rock property and study AvO responses from many modeled interfaces.

For top carbonate, the results implied that AvO effects are bigger when shale type is soft. Also, shale type can be differentiated. For intra carbonate, the AvO effects are minimal between the two fluid types. Monte Carlo modeling showed that gas-water contacts can have different AvO response compared to intra carbonate. However, between the two types of gas-water contacts, i.e. changing porosity and constant porosity across the interface, their AvO responses are very similar.

The modeling results were tested against well synthetics to verify whether they could be observed when there were wavelet effects, i.e. tuning and interference. Well synthetics supported that AvO effects are bigger in top carbonate when the shale type is soft. However, shale type is not as easy to differentiate. Intra carbonate well synthetics were not studied because it was difficult to identify an isolated interface. Gas-water contacts synthetics did not support that the interface has different AvO response than intra carbonate, but they verified that the interface has similar AvO response even when porosity varies.

The inconsistency between modeling results and well synthetics could be because of the simplicity of the modeling used in this project. Several improvements were suggested.

Status of Exploration on Shale Gas Resources in India

A. Boruah* (University of Baroda, Gujarat, India)

Natural gas is rapidly substituting crude oil to suffice the growing energy requirement of today's world. The rising oil prices, high input cost in exploration and production of hard oil resources and relative abundance of gas resources have fuelled the interest towards gas resources. But the consumption of natural gas is increasing rapidly and the growing gap between natural gas consumption and supply has spurred interest in development of unconventional gas resources. Coal Bed Methane, Basin Centred gas, shale gas, underground coal gasification (UCG), gas hydrate are the important unconventional natural gas resources. India is having the immense prospects of unconventional shale gas resources. Commercial exploration of these shale gas resources can effectively make the global natural gas curve more elastic.

The data base on the shale gas potential in India is rather sketchy and requires exhaustive investigations of all the shale beds having significant organic matter and maturity. The present paper deals with the investigations and evaluations of shale gas

resources of prospective sedimentary basins in India. It also attempts to discuss the gas generation and retention mechanisms within shale rock. The available data suggests that the shale gas evaluation requires detailed study of the; (i) type and amount of organic matter, (ii) presence of trace elements which can enhanced the chemo-genesis, (iii) magnitude and duration of thermal maturity, etc. Thermal maturity, sorbed gas fraction, reservoir thickness and geographic extent, total organic content, volume of gas in place, mineralogy, water saturation, fracture types, reservoir heterogeneity etc are the controlling factors in shale gas production. But both the geological and geochemical parameters may show wide variations in different shale gas systems and even most of the world's commercial shale gas reservoirs exhibit wide ranges of these parameters, hence making it more difficult for establishing the resource potential of the shale gas.

Time-Pressure Correlation to Estimate Dewatering Time for Coalbed Methane Reservoir at Saturated and Undersaturated Condition

D.C.I. Hutami* (Institute Technology of Bandung), I.K. Alhamzany (Institute Technology of Bandung), I.G. Permana (Institute Technology of Bandung), S.K.H. Wicaksono (Institute Technology of Bandung), H.W. Alam (Institute Technology of Bandung) & U.W.R. Siagian (Institute Technology of Bandung)

Introduction

Coalbed Methane (CBM) is methane gas that is formed naturally during coalification process and trapped within the coal matrix. Coalbeds Methane (CBM) usually is naturally fractured, low pressure, water saturated gas reservoir. During the progression of coalification from peat to anthracite, methane and water may be generated. The amount of water produced from most CBM wells is relatively high compared to conventional natural gas wells because coal beds contain many fractures and pores that can contain and transmit large volumes of water. The water in coal beds contributes to pressure in the reservoir that keeps methane gas adsorbed to the surface of the coal (Rice and Nuccio, 2000).

Initially the natural fractures of the coal are typically water saturated. At undersaturated condition, when reservoir pressure is above critical desorption pressure, only water is produced. This water has to be removed in order to achieve any significant gas production. Dewatering of the coal seam reduces the hydrostatic pressure of the reservoir, which allows the gas to be desorbed from the coal matrix. At the same time, lowering the water saturation level of the reservoir increases the relative permeability of gas, thereby permitting the desorbed gas to flow to the wellbore. Proper dewatering of CBM wells is the key to efficient gas production from these reservoirs. The time required in dewatering stage can last for several months to several years, depending on the level of maturity and moisture content of the coal formation (coalification) itself. Dewatering processing consumes much times and it is not effective for well development time. The problem encountered during dewatering process to determine the time of gas began to flow, where the reservoir is still undersaturated condition. In this paper, authors would like to recognize dewatering time using time-pressure correlation.

Method and Theory

Firstly, we define critical desorption pressure as the pressure when the first gas is released from the coal matrix. Critical desorption pressure, for example as illustrated on Figure 1, is the pressure on the sorption isotherm that corresponds to the initial gas content (Aminian, 2003). By lowering pressure of coalbed methane cleat system in dewatering process until its critical desorption pressure, gas will desorb from the coal matrix.

Secondly, we define dewatering time into two different terms, as shown on Figure 2 and Figure 3, based on the flowing gas presence in dewatering process : (1) the time needed from dewatering process until the first gas desorb and (2) the time needed from dewatering process until the maximum gas production rate.

For saturated condition at typical condition for CBM reservoir, correlation by Thungsungtonkhum (2001) will be employed. At this condition, there will be two phase water and gas production. The correlation shows that gas flow rate and water flow rate will be calculated from the integral function of pressure as Darcy flow because it is assumed there is no diffusion while the cleat is filled by water.

$$q_w = \frac{0,00708kh}{\ln \frac{r_e}{r_w} \mu_w B_w} \int_{p_d}^{p_{atk,rw}=0} k_{rw}(s_w, p) dp$$

$$q_g = \frac{703 \times 10^{-6} kh}{\ln \frac{r_e}{r_w} \mu_w Z} \int_{p_d}^{p_{atk,rw}=0} k_{rw}(s_w, p) dp$$

For undersaturated condition, King and Ertekin correlation will be employed by assuming there is diffusion phenomenon using Fick's Law.

$$q_{gm} = 2,697 \sigma D \rho_c V_c (G_c - G_s)$$

Dewatering time can be determined by plotting between gas rate and time. Then, it will be defined dimensionless dewatering time as :

$$t_D = \frac{t_{dewatering}}{t_{gas \text{ rate is declining} = 1000 \text{ days}}}$$

While, dimensionless for pressure is taken from its correlation with initial pressure (Pi) as :

$$P_d = \frac{P_i - P_d}{P_i}$$

From dimensionless dewatering time and pressure, it will be plotted in one linear graphic to fine the correlation.

Example

From single well reservoir simulation on figure 4, it is shown that CBM production is divided into several stages : dewatering phase, production phase, and declining phase. Production time reached lower production peak comparing with conventional gas reservoir and slowly declining until several years so that CBM has long life time. It is also shown that declining water production in reservoir affect in increasing gas production. From this example, development planning of CBM production needs to be properly done economically.

Conclusions

Authors show correlations indicating the relationship between the initial pressures at saturated and undersaturated condition versus dewatering time. The correlation between pressure and dewatering time shows linear relationship, both for dewatering terminology type 1 and dewatering terminology type 2. The correlation is only valid for coalbed methane field which has similar reservoir properties as like in this paper and it is formed in dimensionless correlation equation.

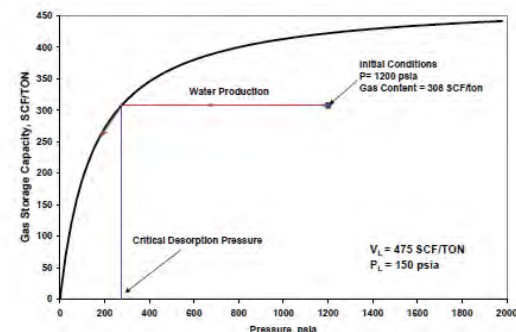


Figure 1: Critical Desorption Pressure in Typical Langmuir Isotherm (Aminian, 2003).

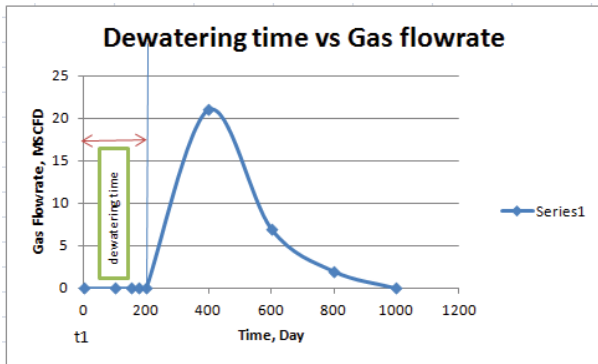


Figure 2: Dewatering time terminology type 1 which shows that dewatering time is defined as the first time gas produced in well.

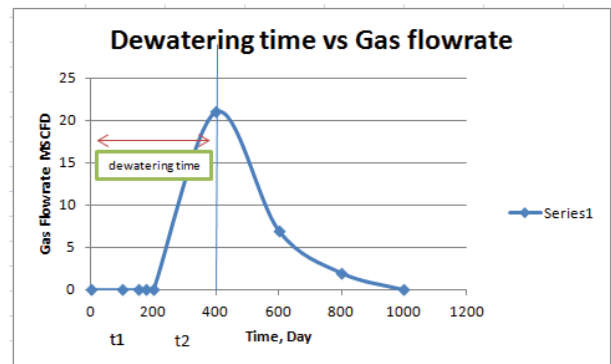


Figure 3: Dewatering time terminology type 2 which shows that dewatering time is defined as the maximum producing gas in well.

Acknowledgments

We would like to thank you to Total E&P Indonesia for sponsoring us to study master degree in Petroleum Engineering ITB.

References

- Aminian, K., 2003. Coalbed Methane – Fundamental Concepts. West Virginia University : Petroleum and Natural Gas Department, 9-10
- Rice, Cynthia A. And Vito Nuccio, 2000. Water Produced with Coal-bed Methane. USGS Fact Sheet FS-156-00 November 2000, 1-2
- Thungsuntonkhum, Witsarut, 2001. Well Deliverability of Undersaturated Coalbed Reservoir. SPE 71068, 3

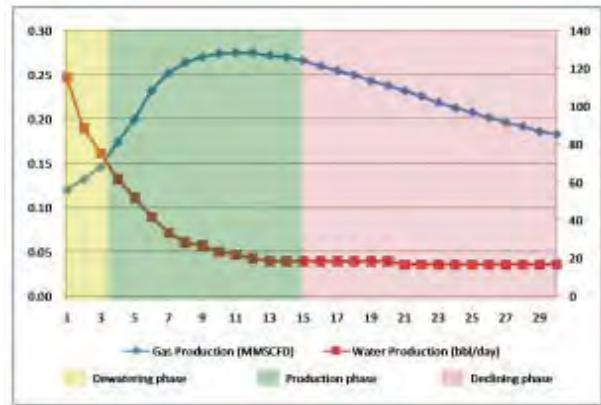


Figure 4: Single well coalbed methane reservoir simulation.

Systematic Evaluation of Play and Prospect Risk Using a New Play-Based Exploration Methodology

A. Neber* (Schlumberger), I. Bryant (Schlumberger), G. Koller (Schlumberger), T. Levy (Schlumberger), M. Neumaier (Schlumberger) & N. Tessen (Schlumberger)

Introduction

Play-based exploration offers a methodology to evaluate the various elements of petroleum systems in a regional context and then incorporate this knowledge into geologically based and objective evaluations of specific prospects. This new methodology results in documented and consistent evaluations of prospects from a portfolio for decision making concerning future activities such as data acquisition, drilling, or divestment. Transforms are used to derive play chance maps from maps of subsurface properties, rather than using traditional common risk segment maps. This method ties the geological concepts of the play directly to the chance that the play, or any element of the play, is adequate at any point within the play area. Working within a dynamic interpretation system in which the underlying play fairway maps can be quickly and easily updated and reincorporated into the play chance maps offers an advance over common risk segment maps which become static “napshots” because they are not easily updated.

We have developed a system that generates chance-of-success maps from maps of the physical elements of the petroleum system—including analysis of dynamic charge and seal chance (Bryant et al. 2012). These maps are expressed in probability units, so that simple map multiplication provides a map of overall play chance of success, but all the elements that went into that final map are readily available for discussion and, more importantly, for inclusion into the evaluation of prospects within the play. Since the maps are derived from data in a software environment that supports model-based integration, the data and interpretations used to generate the play chance assessments are stored and available for audit or revision. Similarly, new data can be readily incorporated and the play chance maps updated (Lodola et al. 2012).

Within the same application, a prospect assessment tool is used to sample the elements of play chance from the play chance maps and inputs to volumetric calculations from the play fairway maps for each prospect in the play, thereby insuring prospect evaluations are consistent with the regional play analysis. Prospect-specific parameters are combined with the play-derived parameters, and Monte Carlo simulation is used to simultaneously calculate chance of success and associated hydrocarbon volumes within the same process. The input frequency function for each parameter uses the entire range of possibilities but then is truncated at an appropriate cut-off value for each parameter. Only the values above the cut-off are sampled, assuring all resulting iterations are made up only of success case inputs.

The integration of the play and prospect evaluations assures the objectivity and consistency needed to make confident business judgements when comparing prospects.

Method

A simple method is used to transform maps of physical properties to probability maps, as shown in Figure 1. The interpreter assigns a probability that values on the input map(s) represent a point where that factor will be “adequate”. Probabilities are assigned to high and low values of a mapped property.

The algorithm in the software tool uses this function to scale the original geological maps to play chance maps. In the presented example, net reservoir thickness is being used as a proxy for reservoir presence. The interpreter has used his experience of the play to assign a range of chance of adequacy to the net thickness values. The interpreter has determined that where less than 25 m net thickness is mapped, there remains a low chance there will be adequate reservoir, in this case 20% (Figure 1).

Where the input map shows more than 50 m of net thickness, the interpreter has assigned a probability of 100%, meaning that it is certain that the reservoir will be adequate in this area. Once these parameters are set, the “Run” button transforms the map of net thickness to a chance map displaying the chance that the reservoir is present, in probability units (zero to 100%), with the lowest value in this example being 20% (Figure 2).

Chance maps for all the key elements are created in a logical, geologically based tree (left side, Figure 1). The key elements may themselves be the result of combining several subelements that make geological sense to use as proxies for each of the elements. In Figure 1, there are five elements multiplied together to give the overall play chance map. Each of these elements are the result of a logical, documented process in which subelements are combined using different ranges and different mathematical operations. Once the chance maps are created for all elements of the play chance, they are combined using the “Multiply” function (Figure 1), to generate a play chance map for the play.

Since all of the subelement maps are created in the same integrated platform, it is easy to revise even subelement maps with new information and regenerate the play chance map using that new interpretation. Interpretations of the geology that went into the play chance are well documented and ready for revision or the creation of new scenarios.

Polygons representing license boundaries may be superimposed on any or all of the play chance maps to calculate the chance of success for different blocks offered in a licensing

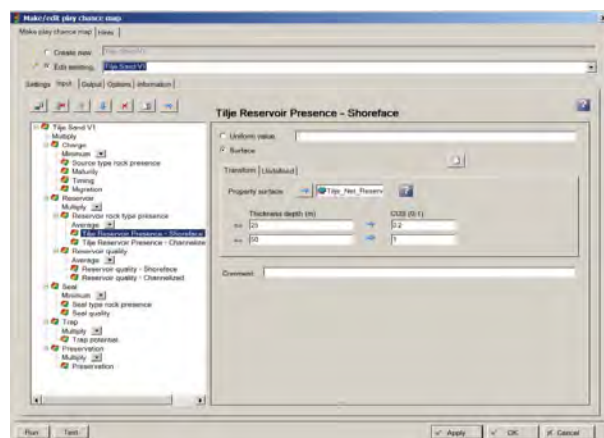


Figure 1: Screen capture illustrating the interface used to generate and combine play chance maps for each of the elements of exploration risk in a play assessment. The play elements and the multiply capability are in the tree to the left; chance of success is entered in the COS field.

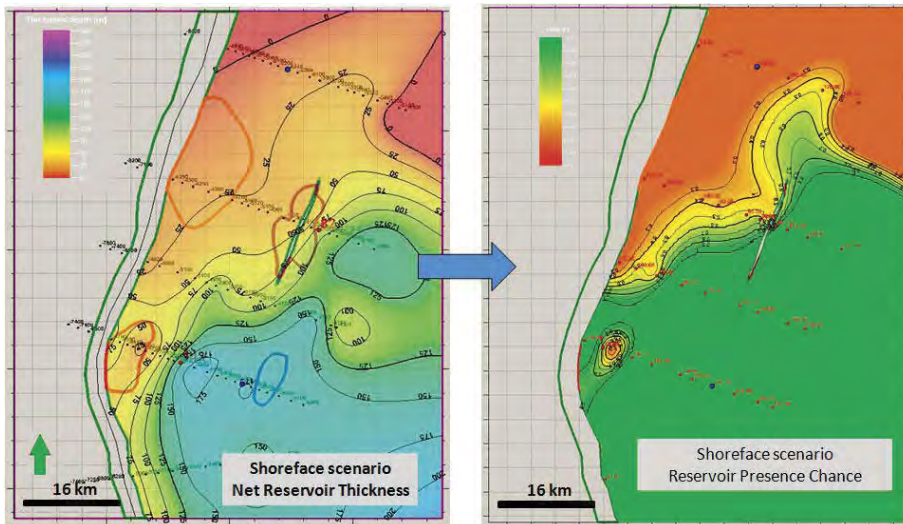


Figure 2: The mapped net reservoir thickness of the potential reservoir (left) is converted to a play chance map of reservoir presence chance (right), using the panel shown in Figure 1. Note how the map reflects the play's geology.

round. Similarly, polygons representing the prospect may be used to sample the chance of adequacy for any particular element or subelement (e.g., reservoir presence chance, charge chance, and overall play chance) for ranking of the opportunities. Similar processes can be used to extract information for the geological elements themselves for use in probabilistic volumetric calculations (e.g., porosity, thickness, and other play-defined properties) for use in a prospect assessment tool that is part of the same application.

The geoscientist can combine these play-defined chance factors with estimates of prospect-specific chance factors to calculate a prospect's chance of success (Figure 3). The combined play/prospect chance factors provide, within the same integrated tool kit as the play chance and play fairway maps, inputs for the probabilistic volumetric calculation tool which uses Monte Carlo simulation to determine not only the probabilistic ranges for volumes, but the chance of success for the prospect.

The input frequency distributions for the volumetric factors are asymptotic and shaped by the geoscientist to represent the degree of confidence in the interpretation. Fixed distribution shapes that use statistical functions, like log normal or triangular, to control the Monte Carlo sampling are replaced by a curve that is shaped by the geoscientist to represent the geological concepts. The inputs for minimum, peak, and maximum values on these distribution curves can be sampled directly from the play fairway maps for the volumetric inputs. Where the input distributions fall below the regional cut-off for that parameter, the distribution is truncated at that cut-off such that only "successful" input samples are used in any Monte Carlo iteration, and the low-end "success" input values are properly sampled to calculate potential reward volumes (Figures 3 and 4). Prospect chance of success for any input factor is derived from this same distribution by relating the area below the cut-off to the total distribution area. These are combined with the play-level chance to give the overall prospect chance of success.

This results in the calculation of probabilistic volumes and chance of success being determined in a single integrated process with a clear documented link between the volume inputs and the chance factors assigned for any prospect chance element (Figure 4). Statistics also identify the most important factors affecting the chance of success and the range of prospect volumes, facilitating documented decisions on how to pursue the opportunities that best fit the company's strategy.

Using this same methodology for all of the prospects in

a play facilitates objective comparison of each prospect and insures that the prospect assessments are consistent with the regional play evaluation.

Furthermore, since the prospect assessment remains linked to the data and interpretations in the same application, an audit trail exists. This linkage also enables rapid update of each of the prospects in a play should new data become available or interpretations change at the play level.

Conclusions

We have demonstrated how play chance maps can be generated for every element of play chance and combined within one software application to objectively build an assessment of overall play chance.

The methodology differs from traditional common segment risk mapping in that the chance-of-success maps are rigorously connected to the data and interpretation used to generate them.

We have shown how the maps generated in the play analysis may be used to provide input to prospect evaluation within the same software application. By using the maps in this way, all prospects within the play are consistent with the play concepts and, therefore, each other. Prospect-specific parameters are combined with the input derived from the play analysis in a probabilistic prospect assessment tool that resides within the same application. Since the prospect assessment is calculated in the same environment that holds the data and interpretations, it is possible to identify the volumetric elements that have the greatest impact on both chance of success and the uncertainty in the estimation of potential prospect volumes.

References

- Bryant, I., Levy, T., Neumaier, M., and Tessen, N., 2012. A Novel Approach to Incorporate Full Petroleum System Analysis into Play Risk Assessments. Abstract D005 presented at the EAGE Workshop on Petroleum Play Assessment, 13–15 February 2012, Malaga, Spain.
- Lodola, D., Martin, R.J., Casey, D.M., Davies, R.B., Sharland, P.R., and Simmons, M.D., 2012. Regional Evaluation of the Khuff Gas Fairway using a Shared Arabian Plate Earth Model and Petrel 2011. Abstract B003 presented at the EAGE Workshop on Petroleum Play Assessment, 13–15 February 2012, Malaga, Spain.

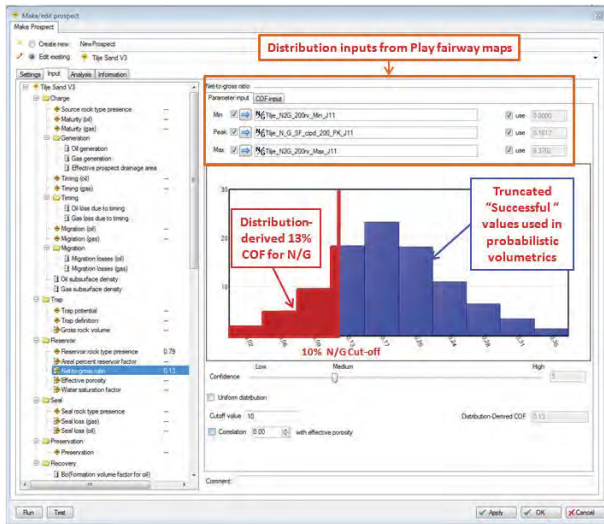


Figure 3: Screen capture illustrating the methodology used to combine play chance of success and prospect-specific parameters for prospect evaluation. COF is chance of failure. The distribution is net-to-gross ratio (N/G).

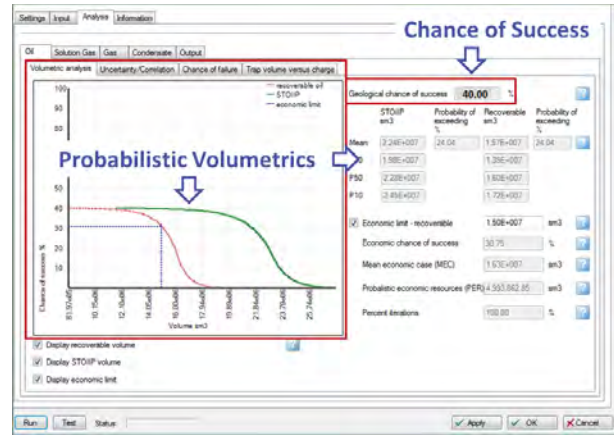


Figure 4: Screen capture illustrating the result of simulating 3000 iterations of the combined playdefined and prospect-specific parameters for an exploration prospect.

Systematic Application & Play-based Exploration Methodology Using ArcGIS in Sabah Exploration Block SB309 & SB310

S. Jamil* (PETRONAS), A. Ngau (Talisman Malaysia Limited) & C.H. Tan (Talisman Malaysia Limited)

Introduction

With discoveries harder to find, geoscientists are collecting more data than ever before and examining their findings with greater scrutiny. The key is to keeping the whole process efficient and consistent.

Play fairway mapping using play-based exploration methodology has been used to evaluate the remaining hydrocarbon potential of the Sabah basins within Blocks SB309 and SB310. It provides a consistent view of their potential and helps geoscientist to develop exploration portfolios that balance risk, prospect size and acreage availability. The study area is located in offshore Sabah Basin (Figure 1), where more than 50 exploratory wells have been drilled with variable success. In-house well failure analysis suggests the presence of adequate reservoir and valid structural trap hence the risks are perceived to be either one of the following; a) Faults Seal Failure, b) Access to charge migration.

The present study aim to improve the understanding of the basin through application of a systematic analysis of all the petroleum risks in the play fairway mapping. It is our hope therefore, that we will be able to assess the relative risk between areas, and properly rank all the ideas/leads and prospect in the study area consistently and systematically.

Methodology

Regional depth structure maps of 10 horizons (Stage III, Stage IVA-IVF and seabed) interpreted from all available 2D seismic data have been used. Stratigraphically, the study area is covered by thick successions of sandstone and shale/mudstone of early Miocene to Pliocene age. Study areas covering more than 12,000 sq km with well calibrations from about 50 wells drilled in the area have been utilised. Most of the wells penetrated no deeper than 3000m and deeper horizons were assigned according to the regional geological understanding and geological correlations.

Play-based exploration methodology demands a thorough understanding of the whole basin from the perspectives of structural (timing and tectonic history), stratigraphy and sedimentology. Several play types have been identified. This presentation will only discuss the shelfal oil play. Other types

of play identified in the study area are Basin Slope Channel and Basin Floor Fan Turbidite play.

Four petroleum system elements, namely Source, Reservoir, Trap and Seal were systematically analysed for their relative risks based on quality, quantity and confident level in the available data.

Each element will have all the defined risk polygons that took into account quality, quantity and confidence levels in the description of risks as well as the risk factors (Figure 2) are captured in the attribute tables in ArcGIS. The supporting data for risks may come from variety of sources, maturity, forms and types. Among them are geological (well data, logs, core, drilling), geochemical, geophysical, remote-sensing, gravity-magnetic and analogue data. It is important to consider element of data confidence in the risking process as it implicitly implies quantity, maturity and uncertainty in the data and the geological and/or geophysical model. By the end of the exercise, multiple polygons and sub-polygons, each with its own risk factors that have been qualified and quantified by the risking exercise described above will be generated for the same the Area of Interest (AOI) representing each play. The composite risk map (CRM) (Figure 3) is then generated, and the resultant map was the product after all the petroleum risk element maps for the play was convolved through a simple multiplication done on ArcGIS. The final polygons in the CRM can be displayed using simple four to six-color scheme (Figure 2) that reflects the degree of associated risks, red being high risk and green, low risk. In practice, risk for structure or closure are done in greater detail at prospect level.

Conclusion

1. Play based exploration methodology was successfully applied in a consistent manner for regional play fairway analysis in Sabah Blocks SB309 & SB310.
2. Method allows differentiation and relative ranking of risk between plays, stratigraphy and area within the held acreages.
3. ArcGIS is a good and right tool for integrating well, geology and geophysical data in play risk analysis exercise.
4. With increased exploration efforts, it is an effective way of reducing risk.

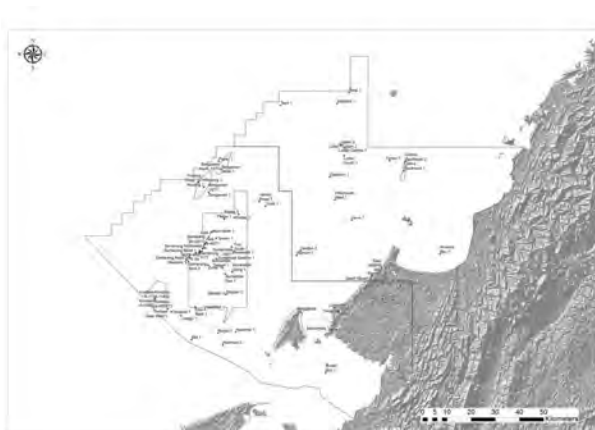


Figure 1: Location map of the study area.

Play Risk Mapping: Risk Matrix

Risk Range	Data	Models/Analogues	Confidence	Basis
1-2	Extensive and consistent	Positive alternative models possible. Uncertain analogues	High	Quality Data & Uncertain Analogues
3-4	Reasonable consistent	Reasonable alternative models possible. Uncertain analogues	Medium	Soft Data & Uncertain Analogues
5-7	Data has a positive bias	Negative alternative models possible. Uncertain analogues	Uncertain	Soft Data & Uncertain Analogues
8-9	Reasonable Data, but with negative bias	Ability of models strongly negative. Negative analogues that are similar	Low	Quality Data & Uncertain Analogues
>9	At the strongly negative	No alternative models possible. Most strongly negative results in analogues	At Question	Very Quality Data Data

*Extensive and consistent (< 1; > 9) require high confidence in high quality, hard data.
 *Analogues and models typically result in mid range values (.3 to .7)

Figure 2: Risk Matrix used in the play risk mapping exercise.

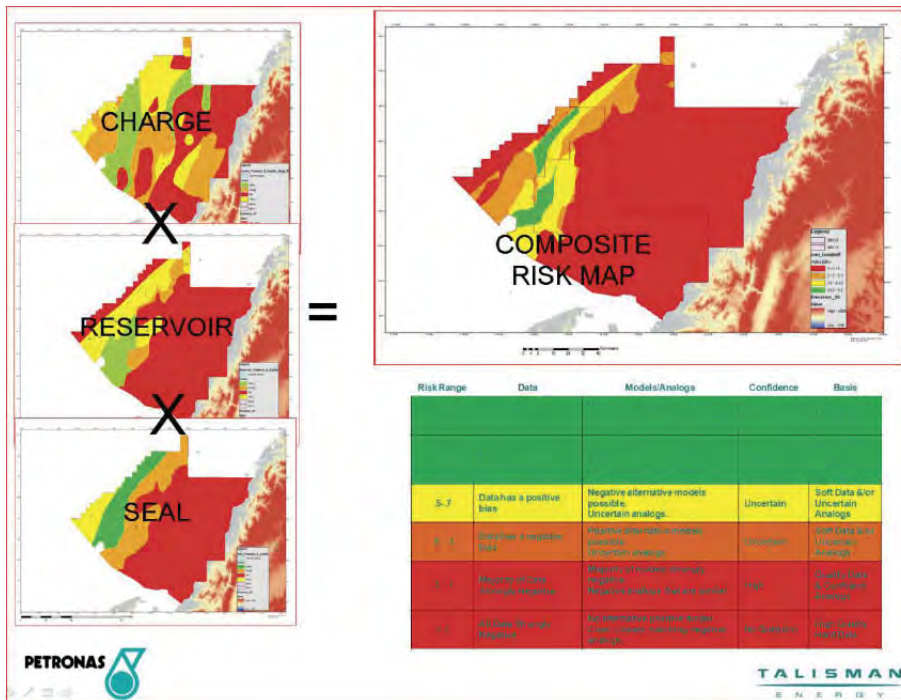


Figure 3: Composite Risk Map (CRM) of the Shelfal Oil Play by convolving individual risk map elements.

Acknowledgement

1. Petroliaim Nasional Berhad (PMU) for permission to use and release of the data
2. To Talisman's Quality and Assurance Team for providing valuable guidance in the preparation of the play risk assessment
3. To all colleagues in Talisman Sabah Exploration team for the valuable inputs and tireless effort in completing the regional basin play risk assessment.

References

Exprodat, 2010. Play Fairway Mapping with ArcGIS Exprodat Training Course, 7 - 140

Deepwater Reservoir Geometry and Characterisation: Analogue from the Semantan and West Crocker Formations

H. H. Ismail* (PETRONAS Research Sdn Bhd), M. Madon (PETRONAS Research Sdn Bhd), Z.A. Abu Bakar (PETRONAS Research Sdn Bhd) & M.S. Leman (National University of Malaysia)

Introduction

This paper is aimed to highlight the deepwater sedimentary successions as potential analogue for deepwater reservoir geometry and characterisation. The understanding of sandbody geometry, heterogeneity and characterisation of deepwater reservoirs is important for better prediction of gas/chemical movement for EOR purposes especially in the Sabah Basin. In Malaysia, the main deepwater formations include the Semantan and West Crocker Formations which preserve excellent deepwater successions. The Semantan Formation is well exposed in the central Pahang whereas West Crocker Formation is exposed in the northwest Sabah. The details of the studied locations are shown in figure 1.

Geological Background of the Semantan and West Crocker Formations

The Semantan and West Crocker Formations have been interpreted as deep-marine sediments based on previous sedimentological and palaeontological studies. The Semantan Formation is well exposed in the Temerloh-Mentakab area and along the East Coast Highway from Lancang to Chenor. The formation is reported to be deposited in Paleo-Tethys ocean during Middle to Late Triassic time (Jaafar Ahmad, 1976; Hutchison, 1989). The convergence between the Eastmal-Indosinia and West Malaya/Sibumasu blocks in Late Triassic resulted in the closure of the ocean (Hutchison, 1989). The Semantan Formation is interpreted as deposited in foreland basin that is associated with eastwards subduction of the West Malaya lithosphere beneath the Eastmal block (Figure 2).

The West Crocker Formation crops out extensively, albeit discontinuously, in northwestern Sabah, around Kota Kinabalu (Collenette, 1957; Stauffer, 1967), and may be considered as the basement to the Northwest Sabah Basin (Mazlan Madon et al., 1999). During the Palaeocene to Early Miocene, deep-marine sediments were deposited in deep-marine setting in the proto-south China Sea. The Early Eocene-Miocene subduction of Proto-South China Sea beneath the Borneo formed the Crocker-Rajang Fold-Thrust belt (Figure 3). The West Crocker Formation was

deposited in a foreland basin that developed along the Oligocene-Miocene subduction zone parallel to the northwest margin of Borneo. The subduction ended after the collision between the Reed Bank-Dangerous Grounds continental blocks and Borneo. The collision in Northwest Sabah is referred to as the Sabah Orogeny which caused uplift of the West Crocker Formation.

Major Deepwater Successions

In deepwater depositional settings, major deepwater successions observed in the formations include mass transport deposits, channelised turbidite sandstones and unchannelised sheet-like geometry of turbidite sandstones. They are important in determining depositional processes and environments in deepwater settings. The examples of the deepwater sedimentary successions, their geometry and characterisation are described below.

Mass transport deposits

Mass transport is a general term used for down-slope movement of sediments under gravity influence in sub-aqueous environment and mainly composed of slides and slumps (Shanmugam, 2006). In the Semantan Formation, mass transport deposits (slumps/slides) are evidenced by the large sandstone blocks within otherwise regularly bedded section (Fig. 4). The slide block of undisturbed sedimentary rock should have derived from continental slope failure which then moved along gliding planes. The facies represents unstable continental slope when the sediments reached high degree of slope angle or triggered by earthquake. This feature is an appropriate analogue for continental slope deposit which is laterally and vertically restricted because the slumped sand bodies sealed by hemipelagic shales.

Channelised turbidite sandstones

The outcrops of the West Crocker Formation in this study area provide good examples of deepwater distributary channels in basin floor fan. The interpretation is made based on the existence of the channels in sheet-like geometry of mid-fan succession. They exhibit erosional scour on top of the underlying beds and



Figure 1: Study area of the Semantan and West Crocker Formations in general location map (A) and in specific location maps (B and C).

infilled by predominantly sandstones facies (Figure 5). The length and width of the channels are difficult to determine in outcrop scale because of the lenticular nature of the channel fill beds. Channel sandstones may have been amalgamated at channel scale giving good analogue of vertical connectivity and lateral continuity towards the basin.

Unchannelised turbidite sandstones

Most of the studied outcrops in the West Crocker Formations exhibit non-channelized deposits that can be an excellent analogue for lobe depositional setting in middle to lower fan. The sandstone beds are thick, massive/graded, amalgamated, sheet-like geometry and non-erosive bases (Figure 6). They were formed by the deposition of turbidite sands that have undergone a long distance transport pathways from continental slope to basin floor fan. As analogue to the subsurface, the sheet-like geometry of reservoir sandstones and good lateral continuity are important characteristics for effective EOR gas/chemical movement from injection well to producing well. Amalgamated sandstones improve the reservoir thickness and connectivity for vertical residue oil migration.

Conclusions

The deepwater deposits of the Semantan and West Crocker Formations have high scientific values mainly for analogue to subsurface deepwater reservoir geometry and characterisation. Major deepwater features observed in the formations include mass transport deposits, channelised turbidite sandstones and unchannelised sheet-like geometry of turbidite sandstones. The mass transport deposits like slide and slumps are vertically and laterally restricted due to hemipelagic shales sealing. Amalgamated channelised turbidite sandstones give good analogue of vertical connectivity and laterally continuous towards the basin. Unchannelised sheet like geometry of sandstones which represents lobe deposits are the most laterally extensive and have good reservoir continuity. This type of sandstones is the most suitable for the implementation of gas/chemical EOR in deepwater reservoirs.

References

Collenette, P., 1957. The geology and mineral resources of the Pensiangan and Upper Kinabatangan area, Sabah, Malaysia, Geol. Survey Borneo Region, Malaysia, Memoir 12.

Hutchison C.S., 1989. Terrains of Cathaysian Affinity. In Geological evolution of South-East Asia, pp. 133-200.

Hutchison, C.S., 2005. Geology of North West Borneo, Sarawak, Brunei and Sabah. Elsevier, UK, pp. 67-80.

Jaafar Ahmad, 1976. The Geology and Mineral Resources of Karak and Temerloh Area, Pahang. Geological Survey of Malaysia Memoir 15, pp. 127.

Leong Khee Meng, 1999. Geological Setting of Sabah. In: The Petroleum Geology and Resources of Malaysia, Petrolim Nasional Berhad (PETRONAS), Kuala Lumpur, pp. 475-492.

Madon, M., Leong, K.M. & Azlina, A., 1999. Sabah Basin, In: The Petroleum Geology and Resources of Malaysia. Petrolim Nasional Berhad (PETRONAS), pp. 501-542.

Shanmugam, G., 2006. Deep-water processes and facies models: Implications for sandstone petroleum reservoirs: Amsterdam, Elsevier.

Stauffer, P.H., 1968. Studies in the Crocker Formation, Sabah, Borneo region, Malaysia. Bulletin of the Geological Survey of Malaysia, 8, pp. 1-13.

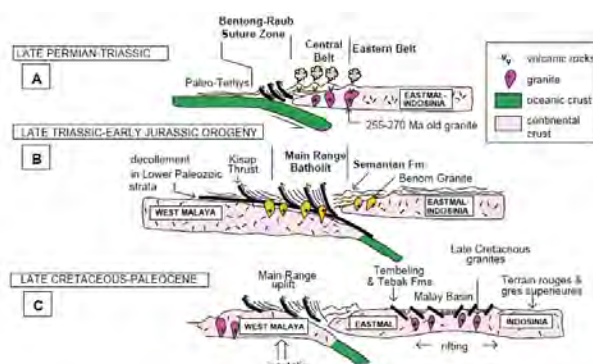


Figure 2: Summary of the tectonic evolution of Southeast Asia, from Late Permian to Early Tertiary (Simplified from Hutchison, 1989).

A. The Paleo-Tethys ocean was narrowing due to subduction beneath Eastmal-Indosinia block. The Semantan Fm. deposited in foreland basin. B. Convergence between the Eastmal/Indosinia and Sibumasu blocks resulted in closure of the Paleo-Tethys ocean and caused uplift of the Semantan Fm. Deposition of terrestrial formations started in Jurassic time. C. The formation of the offshore Malay and Penyu Basins as a result from the rifting of Eastmal and Indosinia blocks.

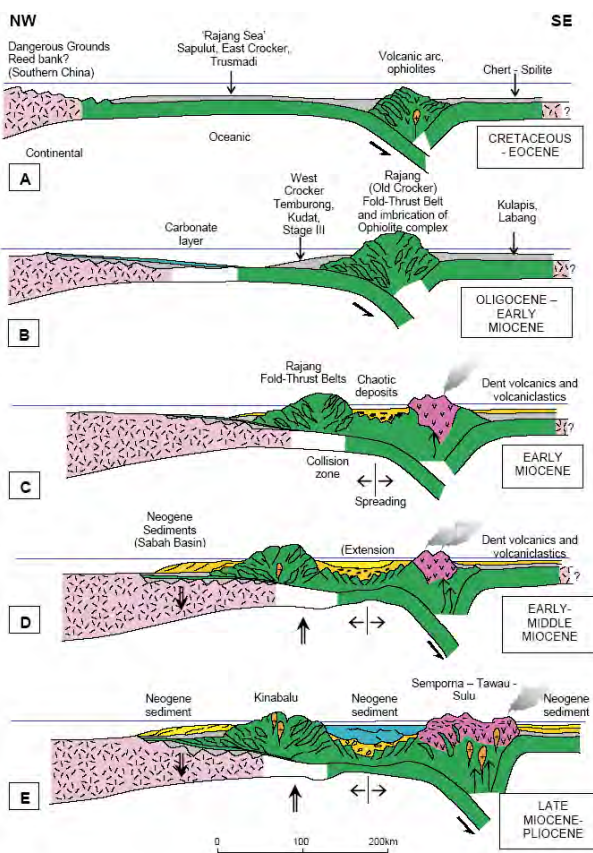


Figure 3: Summary of the tectonic evolution and the formation of the Rajang-Crocker accretionary wedge complex in Sabah (after Leong, 1999; Tongkul, 1991).

A. Extension in the southern continental margin of China resulted in the southeastward subduction proto-South China Sea/Rajang Sea oceanic lithosphere beneath Borneo.

B. Uplift and erosion of the Rajang Fold-Thrust Belt supply sediments to offshore Sabah to form West Crocker and associated formation.

C. Rifting of east Sabah and infilled by shallow marine sediments. The collision of Reed bank terrane with Rajang-Crocker Fold-Belt resulted in uplifting of the West Crocker Formation.

D. Erosion of the uplifted formation supply sediments to Sabah basin in the South China Sea.

E. Intrusion of Kinabalu pluton and active volcanic activity in Semporna, Tawau and Sulu.



Figure 4: The mass transport deposit of the Semantan Formation characterised by large slide block in a muddy matrix. The succession represents depositional environment on a palaeo continental slope.



Figure 5: Channelised turbidite sandstones in the West Crocker Formation characterized by thick, amalgamated and erosional bases. The sequence is interpreted as deposited in middle fan environment.



Figure 6: The outcrop exhibits non-channelised deposits that signify lobe depositional setting in the West Crocker Formation. The sandstone beds are thick, massive/graded, amalgamated, sheet-like geometry and non-erosive bases

Well Log Application in Source Rock Evaluation: Using Committee Machine with Intelligent Systems

M. Verdiyari (Petroleum University of Technology), F. Kamyabi* (Petroleum University of Technology), A. Nazarpour (Petroleum University of Technology) & M.K. Ghassem Alaskari (Petroleum University of Technology)

Introduction

Source rock evaluation consists of assessing the hydrocarbon generating potential of sediments by looking at the sediment's capacity for hydrocarbon generation, type of organic matter present and what hydrocarbons might be generated, and the sediment's thermal maturity and how it has influenced generation. From this, it is possible to begin answering questions about if, how much, what kind, and when hydrocarbon generation has occurred. The analytical methods most frequently used for this purpose are total organic carbon (TOC) content analysis, Rock-Eval pyrolysis, and vitrinite reflectance analysis. The quantity of organic matter is usually expressed as TOC, which is actually the summation of free hydrocarbons, generation potential and residual carbon in the rock. Conventionally TOC is determined by geochemical measurements on organic rich samples of source rocks. Despite of many advantages, this method has some disadvantages, for example: distances between intervals remain analysisless, local studying are expensive and time consuming, and also there is possibility of losing rich samples or sampling of poor and ineffective layers. Moreover, laboratory measurement is not normally used to make real-time drilling decisions because of the lengthy sample preparation, running, and interpretation time. As an alternative, organic rich rocks from petrophysical point of view are characterized by higher porosity, higher sonic transient time, lower density, higher gamma-ray and higher resistivity in compare to organic lean rocks. These physical characteristics of organic rich rocks could be studied in conventional petrophysical well logs. Therefore, petrophysical logs which are fast and cost-effective could be used to estimate the TOC content.

Numerous studies have been done to find a correlation between well log data and organic richness of different rocks. Among them, Beers (1945), Swanson (1960), Fertle (1988), Hertzog et al. (1989) used gamma ray spectral log to identify organic-rich rocks. Schmoker and Hester (1983) proposed to use the density log for estimating organic matter content. Meyer and Nederlof (1984) introduced a method for discrimination of source rocks and non-source rocks involving combination of resistivity, density, and sonic logs, without any effort to quantify organic richness from combination of various logs. Passey et al. (1990) invented a standard method called $\Delta\log R$. This technique employs the overlay of porosity logs (sonic, density, and neutron) and resistivity log for identifying and calculating total organic carbon (TOC). Huang and Williamson (1996) applied artificial neural network (ANN) modeling for source rock characterization. Lately, Kamali and Mirshady (2004) used $\Delta\log R$ and neuro-fuzzy (NF) techniques for determining TOC from well log data. Kadkhodaie et al. (2009) estimated the TOC value with the concept of Committee machine in gas reservoir.

Previous studies demonstrate that they have mainly focused on one or more techniques, independently or using the limited physical well log parameters for estimation. Current study suggests an improved and optimal model for TOC estimation using resistivity, sonic, gamma ray, density and porosity logs by integration of intelligent systems and the concept of committee machine with an example from Pabdeh and Gurpi Formations in

Marun oil field, Iran. This committee machine with intelligent systems (CMIS) combines the results of TOC predicted from intelligent systems. These include, Artificial Neural Network (ANN), Fuzzy Logic (FL) and Neuro-Fuzzy (NF). The optimal combination of weights is derived by a genetic algorithm (GA). The results reveal that the CMIS performs better than all other individual intelligent systems acting alone for predicting TOC.

Methodology

There are several intelligent systems, which depending on the problem to be solved, could be used for modeling and prediction in different disciplines of science. In this study ANN, FL, NF and GA, methods are employed to construct a committee machine for modeling and predicting of TOC from petrophysical data. A CMIS consists of a group of intelligent systems, which combines the outputs of each system and thus reaps the benefits of all work, with little additional computation (Chen and Lin, 2006). Therefore, performance of the model could be better than the best single network. A schematic diagram of CMIS is shown in Figure 1.

Proper combination of the intelligent systems contribution (weight) in a CMIS could be obtained by a GA.

Case Study

Rock sample of Pabdeh and Gurpi Formations in Marun oil field of Iran prepared. Geochemical parameters measured with Rock Eval 6 and outliers removed from data points. Well logs of corresponding depth is extracted from full set well logs after removing bad hole data. Finally 98 data accepted to be used as a proper input for intelligent systems. 67 TOC data points used as a training set and 31 points divided as a test data (Figure2). Five parameters (RIIId, DT, GR, RHOB, and NPHI) of well log selected as an input for predicting TOC. The fitness function for GA was defined as below:

$$MSE_{CMIS} = \sum_{i=1}^n 1/n (w_1 o_{1i} + w_2 o_{2i} + w_3 o_{3i} - T_i)^2 \quad (1)$$

This function shows the MSE of CMIS for training step predictions where w_1 , w_2 , and w_3 are the weight factors corresponding to ANN (o_{1i}), FL (o_{2i}), and NF (o_{3i}) predictions, respectively. T_i is the target values (measured TOC) and n is the number of training data (98 samples).

After 2900 generations, change in the fitness function values over Stall generations was insignificant and the mean and best fitness values were fixed in 0.00042974 and 0.0042971, respectively. Then, the weights obtained from GA were applied

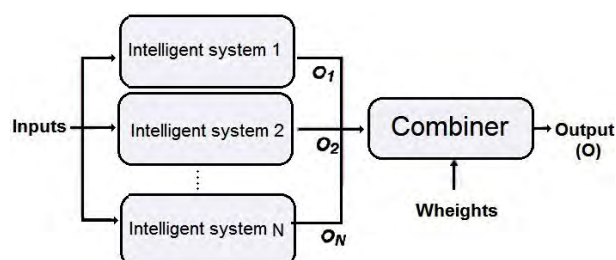


Figure 1: Schematic diagram of Committee machine with Intelligent Systems (CMIS).

to the test dataset predictions of intelligent systems.

Finally overall estimation of TOC by CMIS was calculated as below:

$$TOC_{cmis} = 0.253 TOC_{from ANN} + 0.443 TOC_{from FL} + 0.289 TOC_{from NF} \quad (2)$$

The MSE of predicted TOC from CMIS is 0.0042 that shows an improvement in comparison with ANN, FL and NF (Table 1). R2 correlation between measured and CMIS predicted TOC is increased up to 0.8978 (figure 2). A comparison between measured and CMIS predicted TOC versus depth for the test data is shown in figure 3. Performance of different empirical and intelligent systems on test data is summarized in Table 1.

Conclusions

- Intelligent systems have been successful for making a quantitative correlation between TOC and petrophysical data. The MSE of NN, FL and NF methods for estimation of TOC for the test data are 0.006, 0.0057, and 0.0053, which correspond to the R2 values of 0.8660, 0.8845, and 0.8861, respectively. Among the intelligent systems, which are used, NF model has provided more accurate results than those of the others for the test data.

- The optimal combination of the weights in CMIS was obtained by a GA. The GA derived weights for NN, FL and NF experts are 0.253, 0.443, and 0.289, respectively. MSE of the CMIS for the test data is 0.0045, which corresponds to the R2 value of 0.8978. This indicates that CMIS had an improvement for the estimation of TOC. Therefore, CMIS performs better than any one of the individual intelligent systems acting alone for TOC predicting problem.

- Some over and under estimation seen in certain intervals in all the three intelligent systems. This happens when the small number of data points is used, so, the rock heterogeneity, fluid distribution and mineral change couldn't be recognized clearly by intelligent systems.

- Due to high costs of Rock-Eval pyrolysis, a limited number of samples were used in this study. However, intelligent systems predictions for TOC were satisfactory. So, it could be concluded that when there is a logical relationship between input and output data (such as those mentioned for TOC and petrophysical data), intelligent systems could recognize the patterns even with limited data.

- The CMIS introduced in this study is able to estimate TOC from well log data for other wells of Marun oil field, which have not been cored or their TOC's are not measured.

Acknowledgements

The authors would like to thank the Petroleum University of Technology (PUT), Shahid Chamran University (SCU) and National Iranian South Oil Company (NISOC) for sponsoring, data preparation, and supporting this study.

References

Beers, R.F., 1945. Radioactivity and organic content of some Paleozoic shales. American Association of Petroleum Geologists Bulletin, 26, 1–22.

Chen, C.H., Lin, Z.S., 2006. A committee machine with empirical formulas for permeability prediction. Computers and Geosciences, 32, 485–496.

Fertle, H., 1988. Total organic carbon content determined from well logs. Society of Petroleum Engineers Formation Evaluation, SPE paper NO.15612, 407–419.

Hertzog, R., Colson, L., Seeman, B., O'Brian, M., Scott, H., Mckeon, D., Wraight, P., Grau, J., Schweitzer, J., Herron, M., 1989. Geochemical logging with spectrometry tools. Society of Petroleum Engineers Formation Evaluation, 4, 153–162.

Holland, J.H., 1975. Adaptation in Natural and Artificial Systems. University of Michigan Press, Ann Arbor, USA, 183.

Kadkhodaie Ilkhchi, A., Rahimpour Bonab, H., Rezaee, M.R., 2009. A committee machine with intelligent systems for estimation of total organic carbon content from petrophysical data: An example from Kangan and Dalan reservoirs in South Pars Gas Field, Iran. Computers & Geoscience, 35, 459–474

Kamali, M.R., Mirshady, A.A., 2004. Total organic carbon content determined from well logs using Dlog R and neurofuzzy techniques. Petroleum Science and Engineering, 45, 141–148.

Meyer, B.L., Nederlof, M.H., 1984. Identification of source rocks on wireline logs by density/resistivity and sonic transit time/resistivity cross plots. American Association of Petroleum Geologists Bulletin, 68, 121–129.

Passey, O.R., Moretti, F.U., Stroud, J.D., 1990. A practical modal for organic richness from porosity and resistivity logs. American Association of Petroleum Geologists Bulletin, 74, 1777–1794.

Schmoker, J.W., Hester, T.C., 1983. Organic carbon in Bakken Formation. United States portion of Williston Basin. American Association of Petroleum Geologists Bulletin, 67, 2165–2174.

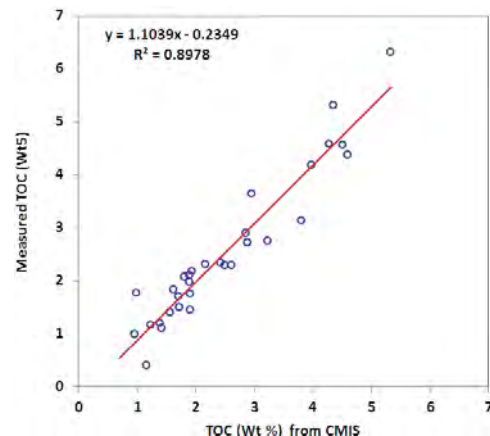


Figure 2: Correlation coefficient between measured and CMIS predicted TOC.

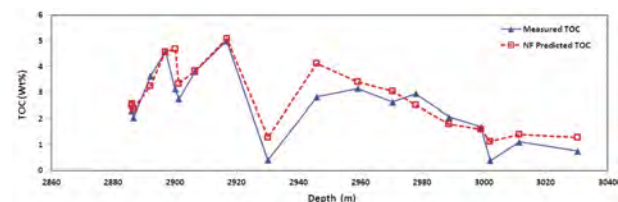


Figure 3: A comparisons between measured and NF predicted TOC versus depth in test data.

Table 1: Summary of performance of different empirical and intelligent systems on test data.

Methods	R2	MSE
Back Propagation Neural Network (BPNN)	0.8660	0.0060
Takagi-Sugeno Fuzzy Interface System (TS-FIS)	0.8845	0.0057
Neuro – Fuzzy (NF)	0.8861	0.0053
Simple Average of BPNN, TS-FIS and NF	0.8878	0.0049
Committee Machine with Intelligent Systems (CMIS)	0.8978	0.0042

Geochemical Evaluation of Oil Reservoirs in the World's Largest Gas Field from Persian Gulf, Iran

P. Hassanzadeh* (NIOC-EXP), M. Khaleghi (NIOC-EXP), A. Ahanjan (NIOC-EXP),
M. Kobraei (NIOC-EXP) & R. Bagheri Tirtashi (NIOC-EXP)

Introduction

The South Pars / North Dome field is a natural gas condensate field located in the Persian Gulf. It is the world's largest gas field, shared between Iran and Qatar (Figure 1) [CEDIGAS]. According to the International Energy Agency (IEA), the field holds an estimated 1,800 trillion cubic feet (51 trillion cubic metres) of in-situ natural gas and some 50 billion barrels (7.9 billion cubic metres) of natural gas condensates [Aali et al. 2006]. In addition to natural gas condensate reserves of South Pars field, oil bearing layer are also identified in both Iranian and Qatari sectors of the field in Cretaceous reservoirs (Figure 2).

This gas field covers an area of 9,700 square kilometres (3,700 sq mi), of which 3,700 square kilometres (1,400 sq mi) (South Pars) is in Iranian territorial waters and 6,000 square kilometres (2,300 sq mi) (North Dome) is in Qatari territorial waters (IEA, 2008).

In this article hydrocarbon potential of probable source rock formations for Oils is investigated in the South Pars field which is southern extension of the North field of Qatar Country. This field is located in Persian Gulf waters and is actually the northern extension of Qatar Arc Paleohigh where geological history of source rock formations is different from nearby area regarding depositional setting, burial history and source rock maturity. In this study, Dariyan (Lower Cretaceous), Gadvan (Lower Cretaceous), Fahliyan (Lower Cretaceous), Surmeh (Upper-Middle Jurassic) and Diyab (Upper Jurassic) formations as source rock candidates, which underlay Upper Dariyan and Mauddud members, respectively, were sampled in two drilled wells of the South Pars field for routine geochemical analysis to investigate hydrocarbon potential of these formations and source rock identification of trapped oil in the Upper Dariyan and Mauddud members.

Beside geochemical analysis of candidate source rocks, oil samples of Upper Dariyan and Mauddud reservoirs and hydrocarbon extracts from core samples of different oil wells have been analyzed.

Based on Rock Eval analysis, except Dariyan and Gadvan source rock samples, other possible source rocks have shown low TOC values. But Maturity parameter (Tmax) of Dariyan and Gadvan samples do not reach 430 °C which is considered as start of oil window. Therefore, it cannot be identified good

source rock in Iranian Sector of Persian Gulf for Oil layers of South Pars Filed.

According to geochemical results, Mauddud reservoir oil of South Pars filed originated from a marine source rock of Carbonate-Marl Facies with type II Kerogen. Age of the source rock is Middle-Upper Jurassic or Cretaceous. Regarding age of the proposed reservoirs (Middle Cretaceous) and not hydrocarbon potential of candidate source rocks in Iranian sector of South Pars filed based on Rock Eval Analysis, it seems that Hanifa (Upper Jurassic) and Araej (Middle Jurassic) are source rock formations. Therefore hydrocarbon accumulated in Upper Dariyan and Mauddud Reservoirs are migrated to the upper carbonate reservoirs in the crestal part of the Qatar Arc.

Method

Thirty-two ditch cutting from four wells were provided by National Iranian Oil company (NIOC). The Petroleum potential and generation of the formation was evaluated using Rock-Eval 6 pyrolysis. The acquisition parameters S1 (free hydrocarbon), S2 (pyrolysed hydrocarbon resulting from the decomposition of Kerogen), S3 (expulsion of CO₂), and Tmax (the temperature at which the S2 peak occurs) were measured to determine the level of thermal maturation and source rock potential. Based on Rock eval pyrolysis, twenty-two samples selected for organic petrography (Vitrinite reflectance measurement) to assess thermal maturation of best samples. Complementary chemical analysis (Extraction, Gas chromatography, Gas chromatography-Mass Spectrometry, Carbon Isotope) have been done on twenty samples. Moreover, hydrocarbon extracted from sixteen core samples (Mauddud, Upper Dariyan, Lower Dariyan, Gadvan, Fahliyan) and three oil samples from U.Dariyan and Mauddud reservoirs of South Pars filed have been analysed for Oil-Source Rock Correlation.

Conclusions

Preliminary and Complementary geochemical analysis of possible source rocks (Dariyan (Lower Cretaceous), Gadvan (Lower Cretaceous), Fahliyan (Lower Cretaceous), Surmeh (Upper-Middle Jurassic) and Diyab (Upper Jurassic)) and correlation with extracted hydrocarbon and oil samples of Mauddud and Upper Dariyan reservoirs of South pars filed have shown that none of the possible source rocks in Iranian Territory



Figure 1: Location of the South Pars Field (Ghasemi-Nejad et al. 2009).

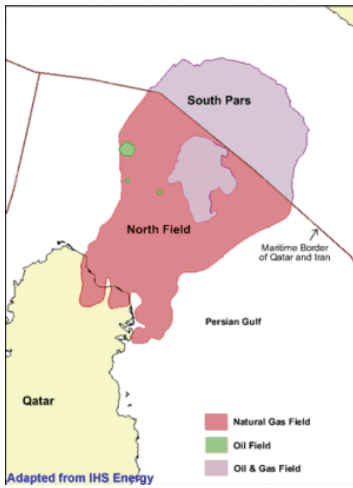


Figure 2: South Pars/North Dome Filed and Distribution of Gas and Oil Reserves (IHS Energy).

of Persian Gulf have good hydrocarbon generation potential. Therefore, mentioned formations have been excluded as a source for oil accumulated in Cretaceous reservoirs of this filed. On the other hand, Qatar introduce Hanifa and Araej formations as source rocks for hydrocarbon accumulated in Jurassic and Cretaceous reservoirs in North Dome filed. As a result, it can be inferred that hydrocarbon probably generated from these two formations of the nearby through and flanks of the Qatar Arc, where the burial depth and temperature increase, in down dip area are migrated to the upper carbonate reservoirs in the crest part of the Qatar Arc.

Table 1: Wells and number of samples in the database.

Well name	Cutting	Core	Oil
SPO#1	-	7	
SPO#2	18	6	2
SPO#3	18	3	
G-3	6	-	
SP-5	1	-	
SP0 A-6	-	-	1

Acknowledgements

The authors would like to appreciate NIOC Research and Technology Directorate for its financial support given to us in this research and for the permission to publish this paper.

References

Aali, J., Rahimpour-Bonab, H., 2006. Geochemistry and origin of the world’s largest gas field from Persian Gulf, Iran. *Journal of Petroleum Science and Engineering*, 50, 161-175.
 CEDIGAZ: Current status of status of the World’s gas giants
 Ghasemi-Nejad, E., Head, M.J. and Naderi, M., 2009. Palynology and Petroleum Potential of the Kazhdumi Formation (Cretaceous: Albian-Cenomanian) in the South Pars Field, Northern Persian Gulf. *Marine and Petroleum Geology*, 26, 805-816.
 IEA, World Energy Outlook 2008. Chapter 12 - Natural gas resources and production prospects, p.298
www.energy.ihs.com

Common Liptinitic Constituents of Mukalla Coals in The Offshore Qamar Basin, Eastern Yemen: Implication for Hydrocarbon

M. Hakimi* (University Of Malaya) & W.H. Abdullah (University Of Malaya)

Qamar Basin is a petroliferous Mesozoic basin in Eastern Yemen. The origin of the hydrocarbons in the basin is not fully understood. The Qamar Basin is dominated by a thick Mesozoic and Cenozoic sedimentary sequence, but wells have not penetrated deeper than the Upper Cretaceous Mukalla Formation in the offshore Qamar Basin. The Mukalla Formation is composed of sandstones, organic-rich shales and coal seams. However, published data related to geochemical and petrographic characteristics of the Mukalla coals are very limited. To rectify this, the Mukalla coal deposits of offshore Qamar Basin, selected from three exploration wells, have been evaluated in this study. This presentation will identify and describe the type of common liptinitic constituents of the Mukalla coals and their relation to hydrocarbon generation potential. The Mukalla coal samples analysed range in maturity from 0.65 to 0.85 %. They are characterised by a high total organic matter content (36-80 wt. %) and possess excellent hydrocarbon generating potential. Kerogen typing carried out on whole rock samples revealed that the Mukalla coal samples consist predominantly of type III vitrinitic kerogen and type II liptinitic kerogen. Vitrinite is the most abundant maceral in the studied coal samples of the Mukalla Formation. All coal samples of the Mukalla Formation, however, contain significant amount of liptinitic macerals particularly sporinite, suberinite, resinite, liptodetrinite, cutinite and exsudatinite (Fig.1). These macerals are dominant type II

kerogen within the studied samples. The kerogen type was also characterised by Rock-Eval pyrolysis analysis. The Mukalla coals contain predominantly a mixture of type II-III kerogen with minor contributions from type II and type III (Fig. 2). This is indicated by hydrogen index values that range from 130 to 410 mg HC/g TOC, thus in support of the kerogen types as were identified based on petrographic method. A number of petrographic features in the Mukalla coals are commonly considered to indicate oil generation were observed. Such features include the occurrence of exsudatinite and oil haze. The development of exsudatinite that displays intense yellow-orange fluorescence in the Mukalla coals is taken to represent a peak mature stage of liquid hydrocarbon generation which takes place at about 0.85 % Ro. This falls within the generally considered "peak oil window" that commonly occurs within 0.6-0.9% vitrinite reflectance values).

Acknowledgements

The authors would like to thank the Petroleum Exploration and Production Authority (PEPA), Yemen for providing the cuttings samples for this study. The authors are more grateful to the Department of Geology, University of Malaya for providing facilities to complete this research. Special thanks are offered to Mr. Peter Abolins PETRONAS Carigali, Kuala Lumpur for his helpful comments on an earlier version of the extended abstract.

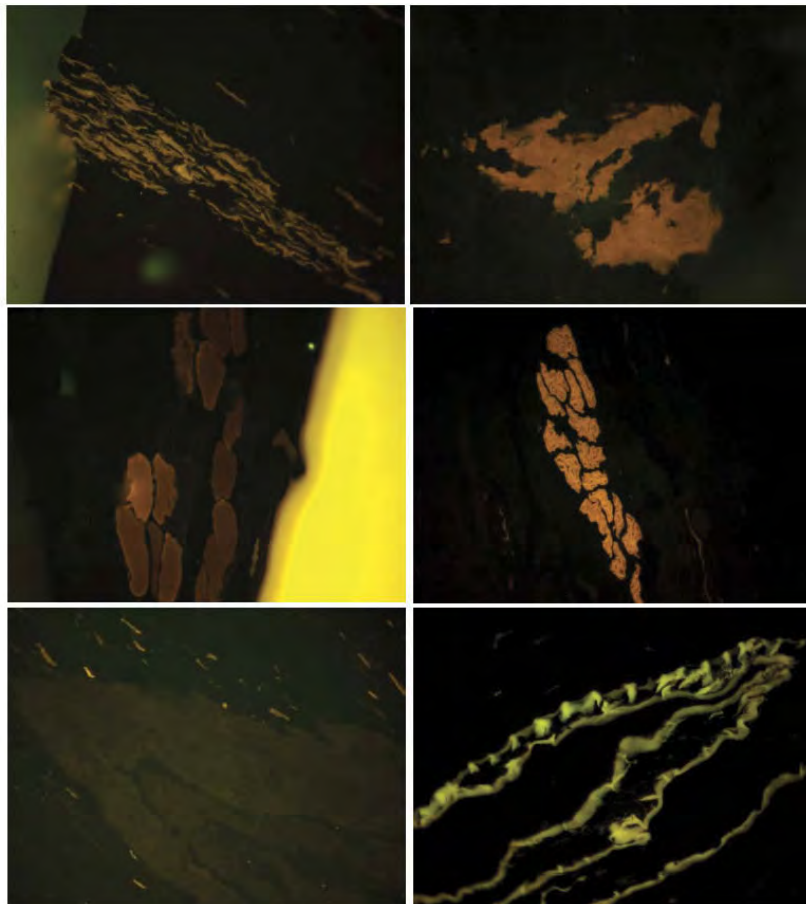


Figure 1: Photomicrographs of macerals from Upper Cretaceous Mukalla coals, offshore Qamar Basin, Eastern Yemen.

Generating a New Approach for Continuous Reservoir Model Updating: Non-Gaussian Priors & Nonlinear Data Functions in EnKF

S. Forghany* (Research Institute of Petroleum Industry (RIPI)), A.A. Asgari (Research Institute of Petroleum Industry (RIPI)) & T. Behrouz (Research Institute of Petroleum Industry (RIPI))

Introduction

Reservoir management of modern oil and gas fields requires periodic updates of the simulation models to integrate in the geological parameterization production data collected over time. To achieve this goal, it is necessary to reconcile geological models to the dynamic response of the reservoir through history matching. In these processes the challenges nowadays are many. First, a coherent view of the geomodel requires updating the simulation decks in ways consistent with geological assumptions. Second, the management is requiring more and more often a probabilistic assessment of the different development scenarios. This means that cumulative distribution functions, reflecting the underlying uncertainty in the knowledge of the reservoir, for key production indicators, e.g. cumulative oil production at Stock Tank condition (STC), along the entire time-life of the field, are expected outcomes of a reservoir modeling project. Therefore, decision making, based on most current information, requires frequent and rapid updates of the reservoir models. The knowledge of the reservoir properties is initially very vague. Hence, a multivariate stochastic model should be used to describe the spatial variability of the reservoir properties such as porosity, permeability, lithology, initial reservoir pressure and fluid saturation. In addition, the stochastic model should represent the pressure and fluid saturation changes in accordance with the fluid flow model. The requirement for these reservoir simulation models should be that they are conditioned to reservoir specific observations (e.g. production history, pressure and 3D seismic), and the aim is to adjust the model in such a way that the simulated performance of the model matches the observed history. These conditioned models provide the basis for an uncertainty assessment through an ensemble of simulation studies, which, in turn, may be used to evaluate different recovery strategies. This is a history matching process and since it is known as an inverse problem, a Bayesian framework is suitable for finding a solution. A Bayesian framework for stochastic reservoir characterization includes a prior model and a likelihood function and both define the posterior model. The prior model typically involves the geological knowledge of the reservoir properties and should give a reasonable description of the prior uncertainty. The likelihood function normally includes both a forward modeling of the data acquisition procedure and a measurement error term which takes into account the uncertainty connected to the acquisition instruments.

Theory

In this study we present a sequential data assimilation procedure, based on a Bayesian framework, where the model parameters and the state variables are updated continuously in time. It is called Ensemble Kalman Filter (EnKF) for data assimilation. It is a Monte-Carlo approach that works with an ensemble of reservoir models. Specifically, the method utilizes cross-covariances between measurements and model parameters computed directly from the ensemble members to sequentially update the reservoir models. In spite of all its favorable properties, the current implementation of EnKF approach comes with its own share of challenges and limitations.

The application of ensemble Kalman filter is quite well when the prior probability distributions are Gaussian, and when the relationships between the model parameters, state variables and observation variables are approximately linear. In a comparison of several different algorithms for data assimilation, it was concluded that the EnKF is to be preferred for strongly nonlinear problems. Still, violations of one or both of these two assumptions may introduce severe problems when using the EnKF for data assimilation in multiphase flow reservoirs. In this paper we will separately examine approaches for dealing with nonlinearity in the dynamical system, and the complex non-Gaussian distributions for model parameters (e.g. reservoir models characterized by a facies distribution). Methods for dealing with these issues in the state variables for EnKF can be categorized into three approaches: transformation of the state variables, reparametrization of the state variables and iterative filters. We will address each of these approaches in turn.

The main significance of this approach is that based on a Bayesian framework, when new data become available, the current model and the data are assimilated to improve the model and with considering the above-mentioned approaches, we can tackle the problems of multiphase and complex non-Gaussian distributions for the model parameters. The idea is that the quality of the model will continuously improve with time. The focus lies on the fact that the model is not rerun after each update to check whether it matches the history (no backward integration in time). On the other hand since EnKF does not need either history matching gradients or sensitivity coefficients, any reservoir simulator with restarting capabilities can readily be used in an EnKF workflow.

Case Study

To demonstrate how the history matching phase of a reservoir study is being performed without the model being rerun after each update, the authors have accomplished a few cases.

Our methodology development which improves the model by EnKF workflow is based on synthetic cases. Using generic cases for methodology development is advantageous since the properties of the "true" case is known exactly and can be used as comparison for the estimates given by the EnKF method. In one of the cases that is provided here, a forward run of the simulation through the whole production history was performed using both the 100 initial ensemble members and the 100 estimated ensemble members. Figure 1 illustrates the GOR data results for these cases. The improvement obtained using the estimated ensemble is clearly seen in this figure.

Conclusions

From the material presented in this paper it can be concluded that the main challenges when using the EnKF to update reservoir simulation models are related to the low rank representation of the model covariance matrix, non-Gaussian prior models, strong nonlinearities in the forward model and the application to large scale field models. These issues and the approaches to deal with them have been considered in detail. As a result of using EnKF method and having dealt with non-Gaussian priors

and nonlinear data functions, effective updating of reservoir simulation models and prediction of future performance with the idea of continuously updating the models, without having to rerun from time zero becomes more practical specially in a closed-loop reservoir management setting.

References

- Anderson, J. L., 2003. A Local Least Squares Framework for Ensemble Filtering. *Monthly Weather Review*, 131 (4), 634-642.
- Aurdal, T., Cheng, N., Sagen, J., and Muller, J. 2001. History Matching of Gas Tracer Data to Identify and Estimate Gas Storage Volumes in a North Sea Oil Field. *Canadian International Petroleum Conference*, Calgary, Canada.
- Bianco, A., Cominelli, A., Dovera, L., Nævdal, G., and Valles, B. 2007. History Matching and Production Forecast Uncertainty by Means of the Ensemble Kalman Filter: a Real Field Application. *The SPE/Europec /EAGE Annual Conference and Exhibition*, London, United Kingdom, SPE paper number 107161.
- Evensen, G. 2006. *Data assimilation: The Ensemble Kalman Filter*, Springer.
- Illiassov, P.A. and Datta-Gupta, A. 2002. Field-scale characterization of permeability and saturation distribution using partitioning tracer tests: The Ranger Field. *SPE Journal* 7 (4), 409-422.
- Liu, N. And Oliver, D. S., 2005. Ensemble Kalman Filter for Automatic History Matching of Geologic Facies. *Journal of Petroleum Science and Engineering*, 47 (3-4), 147-161.
- Nævdal, G., Johnsen, L.M., Aanonsen, S.,M. and Vefring, E.H. 2005. Reservoir Monitoring and Continuous Model Updating Using Ensemble Kalman Filter. *SPE Journal*, 10 (1), 66-74.
- Nævdal, G., Mannseth, T., and Vefring, E., 2002. Near well reservoir monitoring through ensemble Kalman filter. *Proceeding of SPE/DOE Improved Oil recovery Symposium*, Tulsa, Oklahoma, SPE paper number 84372.

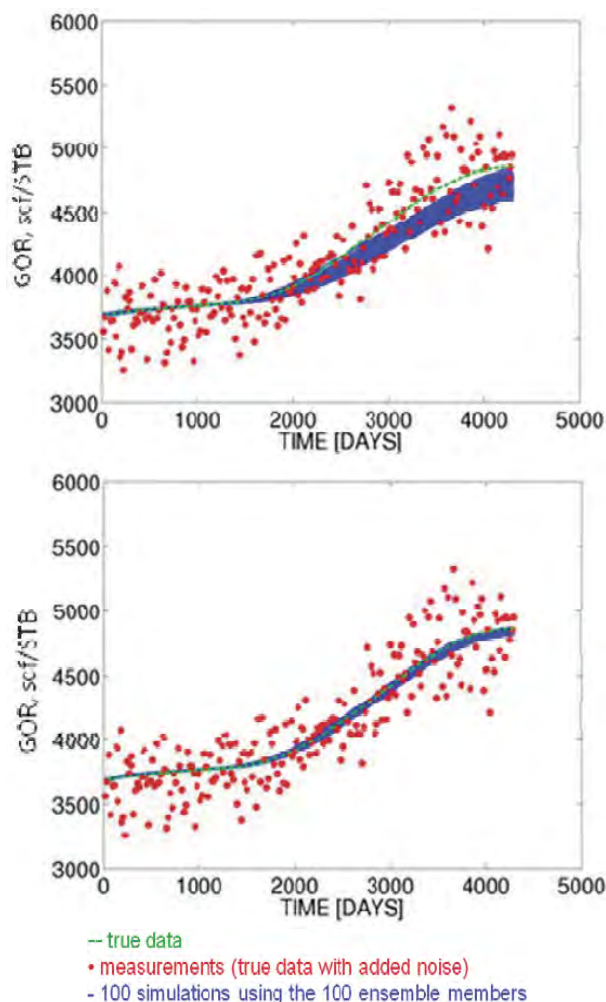


Figure 1: The history match of a generic GOR data with the initial ensemble (top) and with the estimated ensemble (bottom). An improvement is seen using the estimated ensemble, but in both of the graphs the uncertainty represented by the bandwidth of the blue curves is small.

Diverse Origins of Carbonate Cements Revealed By Carbon and Oxygen Isotopic Analysis

D. M. Ince* (PETRONAS Carigali Sdn Bhd)

Well X, drilled in Block SB 305 in the Sandakan Basin tested a large inversion structure the upper portions of which are cut by a major unconformity. Intraformational seals retain hydrocarbons at levels unaffected by the erosional episode.

Two cores were recovered from Lower Miocene reservoir sections. The reservoirs are of shallow marine facies and show extensive bioturbation with distinctive forms such as Ophiomorpha present. Less bioturbated intervals show potential hummocky cross bedding, recording the influence of storm waves, transporting sediment from the coastal to shallow offshore areas.

Core one is highly unusual for a Miocene reservoir section anywhere in Malaysia in that it is extensively cemented by porosity occluding carbonate cements. Visual examination indicates that both dolomite and calcite are present and suggests that the cementation history is complex and multigenerational.

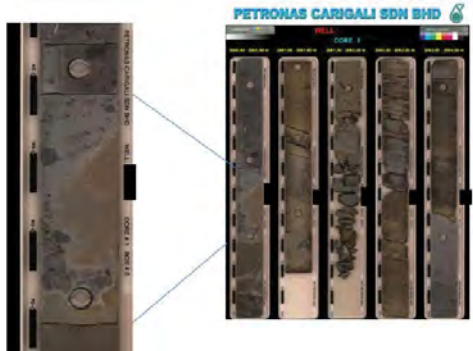
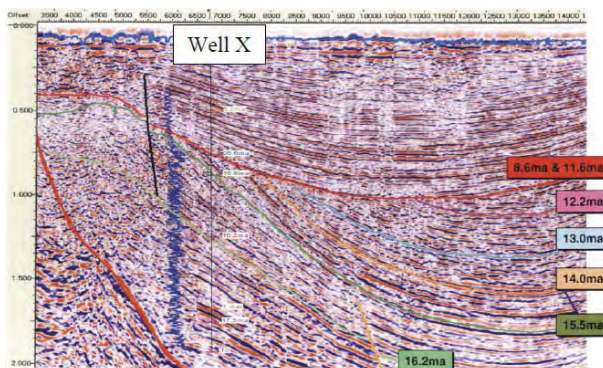
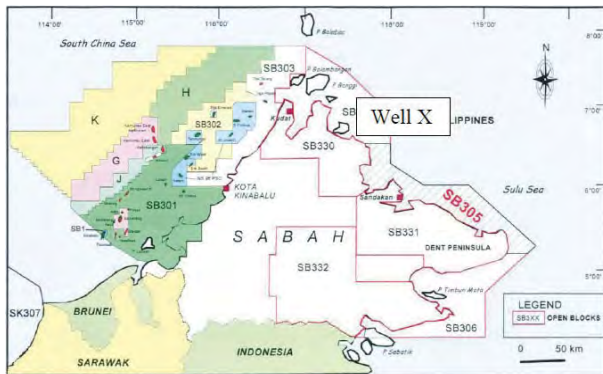
Cementation and mechanical compaction are two major diagenetic processes for these sandstones. Fe-calcite and/or authigenic siderite are common in calcite-rich sandstones and calcite/siderite-rich sandstones. Authigenic minerals are relatively rare in other sandstones, and include pyrite and Fe-calcite. Understanding the origins and thus possible distribution of these cements is important for reservoir characterisation and modelling.

Siderite is common in this sandstone and mostly occurs in a grain-coating manner. Fe calcite is common as well, occluding intergranular areas and fractures. It is apparent that Fe-calcite formed after siderite.

While petrographic analysis allows determination of the nature and relative timing of cement precipitation it does not give information on the thermal conditions or potential origins of the cements. To this end isotopic analysis was carried out to constrain possible sources of the carbonate in the cements (marine; basinal water-rock interaction; meteoric; mixtures) and constrain the range of possible precipitation temperatures and precipitating water $d^{18}O$ values for the authigenic carbonate cements. Although not conclusive, these data could be used to check consistency with a high (late) or low (early) temperature of precipitation.

Synthesis suggests the early, nodular dolomites may have formed shortly after deposition and early, shallow burial of the reservoir sandstones – possibly associated with the 15.5Ma regional up-lift (when there may have been mixing of meteoric waters in the reservoir sandstone). The later ferroan calcites may have formed during the period of resumed burial from about 12Ma until the structuration of the area associated with the 8.6Ma event and subsequent hydrocarbon expulsion and migration.

Future work will integrate the results of the isotope analysis with thermal modelling of the well and surrounding areas to determine the applicability of this technique to any future situations where understanding a complex diagenetic history is important for reservoir characterisation.



Ma		18		17		16		15		14		13		12		11		10		9		8		7		6	
<p>REGIONAL EVENTS</p> <p>Filling and deposition of syn-rift shallow marine to coastal plain sediments</p> <p>Uplift and erosion giving 15.5Ma unconformity</p> <p>Progradation and aggradation of post-rift delta system</p> <p>8.6Ma event (uplift and faulting)</p> <p>Hydrocarbon expulsion and migration</p>																											
<p>NYPHE-2 RESERVOIR</p> <p>Sandstone deposition, 16.2 Ma - 17.5Ma</p> <p>Shallow burial</p> <p>Structure associated with regional up-lift.</p> <p>Resumed burial diagenesis</p> <p>Structure of Nympha field</p> <p>Gas migration into Nympha accumulation</p>																											
<p>PARAGENETIC SEQUENCE</p> <p>Nodular dolomite</p> <p>Fractures</p> <p>Pyrite and siderite</p> <p>Framework grain dissolution</p> <p>Ferroan calcite</p>																											
<p>ISOTOPIC INTERPRETATIONS</p> <p>Nodular dolomite is early diagenetic cement, with Ca and Sr possibly derived from dissolution of Miocene marine carbonates and possibly precipitating from mixed meteoric-marine water at low temperatures (<36°C).</p> <p>Ferroan calcite is burial diagenetic cement incorporating organo-sourced C, and Ca and Sr derived from dissolution of diagenetic cement formed over a period of time, at higher temperatures than the nodular dolomite. Possible minimum precipitation temperatures range from 50°C to 64°C.</p>																											

Conceptual Geology of Dulang Using Sedimentology, Stratigraphy and Netsand Distribution

S. C. Kurniawan* (PETRONAS), K. Saraton (PETRONAS) & U. Deliza Aleesha (PETRONAS)

Dulang field is located in offshore Terengganu, 170 km North Eastern part of Kemaman Base and 2 km North West of the Semangkok field. Dulang field was discovered in 1981 by EPMI Esso Malaysia by well no.1 with oil and gas being discovered in E reservoirs. Different fault blocks of the field were put on production in stages and currently the field has 4 platforms (A, B, C and D) with total of 148 wells. The field is divided into 3 main units namely Dulang West, Dulang Unit and Dulang East. The major NS trending normal faults together with NW-SE and W-E further sub-divide the field into 18 sub-fault blocks with vertical displacement of more than 100 meters. The objective of this study is to map all the major reservoirs honoring all the available well data and other regional data to have better understanding of the depositional environment and generate a conceptual geological model for Dulang field which after validation will be incorporated into the 3D static model. The current model is based on the understanding that the sands are continuous throughout the field and has been compartmentalized by the existing faults. This study would clearly delineate the sands their continuity, lateral extent, pinchouts for all the major reservoirs which would give a better understanding on the field compartmentalization and also on the continuity of the sands which is crucial for the success of the EOR process being implemented for the field. By incorporating the findings from this study would not only help building a robust static model but also help in enhancing the oil recovery from all the major reservoirs.

Some common practices to interpret the depositional environment for building static models are using core descriptions, regional geological understanding, analogue, bio-

stratigraphy, and log data, including dipmeter images and log patterns. For this mature field with 148 wells and dense well spacing of about 800 m between the wells for all the major reservoirs. The classical methods of mapping net sand and gross sand thicknesses after careful correlation and dividing the reservoirs into sub-layers based on the intercalated shale layers are very useful to interpret the continuity and lateral extent of sands. Also patterns from these maps combined with the log motif have helped the team in identifying the depositional pattern including the direction of the source of sedimentation. These maps were useful in identifying the vertical and lateral compartmentalization in the field for all the major reservoirs thus helpful for better reservoir characterization in EOR Project (Figure 1).

Apart from using the core data from 11 wells and the log motif for all the reservoirs from the 148 wells in the field, the thickness maps prepared, have been used to predict the lateral extents and the continuity of the sand bodies for a better depofacies interpretation and reservoir characterization. All the available subsurface data such as petrophysical, pressure and production data has been incorporated to validate the maps prepared which explain the past production and performance of the wells and the field. Hence, the study after incorporating into the 3D static model is expected to give a better history match while simulation and thus predicting the reservoir performance to achieve successful EOR project.

Acknowledgments

Dulang RS & RI team members, PEG and Mr. Bhargava Ram Oruganti

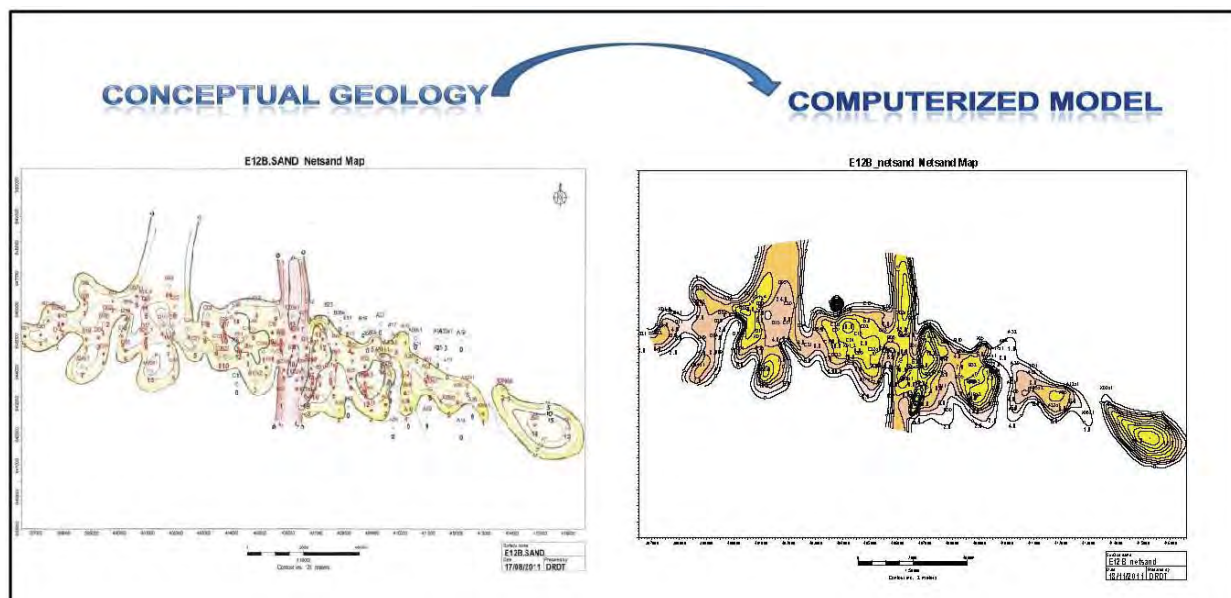


Figure 1: Conceptual geology generated from the available geological data, well log, petrophysical, pressure and production data, then translated into manual mapping to guide computerized geological model for better reservoir characterization in EOR project.

Reservoir Characterization Enhancement Through Integrated Wellbore-Reservoir Flow Model and Pressure Transient Analysis

K. Khadivi (Sharif University), R. Masoudi* (PETRONAS), M. Soltanieh (Sharif University) & F.A. Farhadpou (Sharif University)

Reservoir description and reliable characterization in complex and heterogeneous reservoirs is commonly seen as a challenge in the field development plans. The geological models are usually constructed based on mainly the static information, i.e., Geophysical, Geological and Petrophysical information in the static condition with high level of subsurface uncertainties. Incorporating the dynamic information, such as well test, DST, production test, etc., into the geological model can further enhance the representativeness of the produced geological model.

In this work, a methodology has been proposed using an integrated wellbore-reservoir model, which has been coupled with the numerical pressure transient analysis for improving the reservoir characterization in vertically heterogeneous reservoirs. Challenges and concerns of the pressure transient analysis in vertically heterogeneous reservoirs is studied and examined first. The method includes a separate model for the free fluid flow in the wellbore, which is found essential to allow for hydraulic communication and mixing of the fluid issuing from different reservoir layers. A two dimensional model coupling Darcy flow in the reservoir with Navier-Stokes flow in the wellbore is developed and solved by the finite element technique.

The coupled wellbore-reservoir flow model is used to analyze a layered reservoir with an abrupt change in permeability and a thick formation showing a gradual change in permeability with depth. The model presented captures the wellbore storage effect directly and can handle wells with partial or complete perforations. The results obtained show that the coupled wellbore-reservoir model enables the development of numerical well test procedures capable of delivering the extent of vertical heterogeneity in both isotropic and anisotropic formations enhancing the heterogeneity capturing in the geological model.

Introduction

The transient analysis of the pressure response measured by downhole pressure gauges (well testing) is an important and well established tool for characterization of underground petroleum reservoirs. Conventional well test analyses (Gringarten et al., 1979; Bourdet, 2002) are based on restrictive assumptions that lead to idealised flow characteristics that admit an analytical solution of the onedimensional diffusion equation and obviate the need for direct description of the well bore dynamics.

For instance, in a spatially homogeneous reservoir with full well completion, the flow is purely radial and the well is taken as a simple line source. In the case of a partially completed well, the flow is idealised by a combination of spherical and radial flow characteristics and deviation from pure radial flow is handled by the introduction of a (pseudo) skin (Brons and Marting, 1961; Moran and Finklea, 1962).

The approximations employed in conventional well test analysis are difficult to justify for real formations, which often exhibit significant porosity and permeability variations in both areal and vertical directions. For reservoirs with only radial heterogeneity, it is possible to develop approximate (semi)-analytical one-dimensional solutions that account for the radial heterogeneity without a separate well flow model. An excellent description of what can be recovered for a radially heterogeneous

reservoir has been given by Levitan (2002). There are, however, no obvious simplifications that can be used for a reservoir with significant vertical heterogeneity.

For instance, consider a radially homogeneous reservoir that exhibits the vertical heterogeneity shown in Figure 1; this behaviour is observed in typical fining or coarsening upward of clastic reservoirs (Van Wagoner, et al., 1990; Emery and Myers, 1996). In particular, the porosity is assumed to improve linearly with depth and the permeability is assumed to be locally isotropic, $k_{rr} = k_{zz} = k$, and taken as an exponential function of the local porosity.

Our aim is to demonstrate that reliable well test analysis for reservoirs with appreciable vertical heterogeneity requires a 2D treatment of the reservoir flow coupled with a separate wellbore flow model. In particular, the errors incurred by conventional treatment of vertically heterogeneous reservoirs will be highlighted using simple case study. A numerical well test procedure that couples the 2D finite element solution of reservoir flow with the Navier-Stokes description of the flow in the wellbore is developed. The coupled wellbore-reservoir model provides an accurate and reliable means for dealing with vertically heterogeneous reservoirs.

The Coupled Wellbore-Reservoir Flow Model

Fluid velocity in the spatially heterogeneous reservoir is, in general, very low and momentum effects can be safely neglected. Flow in the reservoir is therefore driven by the gradient in hydraulic potential and is well approximated by the three dimensional (3D) diffusion equation that describes the temporal and spatial pressure changes in the 3D reservoir,

$$\rho\phi C_t \frac{\partial p}{\partial t} = \nabla \cdot \left(\rho \left(\frac{k}{\mu} (\nabla p_d + \rho g \nabla D) \right) \right) \quad (1)$$

Here, \vec{u}_d is the (superficial) Darcy velocity vector, p is the reservoir pressure, μ and ρ are the fluid viscosity and density respectively, g is the magnitude of the acceleration due to gravity, ∇D is a unit vector in the direction over which gravity acts, ϕ denotes porosity, C_t is total compressibility factor and k is the symmetric and positive definite 3D permeability tensor.

The weakly compressible (laminar) Navier-Stokes equations (Bird, Stewart and Lightfoot, 2002) will be used to describe the variation in velocity, \vec{u} , and pressure, p , of the freely flowing fluid inside the wellbore,

$$\frac{\partial \vec{u}}{\partial t} + \nabla \cdot (\rho \vec{u}) = 0$$

$$\rho \frac{\partial \vec{u}}{\partial t} + (\rho \vec{u} \cdot \nabla) \vec{u} = -\nabla p + \nabla \cdot (\mu (\nabla \vec{u} + (\nabla \vec{u})^T)) - \left(\frac{2}{3} \mu - k_{dv} \right) (\nabla \cdot \vec{u}) + \rho g \nabla D \quad (2)$$

The dilatational viscosity, k_{dv} , is usually very small and will be ignored. The flow dynamics of the wellbore and that of the reservoir are strongly coupled at the perforations. In particular, there can be no mass accumulation at the interface between the wellbore and reservoir and the pressure must also be the same on either side of the perforations.

In general, a 3D numerical solution of equations (1) and (2), subject to appropriate initial and boundary conditions, is required to analyze the pressure response of a gauge placed in the wellbore. The computational burden can, however, be significantly reduced by imposing suitable boundary conditions

for a 3D cylindrical reservoir with a centrally located well shown schematically in Figure 2. The individual perforations are not modeled but it is assumed that there is uniform flow across the reservoir layer. We assume that the circumference of the wellbore is symmetrically perforated along all or part of its interface with the reservoir layer. It is further assumed that the top and bottom surfaces of the reservoir layer are sealed and uniform (either constant pressure or no flow) boundary condition is imposed at the outer limit of the reservoir. With such boundary conditions, the problem is geometrically and physically symmetric and there can be no flow in the θ -direction. Flow within the well and the reservoir can therefore be characterized by focusing on one-half of a 2D vertical cross section, as shown in Figure 2. The boundary conditions for equations can be stated as:

$$\vec{n} \cdot \nabla \vec{u}_d = 0, \text{ no flow at the top and bottom of reservoir surfaces,}$$

$$\vec{n} \cdot \nabla \vec{u}_d = 0, \text{ or } p = \text{constant outer limit of the reservoir } (r = r_e)$$

$$p_d = p, \text{ identical wellbore and reservoir pressure at perforations } (r = r_w)$$

$$\vec{u} = \vec{u}_d, \text{ identical velocity vector in wellbore and reservoir at perforations}$$

$$\frac{\partial v}{\partial r} = 0 \text{ and } \frac{\partial p}{\partial r} = 0, \text{ axial symmetry at centerline of the wellbore } (r = 0)$$

$$u = 0 \text{ and } v = 0, \text{ no slip conditions at all solid surfaces of the well tubing}$$

$$\vec{u} = \vec{u}_0, \text{ specified discharge rate from the top surface of the wellbore} \quad (3)$$

Given the spatial variations of porosity and permeability in the reservoir, the numerical solution of equations (1) and (2) with boundary conditions (3) can be obtained using finite difference, finite volume or finite element techniques (Zienkiewicz, 2005). The results presented in this article were obtained using the COMSOL Multiphysics finite element package version 3.5 (COMSOL, 2008). The numerical procedure was validated by comparing the numerical results for various examples with a homogenous reservoir that admit an analytical solution (Crank 1975; Carslaw and Jaeger, 1959; Bourdet, 2002).

Results and Discussion

We present an example that demonstrate the necessity of coupling a separate wellbore flow model to the reservoir flow model for reliable analysis of vertically heterogeneous reservoirs. In particular, the porosity is assumed to improve linearly with depth and the permeability is assumed to be locally isotropic, $k_r = k_z = k$, and taken as an exponential function of the local porosity,

$$\phi(z) = 0.06 - 0.0012z \text{ and } k(z) = 5.066 \exp(20\phi(z)) \text{ [md]}$$

The critical importance of including an explicit wellbore flow model in the analysis of a reservoir with significant vertical heterogeneity is clearly brought out by considering the pressure response from gauges placed at different depths in the wellbore, see Figure 3. In principle, the pressure response from such gauges should only differ by a constant amount equivalent to the head of fluid between them. This means that the log-log pressure derivative plots must be identical and independent of

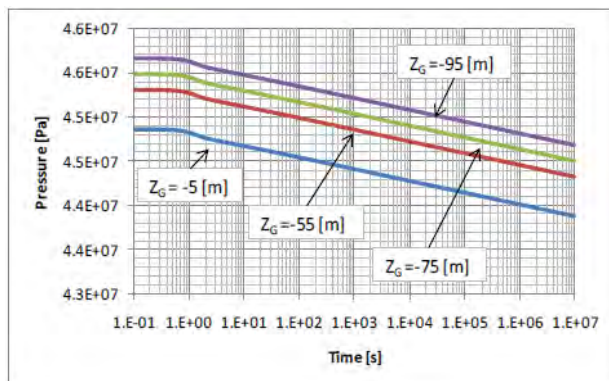


Figure 3: Pressure and pressure derivative plots calculated using the coupled wellbore-reservoir flow model for gauges placed at different heights for a reservoir with vertical heterogeneity shown in Fig. 1.

the gauge location. This is confirmed in Figure 3 that shows the pressure and pressure derivative plots obtained from the coupled wellbore-reservoir model for four gauges placed 5, 55, 75 and 95 meters below the datum height ($z = 0$). As expected, the pressure responses are parallel to each other and exactly the same log-log pressure derivative plot is obtained independent of the gauge depth. A numerical well test procedure capable of capturing the vertical heterogeneity is readily established.

The solution of the nonlinear Navier-Stokes equations in the wellbore complicates the numerical procedure significantly. We may therefore be tempted to only solve the 2D reservoir model, eq.(1), by representing the well as a line source and employ the uniform discharge rate boundary condition used in conventional 1D analysis,

$$\vec{n} \cdot \left(-\frac{k}{\mu} (\nabla p_d + \rho g \nabla D) \right) \Big|_{r=r_w} = \frac{q_s}{2\pi r_w h} \text{ at the perforation} \quad (4)$$

This procedure, however, results in gross misinterpretation. Figure 4 shows the pressure and pressure derivative plots

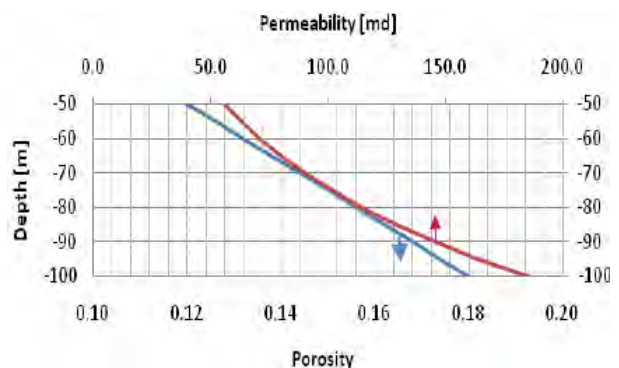


Figure 1: Vertical variation of porosity and permeability in the reservoir.

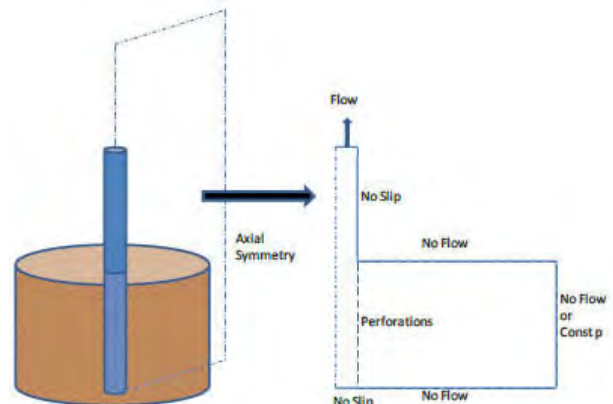
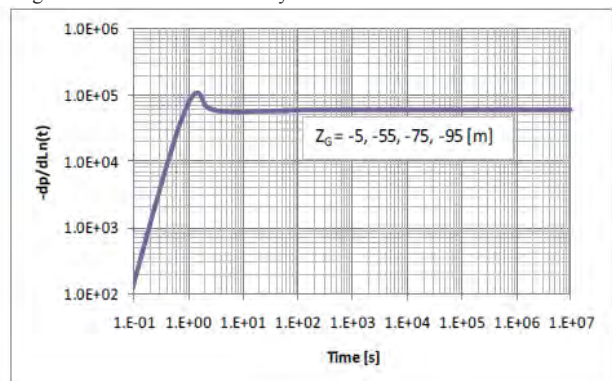


Figure 2: Schematic of a 3D cylindrical reservoir with a central well.



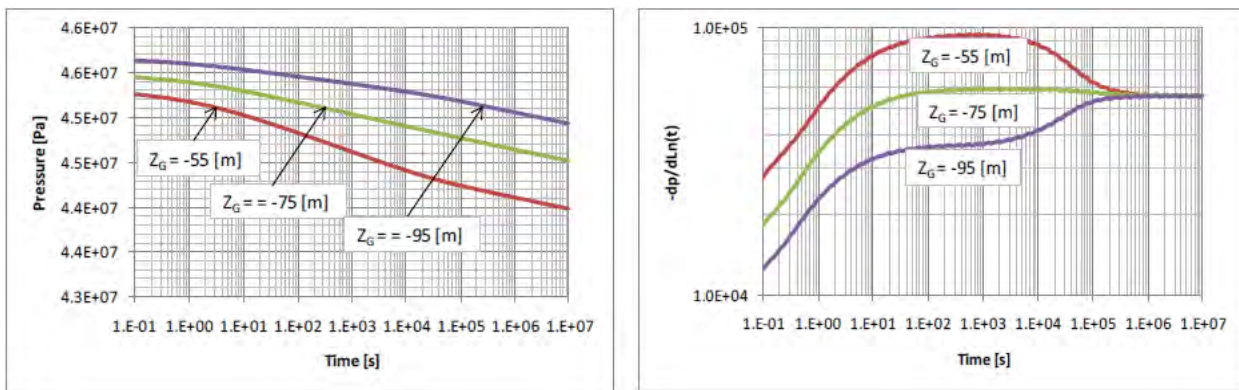


Figure 4: Pressure and pressure derivative plots calculated with a line source well for gauges placed at different heights for a reservoir with vertical heterogeneity shown in Fig. 1.

obtained in this case for three gauges placed near the top, in the middle and close to the bottom of the reservoir layer. The pressure curves are not strictly parallel and the pressure derivative plots for the three gauges are radically different, which is physically incorrect. This is simply because the variation in permeability with depth is not taken into account. In the absence of a wellbore flow model there is no hydraulic communication between the different reservoir layers, which means that each reservoir layer is assumed to flow independently at a constant rate. In fact, there is non-uniform flow across a vertically heterogeneous reservoir, which cannot be captured with line source well model. Consequently, the pressure derivative response becomes dependent on the gauge location, which is clearly incorrect. Evidently, a numerical well test analysis based on a 2D reservoir with a line source well will produce erroneous results. Therefore, a wellbore flow model is essential to provide the hydraulic communication between the different layers of a vertically heterogeneous reservoir.

Conclusions

Transient pressure analysis is a well-established technique for characterization of petroleum reservoirs. Conventional analyses are based on analytical or semi-analytical solutions of the one dimensional diffusion equation under suitable simplifying assumptions. In particular, the formation is assumed to be vertically homogeneous (with depth averaged properties) with a vertically uniform flux through the perforations. This assumption is inappropriate for reservoirs with substantial vertical heterogeneity because the instantaneous rate of influx through the perforations changes with depth and cannot be taken as uniform. The free fluid in the wellbore provides a medium for hydraulic communication between the different reservoir layers, which may have radically different flow properties. Reliable pressure analysis for vertically heterogeneous reservoirs requires a multidimensional description of the flow within the reservoir coupled with an explicit description of the free fluid flow within the wellbore. A two dimensional coupled wellbore-reservoir flow model was developed and solved with the finite element technique. A thick formation with gradual change in permeability was considered. The results obtained confirm that the coupled wellbore-reservoir flow model can be used to develop reliable numerical well test procedure that can deliver the extent of vertical heterogeneity.

References

- Bird R. Byron, Stewart Warren E., 2002. Lightfoot Edwin N., Transport Phenomena, Second Edition, New York, John Wiley & Sons, Inc.
- Bourdet, D., 2002. Well Test Analysis: The Use of Advanced Interpretation Models - (Handbook of petroleum exploration and production), First Edition, Amsterdam, Elsevier Science B.V.
- Brons F. and Marting V. E., 1961. The Effect of Restricted Fluid Entry on Well Productivity, J. Pet. Tech., Feb., 172-174; Trans. AIME, 222. SPE-1322-G.
- Carlsaw H.S. and Jaeger, J.C., 1959. The conduction of Heat in Solids, Second Edition, Oxford, Clarendon Press.
- COMSOL Multiphysics, 2008. Reference Guide Version 3.5, COMSOL AB., Stockholm.
- Crank J., 1975. The Mathematics Of Diffusion, Second Edition, Uxbridge, Oxford, Clarendon Press.
- Emery, D., and K. Myers, 1966. Sequence Stratigraphy: Oxford, Blackwell Science, 297 p.
- Gill, P.E., W. Murray, and M.H. Wright, 1981. Practical Optimization, London, Academic Press
- Gringarten A.C., Bourdet D.P., Landel P.A., and Kniazeff V.J., 1979. A Comparison Between Different Skin and Wellbore Storage Type-Curves for Early-Time Transient Analysis. Paper SPE 8205 presented at the SPE Annual Technical Conference and Exhibition, Las Vegas, Nevada, 23-26 September 1979.
- Levitan M.M., Crawford G.E., 2002. General Heterogeneous Radial and Linear Models for Well-Test Analysis", SPE Journal, June 2002, Volume 7, Number 2: 131-138, SPE 78598-PA
- Moran J. H. and Finklea E. E., 1962. Theoretical Analysis of Pressure Phenomena Associated with the Wireline Formation Tester. J. Pet. Tech., Aug., 899-908. Trans. AIME, 225.
- Van Wagoner J. C., Mitchum R. M., Campion K. M., and Rahmanian V.D., 1990. Siliciclastic sequence stratigraphy in well logs, cores, and outcrops: concepts for high-resolution correlation of time and facies: AAPG Methods in Exploration 7, 55 p.
- Zienkiewicz O.C., Taylor R.L. and Zhu J.Z., 2005. The Finite Element Method: Its Basis and Fundamentals, Sixth edition, Oxford, Elsevier Butterworth-Heinemann.

EB Field: Doubling a Marginal Field's Reserves by Understanding the Application of "Enabling" Technology

K. Afzan* (Newfield Peninsula Malaysia Inc), O.T. Suan (Newfield Exploration Company),
M. Lambert (Newfield Sarawak Malaysia) & B. Goodin (Senergy Australia Pty Ltd)

Introduction

The EB Field is located 160 miles northeast of Terengganu, Malaysia. The primary oil reservoir is Tertiary age and is regionally extensive, highly porous and permeable sandstone. EB Field is considered a marginal field development. It is a particularly challenging development due to the thin oil column (14 meters) which is entirely within the transition zone. Other challenges include unfavourable crude quality, a large gas-cap, extensive bottom water, a low relief structure, and a shallow poorly consolidated sandstone reservoir.

Developing such a marginal field requires extensive reservoir simulation to plan the optimal well spacing, counts, lengths, landing depths, and withdrawal rates. To implement the plan, drilling and geosteering technologies must achieve open-hole horizontal sections exceeding 2,000 meters. Completions require Stand Alone Screens (SAS) and Inflow Control Devices (ICD) to prevent sand production and to distribute the drawdown evenly along the entire well length.

After the initial development extensive field trials were conducted to measure well drawdown, water breakthrough timing, and water-cut increase. Production Logging Tools (PLT) and tracer technologies are applied to confirm that the entire horizontal section contributes to total fluid inflow. Results are used for refining the simulations and optimizing the next phase of development.

At the end of 2010 the field has two and a half years of production history from two successful phases of development (14 wells drilled). The oil production build-up and rate are performing better than expected, doubling the reserves forecasted at project sanction time.

Geology

EB Field is a shallow broad 4,500 acre three-way dip closure bounded to the west by a high-angle fault complex. The reservoir is comprised of lowstand braided fluvial sandstones capped by transgressive lacustrine deltaic sandstones and shales (Figure 1). Median net to gross in the fluvial and deltaic sandstones is 98 and 30 percent respectively. A field-wide, low permeability shaly siltstone 9 to 15 meters thick separates the deltaic and fluvial sandstones. The fluvial sandstones have high median porosity and permeability (30 percent and 1,400 mD respectively). The overlying deltaic sandstones have relatively lower porosity and permeability (median 25 percent and 180 mD). Early appraisal wells defined the structure and stratigraphy and encountered the gas-oil contact (GOC) and oil-water contact (OWC).

Challenges

Determining the optimal development and recovery factor (RF) for this type of reservoir is challenging as there are no analogues in the Malay Basin (and few analogues worldwide). EB Field development challenges are as follows.

Depletion Strategies

- Reservoir pressure maintenance and gas and water contact movements.
- Vertical positioning of horizontal wellbores to minimize gas and water coning.

- Optimal well count and spacing that maximizes RF but minimizes interference.
- Effective length of horizontal wells.

Reservoir Management

- Optimum withdrawal rate based on GOR and water cut performance.
- Optimum gas injection volumes to manage reservoir pressure.

Drilling and Completion

- Ability to drill long (greater than 2,000 meters) horizontal wells while maintaining the horizontal and vertical position of the drillbit within a narrow window (+/- 1 meter).
- Managing mud weight and Equivalent Circulating Density (ECD) for borehole stability and effective cleaning without hydraulically fracturing the unconsolidated formation.
- Selection and correct installation of sand control technologies in extended reach wells.

Solutions: Pre-development

Full field model (FFM) simulation and sector modelling are used to quantify the range of recovery factors (RF) for different depletion strategies under different geological scenarios. It was known that low permeability shaly siltstones occur between the overlying deltaic sandstones and the underlying fluvial sandstones. However, it was unclear how laterally extensive the siltstones were and if they compartmentalized the gas-cap. An additional uncertainty was the extent and strength of the aquifer.

Smaller sector models better represent the performance of single or multiple wells (Figure 2). This is because finer areal gridding and thinner layering are imposed on the sector model to facilitate small-scale reservoir dynamics while keeping a lower overhead than the FFM. Horizontal well completion design was driven by reservoir simulation results from Multi-Segment Well (MSW) modelling which mimics the performance of Inflow Control Devices (ICD).

Describing fluid dynamics in the transition oil zone is crucial for predicting RF in this thin oil column reservoir. The sector models predict the horizontal wells will produce water almost immediately because the completion is in the transition zone with 40% water saturation. Later, the relative permeability function curves were validated against the actual water production performance and subsequently used for the predictions.

Solutions: Early Development

Phased drilling programs permitted early learnings to be systematically applied so that the overall field development was optimized. Early phases allowed for field testing of drilling, completion, and reservoir parameters while preserving the flexibility for refinements in later phases. Seven wells were drilled as Phase-1 and covered the entire structure to confirm the extent of closure, reservoir continuity and quality, and fluid contacts. As drilling, geosteering, and completion practices were progressively refined, the horizontal length of the wells increased up to 2,100 meters. Two wells were drilled at a close spacing for pressure interference test to assess the well spacing effect.

A wide range of enabling technologies was selected to

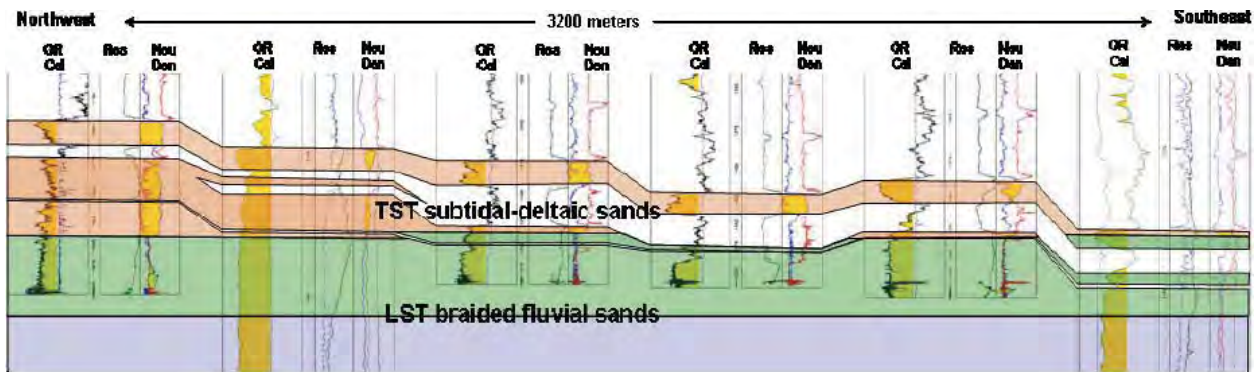


Figure 1: NW-SE section through EB Field showing stratigraphy and fluid contacts.

overcome drilling and completion challenges. For example, keeping the drill bit within the required tight vertical window was achieved with a point-the-bit Rotary Steerable System (RSS). The drill bit position was also optimized with specific geosteering techniques, advanced Logging-While-Drilling (LWD) tools, and Real-Time-Operations (RTO) monitoring from the office. Due to inherent MWD survey error, geosteering focused on the relative position of the bit within the transition zone using resistivity modelling.

A Synthetic-Based-Mud (SBM) provided the required fluid properties for drilling the extended reach wells, using fine ground barite for rheology and filter cake flowback properties. For hole cleaning and stability, the required mud weight and Equivalent-Circulation-Density (ECD) were achieved through optimizing well design, bottom hole assembly (BHA) design, and drilling parameters.

Premium Stand-Alone-Sand-Screen (SAS) systems provided the required level of sand control for long horizontal wells (greater than 2000 meters of screen interval) while permitting filter cake to be flowed back through the screens once the well commences production. Inflow-Control-Devices (ICDs) were installed to control fluid inflow and pressure drop along the entire horizontal well length. Managing pressure drop should reduce gas and water coning along the wellbore.

Solutions: Measuring Performance

Production and reservoir pressure data were measured frequently to understand the reservoir behaviour in different quadrants of the field. Non-permanent, wireline retrieved Downhole Pressure Gauges (DPG) were installed in five wells to measure field-wide pressure decline during early production and record well pressure drawdown at the sand face. Fluid withdrawal rates were progressively increased in each well while the DPG measured the water-cut response as a function of pressure drawdown. Production Logging Tools (PLT) and chemical tracers were run in selected wells to assess the inflow profile along the horizontal section, with special focus on toe contribution. Gas injection volume was carefully monitored, together with the water-cut and GOR performance. This ensures injection and production performance was aligned to the reservoir management requirement of injecting 90 percent of produced gas.

Solutions: Incorporating Learnings

The 3D static model was updated with newly acquired geological information throughout the phased drilling. The new wells confirmed that the low permeability shaly siltstone did extend across the entire field creating a vertical barrier between the overlying deltaic sandstones and the underlying fluvial sandstones, thus reducing the size of the effective gas cap. The

well data also confirmed that reservoir quality, fluid contacts, and the transitional oil zone were similar field wide. The targeted placement of the Phase-1 wells reduced the uncertainties related to structure, reservoir continuity and quality, and the lateral extent of the tight siltstone barrier. As a result, there is high confidence in the resulting resource assessment.

The static model was subsequently conditioned for FFM reservoir simulation and all production performance and pressure data were incorporated and history matched. The history matching process is important to calibrate the relative strength of the bottom water drive and the gas-cap, and to quantify the amount of gas injection required to achieve maximum recovery. During the process, the design of the ICD, which includes port size and the number of open ports, was refined using updated sector models which incorporated the PLT results and utilized the MSW module.

Numerous cases were then simulated on the updated history-matched model to optimize the remaining development program, with particular emphasis on well spacing, landing depth, horizontal length, production rates, and GI/GP. Well and reservoir performance to date indicate that RF can increase further with additional development wells.

Results to date

Due to their positions within the transition zone the Phase-1 wells did have water breakthrough, but much later than predicted by the reservoir simulation. The dynamic model was updated with the early production results and it predicted a further delay in water-cut if the wellbores were shifted up one to two meters. This was tested midway through Phase-1 and indeed higher initial production rates were realized and a further delay in water-cut break-through was observed.

The GOR performance is not as high as predicted in the early reservoir dynamic model. This is likely due to the smaller effective gas cap created by the tight siltstone barrier that separates the deltaic sandstones from the fluvial sands. This barrier was initially believed to be a local buffer to gas encroachment; however it is now believed to be a field-wide barrier prohibiting gas encroachment.

DPG data confirms low pressure drawdown ranging from 20 to 100 psi, which includes the pressure drop across the ICDs. This equates to "world class" Productivity Indices (PI) for the wells in the range of 100 bpd/psi to 300 bpd/psi. When withdrawal rates were increased, the measured drawdown and water-cut did not increase linearly. Continued adjustments helped pin point the optimum withdrawal rate utilizing reservoir dynamic model.

Both the Operator and the Regulatory Body were concerned about flow contribution from the entire length of these long-

reach horizontal wells. To address this issue, the Operator investigated the horizontal well contribution using both tracer and PLT technologies. While providing only indicative non-quantifiable results, the tracer did confirm expected levels of inflow contribution from the toe of horizontal wells with lengths greater than 2,000 meters. In order to further understand and to quantify the inflow contribution of the long horizontal wells, the Operator conducted production logging in two wells using tractor conveyed production logging tools (PLT). The PLT results confirmed that the entire completed horizontal interval including the toe is contributing as designed. Furthermore, the pressure drawdown derived from the PLT shows the entire wellbore has the same drawdown, thus minimizing the effect of hot spots and further confirming the application of ICD technology and ICD port design.

Conclusion

EB Field development results are very encouraging and the final estimated ultimate recovery is projected to be double what was listed in the initial Field Development Plan. The production build-up and sustained rates have exceeded expectations. Reservoir and well performance information, such as pressure trending, well interference, and water-cut and GOR trends, are all very positive. Currently a third phase of development is under way.

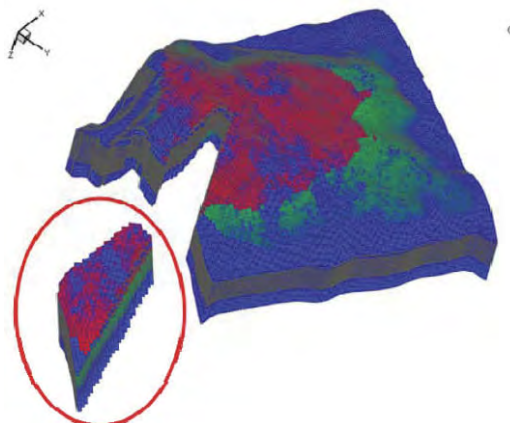


Figure 2: Full field model (FFM) and extraction of Sector Model with pressure boundaries for Multi-Segment Well (MSW) modelling of Inflow Control Devices (ICD).

Unravel New Exploration Opportunity in Central Luconia

A.H.W. Abdullah* (PETRONAS), J. Singh (PETRONAS), S. Osman (PETRONAS) & C. Abdullah (PETRONAS)

A recent exploration well, Well-D, has discovered the potential of hydrocarbon in Cycle V clastic reservoir in Central Luconia which has been well-known of its pool of gas-prone carbonate build-ups.

The low-stand Intra Cycle V which was embedded between marine shale was penetrated, evaluated and an oil sample was obtained. The same clastic reservoir was also penetrated by a nearby well previously, Well-O, drilled before Well-D, and gave gas show but low poro-perm quality was observed (Figure 1).

The reservoir of Intra Cycle V sand previously was interpreted and mapped. The reservoir appears to have high amplitude, high continuity and low frequency character on seismic. The seismic interpretation is supported by a geological model that indicates an incised valley feeder channels system, bounded by major fault at the west, forming a monocline structure that dips eastward (Figure 2).

Intra Cycle V sand has different petroleum system from of the carbonates discoveries in this province. The source rock, particularly, is believed to be charged laterally within the Cycle V interval, which differs from the Pre-Cycle IV source that charged the carbonates build-ups.

As both exploration wells, Well-D and Well-O, penetrated at a structurally down-dip location of the feeder channels system, upside potential is believed yet to be explored. There's also stratigraphic play that lies lateral of the incised valley system. The fan system that the incised valley feeder channel progressed into, is fault bounded and yet to be tested (Figure 3).

An Intra Cycle V clastic reservoir finding opens up new exploration opportunities in Central Luconia province.

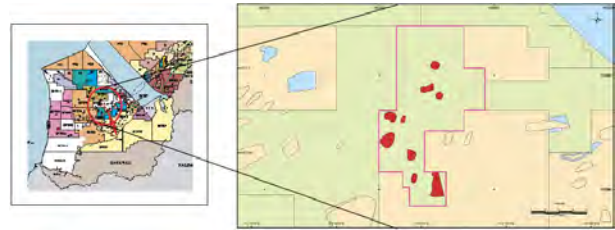


Figure 1: Map showing both Well-D and Well-O in Sarawak, Malaysia.

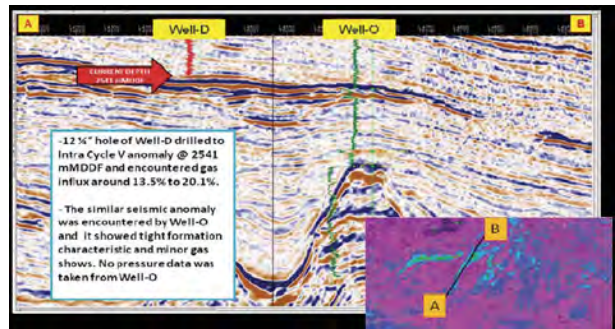


Figure 2: Seismic showing the feeder channel of Intra Cycle V sand.

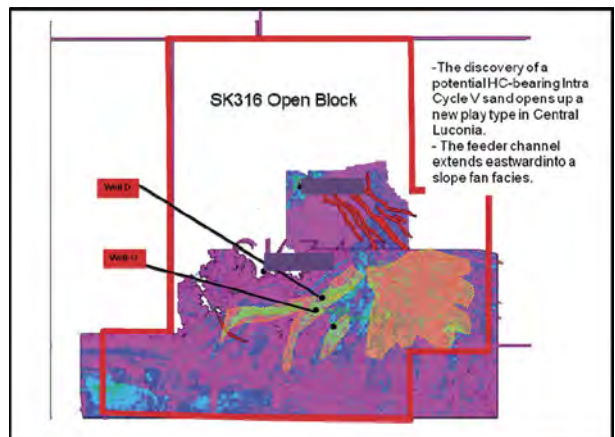


Figure 3: Intra Cycle V sand distribution.

Structuration & Stratigraphic Influence in Post Carbonate Trap Geometry of 'K' Prospect, SK315 Block, Offshore Sarawak

K.A.K. Amry* (Petronas Carigali Sdn Bhd), M.S.M. Sharir (Petronas Carigali Sdn Bhd),
S. S. Wafa (Petronas Carigali Sdn Bhd) & A.M.S. Azlan (Petronas Carigali Sdn Bhd)

Introduction

What can we do in an overly matured basin like the Central Luconia province? With top oil and gas companies having explored the area exhaustively, there exists a crucial need to find better ways or implement new mindsets of seeking and finding hydrocarbons (HC).

In an area well known to house carbonate plays, the existing platforms and pinnacles have already been drilled and tested for HC. Even the pre and post carbonate levels of structural plays have been extensively drilled. If all conventional plays are already tested and we still need to find more HC, the question will be "what else are we still missing?" Therefore, finding new plays are necessary.

Presence of Low Resistivity HC was currently proven through a couple of wells successfully drilled by PETRONAS. This aspect was actually overseen by previous operators in the area; however, the wells yielded hundreds cubic feet of gas. Thus, a new approach has been adopted to look at the stratigraphic plays within the area. A detailed seismic interpretation and mapping were done in order to extract accurate amplitude for seismic attribute analysis.

Method

RMS amplitude maps were generated for the targeted reservoirs at Near Stack and Far Stack from a very thin window of only around 10ms above and below. The amplitude maps were overlain by depth maps of the same horizons. AVO Inversion for the Cycle V/VI reservoir was also generated. However, there were anomalies in other locations including 'K' Field, but not in the offset and target well. This trait was attributed to the possibility that these wells could most likely house multiple

layers of shallow gas of stronger amplitudes that potentially shadowed or masked these particular reservoirs.

Examples

Recently, PETRONAS drilled 'K' Prospect in offshore Sarawak and made a HC discovery in shallow reservoirs where the depth ranged from 600m to 1100m. Two Plays were identified - Cycle VI Structural Stratigraphic Play and Cycle V/VI Stratigraphic Play.

The Cycle VI reservoir showed a strong amplitude response where amplitude anomalies conformed to the structure on the northern and western parts related to fluid change with the southern section displaying facies change. The reservoir was trapped by NE-SW normal faults separating the western and eastern blocks.

The Cycle V/VI reservoir was purely stratigraphic and exhibited non-conformance to structure. Strong amplitude from PSTM Far Stack proved to be HC bearing sands. Amplitude shut off corresponded to free water level and this was confirmed by the presence of water in another well at the edge of the amplitude. The seismic facies was interpreted as Convergent Thinning High Amplitude (Cth) facies with the traits of a parallel high amplitude reflector and thinning on the side. It was interpreted to represent distal lower shoreface sheet sands of interbedded sandstone and shale with high N/G of 50%-80% and porosity of 25-33%.

These interbedded sandstone and shale reservoirs aged Miocene to Early Pliocene prograded perpendicular to the W-E paleo-coastline during the depositional. Source rock is mainly from the older pre-carbonate levels consisting of terrestrial and marine of Cycle I, II and III formation.

SEISMIC LINES vs ATTRIBUTES

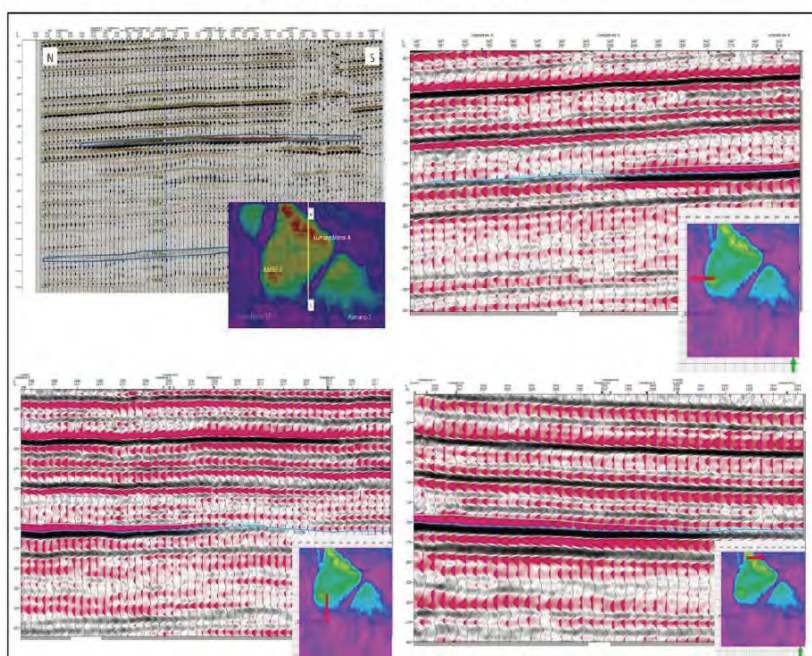


Figure 1: Strong amplitude from PSTM Far Stack proved to be HC bearing sand. Amplitude shut off correspond with free water level and this is confirmed with the presence of water in KMSE-2. Convergent Thinning High Amplitude (Cth) facies with the characteristics of a parallel high amplitude reflector and thinning on the side. It is interpreted to represent distal lower shoreface sheet sand of interbedded sandstone and shale with high Net to Gross (80%) and porosity (33%).

DEPTH STRUCTURE MAP 680 SAND

AMPLITUDE MAP 680 SAND

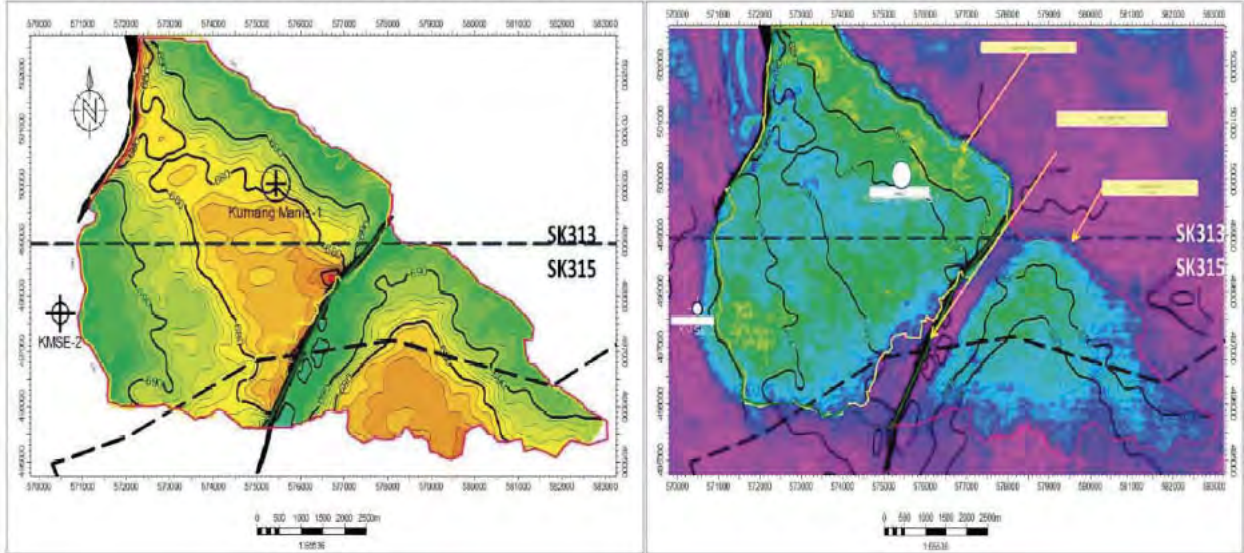


Figure 2: The amplitude anomalies is conform to the structure on the northern and western part which relate to fluid change while southern is representing facies change. The Free Water level (FWL) is at 699m. 680 Sand is a lower shoreface sheet sand. In term of volumetric calculation, 1C area is the bright amplitude within the upthrown block. 2C is the area extend to the fault on the side where the bright amplitude is still above the FWL. The prograding sequence was perpendicular to the W-E trending paleo coast-line during depositional of sediments.

Cycle VI and Cycle V/VI reservoirs have low resistivity readings of four and two ohm respectively that were normally regarded as unpromising reservoirs. Analysis indicated that the reservoirs were thinly bedded which camouflaged the reading of tools to be of shale dominant beds. Samples were taken and production test have proven the existence of HC in the area.

Conclusions

The recent discovery proved there was high potential of shallow HC in Central Luconia, Offshore Sarawak. It basically opens up new opportunities for shallow HC reservoir prospectivity initiatives.

Acknowledgements

We would like to extend our appreciation to Chow Kok Tho, Jamlus Md Yasin, Mazman Abu Bakar, Goh Leong Kee, Nurul Saadah, Noor Iryani, Ahmad Din, Phillip Gordon Cassidy, Rusli Din for their respective contributions in this study.

References

- KM-1 Well Proposal, PCSB in-house report, May 2011
- KM-1 Well Evaluation Report, PCSB in-house report, December 2011
- Chopra, S., Marfurt, K.J. 2007. Seismic Attributes for Prospect Identification and Reservoir Characterization, Society Exploration Geophysics Developments Series No. 11, Stephen, J.H., series editor and volume editor, 99-122.

Sedimentological Characterization of Deeper Group M Reservoirs in Malay Basin

S. A. M. Yusak* (Petronas Carigali Sdn Bhd)

With the proven resources established in the shallower stratigraphic intervals in Malay Basin, the focus has now shifted to the plays in deeper reservoirs. This paper focuses on the sedimentological characteristics of the deeper Group M, the deepest penetrated sedimentary sequence in the study area with hydrocarbon discovery. The early Oligocene Group M top is well demarcated by a regional shale marker (M shale) and has been divided in to subunits from M10 to M110 based on wireline log characteristics in the drilled wells (Fig. 1). The sediments of Group M were laid down in the early rifted continental sequence in alluvial to lacustrine environments.

The sedimentological characteristics were defined using core (conventional and sidewall) and wireline log signatures from three key wells. Based on available conventional core data, wireline logs and limited biostratigraphic control, the depositional setting for the studied interval was characterized by an active braided fluvial system draining in to lake. The recognized key subenvironments within this system include braided fluvial channels and in-channel bars, lacustrine mouthbars, and open lacustrine muds. The stacked and repetitive nature of the environments especially for the deeper M110 indicates an active progradation. The inferred environments and well log correlations show that the sand bodies are laterally extensive with sheet geometry.

Based on petrographic studies, the sandstones are fine to coarse grained, subangular to subrounded, compositionally immature lithic and feldspathic arenites (Fig. 2) and diagenetically altered with presence of silica and carbonate cements, authigenic kaolinite with subordinate illite. The sandstones were derived from metamorphic and igneous basement rocks with a

contribution from pre-existing sedimentary rocks. The evolution of depositional system and the sandstone compositions for the Group M sediments were primarily controlled by the interplay between the syn-rift tectonics and available accommodation space and probably influenced by climatic and lake level fluctuations.

In general, good reservoir quality is shown by braid plain to channel sandstone, with some proximal mouthbar to lacustrine shoreface sediments also showing good reservoir quality (Fig. 3). For the deeper M110 unit, limited sidewall cores are available for evaluation; the general porosity values are moderate to poor whereas the permeability values are low (Fig. 4). The primary controlling factors for reservoir quality in the deeper Group M sandstones are depositional facies, grain size variations and diagenesis. The study has helped in understanding the controls on reservoir characteristics and to evaluate the use of appropriate technology like hydraulic fracturing for possibly enhancing the production in the discovery wells.

References

- Rees, A. J., Bishop, S. N and Watkins, C. A., 2006. Integrated reservoir Study, Well C, Malay Basin. Report No. 9417/I, Project No. Id/GK436, Fugro Robertson Limited, UK
- Mazlan B. H.J. Madon., Peter Abolins., M. Jamal Hoesni and Mansor Bin Ahmad, 1999. Malay Basin. In: The Petroleum Geology and Resources of Malaysia. PETRONAS, Kuala Lumpur, 171-217.

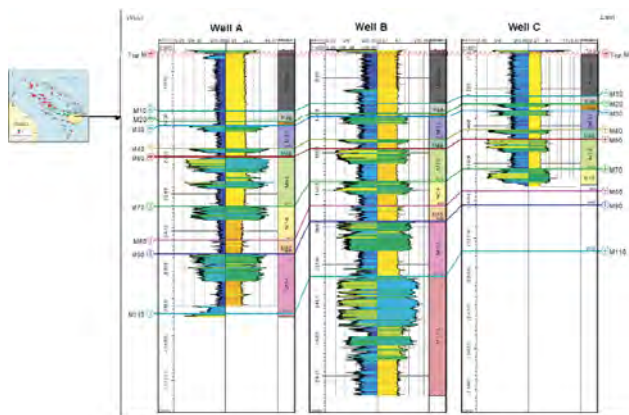


Figure 1: Stratigraphic correlation showing the distribution of Group M in the drilled wells.

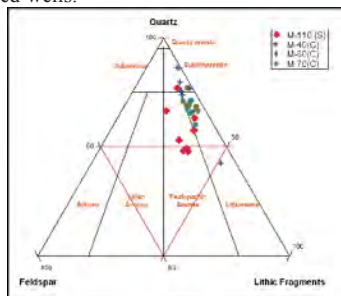


Figure 2: Sandstone compositions of representative core samples from penetrated Group M in the study area.

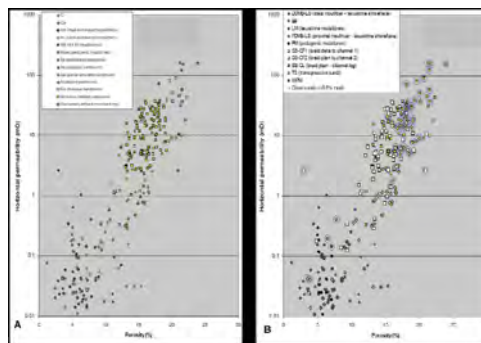


Figure 3: Controls on reservoir quality as shown by Group M40-70 in Well C showing (A) Distinct grain size and facies association, and (B) Better reservoir quality samples are associated with braid plain to channel sandstone, with some proximal mouthbar to lacustrine shoreface sediments also having good reservoir quality.

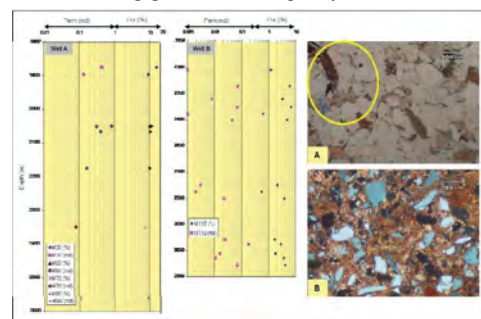


Figure 4 Porosity-permeability variations for Group M30-90 (Well A) and M110 (Well B) units. The variations are controlled by facies and grain size variations with the coarser sandstones preserving porosity (A) and the sandstones with higher matrix content having lower porosity (B).

The Exploration Strategic Potential of Rajang Delta System

Z. Ibrahim* (PETRONAS Exploration), B.H. WEI (PETRONAS Exploration) & A. Rauf (PETRONAS Exploration)

The better understanding of the Rajang Delta depositional history will open the opportunity of future exploration. Our current paleogeographic model of the Rajang Delta is derived from a wider regional stratigraphic review which spliced the East Natuna and the whole Luconia basin to become a single united geological region. In this study we established the same stratigraphic markers of the Sarawak basin (Cycle-I up to Cycle-VIII) in the East Natuna in order to come up with sequential stratigraphic basin evolution on both regions as an integrated linked geological event since late Oligocene. The tectonic activity and sea level fluctuation are concluded as the important geological processes which controlled the depositional history of the Rajang Delta. Two regional scaled normal fault systems are considered as the main boundaries of the Rajang Delta, namely Segitiga Fault and the Jintan Fault. The Late Oligocene rifting created the accommodation space for the deposition of the Cycle-I and Cycle-II stratigraphic intervals. This the initial stage of the depositional history of the Rajang Delta system, where both major fault systems bounded the coastal plain and deltaic environment in the NW and SE side respectively. A major extensional tectonic took place after deposition of Cycle-II in the late early Miocene, which marked the second tectonic phase. During this phase, a series of horsts and grabens were formed in the whole region of the study area. Generally, the whole region of the study area was exposed to the sub-areal erosion during this time, which reworked the previous older deposits. And therefore, major angular unconformity

(MMU) is observable in the whole region of the study area, except if it is deeply buried by younger deposits. The Cycle-III deposition took place during the marine transgression over the MMU, when carbonate deposited in the Segitiga Platform and west margin of the Central Luconia Basin. The absence of the carbonate between the two platforms is interpreted as the environment was too muddy in the SW proximal area, and the environment was starving to become condensed section in the NW distal area. The tectonic was interpreted very stable during the deposition of Cycle-III. Series of paleogeographic maps from Cycle-I are consistently showing the progressive movement of the bathyal environment southwestward to suggest shelf edge retrogradation since Late Oligocene. until the maximum flooding took place in the middle of Cycle-IV (TB2.4). This event of the maximum flooding is marked as the most advancing bathyal environment on the paleogeographic maps. Progradational sequence of Cycle-V marked the sea level drop, followed by shortlived transgression during the Cycle-VI. The broad neritic marine shelf was frequently exposed and incised during sea level fluctuation since Cycle-V. The incised valley fill deposits are proven as potential target by discovery of the Dara field, which tested the Cycle-VII sands. The presence of broad neritic marine shelf since Cycle V open the opportunities for future stratigraphic exploration of the incised valley fill targets in the area. Furthermore, the presence of the lowstand delta yet to be verified by further study.

Shallow Reservoirs, the Neglected Play in the Malay Basin - A Case Study from the A Field

S. H. So* (PETRONAS Carigali Sdn Bhd), S. Shahr (PETRONAS Carigali Sdn Bhd) & N. Ahmad (PETRONAS Carigali Sdn Bhd)

Malay Basin has been one of the prolific hydrocarbon basin in Southeast Asia since 1960's. Being a matured basin now, the hydrocarbon exploration in Malay Basin has become more and more challenging, innovative approaches are required, to identify a new play type for example is becoming more relevant in current scenario. In order to further explore the remaining hydrocarbon potential, mapping and screening have been carried out in the Southern Malay Basin with the main objective to identify the upside potential within the existing fields and inter-fields area. The X Field was one of the chosen field that indicated positive findings. Despite of the recent efforts on identifying deeper play potential, the shallow reservoirs (Group B) in X Field are also showing promising results.

The X Field is located in the Southern flank of Malay Basin, offshore Peninsular Malaysia. The X structure comprises of a heavily faulted Northeast -Southwest trending elongated anticline with a four-way dip closure. The X Field was first discovered in 1975 by Company A through the X-1 exploration well at the crestal part of the anticline. The field encountered non-associated gas in group H, I, J, K and L reservoirs (Upper Oligocene to Early Middle Miocene). Four appraisal wells were drilled from 1992 to 2010 to firm up the accumulation (Figure 1). To-date a Field Development Plan (FDP) is ongoing for the development of group H, I, J, K and L reservoirs within the X proper (near crestal area).

The Group A and Group B, above the Middle-Upper Miocene Unconformity, consist of predominantly marine clays and silts deposited during an overall marine transgression in nearshore to shallow marine environments from Late Miocene to Quaternary (PETRONAS, 1999). Two strong events within

the Group B were interpreted namely Intra B-I (~ 450 m) and Intra B-II (~550 m). The Intra B-II is composed mostly of channel features trending Northeast-Southwest with interpreted seismic facies of sub-parallel, semi- continuous, and wavy high amplitude reflection interpreted as lower coastal plain. The Intra B-I seismic facies of parallel, continuous, high amplitude and high frequency are interpreted as silty marine sheet sand. PCSB has done an Integrated Regional Study of the Malay Basin (IRS) in 2005 using seismic sequence approach where the interpreted SB 2100 marker is equivalent to the Group B from the EPIC, 1994. Findings from the IRS together with wireline logs and mud logs data supported the interpreted Group B depositional environment as lower coastal plain to nearshore marine with sediment provenance from the Northeast direction of the basin.

DHIs such as flats plot and polarity reversal were identified in both Intra B-I and Intra B-II (Figure 2 and 3). The seismic attributes analysis that has been carried out was very convincing to support the shallow potential in Group B as the amplitude anomaly showing possible gas responses (Figure 4). Besides the gas indication from the seismic attributes analysis, the gas chromatograph from the mud logs also showing indication of gas shows, where wells that penetrated the amplitude anomaly indicates higher gas reading, while lower gas readings were observed in the wells located beyond the mapped amplitude (Figure 5). However, no further formation evaluation has been carried out to evaluate the Group B potential.

In conclusion, the upside potential within the X Field is very encouraging using amplitude conformable to the structure spill as indication of gas accumulation which spans over 200 km2. Nevertheless, reservoirs quality (poro-perm) remains as

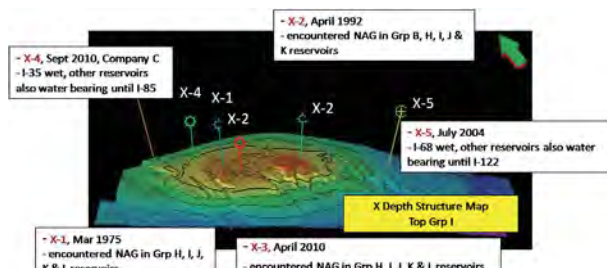


Figure 1: This figure showing the exploration history of the X Field with well location on Top Group I Depth Structure Map.

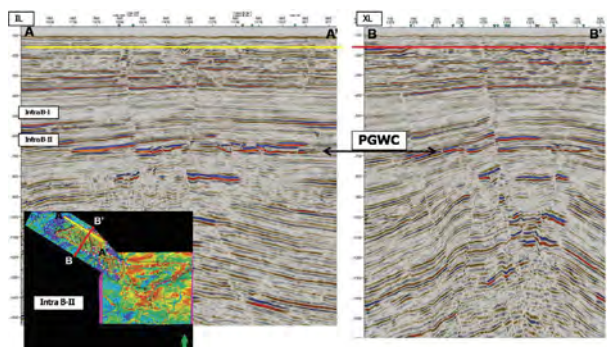


Figure 2: The flatspot or possible gas water contact (PGWC) identified from the Intra B-II horizon.

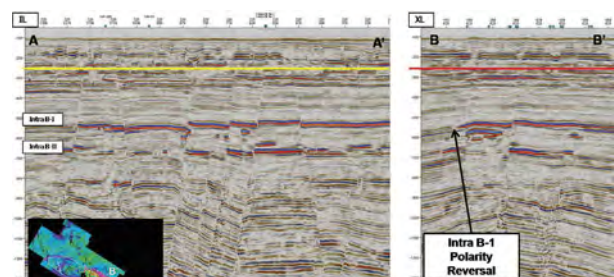


Figure 3: Polarity reversal observed from the Intra B-I horizon.

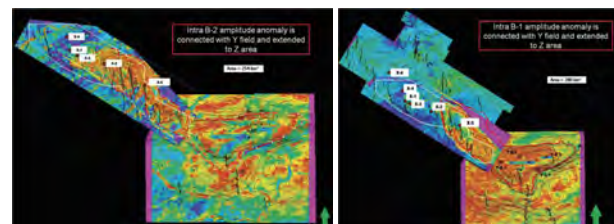


Figure 4: a) Intra B-II RMS amplitude anomaly conformable to the structure. b) Intra B-I RMS amplitude anomaly conformable to the structure.

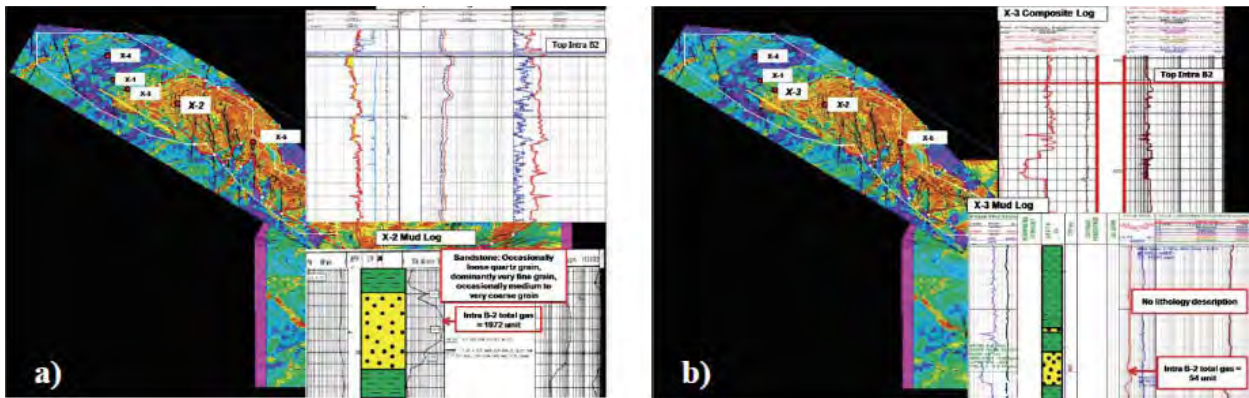


Figure 5: a) X-2 well located on the amplitude anomaly observed significant amount of gas shows in the Intra B-II. b) X-3 well located outside the amplitude anomaly, no gas shows observed in the Intra B-II.

the primary uncertainty for the Group B reservoirs as expected in silty sandstone environment. Draw-down pressure for the shallow reservoir during production is still under study where proper production testing and further formation evaluation is mandatory to conclude the true commerciality of this play.

References

- EPIC, 1994. Regional Study of the Malay Basin - Final Portfolios. Esso-PETRONAS Integrated Collaborative Study, Unpublished report, Esso Production Malaysia Inc.
- Mazlan Madon, Peter Abolins, M. Jamal Hoesni, and Mansor Ahmad, 1999. Malay Basin. The Petroleum Geology and Resources of Malaysia, Petroleum Nasional Berhad, Kuala Lumpur, Malaysia, p. 173-212.
- PCSB, 2005. Integrated Regional Study of The Malay Basin. Unpublished. PETRONAS Carigali Sdn. Bhd..
- PCSB, 2010. X Conceptual Development Plan. Unpublished, PETRONAS Carigali Sdn. Bhd, p. 4-83.

Pre-Tertiary Fractured Basement of Mega Host Block A, Malay Basin in Light of Current 3D Seismic Data Interpretation

N. H. Ngoc (PEG/ PETRONAS Carigali Sdn Bhd), S. A. Aziz (PEG/ PETRONAS Carigali Sdn Bhd), P. N. Bt. Mokhtar (PEX/ PETRONAS Carigali Sdn Bhd)

Pre-Tertiary fractured Basement in Mega host block A, Malay Basin is a large high meta- sediment structure, which became the considering HC objective for a long time. Since 1973 when the first time Oil has been discovered in the Basement by A-01 well, ten Exploration wells named from A-01 to A-10 have been drilled to penetrate inside the basement with different depths. Different well results for the basement target shows that distribution and characters of fracture systems are very complicated and many studies covering different disciplines have been performed to determine the HC potential of the Basement for the area. In this paper the authors would like to present new results of 3D seismic data interpretation to predict high HC potential zones in the study area. Some of the presented data have been applied to design the latest basement appraisal wells for the area with promising results.

The study area is covered by a large 3D seismic survey, which was acquired by eight streamers of 4800m length with acquisition bin side of 6.25m X 18.75 m. The 3D seismic data initially was processed by 3D PSTM processing sequence and then was reprocessed by both Kirchhoff PSDM and Beam PSDM methods. Good imaging of top and inside Pre-Tertiary Basement provided by 3D Beam PSDM processing (Figure 1)

permit us to apply the “From seismic interpretation to tectonic reconstruction” method, which was presented with more detail in the November 2009 AAPG’ IEC in Rio de Janeiro, Brazil to get detail basement mapping and to predict the fault systems with high potential of generating the large aperture (Macro) fractures.

Besides of macro fractures, others fracture characters as: Fracture density, continue & intersection of different fracture systems were also tried to be predicted. For this purpose a large number of 3D seismic attributes have been tested, at the results, relative Acoustic Impedance was considered as the best attribute for prediction of high fracture density areas and reasonable attribute to predict the continue and intersection of different fracture systems (Figure 2). To predict the continue and intersection of different fracture systems, ant tracking attribute which was generated by new work flow proposed by the authors was considered better (Figure 3).

Based on integration of the above seismic attributes, in the mega basement host block A different areas with different fracture characters and consequently different HC potential were identified and outlined. Well data have been used to check and to confirm the predicted results.

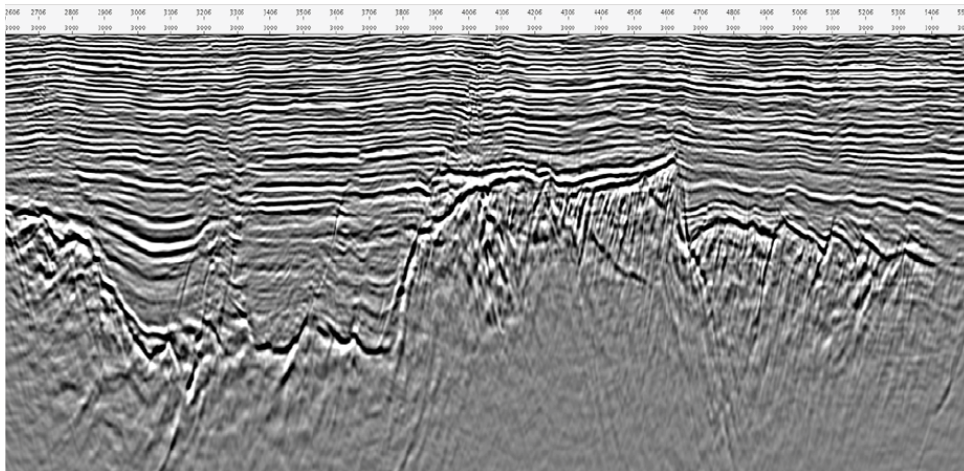


Figure 1: Good imaging of top and inside Pre-Tertiary basement of 3D seismic section processed by Beam PSDM.

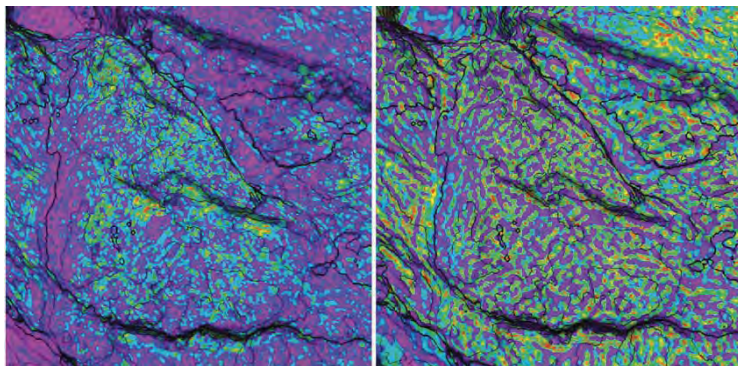


Figure 2: Ave. Magnitude RAI attribute (Left) could predict high fracture density zones, while Maximum Amplitude RAI attribute (right) could predict continue & intersection of different fracture systems.

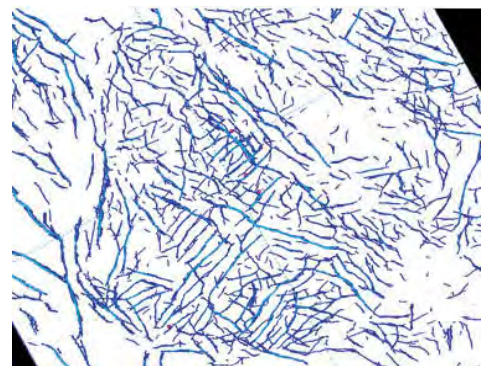


Figure 3: Ant Tracking Time Slice better images continue and intersection of different fracture systems.

3D Near-Wellbore Structural Modeling, Natural Fracture Characterization and in-Situ Stress Analysis in A Complex Thrust

R. Dashti* (Schlumberger)

Introduction

Borehole images are well known to provide high resolution picture of the geology at subsurface. However, upscaling and linking these data to field scale models have always been a challenge whilst of paramount importance particularly in the case of poor seismic data and complex structure. In this study, using a new technique results of borehole images analysis in two wells are integrated to determine the structural configuration of a complex hydrocarbon-bearing structure through construction of a 3D near wellbore fault system and surfaces. Also natural fracture system and in-situ stresses are characterized in incorporation with dipole shear sonic data.

Background

In 2010 an operator drilled two exploration wells in an under-explored area of the Baram Delta Basin, onshore Brunei Darussalam. Both wells (Wells A&B) encountered hydrocarbons in different zones. Prior to the drilling of the two exploration wells an accurate structural interpretation had been hampered by the low-quality of available 3D seismic data and a limited control by older wells in the area. Therefore, a high degree of uncertainty existed regarding structural configuration of faults and reservoirs. Many questions about the character of the natural fracture network and in-situ stress directions and magnitudes had yet to be answered.

Single Well Image Analysis

Two wells (A&B) in these studies were drilled along a slightly S-shape trajectory with maximum 20 deg deviation. In both wells FMIHD* was acquired, processed and interpreted to recognize structural dip, faults, fractures and stress-induced features. Results of this analysis in each well was then checked against the wellbore trajectory to understand the relationship between type and variations of observed structural features with each structural zone/location the well passes through.

Schematic Structural Configuration

Subsequent to single well image analysis, results of the two wells were then integrated to construct the conceptual structural configuration. The main aim of this task was to visualize the changes in structural dip (i.e. structural zones) and the fault zones geometry based on the two wells observations and to investigate how it can be incorporated into a conceptual thrust anticline model which is consistent with regional tectonic setting. Then, this would be used later as the basis for the 3D near wellbore structural model. In this process, regional tectonic as well as outcrop reservoir analogue were carefully investigated and integrated with subsurface results (figure 1).

3D Near Wellbore Structural Modelling

Newly developed technique of eXpandBG* embedded in the Petrel* 3D environment was utilized to integrate the results of structural analysis in two wells to generate a near-wellbore structural model including major thrust plane and reservoir surfaces. This was performed wrt the schematic structural configuration made previously. The workflow of this task include dip sequence analysis, structural plane computation, structural axis delineation, structural unit and elements determination, fault plane generation, isopach map creation and finally structural dip projection and surface creation.

The workflow of 3D near-wellbore structural modelling is illustrated in the figure 2. Since the geometry of the structure and the stratigraphic position of the reservoirs are primarily controlled by the main thrust, only this fault plane was generated and incorporated into the model.

Natural Fractures Characterization

Natural fractures were abundant and readily detected, oriented and classified based on FMIHD images in both studied wells. Various types of fractures were found to create a complex

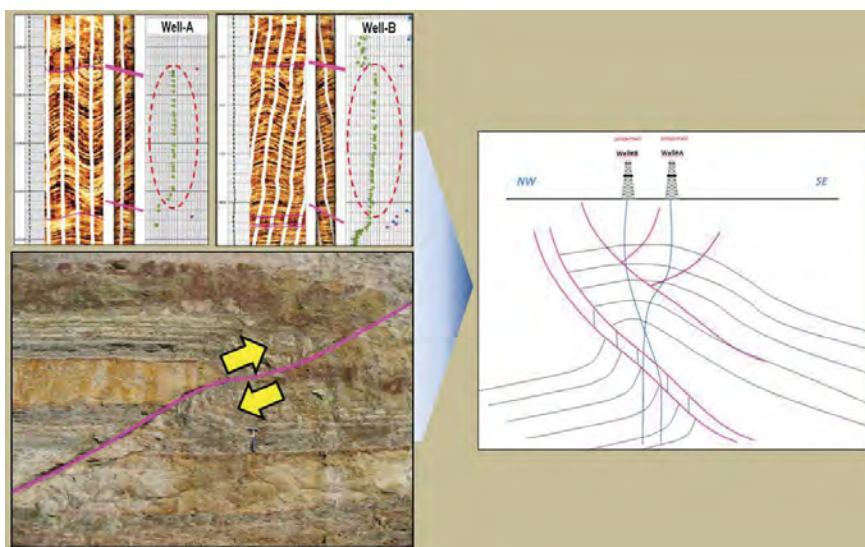


Figure 1: Schematic structural configuration was generated using image analysis results in two wells and with reference to regional settings and outcrop reservoir analogue study.

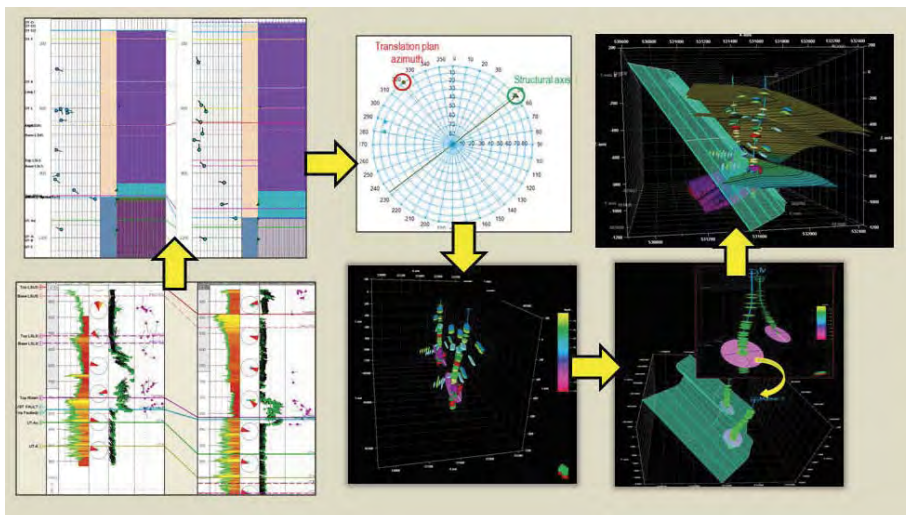


Figure 2: Summarized workflow for generating 3-D near-wellbore structural modeling.

fracture network. Almost all of these fractures are electrically conductive on the image logs and hence likely to be open in nature. These results were correlated with anisotropy analysis using dipole shear sonic data to locate the main fractures corridors, where maximum energy and time anisotropy shows good match with concentration of natural fractures on FMI.

The majority of fractures (with medium to high dip angle) are fault-related, while the rest are fold-related. The latter type of fractures is more common in the well B. This can be attributed to comparatively more structural curvature at the location of this well. It may also be inferred from fracture-breakout relationship analysis. Fault-related fractures in thrust system (the current case) are aligned parallel to Sh_{min} (fault strike), while fold-related fractures (type I) are dominantly parallel to Sh_{max} (figure 3).

In-Situ Stress Analysis

Borehole breakouts identified in both studied wells were analyzed to study the direction of in-situ stress in the study area. This part of the analysis revealed a slight drift of Sh_{min} direction across the main thrust from NNE-SSW below to more NE-SW trending above. These results shows good agreement with the SH_{max} direction inferred from fast shear azimuth derived from Sonic Scanner data (figure 4).

Conclusions

- Using new technique of eXpandBG it is now possible to generate near-wellbore structure model using results of borehole image analysis. This can be of prime significance when surface seismic data are poor and cannot reveal a clear picture of subsurface.
- The natural fracture system in the reservoir has been inferred to comprise both fault- and fold-related fractures. Fold-related fractures are more common in Markisa-1 well probably due to a higher surface curvature.
- Breakout analysis and sonic scanner fast shear azimuth showed changes of stress direction across the thrust zone.

References

- PETRONAS, 1990. Petroleum geology and resources of Malaysia
 Price and Cosgrove, 1990. Analysis of geological structures, Cambridge press.

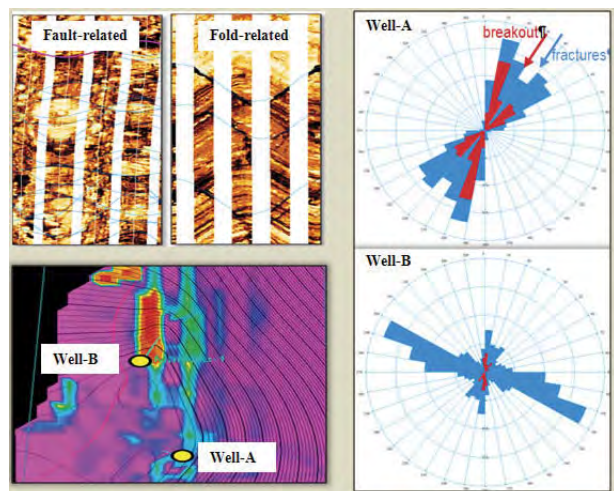


Figure 3: top-left, examples of fold and fault related fractures, bottom-left, location of wells A&B on the curvature map, right, comparison of strike direction of natural fractures and borehole breakouts.

CRS-Stack and NIP-Wave Tomography Implemented to the SH-Wave Reflection Seismic Data for Shallow Hydrocarbon Prospecting

M. R. Sule (Institut Teknologi Bandung), A.A. Valencia* (Institut Teknologi Bandung),
A. Hendriyana (Institut Teknologi Bandung), U. Polom (Leibniz Institute for Applied Geophysics) &
C.M. Krawczyk (Leibniz Institute for Applied Geophysics)

Introduction

Most of exploited hydrocarbon reservoirs are situated at the depth of around 2,000 – 3,000 m. The use of P-wave reflection seismic is suitable for that depth interval and commonly implemented in the oil and gas industries. However, it is believed that there are still many shallow hydrocarbon reservoirs in the world, which become economically to be exploited in a near future. The challenges in the shallow hydrocarbon prospecting by using seismic method include: (1) how S/N ratio in the seismic data could be improved; and (2) how thin layers (and hydrocarbon reservoirs) situated at near surface could be better detected. The use of CRS-Stack and NIP-wave tomography methods to the SH-polarized shear wave reflection data could be a good solution of above challenges. The SH-wave reflection could detect thinner layers, since its velocity is much slower than P-wave, which makes the wavelength shorter. Shorter the wavelength, better resolution of seismic section will be obtained.

As initial experiment, this combined technique is implemented to SH reflection seismic data acquired from Trondheim, Norway, in which the seismic line was conducted below the infilled and paved harbour area (Polom et al. 2010). A land streamer system of 120 channels (geophone interval of 1m) was used in combination with a shear-wave vibrator buggy. Partial Common Reflection Surface (CRS) Stack and Normal-Incident-Point-wave (NIP-wave) tomographic methods are then applied to this high resolution shallow reflection seismic data in order to obtain enhanced image of subsurface with the target up to 1.2 s (shallow target) and more precise interval velocity section. A ca. 600 m long high-resolution multichannel SH-wave reflection seismic profile was accordingly reprocessed.

This paper will describe only the shear wave seismic main reprocessing that has been conducted by this proposed technique. Interpretation related to the data will not be explained. This technique will be then proposed to be adapted for shallow hydrocarbon prospecting in a near future.

Implementation of partial CRS-stack method

Partial CRS attributes has an ability to provide more detail information about subsurface, which consist of emergence angle and the two radii of wavefront curvatures RNIP and RN. Those CRS attributes extracted from prestack seismic data by using optimization scheme and coherence analysis in order to obtain the best stacking surface in every ZO sample. Since the final product of Partial CRS-Stack is CRS supergathers, which are regularized and have better signal-to-noise ratio compared to original CMP gathers, one could implement velocity analysis after applying this method. Thus, the stacking velocity based on obtained CRS supergathers will be better than the one that is obtained from conventional stacking method.

Common-Reflection-Surface (CRS) stack operators are approximation of kinematic reflection response of a curved reflector's segment with certain orientation and local curvature. Velocity model that is basically required for conventional stacking has been replaced by three parameters for 2D CRS-stack or 8 parameters for 3D CRS-stack. The main task of the CRS-

stack method is to extract those attributes in efficient manner. Two versions of this method have been developed in the past time, e.g. Mueller (1998) and Mann (2002). According to Mann (2002), the three parameters are determined by several steps, in which each step determines one parameter. The determined parameter from a step is then used for next steps, i.e. to extract the remaining CRS attributes. The determined CRS attributes can also be used for subsequent steps, such as velocity model building (Duveneck, 2004; Kienast et al., 2007) and determination of migration aperture (Jaeger, 2005).

Before CRS-stack is employed to the seismic data sets, pre-processing sequences must be performed, such as low cut filtering to reduce ground roll, spherical divergence correction, deconvolution, refraction static correction and residual static correction. Afterwards, pre-processed gather is stacked using CRS approach and conventional approach for comparison. The seismic section obtained from conventional processing method is seen in Fig. 1 (top).

Three CRS attributes were determined using Extended Search approach (Mann, 2002). The determined CRS attributes are then smoothed along each reflector according to its local orientation, in order to minimize outlier and fluctuated attributes values (Kluever and Mann, 2005). The smoothed CRS attributes are then used either to generate CRS supergather by means of Partial CRS-stack (Baykulov, 2009) or to derive velocity-depth model using NIP-wave inversion (Duveneck, 2004). The resulted stacked section obtained by CRS-stack shows significant improvement in reflector continuity and enhances signal-to-noise ratio. It reveals unidentified feature in conventional stack section (e.g. shown by dashed boxed), as can be seen in Fig. 1 (bottom).

Implementation of NIP-wave tomographic method

Stacked section and two kinematic wavefield attributes section resulted from CRS-Stack method (i.e. emergence angle, α , and radius of curvature of NIP wavefront, RNIP), are then used as input data for velocity-depth determination by implementing NIP-wave tomographic method. Kinematic wavefield attributes extracted from pre-stack seismic gather is prone to outliers and fluctuated values because they are determined independently for each samples and also because of noise contamination, hence, event consistent smoothing is required. More than 1500 data points have been picked from α and RNIP section in automatic manner but guided by coherence and stacked section. Coherence section which quantified fitting degree between pre-stack seismic gather and reflection respond is considered during automatic picking as well as stacked section in order to separate between reflectors and noise or other unwanted event. Very low coherence values correspond to unreliable attribute should be avoided to be picked. Editing has been applied to the picked attributes to remove undesired data. Figure 2 (top) shows the picked reflectors as input data for NIP-wave tomography.

Initial model represented by 1.5D velocity profile was chosen with constant vertical velocity gradient of 0.3 s⁻¹ and $v_0 = 1100$ dm/s at reference datum. Inversion process is carried

out using 100 dm horizontal spacing and 20 dm vertical spacing. Final velocity-depth model was obtained after 10 iterations. The resulted velocity-depth model is depicted in Fig. 2 (bottom). The resulted velocity-depth model is depicted in Fig. 2 (bottom). The picked kinematic attributes do not found at bottom part of the velocity model (> 1200 dm) which is associated with low coherence value, hence the resulted velocity values at that area are not reliable. Duvencek (2004) introduced new terminologies in the tomographic method, namely: $p = \sin(a)/V_o$, $M_{nip} = (\cos a)^2/(V_o \cdot R_{nip})$, and $t_o = t/2$ (V_o is velocity at near surface and t is two-way-time of reflection event). After the tomographic process was carried out, it can be seen that the difference between observed values of p , M_{nip} and t_o (input data) and calculated values (after tomographic process) is very minimum, as can be seen in Fig. 3.

Conclusion

After the seismic obtained from this proposed technique is compared to the results from conventional method, it can be seen very clearly the advantages of CRS-stack method. The profile under investigation here shows layered sediments down to 120 m depth and the bedrock below. The shearwave velocities could be translated into dynamic shear-modulus values, yielding zones of lowered stiffness. The CRS attributes which required during stacking are utilised for further processing, i.e. velocity model building. NIP-wave tomography that utilised CRS attributes offers promising, efficient and accurate way to derive velocity model because kinematic information picked from stacked section with improved signal-to-noise ratio. Besides that, CRS attributes can be used to predict stationary point and Fresnel zone width which helpful for migration process. Application of CRS-stack and NIPwave tomography to this SH reflection seismic data has gained interesting results, i.e. provide a nearly direct proxy for in situ soil stiffness, a key geotechnical parameter. The obtained velocity model could then be used as input for Prestack Depth Migration, since the velocity model is more precise than the conventional stacking velocity. Finally, this approach could be proposed as promising tool for shallow hydrocarbon prospecting in the future.

Acknowledgment

This research is funded by ITB Research and Innovation Grant 2011 on "S-wave reflection seismic data processing for high precision near surface imaging".

References

- Baykulov, M., 2009. Seismic imaging in complex media with the common reflection surface stack. Dissertation. Hamburg University.
- Duvencek, E., 2004. Tomographic determination of seismic velocity models with kinematic wavefield attributes. Logos Verlag Berlin.
- Jaeger, C., 2005. Minimum-aperture Kirchhoff migration with CRS stack attributes. Logos Verlag Berlin.
- Kienast, T., Spinner M., Mann, J., 2007. CRS-based minimum-aperture time migration – a real data example. EAGE 69th Conference & Tech. Exhibition, London 11-14 June 2007.
- Cluever, T. and Mann, J., 2005. Event-consistent smoothing and automated picking in CRS-based seismic imaging. 75th SEG annual Meeting, Houston.
- Mann, J., 2002. Extensions and applications of the common-reflection-surface stack method. Logos Verlag Berlin.
- Mueller, T., 1998. Common reflection surface stack versus NMO/stack and NMO/DMO/stack. Extended abstract 60 Annual

- internat. Mtg., Eur. Assn. Geosci. Eng. Session 1-20.
- Polom, U., Hansen, L., Sauvin, G., L'Heureux, J.-S., Lecomte, I., Krawczyk, C.M., Vanneste, M. & Longva, O., 2010. High-resolution SH-wave seismic reflection for characterization of onshore ground conditions in the Trondheim harbor, central Norway. In R.D. Miller, J.D. Bradford & K. Holliger (eds.), Advances in Near-Surface Seismology and Ground-Penetrating Radar, SEG, Tulsa, p. 297-312.

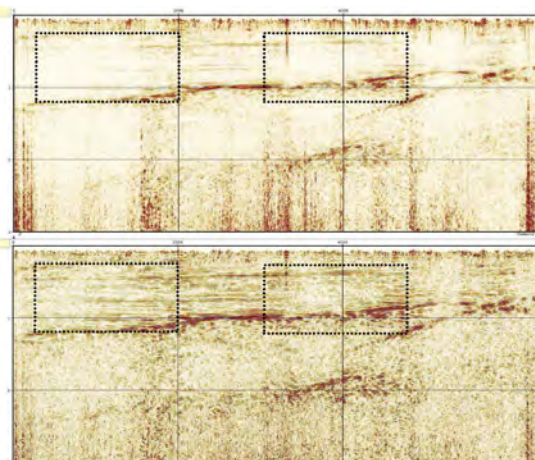


Figure 1: The difference between stack section obtained from conventional stacking method (top) and from Partial CRS-Stack method (bottom). The reflection continuities and S/N ratio are enhanced in the result of Partial CRS-Stack method.

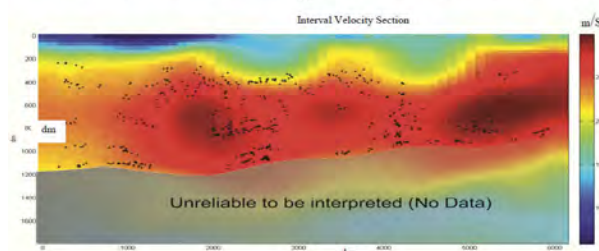
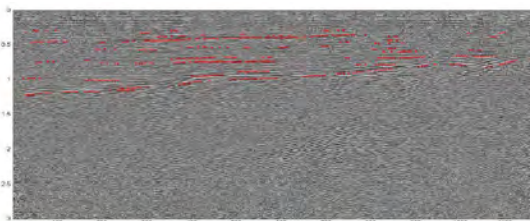


Figure 2: Picked reflectors as input data for NIP-wave tomography (top) and velocity-depth model resulted from NIP-wave tomography (bottom). Black dots situated in the bottom figure denote modelled NIP location using final velocity model. Since there is no NIP locations situated in the depth of 120 m and deeper parts (below the black line), the corresponded velocities are unreliable part of tomogram to be interpreted.

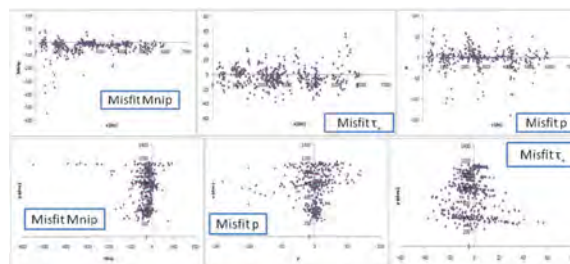


Figure 3: Misfit of M_{nip} , t and p for profile function (top) and depth function (bottom). Here it can be seen very obviously that the misfits are poled around zero.

Workflows to Improve the Resolution of Post-Stack Seismic Data and Attributes from the Malay Basin

A.E. Barnes* (PETRONAS Research Sdn Bhd), M.F. A. Rahim (PETRONAS Research Sdn Bhd) & A.R. Ghazali (PETRONAS EXPLORATION/ PETRONAS Carigali Sdn Bhd)

Introduction

As Malaysia moves towards enhanced oil recovery, it becomes more important to extract as much information as possible from existing seismic data over producing fields. A straightforward and cost-effective means to help achieve this is to enhance the resolution and interpretability of seismic data through modern methods of post-stack interpretive data processing and seismic attributes.

Two key tools of interpretive processing are spectral blueing and coherency filtering. Spectral blueing increases seismic data resolution by increasing the bandwidth and boosting the high frequencies. Coherency filtering improves the interpretability of seismic data by removing incoherent noise. These tools are employed together in a workflow to enhance seismic data. Seismic attributes derived from coherency filtered seismic data are cleaner and show more detail. This is particularly true of structural attributes, such as discontinuity, curvature, and relative amplitude change. Attributes are further enhanced through specific workflows that reveal finer detail in the data.

The tools and attributes described here are widely available in commercial software packages, but their practical application remains limited. We present data examples from several fields in the Malay basin that demonstrate the effectiveness of straightforward workflows built with fairly standard tools for improving post-stack seismic data for detailed analysis.

Method

Post-stack seismic data is readily improved for interpretation through coherency filtering and spectral blueing. The improved seismic data have better resolution and serve as input to produce cleaner seismic attributes. Attributes are often further enhanced through various filters.

Modern coherency filters or "structurally-oriented filters" smooth seismic data along reflection dips while preserving faults and other sharp discontinuities (e.g., Höcker and Fehmers, 2002). Horizon and fault interpretation become easier and more reliable with coherency filtered data, and seismic attributes are cleaner when derived from such data (Sheffield and Payne, 2008; Henning et al., 2010).

Spectral blueing makes the average spectrum of a seismic dataset roughly match the average spectrum observed in well logs (Blache-Fraser and Neep, 2004). It acts to broaden the spectrum of the seismic data, favouring high frequencies. The idea is simple. The earth's reflectivity tends to be fractal, so its amplitude spectrum approximates a power law that mildly boosts high frequencies. The power law exponent varies somewhat regionally, but tends to be fairly stable within a seismic survey. Once the exponent has been chosen, the amplitude spectrum of the seismic data is determined within specified band-limits. Assuming no phase corrections are required, each seismic trace is then reconstructed with its "blued" amplitude spectrum and original phase spectrum. Spectral blueing enhances the vertical resolution to make smaller stratigraphic features clearer.

Spectral blueing tends to boost high frequency noise as well as signal, and therefore it is best run in a workflow with coherency filtering. We obtain good results with a coherency filter to clean the data, followed by spectral blueing to boost vertical resolution, and followed by a second coherency filter to remove incoherent noise that is boosted inadvertently by spectral blueing (Figure 1).

Structural seismic attributes complement standard seismic data by revealing faults, channels, gas chimneys, and other details hidden in the data. They are more effective when derived from coherency filtered data. The most useful attributes for mapping structural detail are discontinuity, curvature, and relative amplitude change (Chopra and Marfurt, 2007; Barnes et al., 2011). Discontinuity attributes are the work-horse attributes for structural interpretation and the most amenable to improvement. Their resolution is often increased along horizontal slices through Laplacian filtering, which sharpens the discontinuities and is fast. However, Laplacian filtering does not improve the vertical connectivity of fault segments in discontinuity attributes. Achieving that requires more powerful methods, such as ant tracking. Ant tracking transforms a discontinuity attribute into a fault attribute, often revealing fault details not apparent in the original attribute (Pedersen et al., 2003). Ant tracking is most successful with clean discontinuity attributes, from which non-fault discontinuities have been removed (Figure 1).

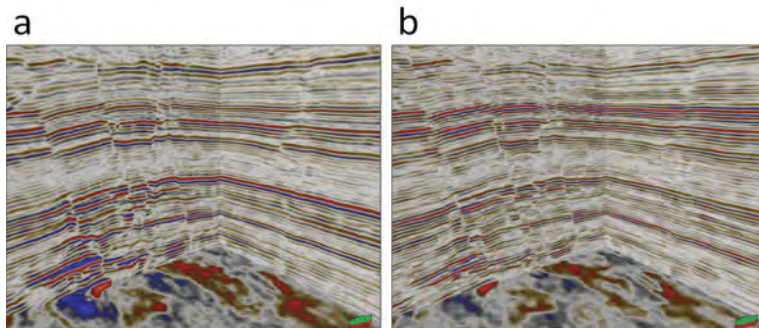


Figure 2: A comparison of (a) original seismic data, with (b) seismic data improved through processing with coherency filtering, spectral blueing, and a second pass of coherency filtering. The processed data have cleaner reflections, better vertical resolution, and sharper faults.

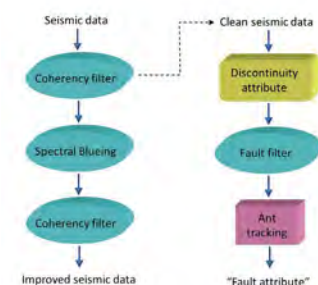


Figure 1: Workflows to improve post-stack seismic data for interpretation and to make a "fault attribute" from a discontinuity attribute. Filters for discontinuity attributes sharpen the discontinuities or remove non-fault discontinuities in preparation for ant tracking.

Relative amplitude change attributes record detail hidden in the seismic amplitudes. They have high resolution because they employ small operators, but they are prone to noise. Median filtering with a short vertical operator is a simple solution for removing noise in relative amplitude change that preserves faults and other structural features.

Discontinuity and amplitude change attributes employ first order derivatives, but curvature attributes employ second order derivatives. Curvature therefore naturally has higher resolution, and, for the same reason, is more prone to noise in the data. It is almost essential that curvature attributes be derived from clean seismic data. They usually do not require further enhancement.

Examples

Figure 2 shows seismic data from a field in the Malay basin before and after enhancement by a workflow that comprises coherency filter, spectral blueing, and a second coherency filter. The continuity and vertical resolution of the data are considerably improved, and faults are sharper. Seismic data nearly always benefits from coherency filtering. However, some coherency filters are overly sensitive to amplitude changes, and all coherency filters in current use have difficulty distinguishing structural detail, such as closely spaced en echelon normal faults. Spectral blueing is likewise usually beneficial, but it is not always suitable for attribute computations. For example, faults seem to be detected better with low frequencies than with high frequencies, and thus spectral blueing might degrade derived discontinuity attributes. We find that a single pass of coherency filter suffices to improve most structural attributes.

Figure 3 shows an example of how a discontinuity attribute is greatly improved for fault interpretation by deriving the attribute from coherency filtered data, and then transforming it into a “fault attribute” through filtering and ant tracking. This workflow makes major faults much sharper and clearer, and reveals many smaller faults that are not visible on the original discontinuity attribute. It also enhances the acquisition footprint along inlines, which is a common problem (lower part of Figure 3d).

Conclusions

Powerful methods of coherency filtering and spectral enhancement are becoming widely available in commercial software, allowing the seismic interpreter to easily increase the resolution and continuity of post-stack seismic data. These methods should be employed routinely. Using a workflow comprising these methods, we significantly improve the interpretability of a field dataset from the Malay Basin. Further, discontinuity, relative amplitude change, and curvature structural are sharper and cleaner when derived from coherency filtered data. Laplacian filters sharpen discontinuity attributes further, and reveal finer structural detail. Laplacian filtering is simple, fast, and effective for time slices, and should be tested routinely. For purely fault interpretation, discontinuity attributes can be transformed into fault attributes by a workflow that applies a filter to reduce non-fault discontinuities, followed by ant tracking to connect fault segments. This makes faults easier to track and reveals greater fault detail than can be seen on standard discontinuity attributes.

Acknowledgement

We would like to thank PETRONAS Research and PETRONAS E&P Technology Centre for permission to prepare and present this paper.

References

- Barnes, A.E., Cole, M., Michaels, T., Norlund, P. and Sembroski, C., 2011. Making seismic data come alive. *First Break*, 29(6), 33-38.
- Blache-Fraser, G. and Neep, J., 2004. Increasing seismic resolution using spectral blueing and colored inversion: Cannonball field, Trinidad. 74th SEG Annual Meeting, Expanded Abstracts, 23, 1794-1797.
- Chopra, S., and Marfurt, K.J., 2007. Seismic attributes for prospect identification and reservoir characterization. SEG, Tulsa.
- Henning, A.T., Martin, R. and Paton, G., 2010. Data conditioning and seismic attribute analysis in the Eagle Ford Shale Play: Examples from Sinor Ranch, Live Oak County, Texas. 80th SEG Annual Meeting, Expanded Abstracts, 1298-1301.
- Höcker, C. and Fehmers, G., 2002. Fast structural interpretation with structure-oriented filtering. *The Leading Edge*, 21, 238, 240, 242-243.
- Pedersen, S.I., Randen, T., Sonneland, L. and Steen, O., 2002. Automatic fault extraction using artificial ants. 72nd SEG Annual Meeting, Expanded Abstracts, 512-515.
- Sheffield, T.M. and Payne, B.A., 2008. Geovolume visualization and interpretation: What makes a useful visualization seismic attribute? 70th SEG Annual Meeting, Expanded Abstracts, 849-853.

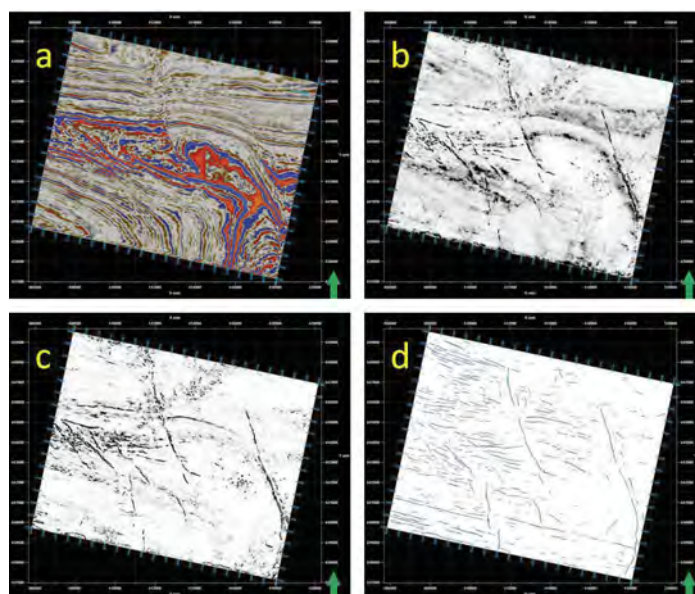


Figure 3: Time slices at 1200 ms illustrating how resolution of a discontinuity attribute is improved. (a) Original seismic data. (b) Discontinuity attribute derived from the original data. (c) Discontinuity attribute derived from the seismic data after coherency filtering. (d) Fault attribute derived from (c) through filtering and ant tracking.

Integrated Fluid Analysis Technique to Improve Evaluation on Fluid Potential in Downthrown Structure Prospect

T.A. Tiur Aldha* (Petronas Carigali Sdn Bhd) & G.T. Gunawan Taslim (Petronas Carigali Sdn Bhd)

This paper describes the process of integrated fluid analysis applied on pre-drilling of appraisal well in downthrown structure area. An integrated study involving seismic attribute analysis and reservoir characterization tools in Peninsular Malaysia provided an understanding of the structure, reservoir continuity and quality of three mature reservoirs that optimized new drilling location of appraisal well.

High amplitude anomaly found from attribute extraction of full stack seismic data has been brought to detail validation of fluid analysis on prospect area. The fluid properties determination in Amplitude Variations with Offsets or Angle (AVO/AVA) study has been extended to quantify its probability whether it is reliable or not. AVO uncertainty analysis is the extended process for analyzing and understanding the uncertainty in the conventional AVO analysis.

The combination of conventional seismic attribute analysis, AVO modeling and AVO uncertainty analysis are then discussed on this paper to show how this technique can be implemented using pre-stack seismic data. Finally, the technique has been proven and successfully implemented based on recent an appraisal well drilling result in AB Development Field of Offshore Peninsular Malaysia. Oil and gas hydrocarbon have been encountered in 20 meter thick of marine sandstone reservoir.

of full stack seismic data suspected as hydrocarbon anomaly as similar response to main structure of producing field. The high amplitude anomaly was validated with AVO conventional method then extended to AVO uncertainty analysis techniques to provide integrated fluid analysis for optimizing drilling location of appraisal well.

The AB Field is located in Offshore South China Sea, eastern flank of Malay Basin, Peninsular Malaysia. The field was discovered in 1992 that encountered oil and gas in I and J group sands and has been produce since 2007. Total 8 wells have been drilled on this field. Additional one infill well and one appraisal well were drilled recently on 2010. The field is covered by 178 sqkm 3D seismic survey. Three main horizons of top markers that representing 3 major producing reservoirs have been mapped. The target area is marine sandstone on shore face environment. Structurally the field is four way dip closure bounded by 2 major faults on west and eastern parts as resulting of rifting system on this area.

Prior to development drilling campaign, an appraisal well was proposed on eastern prospect where structurally located on downthrown of normal fault block of main field structure. Geologically the sand trend development from west to east is improved in term of net to gross. Seismic attributes maps from full stack seismic data revealed similar respond with the main field that suggested sand fairway extends into eastern fault block prospect. The study then continued to further analysis on fluid involving integrated AVO analysis.

Introduction

This paper provides a case study from AB field, where an east prospect was identified from seismic attribute maps

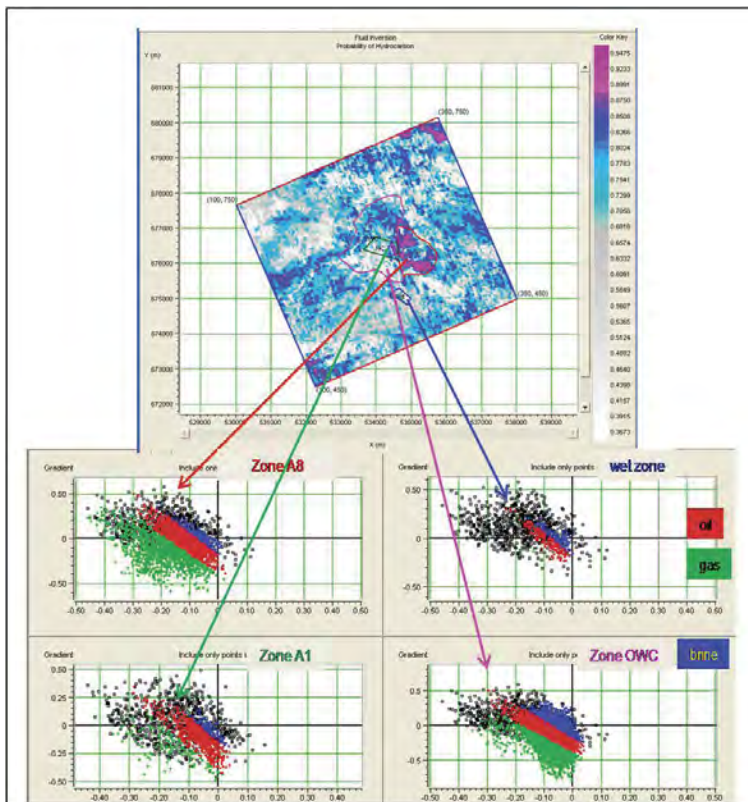


Figure 1: Showing probability map of I-1 sand after calibration to real data from the well that performed trend analysis and Monte Carlo simulation. The polygon of 4 zones on the map were fitted with the real situation of fluid properties including brine sand area.

Data Base and Work Flow

Available seismic and well data in the AB filed included 2005 reprocessed 3D PSTM seismic data comprises of near and far angle stacks, 2 well data of AB-1 and ABA-1; and 2 check shot surveys. Sonic V_p were available for those 2 wells but shear wave V_s is not available. Petrophysical data has been provided to support the rock physic model and fluid replacement modelling.

The following workflow was proposed to accomplish the objectives for the study area: (1) collection of data, well and seismic data including horizon interpretation; (2) log editing; (3) rock physic and fluid replacement modelling; (4) AVO modelling, comprises of few cases: wet, gas, oil, oil & gas cases; (5) well tie and synthetics; (6) Monte Carlo simulation; (7) Hydrocarbon probability; (8) seismic data conditioning; (9) attribute extraction; (10) calibration to real data; (11) Hydrocarbon probability maps; (12) identification and final review on target location. Key results of supporting analyses included (1) detailed correlation of sands; (2) detailed interpretation of faults and horizon in time and depth domains; (3) petrophysics, calibrated to be consistent with existing wells information over the production field area.

In performing fluid substitution and AVO modelling, shear wave velocity is critically needed. However, the absence of S-wave velocity on this field creating a special process of S-wave estimation. It is estimated based on Biot-Gassman relationship in the process of fluid substitution in hydrocarbon-saturated reservoir. In addition, Castagna relationship has been used also with assumption brine-filled rocks. The measurable properties

of P-wave velocity and density including porosity are used to calculate the saturated bulk modulus and shear modulus.

Attribute extraction of minimum amplitude on PSTM near and far stacks on reservoir interval were performed on three reservoir intervals. The results on amplitude map trend were calibrated to trend analysis and Monte Carlo simulation from 2 well data (figure-1). This process allows us to investigate the uncertainty in AVO predictions. By using Bayes' theorem, probability maps were then produced for different potential pore fluids.

Discussion and Conclusions

Based on the probability maps, the I-1 from I group sands has the highest probability on hydrocarbon potential followed by J-4 from J group sands then J-8 from J group sand has less hydrocarbon potential. Probability maps as final products then have been utilized for optimizing appraisal well location. The post drilling result showed the oil and gas has been encountered successfully from I-1 and J-4 reservoirs inside 20 meter gross-sand thickness.

Acknowledgments

The authors would like to thank Petronas Carigali Sdn Bhd and Newfield managements for permitting them to publish this material. In addition we would like to thank Mr Rizal Bakar and Mr Ravi from Specialized Study Group for many helpful discussion and suggestions.

Integration of Sequence Stratigraphy and Elastic Inversion Improved Understanding on Reservoir Characterization

N.M. Mohamud* (PETRONAS Carigali Sdn Bhd), O.A.M. Mahmud (PETRONAS Carigali Sdn Bhd), N.A.R. Razali (PETRONAS Carigali Sdn Bhd) & M.H.M.N. M Nor (PETRONAS Carigali Sdn Bhd)

Introduction

Understanding the geological model is important throughout the exploration, appraisal and development phase of hydrocarbon. A good geological model requires integration and manipulation of all available seismic, well logs, geology and engineering data. Such models are best derived in the context of sequence stratigraphic framework. This paper will present a case study of which sequence stratigraphy and elastic impedance volume was used to understand the reservoir properties and performance in Menggatal field, Offshore Sabah.

Methodology

A geological model is best constructed using sequence stratigraphy technique, since it provides a platform to enable the interpretation of stratigraphic section that considers sedimentology and chronostratigraphy. Sequence stratigraphy interpretation from regional 2D seismic data was carried out to establish a geological model that honours the Menggatal-1 well result. Shingled turbidite model deposited in the prograding complex during the Late Miocene Stage IVD is suggested in Menggatal field (Figure 1). Well log sequence stratigraphy was also utilized to validate seismic interpretation (Figure 2) and accurately tie well log to seismic.

Forward modelling of synthetic angle stacks indicated mismatch with far angle stacks. This mismatch indicates that simultaneous inversion results are not reliable. Therefore elastic inversion of far angle stack was performed. Elastic attributes contrast analysis at Menggatal-1 well location indicated that EI

(30°) contrast is higher than acoustic impedance (AI) contrast for gas-sand/brine sand interface in comparison to overlying shale/gas sand and shale/brine sand interfaces.

An elastic impedance volume that integrates geological, petrophysical and engineering data was generated to estimate the elastic impedance (EI) attributes for lithofacies discrimination, and predicts the extension of hydrocarbon bearing sand in Menggatal field. An iterative approach that integrates the elastic impedance volume and sequence stratigraphy derived model was then performed, to interpret the reservoir properties and performance in Menggatal.

Interpretation and Analysis

Figure 3 summarize the observations from the EI volume. The gas sands in Menggatal were interpreted to have low EI values in comparison with the surrounding shale and brine sands. Predicted flat spot of Sand 4 from the seismic corresponds with free water level at well location. The EI volume enables interpretation of free water level of shallower reservoir in Menggatal field (Figure 3).

The integration of elastic impedance interpretation constrained by sequence stratigraphic derived model, suggested better developed reservoirs are present, away from Menggatal-1

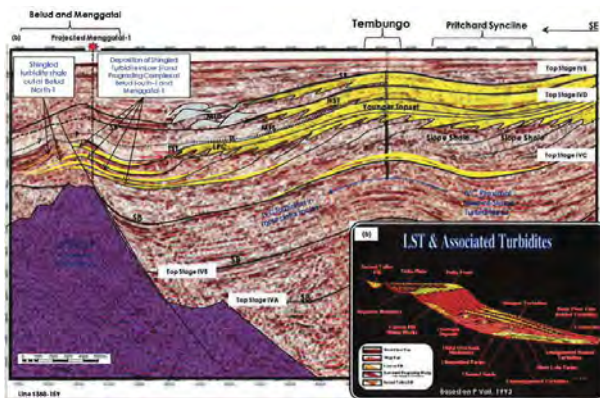


Figure 1: A regional 2D seismic line SB88-159 was used in the sequence stratigraphy interpretation. This seismic line goes through from Bunbury (SE) to Pritchard Syncline, Tembungo Field and Belud and Menggatal area in the NW Sediment direction is observed from SE to NW direction. Sequence boundaries (SB), transgressive surface (TS), low stand prograding complex (LPC), and highstand system track (HST) can be identified from this line. Deposition of shingled turbidites is observed in the low stand prograding complex of Late Miocene Stage IVD. When prograding complex receives a large volume of sand supply, the system can become overloaded and minor short-term lowstands will result in multiple thin shingled turbidite sands at the toes of the prograding complex clinoforms (Sangree .et. ai, 1992). The shingled turbidite model was also proposed by Vail, 1993 (Cramez and Hutchings,2001) (Figure 1c).

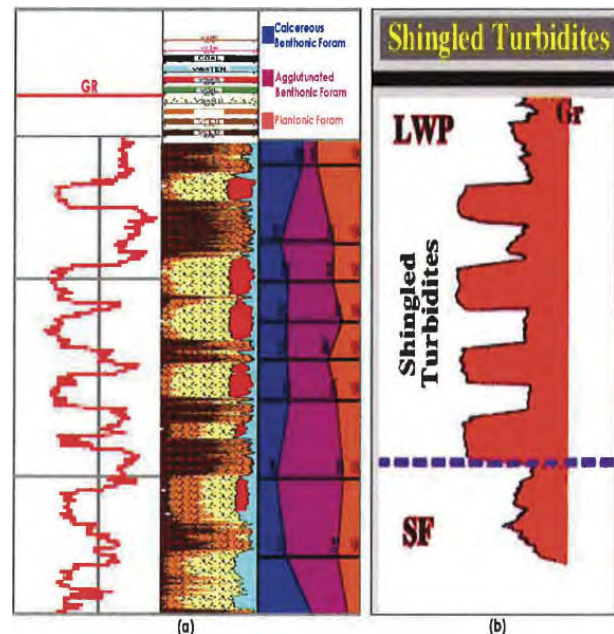


Figure 2: Well log sequence stratigraphy was used to validate seismic interpretation. Menggatal-1 well log pattern (Figure 2a) shows similar stacking pattern of the shingled turbidite model proposed by Cramez and Hutchings, 2001 (Figure 2b). The stacking pattern of the shingled turbidite is characterized by cylindrical boxy shaped sandstones separated by significantly shaly intervals. The presence of high diversity assemblages with deep water agglutinants and calcareous benthonic forams associated with common planktonics in Menggatal-1 well suggest that the sediments were deposited within upper to lower bathyal environmental realm.

well location (Figure 4a and 4b). An iterative approach was carried out to establish the facies model and qualitatively interpret the net sand in Menggatal (Figure 4c and 4d). The interpretation of EI volume also suggested gas sands presence at the adjacent fault block (Figure 3). As a result, this integration enables more accurate resource estimation and quantification of risk and uncertainty in Menggatal field.

Conclusions

The interpretation of reservoir properties and performance from the elastic impedance volume are best done in a realistic geological context that is provided by sequence stratigraphy.

Acknowledgment

The authors would like to thank PETRONAS and PETRONAS Carigali Sdn Bhd management for permission to publish this article.

Reference

- Cremez, C., and Hutchings, W., 2001. Turbidite Systems in Hydrocarbon Exploration, Universidade Fernando Pessoa Porto, Portugal short course, viewed on 10th January 2012, <http://homepage.ufp.pt/bibliotecaiWEBTurDiDepSystems/Index.htm>.
- Sangree, J.B., Mitchum, R.M, Vail, P.R., 1992. Application of Sequence Stratigraphy to Hydrocarbon Exploration, pre-print of paper presented at Sequence Stratigraphy of European Basin Conference Dijon, France.

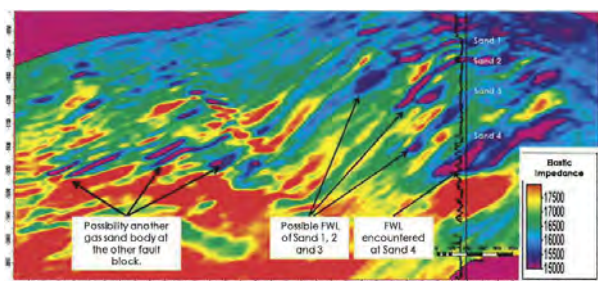


Figure 3: Elastic impedance volume in line across Menggatal-1 well show gas bearing sand has low EI value in comparison with the incasing shale and brine sand in 4 reservoir sands (Sand 1-4). Sand 4 encountered FWL at the well location. Possible FWL could be interpreted at Sand 1, 2 and 3. There is also possibility of gas sand at the adjacent fault block that has similar EI anomalies as the gas sand encountered at the well location.

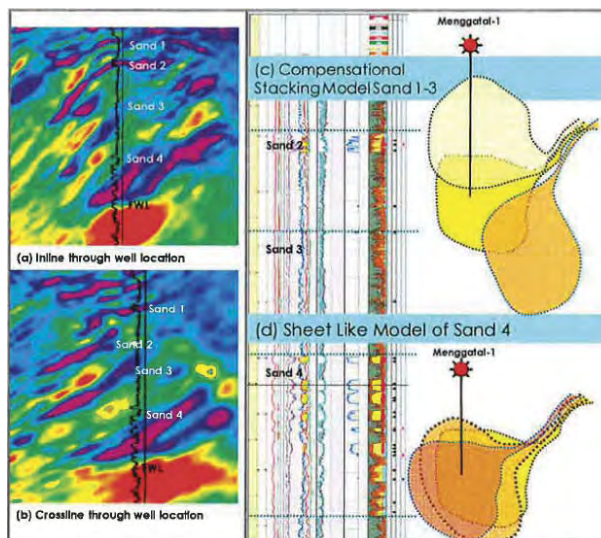


Figure 4: Figure 4 shows the respective inline and crossline at Menggatal-1 well location. In Figure 4a and 4b it can be seen that a better developed reservoir is present away from the well location. Two models for net sand distribution were proposed in Menggatal field; figure 4c: compensational stacking model for Sand 1, 2 and 3; figure 4d shows the sheet like model for Sand 4. This facies model for net sand distribution was done qualitatively by comparing the well log (Figure 4c and 4d) and elastic impedance volume (Figure 4a and 4b).

An Efficient Development 2011 Case History from the Gulf of Thailand

R. C. Roever* (Coastal Energy), J. Moon (Coastal Energy), R. Ripple (Coastal Energy), D. Cox (Coastal Energy), N. Htein (Coastal Energy), J. Mitchell (Coastal Energy), S. Rubio (Coastal Energy), J. Pringle (CEC International, Ltd. (Thailand)), R. The (CEC International, Ltd. (Thailand)), G. Peace (CEC International, Ltd. (Thailand)) & A. Laird (CEC International, Ltd. (Thailand))

From January to December 2011, Coastal Energy (CEC International, Ltd.) has discovered, appraised and started production from the Bua Ban North field. This project encompassed drilling and completing 21 wells with a subsequent hook-up to two Mobile Offshore Producing Units (MOPUs) and Floating Storage Options (FSOs). By year end, average daily oil production over the last five months had increased by over 70% from the previous seven months. The development of this new Lower Miocene field has added Proven plus Possible(2P) Stock Tank Original Oil in Place(STOOIP) of 204MMBO with recoverable reserves of 67MMBO to CEC's G5/43 permit which encompasses the offshore Songkhla Basin. It is located downthrown to the western margin bounding fault of the basin some five to ten kilometers north of the main Bua Ban field. (Figure 1) Prior to 2011, CEC exploration and production efforts were focused primarily on the Lower Oligocene and Eocene sands which are the producing reservoirs for the Songkhla A and Bua Ban fields. These two fields were developed utilizing an early production concept as well going from zero production in 2008 to 10,000BOPD in 2010. They provided a valuable learning curve for the 2011 success.

The general development scenario used by CEC for the Songkhla Basin is to select a central location from which to drill a prospect. In the event of a discovery, the appraisal and development drilling can proceed immediately. All wells are directionally drilled and designed as a three hole-section free standing through a slotted Caisson Deck, which can be tied back to a MOPU. It is planned to produce the well, however there is also an option to sidetrack to additional targets. All completions included the installation of Electric Submersible Pumps (ESPs). Using this type of early development concept requires daily cross discipline cooperation between drilling, engineering and geoscience to ensure operations run efficiently.

The challenges for the geoscientist are varied. Much depends on the geology and geophysics of the individual basin, its petroleum system and the prospects. Initially, one of the main challenges is the selection of the central location. One must consider the primary and secondary objectives, their target depths and structural configuration as well as any shallow hazards. Once that location is determined the main challenge consists of assimilating the drilling, log and pressure analysis into any ongoing structural mapping and analysis of the 3D seismic. This integration is critical for real time decision making and additional well path planning. The difficulty of this particular challenge is dependent on the time it takes to drill, evaluate and complete a well. In the case history for the Bua Ban North field to be described, the average drilling time for each well to total depth was ten to fifteen days, which results in a continuous flood of data for the geoscientist.

In order to understand this development and its challenges, some background will be provided regarding the exploration history as well as the geological setting for G5/43 in the Gulf of Thailand's Songkhla Basin. The Songkhla Basin is one of three narrow early Tertiary rift basins inboard of the main Gulf of Thailand rift, Pattani Basin. It is a N-S trending half-graben

(40x20kms.), with the controlling fault system along its western edge and contains up to 13000 feet of sedimentary section with the early section dominated by lacustrine sediment systems. Dating of the oldest sedimentary fill was obtained from the Benjarong-1 well where clays from a core in the syn-rift sequence gave a late early Eocene age. Structures are mainly tilted fault blocks or anticlinal folds related to roll-over into faults. Heat flows are relatively high with an average temperature gradient of 2.5 deg F/100 feet. This has facilitated the expulsion of large quantities of waxy crude oil typical of algal lacustrine source rocks. Throughout the 70's and 80's exploration was limited in the area as the focus was on the Miocene gas in the central Gulf's Pattani Basin. In the early 90's, Premier Oil was the first to actively explore the Songkhla Basin. They drilled five wells with only one dry hole. Two wells(Songkhla-1 and Bua Ban-1) flowed oil at significant rates (1500 and 768 BOPD respectively) on drill stem tests, one well(Songkhla Southwest-1) encountered a small oil column but did not flow to the surface on testing and another well(Benjarong-1) encountered a significant oil column, but was not tested. Reservoir objectives for all were the Lower Oligocene sands at depths of 7000-8000 feet TVD. The results were considered marginal and there was no further activity until Coastal's Thailand application. Concession G5/43, awarded in July 2003 to a CEC subsidiary (NuCoastal Thailand Ltd) is located offshore eight kilometers from the Songkhla village in the south and 50 kilometers from the Island of Ko Samui in the north. Water depths range from 50-100 feet. Originally a large concession of 17,100 km², it is currently two areas totaling 4775 km² following required relinquishments. (Figure 1) The southern portion covers most of the Songkhla Basin and is the focal point of CEC's current exploration and development. In 2005, three wells were drilled to appraise the Bua Ban 1 discovery. These wells were followed by a 3D survey (334km²) in 2006 covering this Bua Ban trend and the western half of the basin. The eastern half had previously been covered by Premier's 1989 3D survey (327km²).

Phase One development of the Songkhla A field commenced in September 2008 with three wells, 2 targeting the Lower Oligocene and 1 targeting the Eocene. All wells were completed and first oil commenced in February 2009 at 6000 BOPD. With the rig released, Phase Two did not begin until September 2009 with the arrival of Atlantic's Vicksburg jack-up. This phase included the drilling of 3 more development wells and 2 water injectors. The Songkhla Basin oils are waxy and viscous in nature with an API gravity around 30 degrees and no gas in the petroleum system. This crude type coupled with a nearly fresh water drive can create early water breakthrough. Thus, selection of perforation intervals when completing a well is an important challenge for the engineer. Also, water injection and handling capacities are an important consideration in facility design.

Having retained the Vicksburg, the rig moved in 2010 to the western side of the basin to further appraise and develop the Bua Ban field with the drilling of 11 wells. One of the geoscience challenges on the western side is the variable distribution of the Lower Oligocene sands in conjunction with a complex faulted

structure. Well path design becomes a critical component to an efficient development. One of the benefits of deviated wells is the section traversed in the shallow Miocene section above the target Lower Oligocene may catch a fault block different than that of a vertical well. To capitalize on this, it is important to have a complete and careful petrographic analysis over the entire length of the wellbore that can be integrated into the mapping. A key example of this is the Bua Ban C-03 well which encountered a thin Lower Miocene pay sand. Integrating this new information with detailed mapping at the Lower Miocene revealed an additional location that could be targeted with the well Bua Ban C-11. This well further confirmed the Lower Miocene as a new viable reservoir target in the Songkhla Basin.

Still under contract, the rig moved five kilometers north to the Bua Ban North A and B prospects in 2011. These two prospects were originally developed with Lower Oligocene/Eocene objectives, thus the central locations were selected based on that mapping. However, given the success with the Lower Miocene at the Bua Ban C-11 area, the detail structural mapping at this level was used extensively in the well path planning. While the Lower Oligocene results were disappointing at Bua Ban D-01, by tagging a Lower Miocene fault block in a closed position 32 feet of net pay was logged at that level. Following a second disappointing Lower Oligocene well, two additional wells, both successful, were planned and drilled to test only the Lower Miocene section in different fault blocks. In fact, the Bua Ban D-03 logged 125 feet of net pay in five different intervals. This scenario was repeated with the move six kilometers north to Bua Ban North B prospect in that the Bua Ban E-01 had disappointing Lower Oligocene results but discovered 31 feet of net Miocene pay. The following seven wells were all designed to appraise and develop the multiple Lower Miocene reservoirs with excellent results. The Bua Ban E-05 encountered 178 feet of net pay with average porosity of 27%, while the E-08 confirmed a significant eastern block with 85 feet of net 28% porosity pay in only one zone. The shallow depths (3100-4600 feet TVDSS) of the Miocene reservoirs as well as the opposing fault plane dips created a unique challenge in planning the well paths. It is difficult to penetrate each zone in the optimum location with one well bore, thus creating the need for additional wells. This problem requires close cooperation

between drilling, engineering and the geoscience discipline in order to minimize the number of wells. The exploration/appraisal of these two prospects totaling 12 wells had been accomplished in four months, March thru June. These efficiencies were possible due to a rig and crew that had gained experience since starting on Songkhla A in 2009. Logging and completion programs were essentially the same throughout, although the shallow depths and deviated wellbores sometimes precluded using certain tools. The geoscience challenge throughout was incorporating all the data in order to determine whether it was one or two fields as well as to keep progressing towards early production. A Miocene sand correlation was established for the different productive intervals as well as synthetic seismograms which enabled more detailed mapping. The density and resistivity curves proved to be excellent tools for the higher porosity productive sands. While the MOPU was being installed at E, additional wells, including the first horizontal were planned and drilled at the D location which confirmed the continuation of the western fault block between North A and B as well as the oil water contact for the eastern block. The horizontal well is considered a solution to the early water breakthrough challenge previously identified as well as increasing production. First oil from the North B MOPU began in July and was producing close to 8000 BOPD by September. The second MOPU was installed and began production at the end of December. All the data continues to be integrated in order to better understand some of the productive fault relationships. A further challenge to fully utilizing the 3D seismic is the absence of any gas in the petroleum system, thus precluding the use of any pre-stack data for Amplitude Versus Offset (AVO) analysis which could have aided in defining the different productive zones and contacts.

In summary, most of the geoscientific challenges encountered in developing this field were not unique, however, the time period in which they needed to be addressed was critical. New technologies were not required, instead established exploration and development practices were utilized in a rapid, detailed and integrated manner. This geoscience integration with the drilling and engineering expertise has made for an efficient and timely development of a significant new field offshore Thailand, which will provide the template for future exploration.

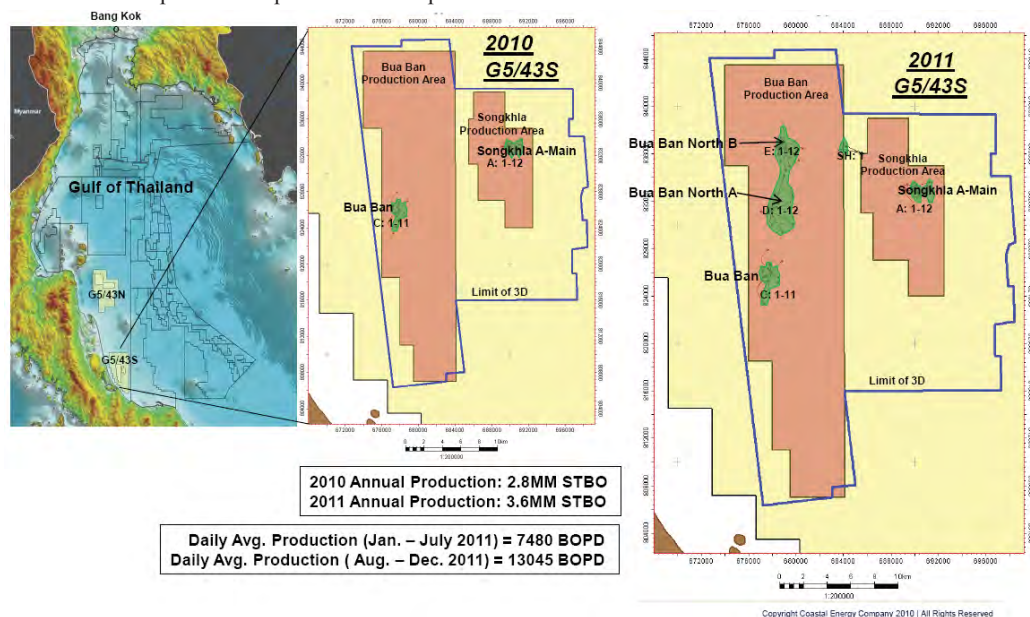


Figure 1: Coastal Energy Gulf of Thailand G5/43 Asset

Reservoir Characterisation of Mishrif Formation of Garraf field, Iraq, using 3D seismic and AI Inversion

M. Embong (Petronas Carigali Sdn Bhd), M. Higashi* (Petronas Carigali Iraq Holding BV), H.H. Abu Bakar (Petronas Carigali Iraq Holding BV), K.A. Zamri (Petronas Carigali Iraq Holding BV), F.H. M Ali (Petronas Carigali Iraq Holding BV), S. Moriya (Petronas Carigali Iraq Holding BV), S.B. M Said (Petronas Carigali Iraq Holding BV) & A.T. Patrick Panting (Petronas Carigali Sdn Bhd)

The Middle Cretaceous Mishrif reservoir consists of coarse-grained limestone deposited within a carbonate ramp in the Garraf field in central Iraq. The main oil bearing reservoir, Lower Mishrif, is controlled by gentle structural and stratigraphic trap. Understanding of the lateral and vertical changes in facies and porosity is very important to designing an optimum development strategy for the field. 3D seismic and AI inversion revealed reservoir geometry and lateral changes in porosity.

3D seismic data of about 500 km² was acquired in 2008-2009 by OEC (Oil Exploration Company in Ministry of Oil, Iraq). Data processing including pre-stack time migration (PSTM) was conducted in 2010 with excellent data quality result. Sparse spike inversion was adopted to convert PSTM to AI (Acoustic Impedance) volume calibrated using 3 existing well data.

3D seismic result shows good quality for seismic interpretation and attributes analysis. The AI result enhanced the resolution and showed better delineation of the stratigraphic feature such as reservoir pinch out and terminations. AI corresponds well with facies and/or porosity change as proved by well log analysis and geological interpretation.

This paper will demonstrate the reservoir characterization workflow, the importance of regional understanding, data integration and subsequently reservoir characterization results.

Introduction

The Development and Production Service Contract for the Garraf Contract Area was signed between South Oil Company, North Oil Company, PETRONAS Carigali Sdn. Bhd, and Japan Petroleum Exploration Co. Ltd (JAPEX) in January 2010.

Garraf field is situated in the southern part of Iraq, in the Thi Qar Governorate, some 5 km Northwest of Al Refaei city and 85 km north of Nasiriya (Figure 1). Garraf is an anticlinal structure aligned northwest – southeast, about 31 km long and 10 km wide in the Mesopotamian foredeep. Three wells have been drilled in this from 1984 to 1987.

Medium – heavy oil has been confirmed in multiple Cretaceous reservoirs; carbonates of the Mishrif and Yamama formations are the main reservoirs whereas sandstones of the Ratawi and Zubair formations are subordinate reservoirs.

The Mishrif reservoir, at the depth of ca. 2,200 mMD, consists of coarse-grained limestone deposited in a carbonate ramp. Heavy oil occurs in 2 separate pools, i.e. the Middle Mishrif and the Lower Mishrif. Lower Mishrif is a combination trap of structural and stratigraphic with lateral pinch out and facies changes. In this study, we focus on Lower Mishrif reservoir.

3D seismic data

The 3D seismic data of about 500 km² was acquired in 2008 and 2009 by OEC (Oil Exploration Company in Ministry of Oil, Iraq) in the scheme of joint study between Ministry of Oil and JAPEX. The 3D data was processed to PSTM (Pre-Stack Time Migration) in 2010. In processing flow, relative amplitude was preserved for quantitative attribute analysis and careful statics

correction was conducted due to low relief and gentle structure. The processed data quality is excellent and shown in Figure 2.

Time-structure map

We tied the well data to the seismic data by synthetic seismograms and picked horizons throughout the seismic volume. The continuity of reflection wave was good and no major fault was interpreted at Mishrif level. Figure 3 shows the time-structure map of top Lower Mishrif reservoir. The Lower Mishrif structure gently tilts and deepens toward north-east with less than 1.5 degree dip. The Garraf field locates on a gentle anticline with the trend of north-west to south-east and the structure relief is very small (about 12 ms). As we explain later on AI volume, the reservoir pinches out toward western area.

Rock physics

Figure 4 show the crossplots of Acoustic Impedance (AI) versus porosity in Lower Mishrif formation. It is clear that there is a linear relationship between porosity (Y axis) and AI (X axis) and correlation coefficient is -0.86; that is reservoir rocks with higher porosity have lower AI. Since seismic data is the response of AI, which is the product of density and Pwave velocity, the fact that there is a straightforward relationship between porosity and AI is a favorable sign to predict porosity from seismic data.

There is no gas cap for the reservoir and no effect of gas on AI. The reservoir consists of carbonate (bioclastic boundstone, grainstone, packstone, wackestone, and lime mudstone) and no shale. Therefore AI corresponds well with facies and/or porosity change in carbonate rather than fluid content.

Acoustic Impedance (AI) inversion

Seismic inversion was performed on 3D PSTM seismic volume as in-house work of PETRONAS Carigali Sdn Bhd. in 2011. Although there are several algorithms for seismic inversion, we adopted a constrained sparse spike inversion to convert the seismic trace into acoustic impedance. The low frequency impedance models were constructed with the interpreted seismic horizons and 3 well log data.

Figure 5 is an example of the seismic inversion results; the original PSTM seismic section of cross-line 566 is displayed on the left panel (a) and the inverted impedance section is displayed on the right panel (b). The merits of this method are that; 1) It is possible to integrate well logs with seismic data and obtain acoustic impedance, which is easier to relate to lithology or reservoir parameters such as porosity than the original seismic reflectivity. 2) It is possible to obtain a higher resolution on impedance sections than original seismic sections, by suppressing tuning effect.

In Figure 5(b), The zone of interest, Lower Mishrif indicated by an arrow, shows low impedance with yellowish color and lateral change of AI value is observed in Lower Mishrif reservoir. In addition, the AI result enhanced the resolution and showed

better delineation of the stratigraphic feature such as reservoir pinch out (shown in circle in Figure 5(b)). The thickness of the reservoir is about 40 m and AI volume able to resolves top and bottom of the reservoir. In this study, PSTM volume was used first for preliminary horizon interpretation and AI volume was used for detailed horizon interpretation in reservoir level.

Figure 6(a) shows the comparisons of original well log and AI Inversion results. Figure 6(b) shows cross-plot of seismic AI versus well log AI in Lower Mishrif of three wells and the correlation coefficient is 0.80. Both figures show the detailed and accurate correlation of the estimated seismic impedance with the well impedance log.

Attribute mapping

Figure 7 shows the predicted porosity map of Lower Mishrif reservoir. The porosity was converted from average AI within the reservoir using linear formation derived from well log AI and well log porosity relationship shown in Figure 4. The porosity map shows fine details of porosity variation in the range from 12 to 30 % which indicates carbonate facies changes in different depositional environment. Two high-porosity areas (bright red or yellow color) with trend of north-south are observed on the porosity map. The reservoir facies in this highporosity area is interpreted as porous bioclastic boundstone or rudist grainstone/packstone dominated facies in the depositional environment of rudist reef or shoal, taking into account of core information at wells. The low-porosity area in the map is interpreted as shallow open marine or lagoon where wackestone dominate.

From regional geological point of view, Garraf field is located within the high energy belt (reefs, shoals, & foreereef) on the paleogeographic map showing the depositional environments of Mishrif formation, and a shallow open marine connection led to a deeper water basin toward east (Aqrawi et al, 1998). This high energy belt is parallel with Paleoshoreline trend in north-south, and it is conforming to the trend of high-porosity area and pinch-out line on the predicted porosity map.

Higher porosity means consequent higher permeability and the well productivity located on the high-porosity area is estimated to be good. Therefore the development strategy of Garraf field including development and injection well locations will be optimized using the porosity map of the reservoir.

One of the most difficult and important problems for Mishrif geological modeling is in the fact that the interpreted Oil Water Contact (OWC) is apparently deeper than the structural spill point depth at south-west flank of the Garraf anticline (Figure 3). The combination of structural and stratigraphic trap model was adopted to solve the above problem. Lower Mishrif reservoir pinches out toward west and reservoir quality deteriorates toward south.

The conclusion of the stratigraphic trap model greatly relies on high quality 3D seismic, AI results and the core facies description. They enabled to depict depositional patterns and lateral facies and property changes in the Mishrif.

Workflow of reservoir characterization

The following is the workflow of reservoir characterization integrating several data such as well log, seismic, core, and regional geological knowledge in this study.

- 1) Preliminary seismic interpretation on PSTM volume
- 2) Acoustic Impedance (AI) inversion
- 3) Secondary seismic interpretation on AI volume to refine
- 4) Depth conversion of time structure maps and AI volume
- 5) Structural modeling of reservoir

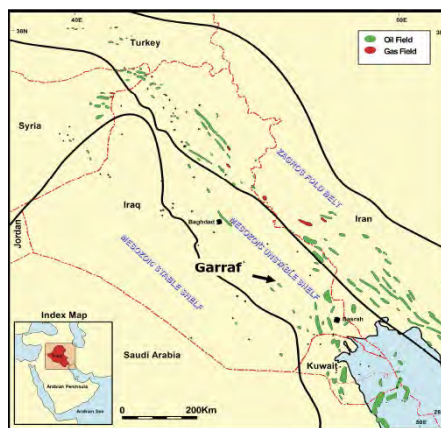


Figure 1: Location of the Garraf field.

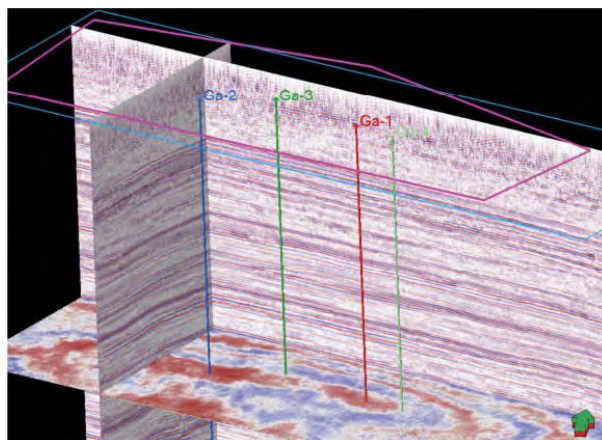


Figure 2: 3D view of seismic volume (PSTM) showing In-line 2500, cross-line 820, and timeslice 2030ms. Three exploration and appraisal wells were located on structure high were used for the study.

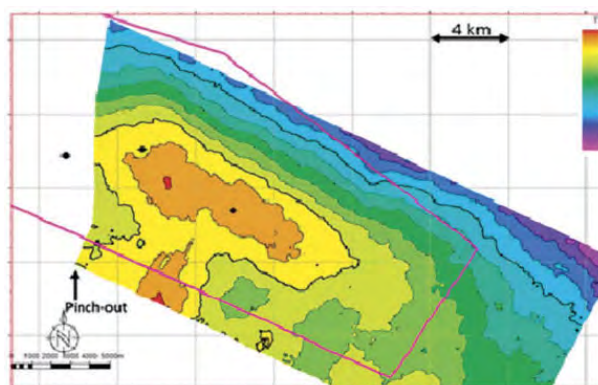


Figure 3: Time-structure map of top Lower Mishrif reservoir with contour interval 10ms. The Garraf field locates on a gentle anticline with the trend of north-west to south-east. The reservoir pinches out toward west.

- 6) Rock physics analysis to link AI to reservoir parameter like porosity
- 7) Lateral and vertical facies changes estimation
 - a. Core / log facies analysis
 - b. AI attribute analysis of 3D seismic
 - c. Regional geological knowledge
- 8) Property modeling including distribution of reservoir properties (porosity, facies and permeability)

Further works

This study was conducted in the early stage of development using existing 3 wells and 3D seismic. We plan further validation of seismic AI by new appraisal and development well data and re-run of inversion with new wells data using other inversion methodology such as model base inversion or stochastic inversion. We also would like to try elastic inversion using angle-limited PSTM volume and S-wave log for better facies estimation.

Conclusion

The interpretation and analysis of 3D seismic data provided a superior definition of the structural and stratigraphic trap and better understanding of Lower Mishrif L1 reservoir in the Garraf field.

Key factors of this study include the follows;

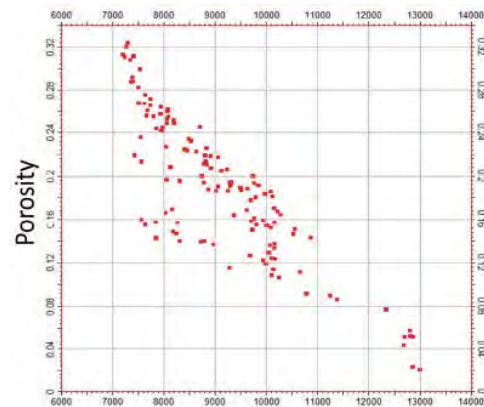
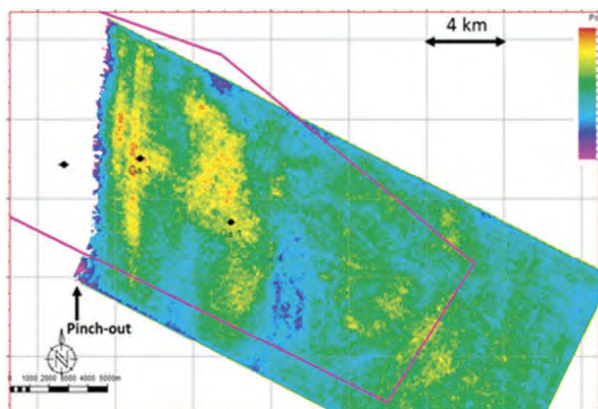
- 1) Rock physics study showed that porosity and AI are well correlated in this field.
- 2) The AI result enhanced the resolution and showed better delineation of the stratigraphic feature such as reservoir pinch out.
- 3) The AI results were used as the input data for porosity and facies modeling for Lower Mishrif reservoir integrating core and well log data.
- 4) The predicted porosity distribution from AI will be used for optimization of field development.
- 5) This study confirmed the effectiveness of AI inversion in the Garraf field.

Acknowledgement

The authors thank South Oil Company, North Oil Company, Oil Exploration Company (OEC), PETRONAS Carigali Sdn. Bhd, and Japan Petroleum Exploration Co. Ltd (JAPEx) for permission to publish this work.

References

- Aqrawi, A.A.M., Thehni, G.A., Sherwani, G.H. and Kareem, B.M.A., 1998. Mid-Cretaceous Rudist-Bearing Carbonates of the Mishrif Formation: An Important Reservoir Sequence in the Mesopotamian Basin, Iraq. *Journal of Petroleum Geology*, 21, 1, 57-82.
- J.J.M. Buiting and M.Bacon, 1997. Using Geophysical, Geological and Petrophysical Data to Characterize Reservoirs in the North Sea, 5th Conference on Petroleum Geology of NW Europe, N97033
- R.B. Simono, M.J.Mashayekhi, R.Morton, P.Crookall, B.Vos, P.Van der Made, 2004. Combined Reservoir Characterization and Modeling, EAEG 66th Conference, A014



Well Log AI

Figure 4: Acoustic Impedance (AI) versus porosity of 3 wells in Lower Mishrif showing good linear relationship (correlation coefficient -0.86). AI and porosity values were re-sampled to 1 to 2 m in 3D modeling procedure.

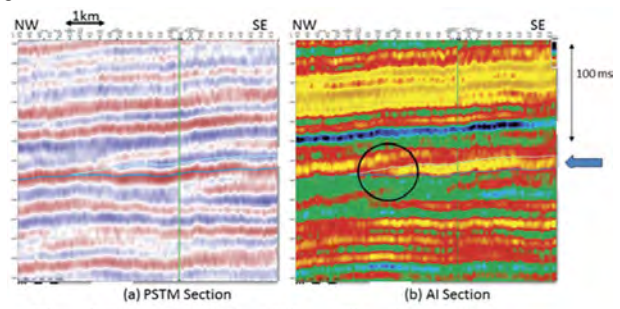


Figure 5: (a) PSTM seismic section. (b) AI section. The zone of interest indicated by an arrow shows low impedance with yellowish color. The AI result enhanced the resolution and showed better delineation of the stratigraphic feature such as reservoir pinch out (shown in circle).

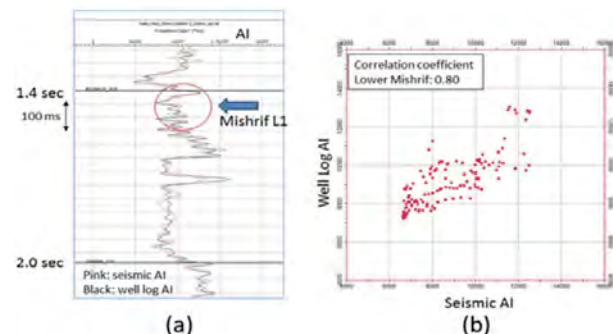


Figure 6: (a) Comparison of seismic AI versus well log AI. Pink line means seismic AI and black line means well log AI. (b) Cross-plot of seismic AI versus well log AI in Lower Mishrif of three wells (correlation coefficient 0.80). Both figures showing the detailed and accurate correlation of the estimated seismic impedance value with the well impedance log.

Figure 7: Predicted porosity map of the Lower Mishrif reservoir. Porosity variations indicate carbonate facies changes in different depositional environment. High-porosity area are interpreted as high energy belt of rudist reefs or shoals.

Geo-Information & GIS: Adding Value to Exploration and Development Activities

G.G. Tan* (Sarawak Shell Berhad)

Geographic Information System (GIS) has always had a role to play in the search for hydrocarbons – and use of GIS in the exploration industry is increasing. One of the main reasons is because of the availability of more tools that help explorers to work effectively within the GIS environment, through integration of many different data types, conducting advanced analysis, and creating accurate, quality results. The questions posed by exploration activities and the answers offered by GIS are often a natural fit. Exploration teams need to integrate and make sense of the abundance of geological and geochemical information. GIS supports this complex workflow by managing and analyzing the data and displaying it in a spatial context. Applications that are relevant to Exploration are also applicable for other Geoscience communities.

The diagram Fig.1 shows an example of Tellus tool, developed by Fugro Robertson as an extensive play fairway and petroleum systems database. Tellus is designed to provide New Ventures groups and explorationists with a comprehensive and consistent tool for understanding play and basin scale petroleum geology worldwide.

GIS has become an invaluable tool for integration for many different data types. The spatial data search is a major advantage of using GIS compared to other types of software. The spatial query capability is possible because GIS maintains a link between spatial features and related nonspatial attributes. By using the commonality between multiple layers to search their relationships, carried out through its ability to combine different map layers and observe them simultaneously to discover their relationship.

With this process, associations and patterns between data sets that are otherwise unknown can be uncovered. This type of work allows one of the core functionalities to stand-out: spatial analysis. Exploring and discovering spatial association between data layers is ultimately used for prediction of suitable areas for a specific target and to derive valuable information. The prediction is made based on various mathematical and statistical models.

Geosciences projects often maintain many various types of data sources (geology, geophysics, wells, cultural, etc.). The main activities where GIS is usually involved in geosciences projects are in data management, visualization, spatial analysis, and decision support system. Today's GIS developments allow wider and deeper contribution of GIS to geosciences projects. The six fundamental activities of GIS that can be applied in geosciences applications:

- i. data management (involving data modeling, data compilation, and database construction);
- ii. data visualization (viewing data, production of on-screen or hard-copy maps and discovering spatial patterns);
- iii. spatial data search (query based on attributes or spatial information);
- iv. integration through spatialization of various data types and sources;
- v. analysis of data; and
- vi. forecasting and prediction, particularly to support decision making based on many factors of spatial information.

The diagram Fig.3 above shows a very good example how the OGP industry-wide Seabed Survey Data Model (SSDM) brought data acquisition directly into a GIS ready product and gained time from more streamlined Geo-Information Management. Oil and gas (O&G) companies aim to manage seabed survey data based on sound geo-information management principles and practices.

Historically, geographical features interpreted from seabed survey have been delivered in unstructured CAD files that have led to many difficulties in the management of survey data. These issues include the fact that data from different surveys has been difficult to integrate and share with joint venture partners. In view of these needs, the OGP Seabed Survey Data Model (SSDM) Task Force was formed in 2010 to define a standard GIS data model for seabed survey. This model can be used as a deliverable standard between O&G companies and survey contractors, as well as a sound data model for managing seabed survey data at an enterprise level within O&G companies.

On the other hand, the current GIS standards for geosciences applications are distinguished by the following criteria: it is built on non-proprietary object-based components, it uses industry-standard database systems, supports full functionality on a desktop-based GIS, opens for further development and is highly interoperable with other systems (see Fig.4), and supports web-based mapping (WebGIS). This enables wider data sharing and mash-ups with other systems, and integration with specialized programs for geologic modeling (e.g. Petrel). The object-based components also meant that GIS system can be configured to fit enterprise or small project requirements since it is modular and scalable. It is modular in the sense that you acquire the system in pieces, and it is scalable since it can be deployed on an individual desktop or across a globally distributed network of people. Typical geoscience users will require the full capability and functionalities of a desktop GIS. Casual users who require



Fig 1: Tellus is Fugro Robertson's basin and play evaluation tool for New Ventures screening

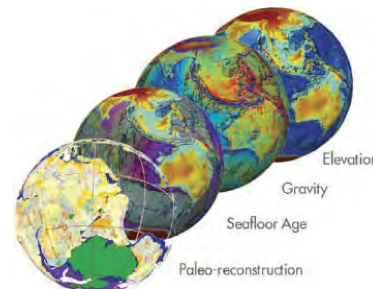
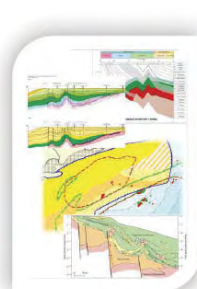


Fig 2: Multi-scale data analysis.

GIS for simple data browsing, visualization or access to pre-set map services, will be best suited to an internet mapping or WebGIS solution. WebGIS is especially best for sharing common data views around multiple geographic locations.

How then do we maximize the capabilities of GIS? How do we leverage these tools to add value to our modern way of work? This presentation aims to answer some of these questions as well as take a look at how GIS technology is used every day in Shell, especially in Exploration and increasingly applied for Development projects, and across the E&P lifecycle. The technology itself is embedded in several exploration toolsets/databases, including Basin Play Analysis and also external vendor technology such as Petrel.

References

- Bonham-Carter, G.F., 1994. Geographic Information System for Geoscientists: Modelling With GIS, Delta Printing Ltd., Ontario, 398 pp.
- Bonham-Carter, G. An Overview of GIS in the Geosciences, in T.C. Coburn and J.M. Yarus (eds.), Geographic Information Systems in Petroleum Exploration.
- Lucas D. Setijadj. GIS for Subsurface Modeling, <http://www.esri.com/industries/mining/pdf/subsurface-modeling.pdf>

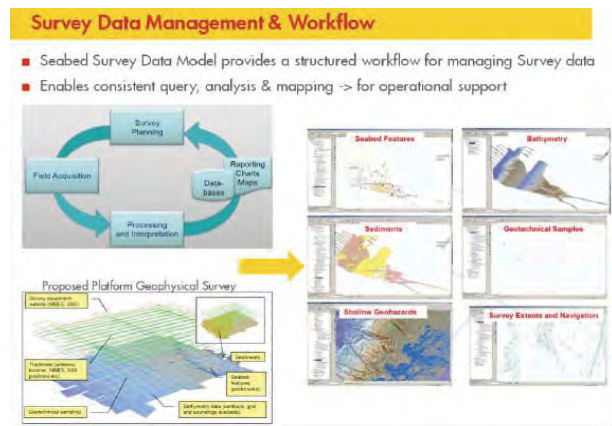


Fig. 3: Seabed survey data model (SSDM)

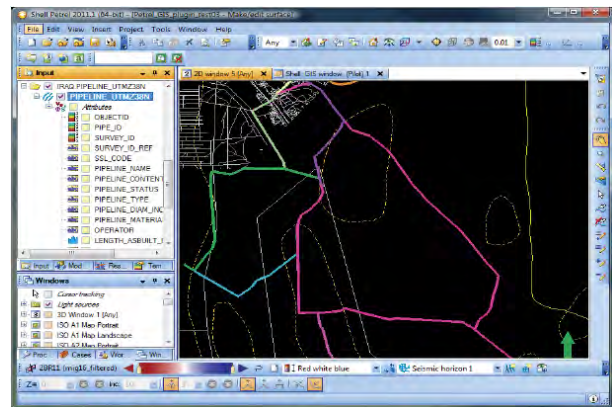


Figure 4: Petrel – ArcGIS Interoperability testing.

A Structured Approach Towards Quantification of Subsurface Parameter Ranges

A.J.W. Everts* (Leap Energy Partners Sdn. Bhd.), L. Alessio (Leap Energy Partners Sdn. Bhd.), P. Friedinger (Leap Energy Partners Sdn. Bhd.) & F. Rahmat (Leap Energy Partners Sdn. Bhd.)

Introduction

Objective of this paper is to illustrate how a structured approach towards quantifying the expectation ranges of key subsurface parameters, differentiating between true uncertainty and mere variability and recognizing the possibility of biases in our subsurface data, can lead to significantly improved asset management, i.e., better reservoir models, improved accuracy of resource estimates, more objective assessment of appraisal value etc.

In the exploration/appraisal stage especially offshore, wells are scarce and therefore well-based property estimates are typically complemented by indirect evidence from seismic. On the other hand, developed fields especially onshore or resource plays may have a much higher well density but with a distribution clustered around interpreted reservoir sweet spots or chosen surface development sites. With this limited 'ground truthing', our challenge is to make as accurate as possible assessments of the subsurface parameters in our fields.

Determining Field- or Block-Wide Parameter Averages

For an accurate assessment of volumetric resource ranges, one needs to determine expectation ranges for the field- or block-wide averages of all key reservoir properties. For fields in the exploration or appraisal phase especially where wells have been drilled on seismic amplitude anomalies, data representativeness is an issue that may easily lead to over-optimism and underestimation of the uncertainty range. Figure 1 shows a typical example of wells drilled on seismic amplitudes within a closure. Rather than using net pay ranges seen in the wells as direct input for the field's net pay as a whole, a more appropriate approach would be to establish via a combination of well data cross-plotting and seismic modelling, a range in possible relationships between amplitude and net pay and from there, convert the amplitude map into range in average net pay values for the field.

On the other hand, in fields with high well density such as resource plays, it is important to distinguish between reservoir

variability which may be very profound from well to well, and genuine remaining uncertainty on the field property averages. Here, we can use the concepts of sampling statistics to work out confidence curves around the mean given the availability of well data (Alessio et al, 2010). These confidence curves can also be used to quantify the impact of further data gathering on uncertainty reduction and hence, be a powerful tool in Value Of Information assessment.

Defining Data Distribution Models for 3D Reservoir Models

Geostatistical property mapping in 2D or 3D typically uses distribution models fit to well data, in combination with transforms to reflect of spatial trends e.g., facies conditioning, depth trends or seismic inversion-based trends. However, where well data is scarce, clustered or sampling anomalous parts of the reservoir, distribution models based on wells alone may not be representative and give rise to inappropriate reservoir property mapping. Statistical techniques like data de-clustering can be used to overcome sampling biases but these techniques are rarely deployed.

Using state of the art modelling tools, 3D reservoir modelling studies often stochastically simulate the impact of parameter distribution uncertainty via introduction of a "random seed". However, one needs to recognize that a "random seed" only addresses the localized distribution pattern away from wells and especially if the closure area is large, localized anomalies introduced by a "random seed" may cancel out and as a result, subsurface uncertainty is underestimated. Uncertainty on spatial (lateral e.g., seismic constrained) or vertical trends can be equally or more important than localized variability and needs to be included in a holistic subsurface uncertainty assessment workflow. Similarly, measurement uncertainties of the parameters themselves, e.g., petrophysical evaluation uncertainty or in unconventional resource plays, analytical uncertainty on parameters like gas content, can have a profound impact that goes way beyond the localized variability simulated using "random seed" techniques.

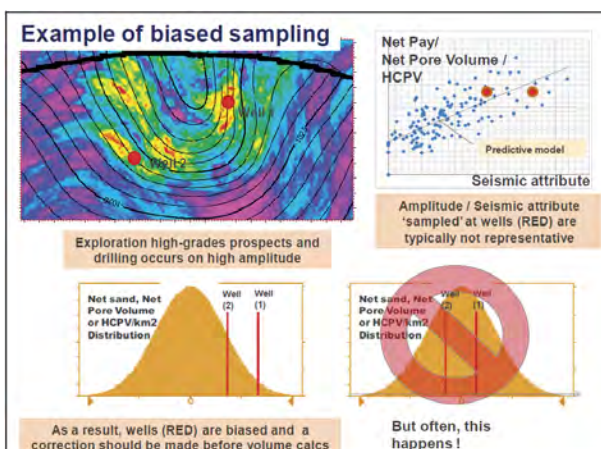


Figure 1: Example of biased well sampling where appraisal drilling targeted seismic amplitude anomalies.

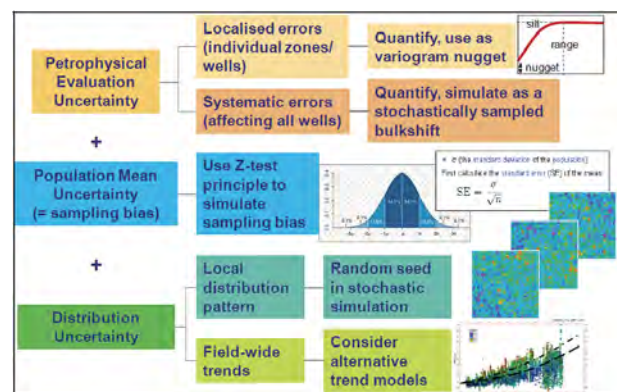


Figure 2: Holistic approach in reservoir-model based simulation of subsurface uncertainty.

Conclusions

Provided all the potential sources of subsurface uncertainty are understood and potential data limitations and biases are recognized, these limitations and potential pitfalls can be overcome by a structured approach that relates back to the principles of sampling statistics and also, by following a holistic approach (Figure 2) that addresses not only distribution uncertainty but also sampling biases and measurement uncertainty on the parameters themselves.

References

Alessio, L., Everts, A. and Rahmat, F., 2010. Uncertainty Management: a Structured Approach towards Recognizing, Quantifying and Managing Sampling Biases in Subsurface Unknowns. Proceedings, Indonesian Petroleum Association, Thirty-Fourth Annual Convention & Exhibition, May 2010

Paper P38

Biostratigraphic Real-time Well-site Support for a NW Palawan, Offshore Philippines Appraisal Well

C.T. Naih* (Sarawak Shell Berhad), J.J. Lim (Sarawak Shell Berhad) & R. Sandom (Sarawak Shell Berhad)

Real-time biostratigraphic well-site support has been successfully applied in appraisal well, NW Palawan, offshore Philippines (Figs.1), to guide the Shell’s Malampaya team to pick the 9 5/8” casing point approximately 50m above the targeted Nido carbonates.

Pre-drill evaluation of available legacy Miocene biostratigraphic data from exploration well demonstrated that nannoplankton and especially quantitative planktonic foram events could play a key role in following the stratigraphy of the well section penetrated and confidently locate the 9 5/8” casing point. In order to test the repeatability of biostratigraphic events, an exercise in a real-time environment was carried out in SSB’s Geological Laboratory in Lutong, Sarawak.

Based on the results of this exercise, the full integration in the subsurface geological model and the fact that the biostratigraphic results could be obtained within 1.5 hours (ca. 30 meters) behind the bit, it was decided by the Shell’s Malampaya team to request real-time biostratigraphic support,

rather than running an expensive VSP tool.

Real-time biostratigraphic started directly below the Matinloc Conglomerates. Pagasa shales directly below the conglomerates yielded planktonic foram SN10 (*Globorotalia fohsi peripheroacuta*, *Globorotalia fohsi peripheroronda*, *Globorotalia archeomenardii*) zonal assemblages of Langhian (Middle Miocene) age. Top SN9 (*Praeorbulina glomerosa circularis*) was encountered 150m above prognosis and reinforced an update of the velocity model of the Pagasa shales. The top of the SN8 zone of Langhian-Burdigalian age (*Globigerinoides diminitus*) was found 10m above prognosis. The targeted intra SN8 quantitative event increase in (*G. fohsi peripheroacuta*, *G. fohsi peripheroronda*, *Praeorbulina sicana*, *Globigerinoides diminitus*, and *Praeorbulina transitoria*) was encountered 16 meter above prognosis in the Lower Pagasa (Figs. 2).

Biostratigraphic quantitative events proved to be a valuable tool to support the drilling activities in the Camago area.

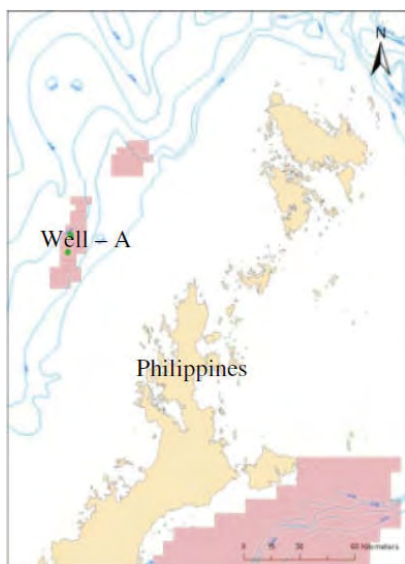


Figure 1: Location Map of Well - A.

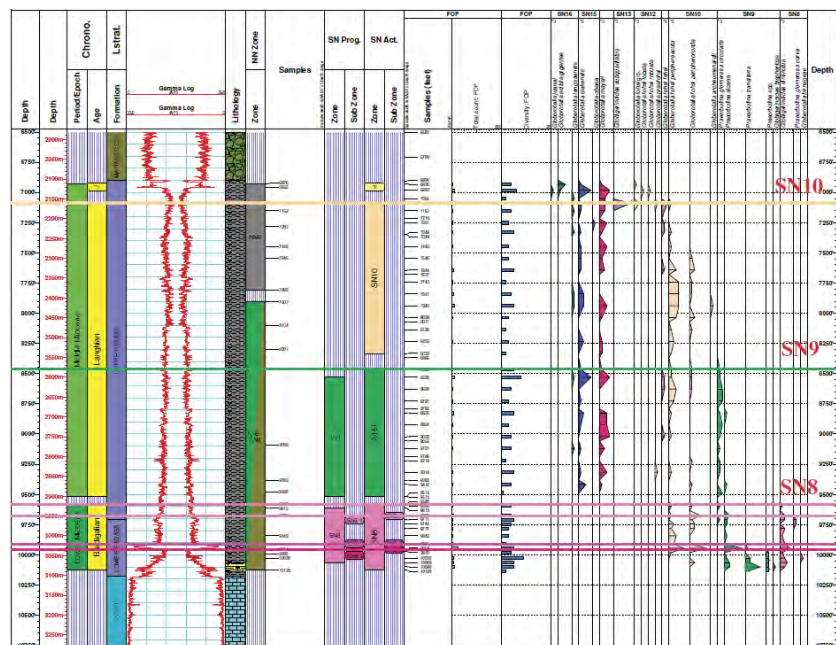


Figure 2: Micropalaeontology Distribution Chart of Well - A.

A Sedimentologic and Petrographic Perspective of the Miocene Stage IVA from the Klias Peninsula to Labuan Island

T.D. Lukie* (Talisman Malaysia Ltd) & A. Balaguru (Talisman Malaysia Ltd)

The Miocene outcrops in NW Sabah provide an opportunity to study the rocks equivalent to the offshore reservoirs undergoing exploration. The primary target for most exploration is the Stage IV (Figure 1) and it ranges in thickness from 3 to 5 kms and comprises interstratified sandstones and shales deposited within marginal marine to shoreface environments. The Stage IVA which is the focus of this study, sits on the Middle Miocene Unconformity (MMU), also known as the DRU (Deep Regional Unconformity) and marks the onset of the next major phase of sediment accumulation (after Early Miocene Stage III) in NW Sabah.

The Stage IVA is well exposed for study on the Klias Peninsula and Labuan Island (Figure 2). The outcrop sections at Batu Luang on the Klias peninsula, and the outcrops at Bethune Head, Ganggarak Quarry and Layang Layangan Beach provide a look at a nearly complete sequence within the Stage IVA. At Batu Luang the MMU is exposed with 34 metres of braided to gravel-meandering fluvial conglomerates cutting into dark grey to black shales containing sideritized silt- to sandstone stringers. The MMU is not exposed at the Bethune Head location; however, it is visible at both the Ganggarak and Layang Layangan localities. At these locations, the MMU is represented by braided to coarse-grained meandering deposits cutting into underlying Stage III shelf edge delta front/prodelta to slope deposits.

The fluvial deposits range from pebble to cobble-sized conglomerates at Batu Luang to medium-very coarse-grained sandstones and pebbly-sandstones in Labuan. The upper portion of the fluvial succession at Labuan is capped by levee to overbank deposits with local coals as seen at Ganggarak Quarry. The top of the fluvial succession is marked by the presence of a highly bioturbated sandstone with sand-filled burrows in the underlying shales (Glossifungites) at Batu Luang and a thin tidal flat succession at Bethune Head marking the onset of transgression and the top of the lowstand systems tract (LST).

Preserved section above the fluvial deposits is only found at the Batu Luang and Bethune Head locations. This section at Batu Luang is composed of bioturbated, trough cross-bedded to swaley-bedded sandstones interstratified with shale-dominated sections containing thin sandstone interbeds. This upper section is interpreted as deltaic deposits comprising distributary channels, delta front sands, interdistributary/shallow bay deposits and prodelta sediments at Batu Luang and distal deltaic to lower shoreface/offshore deposits at Bethune head. The top of this section is best observed at Bethune Head and is marked by a relatively thick marine shale which within lies the maximum flooding surface (MFS). The MFS was identified by the overall increase in coarsening-upward sand successions above this shale. At Batu Luang the MFS is identified at the top of a prodelta shale-prone section containing bioclasts stringers above which resides a thin section of tidal flat sediments. The MFS, by definition, caps the transgressive systems tract (TST) and the fining-upward sequence.

The section above the TST is made up of inter-stratified sandstones and shales comprising tidal flats, distributary channels and delta front sands at Batu Luang. The more distal outcrop at Bethune Head is composed of coarsening-upward packages dominated by deltaic sediments including distributary mouthbars, delta front, distal delta front and prodelta sediments. These prograding sands packages represent the clinofolds of the delta as it progrades into the basin and is part of the highstand systems tract (HST).

The sandstones in the IVA are typically fall into the quartz-dominated, sub-lithic arenite classification (Figure 3; sensu Potter et al., 1987). The bulk of the detrital mineralogy consists of quartz, lithic rock fragments (granitic, metamorphic, chert and sedimentary), K-feldspar, plagioclase, organics and traces of phosphate, glauconite, muscovite and heavy minerals such as zircon, tourmaline. Matrix illite is observed in some samples and it is likely a mixture of detrital illite and pseudo-

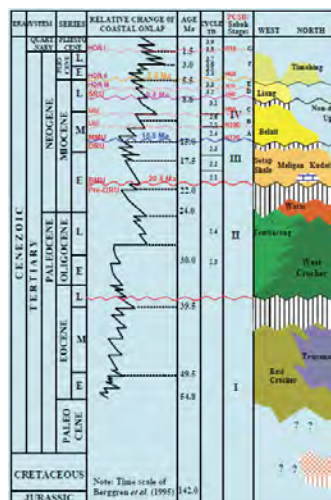


Figure 1: Stratigraphic chart for NW Sabah (Balaguru, 2006).

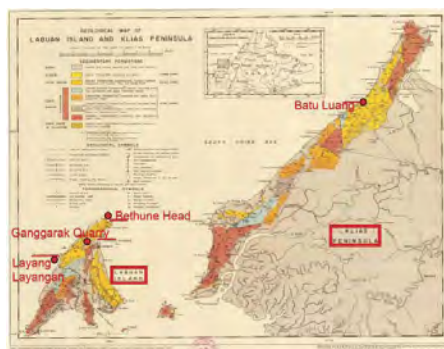


Figure 2: Geological map of Klias Peninsula and Labuan, Sabah. Red dots indicate the outcrop locations (Wilson, 1964).

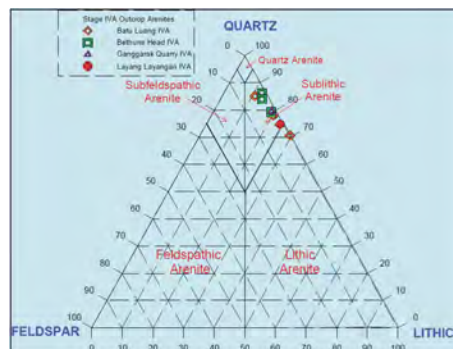


Figure 3: Classification of the Miocene Stage IVA arenites as sampled from outcrop; classification scheme of Pettijohn et al. (1987).

matrix (squashed mud clasts). Evidence of diagenesis is in the form of thin quartz overgrowths and traces of siderite, pyrite, and pore-lining illite. Dissolution of unstable grains (feldspars and unstable lithics) is also observed which creates a secondary pore-system that enhances the total porosity.

The reservoir quality of the sandstones changes with the facies and environments. The lowstand fluvial sands tend to be coarser grained, but more poorly sorted than the deltaic sands. The deltaic sands are finer grained, but tend to be better sorted than the fluvial sands, likely due to the wave-activity modifying the sands. Although the lowstand sands have relatively good reservoir quality, the shelf sediments are dominated by the transgressive and highstand deposits making them more targetable than the lowstand deposits contained within incised-valleys feeding deepwater systems.

References

- Balaguru, A., 2006. Orogeny in Action: Tectonic Evolution and Stratigraphy of Sabah, Seismic and Outcrop Evidence, Petroleum Geoscience Conference and Exhibition (PGCE) Abstract.
- Pettijohn, F.J., Potter, P.E., and Siever, R., 1987. Sand and Sandstone, 2nd Edition, Springer-Verlag, New York, 572pp.
- Wilson, R.A.M. and Wong, N.P.Y., 1964. The Geology and Mineral Resources of the Labuan and Padas Valley Area, Sabah, Malaysia, Memoir 17, Geological Survey Borneo Region, Malaysia, 150pp.

Paper P40

An Integrated Approach Towards Delineating Hydrocarbon Prospectivity in Untested Fault Blocks Within a Brown Field. A Case Study in B Field, Offshore Sarawak, Malaysia

A. Azami* (Petronas Carigali Sdn Bhd), A. Hashim (Petronas Carigali Sdn Bhd), N. Alias (PETRONAS Petroleum Management Unit), N. Ujal (Petronas Carigali Sdn Bhd), M. Bhattacharya (Petronas Carigali Sdn Bhd), A. Roy (Petronas Carigali Sdn Bhd), S. Pamungkas (Petronas Carigali Sdn Bhd) & T.. Aldha (Petronas Carigali Sdn Bhd)

B Field is located approximately 80 km from Bintulu in water depth of about 90 feet, Balingian Province, offshore Sarawak, Malaysia. It was discovered in 1976, with first oil achieved in 1984. Since then, more than 70 wells have been drilled, with production coming from three main accumulations: B North, West, and Northwest. A fourth accumulation, B East was recently discovered in 2006. Structurally, B Field is heavily faulted, with the southwest to northeast and associated antithetic faults giving rise to numerous compartmentalizing fault blocks among the adulating anticlines and synclines. Furthermore, channelized sand bodies add another level of complexity towards understanding the hydrocarbon distribution in B. The reservoirs of interest are on Late Oligocene to Early Miocene in age and occur at an average depth between three to five thousand feet subsea. Depending on the stratigraphic succession, these Cycle II reservoirs are interpreted to have been deposited in a Lower Coastal Plain environment, with channel morphologies ranging from braided streams to meandering and distributary channels.

In order to mitigate the uncertainty associated with reservoir presence (sand distribution) and hydrocarbon occurrences in untested prospective fault blocks, a holistic integrated approach was adopted. By rationalizing all available geological, geophysical and production data, an attempt was made to produce a cohesive and consistent geological conceptual model able to predict hydrocarbon presence beyond the proven areas. The workflow began by understanding the depositional environment of the field as observed from well logs and core data. Possible channel widths were established by comparing the observed data with analogs from available literature. A general provenance direction was also known from the understanding of regional geology and dipmeter data. Reservoir morphology was further delineated by using seismic attributes such as RMS of amplitude

and sum of negative amplitudes, applied on the angle stack seismic data. Observed anomalies between the near and far stack seismic data allowed us carve-out prospective areas away from known hydrocarbon pools of B Field. These anomalies were further validated by comparing with the well logs and petrophysical data from nearby producing areas. Furthermore, the area and zones of interest were subjected to an AVO study in order to assess the hydrocarbon occurrence probability. The volumes were calculated and risked accordingly in order to account for the remaining uncertainties. The identified prospects have been consistently supported by the available data and studies, and this has led to the finalizing of a drillable location about five kilometers Northwest of nearest platform. The target is situated on an isolate horst block of a plunging anticline with the northerly plunging axis. B field has yet to prove the viability of a stratigraphic and structural combination trap. A sound integrated approach as adopted here has a potential for probing hydrocarbon reserves in this new plays types.

Conclusions

A sound integrated approach as adopted here has a potential for probing hydrocarbon reserves in this new plays types.

Acknowledgements

Bayan team members, PEG management, PEB management and Specialized Study group (PEG).

References

- PETRONAS, 1999. The Petroleum Geology and Resource of Malaysia. Petroliaam National Berhad, Kuala Lumpur, Malaysia.

Integrated Geoscience Interpretation of Selected Group B Sands In Beta Field, Malay Basin

C.H. Sim* (ExxonMobil Exploration and Production Malaysia Inc) &
F. Fahmi (ExxonMobil Exploration and Production Malaysia Inc)

Introduction

Beta Field is a non-associated gas field located about 220 km north of Kerteh in water depth of 60 meters. The field was discovered in 1970 and development of the Group "B" sands began in 2003 with first gas in March 2003. The Group B sands were not targeted during the initial field development. The field is a broad, low relief high side fault dependent closure in the northern part of the Malay Basin. In this paper we will briefly examine future development of the shallow and likely unconsolidated B-A, B-B, B-C, and B-D reservoirs in Beta Field.

Method and/or Theory

The B-B and B-C reservoirs are interpreted to be laterally amalgamated fluvial channel deposits while the B-D reservoir is interpreted to be fluvial channels and overbank deposits. 3D seismic and well datasets were used to delineate the geometry of channel thickness and shape of the B-C reservoir, the channel margins and the associated younger mud filled channels. The B-A, B-B and B-C sands exhibit pronounced Class 3 AVO response but only the B-C sand is gas-bearing. The AVO response is studied via map-based amplitude responses, seismic gathers response and AVO modeling. The AVO response of

the B-A and B-B sands is interpreted to be caused by low gas saturation. This is used for risking similar AVO anomalies in untested areas of Beta field.

3D seismic attribute maps and spectral decomposition analysis are also used to differentiate the hydrocarbon response from coal and delineate B-D incised valley boundary. High frequencies (50 - 60 Hz) responses relates to deposition of the regional B-D coal while low frequencies (10 - 30 Hz) spectral decomposition shows DHI of the gas bearing reservoir. Snapshots of varying frequencies are used in the Spectral Decomposition Analysis of the B-D reservoirs. Seismic images at this depth are poor due to shallow gas attenuation. Characterizing individual smaller channels of the B-D reservoirs from 3D seismic data is difficult and thus crestal wells are used for reservoir trend.

Conclusions

In summary, integrating the geoscience interpretation, fully evaluating the AVO responses, including formation evaluation of the shallow and unconsolidated sands and geologic modeling, allows the Beta field team to better characterize the Beta field Group B gas resource and risks/uncertainties associated with the upcoming drilling program.

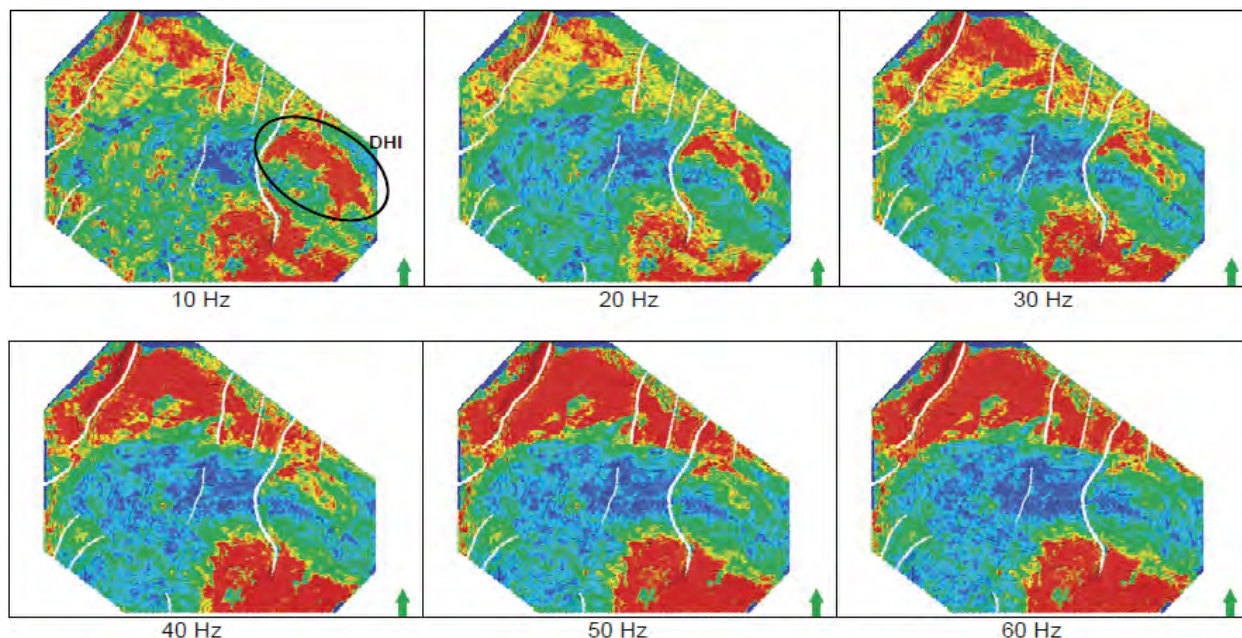


Figure 1. Beta Field B-D Reservoir: Snapshots of varying frequencies in seismic spectral decomposition analysis. Lower frequencies are associated with DHI while higher frequencies are due to coals.

Geohazards Assessment, Data Integration and Visualization via ArcGIS

M. Zulkifli* (Sarawak Shell Bhd), D.A. Bean (Sarawak Shell Bhd) & T.K. Tiong (Sarawak Shell Bhd)

Geohazards are geological features on the seafloor or in the subsurface that may pose drilling and/or development-related issues (e.g. infrastructure placement). Geohazards are conventionally assessed qualitatively via seismic interpretation and the evaluation of site survey geophysical data such as high resolution 2D seismic, multibeam bathymetry and side scan sonar. ArcGIS technology enables improved analysis of geohazards through spatial analyst tools and data integration. The Shell UIA Geohazards Team has developed several improved methods of assessing geohazards via ArcGIS that simplify standard procedures and accelerate project delivery.

ArcGIS integrated methodologies include: 1) geohazards screening tool for the Northwest Borneo region, 2) geohazards risk assessment workflow, and 3) techniques for predictive mapping of seafloor habitats. The screening tool leverages on

advanced ArcGIS data management practices and improves accessibility of historical geohazards information. As a result, the geohazards screening tool enables rapid preliminary screening of geohazards for exploration and development planning. The geohazards risk assessment workflow provides risk quantification at any given location within an evaluated area through a weighted risk map deliverable. The weighted risk map improves geohazards visualization and understanding of areas by combining multiple risks into a single ranked risk layer. ArcGIS has also enabled extrapolated mapping of seafloor biological habitats by integrating environmental data with seafloor geophysical data. The outcome is the extension of seafloor habitat information beyond existing environmental data points to minimize environmental impact of infrastructure and wells.

The Evolution of Tiltmeter-Based Reservoir Monitoring: From Risk Mitigation to Production Optimization

S Marsic* (Pinnacle, a Halliburton Service), M. Machovoe (Pinnacle, a Halliburton Service) & W. Roadarmel (Pinnacle, a Halliburton Service)

Introduction

Tiltmeter technology has proven extremely valuable in heavy oil recovery fields as shown by the increasing installations worldwide, a 15+ year history of monitoring success in regions such as the San Joaquin Valley in California, and now an increasing regulatory demand for its operational use. The use of tiltmeter diagnostics has been a widely accepted tool for mapping of fracture stimulation treatments, but also fulfils a need for a cost effective, near real-time reservoir surveillance tool in thermal enhanced oil recovery (EOR) environments. Tiltmeter-based reservoir monitoring serves as an early warning system for out of zone steam migration and as a diagnostic to help improve operating and recovery efficiency.

Theory and Method

Nearly every reservoir-level process generates and propagates outward a pattern of strain that can be detected using sensitive deformation monitoring technologies. Tiltmeter-based reservoir surveillance has been successfully used throughout the world for nearly 20 years to precisely monitor fracturing stimulation-induced rock deformations which are then used to infer hydraulic fracture orientation and geometry (Wright et al. 1998; Davis et al. 2001). In a similar way, changes in reservoir volumes, such as those produced by fluid production, injection, and thermal processes such as steam flooding, Cyclic Steam Stimulation (CSS), Steam Assisted Gravity Drainage (SAGD), and CO₂ Sequestration (CCS) also generate unique and measurable patterns of formation deformation (Du and Olson 2001; Du et al. 2008). These patterns, or deformation fields, can be measured at the earth's surface with an array of tiltmeter instrumentation. By solving a geophysical inverse problem, precisely measured surface deformation can be used to solve for reservoir-level strain changes (Figure 1). By bringing the surface deformation measurements down to the reservoir level to identify and characterize fluid migration pathways, volumetric strain, pressure fronts, or even the thermal fronts, operators and asset managers are able to improve their understanding of how different storage and recovery methods work in different types of reservoirs at a significant cost savings over traditional monitoring technologies.

The primary goal of many tiltmeter-based microdeformation deployments is risk mitigation, specifically identifying, characterizing and reporting on out of zone fluid migration (Davis et al. 2000; Marsic et al. 2011). Beyond identifying these events, microdeformation diagnostics work in concert with other wellbore measurement devices such as flow and pressure gauges, seismic/microseismic mapping, distributed temperature and pressure sensing (fiber optic) and radioactive tracer surveys. These supplemental technologies can help identify damaged wellbores or extensive reservoir damage and paint a more complete picture of fluid, temperature and pressure changes within the reservoir. Benefits of this combined approach in EOR environments result in overall cost reduction, reduced mechanical failures, and improved production economics.

A secondary goal of tiltmeter-based reservoir monitoring has been realized by many operators once they began focusing on

their recovery strategy in an integrated fashion with identifying and controlling out of zone EOR injection activities. CAPEX and OPEX costs associated with EOR steam generation are quite expensive. Maintaining fluid conformance within target zones and preventing out of zone fluid growth all have economic costs associated with them as ultimately this is lost money for a given project. Injecting into non-producing sands, contacting a common zone with multiple injections or losing steam to a pressure sink also affects project economics. The geomechanical inversion of surface-based reservoir monitoring diagnostics can provide a cost effective way to evaluate the performance of EOR projects by providing information for engineers and asset managers to react to and make more informed operational decisions. Traditionally, wells that produce the most oil are prioritized on the steam injection list. Tiltmeter-based reservoir monitoring best practices now dictates equal consideration for wells that create the most surface deformation (as a result of out of zone steam migration) and wells that are known communicators (with other wellbores and stimulation zones) with the most prolific producing wells when injections are scheduled. Operators can now fully realize the potential of pushing the injection envelope since a comprehensive understanding of the reservoir and subsurface fluid behavior allows them to optimize injection and production with their respective effects on the surface (dilation and subsidence). The long term impacts of these daily injections are also considered since the constant heating and cooling of thermal injection wells cause undue strain to wellbore materials with consequences eventually leading up to potentially expensive casing or cement failure. The formerly blind steam emplacement and fluid balance calculations can now be managed through improved modeling techniques by measuring the surface deformation and strain calculations. Through this novel approach utilizing tiltmeter data and keeping a close eye on net fluid balances, zones of significant subsidence or heave can be monitored and reversed by altering the injection and production cycles. Optimizing these injection cycles to minimize well strain will reduce the workover costs as well as reduce well abandonments that would normally be required once the reservoir and well damage is permanent. By accurately identifying damaged well casings, zones with damage can be squeezed out with cement rather than abandoned if caught in time.

Within this paper a case study (Field A) is presented where daily tiltmeter results play an integral role in helping engineers and field operators keep on top of cyclic well steaming strategies both in a risk mitigation and production enhancement capacity. Tiltmeter results not only highlight regions where shallow events may be occurring, they are able to detect out of zone growth within hours of steam initiation and identify potential source well candidates. If significant time can be saved in identifying problem areas, more resources can be applied to strategically moving steam around the field in a way that enhances overall production levels at a reduced fluid injection cost. The premise here is that the overheating of one area versus the under stimulation of another area often goes undetected, thereby increasing OPEX without realizing maximum recovery of the

asset. Tiltmeter-based microdeformation monitoring serves to change this dynamic.

Tiltmeter-based microdeformation techniques often work best while in concert with other technologies. To bring additional value to the existing tiltmeter deployment, Field-A was equipped with Differential Global Positioning System (GPS) monitoring as well as a satellite-based Interferometric Synthetic Aperture Radar (InSAR) campaign to enhance the results provided by the existing reservoir monitoring operation. Three continuous survey grade GPS stations were installed to provide millimeter-level 3-D motion observables for tiltmeter and InSAR integration and data correction (Davis et al. 2008). InSAR deliverables are processed and delivered on a periodic basis to provide broad aerial surveillance over the field as well as to provide insight into deformation along and beyond the margins of the tiltmeter array where out of zone event activity may be undetected. As with the tiltmeters, all GPS and InSAR microdeformation diagnostics and geomechanical analytics are integrated, analyzed, and reported to the operator of Field A for further evaluation of current operations.

Conclusions

It is important to highlight that there is no one “silver bullet” for monitoring complex reservoir-level processes. As with any technology there always are drawbacks and limitations. However, when deployed correctly and in the right environment, microdeformation monitoring has proven to be a reliable and cost effective methodology for obtaining information on reservoir behavior which can greatly help mitigate risk and improve operational efficiencies.

Acknowledgements

The authors thank Eric Davis, Zeno Philip and Tony Singh at Pinnacle for their input and project support.

References

- Davis, E.J., Marsic, S.D., Roadarmel, W.H., 2008. Combining InSAR and GPS for Improved Surface Deformation Monitoring, WHOC 2008-306 presented at the World Heavy Oil Congress, Edmonton, Alberta March 10-12.
- Davis, E.J., Marsic, S.D., McColpin, G., 2010. Use of deformation based reservoir monitoring for early warning leak detection, presented at the 2010 International Conference on Greenhouse Gas Technologies (GHGT10) held in RAI Amsterdam, The Netherlands, September 19 – 23.
- Du, J. and Olson, J.E., 2001. A poroelastic reservoir model for predicting subsidence and mapping subsurface pressure fronts, *Journal of Petroleum Science and Engineering* 30, 181-197.
- Davis, E., Wright, C., Demetrius, S., Choi, J., Craley, G., 2000. Precise Tiltmeter Subsidence Monitoring Enhances Reservoir Management, SPE 62577 presented at the SPE/AAPG Western Regional Meeting, Long Beach, CA, 19-23 June

Davis, E., Wright, C., Demetrius, S., Choi, J., Craley, G., 2000. Precise Tiltmeter Subsidence Monitoring Enhances Reservoir Management, SPE 62577 presented at the SPE/AAPG Western Regional Meeting, Long Beach, CA, 19-23 June.

Du, J., McColpin, G.R., Davis, E.J., Marsic, S.D., 2010. Model Uncertainties and Resolution Studies With Application to Subsurface Movement of a CO₂ Injection Project in the Krechba Field Using InSAR Data”, *Journal of Canadian Petroleum Technology*, V. 49, No. 6, 31-37.

Marsic, S., Roadarmel, W., Machovoe, M., Davis, E., 2011. Improving Reservoir Monitoring in EOR Environments Using Microdeformation Based Technologies, SPE WVS-022 presented at the 2011 South American Oil and Gas Congress, Maracaibo, Venezuela, 18-21 October 2011.

Wright, C.A., Davis, E.J., Minner, W.A., Ward, J.F., Weijers, L., Schell, E.J., Hunter, S.P., 1998. Surface Tiltmeter Fracture Mapping Reaches New Depths - 10,000 Feet and Beyond? SPE 39919, SPE Rocky Mountain Regional / Low-Permeability Reservoirs Symposium, 5-8 April 1998, Denver, Colorado.

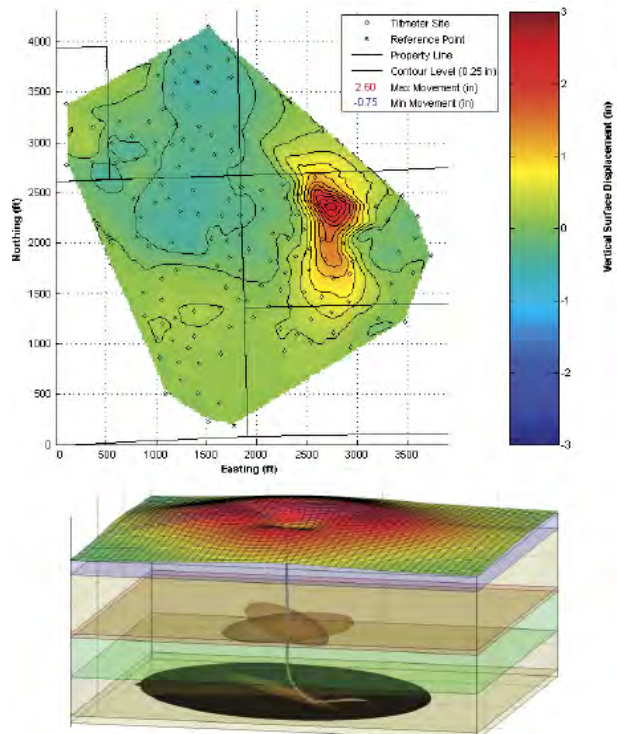


Figure 1: Example of a one-month tiltmeter based deformation output at Field-A used to track surface elevation changes (top). Ground displacement observations on up to an hourly basis are obtained from the field via automated radio telemetry for daily evaluation and analysis. Results can be presented in a variety of formats, database entries, GIS and interactive 3D visualizations (bottom).

Application of Seismic Inversion to Mitigate Reservoir Heterogeneity Uncertainty for Optimized Well Planning

M.F.M.F. Mohd Fuad* (ExxonMobil Exploration & Production Malaysia Inc.),
 F.F. Fahmi (ExxonMobil Exploration & Production Malaysia Inc.) &
 A.G.W. Williams (ExxonMobil Exploration & Production Malaysia Inc.)

Introduction

A seismically-derived sand/shale indicator volume was incorporated in the construction of a geologic model used in well placement optimization and production forecasting for the T gas development project. T gas development involves production of dry, non-associated gas (NAG) from two new satellite platforms to the main regional hub, and subsequently transported onshore for power generation in peninsular Malaysia.

T field is located in the Malay basin, approximately 200 km offshore Terengganu, Malaysia. The NAG reservoirs in field T are lower to middle Miocene siliciclastic sediments with more than 70% of the original gas in-place in the middle Miocene D/E reservoirs. The D/E reservoirs span more than 30 km long across three fields in a megastructure in the southern part of central Malay basin. Top of reservoir is approximately at 700m TVDss and up to 130m of gas column was encountered across the megastructure.

Methodology

The stratigraphic framework of the D/E reservoirs can generally be split into two parts; a lower section containing dominant fluvial-deltaic depositional elements, and an upper section containing a transition of subtidal bar to marginal marine deposits. The lower section is generally higher quality (>30% porosity, multi-Darcy permeability) relative to the upper section and is expected to deliver the bulk of reserves for the project. However, the lower section is potentially more discontinuous laterally with discrete point bars indicative of meander channels observed in 3D seismic. Conventional methods of two-dimensional mapping and attribute extraction may not capture the granularity of these depositional elements. Therefore, a volumetric approach was then taken to capture the lateral and vertical heterogeneities observed in the seismic data.

Rock property analysis indicates that inverted seismic data can be used to differentiate up to 4 classes of seismic facies; good gas-bearing sand (>100mD permeability), intermediate gas-bearing sand (<100mD permeability), and shale. This is mainly attributed to the excellent reservoir quality and shallow burial depth which minimizes attenuation effects from shallower zones and reduces transmission losses. Seismic-to-well ties performed on 6 exploration wells in the field yield high correlation coefficient (0.6-0.8) on near angle stacks. On each angle stack, the average wavelet used in the inversion had a peak frequency of 50 Hz and phase close to zero. The resulting simultaneous inversion resulted in high cross-correlation between inverted synthetics and actual traces, ranging between 0.96 in the near stacks and 0.99 in the far stacks.

The aim of simultaneous inversion was to generate a sand-indicator attribute, the Vp/Vs volume (ratio of compressional velocity over shear velocity). The Vp/Vs volume was found to have a high linear correlation (CC=77.8%) to shale volume logs generated from well data within the gas column. This relationship was then used to calculate a sand/shale volume through a linear multiattribute transform. A lithofacies volume was then built from the sand/shale volume by determining appropriate cut-offs observed from well data. Porosity, permeability, and saturation properties were then populated based on the seismically-derived facies volume and calibrated to well and core data.

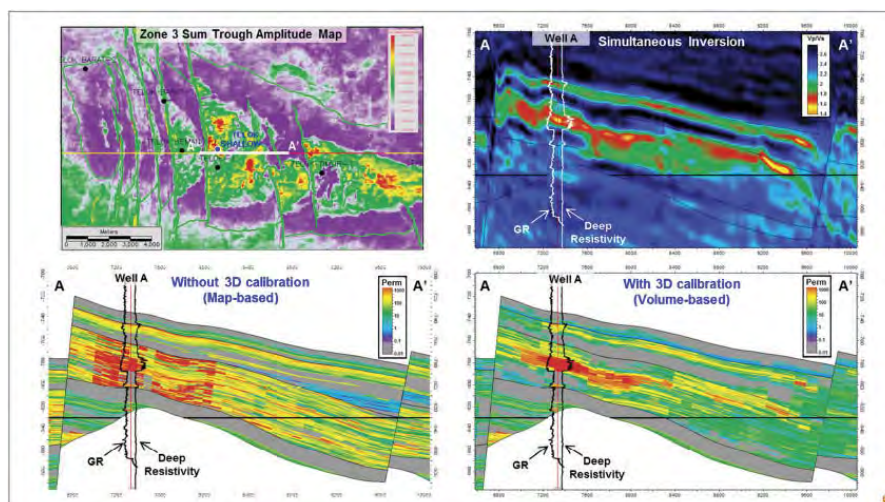
The Vp/Vs volume, built from simultaneous inversion, has enhanced our understanding of the vertical stacking geometries and lateral distribution of lithofacies in a complex fluvial-deltaic depositional environment. Understanding this distribution improves the ability to mitigate facies uncertainty, optimize placement of the gas producer wells, and potentially improve our net sand prediction and production capabilities.

Conclusions

The Vp/Vs volume, built from simultaneous inversion, has enhanced our understanding of the vertical stacking geometries and lateral distribution of lithofacies in a complex fluvial-deltaic depositional environment. Understanding this distribution improves the ability to mitigate facies uncertainty, optimize placement of the gas producer wells, and potentially improve our net sand prediction and production capabilities.

Acknowledgements

Many thanks to Petroliaam Nasional Berhad (PETRONAS) for allowing us to publish the data and PETRONAS CARIGALI SDN.BHD. (PCSB) for sharing the 3D seismic data. I would also like to thank the various personal contributors in ExxonMobil.



Key features of TEM and EM-IP investigations in South-East Asia

Y.A. Agafonov* (Irkutsk Electroprospecting Company), I.V. Bouddo (Irkutsk Electroprospecting Company), I.V. Egorov (Irkutsk Electroprospecting Company) & M.M. Salleh (Onyx Engineering)

Introduction

Currently in South-East Asia most of the hydrocarbon discoveries are associated with deposits of the shelf zone. Recently however the amount of exploration work on the mainland is growing. Among the geophysical methods used are seismic, magnetic and gravity surveys. This geophysical complex is complimented by electromagnetic survey (EM) to solve structural and fluid related oil and gas exploration problems, develop recommendations for the deep drilling wells location. The study of geoelectric parameters of the section (electrical resistivity and induced polarization factor) facilitates mapping the structural characteristics of the sedimentary cover, fault zones and highlight areas promising to search for hydrocarbon deposits.

This paper reports the characteristics of an onshore EM survey recently conducted in the South-East Asia region. The survey area is located on Northern part of the Borneo island (Sarawak, Malaysia) and is characterized by specific natural and geographical conditions and therefore the production work was complicated by several factors. Through the analysis of EM data the different types of noise interfering with electromagnetic data were estimated as well as the geological features of the investigated area were considered. A wide range of variation in the conductivity and thickness of sedimentary cover demanded high acquisition effort while carrying out field electroprospecting works.

Noise nature and interference features

High urbanization: Most of the TEM and EM-IP survey lines were located near industrial projects, housing areas, power lines and pipelines. As a consequence transient EM signals were affected by periodic noise with a frequency of 50 Hz as well as its multiple harmonics. An example of the signal and spectrum affected by the interference of industrial noise is shown below in (Fig.1).

In case of a constant periodical noise distortion usual summation algorithms including the robust averaging are not proper and have a very low efficiency. For the signal averaging a special algorithm was developed based on rejection of the periodical noise. The algorithm calculates the characteristics of the interference by using the exact formulas giving the values of the period, amplitude and phase noise (equation based on knowledge of the period of time elapsed between successive pulses), the synthesis of further interference with the calculated characteristics and subtracting it (and associated harmonics) from the original signal. The application of this algorithm enables to reduce interference to the order of $\approx 10^4$ - 10^5 times. Figure 2 shows the efficiency of periodical noise elimination.

The increased interference of natural processes on the EM signals: EM survey was also complicated by the impact of atmospheric (impulsive, sporadic noise) and telluric currents (low-frequency trend - change the signal level). As we are aware, the strongest and most frequent lightning discharges occur in tropical and equatorial regions of the world [1]. There was a strong influence of thunderstorm activity because the survey area was located in the equatorial zone. Emerging at the same time as the transients were non-periodic sequence of spikes excited

by transient voltage. Electrical signals produced by lightning discharges led to a strong signal distortion (Fig.3B). To improve the signal to noise ratio, different algorithms for summing and averaging the signal, such as the weighted summation and sigma, robust estimates were applied.

The origin of magnetotelluric fields explains the impact of the ionosphere on the flux of charged particles and the deformation of the Earth's magnetosphere. The influence of telluric currents leads to a change in signal level (Fig.3C). The higher influence of the trend effect was observed on conductive sections with a total conductivity up to 200-250 Sim. To minimize low-frequency trend interference an special algorithm was applied. It was based on the knowledge that the form of positive and negative pulses is identical and their difference is due to the influence of low-frequency component. In this analysis, all of the signals implementation obtained during the recording were considered.

The presence of certain types of noise in the collected signals in addition to physical and geographical conditions and proximity to urban areas also largely depends on the type of sensor. For example, the signals obtained with induction sensors (ungrounded loops) are less susceptible to the appearance of low-frequency trend in comparison with the signals received from the grounding line.

Tough natural and geographical conditions

The survey was carried out in mountainous terrain with absolute elevations of 300-500 m. Most of the territory was in the jungle. Undulating terrain, high temperatures, and rain affected the process of data acquisition.

Abrupt changes in geoelectrical properties

Sedimentary cover in the survey area is composed of the Neogene-Miocene rocks (sandstones and shales, reef build-up), and the basement comprised of metamorphosed sandstones of Mesozoic time. The total conductance of the section ranges from 80 to 250 Sim. Study area was located in a zone complicated by

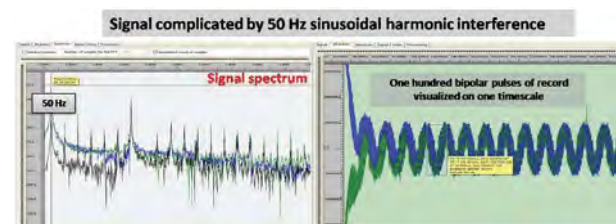


Figure 1: Industrial noise and TEM signals distortion.

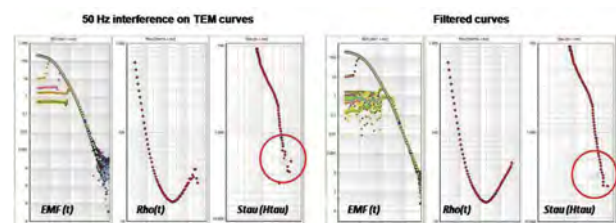


Figure 2: The efficiency of periodical noise reducing.

series of major faults, which is reflected in a significant change in the geological structure of sedimentary cover and variety of the geoelectric models.

As a result, the study area was differentiated into separate territories for the purpose of analysis. Figure 4 shows typical curves for Rho (t) and St (Ht), which reflect the characteristics of the geoelectric sections within designated zones.

Zone 1 and Zone 4 are characterized by the same value of the total conductance of the section which is about 200 Sim but differ through a combination of thickness and geoelectrical properties of the individual horizons. The original model for both areas consists of three main geoelectric layers $\Sigma S1 > \Sigma S2 > \Sigma S3$. Zone 2 has a lower total conductivity up to 100 - 120 Sim and a four-layer model of the geoelectric structure of the section $\Sigma S1 > \Sigma S2 < \Sigma S3 > \Sigma S4$. Zone 3 is characterized by a gradual increase in conductivity to a depth of 4 kilometers, without showing contrasting horizons indicating a homogeneous structure of the section. Thus, the area of study is characterized by high variability of geoelectrical properties.

The low degree of geological and geophysical knowledge of the survey block

The mainland of the block is characterized by almost complete lack of drilled wells, logging data and other geophysical studies which affects the interpretation of data.

The start model for the EM inversion was built using a combination of the scanty geological and geophysical inputs to supplement the resistivity data. Lack of apriori geological

knowledge seriously compromises the building of the start model. Conductivity curves were used to identify the main geoelectric boundaries and to calculate the appropriate power and resistance.

Figure 5 shows an example of calculating the parameters of the starting model together with the preliminary results observed from the EM inversions.

Conclusions

An onshore EM survey was conducted in Sarawak region of Malaysia with the inductive and galvanic transmitters and receivers of electromagnetic field that is adapted to the geoelectric conditions of the South-East Asia. Interpretation of anomalies of the electrical resistivity and polarizability parameters allowed studying the geological structure of sedimentary cover. The efficiency of the electromagnetic methods in specific natural and geographical conditions of South-East Asia is described. High quality of the field data is was acquired through application of the special mathematical algorithms for processing and interpretation of EM data with high amplitude noise. The distribution of the resistivity anomalies and behavior of geoelectric layers is expected to compliment HC exploration in the area with poor information about structure and low geological and geophysical knowledge.

References

MN Berdichevsky, VI Dmitriev, 2009. Models and methods of magnetotelluric. 780 pp.

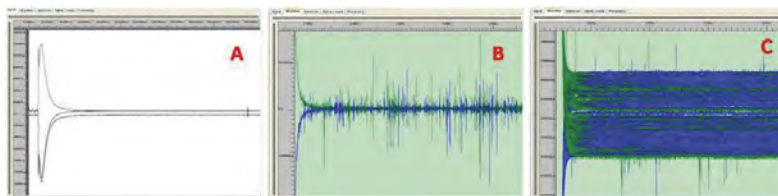


Figure 3: Atmospheric and telluric interference: A - not distorted signal, B- impulse noise, C - trend impact.

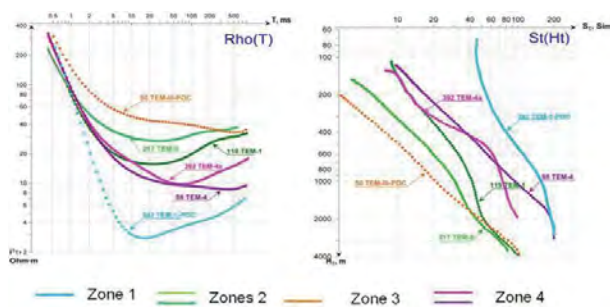
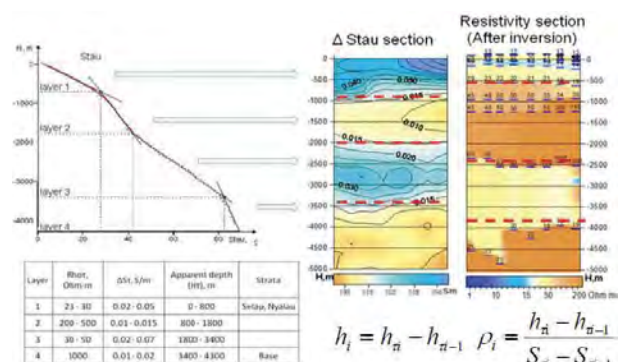


Figure 4: Typical TEM curves for different zones.



where i - number of layers, St_i and Ht_i - absciss and the ordinate of the point of inflection St (Ht), corresponding to the i -layer.

Figure 5: Parameters calculation of the initial model.

CSEM Application in Carbonate Environment: A Case Study

A. S. Saleh* (PETRONAS Carigali Sdn. Bhd.), S. K. Chandola (PETRONAS Carigali Sdn. Bhd.), P. K. Lee (PETRONAS Carigali Sdn. Bhd.), T. Velayatham (PETRONAS Carigali Sdn. Bhd.), P. Kumar (PETRONAS Carigali Sdn. Bhd.), M. S. Wahid (PETRONAS Carigali Sdn. Bhd.) & J. Beenfeldt (EMGS Sdn. Bhd.)

Introduction

Application of Controlled Source Electro Magnetics (CSEM) method as a derisking tool has found increasing application, particularly in deep water environment. CSEM provides resistivity distribution in the subsurface to differentiate between hydrocarbon and brine-filled reservoirs. However, the application of CSEM method in carbonate reservoirs has been rare due to the inherent inhomogeneity associated with carbonates. Variations in density, porosity and cementation may cause significant variation in carbonate resistivity, without any real change in hydrocarbon saturation. Therefore, successful application of CSEM in carbonates would require in-depth understanding of the linkage between resistivity and rock properties to explain the observed resistivity anomalies.

PETRONAS carried out its first ever CSEM survey, one of the first in the world, in a carbonate environment offshore Cuba, in 2010. The main objectives of the CSEM survey were: (i) to extend the application domain of the technology to carbonate reservoirs and (ii) to get a better understanding of the key risks associated with the four hydrocarbon prospects (C-1, C-3, C6 and C-9) identified on the basis of seismic and other G&G analysis, the nearest drilled well being ~300 km away from the study area. The major play types in the study area consist of foredeep inverted structures, sub-thrust play and shelf-slope fairway. Of these, the first one is considered as having lowest geological risk due to better reservoir development, thickest seal and its proximity to the potential source rocks. Based on these considerations, prospect C-1 was identified as the frontline candidate for drilling prior to conducting the CSEM survey.

Method and Theory

Survey Design & Data Acquisition

The water depth in the survey area ranged from 2100m-2700m which is considered favorable for CSEM application due to better suppression of airwave. 3D feasibility modeling was carried out prior to selecting the optimal survey geometry, to maximize the sensitivity of the measurements towards different survey layouts. The survey layout selected for the data acquisition consisted of dense 3D-grid of EM

receivers with closely spaced source tow lines to provide good azimuthal coverage for optimally capturing the anisotropy (Fig.1). Horizontal Electric Dipole (HED) source was deployed for generating EM waves using standard square waveform with maximum energy concentrated at 0.2, 0.6, 1.0 and 1.8 Hz. Good signal-to-noise ratio was observed on Electric & Magnetic components up to source-receiver offset of 15 km.

EM Inversion

EM inversion is the most crucial part of the data analysis workflow. The main challenge encountered while performing inversion of the EM data was the extremely high and variable resistivity values observed especially at the target level. The earth models for 3D inversion were constructed using series of 1D and 2.5D inversion to minimize the uncertainties in the start model. At this stage, a comparison was made between 2.5D inversion of electric and magnetic data using multiple start models as a consistency check to see whether both of the dataset produce similar resistivity distribution. The results were nearly consistent and therefore, it was decided to invert electric data only considering its higher signal to noise ratio and redundancy of the electric data measurement.

The initial unconstrained 3D inversion runs performed using layered resistivity model, were successful in establishing the resistivity of the shallow section. The resistivity value thus obtained for the shallow section were then included in subsequent inversion runs to minimize inversion effort on shallower section and improve the misfit for the deeper section, especially at the target level. 3D constrained inversion was then performed. The final inversion result showed a good misfit for all the prospects and the inversion workflow proved to be successful in handling the high carbonate resistivity. A post-inversion analysis was also performed in an attempt to establish the relationship between saturation and porosity through Archie's equation by using the measured resistivity value and other parameters estimated from petrophysical study. The 3D inversion results for C-1 are particularly interesting since they show a lower resistivity at the crest of the structure as compared to the flanks. The crest of the structure is also associated with lower seismic interval velocities (Fig.2). These observations can be explained either

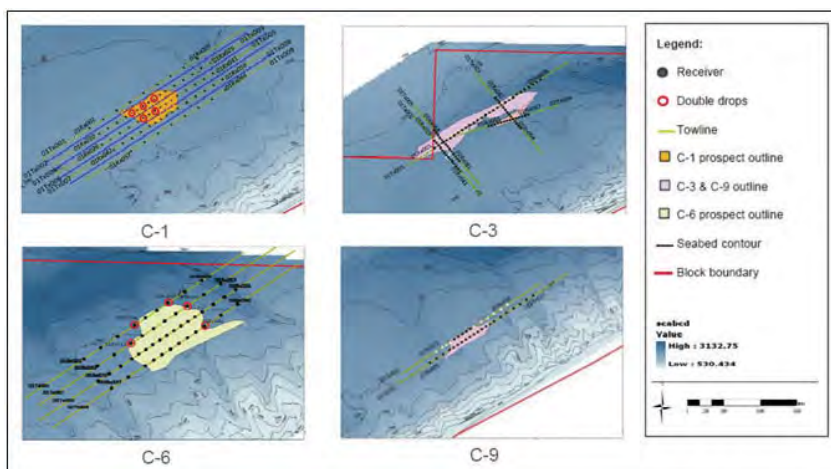


Figure 1: CSEM survey layout adopted for different prospects.

by the possibility of porous, hydrocarbon-bearing carbonates at the crest or a brine-saturated carbonate formation with a low porosity (assuming average value of cementation factor, saturation exponent and tortuosity). Hence, this result is encouraging in terms of the geological risking of the prospect C-1. Post-drilling calibration study using the well, CSEM and seismic data is expected to lead to better understanding of the petroleum system and rock properties in this area.

Conclusions

The maiden CSEM survey conducted by PETRONAS in carbonate reservoirs, has given useful information about the resistivity distribution in the subsurface and has successfully supplemented the G&G risk assessment. A customized inversion workflow, supported by strong R&D efforts successfully handled the high resistivity values. Interesting conductive anomaly has been observed over prospect C-1, supported by lowering of seismic interval velocity, which needs to be confirmed with drilling. An effort has also been made to establish the linkage between resistivity and rock properties for carbonates. Further studies are intended based on the calibration provided by the results of the forthcoming drilling campaign.

Acknowledgements

Authors are grateful to the management of PETRONAS and CUPET for granting the permission to publish and present this work. Direct and indirect contribution made by several colleagues in PETRONAS Carigali, CUPET and EMGS, during the course of this work, is also duly acknowledged.

References

Vossepoel, F., Darnet, M., Gesbert, S., Gonzalez, E., Hindriks, F., Kelly, R., Sandrin, A., Jensen, L. and Uldall, A., 2010. Detecting Hydrocarbon in Carbonates: Joint Interpretation of CSEM and Seismic. SEG Denver 2010 Annual Meeting, Extended Abstracts, 2010.

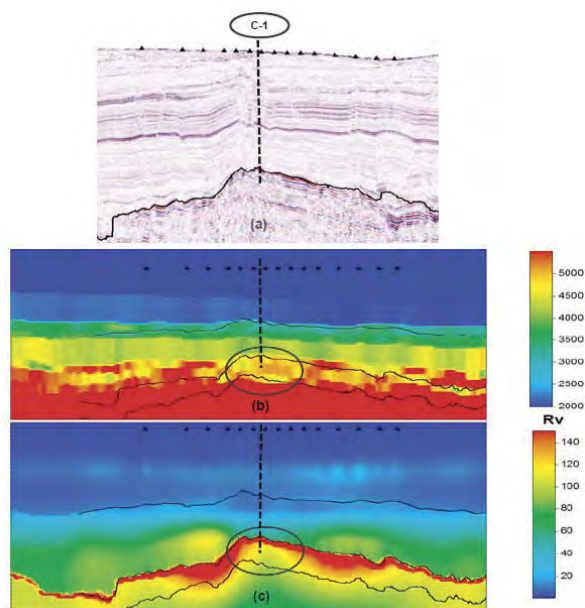


Figure 2: a) Seismic section through prospect C-1. b) Seismic interval velocity profile over prospect C-1. Lower interval velocity over the prospect is marked with a circle. c) 3D constrained EM inversion cross-section over prospect C-1. The conductive anomaly over the structure is marked with a circle. Black triangles are EM receiver locations.

Student Programme (GeoQuiz)

The QeoQuiz held on the first day of PGCE2012 saw strong competitions from 24 teams of contestants comprising undergraduates from eight universities. The QeoQuiz was won by Ling Hwei Chih and Yong Joy Anne from University of Malaya.



The Petroleum Geoscience Conference & Exhibition is an annual event that we Geology students look forward to. This year, it was extra special for me because my friend and I were chosen to represent University Malaya for the GeoQuiz. The prizes were very alluring, two iPad 2 to be won and the winners will also get the chance to attend the Gala Dinner held at the Mandarin Oriental Hotel.

Going into the competition we were hopeful yet apprehensive at the same time. Winning was of course, first and foremost on our minds but our competitors were quite formidable. Besides us, representatives from other universities all over Malaysia and even Indonesia were also participating.

In order to prepare for the quiz, we studied and kept up to date with current news on the industry. We planned our strategy and even came up with questions of our own that we thought could possibly be asked. That was the extent of our passion to win.

The quiz was an exciting and nerve-wracking event. It required speed and quick thinking to be able to answer the questions. As more and more teams were disqualified as the quiz progressed, we surprised ourselves with the fact that we were still one of the few teams remaining. When it came down to the last two teams, we were nervous but our resolve to win was stronger than ever.

We were ecstatic when the timer rang and we saw that we have bested the other team. The events that followed were definitely one of the highlights of our life. We were invited to the Gala Dinner as part of the prize, hosted at Mandarin Oriental Hotel. The theme of the night was Moroccan and the event was hosted by Harith Iskandar and Sheila Majid was the guest performer.

It was truly a wonderful experience, not only because of the prize; but to be able to apply our knowledge successfully, we felt that we had done justice to our lecturers. Our victory was not ours alone, but shared by all our coursemates and lecturers.

Yong Joy Anne

The Petroleum Geoscience Conference & Exhibition 2012 is a prestigious annual event of the petroleum industry in Asia. Every year, PGCE offers special student programmes, which come with various activities, quizzes and presentations by experienced practitioners from the industry. The GeoQuiz was organized to challenge students' mind, and for the first time, participants from both local and international universities were selected.

Conducted using the buzzer system, I felt that this year's quiz is much more exciting than before. The quiz includes 3 rounds where the weightage of the marks for each question increases each round. This further intensifies the excitement of the quiz.

My teammate and me worked together for the quiz and hoped to be qualified for the next round. With the loud cheers and supports from our friends, we finally managed to secure a place in the final round, facing off the last team from UTP. It was a competitive round; however my team managed to conquer the final round questions with the highest marks.

I'm really happy that we made our university proud by winning the GeoQuiz 2012. We received our prizes at the PGCE Gala Dinner in the evening, where the event was hosted by Harith Iskandar. The night gets better with live band performance by our singing diva Dato' Sheila Majid.

Apart from winning the prize, both the quiz and dinner was a superb and unforgettable experience that I can never forget! Hence, I strongly hope that this quiz will be continued as a tradition for student program in the future.

Ling Hwei Chih



CERAMAH TEKNIK TECHNICAL TALK

Tectono-stratigraphy and development of the Miocene delta systems on an active margin of northwest Borneo, Malaysia

Dr. Allagu Balaguru (Sabah Exploration, Talisman Energy, Malaysia)

25 April 2012

Makmal Peta, Bangunan Geologi, Universiti Kebangsaan Malaysia, Bangi

Abstract: The Paleogene regional tectonic setting of Sabah is very complex with southeasterly subduction of the proto-South China Sea in NW Borneo (Hall 1996), followed by a period of continued deposition of deep marine Rajang Group turbidites. The Late Eocene tectonic deformation is characterized by folding, thrusting and regional uplift related to the collision of the Luconia Continental Block against NW Borneo (Sarawak Orogeny; Hutchison, 1996).

Barckhausen & Roeser, (2004) reinterpreted paleomagnetic data and concluded that the sea floor spreading in the South China Sea, which began at 32 Ma, had already ceased by 20 Ma. This indicates that subduction ceased in the Early Miocene as opposed to the previously interpreted Middle Miocene (Brias *et al.* 1993) when the Dangerous Grounds micro-continental fragments collided with NW Borneo (Clennell, 1996; Hutchison *et al.*, 2000. This predates the timing of the Sabah Orogeny including the earlier 20 Ma timing proposed by Balaguru & Hall (2008), and it coincides with the Base Miocene Unconformity (BMU) in Sabah. The Early Miocene (22-20 Ma) deformation is a major tectonic event involving the formation of the Sabah mélanges significant uplift and erosion; patches of Burdigalian limestone formed during this uplift. This period was followed by a change in depositional environment from deep-water clastics to a shallow-water deltaic setting.

The Miocene to recent regressive fluvio-deltaic systems have been progressively deformed and overlie the Oligocene Crocker accretionary complexes generally regarded as the economic basement (Stage II or TB1.5sb). The Oligocene comprises slightly metamorphosed, highly deformed deep-water turbidite sediments known as the Crocker and Temburong Formations of onshore equivalents.

The overlying Neogene section has an unconformable relationship with the underlying section and can be divided into three deltaic complexes that generally young from east to west. The Meligan Delta (Stage III or TB 2.1-2.3) is the oldest and it accumulated in the mid-Early Miocene, forming the sand-dominant Meligan and shale-dominant Setap formations. The Meligan Formation is dominated by thick sandy deltaics with subordinate sandy shallow marine facies; the Setap Formation contains thin interbeds of sandstone within an overall shaley succession representing the distal equivalent facies of the Meligan Delta. All of offshore Sabah was under slope- to deep-marine conditions during Early Miocene to early Middle Miocene time.

A significant Middle Miocene unconformity (also known as Deep Regional unconformity) (MMU/DRU) separates the Meligan Delta from the overlying middle to late Miocene Champion Delta (Stage IV-ABC). This stage generally is characterized by coastal aggradation and progradation sequences comprising the onshore outcrop equivalents of the Belait, Miri and Sibuti Formations of NW Sabah. The Stage IVA (TB2.4-2.5) is a widespread regressive lower coastal plain to marginal marine (deltaic to shoreface) succession, whereas the Stage IVB (TB 2.6) is a major transgressive sequence of offshore marine deposits. The Stage IVC (TB3.1) is a major regressive sequence with widespread coastal to shallow marine and deep-water deposits followed by a period of prolonged sea-level lowstand. The Belait and Miri Formations are dominated by fluvio-deltaic sandstones with laterally equivalent coastal plain to marine sandstone successions that comprise the topsets of the Champion Delta depositional system. The Lambir and Seria formations are lithologically similar, but contain more fine-grained sandstone interbedded with mudstone representing the foresets of the delta. The shale-dominated marine deposit of the Sibuti Formation represents the distal equivalent or bottomsets of this relatively large delta system. Outcrop studies indicate that the Champion Delta is a complex NW prograding delta system with stacked sequences (from bottom to top) of fluvial sands, marginal marine (estuarine & deltaic) and shoreface deposits.

The Baram Delta succession is the youngest of the three deltaic systems. The late Miocene Shallow Regional Unconformity (SRU) separates the Champion Delta sequence from the younger Baram Delta (Stage IV-DEFG) succession; this most prominent unconformity in Sabah coincides with significant regional uplift and erosion. Stage IV (DEFG) of the Late Miocene to Pliocene is composed of stacked fluvio-deltaic sequence of the Baram Delta System with equivalent offshore shales and deep-water turbidite deposits. The late Miocene to Pliocene was a period of active regression with moderate aggradation punctuated by short periods of minor transgression. The deposits

include the onshore equivalent of the Liang Formation of NW Sabah and Brunei that unconformably overlies the Belait and Seria formations. The Liang formation also consists of fluvial sandstones and conglomerates, marginal marine sediments and shoreface sandstones and shales.

Integrated evaluation indicates that the NW Borneo Delta province evolved during the Early Miocene to present day from a foreland basin to a shelf margin. Multiple phases of compressional folding and faulting events have affected the region, causing uplift of the hinterland, large deltaic progradational events, and inversion of gravity-related faults. New geological mapping, detailed field studies and reinterpretation of existing data suggest that the region consists of west-vergent fold-thrust belts formed in the Early Miocene with syn- and postdeposition of the large Meligan, Champion and Baram Delta Systems on an active margin in NW Borneo. Most folds are detached, buried and thrust cored anticlines and they are younging towards west. The Labuan and Jerudong/Morris anticlines and Belait syncline formed during the Late Miocene as fault-bend and fault propagation folds. The prodelta shale was progressively buried by the prograding delta front and likely became overpressured and mobilized above reactivated basement structures during Pliocene, further complicating the deformation style. Pliocene- Pleistocene inversion on NNE- and N-trending structures with continued growth on NE-trending structures is most likely controlled by the regional NW-trending sinistral shear zones. Flower structures and thrust cored anticlines were developed above the reactivated structures. This study provides new insight into the tectonic evolution of rapidly prograding Tertiary delta systems and reveals how the compressional tectonics have migrated basinward as the delta system prograded.

CERAMAH TEKNIK TECHNICAL TALK

Geobencana Gempa bumi & Tsunami – Peringatan daripada Al-Quran & Al-Hadis

Prof Madya Dr Tajul Anuar Jamaluddin (Program Geologi, Universiti Kebangsaan Malaysia)

23 Mei 2012

Bangunan Dewan Anuar Makmur, Universiti Kebangsaan Malaysia, Bangi

Abstrak: “Geobencana” ditakrifkan sebagai proses semulajadi bumi yang boleh menyebabkan kehilangan nyawa, kemalangan jiwa, kerosakan harta benda dan ekonomi serta menjejaskan kualiti alam sekitar. Antara jenis geobencana atau bencana alam yang sering kita dengar dari serata dunia termasuklah gempabumi, tsunami, tanah runtuh, letusan gunung berapi, banjir, banjir lumpur, hakisan pantai, tanah mendap, kebakaran hutan dan sebagainya. Kini rekod menunjukkan kejadian geobencana semakin kerap terjadi dan keamatannya semakin tinggi. Apabila berlaku bencana besar kepada alam ini, pemusatan fikiran kita bukan hanya kepada banyak mana kemalangan jiwa atau kerugian hartabenda yang terlibat, malah kepada sebab musabab yang membawa kepada bencana tersebut. Masyarakat di seluruh dunia sibuk membahaskan tentang kekerapan kejadian bencana alam dan merumuskan pelbagai factor penyebab dan pencetusnya. Antara factor penyebab yang paling popular mengikut penjelasan saintis adalah fenomena pemanasan global, perubahan iklim, penipisan lapisan ozon, pertambahan populasi penduduk bumi dan kekurangan sumber bahan bumi. Daripada pelbagai penyelidikan, pelbagai kaedah mitigasi telah dicadangkan sebagai persiapan menghadapi bencana untuk mengurangi risiko bencana. Daripada mitigasi berupa perancangan, polisi, akta, piagam dan garis panduan hinggalah kepada mitigasi berstruktur yang menggembelingkan kemajuan kejuruteraan, sains dan teknologi. Pelbagai persidangan, seminar dan forum dianjurkan saban tahun, terutama selepas bencana gempabumi/tsunami berskala global yang berlaku di Aceh pada 26 Dis 2004, baik diperingkat tempatan, serantau dan antarabangsa. Malangnya, amat sedikit sekali yang cuba mengaitkannya dengan keterangan dan peringatan yang diberikan oleh Allah s.w.t melalui kitab suci Al-Quran dan RasulNya Nabi Muhammad s.a.w.

Ilmu manusia tentang rahsia alam amat terbatas. Al-Quran adalah mukjizat teragung dan merupakan sumber ilmu serta pedoman hidup kepada umat Muhammad s.a.w. Semakin berkembangnya sains dan teknologi kini, para saintis telah banyak membuat penemuan baharu yang semakin membuktikan kebenaran al-Quran. Dalam hal-hal yang berkaitan dengan kejadian bencana alam, banyak keterangan dan peringatan boleh didapati daripada al-Quran. Kisah-kisah di dalam al-Qur’an ada menceritakan tentang beberapa kaum atau umat nabi-nabi yang terdahulu yang ditimpa bencana yang dahsyat sehingga ada yang terus berkubur bersama-sama tamadun yang mereka bina. Kita mungkin tertanya-tanya apakah bencana ini merupakan fenomena alam semulajadi atau ianya suatu bala yang ditimpakan ke atas manusia? Jawapan kepada persoalan ini cuba dikupas di dalam kertas ini berpandukan kepada keterangan, pengkisahan dan peringatan yang terkandung di dalam al-Quran dan beberapa Hadis yang disampaikan oleh Rasulullah s.a.w.

MALAM EG PRACTICE

Geologist's Input in Hillside Development in Malaysia

Philip Tiong (G&P)

Engineering Geology Practice in Hong Kong

Jack Pan (G&P)

30 May 2012

Department of Geology, University of Malaya

Malam Engineering Geology Practice was held on 30th May 2012. Two practitioners with more than ten years experience in industry were invited to share their experiences. Mr. Philip Tiong gave a brief history on the development of various guidelines on hillside development in Malaysia. He then gave a detailed account on the geological terrain mapping developed by the Minerals and Geoscience Department, which is used by local authorities for the assessment of development planning proposals. Mr. Jack Pan, who is a professional engineer, talk about the practice of engineering geology in Hong Kong. The technical talks were chaired by Mr. Tan Boon Kong, Chairman of the Working Group on Engineering Geology, Hydrogeology & Environmental Geology. The lecture was followed by lively discussions.



VISIT TO PENJOM GOLD MINE

The visit to Penjom Gold Mine on the 12 May 2012 was organised by En. Zakarai Endut, Chairman of the Engineering Geology Working Group. The visit attracted 18 participants from local university such as University Malaya, University Kebangsaan Malaysia and University Malaysia Kelantan, as well as private practitioners. Among others are The transportation was provided by Jabatan Mineral and Geosains (JMG) but some of the participants come with their own transport. A trip to Penjom takes 2 and half hours from Society office at University Malaya. Upon arrival to the mine, the participants were given a briefing on safety and the background of the Penjom Gold Mine. It was followed by a tour of the mining pit, the mill and the laboratory. Below is a brief background of the Penjom Gold Mine.

Penjom Gold Mine is the largest producing gold mine in Malaysia and is currently owned by Indonesian based PT J Resources Nusantara. The mine is situated in Kuala Lipis District, Pahang, and 170 km from Kuala Lumpur. Penjom is located 30 km from the major geological tectonic structure of Bentong Raub Suture, along a NNE splay of this structure. The deposit is hosted within shear veins and associated extension veins, where the good ore grade are associated with felsites intrusive, which provided physical and chemical contrast at contact the with fault and bedding parallel shear. Sedimentary rock host to ore zone is at times highly carbonaceous and produces significant problem to plant processing recovery. However, proper stockpile management and processing technique of Resin-in-Leach (RIL) have overcome this problem with 91% plant recovery achievable depending on the carbon level.



NEW MEMBERSHIP

Full Membership

1. Abd. Razak bin Ahmad
2. Abduwah Zawawi bin Tengku Mohamed Putra
3. Adam Betteridge
4. Ahmad Ziyad bin Elias
5. Ahmed Syafiq Ab Rahman
6. Anisah binti Samion
7. Brund Virlovvet
8. Dehto Anak Kak
9. Hasanuddin bin Wases
10. Jan de Jager
11. Joseph Robert Martin
12. Jufriady Mender
13. Kamarudin bin Samuding
14. Khairil Azhar bin Ghazali
15. Kok Kwi Yen
16. Magdalene Tang Pooi Lee
17. Manan bin Che Jid
18. Marliah binti Musa
19. Nik Mohd Nishamuddin Nik Rahimi
20. Nor Azrina bt Mohd Amin
21. Nor Haliza binti Abdullah
22. Othman bin Kangsar
23. Peter Majid Tandom
24. Rosli Saad
25. Rozlin Hassan
26. Ryan Charles Lafferty
27. Siti Zainab bt Musa
28. Stuart James King
29. Tan Wei Quan
30. Teng King Kuen
31. Wan Mohd Helmy bin Che Alaidin
32. Wong Chee Fui
33. Yee Ah Chim
34. Yeow Yew Heng
35. Zahidi bin Hamzah
36. Zahir Yahya

37. Zhi Fang
38. Zulherry Isnain
39. Zulkili bin Abdul Majid
40. Zulqarnain bin Ibrahim

Associate Membership

1. Jay Dorfman
2. Zulkhairi bin Mat Isa

Student Membership

1. Abdul Manan Abdulah
2. Abdul Rahman bin Rodzi
3. Daniel Lee Tek Aun
4. Habshah bt Ibrahim
5. Hardianshah Saleh
6. Jay Xavier John
7. Junaidi bin Asis
8. Mahmoud Khaki
9. Marsha Sakina
10. Maryam Alsadat Moussavi Alashloo
11. Mohd Amir Asyraf Sulaiman
12. Muhamad Nur Hafiz bin Sahar
13. Nik Nurul Nadiyah Noor Ramli
14. Noorhashima binti Adenan
15. Nur Atikah binti Mohd Ali
16. Nur Liyana binti Hashim
17. Oh Hwee Theng
18. Sabri Abubakar Ali Idriss
19. Samira Ghaheri
20. Sani Kaita Mohammed
21. Siti Noor Aisyah bte Idris
22. Siti Rafhan binti Noor Mahadi
23. Umi Nadiyah bt Harun
24. Wan Noor Farahiyatul Akmal bt Mohd Sani
25. William Lodwick
26. Zaa'elezia Maniff Julian

CHANGE OF ADDRESS

1. Foong Yin Kwan
13 Daydream Place, Eight Mile Plains, Queensland,
4113, Australia
2. Danny Oh
3C Dunsfold Drive, Dunsfold Residences, Singapore
357718
3. Chok Pit Yuen
46, Jalan Mawar 1, Taman Puchong Perdana, 47150
Puchong
4. Allagu Balaguru
45, Jalan Bukit Setiawangsa 7, Taman Setiawangsa,
54200 Kuala Lumpur.
5. Mohd Asraf Hj Khamis
JX Nippon Oil & Gas Exploration (Deepwater Sabah)
Ltd, Petronas Menara 3, Level 51, Kuala Lumpur
City Centre, 50088 Kuala Lumpur
6. Joanes Muda
Jabatan Mineral dan Geosains Malaysia, Jalan Wan
Abdul Rahman, Kenyalang Park, Peti Surat 560,
93658 Kuching, Sarawak
7. Khalid Ngah
18175 Jalan Melati Indah 1, Kemensah Heights,
53100 Kuala Lumpur.

GSM Photographic Competition 2011



First Prize

Mohd Shafiq
Farhan bin
Mohd Zainudin
(Minerals and
Geoscience
Department
Malaysia)

Title: Flute Casts,
brain-like
appearance



Second Prize

Chan Zhijian
(University of
Malaya)

Title: Cave river
formation



Third Prize

Ng Wei Siang

Title: The beauty of rock



Consolation Prize

Chung How Min (Curtin University Miri)

Title: Tusan beach



Consolation Prize

Nizarulikram Abdul Rahim

Title: Wind-stress feature



Consolation Prize

Chung How Min (Curtin University Miri)

Title: Tusan beach



Consolation Prize

Tan Ai Bee

Title: Mulu cave



Consolation Prize

Ling Hwei Chih
(University of Malaya)

Title: Melange of the
Bentong Raub Suture

GSM Photographic Competition 2012

1st Prize: RM1,000.00

2nd Prize: RM 500.00

3rd Prize: RM 300.00

5 consolation prizes of RM100.00 each

Deadline: 31 December 2012

Email your entry to gsmphotocompetition@gmail.com

Please read the rules and regulation.



Geological Society of Malaysia Persatuan Geologi Malaysia Photographic Competition 2012

Rules and regulations:

1. This photographic competition is open to all members of the Society, as well as the general public.
2. The purpose of the competition is to promote interest in the geology of Malaysia. We are especially interested in photographs that showcase the beauty and uniqueness of Malaysian geology, including geological landscapes, outcrops, specimens and photomicrographs of rocks, minerals and fossils. The subject matter and scene should be directly related to the geology of Malaysia, and located within Malaysia.
3. Judging will be based on artistic merit, originality and quality, as well as geological content.
4. Entries are to be submitted in the form of digital images in JPEG, TIFF, PSD or PNG file format. Maximum file size is 15 Mb and it is recommended that the image size be no smaller than 5 megapixels.
5. The subject matter and scene should be accurately depicted in the photograph. Limited digital adjustments (dust removal, cropping, level, saturation, colour balance and contrast, etc.) and black & white conversion are acceptable. Montages or blending of multiple photographs is not allowed, with the exception of panorama, HDR and DOF stacking.
6. Each contestant may submit up to ten entries, and multiple entries are accepted. However, each contestant will be limited to winning two prizes.
7. The prizes are as follows:
 - 1st Prize: RM1,000.00
 - 2nd Prize: RM 500.00
 - 3rd Prize: RM 300.00
 - 5 consolation prizes of RM100.00 eachEach prize winner will also receive a certificate
8. By submitting the entry, the contestant acknowledges that he/she is the photographer, and sole owner of the photograph. By submitting the entry, you also grant the Geological Society of Malaysia the non-exclusive right to use your photographs. The winning photographs will become the property of the Society.
9. Closing date: All entries must reach the Geological Society of Malaysia before the 31 December, 2012.
10. The decision of the judges is final. The organizers reserve the right to make adjustments to these rules and regulations if deemed necessary.
11. Entries in CD should be carefully packed and mailed to: The Organizer, GSM Photographic Competition 2012, c/o Department of Geology, University of Malaya, 50603 Kuala Lumpur, or email to gsmphotocompetition@gmail.com. Each entry must be accompanied by the following information in a text file:
 1. Name
 2. Address
 3. Profession
 4. Affiliation/Institution
 5. Telephone & fax
 6. Email address
 7. Image file name
 8. Title of photograph
 9. Description/Geological information
 10. Locality
 11. Camera & setting
 12. Digital adjustment (if any)

GEO-INTRO 2012



21st April 2012
SM Sains Selangor, Cheras



Geo-Intro is an annual event organized by the AAPG University of Malaya Student Chapter since the year of 2010. Its objective is to promote the subject of Geology to secondary level students as their future choice of study. Geo-Intro – The Earth Demanding Us, was organized and held on the 21st April 2012 at SM Sains Selangor, Cheras. This event was kindly sponsored by Talisman Energy Inc., and was free to all participating students.

There were a total of 90 participating students from SM Sains Selangor. The event started at 8.00 am and ended at 2.30 pm, with a short morning break at 10.30 am and lunch session at 1.30 pm. The students were given brief introduction on AAPG and its history, together with the activities and programmes organized by the student chapter.

The speaker for the talk was Mr. Tan Chun Hock from Talisman. Currently he is an exploration geologist, which mainly works on the Sabah exploration blocks. In his talk, Mr. Tan explained the oil and gas industry in general, including the core areas for operations and global exploration; type of petroleum and overall petroleum system; global oil prices trend and world liquids production outlook, where oil demand is expected to be increasing and unconventional sources may be as important as conventional sources in the future. Upon ending his talk, Mr. Tan also shares his personal experience throughout his career with the students and what it takes to be a geologist. After the morning break, students were divided into groups to visit the exhibition booths prepared by the committee. There are five booths exhibiting minerals, rocks, fossils, maps and geological tools, and a Talisman booth. The exhibition ended at 12.15 pm and was followed by an interaction and experience sharing session between the committee and the students. The last activity of the event was a short photography session, followed by a lunch provided for the students.

Ling Hwei Chih
Event Secretary of Geo-Intro 2012
University of Malaya Student Chapter of AAPG

Sponsored By:

TALISMAN
ENERGY



UPCOMING EVENTS

August 5-10, 2012: 34th International Geological Congress (IGC) in Brisbane, Australia. The primary IUGS conference that is held every 4 years. See the information above, and visit the Congress website at: <http://www.34igc.org/>

August 15-17, 2012: The 10th Symposium on Engineering Geology and the Environment. Villa Carlos Paz City, Cordoba Province, Argentina. Organized by: The Asociación Argentina de Geología Aplicada a la Ingeniería (ASAGAI), Argentina National Group of the International Association for Engineering Geology and the Environment (IAEG). Download the flier from: http://www.iaeg.info/index.php?option=com_content&view=article&id=106:10th-symposium-on-engineering-geology-and-the-environment&catid=44:announcements&Itemid=88. Contact email address for enquiries: simposio@asagai.org.ar

September 3-7, 2012: Coring and Core Analysis, Kuala Lumpur, Malaysia. Tel: 603 21684751; email: ap-enquiries@petroskills.com; www.petroskills.com

September 3-7, 2012: Production Technology for Other Disciplines, Kuala Lumpur, Malaysia. Tel: 603 21684751; email: ap-enquiries@petroskills.com; www.petroskills.com

September 3-14, 2012: Production Operations 1, Kuala Lumpur, Malaysia. Tel: 603 21684751; email: ap-enquiries@petroskills.com; www.petroskills.com

September 7-20, 2012: Primary Cementing – Cementing 1, Kuala Lumpur, Malaysia. Tel: 603 21684751; email: ap-enquiries@petroskills.com; www.petroskills.com

September 10-14, 2012: Seismic Interpretation, Kuala Lumpur, Malaysia. Tel: 603 21684751; email: ap-enquiries@petroskills.com; www.petroskills.com

September 10-14, 2012: Cementing Practices – Cementing II, Perth, Australia. Tel: 603 21684751; email: ap-enquiries@petroskills.com; www.petroskills.com

September 10-14, 2012: Integration of Rocks, Log and Test Data, London, UK. Tel: 603 21684751; email: ap-enquiries@petroskills.com; www.petroskills.com

September 10-14, 2012: Completions and Workovers, Kuala Lumpur, Malaysia. Tel: 603 21684751; email: ap-enquiries@petroskills.com; www.petroskills.com

September 16-19, 2012: AAPG2012 International Conference & Exhibition. Marina Bay Sands Expo and Convention Center, Singapore. <http://www.aapg.org/singapore2012/>

September 17-19, 2012: Operating Company/Service Company Dynamics: How E & P gets Done, Kuala Lumpur, Malaysia. Tel: 603 21684751; email: ap-enquiries@petroskills.com; www.petroskills.com

Lumpur, Malaysia. Tel: 603 21684751; email: ap-enquiries@petroskills.com; www.petroskills.com

September 17-21, 2012: Well Log Interpretation, Kuala Lumpur, Malaysia. Tel: 603 21684751; email: ap-enquiries@petroskills.com; www.petroskills.com

September 17-21, 2012: Petroleum Risk and Decision Analysis, Kuala Lumpur, Malaysia. Tel: 603 21684751; email: ap-enquiries@petroskills.com; www.petroskills.com

September 17-21, 2012: EPEX-World: The E & P Executive Business Simulation, Kuala Lumpur, Malaysia. Tel: 603 21684751; email: ap-enquiries@petroskills.com; www.petroskills.com

September 17-28, 2012: Drilling Practices, Kuala Lumpur, Malaysia. Tel: 603 21684751; email: ap-enquiries@petroskills.com; www.petroskills.com

September 19-20, 2012: European Base Oils & Lubricants Summit, Europe. ACI's Energy Events, email: jkorfanty@acieu.co.uk

September 19-20, 2012: Smart Grids, Europe. Contact: ACI's Energy Events, email: jkorfanty@acieu.co.uk

September 24-28, 2012: Carbonate Reservoirs, London, UK. Tel: 603 21684751; email: ap-enquiries@petroskills.com; www.petroskills.com

September 24-28, 2012: Structural Styles in Petroleum Exploration, Kuala Lumpur, Malaysia. Tel: 603 21684751; email: ap-enquiries@petroskills.com; www.petroskills.com

September 24-28, 2012: Production Geology for Other Disciplines, Kuala Lumpur, Malaysia. Tel: 603 21684751; email: ap-enquiries@petroskills.com; www.petroskills.com

September 24-28, 2012: Drilling Fluids Technology, Kuala Lumpur, Malaysia. Tel: 603 21684751; email: ap-enquiries@petroskills.com; www.petroskills.com

September 24-28, 2012: Shaly Sand Petrophysics (Intermediate), Kuala Lumpur, Malaysia. Tel: 603 21684751; email: ap-enquiries@petroskills.com; www.petroskills.com

September 30-October 4, 2012: Oil and Gas Reserves Evaluation, Kuala Lumpur, Malaysia. Tel: 603 21684751; email: ap-enquiries@petroskills.com; www.petroskills.com

October 1-5, 2012: Petroleum Geochemistry: Tools for Effective Exploration and Development, London, UK. Tel: 603 21684751; email: ap-enquiries@petroskills.com; www.petroskills.com

October 1-5, 2012: Analysis of Structural Traps in Extensional Settings, Kuala Lumpur, Malaysia. Tel: 603 21684751; email: ap-enquiries@petroskills.com; www.petroskills.com

October 1-5, 2012: Basic Drilling Technology, Kuala Lumpur, Malaysia. Tel: 603 21684751; email: ap-enquiries@petroskills.com; www.petroskills.com

October 1-15, 2012: Petroleum Systems: Modeling the Past, Planning the Future, Nice, France. American Association of Petroleum Geologists, P.O. Box 979, Tulsa, Ok, USA; email: education@aapg.org

October 8-12, 2012: Geochemical Techniques for Solving Reservoir Management and Field Development Problems, London, UK. Tel: 603 21684751; email: ap-enquiries@petroskills.com; www.petroskills.com

October 10-11, 2012: Global Geothermal Energy Summit, Europe. ACI's Energy Events, email: jkorfanty@acieu.co.uk

October 15-19, 2012: Foundations of Petrophysics, Kuala Lumpur, Malaysia. Tel: 603 21684751; email: ap-enquiries@petroskills.com; www.petroskills.com

October 15-19, 2012: Wireline Formation Testing and Interpretation (Specialized), Kuala Lumpur, Malaysia. Tel: 603 21684751; email: ap-enquiries@petroskills.com; www.petroskills.com

October 15-19, 2012: Reservoir Management for Unconventional Reservoirs, London, UK. Tel: 603 21684751; email: ap-enquiries@petroskills.com; www.petroskills.com

October 15-19, 2012: Petroleum Project Management: Principles and Practices, Kuala Lumpur, Malaysia. Tel: 603 21684751; email: ap-enquiries@petroskills.com; www.petroskills.com

October 16, 2012: Sustainability Day, Europe. ACI's Energy Events, email: jkorfanty@acieu.co.uk

October 17-18, 2012: The 2012 Tight & Shale Gas Summit, Europe. ACI's Energy Events, email: jkorfanty@acieu.co.uk

October 22-24, 2012: Capillarity in Rocks, Kuala Lumpur, Malaysia. Tel: 603 21684751; email: ap-enquiries@petroskills.com; www.petroskills.com

October 29-November 2, 2012: Applied Seismic Anisotropy for Fractured Reservoir Characterization, Kuala Lumpur, Malaysia. Tel: 603 21684751; email: ap-enquiries@petroskills.com; www.petroskills.com

October 29-November 2, 2012: Basic Reservoir Engineering (Basic), Kuala Lumpur, Malaysia. Tel: 603 21684751; email: ap-enquiries@petroskills.com; www.petroskills.com

October 29-November 2, 2012: Well Stimulation: Practical and Applied, Kuala Lumpur, Malaysia. Tel: 603 21684751; email: ap-enquiries@petroskills.com; www.petroskills.com

October 30-November 2, 2012: International Conference on Ground Improvement and Ground Control: Transport Infrastructure Development & Natural Hazards Mitigation, Innovation Campus, University of Wollongong, Australia. ICGI Conference Secretariat, Faculty of Engineering, University of Wollongong, Wollongong. Tel: 02 42215852; Fax: 02 42213238; email: icgi_2012@uow.edu.au

November 6-8, 2012: UNESCO World Heritage Convention 40th Anniversary Celebration. Kyoto, Japan. This final 40th anniversary celebration event will focus on the outcomes of the different workshops and studies undertaken during the celebrations and will reflect on the future of the Convention. For details of the celebration events check the special UNESCO 40th anniversary website at: <http://whc.unesco.org/en/40years>

November 19-21: Group on Earth Observations (GEO) Task SB-01 "Oceans and Society: the Blue Planet" Symposium, São Paulo, Brazil. http://www.earthobservations.org/about_geo.shtml

November 20-21, 2012: International Mine Management 2012 Conference (IMM 2012). Melbourne, Australia. Organised under the management of The Minerals Institute (AusIMM). The call for papers has been issued, deadline for submission 20 February 2011. Conference details on the web at: <http://ausimm.com.au/imm2012/>

December 5-7, 2012: International Petroleum Technology Conference (IPTC), China World Exhibition Hall in Beijing, China. <http://iptcnet.org/2012/>

January 5-8, 2013: The Second Symposium on the Geological Resources in the Tethys Realm. Aswan, Egypt. The latest flier can be download from the webpage at: <http://www.emwis.net/thematicdirs/events/2013/01/tethys-geological-society-meeting>

April 22-24, 2013: The International Congress on Disaster Risks and Sustainable Territorial Development" (CIRiDe). Catamarca, Argentina. <http://www.scribd.com/doc/97125986/i-Circular-Ciride>

May 19-22, 2013: AAPG 2013 Annual Convention & Exhibition, Pittsburgh, PA USA. <http://www.aapg.org/meetings/>

October 6-7, 2013. International Conference VAJONT 1963-2013 - "Fifty years of increasing knowledge on giant and catastrophic landslides", Padova, Italy. <http://www.vajont2013.info>

Geological Society of Malaysia Publications

GENERAL POLICY

Papers should be as concise as possible. They may include original results of basic, applied and policy research of national or international significance, current reviews, or discussions on techniques, research programs, organisations, information, or national and international policies in geoscience.

SUBMISSION OF PAPERS

Only papers that have not been published elsewhere will be considered for publication. Authors must agree not to publish elsewhere a paper submitted and accepted. All papers will be subjected to review by two or more reviewers. Authors wishing to include published and unmodified figures or text passages are required to obtain permission from the copyright owner(s). Authors of English papers are strongly urged to have their manuscript edited for language before submission by a person whose first language is English.

The Editor reserves the right to reject all or any part of the paper submitted. The Geological Society of Malaysia assumes no responsibility for statements made by authors.

Three (3) original copies of the paper should be submitted to:

The Editor,
Geological Society of Malaysia
c/o Department of Geology
University of Malaya
50603 Kuala Lumpur,
Malaysia
Tel: (603) 7957 7036
Fax: (603) 7956 3900
Email: geologicalsociety@gmail.com

MANUSCRIPT

The paper can be written in Bahasa Malaysia (Malay) or English. For English papers, use either British or American spelling but not a combination of both. The paper should be checked thoroughly for spelling and grammar. The manuscript must be printed at 1.5 spacing in a single column on one side of A4 paper. All pages should be numbered. Length of paper should be between 3,000 and 6,000 words for the *Bulletin* and between 2,000 and 3000 words for *Warta Geologi*, excluding tables and illustrations. Metric units should be used and all non-standard symbols, abbreviations and acronyms must be defined.

TITLE

Title must be informative and reflects the content of the paper. Title in Malay should include an English translation. It should be concise (less than 20 words). Avoid using abbreviation in the title.

AUTHOR'S ADDRESS

Addresses of all authors must be provided. The addresses should be sufficient for correspondence. Please include email address, telephone and fax of the corresponding author.

ABSTRACT

Abstract in both Malay and English, each in one paragraph and should not exceed 300 words. It should clearly identify the subject matter, results obtained, interpretations discussed and conclusions reached.

KEYWORDS

Please include 3 to 8 keywords that best describe the content of the paper.

REFERENCES

In the text, references should be cited by author and year and listed chronologically (e.g. Smith, 1964; Jones *et al.*, 1998; Smith & Tan, 2000). For both Malay and English paper, all references must be listed in English. Title of non-English articles should be translated to English.

The list of references should only include articles cited in the text. The list should be arranged in alphabetical order. Please ensure that the reference list is complete and the bibliographical details are accurate. The references should be in the following manner:

Journal article:

Suntharalingam, T., 1968. Upper Palaeozoic stratigraphy of the area west of Kampar, Perak. *Geol. Soc. Malaysia Bull.*, 1, 1-15.

Book:

Hutchison, C.S., 1989. *Geological Evolution of South-east Asia*. Clarendon Press, Oxford. 368 p.

Chapter of book and Symposium volume:

Hosking, K.F.G., 1973. Primary mineral deposits. In: Gobbett, D.J. and Hutchison, C.S. (Eds.), *Geology of the Malay Peninsular (West Malaysia and Singapore)*. Wiley-Interscience, New York, 335-390.

Article in Malay:

Lim, C.H. & Mohd. Shafeea Leman, 1994. The occurrence of Lambir Formation in Ulu Bok Syncline, North Sarawak. *Geol. Soc. Malaysia Bull.*, 35, 1-5. (in Malay with English abstract)

TABLES

All tables should be cited in the text and numbered consecutively. Tables should have a title and a legend explaining any abbreviation or symbol used. Each table must be printed on a separate piece of paper. Do not insert the tables within the text. Data in tables should be aligned using tab stops rather than spaces. Avoid excessive tabulation of data.

ILLUSTRATIONS

Please make sure that all illustrations are useful, necessary and of good quality. A maximum of ten (10) illustrations (photographs, graphs and diagrams) are allowed and these should be cited in the text and numbered consecutively as Figures. The papers are usually published in black-and-white but it may sometimes be possible to include colour figures at the author's expense. The scales for maps and photomicrographs should be drawn on the figure and not given as a magnification. Originals should not be greater than A4 size and annotations should be capable of being reduced down to 50 percent. The caption should be listed on a separate piece of paper. Do not insert the illustration within the text.

SUBMISSION OF ELECTRONIC FILES

Authors are required to submit electronic files together with three hardcopies of their papers. Submission should be made using CD-ROM. The CD-ROM should be accompanied with a listing of all files and the software (name and version) used. The file names should reflect the content of the files (e.g. Ali_Fig1.tif). Please make sure that the files and the hardcopies are the same.

PREFERRED SOFTWARE

Text: Microsoft Word. Please save in two versions, Word (.doc) and Rich Text Format (.rtf). Do not insert tables and illustration within the text.

Tables: Microsoft Word or Microsoft Excel. Please submit as separate files.

Illustrations – Vector Graphics: Adobe Illustrator (preferred), CorelDraw and Freehand. Final line thickness should be at least 0.5 point or 0.17 mm. For other software, please submit one copy in the native file format and export one copy as a PDF file with all fonts embedded and one copy as a high resolution TIFF or JPEG image.

Photographs or bitmap (raster) images: Adobe Photoshop. Please save as TIFF or PSD files. Save/scan line art at 600 to 1200 dpi and greyscale figures at 300 to 600 dpi. High resolution JPEG, TIFF or GIF files from other sources are also acceptable. The resolution must be high enough for printing at 300 dpi.

REPRINTS

Twenty five copies of each article published are supplied free of charge. Additional reprints are available at cost price provided that orders are placed prior to publication. Authors will also receive a softcopy of the article published in .pdf format.

WARTA GEOLOGI PERSATUAN GEOLOGI MALAYSIA

Newsletter of the Geological Society of Malaysia

Jilid 38, No. 2 • Volume 38, No. 2 • April–June 2012

KANDUNGAN (CONTENTS)

CATATAN GEOLOGI (Geological Notes)

- AHMAD ROSLI OTHMAN: Fossil moluska Trias Akhir dari kawasan Binjui, Kedah (Late Triassic molluscan fossils from Binjui area, Kedah) 27

PERTEMUAN PERSATUAN (Meetings of the Society)

46TH ANNUAL GENERAL MEETING & ANNUAL REPORT 2011

- 35
- Minutes of the 45th Annual General Meeting (AGM) 36
 - President's Report 40
 - Secretary's Report 42
 - Assistant Secretary's Report 49
 - Editor's Report 51
 - Treasurer's Report 52
 - Auditor's Report 53

PETROLEUM GEOSCIENCE CONFERENCE AND EXHIBITION 2012

- Organizing Committee 66
- Sponsors 67
- Programme 68
- Extended Abstracts 69
- Student Programme (GeoQuiz) 81
- 247

- ALLAGU BALAGURU : Tectono-stratigraphy and development of the Miocene delta systems on an active margin of northwest Borneo, Malaysia 248

- Tajul Anuar Jamaluddin: Geobencana Gempa bumi & Tsunami – Peringatan daripada Al-Quran & Al-Hadis 249

- MALAM ENGINEERING GEOLOGY PRACTICE 250

- VISIT TO PENJOM GOLD MINE 251

BERITA-BERITA PERSATUAN (News of the Society)

- New Membership 252
- Change of Address 252
- Winners of GSM Photographic Competition 2011 253
- GSM Photographic Competition 2012 255

BERITA LAIN (Other News)

- GEO-INTRO 2012 256
- Upcoming Events 257



Published by the GEOLOGICAL SOCIETY OF MALAYSIA
 Department of Geology, University of Malaya, 50603 Kuala Lumpur, MALAYSIA
 Tel: 603-7957 7036 Fax: 603-7956 3900 E-mail: geologicalsociety@gmail.com